

A large concrete dam structure with multiple gates partially open, allowing a massive volume of brown, turbulent water to cascade down. The dam is set against a backdrop of industrial buildings and power lines under a clear sky.

# Manual on Estimation of Probable Maximum Precipitation (PMP)



World  
Meteorological  
Organization

Weather • Climate • Water

WMO-No. 1045

# Manual on Estimation of Probable Maximum Precipitation (PMP)

WMO-No. 1045



**World  
Meteorological  
Organization**  
Weather • Climate • Water

WMO-No. 1045

**© World Meteorological Organization, 2009**

The right of publication in print, electronic and any other form and in any language is reserved by WMO. Short extracts from WMO publications may be reproduced without authorization, provided that the complete source is clearly indicated. Editorial correspondence and requests to publish, reproduce or translate this publication in part or in whole should be addressed to:

Chairperson, Publications Board  
World Meteorological Organization (WMO)  
7 bis, avenue de la Paix  
P.O. Box 2300  
CH-1211 Geneva 2, Switzerland

Tel.: +41 (0) 22 730 84 03  
Fax: +41 (0) 22 730 80 40  
E-mail: [publications@wmo.int](mailto:publications@wmo.int)

ISBN 978-92-63-11045-9

**NOTE**

The designations employed in WMO publications and the presentation of material in this publication do not imply the expression of any opinion whatsoever on the part of the Secretariat of WMO concerning the legal status of any country, territory, city or area, or of its authorities, or concerning the delimitation of its frontiers or boundaries. Opinions expressed in WMO publications are those of the authors and do not necessarily reflect those of WMO.

The mention of specific companies or products does not imply that they are endorsed or recommended by WMO in preference to others of a similar nature which are not mentioned or advertised.

# CONTENTS

	Page
<b>LIST OF FIGURES .....</b>	<b>xiii</b>
<b>LIST OF TABLES .....</b>	<b>xix</b>
<b>FOREWORD .....</b>	<b>xxi</b>
<b>PREFACE .....</b>	<b>xxiii</b>
<b>SUMMARY (ENGLISH, FRENCH, RUSSIAN AND SPANISH) .....</b>	<b>xxv</b>
<b>CHAPTER 1. INTRODUCTION .....</b>	<b>1</b>
1.1 OBJECTIVE OF PMP ESTIMATES .....	1
1.2 DEFINITIONS OF PMP AND PMF.....	1
1.2.1 Definition of PMP .....	1
1.2.2 Definition of PMF .....	1
1.3 Close combination of hydrology and meteorology .....	1
1.4 PMP/PMF ESTIMATION .....	1
1.4.1 Basic knowledge.....	1
1.4.2 Approaches to and methods of PMP estimation.....	1
1.4.2.1 Approaches.....	1
1.4.2.2 Methods .....	2
1.4.3 Main steps for storm and watershed approaches .....	3
1.4.3.1 Approach based on storm area .....	3
1.4.3.2 Approach based on watershed area .....	5
1.5 STORM AND FLOOD DATA .....	5
1.6 ACCURACY OF PMP/PMF ESTIMATION.....	5
1.7 THE MANUAL.....	6
1.7.1 Objective.....	6
1.7.2 Scope .....	6
1.7.3 Application of examples .....	6
1.7.4 Application of computer technologies .....	7
1.8 PMP AND CLIMATE CHANGE.....	7
<b>CHAPTER 2. ESTIMATES FOR MID-LATITUDE NON-OROGRAPHIC REGIONS .....</b>	<b>9</b>
2.1 INTRODUCTION .....	9
2.1.1 Summary.....	9
2.1.2 Convergence model .....	9
2.1.3 Observed storm rainfall as an indicator of convergence and vertical motion .....	9
2.2 ESTIMATION OF ATMOSPHERIC MOISTURE.....	10
2.2.1 Assumption of a saturated pseudo-adiabatic atmosphere.....	10
2.2.2 Surface dewpoints as a moisture index .....	10
2.2.3 Persisting 12-hour dewpoints .....	10
2.2.4 Representative persisting 12-hour 1 000-hPa storm dewpoints .....	11
2.2.5 Maximum persisting 12-hour 1 000-hPa dewpoints.....	12
2.2.6 Precipitable water.....	14
2.2.7 Determination of duration of maximum persisting dewpoint.....	14
2.3 MOISTURE MAXIMIZATION .....	14
2.3.1 Seasonal limitations .....	14
2.3.2 Depth of precipitable water .....	14
2.3.3 Applicability of persisting 12-hour dewpoints for all storm durations .....	14
2.3.4 Maximization of storm in place.....	15

	<i>Page</i>
2.3.4.1 Adjustment for storm elevation .....	15
2.3.4.2 Adjustment for intervening barrier .....	15
<b>2.4 WIND MAXIMIZATION .....</b>	<b>16</b>
2.4.1 Introduction .....	16
2.4.2 Use in non-orographic regions.....	16
2.4.3 Winds representative of moisture inflow in storms .....	17
2.4.3.1 Wind direction .....	17
2.4.3.2 Wind speed.....	17
2.4.4 Wind maximization ratio.....	17
<b>2.5 STORM TRANSPOSITION .....</b>	<b>18</b>
2.5.1 Introduction .....	18
2.5.2 Steps in transposition .....	18
2.5.2.1 The storm .....	18
2.5.2.2 Region of influence of storm type .....	18
2.5.2.3 Topographic controls .....	19
2.5.2.4 Example of determining transposition limits.....	19
2.5.2.5 Adjustments.....	20
<b>2.6 TRANSPOSITION ADJUSTMENTS.....</b>	<b>20</b>
2.6.1 Moisture adjustment for relocation .....	20
2.6.1.1 Reference dewpoint for moisture adjustment .....	20
2.6.2 Elevation adjustments .....	21
2.6.2.1 General storms.....	21
2.6.2.2 Local thunderstorms .....	21
2.6.3 Barrier adjustment .....	21
2.6.4 Example of storm transposition and maximization.....	22
2.6.4.1 Hypothetical situation .....	22
2.6.4.2 Computation of adjustment factor .....	22
<b>2.7 SEQUENTIAL AND SPATIAL MAXIMIZATION.....</b>	<b>23</b>
2.7.1 Definition .....	23
2.7.2 Sequential maximization.....	23
2.7.3 Spatial maximization .....	24
2.7.4 Combined sequential and spatial maximization .....	24
<b>2.8 ENVELOPMENT .....</b>	<b>25</b>
2.8.1 Introduction .....	25
2.8.2 Envelopment .....	25
2.8.3 Undercutting .....	26
<b>2.9 SUMMARY OUTLINE OF PROCEDURE FOR ESTIMATING PMP .....</b>	<b>26</b>
2.9.1 Introduction .....	26
2.9.2 Procedural steps .....	27
<b>2.10 SEASONAL VARIATION OF PMP .....</b>	<b>28</b>
2.10.1 Introduction .....	28
2.10.2 Observed storms .....	28
2.10.3 Maximum persisting 12-hour dewpoints .....	28
2.10.4 Moisture inflow .....	28
2.10.5 Daily station precipitation.....	28
2.10.6 Weekly precipitation data .....	29
<b>2.11 AREAL DISTRIBUTION OF PMP .....</b>	<b>29</b>
2.11.1 Introduction .....	29
2.11.2 Observed storm pattern.....	30
2.11.3 Idealized storm pattern.....	30
2.11.3.1 Areal distribution .....	30
2.11.3.2 Example.....	30
<b>2.12 TIME DISTRIBUTION OF PMP .....</b>	<b>31</b>
2.12.1 Order of presentation .....	31
2.12.2 Chronological order based on an observed storm.....	32

	<i>Page</i>
2.13 CAUTIONARY REMARKS .....	34
2.13.1 Importance of adequate storm sample.....	34
2.13.2 Comparison with record rainfalls .....	34
2.13.3 Consistency of estimates.....	34
2.13.4 Regional, durational and areal smoothing.....	34
2.13.5 Seasonal variation.....	35
2.13.6 Areal distribution .....	36
<b>CHAPTER 3. ESTIMATES FOR MID-LATITUDE OROGRAPHIC REGIONS.....</b>	<b>37</b>
3.1 PRECIPITATION IN MOUNTAINOUS REGIONS.....	37
3.1.1 Orographic influences .....	37
3.1.2 Meteorological influences .....	37
3.1.3 Mean annual and seasonal precipitation .....	38
3.1.4 Precipitation-frequency values .....	38
3.1.5 Storm transposition .....	38
3.1.6 Probable maximum precipitation.....	38
3.1.6.1 Estimation of PMP in orographic regions using the orographic separation method.....	38
3.1.6.2 Modification of non-orographic PMP for orography .....	38
3.1.6.3 Direct orographic correction of PMP in orographic regions .....	39
3.1.6.4 Examples of procedures .....	39
3.2 THE OROGRAPHIC SEPARATION METHOD WITH A LAMINAR FLOW MODEL .....	39
3.2.1 Introduction .....	39
3.2.2 Orographic laminar flow model.....	39
3.2.2.1 Single-layer laminar flow model .....	39
3.2.2.2 Multiple-layer laminar flow model.....	40
3.2.2.3 Precipitation trajectories.....	41
3.2.3 Test of orographic laminar flow model on an observed storm .....	41
3.2.3.1 Ground profile .....	41
3.2.3.2 Inflow data .....	42
3.2.3.3 Air streamlines .....	42
3.2.3.4 Freezing level .....	42
3.2.3.5 Precipitation trajectories.....	43
3.2.3.6 Precipitation computation.....	44
3.2.3.7 Comparison of results .....	46
3.2.3.8 Sources of error.....	47
3.3 APPLICATION OF A LAMINAR FLOW MODEL IN THE OROGRAPHIC SEPARATION METHOD FOR ESTIMATING PMP.....	47
3.3.1 Orographic PMP .....	47
3.3.1.1 Maximum winds .....	47
3.3.1.2 Maximum moisture .....	48
3.3.2 Generalized estimates of orographic PMP .....	48
3.3.3 Variations in orographic PMP .....	49
3.3.3.1 Seasonal variation .....	49
3.3.3.2 Durational variation .....	49
3.3.3.3 Areal variation.....	49
3.3.4 Convergence PMP for combination with orographic PMP.....	49
3.3.4.1 Moisture (dewpoint) envelopes.....	50
3.3.4.2 Envelopes of <i>P/M</i> ratios.....	51
3.3.4.3 Reduction of convergence PMP for elevation .....	51
3.3.4.4 Reduction for upwind barriers.....	52
3.3.4.5 Reduction of point, or 25.9 km <sup>2</sup> , convergence PMP for area size .....	52
3.3.4.6 Construction of convergence PMP index map.....	54
3.3.4.7 Adjustment of index map values for other durations, basin sizes and months .....	55
3.3.5 Combination of orographic and convergence PMP.....	55

	Page
3.4 MODIFICATION OF NON-OROGRAPHIC PMP FOR OROGRAPHY .....	56
3.4.1 Introduction .....	56
3.4.2 Tennessee River basin above Chattanooga, Tennessee .....	57
3.4.2.1 Topographic effects.....	57
3.4.2.2 Derivation of PMP .....	58
3.4.2.3 Seasonal variation .....	58
3.4.2.4 Depth-duration relations .....	59
3.4.2.5 Geographic distribution of PMP .....	59
3.4.2.6 Time distribution of PMP.....	60
3.5 CAUTIONARY REMARKS ON ESTIMATING PMP IN OROGRAPHIC REGIONS.....	63
3.5.1 Basic data deficiencies .....	63
3.5.2 Orographic separation method.....	63
<b>CHAPTER 4. STATISTICAL ESTIMATES .....</b>	<b>65</b>
4.1 USE OF STATISTICAL PROCEDURE .....	65
4.2 DEVELOPMENT OF PROCEDURE .....	66
4.2.1 Basis .....	66
4.2.2 Adjustment of $\bar{X}_n$ and $S_n$ for maximum observed event.....	66
4.2.3 Adjustment of $\bar{X}_n$ and $S_n$ for sample size.....	66
4.2.4 Adjustment for fixed observational time intervals.....	66
4.2.5 Area-reduction curves.....	68
4.2.6 Depth-duration relationships.....	68
4.3 APPLICATION OF PROCEDURE .....	70
4.4 GENERALIZED ESTIMATES .....	70
4.5 CAUTIONARY REMARKS .....	72
<b>CHAPTER 5. GENERALIZED ESTIMATES.....</b>	<b>75</b>
5.1 INTRODUCTION .....	75
5.1.1 Base maps .....	75
5.2 ESTIMATES FOR NON-OROGRAPHIC REGIONS USING GENERALIZED MAPS.....	76
5.2.1 Moisture maximization .....	76
5.2.2 Storm transposition .....	76
5.2.2.1 Storm transposition techniques.....	76
5.2.3 Data smoothing (envelopment).....	77
5.2.3.1 Data smoothing (envelopment) for grid point technique .....	77
5.2.3.2 Data smoothing (envelopment) for the storm limit transposition technique .....	78
5.2.3.3 Preparation of final map.....	78
5.2.4 Supplementary aids .....	79
5.2.5 General remarks .....	79
5.2.6 Summary of procedural steps .....	80
5.2.7 Application of generalized or regionalized non-orographic PMP estimates to specific basins .....	81
5.2.7.1 Temporal distribution.....	81
5.2.7.2 Isohyetal patterns.....	83
5.2.7.3 Isohyetal orientation .....	84
5.2.7.4 Isohyet values .....	85
5.2.7.5 Selection of area of PMP storm for drainage.....	88
5.2.7.6 Stepwise procedure .....	88
5.3 ESTIMATES FOR OROGRAPHIC REGIONS .....	91
5.3.1 Introduction .....	91
5.3.2 PMP for drainages up to 259 km <sup>2</sup> in the Tennessee River basin .....	92
5.3.2.1 Outstanding rainfalls over the eastern United States.....	92
5.3.2.2 Local topographic classification.....	92
5.3.2.3 Broad-scale topographic effects .....	92
5.3.2.4 PMP depth-duration curves for 2.6 km <sup>2</sup> .....	93

	Page	
5.3.2.5	Adjustment for moisture and latitudinal gradient .....	94
5.3.2.6	Six-hour 2.6 km <sup>2</sup> PMP index map.....	94
5.3.2.7	Time distribution of rainfall .....	95
5.3.2.8	PMP for specific basins.....	96
5.3.3	PMP for drainages from 259 km <sup>2</sup> to 7 770 km <sup>2</sup> in the Tennessee River basin .....	96
5.3.3.1	Derivation of non-orographic PMP .....	96
5.3.3.2	Terrain and orographic influences on PMP .....	97
5.3.3.3	Terrain stimulation adjustment.....	98
5.3.3.4	Adjustment for PMP at interface (259 km <sup>2</sup> ) .....	99
5.3.3.5	Areal and time distribution.....	100
5.3.3.6	PMP for specific basins.....	100
5.3.4	PMP estimates for the United States between the Continental Divide and the 103rd meridian.....	102
5.3.4.1	Storm separation method .....	103
5.3.4.2	Orographic factor $T/C$ .....	104
5.3.4.3	Storm intensity factor $M$ .....	105
5.3.4.4	Computation of PMP .....	105
5.3.4.5	Depth-area relations.....	106
5.3.5	PMP estimates for the Colorado River and Great Basin drainages of the south-western United States .....	107
5.3.5.1	Orographic precipitation index .....	107
5.3.5.2	Variation with basin size .....	108
5.3.5.3	Durational variation .....	109
5.3.5.4	Combination of orographic and convergence PMP .....	109
5.3.6	PMP estimate for drainage above Dewey Dam, Johns Creek, Kentucky .....	110
5.3.6.1	Orographic factor $T/C$ .....	110
5.3.6.2	Storm intensity factor $M$ .....	111
5.3.6.3	Computation of PMP for Johns Creek basin.....	111
5.3.7	Generalized estimation of PMP for local storms in the Pacific North-west region of the United States .....	111
5.3.7.1	Brief introduction.....	111
5.3.7.2	Moisture maximization .....	112
5.3.7.3	Elevation adjustment and horizontal transposition adjustment .....	112
5.3.7.4	PMP precipitation depth-duration relation.....	112
5.3.7.5	PMP precipitation depth-area relation .....	113
5.3.7.6	One-hour 2.6 km <sup>2</sup> PMP map of the North-west region.....	113
5.3.7.7	Estimating procedure of local storm PMP for specific basin .....	114
5.3.7.8	Example of local-storm PMP estimation .....	115
5.3.8	PMP estimation in California, United States .....	116
5.3.8.1	Profile .....	116
5.3.8.2	Procedure and example computation of estimating PMP with the general storm method .....	117
5.3.8.3	Procedure and example computation of estimating PMP with the local storm method.....	120
5.3.9	Topographic adjustment.....	125
5.4	ESTIMATION OF PMP FOR SHORT DURATIONS AND SMALL AREAS IN AUSTRALIA .....	126
5.4.1	Introduction .....	126
5.4.2	Comparison of record storms in Australia and the United States .....	126
5.4.3	Use of GSMD depth-area-duration data.....	127
5.4.3.1	Geographic variation .....	127
5.4.3.2	Distribution of PMP in time .....	127
5.4.3.3	Distribution of PMP in space .....	128
5.4.3.4	Seasonal variation .....	131
5.4.4	Steps to calculate short-duration small-area PMP .....	131
5.5	ESTIMATION OF PMP FOR LONGER-DURATION STORMS IN AUSTRALIA .....	132
5.5.1	Introduction .....	132
5.5.2	Establishment of the storm database.....	132

	Page
5.5.2.1	132
5.5.2.2	133
5.5.2.3	133
5.5.2.4	133
5.5.2.5	134
5.5.2.6	134
5.5.3	135
5.5.3.1	135
5.5.3.2	135
5.5.3.3	135
5.5.3.4	136
5.5.3.5	138
5.5.3.6	139
5.5.4	140
5.5.4.1	140
5.5.4.2	141
5.5.4.3	141
5.5.4.4	142
5.5.4.5	142
5.5.4.6	142
5.6	142
5.6.1	142
5.6.2	143
5.6.3	144
5.6.4	144
5.6.5	144
5.6.5.1	144
5.6.5.2	144
5.6.5.3	144
5.6.5.4	144
5.6.6	145
5.6.6.1	145
5.6.6.2	145
5.6.7	145
5.7	145
<b>CHAPTER 6. ESTIMATES FOR TROPICAL REGIONS</b>	<b>147</b>
6.1	147
6.1.1	147
6.1.2	148
6.1.3	148
6.1.3.1	150
6.1.4	150
6.1.5	150
6.1.6	152
6.2	152
6.2.1	152
6.2.1.1	153
6.2.1.2	153
6.2.1.3	153
6.2.2	154
6.2.2.1	154
6.2.2.2	155
6.2.2.3	155
6.2.2.4	156
6.2.2.5	159
6.2.2.6	159

	Page
6.2.2.7 Areal distribution .....	159
6.2.2.8 PMP for specific basins.....	160
6.2.3 Estimation of PMP for India.....	160
6.2.3.1 Introduction.....	160
6.2.3.2 Initial non-orographic PMP values .....	161
6.2.3.3 Adjustments to initial non-orographic PMP values.....	162
6.2.3.4 Final non-orographic PMP values .....	162
6.2.4 Estimating PMP for Chambal, Betwa, Sone and Mahi watersheds in India.....	166
6.2.4.1 Introduction.....	166
6.2.4.2 Estimating PMP for small watersheds .....	166
6.2.4.3 Estimating PMP for medium to large watersheds .....	166
6.2.4.4 Estimating PMP for super large watersheds .....	172
6.2.4.5 Temporal distribution of storms .....	172
6.2.4.6 Example application.....	172
6.2.5 PMP estimation for the Daguangba Project in Hainan Island, China .....	173
6.2.5.1 Introduction.....	173
6.2.5.2 Estimation of orographic components of storms in the Changhuajiang River basin.....	173
6.2.5.3 DAD relations of PMP for non-orographic regions on Hainan Island .....	174
6.2.5.4 Estimation of 24-hour PMP for Daguangba watershed .....	175
6.2.5.5 Analysis of the rationality of PMP estimates .....	178
6.3 CAUTIONARY REMARKS .....	178
<b>CHAPTER 7. ESTIMATION OF PMP USING THE WATERSHED-BASED APPROACH AND ITS APPLICATION IN CHINA .....</b>	<b>179</b>
7.1 INTRODUCTION .....	179
7.2 OVERVIEW OF THE APPROACH .....	179
7.2.1 Main characteristics .....	179
7.2.2 Process .....	179
7.2.3 Project characteristics and design requirements .....	179
7.2.4 Analysis of watersheds, characteristics of storms and floods, and meteorological causes.....	179
7.2.5 Deducing qualitative characteristics of storm models .....	181
7.2.5.1 Importance of correct storm model.....	181
7.2.5.2 Qualitative characteristics.....	181
7.2.5.3 Methods for determining characteristics .....	181
7.2.5.4 Example of qualitative characteristic analysis – San-Hua region, China .	181
7.2.5.5 Similar work in other countries.....	183
7.2.6 Comprehensive analysis using multiple methods .....	184
7.2.7 Realistic results check.....	184
7.2.7.1 Checking each step.....	185
7.2.7.2 Comparison with historical extraordinary storms/floods in the watershed....	185
7.2.7.3 Comparison with adjacent watersheds .....	185
7.2.7.4 Comparison with historical estimation results.....	185
7.2.7.5 Comparison with worldwide storm and flood records .....	185
7.2.7.6 Comparison with results of frequency analysis.....	186
7.2.7.7 Similar work in other countries .....	186
7.3 LOCAL MODEL METHOD .....	186
7.3.1 Applicable conditions .....	186
7.3.2 Model selection .....	186
7.3.3 Model suitability analysis .....	186
7.3.4 Model maximization .....	186
7.3.4.1 Summary .....	186
7.3.4.2 Selection of maximum moisture adjustment factor .....	187
7.3.4.3 Selection of maximum dynamic adjustment factor.....	187
7.3.4.4 Model maximization .....	187
7.3.5 Example calculations .....	188

	Page	
7.3.5.1	Deducing qualitative characteristics of PMP storm models .....	188
7.3.5.2	Model selection .....	188
7.3.5.3	Selection of dewpoints.....	188
7.3.5.4	Calculating the efficiency of the typical storms.....	188
7.3.5.5	Determining maximization parameters.....	188
7.3.5.6	Calculating maximization amplification.....	188
7.3.5.7	Maximizing typical storm.....	188
7.4	TRANSPOSITION MODEL METHODS .....	189
7.4.1	Applicable conditions .....	189
7.4.2	Selection of transposed storms .....	189
7.4.3	Transposition possibility analysis .....	189
7.4.3.1	Comparison of geographical and climatic conditions .....	190
7.4.3.2	Comparison of orographic conditions .....	190
7.4.3.3	Comparison of spatio-temporal distribution characteristics of storms (floods).....	190
7.4.3.4	Comparison of weather causes.....	190
7.4.3.5	Comprehensive judgement.....	190
7.4.4	Spatial distribution of rainfall map .....	191
7.4.5	Transposition adjustment.....	191
7.4.5.1	Common methods.....	191
7.4.5.2	Comprehensive orographic correction method.....	191
7.4.6	Example calculations .....	192
7.4.7	Storm transportation for arid and semi-arid regions .....	193
7.4.7.1	Storm characteristics.....	193
7.4.7.2	Characteristics of PMP estimation .....	193
7.5	COMBINATION MODEL STORM METHOD .....	194
7.5.1	Applicable conditions .....	194
7.5.2	Combination methods.....	194
7.5.2.1	Similar process substitution method.....	194
7.5.2.2	Evolvement trend analysis method.....	195
7.5.3	Analysis of combination scheme rationality.....	196
7.5.3.1	Analysis based on synoptic meteorology .....	196
7.5.3.2	Analysis based on climatology.....	196
7.5.3.3	Comparison with historical extraordinary storm floods in the watershed...	196
7.5.4	Combination model maximization.....	196
7.5.5	Example calculations .....	196
7.5.5.1	Similar process substitution method.....	196
7.5.5.2	Weather system evolution method.....	199
7.6	PMF ESTIMATION .....	200
7.6.1	Introduction .....	200
7.6.2	Basic assumption for deriving PMF from PMP .....	200
7.6.3	Characteristics of runoff yield and flow concentration with PMP .....	200
7.6.3.1	Characteristics of runoff yield .....	201
7.6.3.2	Characteristics of flow concentration.....	201
7.6.4	Methods for converting PMP into PMF .....	202
7.6.5	Influence of antecedent conditions .....	202
7.7	ESTIMATION OF PMP/PMF FOR LARGE WATERSHEDS .....	202
7.7.1	Introduction .....	202
7.7.2	Major temporal and spatial combination method .....	202
7.7.2.1	Introduction.....	202
7.7.2.2	Procedure .....	203
7.7.2.3	Example calculations.....	203

	<i>Page</i>
7.7.3 Storm simulation method based on an historical flood .....	204
7.7.3.1 Introduction.....	204
7.7.3.2 Principles .....	204
7.7.3.3 Procedure .....	204
7.7.3.4 Example calculations.....	205
<b>ACKNOWLEDGEMENTS .....</b>	<b>209</b>
<b>ANNEXES.....</b>	<b>211</b>
ANNEX I. TABLES OF PRECIPITABLE WATER IN A SATURATED PSEUDO-ADIABATIC ATMOSPHERE.....	211
ANNEX II. THE WORLD'S GREATEST KNOWN RAINFALLS .....	218
ANNEX III. THE WORLD'S GREATEST KNOWN FLOODS .....	230
ANNEX IV. GLOSSARY .....	238
<b>REFERENCES AND FURTHER READING.....</b>	<b>245</b>



## LIST OF FIGURES

	Page
Figure 2.1 Pseudo-adiabatic diagram for dewpoint reduction to 1 000 hPa at zero height.....	11
Figure 2.2 Determination of maximum dewpoint in a storm. Representative dewpoint for this weather map is the average of values in boxes.....	12
Figure 2.3 Enveloping maximum persisting 12-hour dewpoints at a station.....	13
Figure 2.4 Maximum persisting 12-hour 1 000-hPa dewpoints for August (Environmental Data Service, 1968).....	13
Figure 2.5 Schematic illustrating concept for alternative moisture adjustment for intervening barrier to air flow (after Hart, 1982) .....	16
Figure 2.6 Transposition limits (heavy dashed line) of 9–13 July 1951 storm. Locations of synoptically similar summer storms marked by X. Light lines indicate maximum persisting 12-hour 1 000-hPa dewpoints (°C) for July. ....	19
Figure 2.7 Example of storm transposition. Long dashed lines indicate maximum persisting 12-hour 1 000-hPa dewpoints (°C) for the same time of year the storm occurred or within 15 days according to common practice (section 2.3.1). ....	21
Figure 2.8 Isohyets (cm) for the 6-hour afternoon storms of 16 June 1965 (solid lines) and 17 June 1965 (dashed lines) in eastern Colorado (Riedel and others, 1969) .....	24
Figure 2.9 Isohyets (cm) resulting from the combination of patterns of the 6-hour storms of 16–17 June 1965 shown in Figure 2.8 (Riedel and others, 1969).....	25
Figure 2.10 Depth-duration envelope of transposed maximized storm values for 2 000 km <sup>2</sup> .....	26
Figure 2.11 Depth-area envelope of transposed maximized 24-hour storm rainfall values .....	26
Figure 2.12 Enveloping DAD curves of probable maximum precipitation for a hypothetical basin .....	26
Figure 2.13 Seasonal variation of probable maximum precipitation in the Upper Tigris River basin in Iraq.....	29
Figure 2.14 Maximization of a pattern storm by the sliding technique for a 5 000 km <sup>2</sup> basin, the point of first contact occurs on the 72-hour curves between about 2 000 and 4 500 km <sup>2</sup> .....	31
Figure 2.15 Example of enveloping DAD curves of PMP and within-storm rainfall depths .....	31
Figure 2.16 Critical isohyetal pattern over 3 000 km <sup>2</sup> basin.....	32
Figure 2.17 Isohyetal profile constructed from data in Table 2.3 .....	32
Figure 2.18 Observed rainfalls expressed as a percentage of PMP in the United States, east of the 105th meridian ≥ 50 per cent of all-season PMP for the 24-hour duration and an area size of 518 km <sup>2</sup> (Riedel and Schreiner, 1980).....	35
Figure 3.1 Simplified inflow and outflow wind profiles over a mountain barrier (United States Weather Bureau, 1961a) .....	40
Figure 3.10 Decrease of maximum precipitable water with duration (after United States Weather Bureau, 1958) .....	51
Figure 3.11 Seasonal envelope of maximum observed dewpoints at Los Angeles, California (after United States Weather Bureau, 1961a).....	52
Figure 3.12 Maximum persisting 12-hour 1 000-hPa dewpoints (°C) for February (United States Weather Bureau, 1961a) .....	52
Figure 3.13 Maximum P/M ratios for combination with orographic storms (after United States Weather Bureau, 1961a) .....	53
Figure 3.14 Ratios of 6-hour and 72-hour precipitation to 24-hour precipitation (United States Weather Bureau, 1961a) .....	53
Figure 3.15 Effective elevation and barrier heights (30.5 m) in northern California (square delineates Blue Canyon orographic model test area; United States Weather Bureau, 1961a).....	54
Figure 3.16 Six-hour 518 km <sup>2</sup> convergence PMP (inches) for January and February (square delineates Blue Canyon orographic model test area; United States Weather Bureau, 1961a).....	55
Figure 3.17 Variation of convergence PMP index with basin size and duration for December (United States Weather Bureau, 1961a) .....	56

	Page
Figure 3.18 Typical orographic rainfall pattern for southwesterly winds. Isolines indicate ratios of orographic to non-orographic rainfall (Schwarz, 1965) .....	58
Figure 3.19 Basin subdivisions for check of topographic effects on basin-wide precipitation volume (Schwarz, 1963).....	58
Figure 3.2 Single-layer laminar flow wind model .....	41
Figure 3.20 March 24-hour 25 900 km <sup>2</sup> PMP (cm; after Schwarz, 1965).....	59
Figure 3.21 Seasonal variation of PMP for 55 426 km <sup>2</sup> as percentage of March PMP (Schwarz, 1965).....	59
Figure 3.22 Depth-area ratios (55 426/ 20 688 km <sup>2</sup> ) for 24-hour rainfall (Schwarz, 1965).....	60
Figure 3.23 Depth-duration relations in percentage of 24-hour rainfall (Schwarz, 1965) .....	61
Figure 3.24 Six-hour PMP storm pattern (mm) for maximum 6-hour increment for total basin (55 426 km <sup>2</sup> ) (Schwarz, 1965); isohyet values are applicable to the March PMP.....	61
Figure 3.25 Nomogram for obtaining isohyet values for maximum 6-hour rainfall increment in pattern storms .....	62
Figure 3.26 PMP storm pattern for maximum 6-hour increment for sub-basin (21 000 km <sup>2</sup> ; Schwarz, 1965); isohyet values are applicable to March .....	63
Figure 3.3 Multiple-layer laminar flow wind model .....	41
Figure 3.4 Blue Canyon orographic laminar-flow model test area in California (United States Weather Bureau, 1966) .....	42
Figure 3.5 Precipitation station elevations relative to adopted ground profile for test area of Figure 3.4 (United States Weather Bureau, 1966).....	42
Figure 3.6 Air streamlines and precipitation trajectories for test case .....	43
Figure 3.7 Maximum 1-hour wind profile and supporting data (United States Weather Bureau, 1961 <i>b</i> ) .....	48
Figure 3.8 Variation of maximum 6-hour wind speed with time (after United States Weather Bureau, 1961 <i>a</i> ) .....	49
Figure 3.9 Six-hour orographic PMP (inches) for January (square delineates Blue Canyon orographic model test area; United States Weather Bureau, 1961 <i>a</i> ) .....	50
Figure 4.1 Km as a function of rainfall duration and mean of annual series (Hershfield, 1965).....	65
Figure 4.2 Adjustment of mean of annual series for maximum observed rainfall (Hershfield, 1961 <i>b</i> ) .....	67
Figure 4.3 Adjustment of standard deviation of annual series for maximum observed rainfall (Hershfield, 1961 <i>b</i> ).....	67
Figure 4.4 Adjustment of mean and standard deviation of annual series for length of record (Hershfield, 1961 <i>b</i> ) .....	67
Figure 4.5 Adjustment of fixed-interval precipitation amounts for number of observational units within the interval (Weiss, 1964) .....	68
Figure 4.6 Examples of (A) isohyetal pattern centred over basin as would be the case for storm-centred depth-area curves, and (B) two possible occurrences of isohyetal patterns over a geographically fixed area as would be the case in development of curves for a geographically fixed area (Miller and others, 1973) .....	69
Figure 4.7 Depth-area, or area-reduction, curves for western United States (United States Weather Bureau, 1960) .....	69
Figure 4.8 Maximum depth-duration curve (Huff, 1967).....	70
Figure 5.1 Contrast in (a) PMP (Schwarz, 1963) and (b) 25-year rainfall patterns (United States Weather Bureau, 1962), both for 24-hour at a point, Island of Hawaii; particularly note differences on north-western coast .....	80
Figure 5.2 Depth-duration interpolation diagrams from study for western United States (United States Weather Bureau, 1960) .....	81
Figure 5.3 All-season envelope of 24-hour 25.9 km <sup>2</sup> PMP (cm; Schreiner and Riedel, 1978); stippled areas are regions where orographic effects have not been considered.....	82
Figure 5.4 Examples of temporal sequences of 6-hour precipitation in major storms in eastern and central United States (Hansen and others, 1982).....	83
Figure 5.5 Standard isohyetal pattern recommended for spatial distribution of PMP for the United States east of the 105th meridian (Hansen and others, 1982) .....	84
Figure 5.60 Montana 100-year 24-hour rainfall (inches) .....	126

	<i>Page</i>
Figure 5.7 Model for determining the adjustment factor to apply to isohyet values as a result of placing the pattern in Figure 5.5 at an orientation differing from that given in Figure 5.6 by more than $\pm 40^\circ$ , for a specific location (Hansen and others, 1982) .....	85
Figure 5.8 Schematic diagram showing the relation between depth-area curve for PMP and the within/without-storm relations for PMP at $1\ 000\ \text{km}^2$ (Hansen and others, 1982) .....	86
Figure 5.9 Six-hour within/without-storm average curves for standard area sizes (Hansen and others, 1982) .....	86
Figure 5.10 Within/without storm curves for PMP at $37^\circ\ \text{N}$ , $89^\circ\ \text{W}$ Tennessee River basin over Chattanooga, Tennessee (Zurndorfer and others, 1986). W for standard area sizes (Hansen and others, 1982) .....	87
Figure 5.11 Isohyetal profiles for standard area sizes at $37^\circ\ \text{N}$ , $89^\circ\ \text{W}$ (Hansen and others, 1982) .....	88
Figure 5.12 Nomogram for the first 6-hour PMP increment and for standard isohyet area sizes between $25.9$ and $103\ 600\ \text{km}^2$ (Hansen and others, 1982) .....	89
Figure 5.13 Example of computation sheet showing typical format (Hansen and others, 1982).....	90
Figure 5.14 Topography classified on basis effect on rainfall, Tennessee River basin above Chattanooga, Tennessee (Zurndorfer and others, 1986) .....	93
Figure 5.15 Adopted $2.6\text{-km}^2$ PMP with supporting data, Tennessee River basin; dashed lines are extrapolations based on relation of Figure 5.16, smooth curve applies uncorrected only to 100 per cent line of Figure 5.18 (Zurndorfer and others, 1986).....	93
Figure 5.16 PMP depth-duration curves for basins up to $259\ \text{km}^2$ in Tennessee River basin (Zurndorfer and others, 1986) .....	94
Figure 5.17 Moisture index chart for north-western portion of Tennessee River basin over Chattanooga, Tennessee (Zurndorfer and others, 1986) .....	94
Figure 5.18 Latitudinal rainfall gradient (in per cent) in south-eastern portion of Tennessee River basin above Chattanooga, Tennessee (Zurndorfer and others, 1986) .....	95
Figure 5.19 Six-hour $2.6\text{-km}^2$ PMP (inches) for Tennessee River basin above Tennessee River basin over Chattanooga, Tennessee (Zurndorfer and others, 1986).....	95
Figure 5.20 Nomogram for depth-duration relations for 24-hour PMP storms, Tennessee River basin (Zurndorfer and others, 1986) .....	96
Figure 5.21 Depth-area relations for small basin estimates, Tennessee River basin (Zurndorfer and others, 1986) .....	96
Figure 5.22 Non-orographic PMP at Knoxville, Tennessee (Zurndorfer and others, 1986) .....	96
Figure 5.23 Twenty-four-hour $2\ 590\text{-km}^2$ PMP percentiles of Knoxville Airport value (meteorological observations made at airport, about $16\ \text{km}$ south of Knoxville; Zurndorfer and others, 1986) .....	97
Figure 5.24 Two-year 24-hour precipitation-frequency map (tenths of inches) for eastern Tennessee River basin (Zurndorfer and others, 1986) .....	97
Figure 5.25 Optimum wind directions for heavy rains (Zurndorfer and others, 1986) .....	98
Figure 5.26 Adjustment chart for optimum wind inflow direction for south-eastern mountainous portion of Tennessee River basin over Chattanooga, Tennessee (Zurndorfer and others, 1986) .....	99
Figure 5.27 Illustration of terrain classification for the eastern Tennessee River basin (Zurndorfer and others, 1986) .....	99
Figure 5.28 Nomogram for determining terrain adjustments for basins larger than $259\ \text{km}^2$ (Zurndorfer and others, 1986) .....	100
Figure 5.29 Variation of terrain roughness adjustment (Figure 5.28) with basin size (Zurndorfer and others, 1986) .....	100
Figure 5.30 Adjustment applied to broad-scale orographic factor for areas near the interface between procedures for areas less than and greater than $259\ \text{km}^2$ (Zurndorfer and others, 1986) .....	101
Figure 5.31 Schematic flow chart for storm separation method (Miller and others, 1984b).....	103
Figure 5.32 Moisture-maximized convergence precipitation (inches) map for state of Colorado east of Continental Divide (Miller and others, 1984b) .....	104
Figure 5.33 Convergence component of the 100-year 24-hour precipitation-frequency values (tenths of inches) for the state of New Mexico east of the Continental Divide (Miller and others, 1984b) .....	105

	Page
Figure 5.34 Orographic factor (T/C) map for the state of Colorado east of the Continental Divide (Miller and others, 1984b) .....	105
Figure 5.35 Storm intensity factor (M) for the state of Montana east of the Continental Divide (Miller and others, 1984b) .....	106
Figure 5.36 Twenty-four-hour 25.9-km <sup>2</sup> PMP estimates (inches) for the northern portion of the state of New Mexico east of the Continental Divide .....	106
Figure 5.37 Schematic diagram of the sub-regional system used in developing depth-area-duration relations (Miller and others, 1984b) .....	107
Figure 5.38 Depth-area-duration relation for orographic region of Missouri and Yellowstone River basins (Miller and others, 1984b) .....	108
Figure 5.39 Twenty-four-hour 25.9 km <sup>2</sup> orographic PMP (inches) for southern Arizona, south-western New Mexico and south-eastern California (Hansen and others, 1977) ....	109
Figure 5.40 Variation of orographic PMP with basin size for Colorado River and Great Basin drainages (Hansen and others, 1977).....	109
Figure 5.41 Adopted durational variation in orographic PMP for Colorado River and Great Basin drainages (Hansen and others, 1977).....	110
Figure 5.42 Isolines on convergence 100-year 24-hours rainfall (cm) for central United States (Fenn, 1985).....	110
Figure 5.43 Depth-area relations for local storm PMP Pacific Northwest states .....	113
Figure 5.44 Idealized isohyetal pattern for local storm PMP areas up to 1 300 km <sup>2</sup> (Hansen and others, 1977) .....	114
Figure 5.45 One-hour 2.6-km <sup>2</sup> local storm PMP in inches for elevations to 1 830 m .....	114
Figure 5.46 Temporal distribution relation for Mud Mountain Dam .....	116
Figure 5.47 Twenty-four-hour PMP isoline map for Auburn watershed (inches) .....	118
Figure 5.48 California DAD region map .....	119
Figure 5.49 Curve of relationship between areal mean PMP and duration for Auburn watershed.....	120
Figure 5.50 Temporal distribution of 72-hour PMP for Auburn watershed.....	121
Figure 5.51 California Wash watershed .....	121
Figure 5.52 Isoline map of PMP for California for local storms with 1-hour duration and storm area of 2.6 km <sup>2</sup> .....	122
Figure 5.53 Corrected percentage of moisture content in air columns for different watershed elevations.....	122
Figure 5.54 Coefficients of correcting PMP for different durations.....	123
Figure 5.55 Isoline map of watershed correction types .....	124
Figure 5.56 Coefficients of area reduction corresponding to Type C .....	124
Figure 5.57 Curve of duration-area PMP relationship for the watershed .....	124
Figure 5.58 Generalized isohyetal map of PMP .....	125
Figure 5.59 Montana storm isohyets (inches) transposed to Cheesman basin .....	126
Figure 5.6 Analysis of isohyetal orientations for selected major storms in United states east of the 105th meridian adopted as recommended orientation for PMP within ±40° (Hansen and others, 1982) .....	85
Figure 5.61 Cheesman 100-year 24-hour rainfall (inches) .....	126
Figure 5.62 Grid of rainfall depth (inches) of Montana storm transposed over the Cheesman basin multiplied by the ratio of the grids of Figures 5.61 to 5.60 .....	127
Figure 5.63 Zones for use with the generalized short-duration method (Australian Bureau of Meteorology, 2003).....	128
Figure 5.64 Generalized short-duration method depth-duration-area curves (Australian Bureau of Meteorology, 2003).....	128
Figure 5.65 Reduction factor for geographic variation from extreme moisture (Australian Bureau of Meteorology, 2003).....	130
Figure 5.66 Temporal distribution for use with PMP estimates derived using the generalized short-duration method (Australian Bureau of Meteorology, 2003).....	130
Figure 5.67 Generalized short-duration method spatial distribution .....	130
Figure 5.68 Monthly percentage moisture adjustment for southern Australia (south of 30° S); areal limit is 500 km <sup>2</sup> .....	132
Figure 5.69 Boundaries between PMP methods.....	133
Figure 5.70 An example of a set of standard area polygons as applied to the 6-day storm, 18–23 January 1974 .....	134

	Page
Figure 5.71 Boundaries between PMP methods and zones – GTSMR .....	135
Figure 5.72 Seventy-two-hour 50-year rainfall intensities over central NSW coast. Isopleths in mm/hour.....	136
Figure 5.73 Convergence component of 72-hour 50-year rainfall intensities over central NSW coast. Isopleths are in mm/hour .....	137
Figure 5.74 Extreme monthly 24-hour persisting dew-point temperature for Brisbane and the standard extreme persisting dew-point temperatures for the GSAM seasons .....	138
Figure 5.75 Extreme monthly 24-hour persisting dew-point temperatures for Broome and the standard extreme persisting dew-point temperatures for the GTSMR seasons .....	139
Figure 5.76 The distribution of amplitude factors defining the degree of mechanism decay expected over the GTSMR zone .....	139
Figure 5.77 An example of the enveloping process for a set of storms (A–F) defined by depth-area curves of their convergence component.....	140
Figure 5.78 Enveloping process to define PMP depth across a range of durations for a specific catchment area.....	143
Figure 5.79 Example of a GSAM design spatial distribution.....	143
Figure 5.80 Twenty-four-hour point PMP in China (mm; Wang J., 2002) .....	146
Figure 6.1 Comparison (Miller, 1981) of observed and estimated precipitable water for Merida, Mexico for layer from surface to 500 hPa; observed values computer from radiosonde observations using data by 500-hPa layers; estimated values determined using surface dewpoint at time of radiosonde obervations and assuming a saturated pseudo-adiabatic lapse rate.....	151
Figure 6.2 Comparison (Miller, 1981) of maximum semi-monthly precipitable water computer from radiosonde observations and that estimates from the surface dewpoint at the time of observation for Merida, Mexico; the period of record is January 1946 to December 1947 and October 1957 and December 1972 .....	151
Figure 6.3 Extreme events related to tropical storms (Schwarz, 1972) .....	153
Figure 6.4 Rain intensification for ground slopes (Schwarz, 1963).....	155
Figure 6.5 Adjustment of non-orographic PMP for elevation and slope, Hawaiian Islands (Schwarz, 1963) .....	156
Figure 6.6 Variation of index PMP with basin size and duration, Hawaiian Islands (Schwarz, 1963) .....	156
Figure 6.7 Mekong River basin and sub-basins (United States Weather Bureau, 1970) .....	157
Figure 6.8 Generalized topography of Mekong River basin; dots show location of precipitation stations (United States Weather Bureau, 1970).....	158
Figure 6.9 Mean May–September (south-west monsoon season) precipitation (mm; United States Weather Bureau, 1970) .....	159
Figure 6.10 Depth–area–duration curves of PMP on Viet Nam coast (United States Weather Bureau, 1970) .....	160
Figure 6.11 Adjustment (percentage) of coastal typhoon rainfall for distance inland (United States Weather Bureau, 1970) .....	161
Figure 6.12 Latitude adjustment of typhoon rainfall as percentage of values at 15° N (United States Weather Bureau, 1970) .....	161
Figure 6.13 Barrier adjustmest of typhoon rainfall (percentage decrease; United States Weather Bureau, 1970) .....	162
Figure 6.14 Adjustment of typhoon rainfall (United States Weather Bureau, 1970) for basin topography (percentage increase or decrease relative to low-elevation south-west monsoon rainfall over flat terrain) .....	163
Figure 6.15 Total adjustment (percentage) of coastal typhoon rainfall (combined adjustments of Figure 6.11 to 6.14; United States Weather Bureau, 1970) .....	164
Figure 6.16 PMP (mm) for 24 hours over 5 000 km <sup>2</sup> (United States Weather Bureau, 1970) .....	165
Figure 6.17 Depth–area–duration values of PMP in per cent of 24-hour 5 000 km <sup>2</sup> PMP (United States Weather Bureau, 1970) .....	165
Figure 6.18 PMP (solid lines) and key depth–area curves typical of major tropical storms (United States Weather Bureau, 1970) .....	166
Figure 6.19 Isohyetal values for maximum 6-hour increment of PMP storm as percentage of average rainfall for area enclosed (United States Weather Bureau, 1970) .....	166

	Page
Figure 6.20 Location of three major storm centres over India and their transposition limits (Rakhecha and Kennedy, 1985).....	167
Figure 6.21 Maximum observed DAD rainfall values for three major storms in India (Rakhecha and Kennedy, 1985).....	167
Figure 6.22 Extreme persisting 24-hour point dewpoint temperatures over India (Rakhecha and Kennedy, 1985).....	168
Figure 6.23 Adjustment factor for distance from coast for non-orographic PMP values in India (Rakhecha and Kennedy, 1985) .....	168
Figure 6.24 Normalized PMP DAD curves for India (Rakhecha and Kennedy, 1985).....	169
Figure 6.25 Calculating grids of Changhuajiang River Basin (Lin, 1988).....	176
Figure 6.26 Isohyetal map of 24-hour 5 000 km <sup>2</sup> PMP for non-orographic regions on the Changhuajiang River Basin (Lin, 1988).....	178
Figure 6.27 Storm isoline map of 24 hour PMP for the Changhuajiang River basin on Hainan Island (Lin, 1988).....	179
Figure 7.1 The process for PMP and PMF estimation (Wang G., 1999).....	182
Figure 7.2 Diagram of the shape of the San-Hua region watershed on the Yellow River (Wang G., 1999).....	185
Figure 7.3 Generalized 700-hPa storm effect system map for 8 p.m. (Beijing time) 16 July 1958 in the catastrophic cloudburst period in the San-Hua region on the Yellow River (Wang G., 1999).....	186
Figure 7.4 Watershed sketch.....	189
Figure 7.5 Diagram of topographic and rainfall profiles .....	194
Figure 7.6 500-hPa situation map for 13 July 1981 (MWR and others, 1995).....	201
Figure 7.7 500-hPa situation map for 15 July 1982 (MWR and others, 1995).....	201
Figure 7.8 500-hPa situation map for 5 June 1956 (MWR and others, 1995).....	202
Figure 7.9 500-hPa situation map for 6 June 1956 (MWR and others, 1995).....	202
Figure 7.10 Daily rainfall map on 13 July 1981 .....	203
Figure 7.11 Daily rainfall map on 15 July 1982 .....	203
Figure 7.12 Daily rainfall map on 5 June 1956.....	203
Figure 7.13 Daily rainfall map on 6 June 1956 .....	203
Figure 7.14 Watershed diagram of design project A.....	205
Figure 7.15 Flood hydrograph of Yichang station in 1870 (Zhao and others, 1983).....	208
Figure 7.16 Simulated rainfall isoline for 13–19 July 1870 (Zhao and others, 1983) .....	209
Figure A.2.1 World's greatest known point rainfalls (Wang G. and others, 2006) .....	221
Figure A.3.1 World's greatest known floods (Wang G. and others, 2006) .....	233

## LIST OF TABLES

	<i>Page</i>
Table 2.1 Dewpoints observed at 6-hour intervals .....	11
Table 2.2 Maximum average depth (mm) of rainfall in 20–23 May 1927 storm.....	20
Table 2.3 Isohyetal profile computation.....	32
Table 2.4 Evaluation of isohyet labels of Figure 2.16.....	33
Table 2.5 Chronological distribution of probable maximum precipitation (PMP) for a hypothetical 3 000 km <sup>2</sup> basin.....	33
Table 3.1 Computation of orographic precipitation over leg 10 of Blue Canyon, California, test area for the 6-hour period 2 p.m. – 8 p.m., 22 December 1955 (hand computation, using 3 p.m. 22 December 1955 sounding at Oakland, California, as inflow data and assuming a nodal surface of 350 hPa) .....	44
Table 3.3 Comparison of observed and computed 6-hour precipitation for the period 2 p.m. – 8 p.m., 22 December 1955 over Blue Canyon, California, test area.....	46
Table 3.4 Probable maximum precipitation (mm) for Tennessee River basin above Chattanooga, Tennessee (Schwarz, 1965).....	60
Table 3.5 Isohyet values (mm) for 6-hour March PMP storm pattern of Figure 3.24.....	62
Table 4.1 Computation of probable maximum precipitation (PMP).....	71
Table 5.1 Shape ratios of isohyetal patterns for 53 major rain events in the eastern United States (Hansen and others, 1982) .....	84
Table 5.2 Sample computation of PMP precipitation estimates for the 7 542 km <sup>2</sup> Clinch River basin above Norris Dam, Tennessee. Centre of basin is 36°42' N 82°54' W.....	101
Table 5.3 Major river basins within the region of the central United States between the Continental Divide and the 103rd meridian used for depth-area relations .....	107
Table 5.4 Values of T/C at the centroid of the drainage above Dewey Dam, Johns Creek, Kentucky.....	112
Table 5.5 Estimated duration of intense precipitation t for selected total length of precipitation period (Fenn, 1985).....	112
Table 5.6 Storm intensity factor M for selected durations (Fenn, 1985) .....	112
Table 5.7 PMP of the drainage above Dewey Dam, Johns Creek, Kentucky.....	112
Table 5.8 PMP profile values (accumulative percentage of 1-hour 2.6-km <sup>2</sup> amount) .....	115
Table 5.9 PMP values of each duration in drainage mean 2.6 km <sup>2</sup> .....	116
Table 5.10 Drainage average PMP value for each duration .....	116
Table 5.11 Increments of drainage average PMP value for each duration.....	116
Table 5.12 Isohyetal label values (mm) for local-storm PMP, White River, Washington (1 041 km <sup>2</sup> ).....	117
Table 5.13 Coefficients of duration – precipitation depth conversion for each DAD region in California .....	118
Table 5.14 Calculated result of PMP for each duration in Auburn .....	119
Table 5.15 Area-duration-reduction coefficients for Sierra Nevada region (percentage).....	120
Table 5.16 Coefficient of area reduction and areal mean PMP for Auburn watershed.....	120
Table 5.17 Accumulated PMP hydrograph and time-interval hydrograph for the Auburn watershed .....	121
Table 5.18 Results of corrected PMP for different durations for the Wash watershed.....	123
Table 5.19 Results of PMP for the Wash watershed with correction to area size .....	123
Table 5.20 Accumulated PMP hydrograph and time-interval hydrograph for the Wash watershed.....	123
Table 5.21 Percentages of isohyets corresponding to type-C correction.....	125
Table 5.22 Isohyet values for the Wash watershed .....	125
Table 5.23 Notable observed depth-area-duration data (mm) for Australia (derived from data in Australian Bureau of Meteorology, 1985).....	127
Table 5.24 Some notable point rainfall totals recorded in Australia (Australian Bureau of Meteorology, 1994, as amended 1996) .....	129
Table 5.25 Initial mean rainfall depths enclosed by ellipses A–H in Figure 5.67 .....	131
Table 5.26 Small-area adjustments used in the GSAM (percentage).....	141

	Page
Table 5.27 Topographic enhancement factors .....	142
Table 5.28 Point-area relation of PMP with different durations in orographic regions in Henan Province, China.....	146
Table 6.1 Frequency factors Km for Chambal, Betwa, Sone and Mahi watersheds .....	169
Table 6.2 PMP for 1- and 2-day durations for Chambal and Betwa watersheds.....	170
Table 6.3 Catchment areas in the Chambal watershed .....	171
Table 6.4 Sub-basin location in the Chambal watershed.....	171
Table 6.5 SPS for the Chambal watershed in India.....	172
Table 6.6 Moisture maximization factors for three typical storms.....	172
Table 6.7 Area reduction factor for storms in the Chambal watershed .....	173
Table 6.8 Calculated results of PMP for the Chambal watershed.....	173
Table 6.9 MAF for each grid of either Chambal or Betwa watershed.....	174
Table 6.10 PMP for each grid of either Chambal or Betwa watershed.....	175
Table 6.11 DAD enveloping relations of typhoon storm extremes in non-orographic regions on Hainan Island (Zhang, 1988) .....	177
Table 6.12 Comprehensive adjustment coefficient for 24-hour storms in the Changhuajiang River basin of Hainan Island (Zhang, 1988) .....	178
Table 7.1 Qualitative characteristics of PMP storm model in the San-Hua region of the Yellow River .....	186
Table 7.2 The areal mean rainfall amount of the July 1958 storm in the San-Hua region on the Yellow River .....	190
Table 7.3 Table of calculation of efficiencies of the July 1958 typical storm in the San-Hua region on the Yellow River .....	191
Table 7.4 Calculation of moisture and efficiency amplifications of the July 1958 typical storm in the San-hua Region on the Yellow River .....	191
Table 7.5 Five-day PMP in the San-Hua region on the Yellow River .....	191
Table 7.6 Key characteristics of PMP for the Manwan project .....	199
Table 7.7 Table of typical storm process sequence in Manwan in 1966.....	200
Table 7.8 Table of combined storm process sequence using similar process substitution method for the 1966 typical storm in Manwan .....	200
Table 7.9 Watershed profiles for four key projects in China.....	206
Table 7.10 Methods for deriving PMP/PMF for four key projects in China.....	207
Table 7.11 Peak and volume of the flood at Yichang station in 1870 (CJWRC, 1997).....	208
Table 7.12 Simulated 1870 storm sequence .....	209
Table 7.13 PMF estimate for Three Gorges (Yichang) – scheme of simulating 1870 historical flood (Jin and Li, 1989) .....	210
Table A.1.1 Precipitable water (mm) between 1 000-hPa surface and indicated pressure (hPa) in a saturated pseudo-adiabatic atmosphere as a function of the 1 000-hPa dew point (°C) .....	213
Table A.1.2 Precipitable water (mm) between 1 000-hPa surface and indicated height (m) above that surface in a saturated pseudo-adiabatic atmosphere as a function of the 1 000-hPa dew point (°C) .....	215
Table A.1.3 Precipitable water (mm) in column of air above specified heights (m) as a function of the 1 000 hPa temperature (°C) (revised May 1981) .....	216
Table A.1.4 Mixing ratios along pseudo-adiabats for specified 1 000-hPa dew points and elevations in meters above the 1 000-hPa level .....	219
Table A.2.1 World's greatest known point rainfalls.....	222
Table A.2.2 World's near-record rainfalls .....	225
Table A.2.3 Maximum observed depth-area-duration data for China, the United States and India (average rainfall in mm) (Wang J., 2002).....	226
Table A.2.4.1. Maximum and near-record known depth-area-duration data for northern and southern China (Wang J., 2002).....	227
Table A.2.4.2. Depth-area-duration data of long-duration and large-area extraordinary storms in China (average rainfall in mm) (Wang J., 2002).....	229
Table A.2.5 Maximum observed depth-area-duration data for the United States (WMO-No. 332)....	230
Table A.2.6 Maximum observed depth-area-duration data for India (average rainfall in mm) (Wang G. and others, 2005) .....	231
Table A.3.1 World's greatest known floods .....	234
Table A.3.2 World's near-record floods .....	237

## FOREWORD

The probable maximum precipitation (PMP), which is a fundamental parameter in the design of a variety of hydrological structures, also has a key role in floodplain management, where it is made to correspond to the extreme potential risk of flooding at a given time and place.

PMP is therefore very useful for hydrologists, to estimate the probable maximum flooding and thereby, for example, to design the most appropriate spillways to minimize the risk of overtopping a given hydraulic structure, such as a dam. In this way, the risks of loss of lives, damages and community impacts can be minimized and managed.

The present publication covers a wide range of methods which can be used to make PMP estimates and it draws heavily on international experience

from many regions of the world. The previous edition was published by WMO in 1986 as an Operational Hydrology Report.

On behalf of WMO, I would therefore like to express my gratitude to all experts involved in its preparation and its publication, in particular to Mr Bruce Stewart, President of the WMO Commission for Hydrology, who led the corresponding review process as requested by the Commission at its twelfth session (Geneva, October 2004).



(M. Jarraud)  
Secretary General



## PREFACE

As President of the Commission for Hydrology (CHy) I am pleased to report that the preparation of the manual was led by Professor Wang Guoan (China). Professor Wang had strong support from a National Committee dedicated to the revision and update of the second edition of the manual. You will find the names of the Chinese members of the Committee under the Acknowledgement (page 211). The other technical reviewers of the draft text, in alphabetical order of the Member country, were:

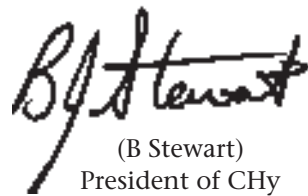
- Cristina Moyano (Argentina)
- David Walland (Australia)
- Van-Than-Va Nguyen (Canada)
- Paul Pilon (Canada) who was also the organizer and chair of a meeting of reviewers held in Canada
- Aaron F. Thompson (Canada)
- Alistair McKerchar (New Zealand)
- Shaukat Ali Awan (Pakistan)
- Louis C. Schreiner (United States of America)

The activities were carried out in association with the Open Panel of CHy Experts (OPACHE) on Hydrological Forecasting and Prediction.

I express my gratitude to authors of the third edition of the manual on estimation of probable maximum precipitation, the editor-in-chief of this revision (Professor Wang) and the reviewers for their contributions to the preparation of the revised manual.

This manual is the first manual of the newly established CHy series of publications: manuals as decided by CHy-XIII in early November 2008. It will be followed by the second CHy Manual on Stream Gauging, which will be the second edition of a report prepared under the old CHy series mentioned by the WMO's Secretary General in his foreword. The first edition of the Manual on Stream Gauging was published in 1980.

CHy is planning to organize demand-driven courses on both manuals during 2010 and the years to come.



(B Stewart)  
President of CHy



## SUMMARY

Probable maximum precipitation (PMP) is defined as the greatest depth of precipitation for a given duration meteorologically possible for a design watershed or a given storm area at a particular location at a particular time of year, with no allowance made for long-term climatic trends.

The first and second editions of this manual were published in 1973 and 1986, respectively. The current edition keeps a majority of the content from the second edition. Newly added content in this third edition primarily results from experiences, since 1986, in directly estimating PMP for the requirements of a given project in a design watershed on probable maximum flood (PMF) in China, the United States of America, Australia and India.

The methods used in China are characterized by integrating hydrological analysis and calculation into estimation of PMP/PMF. The current knowledge of storm mechanisms and their precipitation-producing efficiency remains insufficient to allow precise evaluation of limiting values of extreme precipitation. PMP estimates, therefore, must still be considered approximations. The accuracy, or reliability, of an estimate fundamentally depends on the amount and quality of data available and the depth of analysis.

Procedures for estimating PMP cannot be standardized. They vary with the amount and quality of data available, basin size and location, basin and regional topography, storm types producing extreme precipitation, and climate. There are many regions in various parts of the world for which PMP has never been estimated. It would be impossible at this time to prepare a manual covering all the problems that could possibly be encountered. Nor would it be practicable to prepare a manual that covers all the situations for which past estimates were derived. As a result, this manual introduces some basic models, or basic methods and the conditions under which they are applied, and highlights issues for attention. It is important for professionals to be flexible when using the methods in actual situations. In some cases it is appropriate to make parallel estimates using more than one method, followed by comprehensive analysis in order to acquire reasonable PMP estimates.

The purpose of PMP estimation is to determine PMF for a particular project in a design watershed. There are now two classes of PMP estimation methods. The first class (the indirect method) uses an approach based on storm area. This approach determines PMP for the storm area (the area surrounded by isohyets) and then converts it into PMP for the collecting area of a particular project in the design watershed. Methods introduced in Chapters 2 and 3, and 4, 5 and 6 in particular, mostly fall into this class. The second class (the direct method) adopts an approach based on watershed area. This approach directly estimates PMP for the collecting area of a particular project in the design watershed. Methods introduced in Chapter 7 are in this class, and those in Chapters 2 and 3 are also applicable.

In Chapters 2, 3 and 5, the manual introduces methods for PMP estimation that are widely applicable in middle latitudes to watersheds with areas less than 13 000 km<sup>2</sup> in orographic regions and those with areas less than 50 000 km<sup>2</sup> in non-orographic regions. The methodologies used in middle latitudes are, in most cases, also applicable to tropical regions. Since PMP procedures for tropical regions have not been as extensively applied as in middle latitudes, some possible modifications to traditional procedures have been suggested in Chapter 6.

Methods introduced in Chapter 7 are applicable to PMP estimation for watersheds with various areas and various precipitation durations in orographic and non-orographic regions where floods are caused by storms. In this chapter, some important issues relating PMF estimation are also introduced in a simple manner.

The procedures are illustrated by examples from actual studies done by the National Weather Service (formerly United States Weather Bureau), National Oceanic and Atmospheric Administration, United States Department of Commerce, the Australian Bureau of Meteorology, and water and power authorities in China and India. The examples were chosen to (a) represent a variety of problems; (b) capitalize on studies published in widely distributed and accessible reports; and (c) reflect the availability of basic material such as photographic prints (which minimized the time and cost of preparing the manual). The examples given cover

estimates for specific basins and more generalized estimates for regions, and include PMP estimates for thunderstorms, general (systematic) storms and tropical storms, as well as PMP/PMF estimates for extremely large watersheds.

All of the procedures described, except the statistical procedure, are based on the hydrometeorological approach. This approach consists essentially of moisture maximization and transposition of observed storms and combinations of storms. Precipitation efficiency is sometimes used, as is wind maximization. Storm transposition involves adjustments for elevation, moisture-inflow barriers, and distance from the moisture source. Variations of the traditional approach include the use of an orographic computation model in mountainous regions, the major temporal and spatial combination method, and the storm simulation method based on historical flood for extremely large

watersheds. Methods are described for determining the seasonal variation and temporal and areal distribution of PMP.

Tables of precipitable water in a saturated pseudo-adiabatic atmosphere are included for making various adjustments involving atmospheric moisture. Also included are world record and near-record rainfalls/floods that may be used for making rough assessments of derived PMP/PMF estimates.

Throughout the manual, it is assumed that users will be meteorological and hydrological professionals. As a result, basic meteorological and hydrological terminology and methodologies are not introduced. It is believed that the procedures described are presented in sufficient detail to permit meteorologists and hydrologists, especially those with hydrometeorological training, to apply them to estimating PMP and PMF in standard situations.

## RÉSUMÉ

Les précipitations maximales probables (PMP) sont définies comme étant la hauteur maximale de la lame d'eau qui peut, météorologiquement s'accumuler en un temps donné dans un bassin versant ou une zone de perturbations déterminés, en un endroit particulier et à une certaine époque de l'année, sans qu'il soit tenu compte des tendances climatiques à long terme.

La première et la deuxième éditions du Manuel sont parues respectivement en 1973 et 1986. La présente édition reprend dans une large mesure la teneur de l'édition précédente. Les nouveaux textes qu'elle contient rendent compte, pour l'essentiel, des activités menées depuis 1986 pour estimer directement les PMP dans le cadre d'un projet donné concernant la crue maximale probable (CMP) dans un bassin versant déterminé en Chine, aux États-Unis d'Amérique, en Australie et en Inde.

Les méthodes utilisées en Chine consistent à intégrer l'analyse et le calcul hydrologiques dans l'estimation des prévisions maximales probables et de la crue maximale probable. Nous n'en savons pas encore assez sur les mécanismes qui régissent les averses et sur leur aptitude à engendrer des précipitations pour évaluer avec précision les valeurs limites des précipitations extrêmes, et par conséquent, les estimations relatives aux PMP doivent être encore considérées comme des valeurs approximatives. La précision - ou la fiabilité - d'une estimation dépend essentiellement du volume et de la qualité des données disponibles et de la profondeur de l'analyse.

Il n'est pas possible de normaliser les méthodes employées pour estimer les précipitations maximales probables, car elles varient en fonction du volume et de la qualité des données disponibles, de la superficie et de la situation du bassin versant, de la topographie du bassin et de la région, de la nature des perturbations génératrices de précipitations extrêmes et, finalement du climat. Il existe un peu partout dans le monde des régions pour lesquelles ce paramètre n'a jamais fait l'objet d'estimations, et il serait impossible à l'heure actuelle d'élaborer un manuel qui traiterait de tous les problèmes susceptibles de se poser ou qui aborderait toutes les situations ayant donné lieu par le passé à des estimations. Par conséquent, le présent manuel porte sur des modèles et des méthodes élémentaires et les conditions dans lesquelles ces modèles et ces

méthodes sont utilisés, tout en mettant l'accent sur un certain nombre de questions. Il est important que les professionnels auxquels ce manuel s'adresse fassent preuve de souplesse en situation réelle. Dans certains cas, il est souhaitable de procéder à des estimations parallèles à l'aide de plusieurs méthodes puis à une analyse approfondie afin d'obtenir des estimations de PMP de qualité raisonnable.

L'estimation des PMP a pour but de déterminer la crue maximale probable pour un projet particulier et dans un bassin versant donné. Il existe deux catégories de méthodes d'estimation des PMP. La première – la méthode indirecte – consiste à déterminer tout d'abord les précipitations maximales probables pour la zone perturbée (délimitée par des isohyètes) et à en déduire ensuite les PMP pour l'aide de collecte se rattachant au projet considéré. Les méthodes présentées dans les chapitres 2 à 6, notamment, entrent pour la plupart dans cette catégorie. La deuxième catégorie – la méthode directe – est axée sur le bassin versant et consiste à estimer directement les PMP pour l'aire de collecte rattachée à un projet particulier dans le bassin versant considéré. Les méthodes présentées dans le chapitre 7 entrent dans cette catégorie.

Les méthodes d'estimation des PMP présentées dans les chapitres 2, 3 et 5 sont largement applicables aux bassins versants des latitudes moyennes d'une superficie inférieure à 13 000 km<sup>2</sup>, et situés en région montagneuse, et aux bassins versants d'une superficie inférieure à 50 000 km<sup>2</sup> situés en région de plaine. Les méthodes utilisées aux latitudes moyennes peuvent s'appliquer également, dans la plupart des cas, aux régions tropicales. Étant donné que, pour les régions tropicales les méthodes d'estimation des PMP n'ont pas été appliquées aussi largement que pour les latitudes moyennes, quelques modifications susceptibles d'être apportées aux méthodes traditionnelles sont proposées dans le chapitre 6.

Les méthodes présentées dans le chapitre 7 peuvent être utilisées pour estimer les précipitations maximales probables pour des bassins versants de tailles diverses et des périodes de précipitations variables, en région montagneuse comme en région de plaine, là où les perturbations provoquent des crues. Quelques questions importantes relatives à l'estimation de la crue maximale probable sont également abordées dans ce chapitre.

Les méthodes sont illustrées par des exemples tirés d'études effectuées par le National Weather Service (ex-U.S. Weather Bureau), la National Oceanic and Atmospheric Administration (NOAA), le Ministère américain du commerce, le Bureau of Meteorology australien et les autorités du secteur hydraulique et énergétique en Chine et en Inde. Les exemples ont été choisis: a) pour faire état des divers problèmes rencontrés; b) pour illustrer des études publiées dans des rapports largement diffusés et accessibles; c) pour rendre compte de l'existence de clichés photographiques, entre autre matériel de base, qui ont permis de réduire le temps nécessaire pour élaborer le manuel et les dépenses correspondantes. Ces exemples portent sur des estimations relatives à des bassins particuliers et d'autres, plus générales, qui concernent des régions entières. On trouve notamment des estimations de PMP se rapportant à des orages, à des perturbations de type classique et à des tempêtes tropicales, ainsi que des estimations de PMP/CMP pour d'immenses bassins versants.

Toutes les méthodes décrites, à l'exception de la méthode statistique, sont fondées sur la technique hydrométéorologique, qui fait intervenir essentiellement la maximalisation de l'humidité et la transposition des averses et des combinaisons d'averses observées. On a parfois recours au rendement des précipitations, ainsi qu'à la maximalisation du vent. La transposition d'averses comprend des ajustements pour tenir compte de l'altitude, des

obstacles à l'apport d'humidité et de la distance à la source d'humidité. Des variantes de l'approche traditionnelle consistent à utiliser, un modèle orographique pour les régions montagneuses, la méthode de combinaison spatiotemporelle et la méthode de simulation des averses reposant sur la crue historique pour les bassins versants particulièrement vastes. Sont décrites également les méthodes utilisées pour déterminer les variations saisonnières et la distribution spatiotemporelle des PMP.

On trouve aussi dans le Manuel des tableaux sur l'eau précipitable dans une atmosphère pseudo-adiabatique saturée, qui permettent d'effectuer divers ajustements où l'humidité atmosphérique entre en ligne de compte. Sont également fournis des records mondiaux en matière de précipitations ou de crues et les valeurs approchantes, qui peuvent servir à réaliser des évaluations approximatives des précipitations et des crues maximales probables.

Le Manuel s'adresse aux professionnels de la météorologie et de l'hydrologie et ne contient donc pas d'initiation à la terminologie et aux méthodologies de base utilisées dans ces domaines. On part du principe que les méthodes décrites sont exposées suffisamment en détail pour que les météorologues et les hydrologues, en particulier ceux qui ont une formation en hydrométéorologie puissent les utiliser pour estimer les précipitations et les crues maximales probables dans des situations standard.

## РЕЗЮМЕ

Максимально возможные осадки (МВОС) определяются как наибольший слой осадков за заданную продолжительность, метеорологически возможную для расчетного водосбора или для данной зоны ливней в конкретном месте в определенное время года без учета долгосрочных климатических тенденций.

Первое и второе издание настоящего наставления были опубликованы в 1973 и 1986 гг. соответственно. В нынешнем издании сохранена большая часть материала из второго издания. Новый материал, добавленный в содержание настоящего третьего издания, в основном, подготовлен на основе опыта, накопленного после 1986 г. в выполнении непосредственных оценок МВОС для потребностей отдельных проектов в расчетных водосборах по вероятным максимальным паводкам (ВМП) в Китае, Соединенных Штатах Америки, Австралии и Индии.

Методы, применяемые в Китае, характерны комплексным гидрологическим анализом и расчетом оценки МВОС/ВМП. Современный уровень знаний о механизмах сильных дождей и их осадкообразующей эффективности остается все еще недостаточным, чтобы выполнить точную оценку предельных значений экстремальных осадков. По этой причине оценки МВОС должны, по-прежнему, рассматриваться как приблизительные величины. Точность или надежность оценки коренным образом зависит от объема и качества имеющихся данных и глубины анализа.

Методы оценки МВОС не могут быть стандартизированы. Они изменяются в зависимости от объема и качества имеющихся данных, размеров бассейна и географического положения, топографии бассейна и района, характера ливней, приводящих к экстремальным осадкам, и климата. В различных частях земного шара существует много районов, для которых никогда не производился расчет оценок МВОС. В настоящее время было бы невозможно подготовить наставление, охватывающее все проблемы, с которыми может быть придется столкнуться. Было бы также практически невозможно подготовить наставление, которое предусматривало бы все ситуации, для которых

были рассчитаны оценки в прошлом. Таким образом, в настоящем наставлении представлены некоторые основные модели или базовые методы и условия, при которых они применялись, а также делается акцент на ряде проблем, требующих внимания. Важно, чтобы специалисты проявляли гибкость при применении методов в реальных ситуациях. В ряде случаев необходимо использовать параллельные оценки, применяя сразу несколько методов с последующим всесторонним анализом, чтобы получить приемлемые оценки МВОС.

Целью выполнения оценки МВОС является определение ВМП для конкретного проекта в расчетном водосборе. В настоящее время существует два класса методов оценки МВОС. В первом классе (косвенный метод) применяется подход, основанный на учете площади выпадения ливня. При данном подходе определяется МВОС для территории ливня (площадь между двумя соседними изогиетами) и затем их величины конвертируются в МВОС для водосборной площади конкретного проекта в исследуемом бассейне. Методы, представленные в главах 2 и 3, а также в 4, 5 и 6 в частности, по большей части относятся к данному классу. Во втором классе (прямой метод) используется подход, основанный на учете площади водосбора. Данный подход позволяет непосредственно оценивать МВОС для площади водосбора конкретного проекта в исследуемом бассейне. Методы, включенные в главу 7, относятся к этому классу, и туда же можно также отнести методы, описанные в главах 2 и 3.

В главах 2, 3 и 5 наставления представляются методы для оценки МВОС, которые широко применимы в средних широтах для водосборов с площадями менее 13 000 км<sup>2</sup> в орографических районах и для водосборов с площадями менее 50 000 км<sup>2</sup> в равнинных районах. Методологии, используемые в средних широтах, в большинстве случаев также применимы к тропическим районам. Поскольку методы оценки МВОС для тропических районов не применялись так широко, как в средних широтах, в главе 6 предложены некоторые возможные изменения к традиционным методам.

Методы, представленные в главе 7, применяются для оценки МВОС в водосборах с различными

площадями и с различной продолжительностью выпадения осадков в орографических районах и в равнинных районах, в которых паводки вызываются ливнями. В данной главе также изложены в доступной форме некоторые важные проблемы, касающиеся оценки ВМП.

Методы проиллюстрированы с помощью примеров фактических исследований, выполненных Национальной метеорологической службой (ранее Бюро погоды Соединенных Штатов Америки), Национальным управлением по исследованию океанов и атмосферы (НУОА), Министерством торговли США, Австралийским бюро метеорологии, а также органами управления водными ресурсами и энергетикой в Китае и Индии. Примеры были выбраны, чтобы а) отобразить наличие различных проблем; б) использовать наилучшим образом результаты исследований, опубликованные в широко распространенных и доступных отчетах; и с) отразить доступность исходного материала такого как фотографические отпечатки (что сократило время и затраты на подготовку настоящего наставления). Приведенные примеры охватывают оценки по конкретным бассейнам и обобщенные оценки по регионам, и, кроме того, включают оценки МСОВ для гроз, обычных (регулярных) ливней и тропических циклонов, а также оценки МВОС/ВМП для сверхбольших водосборов.

Все описанных способы, за исключением статистического метода, основаны на гидрометеорологическом подходе. Данный подход включает, в основном, максимизацию влагосодержания и транспозицию данных наблюдений за ливнями и их комбинациями.

Осадкообразующая эффективность иногда используется так же, как и максимизация ветра. Транспозиция ливня предусматривает учет высоты препятствия для притока влаги и расстояния от источника влаги. К вариантам традиционного подхода относятся применение орографической модели расчета для горных районов, основного метода комбинирования пространственно-временных параметров и метода моделирования на основе исторической информации о паводках для сверхбольших водосборов. Описываются методы для определения сезонных изменений и распределения МВОС во времени и по площади.

Для учета различных факторов, касающихся атмосферной влаги, приводятся таблицы общего количества пара в насыщенной псевдоадиабатической атмосфере, которое может выпасть в виде осадков. В наставление включены также мировые рекордные или близкие к рекордным осадки/паводки, которые могут использоваться для грубой проверки расчетных значений МВОС/ВМП.

Все наставление составлено в расчете на то, что им будут пользоваться специалисты в области метеорологии и гидрологии. Таким образом, по всему тексту наставления не разъясняются метеорологические терминология и методология. Предполагается, что описания методов представлены достаточно подробно, чтобы позволить метеорологам и гидрологам, в особенности прошедшим подготовку по гидрометеорологии, применять эти методы для оценки МВОС и ВМП при стандартных ситуациях.

## RESUMEN

La precipitación máxima probable (PMP) se define como la mayor cantidad de precipitación meteorológicamente posible que corresponde a determinada duración en una cuenca hidrográfica o zona de tormenta específicas de un determinado lugar en un período dado del año, sin tener en cuenta las tendencias climáticas que se producen a largo plazo.

La primera y segunda ediciones de este Manual se publicaron en 1973 y 1986 respectivamente. La edición actual conserva gran parte del contenido de la segunda edición. El contenido que se ha añadido a esta tercera edición procede principalmente de las experiencias de estimación directa de la precipitación máxima probable llevadas a cabo desde 1986 para atender las necesidades relacionadas con la crecida máxima probable de un proyecto determinado para una cuenca hidrográfica específica en China, Estados Unidos de América, Australia e India.

Los métodos utilizados en China se caracterizan por integrar el análisis y el cálculo hidrológicos en la estimación de la precipitación y la crecida máximas probables. Los conocimientos actuales sobre los mecanismos de las tormentas y su eficacia para producir precipitaciones no resultan aún suficientes para poder evaluar con precisión los valores límite de las precipitaciones extremas. Así pues, las estimaciones de la PMP todavía deben considerarse como aproximaciones. La precisión, o fiabilidad, de una estimación depende fundamentalmente de la cantidad y calidad de los datos disponibles y de la profundidad del análisis realizado.

Los procedimientos de estimación de la precipitación máxima probable no pueden ser normalizados ya que varían con la cantidad y calidad de los datos disponibles, el tamaño de la cuenca y su emplazamiento, la topografía de la cuenca y de la región, los tipos de tormentas que producen precipitaciones extremas y el clima. Existen numerosas regiones en varias partes del mundo en las que jamás se ha estimado la precipitación máxima probable. En estos momentos resultaría imposible redactar un manual en donde se estudiaran todos los problemas que a este respecto puedan plantearse. Y tampoco sería viable reunir en un manual todas las situaciones que se plantearon al deducir las estimaciones anteriores. En consecuencia, este Manual presenta

algunos modelos o métodos básicos y las condiciones en las que se aplican y pone de relieve cuestiones que requieren atención. Es importante que los profesionales sean flexibles cuando usen los métodos en situaciones reales. En algunos casos conviene realizar estimaciones paralelas, usando más de un método, seguidas de un análisis exhaustivo para así poder contar con estimaciones razonables sobre la PMP.

La finalidad de la estimación de la precipitación máxima probable es determinar la crecida máxima probable para un proyecto dado en una cuenca determinada. Actualmente existen dos clases de métodos de estimación de la PMP. La primera clase (el método indirecto) utiliza un enfoque basado en la zona de tormenta. Este enfoque determina la PMP para la zona de tormenta (la zona rodeada por isoyetas) y la convierte en la PMP de la zona de recogida de un proyecto dado en una cuenca determinada. Los métodos presentados en los Capítulos 2 y 3, y en particular 4, 5 y 6, corresponden a esta clase casi en su mayoría. La segunda clase (el método directo) adopta un enfoque basado en la zona de la cuenca hidrográfica. Con este enfoque se estima directamente la PMP para la zona de recogida de un proyecto dado en una cuenca determinada. Los métodos presentados en el Capítulo 7 pertenecen a esta clase.

En los Capítulos 2, 3 y 5 del Manual se presentan métodos de estimación de la PMP que son de aplicación general en las latitudes medias en las cuencas hidrográficas cuya extensión sea inferior a 13 000 km<sup>2</sup> en las regiones orográficas e inferior a 50 000 km<sup>2</sup> en las regiones no orográficas. En la mayoría de los casos, los métodos usados en esas latitudes también son aplicables a las regiones tropicales. Dado que los procedimientos para medir la PMP en las regiones tropicales todavía no se aplican tan ampliamente como en las latitudes medias, en el Capítulo 6 se han propuesto algunas posibles modificaciones de los procedimientos tradicionales.

Los métodos presentados en el Capítulo 7 son aplicables a la estimación de la PMP en las cuencas hidrográficas con zonas diversas y una duración de la precipitación variable en las regiones orográficas y no orográficas, donde las crecidas son causadas por tormentas. En este Capítulo se presentan también, de manera sencilla, algunas cuestiones

importantes relacionadas con la estimación de la crecida máxima probable.

Los procedimientos se ilustran mediante ejemplos tomados de estudios verdaderos llevados a cabo por el Servicio Meteorológico Nacional (antiguamente United States Weather Bureau), la Administración Nacional del Océano y de la Atmósfera, el Departamento de Comercio de Estados Unidos de América, la Oficina de Meteorología de Australia y las autoridades encargadas de los recursos hídricos y energéticos de China e India. Los ejemplos utilizados se eligieron porque a) representaban diferentes problemas; b) habían sido tomados de estudios publicados en informes de amplia distribución y acceso generalizado; y c) reflejaban la fácil disponibilidad de material básico, como las fotografías de ilustraciones (que redujeron al mínimo el tiempo y el costo de preparación del Manual). Los ejemplos citados se refieren a estimaciones para cuencas específicas y a estimaciones de carácter más general para las regiones, y abarcan valores estimados de la PMP resultante de las tormentas en general y de las tormentas tropicales, así como valores estimados de precipitación máxima probable y de crecida máxima probable para cuencas hidrográficas extremadamente grandes.

Todos los procedimientos descritos, excepto el procedimiento estadístico, están fundados en el planteamiento hidrometeorológico. Este planteamiento consiste fundamentalmente en la maximización de la humedad y en la transposición de las tormentas observadas y las combinaciones de tormentas. Algunas veces se usa la eficiencia de la precipitación, al igual que la

maximización del viento. La transposición de las tormentas implica ajustes de altitud, de las barreras contra el flujo de humedad entrante y de la distancia a partir de la fuente de humedad. Entre las variaciones del planteamiento tradicional se encuentra la utilización de un modelo orográfico de cálculo, aplicable en las regiones montañosas, el principal método de combinación temporal y espacial, y el método de simulación de tormentas basado en crecidas históricas para las cuencas hidrográficas extremadamente grandes. Asimismo, se incluyen métodos para determinar la variación estacional y la distribución zonal y temporal de la PMP.

Se incluyen tablas de agua precipitable en una atmósfera pseudo-adiabática saturada con objeto de hacer varios ajustes en relación con la humedad atmosférica. Asimismo, se incluyen casos récord o cercanos al récord de precipitaciones y de crecidas que pueden utilizarse para realizar evaluaciones aproximadas de estimaciones derivadas de precipitación máxima probable y de crecida máxima probable.

Se ha dado por sentado que los usuarios del Manual serán meteorólogos o hidrólogos. Por ello, en el Manual no se utilizan términos ni métodos meteorológicos o hidrológicos básicos. Se considera que los procedimientos descritos se presentan con suficiente detalle como para permitir a los meteorólogos y a los hidrólogos, y especialmente a los que poseen una formación en hidrometeorología, que los apliquen a la estimación de la precipitación máxima probable y la crecida máxima probable en situaciones tipo.

# CHAPTER 1

## INTRODUCTION

1.1

### OBJECTIVE OF PMP ESTIMATES

The objective of a probable maximum precipitation (PMP) estimate is to calculate the probable maximum flood (PMF) used in the design of a given project at a particular geographical location in a given watershed, and to further provide information that could assist in designing the size (dam height and reservoir storage capacity) of the given project and dimension of the flood-carrying structures (spillway and flood carrying tunnel) of the project.

1.2

### DEFINITIONS OF PMP AND PMF

1.2.1

#### Definition of PMP

PMP is the theoretical maximum precipitation for a given duration under modern meteorological conditions. Such a precipitation is likely to happen over a design watershed, or a storm area of a given size, at a certain time of year. Under disadvantageous conditions, PMP could be converted into PMF – the theoretical maximum flood. This is necessary information for the design of a given project in the targeted watershed.

1.2.2

#### Definition of PMF

PMF is the theoretical maximum flood that poses extremely serious threats to the flood control of a given project in a design watershed. Such a flood could plausibly occur in a locality at a particular time of year under current meteorological conditions.

1.3

### CLOSE COMBINATION OF HYDROLOGY AND METEOROLOGY

PMP/PMF estimation falls within the field of hydrometeorology. It is a method of hydrometeorology used to estimate the design flood, which combines hydrology and meteorology. The work of PMP/PMF estimation requires close cooperation between hydrologists and meteorologists. Any issues arising in PMP/PMF estimation should not be studied from a purely hydrological or purely

meteorological point of view. The concepts and theories of both hydrology and meteorology should be considered. Only in this way can the PMP/PMF estimates be optimized and reflect a balance between safety and cost-efficiency in project design. The studies should also cover all factors that affect PMF, including meteorology, hydrology, geology and topography. Nevertheless, separate analysis of meteorological factors is possible.

The manual contains advances based on the methods and technologies introduced in the literature in recent years and new experience of current practices. Physical models are not usable as they produce low-accuracy estimates of precipitation. The use of numerical weather models for PMP estimation is currently a topic of research (Cotton and others, 2003).

1.4

### PMP/PMF ESTIMATION

1.4.1

#### Basic knowledge

Storms, and their associated floods, have physical upper limits, which are referred to as PMP and PMF. It should be noted that due to the physical complexity of the phenomena and limitations in data and the meteorological and hydrological sciences, only approximations are currently available for the upper limits of storms and their associated floods.

1.4.2

#### Approaches to and methods of PMP estimation

1.4.2.1

##### Approaches

PMP is primarily considered to be the precipitation resulting from a storm induced by the optimal dynamic factor (usually the precipitation efficiency) and the maximum moisture factor simultaneously. There are two general approaches to estimating PMP: one based on storm area (area surrounded by isohyets) and the other based on the specific watershed location (watershed area).

The approach based on storm area (the indirect approach) focuses on the estimation of a group of PMPs with various durations and areas in a wide region (a zone with meteorologically homogeneous

conditions), and then provides a set of methods to convert them into the PMP in the design watershed for the purpose of PMF estimation in high-risk projects (usually reservoirs and nuclear power stations).

The approach based on watershed area (the direct approach) focuses on the direct estimation of PMP with a given duration according to the requirements of a specific project (usually the design of a reservoir) in the targeted watershed. The reason for introducing the specific project here is that different design scenarios could result in the selection of different design PMPs potentially resulting from different causative factors. For instance, if a large high-dam reservoir with powerful regulating and storing capacity is constructed at a site, the total flood volume will be the controlling factor for the project regarding flood control. Therefore, the duration of the design flood will be relatively long, and the storm may be created through the superposition and replacement of several storms. If a small low-dam reservoir with small regulating and storing capacity is constructed at the same site, peak flood discharge will be the controlling factor for the project regarding flood control. The required design flood duration may hence be shorter, and a storm may be created by a single storm weather system or by local violent convection.

#### 1.4.2.2 Methods

There are six methods of PMP estimation currently used:

- (a) The local method (local storm maximization or local model);
- (b) The transposition method (storm transposition or transposition model);
- (c) The combination method (temporal and spatial maximization of storm or storm combination or combination model);
- (d) The inferential method (theoretical model or ratiocination model);
- (e) The generalized method (generalized estimation);
- (f) The statistical method (statistical estimation).

Most can be used in medium- or low-latitude areas, but when used in low-latitude areas (tropic zone), the method for deriving some parameters needs to be properly revised (see Chapter 6).

In addition, two other methods can be used for deriving PMP/PMF in extremely large watersheds.

They are:

- (a) The major temporal and spatial combination method;
- (b) The storm simulation method based on historical floods (see Chapter 7).

The characteristics of and the application conditions for these eight methods are, briefly, as follows.

##### 1.4.2.2.1 *Local method*

PMP is estimated according to the maximum storm of the observed data in the design watershed or specific location. This method is applicable where there are several years of observed data.

##### 1.4.2.2.2 *Transposition method*

In this method an extraordinarily large storm in the adjacent area is transposed to the design area or the location to be studied. The work focuses on two aspects. The first is to ascertain the storm transposition probability, which can be done in three ways:

- (a) By determining the meteorologically homogeneous zone, studying the possible transposition range of the storm and carrying out a detailed analysis of the design watershed conditions;
- (b) By making a variety of adjustments for the transposed storm, based on the differences in geographic and topographic conditions between the original storm occurrence area and the design area. This method, which is widely applied, is used for design areas where high-efficiency storms are rare.

##### 1.4.2.2.3 *Combination method*

This method reasonably combines two or more storms in a local area, based on principles of synoptic meteorology and experience of synoptic forecasting, in order to form a sequence of artificial storms with a long duration. The work focuses on selection of combinations, determination of combination schemes and reasonable demonstration of combination sequences. This method is applicable for deriving PMP/PMF in large watersheds with long durations, and requires strong meteorological knowledge.

##### 1.4.2.2.4 *Inferential method*

The inferential method generalizes the 3-D spatial structure of a storm weather system in the design area to create a simplified physical storm equation for the main physical factor that influences the

storms. According to the available wind field data, the method uses either a convergence model or a laminar model. In the convergence model, it is assumed that the inflow of storm moisture converges to the centre from all sides and rises to create an event. In the laminar model, it is assumed that the inflow of storm moisture crawls along an inclining surface in a laminar fashion and rises to create an event. This method, requiring strong available observation data of upper meteorology in the design area, is applicable for watersheds with an area of hundreds to thousands of square kilometres.

#### 1.4.2.2.5 *Generalized method*

The generalized method is used to estimate PMP for a large, meteorologically homogeneous zone. The procedure involves grouping the observed rainfall of a storm into convergence and orographic rainfall. Convergence rain, which is the rainfall created through atmospheric convergence and rising induced by a passing weather system, is assumed to occur anywhere in meteorologically homogeneous zones. Orographic rain is the rainfall created through orographic rising. The generalization method uses convergence rainfall and the main results are as follows:

- (a) PMP depth, which is shown as a generalized depth-area-duration (DAD) curve (produced via storm transposition);
- (b) PMP spatial distribution, which is a group of concentric ellipses generalized from isohyets;
- (c) PMP temporal distribution, which is a single-peak map of a generalized hyetograph.

This method requires a large amount of long-term data obtained by rainfall self-recorders in the study area. This is a time-consuming and expensive process. However, the method can lead to high accuracy and easy application of PMP results. This method is applicable to watersheds under 13 000 km<sup>2</sup> in orographic regions and 52 000 km<sup>2</sup> in non-orographic regions, and rainfall durations of 72 hours or less.

#### 1.4.2.2.6 *Statistical method*

The statistical method was proposed by Hershfield of the United States. PMP is derived from data from numerous gauge stations in a meteorologically homogeneous zone, using the hydrological frequency analysis method together with the regional generalized method. The procedure differs from the traditional frequency analysis method, resulting in different physical connotations (Wang G., 2004). This method is mainly applicable for watersheds with a collecting area under 1 000 km<sup>2</sup>.

#### 1.4.2.2.7 *Major temporal and spatial combination method*

In this method, the part of the PMP that has the larger influence on PMF temporally (flood hydrograph) and spatially (flood source area) at the design section is treated with hydro-meteorological methods (local, transposition, combination and generalized), and the part of PMP which has the smaller influence is treated with the common correlation method and the typical flood distribution method. Obviously, this method, which can be regarded as a storm combination method, combines both temporal and spatial conditions. It only makes detailed computations for the main part while making rough computations for the secondary part. This method is mainly used for watersheds above the design section and for large rivers with a great difference between upstream and downstream weather conditions.

#### 1.4.2.2.8 *Storm simulation method based on historical flood*

This method produces a storm that could have potentially created the historical flood. This is done through hydrological watershed models. This method is inherently based on the incomplete temporal and spatial distribution information of the known extraordinary flood. It is also based on the assumption that modern synoptic meteorological conditions and synoptic forecast experience are applicable to the historical period. Then, with the extraordinary storm as a high-efficiency storm, the PMP is derived after maximizing moisture. This method is applicable where information about the flood hydrograph at the design section and knowledge of the rainfall, hydrological and flooding situations in some parts of the upstream mainstream and tributaries have been obtained through investigation and analysis of historical literature (books, newspapers, anecdotes and other records).

Local, transposition and combination methods are described in Chapters 2, 3 and 7 of this manual. Various additional methodologies and practices have been introduced in this third edition, including approaches that have been developed and applied in China.

### 1.4.3 **Main steps for storm and watershed approaches**

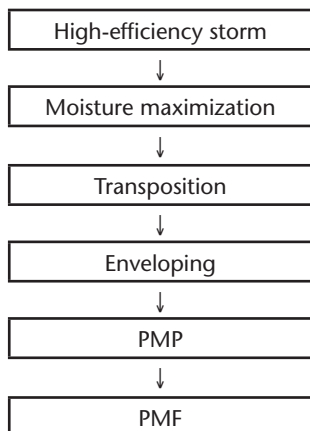
#### 1.4.3.1 *Approach based on storm area*

The generalized estimation method and statistical estimation method are the commonly used

methods that are based on a storm area approach. The former aims to generalize the areal mean precipitation depth within an isohyet while the latter aims to generalize a point (gauge station) precipitation depth. The point can be taken as a mean precipitation depth for an area less than 10 km<sup>2</sup> to derive PMP. The PMP from areal mean precipitation depth within an isohyet and the PMP from a point (gauge station) precipitation depth are then converted to obtain the PMP of the design watershed.

#### 1.4.3.1.1 *Main steps for the generalized estimation method*

The main steps for PMP estimation via this method include (Wang G., 2004):



High-efficiency storm, simply speaking, is a major storm (observed data) with the assumption that its precipitation efficiency has reached its maximum.

Moisture maximization is the process of adjusting the moisture factors of high-efficiency storms to their maximum.

Transposition is the rainfall distribution map transfer of moisture-maximized and high-efficiency storms in meteorologically homogeneous zones.

Enveloping means that enveloping values are taken from the DAD relation plotted according to the transposed storms, thereby maximizing the precipitation depth for various areas and durations.

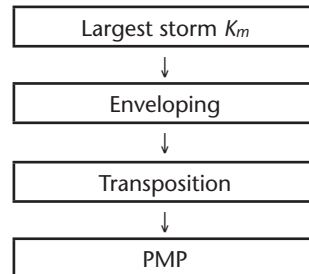
PMP is the possible maximum precipitation that comes from the application of the above DAD enveloping values for the design watershed.

PMF is the assumption that the flood (together with base runoff) created by PMP is the possible maximum flood in the design area.

The methods described in Chapters 5 and 6 are examples of generalized estimation methods.

#### 1.4.3.1.2 *Main steps for the statistical estimation method*

The main steps for PMP estimation via this method include (Wang G., 2004):



Largest storm  $K_m$  is a statistical representation of the maximum value in the observed storm series, given by:

$$K_m = \frac{X_m - \bar{X}_{n-1}}{\sigma_{n-1}} \quad (1.1)$$

where  $X_m$  is the maximum observed storm value;  $\bar{X}_{n-1}$  and  $\sigma_{n-1}$  are, respectively, the mean value and standard deviation computed excluding the extraordinarily large value.

Enveloping shows  $K_m$  values for various durations  $D$  at each gauged station as a dotted line on a correlation plot of  $K_m \sim D \sim \bar{X}_{n-1}$ . The enveloping curve, or the  $K_m \sim \bar{X}_{n-1}$  relationship, varies with the value of  $D$ .

Transposition transposes the  $K_m$  value in the above enveloping curve to the design station. The procedure computes the mean value  $\bar{X}_n$  from the storm series using all the observed  $n$  years at the design station, and  $K_m$  is the value of the design station from the above correlation plot.

PMP is the possible maximum precipitation at the design station, which can be computed with the following formula:

$$\text{PMP} = \bar{X}_n + K_m \sigma_n = \bar{X}(1 + K_m C_{vn}) \quad (1.2)$$

where  $\sigma_n$  and  $C_{vn}$  are, respectively, the standard deviation and the coefficient of variation of the precipitation series for the  $n$  years of data at the design station ( $C_{vn} = \sigma_n / \bar{X}_n$ ).

It can be seen from the above that the statistical estimation method is similar to storm transposition. However, what is transposed is not a specific storm rainfall but, rather, an abstracted statistical

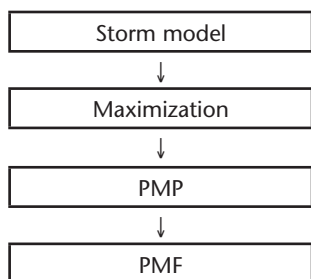
value  $K_m$ . Storm transposition correction is carried out with the mean value  $\bar{X}_n$  and the variation coefficient  $C_{vn}$  at the design station (Wang, G. 2004).

The PMP derived by the above procedure is for a point (assumed as the storm centre), and the areal mean PMP of the design watershed can be obtained from the storm-point area relationship map.

The methods described in Chapter 4 are examples of a statistical estimation method.

#### 1.4.3.2 Approach based on watershed area

The main steps of this approach for PMP estimation are (Wang G., 1999, 2004):



Storm model is a typical storm or ideal model that reflects the characteristics of extraordinary storms of the design watershed, which pose serious threats to flood control in the project. Depending on its sources, it can be categorized as a local model, transposition model, combination model or inferential model. The implications of these models are the same as described in section 1.4.2.2.

Maximization means maximizing the storm model. When the storm model is a high-efficiency storm, only moisture maximization is performed, otherwise both the moisture factor and the dynamic factor need to be maximized.

PMP is the possible maximum precipitation over a design watershed derived from maximization of the storm model.

PMF is the possible maximum flood converted from the PMP over a design watershed.

Methods described in Chapter 7 are examples of this approach. The convergence model and the laminar model are briefly introduced in Chapters 2 and 3 but as they are more theoretical, the two models are not mentioned again in Chapter 7.

These methods, especially those introduced in Chapter 7, require close cooperation between hydrological and meteorological staff.

#### 1.5

#### STORM AND FLOOD DATA

As data on extraordinary storms and floods form the basis for estimating PMP/PMF, it is necessary to extensively collect, process and analyse them. Analysis focuses on the magnitude of numerical values, the spatial-temporal distribution pattern and the synoptic cause. Areal mean rainfall is calculated based on observed rainfall of heavy storms in the watershed. Radars and satellites can provide additional and recent observed rainfall data. Telemetry data are now available and especially useful for regions with scarce data (see for example <http://www.ecmwf.int> and <http://www.cdc.noaa.gov/cdc/reanalysis/reanalysis.shtml>).

Areal mean rainfall is used to develop the DAD curves. Depth-area-duration analysis is performed using the method described in the *Manual for Depth-Area-Duration Analysis of Storm Precipitation* (WMO-No. 237). The method facilitates determining the average precipitation depth of a storm over a given area for a particular time. In PMP studies, the analysis method is extremely useful in studying the hydrological characteristics of a watershed.

Data and information on historical extraordinary storms and floods obtained from field surveys and historical literature should be collected and analysed as rigorously as possible. It should be noted that, particularly when dealing with early, unusual records, great effort should be made to verify the information. In any analysis, the storm volume, its spatial and temporal distributions, and the causative factors of each extraordinary storm should be carefully determined. Similarly, for each extraordinary flood, its peak flood, flood volume, temporal distribution and flood source region should also be determined as clearly as possible.

#### 1.6

#### ACCURACY OF PMP/PMF ESTIMATION

The accuracy of PMP/PMF estimation rests on the quantity and quality of data on extraordinary storms and floods and the depth of analysis and study. Nonetheless, it is impossible to give precise values for PMP and PMF. As yet, there are no methods to quantitatively assess the accuracy of PMP and PMF. Presently, it is most important to analyse, compare and harmonize results of PMP/PMF from multiple perspectives. This task is called a consistency check in the United States (Hydrometeorological Reports 55A, 57 and 59: Hansen and others, 1988; Hansen and others,

1994; and Corrigan and others, 1998) and is termed a rationality check in China (section 7.2.7 of the manual). Results are quality controlled through such a comparison.

When evaluating various PMP estimates, there are some other aspects to consider:

- (a) the amount by which the estimated PMP exceeds the maximum observed rainfall values for the surrounding meteorologically homogeneous region;
- (b) the frequency and severity of recorded storms that have occurred in the region;
- (c) limitations on storm transposition in the region;
- (d) the number of times and character of maximization, and correlations between them;
- (e) the reliability of relations between rainfalls and other meteorological variables in the model;
- (f) occurrence probabilities of individual meteorological variables in the model, though excessive combination of rare occurrences should be avoided.

Although the procedures described here produce PMP estimates to the nearest millimetre or tenth of an inch, this should not be used to indicate the degree of accuracy.

## 1.7 THE MANUAL

### 1.7.1 Objective

The objective of compiling this manual is to make a systematic description of the methods for deriving PMP presently in common use around the world. The manual includes basic ideas, critical links, points for attention and common terms for engineers and designers to refer to in relation to their particular projects.

The manual assumes readers possess knowledge of hydrometeorology; thus basic meteorological and hydrological terms and procedures are not described.

### 1.7.2 Scope

With regard to its regional scope, the manual describes approaches applicable to estimating PMP for rivers with mostly stormy floods in middle and low latitudes, not approaches for estimating PMP for rivers with mostly snow-melt floods in high latitudes.

In terms of area and duration, Chapters 2 to 6 elaborate common meteorological methods for estimating PMP for watersheds with areas less than 50 000 km<sup>2</sup> in non-orographic regions and less than 13 000 km<sup>2</sup> in orographic regions (the statistical estimation method in Chapter 4 generally applies to areas less than 1 000 km<sup>2</sup>) for a precipitation duration of less than 72 hours. In principle, the approaches in Chapter 7 can be applied to estimating PMP for all sorts of areas in both orographic and non-orographic regions and with a variety of precipitation durations. Chapter 7 emphasizes that estimation of PMP should consider the requirements of a given project in the design watershed. Aspects such as critical duration, flood peak and flood volume are important considerations in arriving at an appropriate estimate of PMF.

Chapter 7 provides approaches to address the estimation of PMP for large watersheds with areas between 50 000 km<sup>2</sup> and 1 000 000 km<sup>2</sup> while other approaches have also been used (Morrison-Knudsen Engineers, Inc., 1990).

While methods for PMP estimation in Chapter 7 are used to estimate PMF for a given project in the design watershed, some further attention could have been given to the estimation of PMF in this manual. However, as the focus of the manual is on PMP estimation, it was not considered appropriate to discuss PMF in detail. Therefore, the manual limits itself to highlighting some important features of watershed runoff yield and watershed confluence during PMP by way of background to corresponding methods for PMF estimation. The manual does not discuss issues such as deriving maximum seasonal accumulation of snow and optimal snow-melting rate necessary to produce the PMF in some regions. Standard hydrological references for these aspects include: German Water Resources Association, 1983; Institution of Engineers, Australia, 1987; Cudworth, 1989; United States Army Corps of Engineers, 1996; Wang G., 1999; WMO-No. 233; WMO-No. 168; WMO-No. 425); and web references (for example, <http://www.ferc.gov/industries/hydropower/safety/guidelines/fema-94.pdf>).

### 1.7.3 Application of examples

The manual describes common practical methods for estimating PMP using examples from published reports on PMP for storm areas and watershed areas with different sizes, climates and topographies. There are two main reasons for using such examples: first, they are actual calculations for actual watersheds rather than imaginary cases; and second, these examples are supported by detailed reports,

which give valuable additional information. The content in the manual should be adequate for hydrometeorologists. PMP estimation occurs in many countries, and the manual takes examples from Hydrometeorological Reports (HMR) published by the United States Weather Bureau (renamed National Weather Service in 1970), the Australian Bureau of Meteorology and water and power design organizations in China and India. However, those methods and results discussed should not necessarily be considered superior to those from other countries or organizations.

The examples presented are not intended for direct application in deriving PMP estimates. They aim to explain how to estimate PMP in different cases, including watersheds of various sizes as well as different topographies, climates and quality of data. It is not intended that the method given for any particular situation represents the only solution. Other methods may also be effective. The examples should be regarded merely as recommendations for how to derive PMP estimates. Special attention should be paid to the notes at the end of each chapter.

The importance of meteorological studies in PMP estimation cannot be over-emphasized. Such studies give guidance on regional, seasonal, durational and areal variations and topographic effects.

#### **1.7.4 Application of computer technologies**

As computers have developed so has their use in hydrometeorology. Computers may be used in everything, from analysing and processing data needed for PMP estimation to determining PMP and PMF. In addition, with the use of geographical information systems (GIS), many stages of PMP and PMF estimation can be improved. The manual includes information on the application of computer technologies, in combination with generalized PMP estimation, in south-eastern Australia.

#### **1.8 PMP AND CLIMATE CHANGE**

In assessing the possible impacts of climate change on PMP, the following factors need to be considered: moisture availability, depth-area curves, storm

types, storm efficiency and generalized rainfall depths. Since the PMP methodology is related to very large rainfall events, changes in both observed and projected extreme rainfall should also be considered.

These factors can be assessed using both an event-based approach and a station-based approach. In a study undertaken for Australia (Jakob and others, 2008), some significant increases in moisture availability were found for coastal Australia, and climate models project further general increases, although some regions of decrease were also found. Very few significant changes in storm efficiency were found, although there is a tendency to a reduction in storm efficiency for coastal parts of eastern Australia.

Typically, no significant changes were found in generalized rainfall depths, but a recent event broke previous records (both in terms of storm efficiency and generalized rainfall depth) for the season during which the event occurred (winter).

PMP estimates are robust estimates (typically not based on single outliers). Recent significant rainfall events are regularly screened to check whether including these events in the storm databases would increase PMP estimates. In the Australian case study, there had been no recent cases where PMP estimates had to be updated.

Long-term trends in rainfall extremes were found for only two regions: a decrease in coastal south-western Western Australia and an increase in parts of northern New South Wales. The fact that trends were found for only two regions implies that current generalized PMP estimates are representative of current climate conditions for most of Australia.

Global climate models do not accurately model the trends of late twentieth century Australian rainfall. However, there is an indication that, due to the overall increase in moisture availability in a warming climate, the most extreme rainfall events are likely to increase in the twenty-first century.

Based on the above analysis, the Australian case study indicates that so far we cannot confirm whether PMP estimates will definitely increase under a changing climate.



## CHAPTER 2

# ESTIMATES FOR MID-LATITUDE NON-OROGRAPHIC REGIONS

## 2.1 INTRODUCTION

### 2.1.1 Summary

- (a) Key factors influencing precipitation can be summarized as the moisture factor and the dynamic factor. The moisture factor is usually determined using surface dewpoints. The dynamic factor is usually determined indirectly through data on observed extraordinary storms, but it may be estimated directly using a specific meteorological factor.
- (b) Three methods are usually used in estimating probable maximum precipitation (PMP) in non-orographic regions. The first is local storm maximization. Methods of maximization include moisture maximization and wind maximization. The second is the storm transposition method. Elevation adjustment, barrier adjustment and horizontal displacement adjustment need to be performed in the transposition. The third method is spatial and temporal maximization, where the spatial and temporal distributions of one or more storms are adjusted deliberately using certain principles, thereby forming a new storm sequence to enhance the effect of flood creation. In China this third method is called storm combination.
- (c) The term enveloping means that results obtained from one or several methods are used to draw the depth-area-duration (DAD) enveloping curve, or PMP. It is used to maximize observed storms or hypothesized storms with certain durations and areas in a particular watershed and the result is called the probable maximum storm (PMS).
- (d) Generally, there are two methods for deriving spatial and temporal distributions. The first is the generalized spatio-temporal distribution method. In this method, the temporal distribution is generalized into the single-peak type with the peak slightly behind; and the spatial distribution is generalized into a set of concentric ellipses. The second method is the simulated observed typical storm method. In this case, the spatio-temporal distribution of a certain observed storm is used as the spatio-temporal distribution of PMP.

The above methods are applicable to certain watersheds and generalized estimation in a meteorologically homogeneous zone.

### 2.1.2 Convergence model

The theoretical interrelationship of convergence, vertical motion and condensation is well known. If either the convergence at various heights in the atmosphere or the vertical motion (averaged over some definite time and space) is known, or assumed with a given degree of precision, then the other can be calculated to an equal precision from the principle of continuity of mass.

Observations confirm that the theoretical pseudo-adiabatic lapse rate of temperature of ascending saturated air is an accurate approximation from which to calculate precipitation yield in deep precipitating clouds. The higher the specific humidity, the greater the precipitation yield for a given decrease in pressure. All these factors are basic to the formulation of a convergence model, and several such models have been postulated (United States Weather Bureau, 1947; Wiesner, 1970; WMO-No. 233).

### 2.1.3 Observed storm rainfall as an indicator of convergence and vertical motion

There is a problem in estimating PMP with a convergence model. Maximum water vapour content can be estimated with acceptable accuracy for all seasons for most parts of the world by appropriate interpretation of climatological data. However, there is neither an empirical nor satisfactory theoretical basis for assigning maximum values to either convergence or vertical motion. Direct measurement of these values to date has been elusive. The solution to this dilemma has been to use observed storm rainfall as an indirect measure.

Extreme rainfalls are indicators of maximum rates of convergence and vertical motion in the atmosphere, which are referred to as the storm or precipitation-producing mechanism. Extreme mechanisms for extreme storms may then be determined for basins under study without the need to actually calculate the magnitude of the convergence and vertical motion. The procedures for using

maximizing observed storm rainfall to estimate PMP involve moisture adjustments, storm transposition and envelopment. These are discussed in the following sections.

## 2.2 ESTIMATION OF ATMOSPHERIC MOISTURE

### 2.2.1 Assumption of a saturated pseudo-adiabatic atmosphere

Since many of the extreme, or major, recorded storms occurred before extensive networks of upper-air temperature and humidity soundings had been established, any index of atmospheric moisture must be obtainable from surface observations. Even today, current upper-air observational networks are too sparse to adequately define the moisture inflow into many storms, especially those limited to areas of the size considered in this manual.

Fortunately, the moisture in the lower layers of the atmosphere is the most important for producing precipitation, both because most atmospheric moisture is in the lower layers and because it is distributed upward through the storm early in the rainfall process (Schwarz, 1967; United States Weather Bureau, 1960). Theoretical computations show that, in the case of extreme rains, ascensional rates in the storm must be so great that air originally near the surface has reached the top of the layer from which precipitation is falling within an hour or so. In the case of severe thunderstorm rainfall, surface air may reach the top in a matter of minutes.

The most realistic assumption seems to be that the air ascends dry-adiabatically to the saturation level and thence moist-adiabatically. For a given surface dewpoint, the lower the level at which the air reaches saturation, the more moisture a column of air will contain. The greatest precipitable moisture occurs when this level is at the ground. For these reasons, hydrometeorologists generally postulate a saturated pseudo-adiabatic atmosphere for extreme storms.

### 2.2.2 Surface dewpoints as a moisture index

Moisture maximization of a storm requires identification of two saturation adiabats. One typifies the vertical temperature distribution that occurred in the storm to be maximized. The other is the warmest saturation adiabat to be expected at the same time of year and place as the storm. It is necessary to identify these two saturation adiabats with an indicator. The

conventional label in meteorology for saturation adiabats is the wet-bulb potential temperature, which corresponds to the dewpoint at 1 000 hPa. Tests have shown that storm and extreme values of precipitable water may be approximated by estimates based on surface dewpoints, when saturation and pseudo-adiabatic conditions are assumed (Miller, 1963; United States Weather Bureau, 1960).

Surface dewpoints that represent the moisture inflow into the storm can be used to identify the storm saturation adiabat. The moist adiabat corresponding to either the highest recorded dewpoint observed over a period of 50 years or more for the location and season, or the dewpoint for a specific return period, for example, 100 years (see section 2.2.5), is considered sufficiently close to the probable warmest saturation adiabat. Both storm and maximum dewpoints are reduced pseudo-adiabatically to the 1 000-hPa level (Figure 2.1), so that dewpoints observed at stations at different elevations are comparable. This permits construction and use of tables showing atmospheric moisture as a function of the 1 000-hPa dewpoints (Tables A.1.1 to A.1.3, Annex 1).

### 2.2.3 Persisting 12-hour dewpoints

As moisture inflow has an appreciable effect on storm precipitation, the moisture must be the type that persists for hours rather than minutes. Also, any single observation of dewpoint could be a considerably inaccurate value. Consequently, dewpoint values used to estimate probable maximum and storm moisture should be based on two or more consecutive measurements separated by a reasonable time interval, or a continuous automatic record of dewpoint over a period of time. The so-called highest persisting 12-hour dewpoint is generally used. Other alternatives include the maximum average 24-hour dewpoint, an average 12-hour dewpoint or a 24-hour persisting dewpoint. The highest persisting dewpoint for some specified time interval is the value equalled or exceeded at all observations during the period.

Table 2.1 shows a series of dewpoints observed at 6-hour intervals. The highest persisting 12-hour dewpoint for this example series is 24°C, which is obtained from the period 1800 to 0600. However, if the air temperature had dropped below 23°C during the period 0000 to 0600, the highest persisting 12-hour dewpoint would then be 23°C, which is obtained from the period 1200 to 0000. If available, hourly dewpoints may be used, but such records are sparse. They also add a great deal of work to the surveys for persisting values, especially in the case

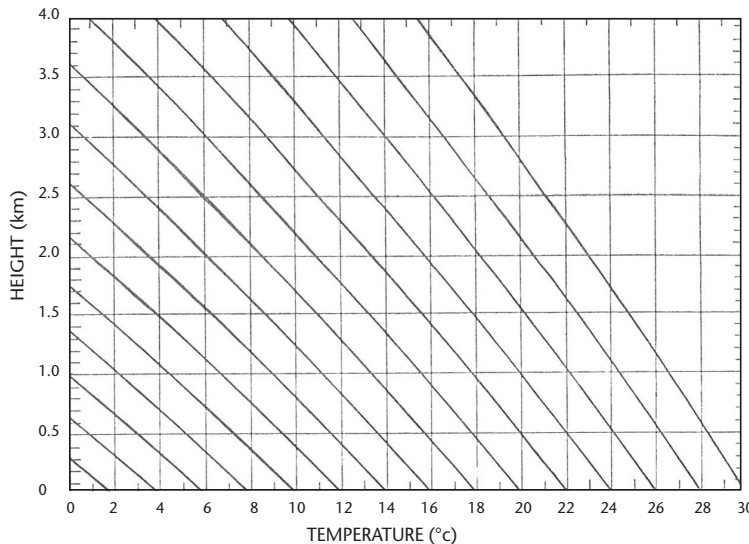


**Figure 2.1. Pseudo-adiabatic diagram for dewpoint reduction to 1 000 hPa at zero height**

of maximum persisting 12-hour dewpoints, which are discussed in section 2.2.5.

#### 2.2.4      **Representative persisting 12-hour 1 000-hPa storm dewpoints**

To select the saturation adiabat representing the storm moisture, the highest dewpoints in the warm air flowing into the storm are identified from surface weather charts. Dewpoints between the rain area and moisture source should be given primary consideration. Dewpoints in the rain area may be too high because of the precipitation, but they need not be excluded if they (a) appear to agree with dewpoints outside the area, and (b) appear to be truly representative of the layer of air where precipitation is forming. In some storms, particularly those with frontal systems, surface dewpoints in the rain area may represent only a shallow layer of cold air and not the temperature and moisture distributions in the clouds releasing the precipitation.

Figure 2.2 schematically illustrates a weather map from which the storm dewpoint is determined. On each consecutive weather map for 6-hour intervals during the storm, the maximum dewpoint is averaged over several stations, as illustrated in the figure. The same stations should be selected for averaging on each of the weather maps.

Occasionally, it is necessary to rely on the dewpoint at only one suitably located station, for example, when the moist airflow into the storm is from a very narrow moist tongue. The distance from the centre of the storm precipitation to the stations selected for determining the storm dewpoint should be limited to that of synoptic scale phenomena, no more than approximately 1 600 km. The average, or single, maximum dewpoints selected from consecutive maps form a series, and the maximum persisting 12-hour storm dewpoint is then determined, as described in section 2.2.3. Care should be taken to ensure that the time period selected for the storm dewpoint is taken so as to allow for transport from the location of the dewpoint stations to the storm site during an interval compatible with observed winds in the storm. The selected dewpoint is then reduced pseudo-adiabatically to the 1 000-hPa level.

If the originally observed values plotted on the weather maps are for stations differing significantly in elevation, a reduction of 1 000 hPa should be made for each station before averaging, however, elevation differences between dewpoint stations in the moist-air inflow are usually small, hence are generally neglected in the selection of the storm dewpoint.

**Table 2.1. Dewpoints observed at 6-hour intervals**

Time	0000	0600	1200	1800	0000	0600	1200	1800
Dewpoint (°C)	22	22	23	24	26	24	20	21

## 2.2.5 Maximum persisting 12-hour 1 000-hPa dewpoints

Maximum values of atmospheric water vapour used for storm maximization are usually estimated from maximum persisting 12-hour 1 000-hPa dewpoints. These dewpoints are generally obtained from surveys of long records – 50 or more years – at several stations in the problem area. In some regions, the maximum dewpoints for each month of the year or critical season may be adequate to define the seasonal variation of maximum atmospheric moisture, but it is generally advisable to select maximum persisting 12-hour dewpoints using semi-monthly or 10-day intervals.

Dewpoint records appreciably shorter than approximately 50 years are unlikely to yield maximum values representative of maximum atmospheric moisture. The usual practice in such cases is to perform a frequency analysis on an annual series of monthly or shorter interval maximum persisting 12-hour dewpoints.

Since values for the 100-year return period have been found to approximate maximum dewpoints obtained from surveys of long records, it is the 100-year values that are generally used for defining the seasonal variation curve, although 50-year values have been used sometimes.

Certain precautions are advisable when selecting maximum dewpoints intended as indices of maximum moisture for storm maximization. These precautions apply regardless of whether the maximum dewpoints are used directly as surveyed, or subjected to frequency analysis. In places and seasons characterized by ample sunshine, sluggish air circulation, numerous lakes, rivers and swamps, a locally high dewpoint may be a result of local evaporation of moisture from the surface and may not be at all representative of atmospheric moisture at upper levels. Such dewpoints should be discarded. To eliminate dewpoints so affected, the surface weather charts for the dates of highest dewpoints should be examined and the dewpoints discarded if they appear to have occurred when the observing station was clearly in an anticyclonic or fair weather situation rather than in a cyclonic circulation with tendencies towards precipitation.

Another precaution is to avoid dewpoints that are too extreme. With very long record lengths, values of dewpoints may occur that are higher than optimum for the processes that produce extreme precipitation amounts. If dewpoints are found that substantially exceed 100-year values, the weather situation accompanying them should be carefully evaluated to ascertain that they are capable of causing extreme precipitation amounts.

All values of maximum persisting 12-hour dewpoints selected directly from surveys of long records are plotted against the date observed, and a smooth envelope drawn, as illustrated in Figure 2.3. When dewpoints from short records are subjected to frequency analysis, the resulting values are usually plotted against the middle day of the interval for which the series is compiled. For example, if the frequency analysis is for the series of semi-monthly maximum persisting 12-hour dewpoints observed in the first half of the month, the resulting 50- or 100-year values would be plotted against the eighth day of the month.

It is advisable to prepare monthly maps of maximum persisting 12-hour 1 000-hPa dewpoints, especially where numerous estimates of PMP are required. Such maps not only provide a ready, convenient source of maximum dewpoints, but also help in maintaining consistency between estimates for various basins. The maps are based on mid-month dewpoint values read from the seasonal variation curves and adjusted to the 1 000-hPa level. These values are plotted at the locations of the observing stations, and smooth isopleths are then drawn, as in Figure 2.4.

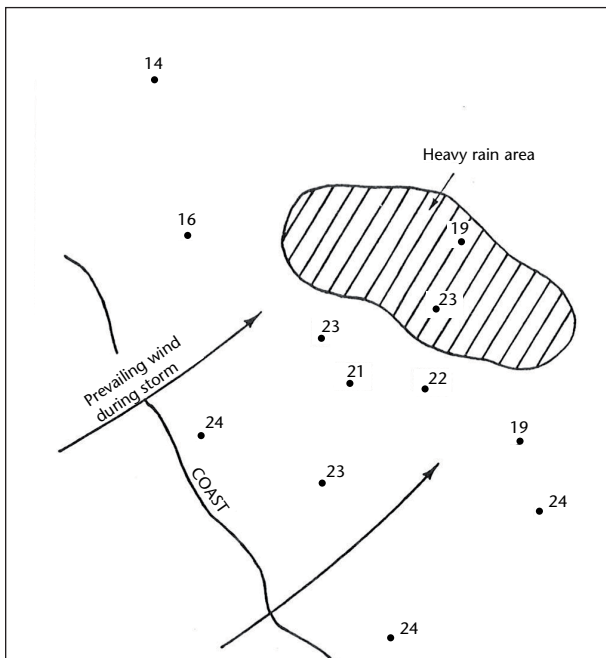


**Figure 2.2. Determination of maximum dewpoint in a storm. Representative dewpoint for this weather map is the average of values in boxes.**

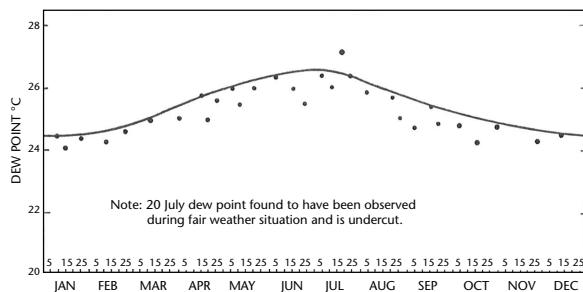


**Figure 2.3. Enveloping maximum persisting 12-hour dewpoints at a station**

Some regions have no dewpoint data, or a period of record so short as to preclude reliable frequency analysis. In these instances, sea-surface temperatures provide a logical base for estimating maximum dewpoints since the chief source of moisture inflow into major storms is water evaporated from the seas or oceans. Sea-surface temperatures may be more representative of atmospheric moisture than inland dewpoints that are affected by local conditions hence may not be representative of the total moisture column.

Estimation of maximum dewpoints from sea-surface temperatures is relatively simple for coastal

regions since there is little modification of the moist air by passage over land surfaces. In the coastal regions of the Gulf of Mexico, for example, maximum persisting 12-hour 1 000-hPa dewpoints range from about 1°C to 2°C below upwind, offshore mean-monthly sea-surface temperatures. The difference increases with distance inland. In Australia, extreme coastal dewpoints are about 4°C below extreme upwind sea-surface temperature values.

The rate of decrease of maximum dewpoints with distance inland depends upon the season of the year, direction of moisture flow during periods of maximum humidity, topographic barriers, and other geographic factors. The decrease must be determined for each month and for each region of interest in order to obtain a reasonably reliable seasonal variation curve. The gradients indicated by maps of maximum persisting 12-hour 1 000-hPa dewpoints prepared for areas with adequate data provide the most useful guidance in determining such dewpoints for areas with very little or no data. Portions of the map of Figure 2.4, for example, would be useful for estimating gradients of maximum persisting dewpoints for other regions of similar geography.

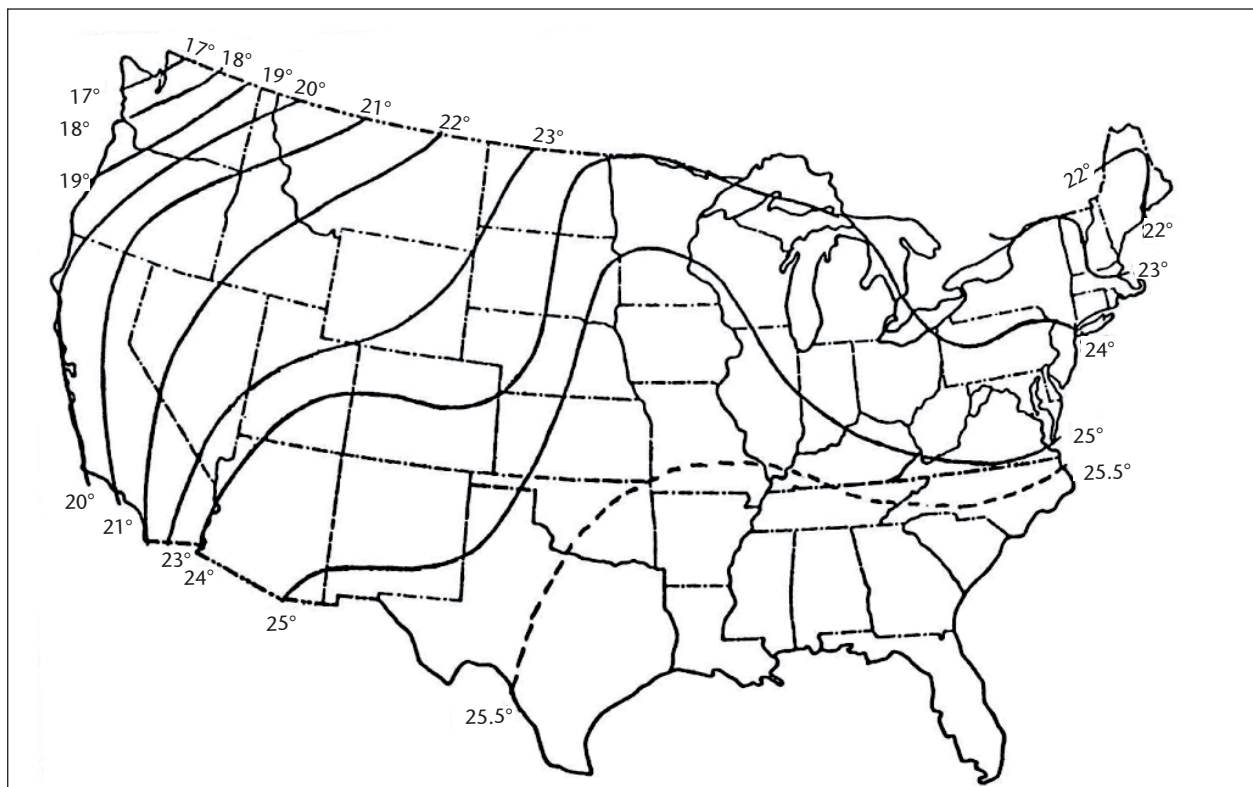


**Figure 2.4. Maximum persisting 12-hour 1 000-hPa dewpoints for August (Environmental Data Service, 1968)**

## 2.2.6 Precipitable water

This is a term used, mostly by hydrometeorologists, to express the total mass of water vapour in a vertical column of the atmosphere. A statement that the air contains 3 cm of precipitable water signifies that each vertical column of 1 cm<sup>2</sup> cross-section from the surface to the “top” of the atmosphere contains 3 g of water in vapour form. If all the water vapour were to be condensed into liquid water and deposited at the base of the column, the accumulated liquid would be 3 cm deep, since the density of water is 1 g/cm<sup>3</sup>. Precipitable water is, in fact, a misnomer, because no natural process will precipitate all the water vapour in the atmosphere. For this reason, the substitute term liquid equivalent of water vapour, or simply liquid water equivalent, is sometimes used.

Tables of precipitable water for saturated air with pseudo-adiabatic lapse rate as a function of the 1 000-hPa dewpoint are presented in Annex 1. These tables are used for moisture adjustments.

## 2.2.7 Determination of duration of maximum persisting dewpoint

For general storms at mid-latitudes, durations are more than 6 hours and periods of stable moisture inflows are long, so 12-hour time intervals are adopted for the selection of representative dewpoints of storms and historical maximum dewpoints. For local storms, storm durations are less than 6 hours, and storm moisture conditions and large-scale moisture inflow relations are not distinct, so 3-hour time intervals are adopted for selection (for example, in the north-west of the United States). In some tropical regions, storm durations are longer, the moisture supply is abundant and inflows are stable, so 24-hour time intervals may be adopted for selection (for example, India).

## 2.3 MOISTURE MAXIMIZATION

### 2.3.1 Seasonal limitations

Seasonal variations in storm structure place limitations on moisture maximization. For example, a winter storm would never be adjusted for the moisture content indicated by the maximum persisting 12-hour dewpoint for the year if that moisture maximum occurs in summer, which is almost always true. In practice, the moisture adjustments are made on the basis of the maximum persisting 12-hour dewpoint for the same time of year as the storm occurrence or, more often, the maximum

persisting 12-hour dewpoint within 15 days of the seasonal maximum. For example, if the maximum dewpoint for maximizing a 15 May storm was being selected from the curve of Figure 2.3, one would use the higher dewpoint indicated for 30 May. Similarly, the maximum dewpoint indicated for 15 September would generally be used for maximizing a 30 September storm.

### 2.3.2 Depth of precipitable water

Tables A.1.1 and A.1.2 presented in Annex 1 show depth of precipitable water between the 1 000-hPa surface and various altitudes or pressure levels as a function of the 1 000-hPa dewpoint. In maximizing storm rainfall, only the depth of precipitable water from the ground to some arbitrarily selected level between 400 hPa and 200 hPa is used. The 300-hPa level is generally accepted as the top of the storm. From the 400-hPa level upwards, the selected level make little difference as there is very little moisture and the effect on the moisture adjustment is negligible. For convenience, Table A.1.3 gives the amount of precipitable water in the column between a specified height and 300 hPa for use in storm maximization. In cases where a mountain barrier lies between the storm area and the moisture source, the mean elevation of the ridge or crest is selected as the base of the moisture column. In most cases, it is advisable to select the storm and maximum dewpoints between the barrier and the storm location.

### 2.3.3 Applicability of persisting 12-hour dewpoints for all storm durations

The dewpoints from a set of stations used to obtain a representative persisting 12-hour storm dewpoint are unlikely to be in the most intense moisture inflow for more than 12–24 hours. After this time the stations where the dewpoints were observed are very likely to be in the cold air because of the displacement of the storm. The selection of different representative 12-hour dewpoints for every 12 hours of a storm is a very tedious task, especially for storm durations of 72 hours and longer. Storm rainfall values adjusted on the basis of 12-hour dewpoints from different sets of stations compared with values from a single set indicate that differences are too small to justify the additional time required in obtaining representative 12-hour dewpoints for different storm intervals.

It should be noted also that the use of different representative dewpoints for a storm requires different maximum dewpoints for the maximizing procedures described below. The use of

representative storm dewpoints for adjusting storm rainfall values over various time intervals – for example, 24-, 48- and 72-hour dewpoints – showed only small differences from the results obtained from the use of the 12-hour representative storm dewpoint. The general practice is to use a single representative persisting 12-hour dewpoint for adjusting the storm rainfall for all durations and sizes of area.

### 2.3.4 Maximization of storm in place

Moisture maximization of storms in place – that is, without change in location – is calculated by simply multiplying the observed storm rainfall amounts by the moisture maximizing ratio  $r_m$ .

This ratio is defined by:

$$r_m = \frac{W_m}{W_s} \quad (2.1)$$

where,  $W_m$  is the maximum precipitable water indicated for the storm reference location and  $W_s$  is the precipitable water estimated for the storm. For example, if the representative persisting 12-hour 1 000-hPa storm dewpoint is 21°C and the maximum is 24°C and the rain area is at mean sea-level (always assumed to be at 1 000 hPa) with no intervening topographic barrier between the rain area and moisture source, then the moisture maximizing ratio is computed from precipitable water values obtained from the Table A.1.1 in Annex 1:

$$W_m = 74.0$$

$$W_s = 57.0$$

$$r_m = 1.30$$

The precipitable water values used in determining  $W_m$  and  $W_s$  are for a moisture column with the base at 1 000 hPa and the top at 300 hPa. If values in Table A.1.3 were used instead of those in Table A.1.1, the resulting value of  $r_m$  would be unchanged.

#### 2.3.4.1 Adjustment for storm elevation

Some correction for storm elevation may be required if the storm elevation is not at mean sea-level. Some studies have not made an adjustment for storm elevation (Hart, 1982; Schreiner and Riedel, 1978) if the elevation of the storm is less than 300 m. This decision is based on the distance to the moisture source, the storm characteristics and the topography of the region. Several procedures have been used. If the previous storm example (section 2.3.4) is assumed to occur some distance from the moisture source on

a broadly sloping plain at an elevation of 400 m still with no intervening topographic barrier between the rain area and the moisture source, then the moisture maximizing ratio ( $r_m$ ) can be computed from precipitable water values obtained from Tables A.1.1 and A.1.2 in Annex 1:

$$W_m = 74.0 - 8.00 = 66.0$$

$$W_s = 57.0 - 7.00 = 50.0$$

$$r_m = 1.32$$

Table A.1.3 provides values between the indicated elevation and the 300 hPa level. This table can be used to compute the maximizing ratio without having to subtract the amount of moisture lost. If this method were used, the computation would be:

$$W_m = 65.7$$

$$W_s = 50.0$$

$$r_m = 1.31$$

The differences result from the degree of precision for data presented in Tables A.1.1 to A.1.3 and should not be considered significant.

#### 2.3.4.2 Adjustment for intervening barrier

If it is now assumed that there is an extensive, relatively unbroken range of hills with a mean crest elevation of 600 m between the rain area and moisture source,  $r_m$  would then be determined as follows using Tables A.1.1 and A.1.2:

$$W_m = 74.0 - 12.0 = 62.0$$

$$W_s = 57.0 - 10.0 = 47.0$$

$$r_m = 1.32$$

Here, the precipitable water in the 1 000-hPa to 300-hPa column is decreased by the water column with a base at 1 000 hPa and a top at 600 m, that is, the elevation of the barrier crest and not the elevation of the rain area. If values from Table A.1.3 were used,  $r_m$  would also be 1.32.

An alternative procedure (Hart, 1982) does not consider the barrier to be completely effective in removing moisture from the airflow reaching a sheltered location if the barrier does not exceed about 500 m. Although the airflow in the vicinity of mountains is not well understood, it can be assumed that the convergent layer is merely lifted by the height of the barrier, but the storm is otherwise not affected. The moisture flow into the area behind the barrier is reduced by the ratio of the

specific humidities of the lifted and original layers. These specific humidities are approximated by the mixing ratios associated with the saturation adiabat for the 1 000-hPa dewpoint.

As further illustrated in Figure 2.5, the moisture inflow behind the barrier is given by:

$$I_1 = \frac{q_1 \# V_1 \# \Delta p_1}{g} \quad (2.2)$$

where  $I_1$  is the moisture inflow;  $q_1$  is the specific humidity;  $V$  is the wind velocity;  $\Delta p_1$  is the depth of the layer in hPa;  $g$  is the acceleration of gravity in cm/s<sup>2</sup>. The flow over the barrier is given by:

$$I_2 = \frac{q_2 \# V_2 \# \Delta p_2}{g} \quad (2.3)$$

Applying the relationship  $V_1\Delta p_1 = V_2\Delta p_2$  and the principle of continuity of mass to these equations shows how the moisture inflow  $I_2$  is reduced by the ratio of specific humidities:

$$I_2 = I_1 \# \frac{q_2}{q_1} \quad (2.4)$$

For the example storm being considered, mixing ratio values from table A.1.4 are used to approximate the specific humidity values and the moisture maximizing ratio can be determined as:

$$W_m = 74.3 \# \frac{17.7}{19.1} = 68.9$$

$$W_s = 57.1 \# \frac{14.5}{15.9} = 52.1$$

$$r_m = 1.32$$

In this example, the moisture maximizing ratio remains unchanged. This alternative procedure can result in different results when storm transposition is involved (see section 2.5).

Whenever possible, however, representative storm dewpoints on the leeward side of the barrier should be used. This is especially advisable in the case of local storms, which do not necessarily require a strong, widespread moisture inflow, but may utilize moisture that has seeped into and accumulated in the storm area during an interval of several days or longer of sluggish circulation prior to the storm (section 5.3.7).

## 2.4 WIND MAXIMIZATION

### 2.4.1 Introduction

Wind maximization is most commonly used in orographic regions when it appears that observed

storm rainfall over a mountain range might vary in proportion to the speed of the moisture-bearing wind blowing against the range. Wind maximization in such regions is discussed in sections 3.3.1.1 and 3.3.1.2.

In non-orographic regions, wind maximization is used infrequently. For these regions, storms can be transposed hundreds of kilometres to synthesize an adequate storm history for a project basin. It is reasoned that moisture inflow rates recorded in extreme storms are at a maximum or near-maximum for precipitation-producing effectiveness, and there is generally no need to maximize wind speeds.

This reasoning follows from the logical assumption that storms with the highest wind speeds do not necessarily produce the most intense precipitation. While hurricanes or typhoons do have high wind speeds and tend to produce heavier rainfall, their moisture content is also much higher. Whether hurricanes with the highest wind speeds produce more rainfall than weaker hurricanes is uncertain, since they generally reach full strength over water. It is known, however, that rainfall from hurricanes over land is not proportional to their wind speeds.

### 2.4.2 Use in non-orographic regions

Wind maximization is occasionally used in non-orographic regions when moisture adjustments alone appear to yield inadequate or unrealistic results.

In regions with limited hydrometeorological data, for example, wind maximization may be used to partly compensate for a short period of record, or when a storm sample may be inadequate due to limitations on storm transpositions. This is because

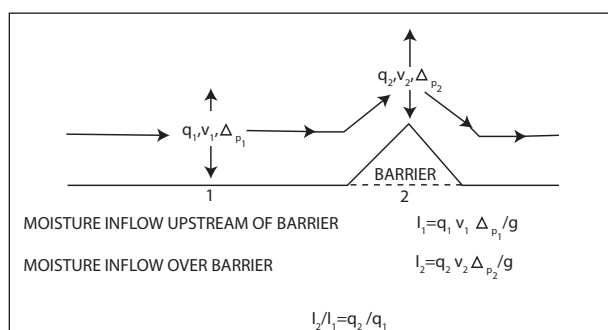


Figure 2.5. Schematic illustrating concept for alternative moisture adjustment for intervening barrier to air flow (after Hart, 1982)

the limited data available are unlikely to include extreme values of dewpoints or outstanding storms equivalent to those that would be observed over a long period of record. The heaviest recorded storms may be relatively weak, and their moisture inflow rates are likely to be less than those associated with maximum precipitation-producing effectiveness. Increasing both wind and moisture yields (to a higher degree of maximization than the moisture adjustment alone) compensates, at least in part, for an inadequate sample of observed data.

Wind maximization is sometimes used when the seasonal variation of maximum 12-hour dewpoints gives a false indication of the seasonal variation of PMP. This is most likely to occur in regions where summers are dry and all major storms are experienced in the cold half of the year. The dewpoint curve almost always peaks in summer, and the seasonal variation of maximum wind speeds must be considered in developing a representative seasonal variation curve of PMP (sections 2.10.3 and 2.10.4). In cases where this is done, individual storms are maximized for both moisture and wind, as described in sections 2.4.3, 2.4.4 and 2.10.2.

#### **2.4.3      Winds representative of moisture inflow in storms**

Low-level winds are generally used to estimate moisture inflow in storms because most of the moisture usually enters the storm system in the lowest 1 500 m. The winds in this bottom layer can be obtained from pilot-balloon or rawinsonde observations. The winds at 1 000 m and 1 500 m are perhaps the most representative of moisture inflow. Upper-air observations, however, have several shortcomings. They have relatively short records and cannot be used for maximizing the older storms. Pilot-balloon observations cannot be made in storms. Upper-air-wind observations are made at considerably fewer stations than surface-wind observations and are hence often inadequate for determining moisture inflow into small-area storms. For these reasons, surface data are often used as an index of wind movement in the critical moisture-bearing layer.

##### **2.4.3.1    Wind direction**

The first consideration in developing wind adjustments is the wind direction associated with moisture inflow during major storms. Only winds from those directions critical for inflow of moisture are considered in deriving wind-adjustment ratios. If more than one direction provides moist-air inflow, separate seasonal maximum wind-speed curves should be constructed for each direction.

This is particularly advisable if the different wind directions bring in moisture for different source regions.

##### **2.4.3.2    Wind speed**

Various measures of wind speed have been used to develop wind maximization ratios. Among them are:

- (a) average wind speed through the moisture-bearing layer computed from representative upper-air wind observations;
- (b) average speed in the moist layer computed from two or three consecutive 6- or 12-hour upper-air wind observations; and
- (c) average surface-wind speed or total wind movement for a 12- or 24-hour period at a representative station, the 24-hour period being preferred because of diurnal variations.

Only wind speeds from critical directions are considered (section 2.4.3.1). Wind observations during the 24-hour period of maximum rainfall are usually the most representative of moisture inflow to storms of that of longer duration. For storms of shorter duration, average winds need to be computed for the actual storm duration only.

#### **2.4.4      Wind maximization ratio**

The wind maximization ratio is simply the ratio of the maximum average wind speed for some specific duration and critical direction obtained from a long record of observations, for example, 50 years, to the observed maximum average wind speed for the same duration and direction in the storm being maximized. The monthly maximum average values obtained from the records are usually plotted against date of observation, and a smooth seasonal curve drawn so that storms for any time of the year may be maximized readily (Figure 2.13, part C). The maximum wind speeds used for maximization are read from the seasonal curve.

Wind records appreciably shorter than around 50 years are unlikely to yield maximum speeds reasonably representative of those obtained from a long record. Frequency analysis is advisable for such short records. The computed 50- or 100-year values, usually the former, are used to construct the seasonal variation curve of limiting wind speed.

Sometimes the moisture values (precipitable water), both maximum and storm-observed, are multiplied by the corresponding wind speeds to provide a

moisture-inflow index. The advantage in this is that the resulting moisture-inflow index curve presents a more readily visualized seasonal variation of PMP (Figure 2.13, part D) than when moisture and wind speed curves are examined separately. Also, when the seasonal variation curves are expressed in terms of percentage of the peak or other value, the moisture-inflow index curve provides a single percentage value for adjusting PMP values for any particular time of year.

## 2.5 STORM TRANSPOSITION

### 2.5.1 Introduction

The outstanding rainstorms in a meteorologically homogeneous region surrounding a project basin are a very important part of the historical evidence on which a PMP estimate for the basin is based. The transfer of storms from locations where they occurred to other areas where they could occur is called storm transposition.

Explicit transposition limits refer to the outer boundaries of a region throughout which a storm may be transposed with only relatively minor modifications of the observed storm rainfall amounts. The area within the transposition limits has similar, but not identical, climatic and topographic characteristics throughout. More restricted transposition limits may be defined if a region has a long record of precipitation measurements from a relatively dense network of gauges and has experienced many outstanding storms. Where the record of storms is more limited, either because of a sparse raingauge network or because of very infrequent occurrence of severe storms during the period of record, then more liberal, though perhaps slightly less reliable, transposition limits must be accepted. A transposition adjustment is a ratio by which the storm-rainfall amounts are multiplied to compensate for differences between conditions at the storm site and those at the project basin.

The restrictions imposed by explicit transposition limits can sometimes result in discontinuities in PMP estimates made for nearby basins. This can result from transposition of storms to one basin but not to the other. Fluid dynamics indicate that the atmosphere does not create vertical walls (or step functions) to extreme storm conditions. Thus, when boundary problems are created by limitations on storm history and transposition boundaries it is necessary to postulate how the atmosphere is "limited" in the region beyond the explicit

transposition limits of the larger storm values. If reasonable explanations cannot be found, regional, areal or durational smoothing is used to eliminate these discontinuities. Implicit transposition is the term given to this smoothing. This is discussed further in sections 2.8 and 5.2.3.

As for the transposition range, storms of some types were transposed over long distances, even intercontinentally, in some studies. For example, in HMR 46 (United States Weather Bureau, 1970), compiled by the United States in 1970, typhoon storms in south-eastern United States that were generated on the Atlantic Ocean were transposed to the Mekong River Basin in Southeast Asia (see section 6.2.2 for details). Design organizations in China also transposed the above-mentioned typhoon storms that occurred in the United States to the Daguangba Project on Hainan Island in 1987. In short-duration, small-area PMP estimation in Australia, thunderstorm rains from the United States in the northern hemisphere were transposed to Australia in the southern hemisphere (Australian Bureau of Meteorology, 1985).

### 2.5.2 Steps in transposition

The transposition procedure involves the meteorological analysis of the storm to be transposed, the determination of transposition limits, and the application of the appropriate adjustments for the change in storm location. The procedure may be divided into four steps, as in the following paragraphs.

#### 2.5.2.1 The storm

The first step in transposing a storm is to identify clearly when and where the heaviest rainfall occurred and the approximate causes in terms of synoptic meteorology. An isohyetal chart, a few key mass rainfall curves, and weather maps serve these purposes. The isohyetal chart may be a simple one, since its primary function is to identify the storm location. Routinely available weather maps may be sufficient to identify the storm causes, especially if the precipitation is closely associated with either a tropical or an extratropical cyclone. In other instances, a detailed analysis may be necessary to identify causes.

#### 2.5.2.2 Region of influence of storm type

The second step is to delineate the region in which the meteorological storm type identified in step 1 is both common and important as a producer of precipitation. This is done by surveying a long series of daily weather charts, or available

climatological summaries for a specific region of interest. Tracks of tropical and extratropical cyclones are generally available in published form, and these may be used to delineate the regions frequented by the various storm types.

#### 2.5.2.3 Topographic controls

The third step is to delineate topographic limitations on transposability. Coastal storms are transposed along the coast with little restriction, but greater care must be used to determine the distance inland the storm should be transposed. This is determined by analysis of the meteorological factors causing the large rainfall amounts and the importance of proximity to the moisture source in this process. Transposition of inland storms is restricted to areas where major mountain barriers do not block the inflow of moisture from the sea unless such blocking prevailed at the original storm site. Adjustments for transposition behind moderate and small barriers are discussed in section 2.6.3. Some limitation is placed on latitudinal transposition in order not to involve excessive differences in air mass characteristics. In estimating PMP over a specific basin, it is only necessary to determine if a particular storm can be transposed to the problem basin, and delineation of the entire area of transposability is not required. It is required, however, in the preparation of generalized estimates discussed in Chapter 5.

#### 2.5.2.4 Example of determining transposition limits

Heavy rainfall over western Kansas, United States, in July 1951, caused large floods over a major portion of the State. The rainfall from this storm was due to the occurrence of various meteorological factors that could just as easily have happened in other parts of mid-western United States (United States Weather Bureau, 1952). After a comprehensive analysis of the major causes of the precipitation in this storm, the weather maps were examined for all other major storms that have occurred between the Rocky Mountains and the Appalachians with characteristics similar to this storm. Specifically, the characteristics were:

- Absence of pronounced orographic effects;
- A general east-west orientation of the frontal system and rainfall pattern;
- No marked wave action or occlusion of a wave during and after the storm period;
- Storm duration of two days or longer;
- Storm precipitation of 180 mm or more at the centre;

- A polar high situated to the north of the storm centre during the rainfall;
- Southward movement of the frontal system at the end of the rain period.

The location of the storms that met these criteria and the final transposition limits assigned for this storm are shown in Figure 2.6. Since a major portion of the rainfall during this July storm fell in nocturnal thunderstorms, the distribution of such storms and their frequencies were used as an additional guide. Study of the moisture inflow indicated that modifications would occur if the synoptic situation existed at elevations much higher than that at which the storm actually occurred.

To the west, transposition was limited to the 914-m contour, the slope is relatively gentle, and it is believed there would be little or no orographic effect on the storm mechanism below this elevation. This limit was set even though two storms synoptically similar were observed further west at higher elevations. However, examination of the isohyetal patterns for the northernmost of these two storms shows that topography was an important contributor to the rainfall. In the case of the more southerly storm, much of the rainfall fell in the outlined transposition limits. However, the main centre to the west was on a slope of the Rockies where orography played an important part. The 914-m contour also coincided closely with the western boundary of the area showing a high frequency of nocturnal thunderstorms.

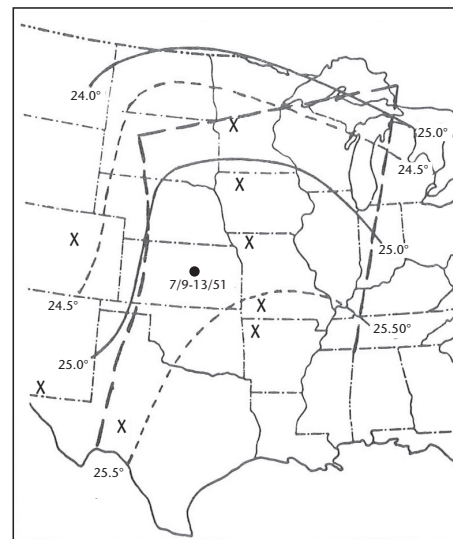


**Figure 2.6** Transposition limits (heavy dashed line) of 9–13 July 1951 storm. Locations of synoptically similar summer storms marked by X. Light lines indicate maximum persisting 12-hour 1 000-hPa dewpoints (°C) for July.

Northern limits were set along a line that coincides with the northern limits of high frequency of nocturnal thunderstorms and also outlines the northern limits of observed storms of this type.

Eastern limits were set at the beginning of the upslopes for the foothills of the Appalachian Mountain chain. East of this line there would be a tendency for the inflow wind to be affected by the beginnings of the Appalachian Mountain chain, thus influencing the storm characteristics.

Southern limits have been set tentatively at the 152-m contour. This line is to the south of all observed storms and the area of high thunderstorm frequency. The exact location of the southern limit is academic, since considerably larger storms of other types have occurred to the south.

#### 2.5.2.5 Adjustments

The final step in transposition is the application of adjustments discussed in the following section 2.6.

### 2.6 TRANSPOSITION ADJUSTMENTS

#### 2.6.1 Moisture adjustment for relocation

The moisture adjustment is the observed storm rainfall amounts multiplied by the ratio of precipitable water for the enveloping, or maximum, dewpoint at the transposed location ( $W_2$ ) to the precipitable water for the representative storm dewpoint ( $W_1$ ), or

$$R_2 = R_1 \left( \frac{W_2}{W_1} \right) \quad (2.5)$$

where  $R_1$  is the observed storm rainfall for a particular duration and size of area and  $R_2$  is the storm rainfall adjusted for transposition. Equation 2.5 incorporates both a transposition adjustment and a moisture maximization. The DAD array of storm rainfall values (Table 2.2) is multiplied by this ratio. Values such as those given in Table 2.2 must be determined separately for each storm, using the appropriate procedures for determining such data (WMO-No. 237). These values should be adjusted for a range of areas from storm-area sizes less than the area of the basin to those exceeding the basin size (see sections 2.8.2, 2.9, and 2.13.4). The moisture adjustment may be either greater or less than unity, depending on whether the transposition is toward or away from the moisture source and whether the elevation of the transposed location is lower or higher than that of the original storm site.

#### 2.6.1.1 Reference dewpoint for moisture adjustment

For reasons given in section 2.2.4, dewpoints between the rain area and moisture source tend to be more representative of the atmospheric moisture content, or precipitable water, flowing into the storm than dewpoints within the rain area. Such representative dewpoints may be a few hundred kilometres away from the storm centre. In maximizing for moisture, the maximum dewpoint used is for the same location as that of the representative storm dewpoint. In transposing, the same reference distance is laid out on the same bearing from the transposition point (Figure 2.7). The referenced dewpoint location is then used to obtain the maximum dewpoint from the maximum dewpoint chart

**Table 2.2. Maximum average depth (mm) of rainfall in 20–23 May 1927 storm**

Area ( $\text{km}^2$ )	Duration (hours)							
	6	12	18	24	36	48	60	72
25 <sup>a</sup>	163	208	284	307	318	328	343	356
100	152	196	263	282	306	324	340	353
200	147	190	251	269	300	321	338	352
500	139	180	234	250	290	315	336	351
1 000	133	171	220	235	278	304	328	341
2 000	124	160	202	215	259	284	308	322
5 000	107	140	172	184	218	241	258	274
10 000	91	118	140	151	182	201	215	228
20 000	66	87	104	114	143	158	173	181

<sup>a</sup>Assigned area for maximum station precipitation.

for calculating the combined maximization and transposition adjustments.

## 2.6.2 Elevation adjustments

An increase in surface elevation decreases the moisture that may be contained in a column of the atmosphere. However, many storms receive most of their moisture in a strong low-level flow 1 to 1.5 km deep, and this inflow is not appreciably affected by relatively small changes in ground elevation. Ranges of low hills or gradually rising terrain may actually stimulate convection and increase rainfall. This effect on precipitation may more than compensate for the decrease in precipitable water with increasing ground elevation. Elevation adjustments for PMP estimates for non-orographic regions in the middle latitudes are discussed in the next two paragraphs.

### 2.6.2.1 General storms

Because the effects of relatively small elevation changes on precipitation is uncertain, there are

different opinion as to whether elevation adjustments should be made for storm transposition over small elevation changes that occur over relatively short distances. A decision as to whether or not to use an elevation adjustment in a certain situation is based on a comparison of major storms in the vicinity of the actual site of the storm to be transposed with those in the area surrounding the project site. For example, if observed major storms at the two sites showed differences in magnitude ascribable only to differences in moisture, omission of an elevation adjustment would be justified. In some studies (Hart, 1982; Miller and others; 1984b; Schreiner and Riedel, 1978), adjustments for elevation differences of about 300 m or less over short distances have not been made. A second consideration involves similar changes over broad, gradually sloping plains. This situation must be considered separately and major storm rainfalls in these regions examined. Again, if differences in rainfall amounts can be ascribed to differences in moisture not involving elevation differences, omission of an elevation adjustment is justified. If it is decided to omit adjustment for elevation,  $W_2$  of Equation 2.5 is computed for the maximum dewpoint at the referenced location (section 2.6.1.1) for the project site and the same column height as for  $W_1$ . If an adjustment is used,  $W_2$  is computed for the same maximum dewpoint just described, but for the column above the ground at the project site, which may be lower or higher than the site of the observed storm. Regardless of whether or not an elevation adjustment is used, transposition involving elevation differences of more than 700 m is generally avoided.

### 2.6.2.2 Local thunderstorms

Intense local thunderstorms are not adjusted for elevation when transposition involves elevation differences of less than around 1 500 m. Since this chapter deals with non-orographic regions, it can be stated simply that no elevation adjustment is made for local thunderstorms. Elevation adjustment for such storms is required in orographic regions, however, and they are discussed in sections 5.3.2.1 and 5.3.7.4.

### 2.6.3 Barrier adjustment

Transposition of a storm from the windward to the leeward side of a topographic barrier normally requires an adjustment for the height of the barrier. This is a common situation, because basins upstream from a proposed dam site are often rimmed by mountains or hills. Transposition of

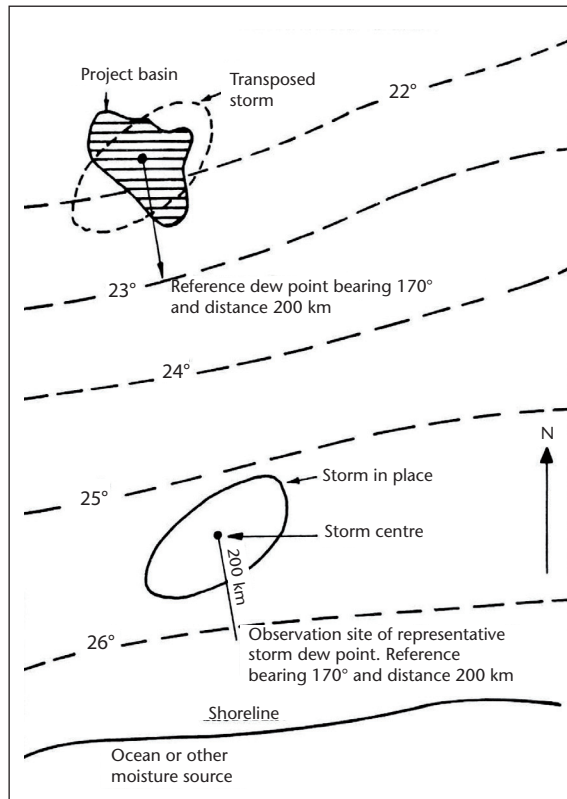


**Figure 2.7 Example of storm transposition. Long dashed lines indicate maximum persisting 12-hour 1 000-hPa dewpoints ( $^{\circ}\text{C}$ ) for the same time of year the storm occurred or within 15 days according to common practice (section 2.3.1).**

storms across barriers higher than about 800 m above the elevation of the observed storm site is generally avoided because of their dynamic influence on storms. Also, barrier adjustments are not used in transposing local, short duration, intense thunderstorms, which can draw in moisture trapped by the barriers prior to the storm. The example of storm transposition presented in the next section includes a barrier adjustment.

#### 2.6.4 Example of storm transposition and maximization

##### 2.6.4.1 Hypothetical situation

Assume that synoptic weather charts associated with major storms indicate that the hypothetical storm pattern shown in Figure 2.7 is transposable to the project basin shown in the same illustration. The average elevation of the storm area is 300 m. The average elevation of the moisture-inflow (south) side of the basin is 700 m, with no intervening orographic barriers. The representative persisting 12-hour storm dewpoint (section 2.2.4) is 23°C, which was observed at a site (Figure 2.7) located at an elevation of 200 m and a distance 200 km from the storm centre on a bearing of 170° (section 2.6.1.1). Reduction of this dewpoint to the 1 000-hPa level (Figure 2.1) yields 24°C.

##### 2.6.4.2 Computation of adjustment factor

The adjustment factor, or ratio, is computed as follows:

$$\begin{aligned} r &= \left( \frac{W_{26}}{W_{24}} \right)_{300} \# \left( \frac{W_{23}}{W_{26}} \right)_{300} \# \frac{(W_{23})_{700}}{(W_{23})_{300}} \\ &= \frac{(W_{23})_{700}}{(W_{24})_{300}} \end{aligned} \quad (2.6)$$

where the subscripts within parentheses refer to the 1 000-hPa dewpoints for which the precipitable water  $W$  is computed, and the subscripts outside parentheses refer to the various pertinent ground elevations forming the bases of the atmospheric columns for which  $W$  is computed. Thus, the term  $(W_{26}/W_{24})_{300}$  represents moisture maximization at the storm site;  $(W_{23}/W_{26})_{300}$  is the adjustment for the difference in maximum dewpoints between the original and transposed locations; and  $(W_{23})_{700}/(W_{23})_{300}$  is the elevation adjustment. Multiplication of all these terms leads to a simple result that all the required adjustments are implicit in the single term  $(W_{23})_{700}/(W_{24})_{300}$ . Referring to Tables A.1.1 and A.1.2 in Annex 1 for a column top of 300 hPa:

$$(W_{23})_{700} = 67.0 - 13.0 = 54.0 \text{ mm}$$

$$(W_{24})_{300} = 74.0 - 6.00 = 68.0 \text{ mm.}$$

$$\text{Hence, } r = 54.0/68.0 = 0.79.$$

If the alternative procedure for adjusting for moisture depletion were used (section 2.3.4.2), the adjustment factor would be computed as follows:

$$\begin{aligned} r &= \frac{\left( W_{26} \# \frac{q_{300}}{q_{s1}} \right)}{\left( W_{24} \# \frac{q_{300}}{q_{s1}} \right)} \# \frac{\left( W_{23} \# \frac{q_{300}}{q_{s1}} \right)}{\left( W_{26} \# \frac{q_{300}}{q_{s1}} \right)} \# \frac{\left( W_{23} \# \frac{q_{700}}{q_{s1}} \right)}{\left( W_{23} \# \frac{q_{300}}{q_{s1}} \right)} \\ &= \frac{\left( W_{23} \# \frac{q_{700}}{q_{s1}} \right)}{\left( W_{24} \# \frac{q_{300}}{q_{s1}} \right)} \end{aligned} \quad (2.7)$$

If this is evaluated using Tables A.1.3 and A.1.4, the result is as follows:

$$\begin{aligned} r &= \frac{\left( 69.7 \# \frac{16.3}{18.0} \right)}{\left( 74.3 \# \frac{18.4}{19.1} \right)} \\ &= 0.86 \end{aligned}$$

This result provides a lesser reduction than assuming all of the moisture is removed by the increased elevation.

If an extensive orographic barrier (section 2.6.3) of, for example, 1 000 m in mean elevation lay between the observed storm site and the project basin,  $(W_{23})_{1000}$  would be substituted for  $(W_{23})_{700}$  and ratio  $r$  would then be  $(68.0 - 18.0)/(74.0 - 6.00) = 0.74$ . The appropriate ratio is then applied to values for a range of area sizes both larger and smaller than the basin size from storm DAD data like those of Table 2.2. Since the elevation of the barrier is higher than discussed in section 2.3.4.2, the alternate procedure discussed by Hart (1982) is not used.

Another alternative procedure for moisture adjustment for storm transposition was used in a study for central and western United States (Miller and others, 1984b). In this study, plots of maximum observed point precipitation amounts versus elevation did not disclose any consistent variation of precipitation over limited ranges of elevations. Thus no adjustment was made for storm precipitation amounts for small areas for changes in elevations of about 300 m or less. For higher elevation changes, adjustments based on the total variation in precipitable water amounts produced amounts that seemed unrealistic, based upon observed storm experience. The vertical transposition adjustment then was restricted to one-half the variation in precipitable water for those changes in elevation that exceed 300 m. This can be expressed mathematically as:

$$R_{VT} = 0.5 + 0.5 \left( \frac{W_{P_{\max, TL, TE}}}{W_{P_{\max, TL, SE \pm 300}}} \right) \quad (2.8)$$

where  $R_{VT}$  is the vertical transposition adjustment;  $TE$  is the transposed/barrier elevation: the elevation of the transposed location or any higher barrier to moist airflow;  $W_{P_{\max, TL, SE} \pm 300}$  is the precipitable water associated with the maximum persisting 12-hour 1 000-hPa dewpoint considering one-half the increase (decrease) in precipitable water for the difference in elevation greater than  $\pm 300$  m from the storm/barrier elevation; and  $W_{P_{\max, TL, SE}}$  is the precipitable water associated with the maximum persisting 12-hour 1 000-hPa dewpoint above the transposed barrier elevation.

In the storm being considered here, the vertical moisture adjustment would be:

$$R_{VT} = 0.50 + 0.50R_{VT} = 0.50 + 0.50 = 0.92$$

In this method, adjustments for moisture maximization and horizontal transposition are treated separately and are done in the manner previously described.

Other storms are adjusted similarly by appropriate ratios, and the results are then treated as described in sections 2.8 and 2.9.

## 2.7      **SEQUENTIAL AND SPATIAL MAXIMIZATION**

### 2.7.1      **Definition**

Sequential and spatial maximization involves the development of hypothetical flood-producing storms by combining observed individual storms or rainfall bursts within individual or separate storms. The combination is carried out by hypothesizing critical sequences with minimum time intervals between individual events (sequential maximization), which also may be repositioned or geographically transposed (spatial maximization).

### 2.7.2      **Sequential maximization**

Sequential maximization is the rearrangement of observed storms or portions thereof into a hypothetical sequence such that the time interval between storms is at a minimum. The storms may have occurred in close succession, or they may have occurred years apart. The procedure is most often used for large basins, where outstanding floods result from a sequence of storms rather than from a single event. For small basins, where rainfall for one day or less may produce the maximum flood, sequential maximization may involve the elimination or

reduction of the time interval between successive bursts in the same storm or in separate storms.

The initial step for sequential maximization is the same for large or small basins. In each instance, a thorough study of the meteorology of major storms in the area of interest is required (Lott and Myers, 1956; Myers, 1959; Weaver, 1962, 1968). Storm types associated with heavy rainfalls in or near the project basin are determined: movement of surface and upper-air lows and highs are examined; depth, breadth, and direction of moisture inflow are determined; vorticity advection is investigated; etc. It is usually impossible to study all major storms with the same degree of detail. In the case of older storms, for example, upper-flow patterns must be estimated from surface data.

The next step is to determine the storm sequences in and near the project basin. For large basins, storm sequences should be examined to determine the shortest reasonable time interval between individual storms of various types. The minimum time interval, usually measured in days, should be determined for each combination of storm types producing heavy precipitation. This interval is a critical factor in the hypothetical storm sequence established. For small basins, the procedure is similar, but concentrates on the interval, usually measured in hours, between bursts in individual storms. In some instances, the combination of bursts from separate storms is a possibility, and the time interval between similar storm bursts should be considered.

After storms have been examined and reasonable minimum time intervals between them determined, pairs or sequences of storms or bursts are developed. Each pair of storms, or individual bursts within a storm for small basins, is examined carefully to insure that meteorological developments following the first storm or burst – that is, movement of lows and highs, overrunning of the basin by cold air, etc – would not prevent the succeeding storm or burst from occurring within critical time limits.

If all the important features of the weather situation at the beginning of the second storm can be developed in a logical manner over a sufficiently large area, the necessary conditions for its onset will have been met. The successive hypothetical synoptic weather maps for the interval between storms or bursts are patterned to the greatest extent possible after the actual maps following the first storm or burst and preceding the second. Synoptic features – such as highs, lows and fronts – are allowed to move and change as indicated by

experience, at a rate somewhat faster than average, but not excessively so. The resulting hypothetical storm sequence is intended to depict a critical, meteorologically possible transition from one storm or burst to another.

While the derived hypothetical storm sequence often consists of two unadjusted observed storms, the PMS is sometimes selected as the second storm of the sequence. In other words, the second storm has been maximized for moisture and perhaps wind so that it is equivalent to PMP for at least one duration and size of area (sections 1.1.4, 2.11.2, and 2.11.3). Sequences of two probable maximum storms are never developed, however, for two reasons. One is that a properly derived PMS has a very low probability of occurrence, and the probability of two such storms occurring in unusually close succession is so remote as to be considered unreasonable. The second reason is that the first PMS would be followed by a meteorological situation unfavourable for the rapid development of the second, and the longer transition period between the two is likely to make the sequence less hydrologically critical than a sequence of lesser storms with a shorter time interval between them.

### 2.7.3 Spatial maximization

Spatial maximization involves the transposition of storms that occurred in or near a project basin to one or more critical locations in the basin to obtain maximum runoff. The procedure involves determining if particular storms can be transposed to critical locations within specified time intervals and combined to produce maximum runoff rates or volumes. As in sequential maximization, the first requirement is a thorough knowledge of the storms causing heavy precipitation over the basin and surrounding region.

The following example of spatial maximization is based on a series of heavy, localized rainfall bursts occurring 14–18 June 1965 in eastern Colorado, United States. During this period, a persistent large-scale circulation maintained a pronounced inflow of moist unstable air into the storm area. Fronts and related synoptic features played a minimal role, as did high-level factors such as vorticity advection (Schwarz, 1967).

Two distinct, severe 6-hour bursts occurred on successive days, 16–17 June. Isohyetal maps for the two bursts are shown in Figure 2.8. The 16 June burst was centred over Plum Creek basin ( $1100 \text{ km}^2$ ), while that of 17 June was centred about 40 km south-east. It is reasonable to assume

that the rainfall centres could have occurred over the same location since the weather situation was very much the same on both days. Combination of the two isohyetal patterns on the basis of this assumption resulted in the pattern of Figure 2.9. In combining the patterns, the principal centre of the 17 June burst was superimposed on that of the 16 June, and the pattern was rotated about  $25^\circ$  anti-clockwise for better agreement with the orientation of the pattern of the 16 June burst (Riedel and others, 1969). In this region, such a rotation is realistic for this type of storm. In other regions and for other storm types, examination of many storms might show that such superposition and/or rotation would not be permissible.

### 2.7.4 Combined sequential and spatial maximization

Sequential and spatial maximizations are generally used in combination, that is, storms or bursts within storms may be repositioned geographically in addition to shortening the time interval between them.

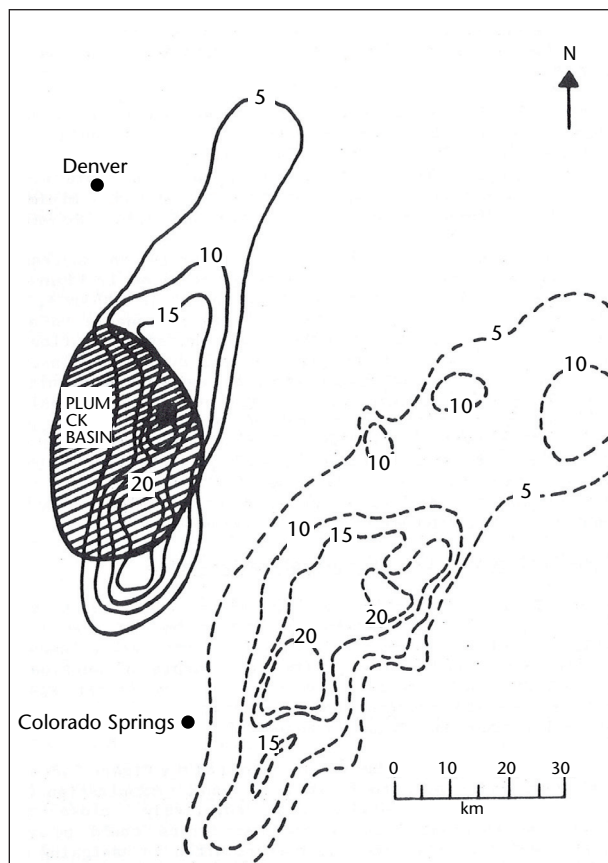


**Figure 2.8. Isohyets (cm) for the 6-hour afternoon storms of 16 June 1965 (solid lines) and 17 June 1965 (dashed lines) in eastern Colorado (Riedel and others, 1969)**

In the study (Riedel and others, 1969) from which the example of section 2.7.3 was taken, the two rainfall bursts were not only maximized spatially by superimposing centres and rotating one of the isohyetal patterns, but also the time interval between them was shortened.

The actual times of the bursts depicted in Figure 2.8 were from 1 p.m. to 7 p.m., 16 June, and from 2 p.m. to 8 p.m., 17 June. Examination of a large number of similar storms occurring in relatively close succession indicated that the interval between the two bursts could be reduced to 12 hours. This shortening of the time interval resulted in assigning an overall duration of 24 hours to the total rainfall for the two bursts, 7 hours less than the observed total storm period of 31 hours.

Examples of the use of sequential and spatial maximization in deriving hypothetical maximum flood-producing storm sequences for large basins may be found in Lott and Myers (1956), Myers (1959) and Schwarz (1961).

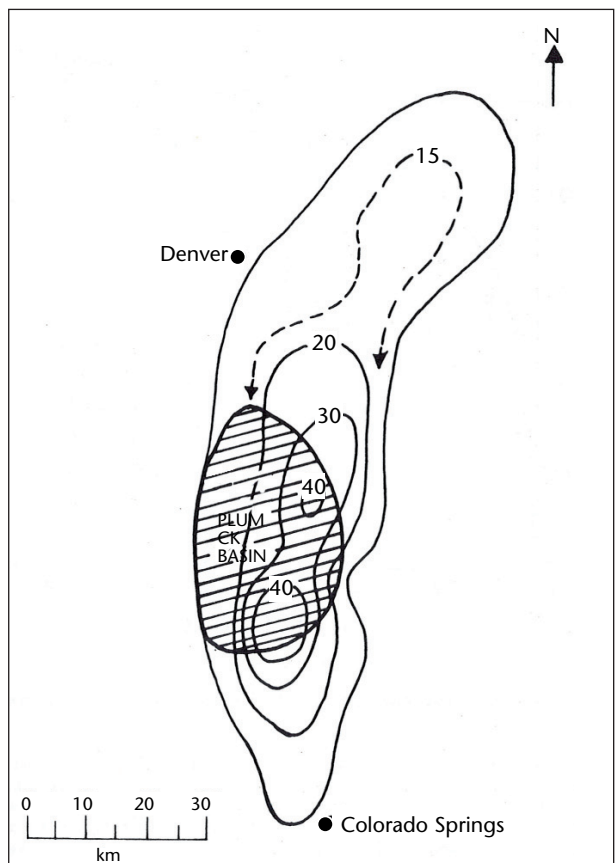


**Figure 2.9. Isohyets (cm) resulting from the combination of patterns of the 6-hour storms of 16–17 June 1965 shown in Figure 2.8 (Riedel and others, 1969)**

## 2.8

## ENVELOPMENT

### 2.8.1 Introduction

The maximization of a single storm and its transposition to a basin presumes that a certain precipitation volume could fall over that basin. Nothing about the relation of this precipitation volume to PMP is revealed, and it could be far less than PMP magnitude. To consider only fewer than a half-dozen or so storms or storm sequences, no matter how sophisticated the maximization and transposition adjustments might be, gives no assurance that the PMP level has been obtained.

The question of adequacy of storm sample for estimating PMP is a difficult one to answer, especially with limited data. It seems logical, however, to expect that an envelope of many rainfall values that have been maximized and transposed to a basin is very likely to yield values indicative of PMP magnitude. This is especially true since no storm is likely to yield extreme rainfall values for all durations and area sizes. It is for these reasons that envelopment is considered a necessary final step in estimating PMP. Any PMP estimates that do not include envelopment, and areal, durational and regional smoothing, might provide inadequate values.

### 2.8.2 Envelopment

Envelopment is a process for selecting the largest value from any set of data. In estimating PMP the maximized and transposed rainfall data are plotted on a graph, and a smooth curve is drawn through the largest values. Figure 2.10 shows a durational envelope of transposed, maximized precipitation values for durations up to 72 hours over a 2 000-km<sup>2</sup> area. The variables are changed in Figure 2.11, which is an areal envelope of transposed, maximized 24-hour rainfall values for areas ranging up to 100 000 km<sup>2</sup>. In developing a full array of PMP DAD data for a basin, it is necessary to envelope both ways, as shown in Figures 2.10 and 2.11. Values read from the enveloping curves (Figures 2.10 and 2.11) are then used to construct a set of DAD curves, as shown in Figure 2.12.

It should be noted that the controlling points determining each curve are usually from different storms. In Figure 2.12, for example, with the exception of the 6- and 12-hour curves, the points controlling the curves at about 2 500 km<sup>2</sup> are typically from different storms than those at 50 000 km<sup>2</sup>. Similarly, the points controlling the short-duration curves are usually from different storms than those controlling the long-duration curves.

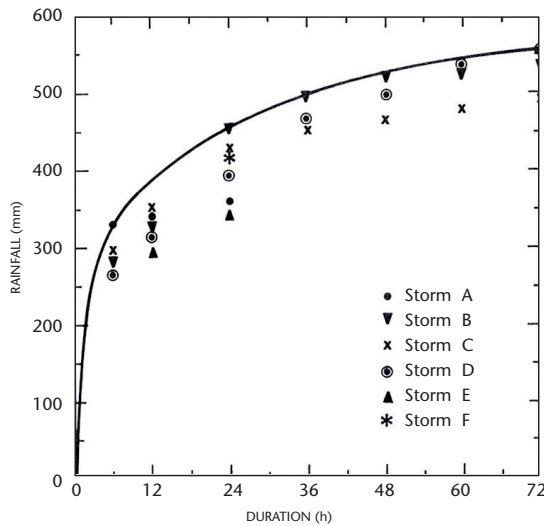


**Figure 2.10. Depth-duration envelope of transposed maximized storm values for 2 000 km<sup>2</sup>**

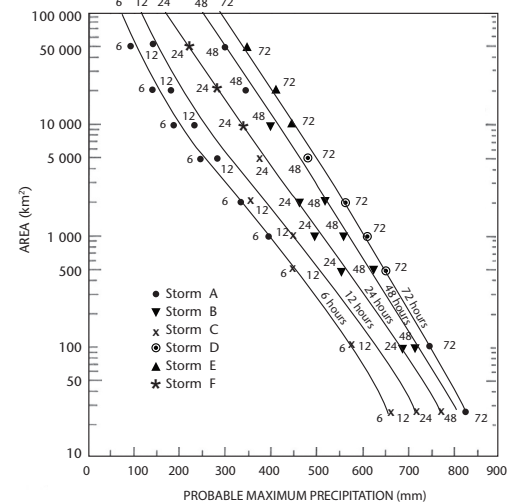


**Figure 2.12. Enveloping DAD curves of probable maximum precipitation for a hypothetical basin**

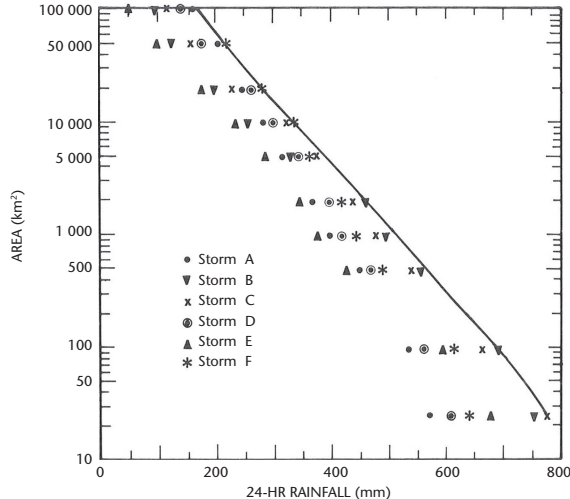


**Figure 2.11. Depth-area envelope of transposed maximized 24-hour storm rainfall values**

To prepare an individual drainage estimate, it is usually sufficient to prepare DAD curves for a range of area sizes from about 0.1 to about 10 times the area of the basin.

### 2.8.3 Undercutting

The data used in constructing an envelope curve are not of equal accuracy or reliability. For example, looking at graphs such as Figures 2.10 and 2.11, the basin under study may lie definitely within the transposition limits of some of the transposed storms, but it may lie within the fringes of the transposition limits of other storms, which leads to somewhat less reliable data from the transposition of those storms to this particular

basin. Under these circumstances, it may be justified to place the curve at somewhat lower values than the extremes. This is called undercutting. Any undercutting should be done only after a careful review of:

- the meteorological characteristics of the storm;
- the transposition limits;
- the moisture and other adjustment factors;
- any other factors that affect the magnitude of the plotted value.

## 2.9 SUMMARY OUTLINE OF PROCEDURE FOR ESTIMATING PMP

### 2.9.1 Introduction

The steps outlined below for estimating PMP over a project basin are applicable only for a non-orographic region with reasonably adequate hydrometeorological data. For most reliable estimates, data should include:

- relatively detailed 6-hour or daily weather maps;
- long records, 50 years or more, of hourly and daily rainfall data from precipitation networks of sufficient density to permit reliable determination of time and spatial distribution of storm rainfall;
- long records of temperature, dewpoint and wind data, both at the surface and, if possible, aloft, although upper-air data are not essential for the PMP estimation procedure outlined here.

It should be kept in mind that the procedure described generally applies only to mid-latitude basins of no more than around 50 000 km<sup>2</sup>. Also, since it is very unlikely that a project basin will have experienced all the outstanding storms of the region in which it lies, storm transposition is always required. When developing the PMP estimate for a basin, a range of storms with areas both larger and smaller than the basin should be considered for all durations so the appropriate degree of envelopment is achieved (section 2.8.2).

## 2.9.2 Procedural steps

The steps are as follows:

- (a) Using weather, topographic, and preliminary total-storm isohyetal maps, determine the explicit transposition limits of storms, as described in section 2.5.
- (b) Survey precipitation records to obtain outstanding storms on record within the region of transposability.
- (c) Make DAD analyses of the storms selected in (b), as described in *The Manual for Depth-Area-Duration Analysis of Storm Precipitation* (WMO-No. 237). The results of the analysis for each storm are tabulated as shown in Table 2.2. (The DAD analysis of storm precipitation is a lengthy and tedious process even when done by computer. A ready file of storm DAD data is a great convenience in making PMP estimates. Some countries maintain a ongoing DAD analysis programme that accumulates a file of DAD data for both old storms on record and new storms as they occur. DAD data for storms in the area of transposability may be readily selected from such files, thus eliminating (b) and (c).)
- (d) Determine the representative persisting 12-hour dewpoint for each appropriate storm, as described in section 2.2.4. Since this dewpoint is usually outside the rain area (Figure 2.2), its distance and direction (or bearing) from the storm centre should be specified (section 2.6.1.1). If wind maximization is indicated (section 2.4), select also for each storm the maximum 24-hour average speed of the wind from the moisture-inflow direction. Multiply the precipitable water  $W$  that corresponds to the representative storm dewpoint by the wind speed to obtain the representative storm moisture-inflow index (Figure 2.13).
- (e) Determine the highest maximum persisting 12-hour dewpoint on record for the location of the reference dewpoint for the transposition site, as described in sections 2.2.5 and 2.6.1.1. Since several storms of different dates and with different reference dewpoint locations must be transposed, it is recommended that the maximum dewpoints for the entire storm season and for the project basin and surrounding areas be determined at one time, as described in section 2.2.5. Preparation of maximum persisting 12-hour 1 000-hPa dewpoint maps, such as Figure 2.4, is advisable. Such maps have an additional advantage in that they yield some indication of the geographic variation of PMP values in a plains area.
- (f) Compute the combined transposition and maximization ratio of the precipitable water  $W$  for the maximum persisting 12-hour 1 000-hPa dewpoint from (e) for the storm date, or within 15 days of it (section 2.3.1), to the precipitable water for the representative persisting 12-hour 1 000-hPa dewpoint for the storm (section 2.6). If wind maximization is involved, compute the ratio of the maximum moisture-inflow index to the representative storm moisture-inflow index.
- (g) Multiply the values for various appropriate areas using DAD data (such as in Table 2.2) for each storm by the appropriate precipitable-water or moisture-inflow index ratio, as determined in (f).
- (h) Plot graphs of the transposed maximized DAD values determined in (g), as shown in Figures 2.10 and 2.11, and insert envelope curves. Use envelope curve values to construct DAD curves of PMP, as shown in Figure 2.12. Although not mandatory, storms providing control points on the PMP curves should be identified, as indicated in Figure 2.12. This will assist with selecting actual storm patterns from

which to determine the time and spatial distribution of the PMP in calculating the design flood.

## 2.10 SEASONAL VARIATION OF PMP

### 2.10.1 Introduction

In those regions where the maximum flood is likely to result from a combination of snowmelt and rainfall, it is necessary to determine the seasonal variation of PMP so that various combinations for different times of the melting season can be evaluated and the most critical combination determined. For example, in a particular region, maximized June storms may provide the controlling points for PMP, but optimum combinations of accumulated snow on ground and melting rates may be found in April. It is then necessary to estimate PMP for April. Since it is not known exactly what time of year is most critical for the maximum snowmelt and rain flood, the usual procedure is to determine the seasonal variation curve of PMP for the entire snowmelt season. The curve then permits a ready adjustment of PMP for use in assessing flood situations at various times during the melting season in order to determine the most critical flood.

There are various ways of determining the seasonal variation of PMP. The more common procedures are discussed here. Selection of a procedure depends on data available. Whenever possible, it is advisable to use several procedures in developing a seasonal variation curve. Cautionary remarks on the representation and use of seasonal variation curves are given in section 2.13.5.

### 2.10.2 Observed storms

The best way to determine the seasonal variation of PMP requires a relatively large number of storms for which DAD data are available and that are fairly well distributed throughout the melting season. Different variations are usually found for small and large areas and for short and long durations. It is, therefore, important to base the seasonal variation on data consistent with the basin size and critical rainfall duration. Because of this, it is often advisable to construct a set of curves rather than a single one. The storm rainfall for a particular size of area and duration is then maximized for moisture, as described in sections 2.3 and 2.6. The maximized data are then plotted against the date of storm occurrence, and a smooth envelope curve is drawn. The rainfall scale is usually converted to a percentage scale expressing

the PMP as a percentage of the peak value or the value for some particular time of year.

### 2.10.3 Maximum persisting 12-hour dewpoints

The seasonal variation of maximum persisting 12-hour dewpoints may be used also to determine the seasonal variation of PMP. This procedure is more applicable to localized thunderstorm PMP than to PMP for large areas and long durations. Precipitable water is computed for the individual maximum 12-hour dewpoints throughout the critical season, or it may be computed for values read from their seasonal variation curve, like Figure 2.3. A shortcoming of this procedure is that it will almost always indicate a peak PMP value in summer, even in regions where summers have little or no rainfall and major storms occur in winter. It cannot be used under these conditions unless wind is also considered (see section 2.10.4).

### 2.10.4 Moisture inflow

In those regions where summers are dry and major storms occur only in the cold half of the year, the seasonal variation of maximum precipitable water (section 2.10.3) gives a false indication of the seasonal variation of PMP when used alone. A wind factor is also required to develop a representative seasonal variation of PMP.

Figure 2.13 shows a seasonal variation curve developed for PMP in the Upper Tigris River basin, where in summer there is very little rain. While the maximum dewpoint and precipitable water curves tend to show minimum values during the cold season, climatological records show that in this region all major general-type storms occur in that season. Weather charts indicate that the heaviest precipitation occurs with surface winds in the south-eastern and south-western quadrants. A survey of a long record of surface winds yielded the maximum 24-hour wind curve in Figure 2.13, part C, which shows peak values in January and February. Multiplication of precipitable water values by wind speed resulted in the moisture-inflow index curve shown in part D. The double peak was confirmed by outstanding recorded storms.

### 2.10.5 Daily station precipitation

An indication of the seasonal variation of PMP may be easily obtained from monthly-maximum daily station rainfall amounts. The use of average maximum values for several stations rather than from a single station is advisable for larger basin sizes. In

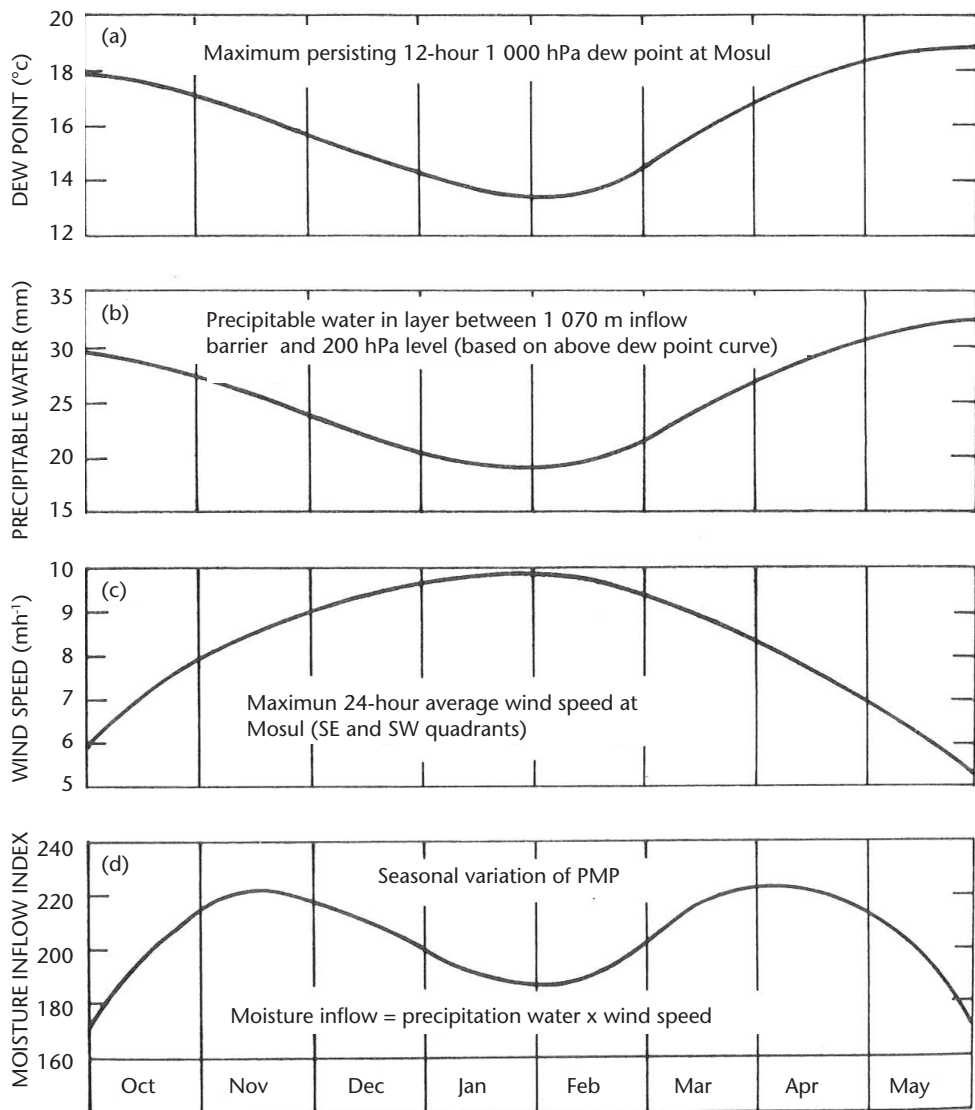


**Figure 2.13. Seasonal variation of probable maximum precipitation in the Upper Tigris River basin in Iraq**

periods of rapid weather transitions, usually early autumn and late spring, it may be advisable to select maximum rainfall values by half-month or 10-day periods. Again, the maximum values are plotted against the date of occurrence, and a smooth seasonal envelope curve is then drawn. The rainfall scale is usually converted into terms of percentage, as in section 2.10.2.

#### 2.10.6 Weekly precipitation data

Occasionally, special summaries of precipitation data may be found which can be used to derive the seasonal variation of PMP. One such summary is average weekly precipitation for given areas, determined by averaging station precipitation within each area for each week of the year over a long period. The

seasonal variation curve of PMP may be based on an envelope of these weekly values. A seasonal variation curve developed in this way would be more applicable to PMP for long durations and large areas.

#### 2.11 AREAL DISTRIBUTION OF PMP

##### 2.11.1 Introduction

Once the PMP values for a particular location have been derived as a table, or enveloping DAD curves like Figure 2.12, areal distribution over the project basin must still be determined. It is not generally recommended that the PMP values be considered as applying to any one storm, especially for the

larger basins. Direct use of the PMP values for all area sizes of a storm pattern within a basin may be unrealistic for the most critical design storm for two main reasons. First, the storm producing maximum rainfall over small areas within a project basin is usually of a different type from that producing maximum rainfall over the same basin as a whole. Similarly, in some climatic regions, different types of storms may provide maximum values for different durations over the isohyetal pattern for the same area size. Second, the shape and orientation of the isohyetal patterns may be different for small area storms than those permissible for the controlling isohyetal patterns for larger area storms.

### 2.11.2 Observed storm pattern

For the above reasons, the hydrometeorologist makes recommendations regarding the storm isohyetal patterns that can be applied to a basin. One or more transposed storms may provide a suitable pattern or patterns, especially when both basin and storm site are topographically similar. A limitation may be placed on the rotation or displacement of the isohyetal pattern. If, as often happens, the transposed or basin storms selected provide points on the PMP DAD curves, no further adjustment may be required. If not, they may be maximized using the sliding technique.

Storms not providing controlling points on PMP DAD curves may be maximized by separately plotting the storm and PMP DAD curves on the same logarithmic scale. The storm curve is then superimposed onto the PMP DAD curve and is slid to the right until the first apparent contact between curves for the same duration occurs, as shown in Figure 2.14. The ratio of any PMP scale value to the superimposed storm scale value is the maximizing factor. Obviously, this factor adjusts the observed storm for greater rain-producing efficiency, as well as for maximum moisture. In Figure 2.14, the first point of contact occurs for 72-hour curves between about 2 000 and 4 500 km<sup>2</sup>, for a 5 000 km<sup>2</sup> basin, but different time and spatial distributions might show a point of first contact for another duration and/or area size.

The coincidence between the storm and PMP DAD curves should be at an area size that approximates that of the basin. Current practice, however, favours bringing average depths for all durations of the storm to PMP levels, as described in section 2.11.3, for an idealized pattern. In applying the procedure to actual storms, care must be taken to ensure that

rainfall depths for areas smaller than the basin do not exceed PMP. If they do, the storm deptharea relations must be altered so that depths nowhere exceed PMP.

### 2.11.3 Idealized storm pattern

An alternative method for fixing the areal distribution of PMP over a basin is based on the assumption that the PMP values for all durations at the total area of the basin could occur in a single storm. This may introduce an additional degree of maximization, because controlling values for all durations at a particular size of area may be from several storms. In order to counter this possibility, the precipitation values for the smaller areas within the basin are maintained at less than PMP, usually being patterned after the deptharea relations of major storms that have occurred over or near the project basin. For example, the dashed within-storm curves of Figure 2.15 (only two shown) set the concentration of rain within a 3 000 km<sup>2</sup> basin for the 6- and 24-hour durations. These curves are generally drawn for all durations by 6-hour intervals. For further discussion of the development of idealized isohyetal patterns see sections 5.2.7.2 and 5.2.7.4.

#### 2.11.3.1 Areal distribution

The areal distribution of a basin's PMP involves the shape and orientation of its isohyetal pattern, and this may be based on observed storms. For basins up to about 1 500 km<sup>2</sup> in flat terrain, an elliptically-shaped pattern with almost any orientation is adaptable and the pattern is usually centred over the basin. For larger basins (up to and even above the limiting size considered in this report), in the middle latitudes of the northern hemisphere, the orientation of the pattern tends to be controlled in a general way by the flow in the middle to upper troposphere. Studies should be performed to determine preferred isohyetal orientation for an individual basin (section 5.2.7.3). The pattern may or may not be centred over the basin, depending on what the history of major basin storms in the region indicates.

#### 2.11.3.2 Example

The critical storm pattern is usually constructed on the assumption that the largest volume of rain over the basin will produce the most critical design flood. This principle also applies to the division of a larger basin into sub-basins for flood computations. In some cases, other centring may be important. For example, a storm pattern centred over a portion

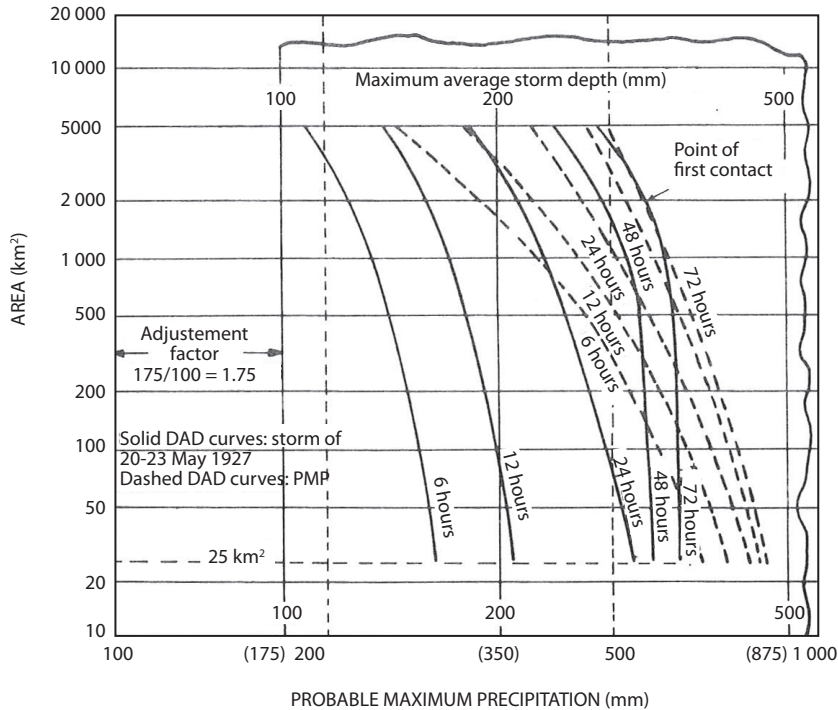


**Figure 2.14. Maximization of a pattern storm by the sliding technique for a 5 000 km<sup>2</sup> basin, the point of first contact occurs on the 72-hour curves between about 2 000 and 4 500 km<sup>2</sup>**

of a basin just upstream from a dam may prove most critical for peak flow. This can only be determined by hydrological trials.

In the general case, hypothetical isohyets are drawn more or less congruent to the basin boundaries (Figure 2.16), and the rain values, or labels, for the isohyets are determined by a procedure that is essentially a reversal of the usual DAD

analysis. For example, given the 6-hour PMP and within-storm DAD curves of Figure 2.15, the isohyetal values for the critical storm pattern superimposed on the outline of the 3 000 km<sup>2</sup> basin of Figure 2.16 can be determined. Table 2.3 shows how the isohyetal profile is computed, and the results are shown in Figure 2.17. The required isohyetal values are obtained as shown in Table 2.4.

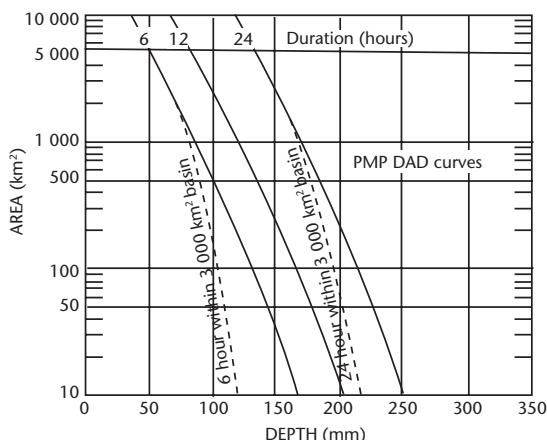


**Figure 2.15. Example of enveloping DAD curves of PMP and within-storm rainfall depths**

## 2.12 TIME DISTRIBUTION OF PMP

### 2.12.1 Order of presentation

An appropriate chronological time sequence of rainfall increments is needed for application of PMP estimates. PMP values, whether presented in tabular form or by DAD curves, are generally given with the maximum accumulated amounts for any duration preceding all other values for the specified duration. In other words, the 6-hour PMP amount given is the maximum 6-hour increment to be found anywhere in the PMP sequence. Similarly, the amounts for 12, 18, 24 hours and longer are the maximum for the sequence. This order of presentation, however, is rarely representative of the chronological order found in actual storms, and

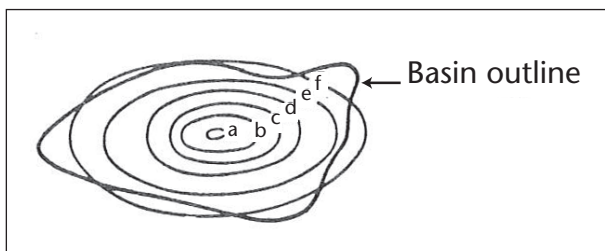


**Figure 2.16. Critical isohyetal pattern over 3 000 km<sup>2</sup> basin**

thus observed storms characteristic of the basin need to be studied to define the correct chronological sequence. Furthermore, it is often unlikely to produce maximum runoff for the amounts of rainfall involved.

#### 2.12.2 Chronological order based on an observed storm

A more realistic, and generally more critical, chronological order is usually obtained from some storm producing critical runoff amounts and rates in or

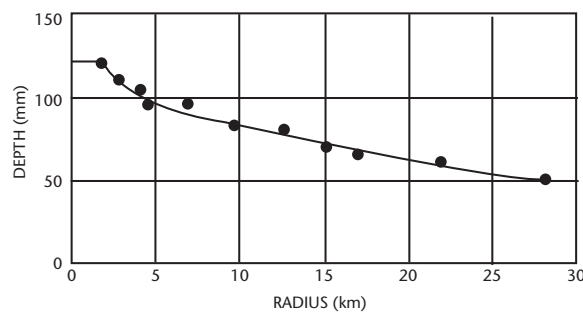


**Figure 2.17. Isohyetal profile constructed from data in Table 2.3**

near the project basin. Table 2.5 presents an example of how the order of the 6-hour PMP increments might be rearranged to agree with the chronological order of a critical observed storm. Note that this procedure leads to rainfall amounts equal to PMP for several durations, hence, higher runoff than would be obtained using a maximized storm as described in section 2.11.2, where usually only one maximized value equals PMP.

**Table 2.3. Isohyetal profile computation**

Total area (km <sup>2</sup> ) <sup>a</sup>	Net area (km <sup>2</sup> ) <sup>b</sup>	Average depth (mm) <sup>c</sup>	Accumulated rain volume (km <sup>2</sup> mm) <sup>d</sup>	Net rain volume (km <sup>2</sup> mm) <sup>e</sup>	Volume area (mm) <sup>f</sup>	Average area (km <sup>2</sup> ) <sup>g</sup>	Equivalent circle radius (km) <sup>h</sup>
10	10	122	1 220	1 220	122	10	1.8
40	30	113	4 520	3 300	110	25	2.8
60	20	110	6 600	2 080	104	50	4.0
80	20	107	8 560	1 960	98	70	4.7
100	20	105	10 500	1 940	97	90	5.3
200	100	100	20 000	9 500	95	150	6.9
400	200	92	36 800	16 800	84	300	9.8
600	200	88	52 800	16 000	80	500	12.6
800	200	84	67 200	14 400	72	700	15.0
1 000	200	81	81 000	13 800	68	900	16.9
2 000	1 000	71	142 000	61 000	61	1 500	21.9
3 000	1 000	64	192 000	50 000	50	2 500	28.2

<sup>a</sup> Column 1: standard sized areas

<sup>b</sup> Column 2: successive subtraction of Column 1 items

<sup>c</sup> Column 3: maximum average depths from 6-hour within-storm curve of Figure 2.15 for area sizes in Column 1

<sup>d</sup> Column 4: product of Column 1 and Column 3 entries

<sup>e</sup> Column 5: successive subtraction of Column 4 items

<sup>f</sup> Column 6: Column 5 divided by Column 2

<sup>g</sup> Column 7: average of two consecutive areas in Column 1

<sup>h</sup> Column 8: radius of circle with area of Column 7

Data from columns 6 and 8 are then used to construct the curve of Figure 2.17.

**Table 2.4. Evaluation of isohyet labels of Figure 2.16**

Isohyet <sup>a</sup>	Enclosed area (km <sup>2</sup> ) <sup>b</sup>	Equivalent radius (km) <sup>c</sup>	Isohyet value (mm) <sup>d</sup>
A	10	1.78	122
B	200	7.98	89
C	500	12.65	77
D	750	15.50	70
E	2 000	25.20	55
F	3 000	30.98	48

<sup>a</sup> Column 1: refers to isohyets of Figure 2.16<sup>b</sup> Column 2: areas enclosed by isohyets of Figure 2.16<sup>c</sup> Column 3: radii of circles equivalent in area to enclosed areas in Column 2<sup>d</sup> Column 4: labels for isohyets of Figure 2.16 as indicated by entering Figure 2.17 with radii of Column 3

When it is thought that there might be more critical possible arrangements of rainfall increments than indicated by observed storms, various other realistic arrangements are examined, and the more likely ones are specified. In developing different arrangements of 6-hour increments, the standard practice in the United States is to maintain PMP magnitude for all durations, that is, the two highest increments in order of magnitude adjacent, the

countries, this practice is not always followed and different temporal distributions based on mass curves for observed severe storms are provided. This practice does not always provide PMP magnitude rain for all durations. It is the responsibility of the meteorologist and hydrologist to determine which arrangement is appropriate for a particular region and will result in the critical design storm for a basin.

**Table 2.5. Chronological distribution of probable maximum precipitation (PMP) for a hypothetical 3 000 km<sup>2</sup> basin**

Duration (hours)	PMP (mm)	6-hour increments		Maximum accumulation
		PMP	Arranged <sup>a</sup>	
6	284	284	16	284
12	345	61	28	345
18	384	39	20	384
24	419	35	12	419
30	447	28	39	431
36	467	20	61	451
42	483	16	284	479
48	495	12	35	495
54	505	10	5	500
60	513	8	8	508
66	521	8	10	518
72	526	5	8	526

<sup>a</sup> Increments in this column are assumed to be arranged according to the sequence of increments in a critical storm producing maximum runoff in the project basin.

Note that maximum accumulation for any given duration may be less than or equal to, but not more than, the summation of PMP increments for the same duration. Thus, for example, the maximum 24-hour accumulation is equal to the PMP value of 419 mm (39.0 + 61.0 + 284 + 35.0). The maximum 30-hour value is only 431 mm (12.0 + 39.0 + 61.0 + 284 + 35.0), whereas the 30-hour PMP value is 447 mm. In this example, only the 6-, 12-, 18-, 24-, 48 and 72-hour accumulations are equal to the PMP values.

three highest adjacent, etc. In Australia and other

## 2.13

### **CAUTIONARY REMARKS**

Preparation of PMP estimates for specific basins requires considerable effort to ensure appropriate values are determined. Where estimates are required for more than one or two basins in a region, generalized PMP studies combined with an applications manual for developing estimates for individual basins is a preferred procedure (see Chapter 5). If individual PMP estimates are prepared, the procedures discussed in this chapter should be followed comprehensively with special notice taken of these cautionary remarks.

#### 2.13.1     **Importance of adequate storm sample**

Transposition and maximization of a few storms is unlikely to yield reliable PMP estimates for an individual basin. It is important that all outstanding storms recorded over the project basin and areas of transposability be used in making such estimates. Comparison of storms in the areas of transposability with those outside should be made. If such comparison indicates that only a few storms within the area reach the magnitude of generally greater storms outside the areas, the transposition limits should be re-examined and relaxed, if at all possible, to include storms in the marginal areas just outside the limits originally determined.

Storm surveys and analyses should be extended to meteorologically comparable regions no matter how far removed from the project basin. If synoptic storm types are kept in mind, far distant areas of the world may sometimes provide better clues to PMP than nearby areas. This not only applies to precipitation data, but to other factors instrumental in developing concepts for understanding storm precipitation-producing mechanisms.

The greater the number of carefully selected extreme storms transposed and maximized, the greater the reliability of the resulting PMP estimates. Under ideal conditions, some two dozen major storms might be important for determining PMP. Of these, probably fewer than half a dozen might provide control points on the PMP DAD curves.

#### 2.13.2     **Comparison with record rainfalls**

The final results of any PMP estimate should always be compared with observed record values. The world record values of point rainfall, presented in Annex 2, very probably approach PMP magnitude. Estimates appreciably exceeding these values, say by 25 per cent or more, may be excessive. Most

estimates of point PMP might be lower than these record values for durations of approximately 4 hours and longer since few basins are so favourably located as to experience rainfalls of these record magnitudes.

Table A.2.3 in Annex 2 presents enveloping values of DAD data from over 700 storms in the United States. Many values are from storms in the southern part of the country near the moisture source – the Gulf of Mexico. These enveloping values from such a large sample of major storms may approach PMP magnitude for this region, especially for areas larger than around 25 km<sup>2</sup>.

It should be noted that PMP values are considered estimates of the upper limit of precipitation potential over a basin. The comparison of these estimates with maximum observed precipitation over a limited geographic region will considerably exceed observed values unless some storms of great magnitude have occurred in the immediate vicinity. Comparisons between PMP estimates and maximum observed precipitation should be made over very large regions and include a range of area sizes and durations. Figure 2.18 shows the results for one area size and duration from such a comparison study for the United States (Riedel and Schreiner, 1980).

#### 2.13.3     **Consistency of estimates**

PMP estimates for various basins in a meteorologically homogeneous region should be compared for consistency. Appreciable differences should be studied to see if they are supported by climatic or geographic factors. If not, it can be concluded that the differences are not valid and the various steps involved in the procedure for estimating PMP should be re-examined thoroughly. When PMP estimates are made basin by basin at various times, consistency is difficult to maintain. The generalized estimates approach, described in Chapter 5, is recommended for achieving consistency.

#### 2.13.4     **Regional, durational and areal smoothing**

It is important when developing PMP estimates to recognize the continuity of the field of precipitation potential. When examining major rainstorms for one area size or duration, it is possible that no storm in a region has occurred with an optimum combination of the factors involved in the precipitation process. For this reason, it is important that a wide range of area sizes and durations be used in developing the DAD relation for the PMP estimate

for an individual basin. Unless some meteorological or topographical explanation can be provided, the relations developed should provide smooth depth-area and depth-duration curves and properly envelop all moisture-maximized rainfall amounts. In a comprehensive study, sets of DAD curves would be developed for surrounding locations to ensure regional consistency.

### 2.13.5 Seasonal variation

Any one of the procedures described in section 2.10, except possibly section 2.10.2, may result in seasonal curves of PMP that are obviously misleading. For this reason, it is advisable to try several procedures to see if there is agreement between the resulting seasonal variation curves. Judgement on whether a derived curve is representative or not should be based on a comparison with actual storms observed at various times during the critical season.

As mentioned in section 2.10, the seasonal variation of PMP differs with duration of storm rainfall and size of area, and several seasonal variation curves may have to be derived for different durations and areas. Also, a seasonal variation curve does not imply that maximized storms can be transposed in time without regard to seasonal limitations on storm types. The curve may be used only to adjust the level of PMP to various times of the year. Storm types and patterns, however, differ from month to month and a July storm, for example, is rarely adaptable to April conditions. Storm transposition in time is usually limited to 15 days, but a longer period, such as one month, may be used when storm data are sparse. In some regions where specific storm types occur over a several month span, for example, the West Coast of the United States in winter, transposition in time of several months may be justified.

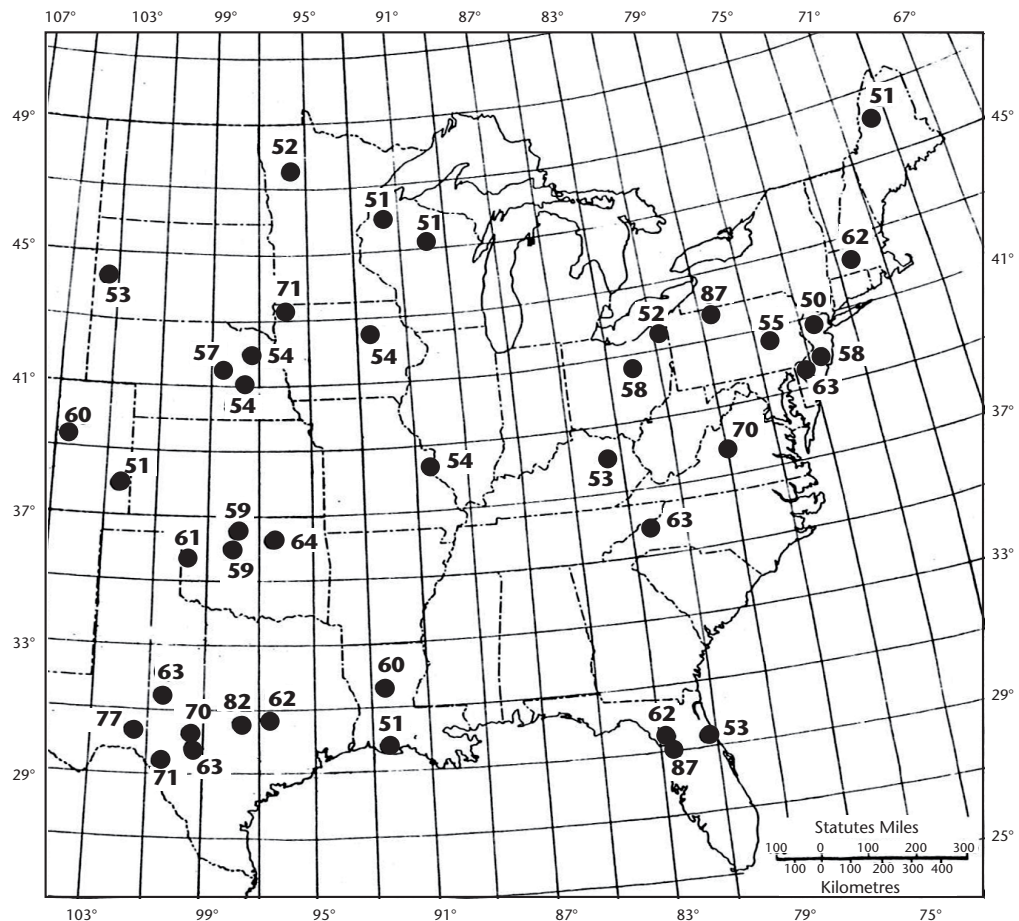


Figure 2.18. Observed rainfalls expressed as a percentage of PMP in the United States, east of the 105th meridian  $\geq 50$  per cent of all-season PMP for the 24-hour duration and an area size of  $518 \text{ km}^2$  (Riedel and Schreiner, 1980).

### 2.13.6 Areal distribution

Two methods of establishing the areal distribution of what may be termed the PMP storm were described in section 2.11. The first, which involves the use of an observed storm pattern maximized by the sliding technique (section 2.11.2), usually equals PMP for only one duration and size of area. The second method, which is used with idealized storm patterns, requires PMP values for the basin area to be equalled for all durations (section 2.11.3). Values for areas smaller than the total basin area are set at less than PMP by the use of within-storm deptharea curves shaped according to observed storms. In general, the larger the basin, the larger the difference between PMP and within-storm curve values for any given area smaller than the basin (Figure 5.10). Conversely, the difference decreases as basin size decreases, so that for basins of no more than a few hundred square kilometres, the areal distribution is frequently accepted as conforming to the PMP curves.

If meteorological conditions are the same, there may seem to be no reason why the rainfall potential over a  $100 \text{ km}^2$  area in a  $25\,000 \text{ km}^2$  basin, for example, should be less than that over a  $100 \text{ km}^2$  area in a  $5\,000 \text{ km}^2$  basin. In the regions where such within-storm curves have been developed, however, storms producing large rainfall depths over areas of  $25\,000 \text{ km}^2$ , in general, do not have embedded large convective cells. In contrast, storms that produce maximum values over areas of approximately  $5\,000 \text{ km}^2$  are more convective in nature with large amounts over small areas within the storm. For this

reason, these within-storm curves indicate lesser small-area depths as basin size increases. The within-storm curves are patterned after actual storms that have occurred over a region and reflect actual storm rainfall distributions. This relation may not be valid in other regions and actual storms must be examined to determine appropriate within-storm curves for any study. The effect of small-area depths on total basin rainfall volume decreases as basin size increases.

An important restriction on the construction of depth-area curves is that their slopes should nowhere indicate a decrease in rainfall volume with increasing area. This applies to all deptharea curves, including PMP.

While most examples of PMP estimation presented in this manual involve areal distribution based on within-storm curves, it should not be inferred that this is the recommended method. Whether the areal distribution is based on an observed storm maximized by the sliding technique, on within-storm curves, on PMP depth-area curves, or on other methods depends on the judgement of the meteorologists, hydrologists and engineers involved in the development of the design for a hydrological structure. A variety of different methods are normally used by the meteorologist to develop estimates of rainfall distribution over the basin. The estimates are then reviewed to ensure they are consistent with storm experience. The hydrologist and/or engineer will then apply the various rainfall distributions to determine which is most hydrologically critical for the design of a particular structure.

## CHAPTER 3

# ESTIMATES FOR MID-LATITUDE OROGRAPHIC REGIONS

Precipitation in orographic regions can be divided into two types: that resulting from the movement of precipitation weather systems, called convergence components or convergence rain; and that resulting from orographic effects, called orographic components or orographic rain.

In estimating probable maximum precipitation (PMP) in a particular watershed or performing generalized PMP estimation for a particular area in an orographic region, data on transposed storms needs to be corrected. This enables the use of data from large storms that occurred in orographic regions and plains in the meteorological homogeneous zone. Depending on the method used to process the influence of orography on precipitation, methods for estimating PMP in orographic regions can be divided into three categories. The first category is the storm separation method. The second category is the method of orographic correction of PMP in non-orographic regions. The third category is the method of direct, detailed correction of PMP in orographic regions. The first two categories are introduced in Chapters 3, 5 and 6 and the third category is introduced in Chapter 7.

### 3.1 PRECIPITATION IN MOUNTAINOUS REGIONS

#### 3.1.1 Orographic influences

The effects of topography on precipitation have been studied for many years. Observations of precipitation and runoff in mountainous terrain in many parts of the world show a general increase in precipitation with elevation. Several features of this increase can be distinguished.

First, there is the increase on windward slopes due to forced lifting of air over mountains. The magnitude of the effect on precipitation varies with the direction and speed of the moist airflow, and with the extent, height, steepness and regularity of the mountain barrier. Breaks in ridges or passes reduce the amount of lifting. Other factors are the extent and height of lower mountains or hills upwind of a slope.

Concomitant with increased precipitation on windward slopes is the decrease on lee areas. Immediately

to the lee of ridges is a spillover zone, where precipitation produced by the forced ascent of moist air over windward slopes can be as great as on the ridge. Because of the relatively slow fall velocity of snowflakes, spillover extends much farther beyond the ridge for snow than it does for rainfall. Beyond the spillover zone, significant reductions can occur in precipitation due to sheltering effects.

A second feature of orographic precipitation, indicated by theory and supported by observations, is that first slopes or foothill regions are preferred locations for the initiation of showers and thunderstorms. This effect results from stimulation of convective activity in unstable air masses by an initial and relatively small lift. Observational data are often too sparse to verify this phenomenon because of the more obvious effects of higher slopes nearby. Coastal station observations sometimes exhibit the effects of small rises in elevation. For example, a comparison of rainfalls at San Francisco, California, United States of America, and the Farallon Islands, approximately 40 km off the coast west of San Francisco Bay, showed that in major storms, rainfall is about 25 per cent greater at San Francisco. This effect was taken into account in a PMP study for the north-western United States (United States Weather Bureau, 1966).

Another effect noticed in orographic regions is sometimes referred to as a funnelling effect. Where there are narrowing valleys or canyons parallel to storm winds, the winds can experience horizontal convergence and resultant vertical lift, initiating or increasing rainfall. For this to occur, it is necessary that mountains adjacent to the valleys or canyons be relatively unbroken and at least moderately high.

#### 3.1.2 Meteorological influences

Experience has shown that general storm precipitation resulting from atmospheric systems that produce convergence and upward motion is just as important in orographic regions as on the plains. Reports of thunderstorms and passages of weather systems during large-area storms in high mountain ranges are indicators of the dual nature of precipitation in orographic regions. Radar, for example, has tracked bands of precipitation moving across the coastal hills and central valley of California into the high Sierra Nevada (Weaver, 1966).

### 3.1.3 Mean annual and seasonal precipitation

Mean annual and seasonal precipitation at different locations in mountainous terrain can be influenced greatly by the varying frequency of relatively light rains. Some weather situations produce precipitation on mountains when little or no precipitation is observed in valleys, and storm precipitation generally has longer durations in the mountains. Thus, the variation indicated by mean annual or seasonal precipitation maps is not necessarily a reliable index of geographic variation in PMP unless adjusted for these biases. An adjustment technique frequently used is based on the mean number of rainy days at stations in the project area and a map showing the average station or point precipitation per rainy day (which is usually defined as any day with measurable precipitation, although a higher threshold value, for example 2 mm, is sometimes used). The most representative mean annual and seasonal precipitation maps are those based on other data in addition to precipitation (Nordenson, 1968; Solomon and others, 1968), and such maps should be used whenever possible.

### 3.1.4 Precipitation-frequency values

Precipitation-frequency values represent an equal probability level of rainfall. The values for the rarer recurrence intervals, for example the 50-year or 100-year recurrence interval, are associated with severe weather systems. Therefore, they are better indicators of the geographic variation of PMP than mean seasonal or annual precipitation maps. Ratios of precipitation-frequency values between those at a storm location and those over an individual basin have been used to adjust rainfall amounts when storms have been transposed in mountainous regions. Since precipitation-frequency values represent equal probability, they can also be used as an indicator of the effects of topography over limited regions. If storm frequency, moisture availability, and other precipitation-producing factors do not vary, or vary only slightly, over an orographic region, differences in precipitation-frequency values should be directly related to variations in orographic effects. This concept was used to adjust convergence PMP for orographic variations in an American study (Miller and others, 1984b) and as an index to the geographic distribution of the orographic component of PMP in other studies (Hansen and others, 1977; United States Weather Bureau, 1961a, 1966).

### 3.1.5 Storm transposition

Because of the dual nature of precipitation in mountainous regions, the similarity between storm

precipitation patterns and topography is limited, varying with the precipitation-producing factors involved. Nevertheless, in mountainous terrain, orographic influences on precipitation can be significant, even in major storms. For this reason, caution should be exercised in transposing storms in such regions because their precipitation patterns are usually linked to the orography where they were observed.

### 3.1.6 Probable maximum precipitation

PMP estimates for orographic regions must be based on two precipitation components:

- (a) orographic precipitation, which results from orographic influences;
- (b) convergence precipitation, which results from atmospheric processes presumed to be independent of orographic influences.

Both components must be evaluated in making PMP estimates in orographic regions.

#### 3.1.6.1 Estimation of PMP in orographic regions using the orographic separation method

The orographic separation method consists of estimating each precipitation component separately and then adding them, keeping in mind some necessary restrictions on their addition (United States Weather Bureau, 1961a). One method, which is described in sections 3.2 and 3.3, involves the use of an orographic model for evaluating the orographic component (United States Weather Bureau, 1961a, 1966). A second method estimates the orographic component using indirect procedures (Hansen and others, 1977). This method is described in section 5.3.5.

#### 3.1.6.2 Modification of non-orographic PMP for orography

Another approach is to first estimate a non-orographic PMP. One technique in this approach is to develop the convergence PMP estimate for the relatively flat regions adjoining the mountains using only storms from non-orographic regions. A second technique is to estimate the convergence component of all storms over a region, both in the orographic and non-orographic portions, and draw generalized charts of convergence PMP. Modifications for terrain influences are then introduced on the basis of differences in storm rainfall data, both in the project basin and surrounding areas, and on sound meteorological judgement derived from storm analyses (Schwarz,

1963, 1965; United States Weather Bureau, 1970; Zurndorfer and others, 1986). The procedure is described in section 3.4 and Chapter 5.

### 3.1.6.3 Direct orographic correction of PMP in orographic regions

This method proposes the direct transposition of the PMP (storm) in an orographic region to a particular position (the storm centre and the storm area axis) in a specific watershed, and then the performance of specific corrections based on the potential influence of the orographic differences on PMP in the two regions. Section 7.4.5 provides details of the methodology.

### 3.1.6.4 Examples of procedures

The remainder of this chapter presents details on procedures used in applying the methods mentioned in the two preceding paragraphs. The general principles involved are discussed, and examples given from published reports. Thus, the examples necessarily are for a particular set of conditions: namely, a certain amount of available data, certain terrain characteristics, and last, but just as important, the meteorological characteristics of the major storms in the regions for which the studies were made.

## 3.2 THE OROGRAPHIC SEPARATION METHOD WITH A LAMINAR FLOW MODEL

### 3.2.1 Introduction

In PMP estimation using the orographic separation method, an orographic model is used to calculate orographic storms. There are only a small number of cases in which the model is applicable for mid-latitude regions, so it must be used with care. Despite its limited application, the method is introduced in detail here because of a dearth of information published elsewhere. Approaches for calculating precipitation convergence components of a weather system using the orographic separation method are also presented in this section.

Sections 3.2 and 3.3 provide results of studies made by the then United States Weather Bureau on PMP for California in 1961 and 1966. Despite the fact that more recent results of PMP for that region are now available (Corrigan and others, 1999), sections 3.2 and 3.3 still use the earlier estimates, figures and tables for consistency with earlier editions of this manual.

### 3.2.2 Orographic laminar flow model

Precipitation released when moist air is forced over a relatively unbroken mountain ridge is the result of a basic process which can be idealized and treated as a two-dimensional problem. The air passing over the mountain crest must accelerate since there is a shallower layer within which air from a deeper upwind layer must be passed. This process has led to an orographic precipitation model in which the airflow, assumed to be laminar, is lifted over the mountain ridge. In regions with a significant amount of convective activity during major storms, this model will not provide reliable results because of the assumption of laminar flow. Another result of this characteristic of the model is to limit its use to temperate regions where tropical storms are not important causes of large storms. The laminar flow model is a storage evaporation model in that the resulting precipitation is the difference between the water vapour inflow at the base of the mountain range and the outflow above the ridge.

At some great height, called the nodal surface, airflow is assumed to be essentially horizontal. The height at which this occurs can be computed theoretically (Myers, 1962). In general, this height is between 400 and 100 hPa for moderately high barriers. A simplified diagram of inflow and outflow winds over a mountain barrier is shown in Figure 3.1.

This model considers the flow of air in a vertical plane at right angles to a mountain chain or ridge. It is what is termed a two-dimensional model. The plane has a  $y$  coordinate in the direction of flow and a  $z$  coordinate in the vertical. The flow may represent an average over a few kilometres or tens of kilometres in the transverse, or  $x$ , direction, which does not appear explicitly in the model. The wind at ground level moves along the surface. The slope of the air streamlines above a given point on the mountain slope decreases with height, becoming horizontal at the nodal surface.

### 3.2.2.1 Single-layer laminar flow model

If it is assumed that the air is saturated, that temperature decreases along the rising streamlines at the moist adiabatic rate, and that the flow is treated as a single layer of air between the ground and the nodal surface (Figure 3.2), the rate of precipitation is then:

$$R = \frac{\bar{V}_1 \left( \bar{W}_1 - \bar{W}_2 \frac{\Delta P_1}{\Delta P_2} \right)}{Y} \quad (3.1)$$

where  $R$  is the rainfall rate in mm/s;  $\bar{V}_1$  is the mean inflow wind speed in m/s;  $\bar{W}_1$  and  $\bar{W}_2$  are the inflow and outflow precipitable water (liquid water

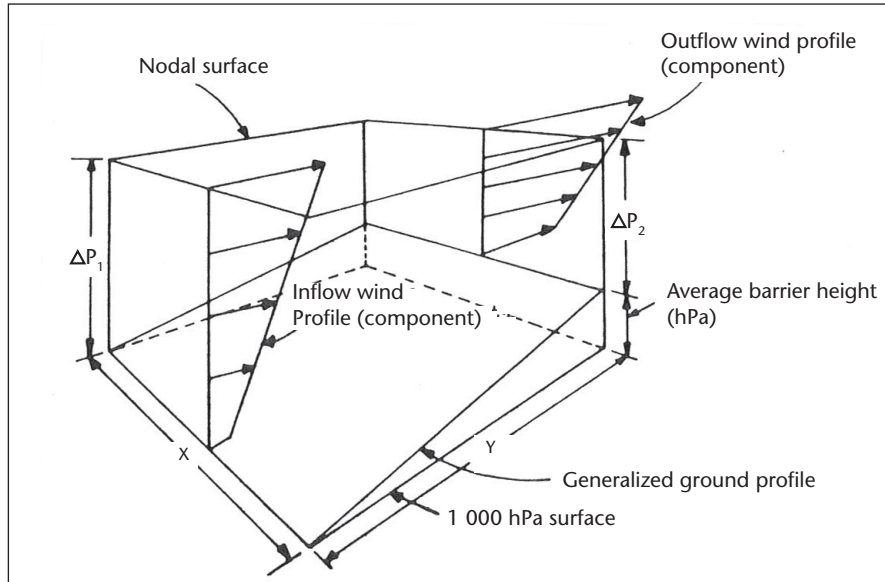


**Figure 3.1. Simplified inflow and outflow wind profiles over a mountain barrier  
(United States Weather Bureau, 1961a)**

equivalent), respectively, in mm;  $Y$  is the horizontal distance in m; and  $\Delta P_1$  and  $\Delta P_2$  are the inflow and outflow pressure differences, respectively, in hPa.

Equation 3.1 is a storage equation: that is, precipitation equals inflow of water vapour minus outflow of water vapour. It may be derived as follows. Consider the mass transport through the slice of space bounded by two identical vertical planes, as in Figure 3.2, a short horizontal distance  $s$  apart. The storage equation for water vapour is:

$$M_r = (M_v)_1 - (M_v)_2 \quad (3.2)$$

where  $M_r$  is the rate of conversion of water vapour to precipitation in g/s;  $(M_v)_1$  is the rate of inflow of water vapour in g/s; and  $(M_v)_2$  is the rate of outflow of water vapour in g/s.

The values of these terms are given by:

$$W_r = R Y s p \quad (3.3)$$

$$(M_v)_1 = V_1 W_1 s p \quad (3.4)$$

$$(M_v)_2 = V_2 W_2 s p \quad (3.5)$$

where  $p$  is the density of water, which is 1.0 g/cm<sup>3</sup>, and  $s$  is in cm. The mass of air flowing in equals the mass flowing out if no allowance is made for the mass of precipitation which falls, which is relatively very small and may be neglected. The continuity equation is expressed by:

$$V_1 \Delta P_1 = V_2 \Delta P_2 \quad (3.6)$$

Combining Equations 3.2–3.6 and solving for  $R$  yields Equation 3.1.

### 3.2.2.2 Multiple-layer laminar flow model

Greater precision requires dividing the air into several layers of flow, as in Figure 3.3, rather than treating it as a single layer. Equation 3.1 applies to each of these layers. Total precipitation is then obtained by adding the rates from all layers. With several layers, it is more convenient to use the storage equation in the following form:

$$R = \frac{\bar{V}_1 \Delta P_1 (\bar{q}_1 - \bar{q}_2)}{Y} \frac{1}{g p} \quad (3.7)$$

where  $\bar{V}_1$  and  $\Delta P_1$  refer to the inflow in a particular layer; and  $\bar{q}_1$  and  $\bar{q}_2$  are the mean specific humidities in g/kg at inflow and outflow, respectively. The mixing ratio  $w$  is often substituted for specific humidity  $q$ . The terms  $g$  and  $p$  refer to the acceleration due to gravity in cm/s<sup>2</sup> and the density of water in g/cm<sup>3</sup>, respectively.

Equation 3.7 is derived from the relation between specific humidity and precipitable water:

$$W = \frac{\bar{q} \Delta P}{g p} \quad (3.8)$$

Substituting this relation into Equation 3.1 yields:

$$R = \frac{\bar{q}_1 \Delta P_1}{g p} - \frac{\bar{q}_2 \Delta P_2}{g p} \frac{\Delta P_1}{\Delta P_2} \quad (3.9)$$

This reduces to Equation 3.7.

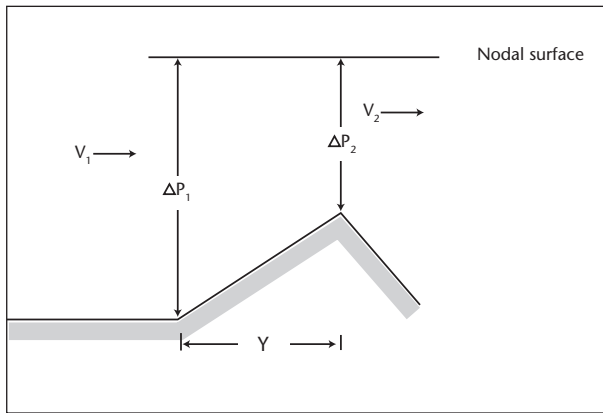


**Figure 3.2. Single-layer laminar flow wind model**

An approximate relation often substituted for Equation 3.7 is:

$$R \approx \frac{0.0102 \bar{V}_1 \Delta P_1 (\bar{w}_1 - \bar{w}_2)}{Y} \quad (3.10)$$

where  $R$  is the rainfall rate in mm/h;  $\bar{V}_1$  is the mean inflow wind speed in knots;  $P_1$  is the pressure difference between the top and bottom of an inflow layer in hPa;  $\bar{w}_1$  and  $\bar{w}_2$  are the mean mixing ratios in g/kg, at inflow and outflow, respectively; and  $Y$  is the horizontal length of the slope in nautical miles (nmi).

Equation 3.10 is derived from the approximate relation between the mean mixing ratio  $w$  and precipitable water  $W$ :

$$W \approx 0.0102 \bar{w} \Delta P \quad (3.11)$$

where  $W$  is in mm;  $\bar{w}$  in g/kg;  $\Delta P$  in hPa; and the coefficient 0.0102 has the dimensions mm/hPa kg/g. Substituting this relation into Equation 3.1 and using larger units of  $V$  and  $Y$  yields Equation 3.10.

### 3.2.2.3 Precipitation trajectories

The distribution of precipitation along a windward slope requires construction of snow and raindrop trajectories from the level of their formation to the ground. These trajectories are considered along with streamlines of the airflow over a ridge, as shown in Figure 3.3. The computation of precipitation trajectories is described in the following example of a test of the orographic model against observed storm rainfall.

### 3.2.3 Test of orographic laminar flow model on an observed storm

The following example of the use of the model was selected from PMP studies for the Sierra Nevada and

Cascade Range near the west coast of the United States (United States Weather Bureau, 1961a, 1966). Figure 3.4 shows a map of the test area with some of the precipitation stations and generalized terrain. Figure 3.5 shows the smoothed average ground elevation profile used for the computations. The elevations of the precipitation stations are plotted to show how well they fit the profile. The storm period selected for testing was the 6-hour period ending at 8 p.m., 22 December 1955. The 3 p.m. upper-air sounding on 22 December 1955 at Oakland, California, approximately 160 km south-west of the inflow end (south-western side) of the test area, was used for inflow data. Precipitation computations will be shown for the last segment, or the portion of the windward slope near the crest. The following steps are recommended in computing orographic precipitation over the slope.

#### 3.2.3.1 Ground profile

Determine the ground profile of the area under consideration and divide it into segments at each break in the profile. Long segments may be subdivided. In Figure 3.6, since the slope is fairly uniform, the first nine segments, or legs, have been made of equal length 9.7 km (5.2 nmi). The length of the last leg is 6.4 km (3.5 nmi), so the total distance from inflow to outflow is 93.3 km (50.3 nmi).

Convert heights of ground profile (Figure 3.5) to pressures by means of the pressure-height curve constructed from the inflow sounding of pressure, temperature and relative humidity. Plot these

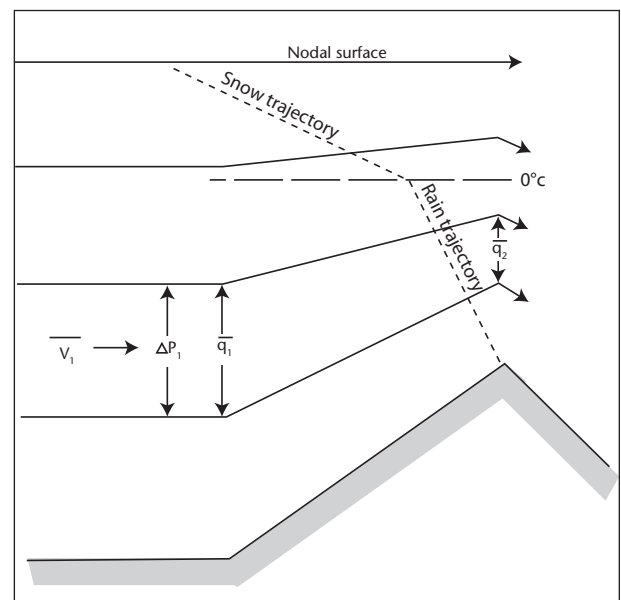


**Figure 3.3. Multiple-layer laminar flow wind model**

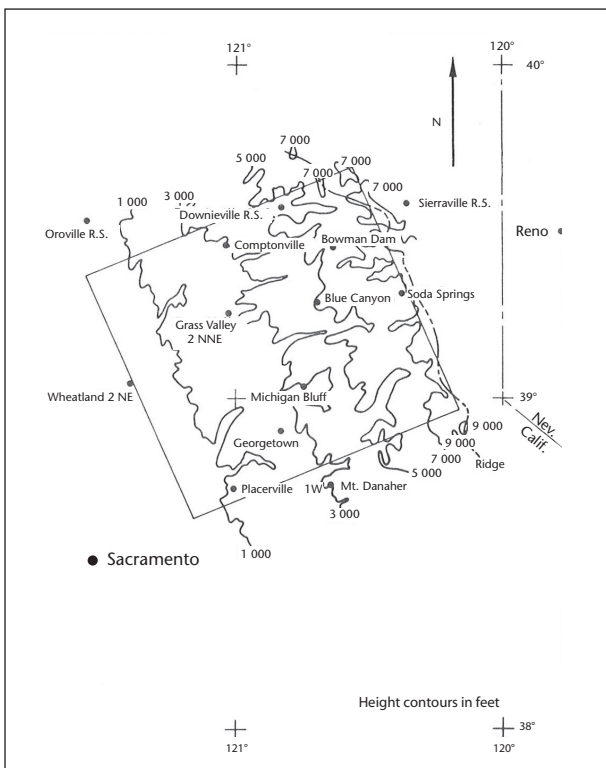


**Figure 3.4. Blue Canyon orographic laminar-flow model test area in California  
(United States Weather Bureau, 1966)**

pressures at the end of each leg, and draw the ground profile as shown in Figure 3.6. (Until some way is found to take downslope motion of air into account in computing precipitation, it is recommended that any downslopes in the ground profile

be drawn horizontal.) Construct verticals at the inflow and outflow ends of the model and at the end of each leg.

### 3.2.3.2 Inflow data

The inflow data used in the example are tabulated in the first eight columns of Table 3.1. These data were obtained from the sounding. The wind speeds are the components normal to the mountain ridge, that is,  $V = V_o \cos(\alpha)$ , where  $V_o$  is the observed wind speed from the observed direction and  $\alpha$  is the angle between the observed direction and the normal to the ridge.

### 3.2.3.3 Air streamlines

Space the streamlines at the inflow vertical in the manner indicated in Figure 3.6. There, the first streamline above the surface streamline is set at 1 000 hPa. Streamlines are then spaced at 25-hPa intervals up to the 800-hPa level, then at every 50 hPa up to the nodal surface, which is assumed to be at 350 hPa. Streamlines at the outflow vertical and intermediate verticals are spaced in proportion to the spacing at inflow. Spacing may be done either graphically or by mathematical interpolation.

### 3.2.3.4 Freezing level

As the air travels along any streamline, its pressure, temperature and mixing ratio at any point on the streamline may be determined from a pseudo-adiabatic chart. Determine the pressure at the freezing point on those streamlines where the 0°C

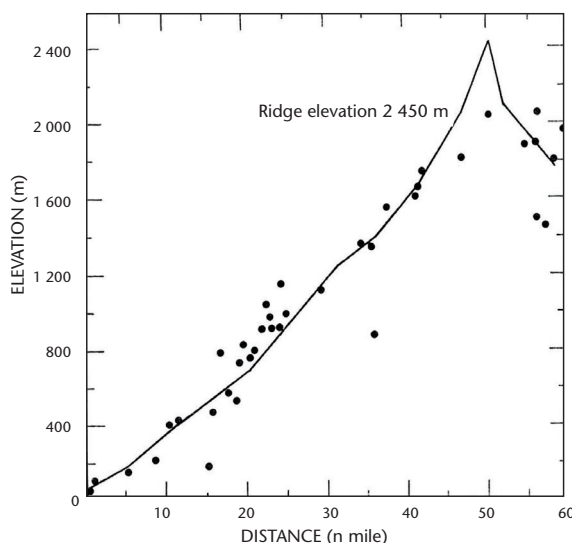


**Figure 3.5. Precipitation station elevations relative to adopted ground profile for test area of Figure 3.4  
(United States Weather Bureau, 1966)**

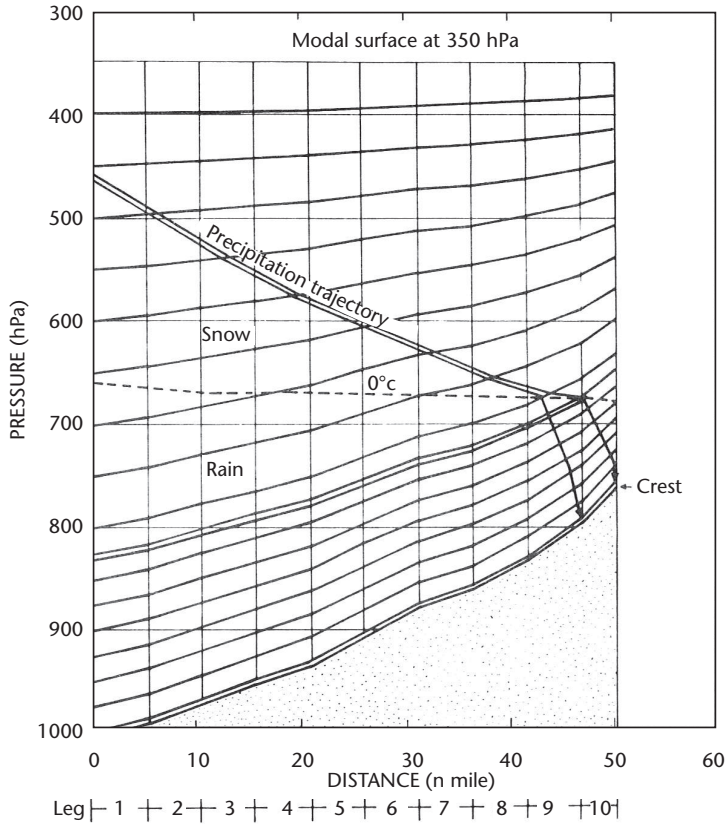


**Figure 3.6. Air streamlines and precipitation trajectories for test case**

temperature occurs between inflow and outflow. (See discussion of Table 3.2 in section 3.2.3.5.) Plot these points on their respective streamlines, and draw the freezing line as shown in Figure 3.6. Precipitation is assumed to fall as snow above the freezing line and as rain below.

### 3.2.3.5 Precipitation trajectories

The path followed by falling precipitation particles is determined by three components: (a) vertical fall due to gravity; (b) horizontal drift caused by the horizontal component of the wind; and (c) vertical rise resulting from the upward component of the wind as it flows along the streamlines.

The average falling rate of precipitation particles in orographic storms affecting the test area has been taken as 6 m/s for rain and 1.5 m/s for snow. For computational purposes, these values have been converted to 2 160 hPa/hour and 453 hPa/h, respectively.

The horizontal drift of precipitation particles while falling from one streamline to another is  $\frac{\bar{V}\Delta P}{\text{rate of fall}}$

where  $\bar{V}$  is the mean horizontal wind speed, in knots, in the layer between streamlines;  $P$  is the thickness of the layer in hPa; and rate of fall is in hPa/hour. Since  $\bar{V}\Delta P$  is constant between any two streamlines, drifts computed at inflow may be used anywhere between the same two streamlines. In Table 3.2, horizontal rain drift (DRR) and horizontal snow drift (DRS) between streamlines are shown in columns 6 and 7. Drifts are in nautical miles (nmi) since  $\bar{V}$  is in knots. The effect of the upward component of the wind is automatically taken into account by the slope of the streamlines.

Precipitation trajectories are computed from the ground up, starting at the ends of the selected legs of the ground profile. Plotting points for two trajectories are computed in Table 3.2: one, called upper (UT), beginning at outflow, or 50.3 nmi from inflow; and the other, called lower (LT), beginning at the end of the ninth leg, or 46.8 nmi from inflow. Columns 8 and 9 of Table 3.2 give accumulated horizontal drifts from the vertical passing through the ground point of each of these trajectories. Columns 10 and 11 give corresponding distances from the inflow vertical.

**Table 3.1. Computation of orographic precipitation over leg 10 of Blue Canyon, California, test area for the 6-hour period 2 p.m.–8 p.m., 22 December 1955 (hand computation, using 3 p.m. 22 December 1955 sounding at Oakland, California, as inflow data and assuming a nodal surface of 350 hPa)**

Inflow data										$\Delta \bar{W}_{LT}$		$\Delta \bar{W}_{UT}$							
P (hPa)	T (°C)	RH (%)	V (kn)	$\bar{V}_{\Delta P}$ (kn)	w <sub>s</sub> (g/kg)	w <sub>I</sub>	P <sub>c</sub>	P <sub>LT</sub>	w <sub>LT</sub>	P <sub>UT</sub>	w <sub>UT</sub>	$\bar{W}_I$	$\bar{W}_{LT}$	$\bar{W}_{UT}$	$\bar{W}_I - \bar{W}_{LT}$	$\bar{V}_{\Delta P} \Delta \bar{W}_{LT}$	$\bar{W}_I - \bar{W}_{UT}$	$\bar{V}_{\Delta P} \Delta \bar{W}_{UT}$	
500	-12.3	77	61.8	59.6	2980	2.96	2.28	475	494	2.28	495	2.28	2.70	2.70	2.70	0.00	0	0.00	0
550	-8.1	82	57.4	62.7	3135	3.80	3.12	529	537	3.12	536	3.12	3.61	3.53	3.52	0.08	251	0.09	282
600	-4.2	88	67.9	62.8	3140	4.65	4.09	543	575	4.09	574	3.92	4.64	4.22	4.20	0.42	1319	0.44	1382
650	-0.6	92	57.6	55.1	2755	5.64	5.19	638	604	5.19	602	4.47	5.72	4.73	4.69	0.99	2727	1.03	2838
700	1.6	94	52.6	49.8	2490	6.64	6.24	692	630	6.24	628	4.90	6.69	5.18	5.11	1.51	3760	1.56	3864
750	5.3	95	47.0	50.1	2505	7.50	7.13	742	656	7.13	654	5.36	7.55	5.51	5.45	2.04	5110	2.10	5261
800	7.9	95	51.1	51.4	1285	8.38	7.96	792	672	7.96	649	5.54	8.20	5.75	5.57	2.45	3148	2.63	3180
825	9.1	96	49.6	49.2	295	8.79	8.44	817	688	8.44	672	5.60	8.50	5.92	5.61	2.58	761	2.89	153
831	9.4	96	48.7	47.2	897	8.92	8.56	823	693	8.56	673	5.62	8.75	6.09	5.69	2.66	2386	3.06	2745
850	10.3	96	45.7	44.2	1105	9.30	8.93	843	703	8.93	680	5.76	9.13	6.34	5.84	2.79	3083	3.27	3613
875	11.4	96	42.7	42.7	1068	9.71	9.32	868	718	9.32	694	5.95	9.44	6.51	6.00	2.95	3151	3.46	3695
900	12.5	94	42.7	41.9	1048	10.20	9.59	888	732	9.59	705	6.05	9.69	6.59	6.06	3.10	3249	3.63	3804
925	13.4	93	41.1	37.6	940	10.52	9.79	911	746	9.79	717	6.07	9.81	6.64	6.09	3.17	2980	3.72	3497
950	14.2	91	34.1	29.9	748	10.80	9.83	929	760	9.83	721	6.10	9.63	6.57	5.94	3.06	2289	3.69	2760
975	15.0	85	25.7	19.4	485	11.10	9.43	941	776	9.43	740	5.78	9.42	6.42	5.76	3.00	1455	3.66	1775
1000	15.5	84	13.1	11.1	56	11.20	9.41	961	790	9.41	753	5.73	9.55	6.48	5.80	3.07	172	3.75	210
1005	15.7	84	9.1			11.27	9.69	971	793	9.69	754	5.87							

Legend: RH = Relative humidity

w<sub>s</sub> = Saturation mixing ratio

w<sub>I</sub> = Mixing ratio at inflow

P<sub>c</sub> = Condensation pressure

LT = Lower precipitation trajectory

UT = Upper precipitation trajectory

$$I = 35\ 841 \quad 39\ 979$$

$$\text{6-hour volume (mm} \times \text{nmi}^2) = 0.0612 \times I = 2\ 193 \quad 2\ 447$$

$$\text{Unit-width horizontal area (nmi}^2) = 46.8 \quad 50.3$$

$$\text{6-hour average rainfall (mm)} = 47 \quad 49$$

$$\text{6-hour average rainfall over last leg (mm)} = \frac{2\ 447 - 2\ 193}{50.3 - 46.8} = 73$$

Rain drift is used below the freezing level; snow drift, above. By coincidence, the lower trajectory (Figure 3.6) reaches the freezing level approximately where the latter intersects a streamline. The upper trajectory, however, reaches the freezing level between the 850- and 825-hPa inflow streamlines. Hence, a streamline passing through the intersection of this trajectory and the 0°C line is constructed. This streamline intersects the inflow vertical at 831 hPa. Since the snow drift in the 831- to 825-hPa layer is 0.65 nmi (Table 3.2), the total drift measured from the outflow vertical to the 825-hPa streamline would be  $2.95 + 0.65 = 3.60$  nmi, which would take the trajectory below the freezing level. Hence, total drift was assumed to be 3.47 nmi, which means that the drift within this layer was assumed to be 0.52 nmi rather than 0.65 nmi. Since the snow in this layer is probably very wet, the falling rate is likely to be between that for snow and that for rain, and the above assumption appears warranted.

### 3.2.3.6 Precipitation computation

After constructing the precipitation trajectories, compute the total volume of precipitation under each trajectory, layer by layer. Subtract the total volume under one trajectory from the volume under the next higher one, and divide the difference by the horizontal area of the ground on which this volume falls to obtain the average depth over this area.

If Equation 3.10 for rainfall rate is multiplied by the area XY it yields the 1-hour rainfall volume. The Y in the numerator and denominator cancel one another, and if area width X is taken as 1 nmi, the 1-hour volume R(XY) or Vol<sub>1 hour</sub> under a particular trajectory is approximately:

$$\text{Vol}_{1 \text{ hour}} \approx 0.0102 \bar{V}_1 \Delta P_1 (\bar{W}'_1 - \bar{W}') \quad (3.12)$$

where  $\bar{W}'$  is the mean outflow mixing ratio at the trajectory (see  $\bar{q}$  in Figure 3.3).

**Table 3.2. Computation of rain and snow drift for computing precipitation trajectories over Blue Canyon, California, test area (based on sounding of 3 p.m. 22 December 1955 at Oakland, California)**

P (hPa)	Inflow data					DRR (nmi)	DRS (nmi)	(UT) $\sum$ DRIFT (nmi)	(LT) $\sum$ DRIFT (nmi)	(UT) 50.30 – $\sum$ DRIFT (nmi)	(LT) 46.80 – $\sum$ DRIFT (nmi)
	V (kn)	$\bar{V}$ (kn)	$\Delta P$ (mb)	$\bar{V}_{\Delta P}$	(1)						
	(2)	(3)	(4)	(5)	(6)	(7)	(8)	(9)	(10)	(11)	
350	97.7	81.9	50	4 095	1.90	9.04					
400	66.1	68.6	50	3 430	1.59	7.57					
450	71.0	66.4	50	3 320	1.54	7.33	51.18 <sup>a</sup>	48.55 <sup>a</sup>	-0.88	-1.75	
500	61.8	59.6	50	2 980	1.38	6.58	43.85 <sup>a</sup>	41.22 <sup>a</sup>	6.45	5.58	
550	57.4	62.7	50	3 135	1.45	6.92	37.27 <sup>a</sup>	34.64 <sup>a</sup>	13.03	12.15	
600	67.9	62.8	50	3 140	1.45	6.93	30.35 <sup>a</sup>	27.72 <sup>a</sup>	19.95	19.08	
650	57.6	55.1	50	2 755	1.28	6.08	23.42 <sup>a</sup>	20.79 <sup>a</sup>	26.88	26.01	
700	52.6	49.8	50	2 490	1.15	5.50	17.34 <sup>a</sup>	14.71 <sup>a</sup>	32.96	32.09	
750	47.0	50.1	50	2 505	1.16	5.53	11.84 <sup>a</sup>	9.21 <sup>a</sup>	38.46	37.59	
800	53.1	51.4	25	1 285	0.59	2.84	6.31 <sup>a</sup>	3.68	43.99	43.12	
825	49.6	49.2	6	295	0.14	0.65	3.47 <sup>b</sup>	3.09	46.83	43.71	
831	48.7	47.2	19	897	0.42	1.98	2.95	2.95	47.35	43.85	
850	45.7	44.2	25	1 105	0.51	2.44	2.53	2.53	47.77	44.27	
875	42.7	42.7	25	1 068	0.49	2.36	2.02	2.02	48.28	44.78	
900	42.7	42.7	25	1 048	0.49	2.31	1.53	1.53	48.77	45.27	
925	41.1	37.6	25	940	0.44	2.08	1.04	1.04	49.26	45.76	
950	34.1	29.9	25	748	0.35	1.65	0.60	0.60	49.70	46.20	
975	25.7	19.4	25	485	0.22	1.07	0.25	0.25	50.05	46.55	
1 000	13.1	11.1	5	56	0.03	0.12	0.03	0.03	50.27	46.77	
1 005	9.1						0	0	50.30	46.80	

<sup>a</sup> Using snow drift<sup>b</sup> Arbitrary (to keep trajectory on or above freezing line)Legend: DRR =  $\bar{V}_{\Delta P}/2 160$  = Horizontal rain driftDRS =  $\bar{V}_{\Delta P}/453$  = Horizontal snow drift

UT = Upper precipitation trajectory

LT = Lower precipitation trajectory

The orographic model is generally used to compute rainfall by 6-hour increments, so Equation 3.12 becomes:

$$\text{Vol}_{6 \text{ hour}} \approx 0.0612 \bar{V}_1 \Delta P_1 (\bar{W}'_1 - \bar{W}') \quad (3.13)$$

where  $\text{Vol}_{6 \text{ hour}}$  is in mm (nmi)<sup>2</sup>;  $\bar{V}_1$  in kn;  $\Delta P_1$  in hPa;  $(\bar{W}'_1 - \bar{W}')$  in g/kg; and the coefficient 0.0612 has the dimensions nmi hour (6 hour)<sup>-1</sup> kg/g mm/hPa.

Table 3.1 shows the computation of orographic rainfall under the two precipitation trajectories shown in Figure 3.6. The following example demonstrates how the table was prepared.

Consider the layer between the streamlines passing through inflow pressures 850 and 875 hPa

( $P = 25$  hPa). The air at 850 hPa has a temperature of 10.3°C, relative humidity 96 per cent, and horizontal component of wind speed parallel to the sides of the selected ground area of 45.7 kn. Plotting 10.3°C at 850 hPa on a pseudo-adiabatic chart, the saturation mixing ratio is seen to be about 9.30 g/kg. The actual mixing ratio is 96 per cent of this, or 8.93 g/kg.

From Figure 3.6, the pressures where the streamline through 850 hPa intersects the two precipitation trajectories are seen to be 703 and 680 hPa. Following the dry adiabat through 850 hPa and 10.3°C upward to where it crosses the saturation mixing ratio of 8.93 g/kg, the condensation pressure is seen to be about 843 hPa and the temperature 9.6°C (not shown). Since the air is now saturated, the moist adiabat is followed

**Table 3.3. Comparison of observed and computed 6-hour precipitation for the period 2 p.m.–8 p.m., 22 December 1955 over Blue Canyon, California, test area**

	Leg										Average
	1	2	3	4	5	6	7	8	9	10	
Horizontal length of leg (nm)	5.2	5.2	5.2	5.2	5.2	5.2	5.2	5.2	5.2	3.5	
Cumulative length (nm)	5.2	10.4	15.6	20.8	26.0	31.2	36.4	41.6	46.8	50.3	
Elevation at end of leg (m)	180	366	543	707	978	1244	1414	1689	2060	2 448	
Observed precipitation (mm)	3	6	13	25	38	46	55	64	67	65	37
Machine-computed precipitation 1	0	14	40	44	55	66	54	60	67	72	46
Machine-computed precipitation 2	1	17	44	45	56	66	55	59	67	69	47
Hand-computed precipitation										73	49

Notes: Elevation at beginning of first leg = 61 m.

Machine-computed precipitation 1 used spacing of streamlines by a method developed by Myers.

Machine-computed precipitation 2 used spacing of streamlines between surface and 350-hPa nodal surface (assumed), along any vertical, proportional to their spacing at inflow.

Hand-computed average precipitation over leg 10 and legs 1–10 based on the same spacing of streamlines as machine-computed precipitation 2.

upward from this point. The saturation mixing ratio on this moist adiabat is about 6.22 g/kg at 703 hPa and about 5.76 g/kg at 680 hPa. The mixing ratio values on the 875-hPa streamline at the lower and upper precipitation trajectories are found in the same way.

For the 850- to 875-hPa layer,  $\bar{V}$  is then seen to be 44.2 kn,  $\Delta P = 1105$  kn mb,  $\bar{W}_1 = 9.13$  g/kg,  $\bar{W}_{LT} = 6.34$  g/kg for the lower trajectory, and  $\bar{W}_{UT} = 5.86$  g/kg for the upper trajectory. The decrease in mean mixing ratio of the layer from inflow to lower trajectory,  $\Delta \bar{W}_{LT} = 2.79$  g/kg and to the upper trajectory,  $\Delta \bar{W}_{UT} = 3.27$  g/kg. For the layer, the value of  $\bar{VPW}$  is 3 083 nmi/hour hPa g/kg between inflow and lower precipitation trajectory and 3 613 nmi/hour hPa g/kg between inflow and upper trajectory.

After values of  $\bar{VPW}$  are computed for all layers for all trajectories, values for each trajectory are summed and multiplied by 0.0612 nmi hour (6 hour)<sup>-1</sup> kg/g mm/hPa to obtain values in mm nmi<sup>2</sup> (6 hour)<sup>-1</sup>. In Table 3.1 these values are 2 193 for the lower trajectory and 2 447 for the upper trajectory. Division by the areas over which these volumes fall gives average depths for those areas. Since unit width is assumed for Figure 3.6, any such area is numerically equal to the sum of the lengths of the legs between inflow and a given precipitation trajectory. For the lower trajectory this is the sum of the lengths of legs 1–9, or 46.8 nmi<sup>2</sup>, which makes the 6-hour average depth over those legs 47 mm. For the upper trajectory,

the volume falls over legs 1–10, or 50.3 nmi<sup>2</sup>, giving a 6-hour average depth of 49 mm. The volume that falls on leg 10 alone is the difference between the volumes under upper and lower trajectories, or 254 mm nmi<sup>2</sup> (6 hour)<sup>-1</sup>. This is distributed over 3.5 nmi<sup>2</sup>, which makes the 6-hour average depth 73 mm.

### 3.2.3.7 Comparison of results

The above procedure has been computerized to facilitate complete computations for numerous areas and soundings. Another computerized version of the orographic model is somewhat more sophisticated than the one just described. Whereas in the example model the height of the nodal surface was assumed and an approximate method used for spacing streamlines at the outflow over a mountain crest, this second computer model uses a nodal surface and streamline spacing based on physical laws of air flow (Myers, 1962). The outflow approximations used in the above example give results comparable with those of the more sophisticated model. Table 3.3 compares the results yielded by the two computerized models for each of the ten legs for a 6-hour period and by the manual application just described for the tenth leg.

The so-called observed precipitation used in the comparison of Table 3.3 refers to the orographic component only. Ordinarily, this would be obtained by subtracting from the observed total precipitation for each leg the precipitation measured in the flat valley upwind of the test area

during the 6-hour period of the test. This valley precipitation (the convergence component of total precipitation), which is sometimes reduced for elevation, is attributed to atmospheric processes not directly related to orography. In the test case described, however, there was no appreciable valley precipitation so no deduction was made from observed precipitation.

### 3.2.3.8 Sources of error

Differences between precipitation computed by the model and observed orographic precipitation (total precipitation minus convergence component) can be attributed to two main sources: (a) errors of input to the model; and (b) sparsity and unrepresentativeness of precipitation data for checking model computation.

#### 3.2.3.8.1 *Input to the model*

Usually, no more than two upper-air observations are made daily. Despite utmost care in interpolating for a particular storm period by referring to the more frequent surface synoptic charts, the question remains as to the representativeness of instantaneous wind and moisture values for even a short period of a few hours. Such inaccuracies lead to errors in computed amounts of precipitation.

In the example given, no allowance was made for the fact that the upper-air sounding station (Oakland) is approximately 160 km from the test area, and moisture and wind values were taken directly from the sounding. Attempts to adjust for wind travel time (averaging less than 2 hours) did not improve results.

#### 3.2.3.8.2 *Observed orographic precipitation*

The uneven distribution of storm precipitation, with respect both to time and to space, the sparseness of the precipitation network, and the usual errors of gauge measurements make it difficult to obtain reliable averages of storm precipitation on slopes. Also, most gauges in orographic regions are located in narrow valleys or on relatively flat sites unrepresentative of nearby elevations or the generalized ground profile. Their measurements, while perhaps acceptably representative of actual precipitation at the gauge sites, are unlikely to represent with any great accuracy the average precipitation falling on the general slope. These various factors make it difficult to obtain reliable values of observed storm precipitation on a slope for comparison with model computations.

## 3.3

### APPLICATION OF A LAMINAR FLOW MODEL IN THE OROGRAPHIC SEPARATION METHOD FOR ESTIMATING PMP

Reference was made earlier to the fact that precipitation in mountainous regions consists of two components: (a) orographically induced precipitation (orographic precipitation), and (b) precipitation produced by atmospheric processes unrelated to orography (convergence precipitation). PMP is computed, therefore, by maximizing and adding the two precipitation components. Caution must be exercised to avoid over-maximizing. Caution must also be used and this model applied only where the assumption of laminar flow is realistic (sections 3.2.1, 3.2.2, 3.4.1 and 3.5.2). In other regions, procedures discussed in section 3.4 or Chapters 5 and 6 may be more appropriate.

#### 3.3.1 **Orographic PMP**

The procedure used in applying the orographic model for computing the orographic component of PMP is the same as that used in testing the model (section 3.2.3) with the exception that inflow winds and moisture are maximum values.

##### 3.3.1.1 **Maximum winds**

If there is a long record of upper-air winds, say 30 years or longer, an envelope of the highest recorded speeds for winds from critical directions for each month or part of the month is usually adequate. The probability of occurrence of any of the envelope values is determined by statistical analysis. Such analysis may be used also to estimate high wind speeds, say for a 50-year return period, when the record is so short as to introduce doubt as to its maximum values being representative of those that would be obtained from a longer record. If the record is so short as to preclude reliable frequency analysis, say less than 10 years, maximum wind speeds may be estimated from surface pressure gradients between suitably located stations. Maximum surface winds so determined may then be used to estimate upper-air wind speeds by means of empirical relations (United States Weather Bureau, 1961a).

Figure 3.7 shows the maximum wind speed profile used for the coastal region of California. The variation with duration (Figure 3.8) was based on that of geostrophically derived winds and of 900 hPa winds at Oakland during selected storm periods.

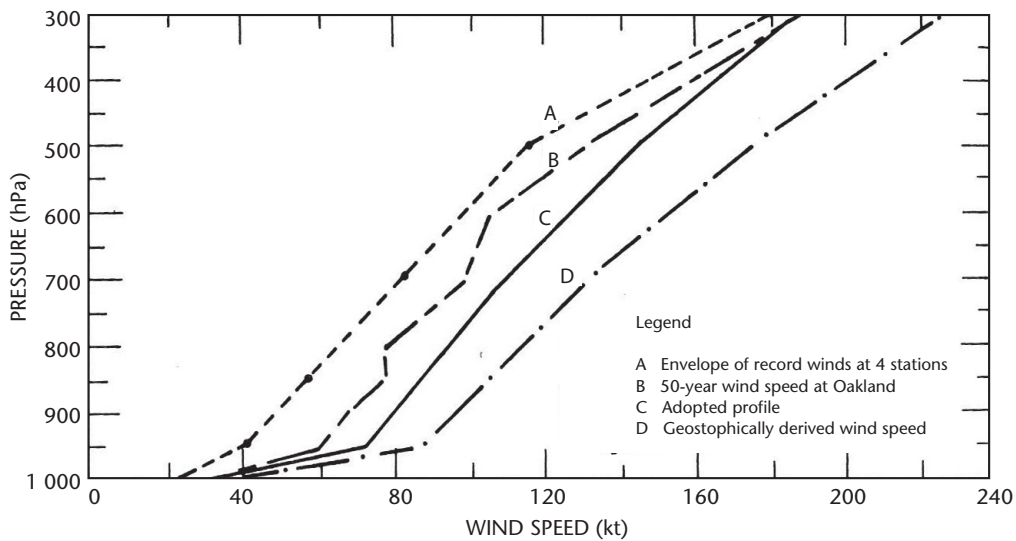


**Figure 3.7. Maximum 1-hour wind profile and supporting data (United States Weather Bureau, 1961b)**

### 3.3.1.2 Maximum moisture

Maximum values of moisture are obtained from maximum persisting 12-hour 1 000-hPa dewpoints. A full discussion of these dewpoints is given in section 2.2.

### 3.3.2 Generalized estimates of orographic PMP

One method of applying the model for developing generalized estimates of PMP is to define terrain profiles over the entire region of interest. If the topography is relatively uncomplicated and all general windward slopes face one most critical moisture-inflow direction, as in the California Sierra Nevada, application of this procedure presents no special problems.

An alternative method is to use the model to compute PMP for selected terrain profiles and to evaluate PMP between them by means of maps, such as mean seasonal, annual precipitation or precipitation-frequency maps, which adequately depict the geographic distribution of precipitation. In this approach, it must be shown first that there is good correlation between computed orographic PMP on the selected computation profiles, or areas, and the values indicated by reference maps used for interpolation.

A somewhat different approach was used (United States Weather Bureau, 1966) for regions where the optimum moisture-inflow direction and orientation of slopes varied from place to place. The procedure

consists of computing PMP for terrain profiles oriented in different directions and then enveloping the greatest values regardless of inflow direction or slope orientation. Relations are then developed for adapting the envelope values to inflow directions and slope orientations critical for a specific basin. A simple but adequate method for making such adaptations is to use a variation with basin size, since the variety of optimum inflow directions and slope orientations tends to increase with size of area. This type of adjustment was used in a study for the north-western United States (United States Weather Bureau, 1966). In the California study (United States Weather Bureau, 1961a), the adjustment was based on the decrease of moisture with increasing width, or lateral extent, of inflow in observed major orographic storms (section 3.3.3).

Generalized estimates of PMP are usually presented on an index map showing isohyets of PMP for a particular duration, size of area and month. Relations are then provided for adjusting the mapped PMP values to other durations, basin sizes, and months.

Figure 3.9 shows the January 6-hour orographic PMP index map developed in the aforementioned California study. This particular map does not specify an area size. In this case, the average index value for any specified basin is obtained by laying an outline of the basin on the index map and then estimating the average of the values within the outline. No further areal adjustment is required unless the width of the basin exposed or normal to the optimum moisture inflow exceeds 50 km (section 3.3.3).

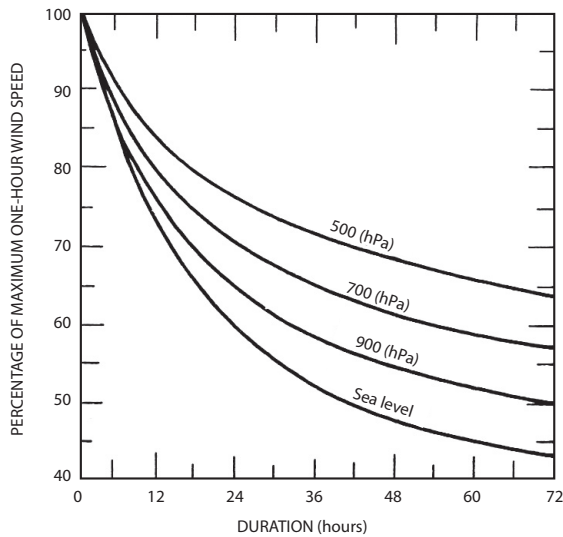


**Figure 3.8. Variation of maximum 6-hour wind speed with time  
(after United States Weather Bureau, 1961a)**

### 3.3.3 Variations in orographic PMP

As mentioned, PMP varies with region, season, duration and size of area. The generalized maps show the regional variation, and no further discussion is required. While the discussion of the other variations presented in this section applies particularly to the orographic separation method, especially as used in the California study given as an example, much of it applies to variations of orographic PMP in general.

#### 3.3.3.1 Seasonal variation

In any region where snowmelt or the occurrence of frozen ground is likely to contribute significantly to the probable maximum flood, it is necessary to determine the seasonal variation of PMP. In orographic regions the seasonal variation should be determined even when snowmelt or frozen ground is not involved in order to ensure that the month of highest potential for total PMP (orographic plus convergence) has not been overlooked. A logical procedure is to compute PMP for each month on the basis of maximum values of wind and moisture in each month. The seasonal variation of major storms recorded over a long period is generally a useful guide in delineating the seasonal variation of PMP.

Evaluation of seasonal variation of orographic PMP by means of the model has several shortcomings. In the transitional seasons (spring and autumn), the usual orographic influences prevail, but stimulation of storm precipitation by upwind slopes or barriers is

often most effective in determining precipitation distribution. The need for generalizing topography leads to differences between computed orographic PMP and that indicated by the actual terrain. For different terrain profiles, seasonal influences may vary with barrier height, steepness of slope and other features. In some cases, a compromise between seasonal variation indicated by computed orographic PMP values and that based on maximum storm rainfall amounts observed at well-exposed stations may yield the most realistic results.

#### 3.3.3.2 Durational variation

Variations in maximum wind speeds and moisture with time are used to determine durational variation of computed orographic PMP. The variation of winds in major observed storms is probably the best type of information to use in establishing variations in the shape of the inflow profile with duration, and this was used in the example study. Variation of moisture with time was based on the durational variation of maximum persisting 1 000-hPa dewpoints (United States Weather Bureau, 1958). Moisture values at upper levels were based on the assumption of a saturated pseudo-adiabatic lapse rate. A common durational variation (Figure 3.10) for all months and regions was adequate for the example study. An additional factor found helpful in some studies (United States Weather Bureau, 1966) is the variation of moisture with duration during major observed storms.

#### 3.3.3.3 Areal variation

The variation of orographic PMP with basin size is controlled by the orography, and therefore, may vary greatly from basin to basin. As stated in section 3.3.2, the averaging of index PMP by superimposing an outline of the basin on the index map eliminates the need for the usual type of depth-area relation. The average index PMP thus obtained usually requires some adjustment for basin size, however, since the intensity of moisture inflow decreases with increasing width of inflow. In the example study (United States Weather Bureau, 1961a), no adjustment was required for basin widths up to 50 km, but a reduction curve for greater widths reduced the basin average index PMP by 15 and 25 per cent for widths of 160 and 300 km, respectively.

#### 3.3.4 Convergence PMP for combination with orographic PMP

The procedure described here for estimating convergence (non-orographic) PMP for combination with orographic PMP was developed for the coastal



**Figure 3.9.** Six-hour orographic PMP (inches) for January (square delineates Blue Canyon orographic model test area; United States Weather Bureau, 1961a)

regions of California (United States Weather Bureau, 1961a), where the critical season for major orographic storms is October to March. The approach, which has been used elsewhere, is basically similar to those used in estimating PMP for non-orographic regions. The greatest precipitation amounts for various durations at stations in the least orographically influenced areas are maximized for moisture. This is done in two steps. First, regional envelopes of maximum persisting 12-hour 1 000-hPa dewpoints are determined for use in evaluating maximum moisture  $M$ . Second, durational envelopes of maximum  $P/M$  ratios at each station are determined for each month. Here,  $P$  is the storm precipitation for a particular duration, and  $M$  is determined from the precipitable water  $W$  for the representative persisting 12-hour 1 000-hPa storm dewpoint (section 2.2.4).

$P/M$  ratios should be computed for several of the highest rainfalls at any particular station because

the maximum rainfall does not necessarily yield the highest  $P/M$  ratio. Maps of maximum moisture and  $P/M$  ratios are then drawn. Multiplication of corresponding values from appropriate pairs of maps yields moisture-maximized rainfall amounts for any required location, or  $(P/M)_{\max}$  multiplied by  $M_{\max}$  equals convergence PMP.

### 3.3.4.1 Moisture (dewpoint) envelopes

Maximum, or 100-year, persisting 12-hour 1 000-hPa dewpoints (section 2.2.5), enveloped seasonally at each station (Figure 3.11) and smoothed regionally (Figure 3.12), are used to establish the level of maximum moisture available for evaluating convergence PMP. In the example study (United States Weather Bureau, 1961a), one mean seasonal variation curve (not shown) was found applicable to the entire region of interest. Different seasonal trends for different portions of a region would affect only the details of application.

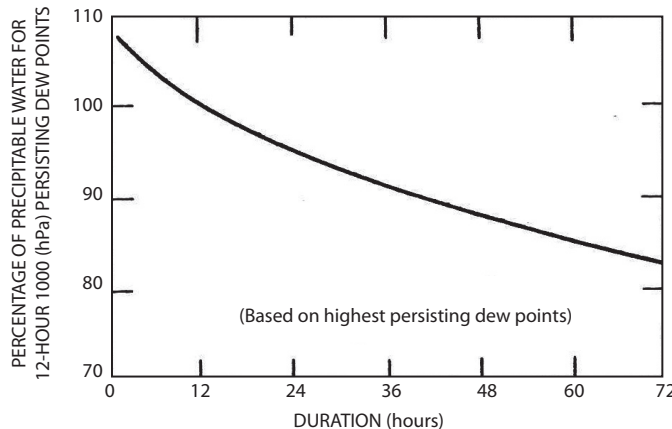


**Figure 3.10. Decrease of maximum precipitable water with duration  
(after United States Weather Bureau, 1958)**

### 3.3.4.2 Envelopes of $P/M$ ratios

Finding suitable station precipitation data uninfluenced by orography is a problem. In the example study, the search was confined to the large flat valley between the coastal mountains to the west and the Sierra Nevada to the east, and to some coastal stations unaffected by nearby steep slopes. Except for a few short intense rainfalls, most data were observation day or highest 24 consecutive 1-hour amounts. Envelope curves of highest  $P/M$  ratios found in the restricted region are shown in Figure 3.13.

Adequate data on intense rainfalls for establishing a seasonal trend in  $P/M$  ratios would have been desirable, but there were not enough of these data in the problem area. However, many plots of maximum 24-hour precipitation at non-orographic stations indicated no definite seasonal trend for any magnitude. On the other hand, such trends did exist for 6- and 72-hour precipitation (Figure 3.14).

It was concluded that seasonal trends of moisture and  $P/M$  ratios for the 24-hour duration must counteract each other since there was no trend in 24-hour precipitation. On the basis of this concept, the greatest 24-hour  $P/M$  ratio was assigned to February, the month having the lowest maximum precipitable water; and ratios for other months were evaluated in proportion to their maximum precipitable water, as indicated by their maximum persisting 12-hour dewpoints.

The ratios of 6- to 24-hour and 72- to 24-hour precipitation (Figure 3.14) were used to establish

$P/M$  ratios for 6 and 72 hours. This was possible since 12-hour moisture, the denominator  $M$  in the ratios, was used for all durations. The durational variation of  $P/M$  ratios is thus the same as the durational variation in precipitation  $P$ . Monthly curves of durational variation of  $P/M$  ratios are shown in Figure 3.13.

### 3.3.4.3 Reduction of convergence PMP for elevation

In the example study (United States Weather Bureau, 1961a), PMP values computed as described in the first two paragraphs of section 3.3.4 were reduced for elevation. For gently rising slopes where storm precipitation was apparently little affected by upwind barriers, the decrease in convergence PMP was assumed to be proportional to the decrease of precipitable water  $W$  in a saturated column of air. This decrease was computed as the difference between  $W$  in a column with the base at the ground elevation, at a point 8 km upwind from the problem area, and that with the base at the ground elevation of the convergence PMP. The 8 km distance upwind marks the average location of the formation of the storm precipitation particles falling on the problem area.

In estimating PMP by methods other than the orographic separation method, the usual procedure is to base the decrease on the difference between observed storm amounts on slopes and in valleys. In one study (United States Weather Bureau, 1961a), the non-orographic, or convergence, PMP was reduced by 5 per cent for every 300 m increase in elevation.

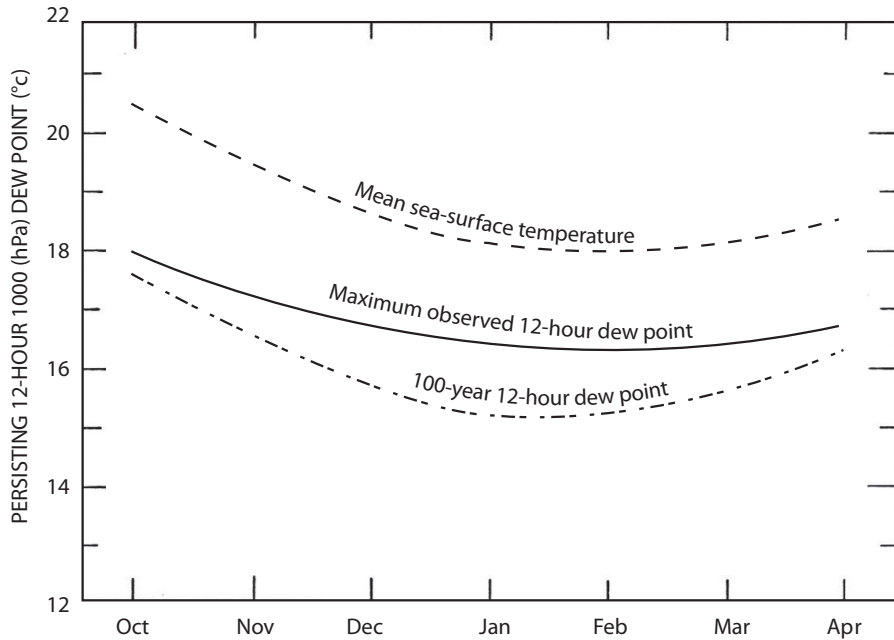


**Figure 3.11. Seasonal envelope of maximum observed dewpoints at Los Angeles, California (after United States Weather Bureau, 1961a)**

### 3.3.4.4 Reduction for upwind barriers

The amount of moisture that a column of air can contain is reduced by shortening the column as it crosses an orographic barrier. Convergence PMP is therefore adjusted for the moisture depletion by upwind barriers. In making the reductions, so-called effective barrier heights are used rather than actual heights. Maps of effective barrier heights (Figure 3.15) differ from actual topographic maps in that they take into account the effect of barriers on air crossing them. Also, since the maps are intended for use in making generalized estimates of PMP, effective barrier height contours naturally smooth out the smaller irregularities in crest height, ridge orientation, and other orographic features. Local features that would seriously affect precipitation over small basins are thus smoothed out.

### 3.3.4.5 Reduction of point, or 25.9 km<sup>2</sup>, convergence PMP for area size

Point precipitation data (arbitrarily accepted as representative for 25.9 km<sup>2</sup>) were used in the derivation of convergence PMP described above. Ideally, the 25.9 km<sup>2</sup> values would be reduced for area size by depth-area relations based on observed storms that produced heavy convergence (non-orographic) rainfalls in the problem area. Sparsity

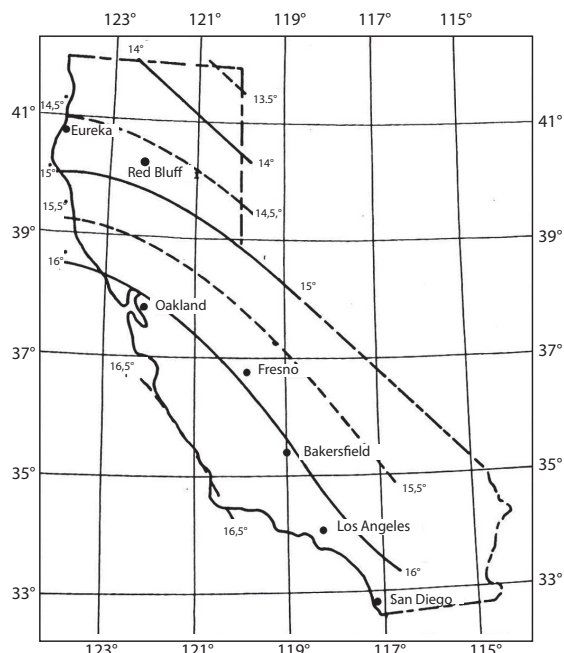


**Figure 3.12 Maximum persisting 12-hour 1 000-hPa dewpoints (°C) for February (United States Weather Bureau, 1961a)**

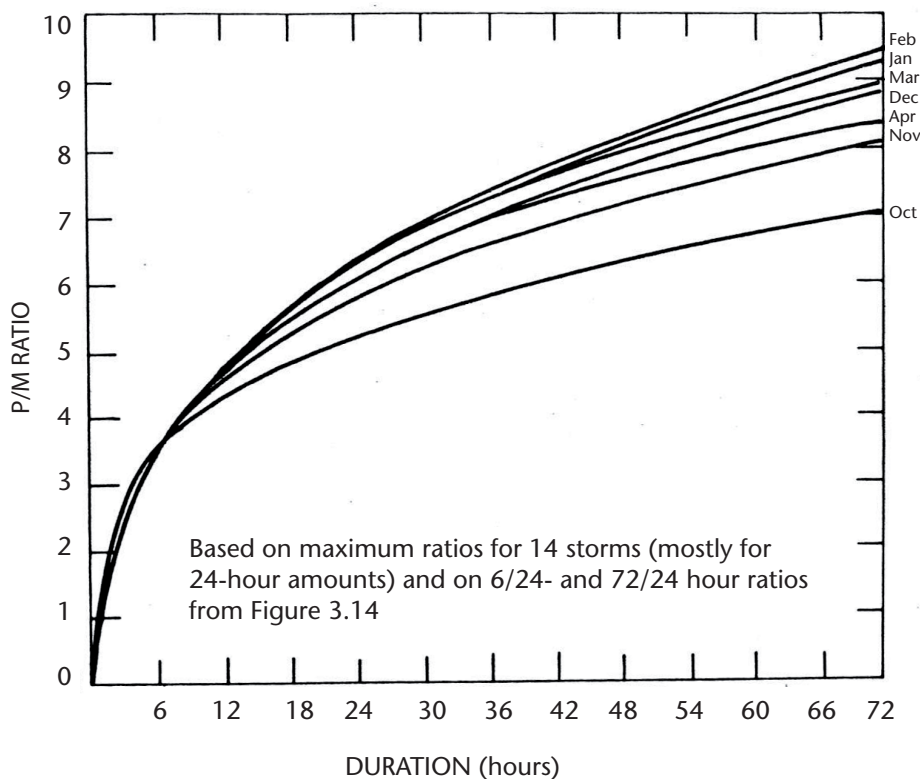


**Figure 3.13. Maximum P/M ratios for combination with orographic storms**  
(after United States Weather Bureau, 1961a)

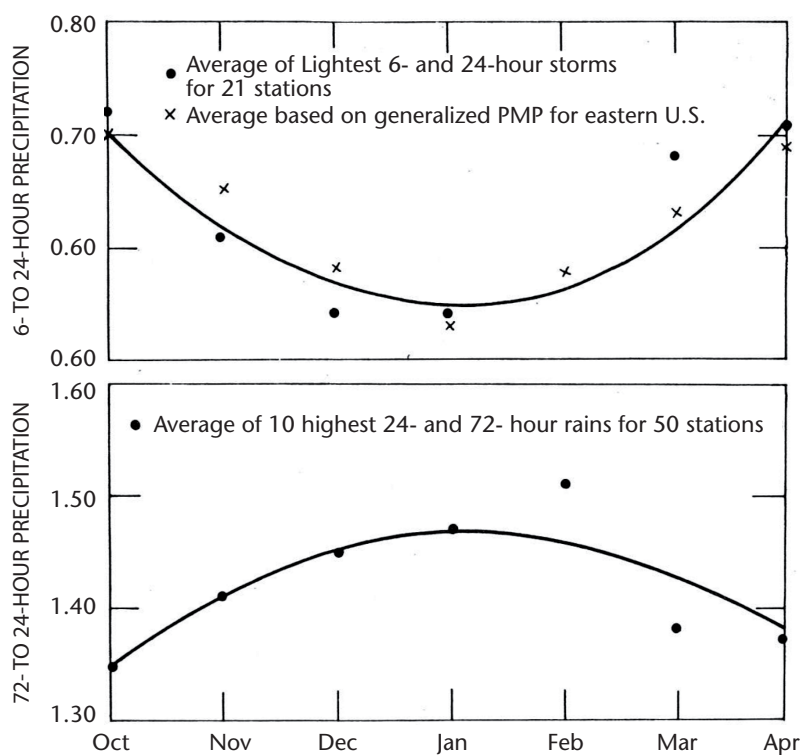


**Figure 3.14. Ratios of 6-hour and 72-hour precipitation to 24-hour precipitation**  
(United States Weather Bureau, 1961a)

of storm-centred data in non-orographic areas in the region of interest, however, precluded the development of such relations. It was therefore necessary to develop depth-area relations for extreme storms (excluding tropical storms) in regions where orography had little or no influence on storm precipitation. These relations were used to adjust the 25.9 km<sup>2</sup> convergence PMP values for area in construction of the index map for this study (United States Weather Bureau, 1961a). They are also used to adjust the values from the index map for various basin area sizes.

### 3.3.4.6 Construction of convergence PMP index map

The steps described below for the construction of the 6-hour 518 km<sup>2</sup> convergence PMP index map (Figure 3.16) for February in the example study apply equally well to similar index maps for other durations, basin sizes and months, if required.

- (a) After an appropriate grid had been drawn on a suitable map base, the maximum moisture for

February was determined for each grid point and plotted. These maximum moisture (precipitable water) values were first obtained from the maximum persisting 12-hour 1 000-hPa dewpoints for February (Figure 3.12), and then adjusted for effective elevation or barrier height (Figure 3.15).

- (b) The adjusted precipitable water value at each grid point was then multiplied by the maximum 6-hour P/M ratio for February (Figure 3.13). The values thus multiplied represent 6-hour 25.9 km<sup>2</sup> convergence PMP.
- (c) The convergence PMP values computed as above were then adapted to 518 km<sup>2</sup> by a reduction factor (0.80) obtained from the depth-area relation (not shown) described in section 3.3.4.5. Isopleths were then drawn on the basis of these areally reduced values, to produce the index map of 6-hour 518 km<sup>2</sup> convergence PMP shown in Figure 3.16. The factors involved in the construction of this map showed little difference in January, so the index map was used without seasonal adjustment for both January and February, and was so labelled.

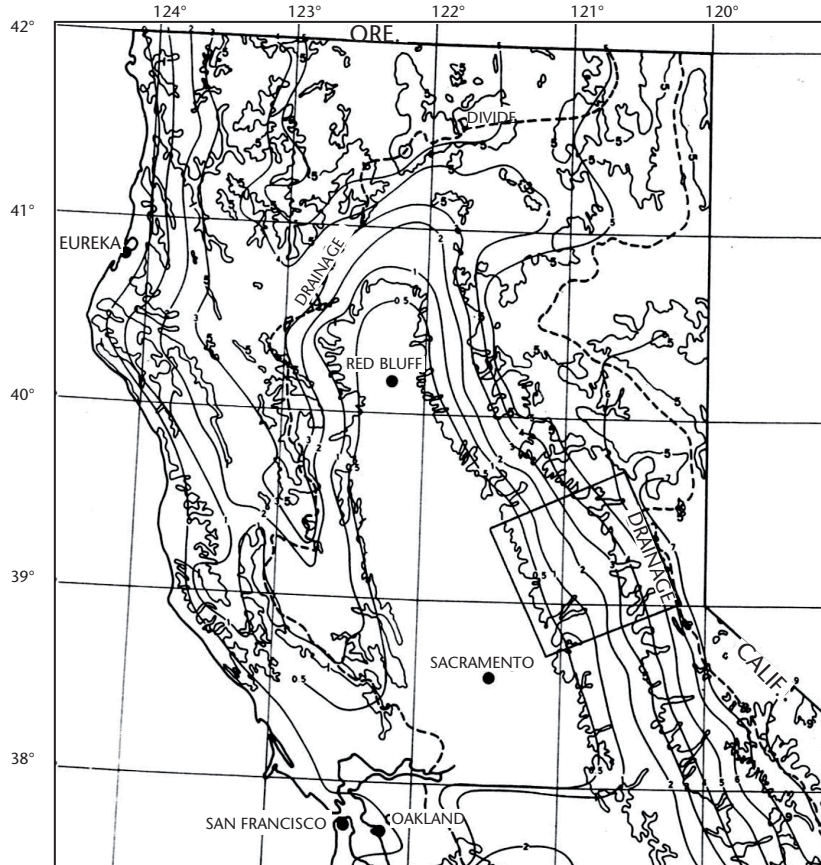


**Figure 3.15. Effective elevation and barrier heights (30.5 m) in northern California (square delineates Blue Canyon orographic model test area; United States Weather Bureau, 1961a)**

### 3.3.4.7 Adjustment of index map values for other durations, basin sizes and months

The convergence PMP index map, constructed as just described, presents 6-hour 518 km<sup>2</sup> values for January and February. Relationships were developed for adjusting these values for different durations, basin sizes and months. This was carried out by means of the following steps:

- (a) Six-hour incremental values of maximum P/M ratios through 72 hours were obtained for each month from Figure 3.13. These values were smoothed and expressed as percentages of the maximum 6-hour P/M ratio for February.
- (b) Durational and seasonal variations for a point, or 25.9 km<sup>2</sup>, were found from durational

(Figure 3.10) and seasonal variations of moisture (precipitable water), expressed as percentages of the 12-hour February moisture (based on maximum persisting 12-hour 1 000 hPa dewpoints) and multiplied by the percentage variation in P/M ratios (from (a)).

- (c) The areal variation (section 3.3.4.5) was then applied to the values obtained in (b) to yield a depth-area-duration relation for each month. That for December is shown in Figure 3.17.

### 3.3.5 Combination of orographic and convergence PMP

Total PMP is obtained by adding the orographic and convergence components. Throughout the development of each component, care must be exercised to minimize the possibility of over-estimating total

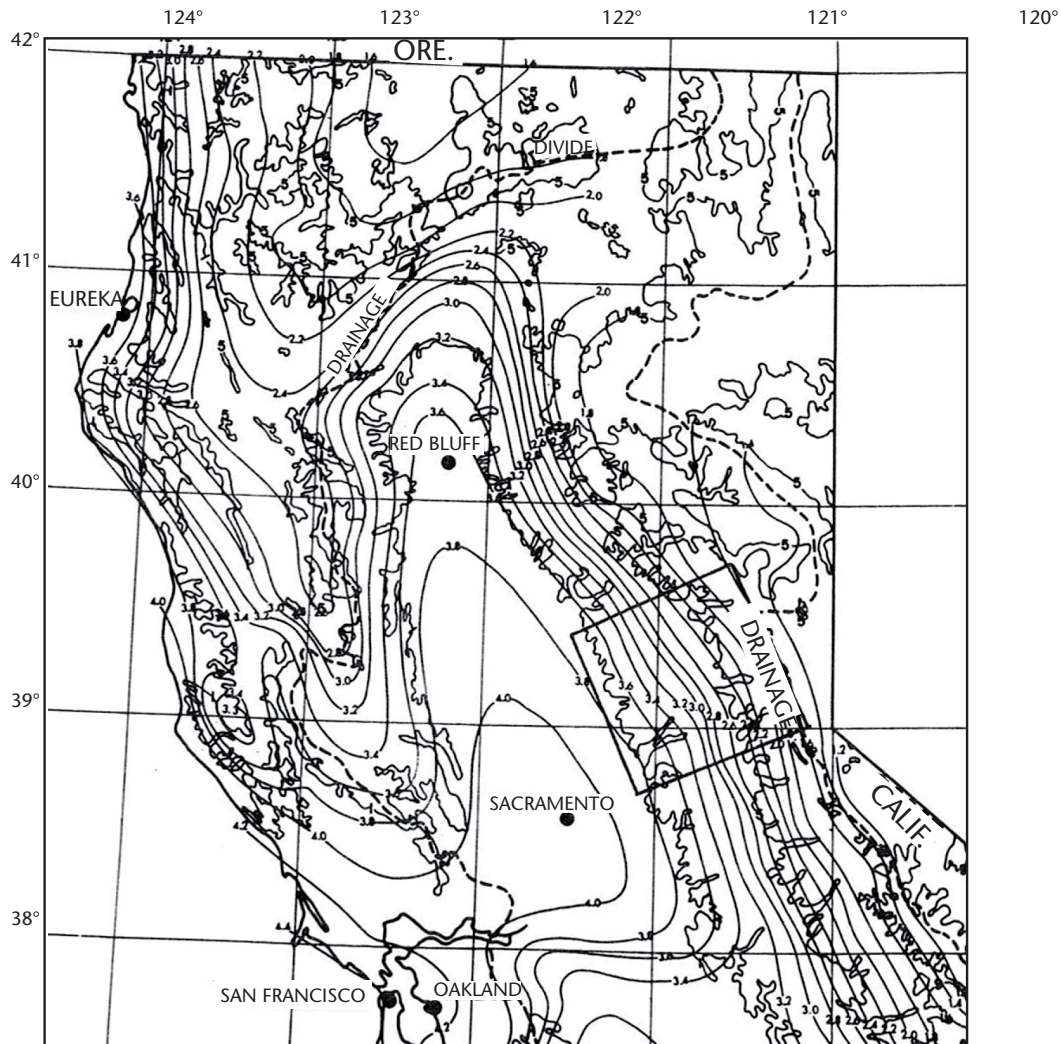


**Figure 3.16.** Six-hour 518 km<sup>2</sup> convergence PMP (inches) for January and February (square delineates Blue Canyon orographic model test area; United States Weather Bureau, 1961a)

PMP. In computing orographic PMP, for example, the model should be tested against observed orographic precipitation only. Testing may be restricted to storm periods showing little or no evidence of convergence precipitation, or the convergence component of total observed precipitation may be estimated (section 3.2.3.7) and subtracted from the total to obtain an estimate of the orographic component.

In estimating convergence PMP, the measure of the storm mechanism, or efficiency, is the *P/M* ratio computed from outstanding storms. As a precaution against over-maximizing, only *P/M* ratios from general storms producing heavy orographic precipitation should be used. Another precaution is to use only maximum persisting 12-hour 1 000-hPa dewpoints observed in major general-type storms for moisture maximization.

### 3.4

## MODIFICATION OF NON-OROGRAPHIC PMP FOR OROGRAPHY

### 3.4.1

### Introduction

Two general approaches for estimating PMP in orographic regions were briefly mentioned in section 3.1.6. One, the orographic separation method using a laminar-flow model, was described in detail in section 3.3. The other, as the title of this section implies, consists of first estimating the non-orographic PMP for the non-mountainous problem region and then applying modifying factors to adjust the non-orographic PMP for orographic effects. The non-orographic PMP may be determined for the plains area in the region of interest, or if there are no broad plains areas it may be estimated as if the mountains did not exist in order to provide a working base.

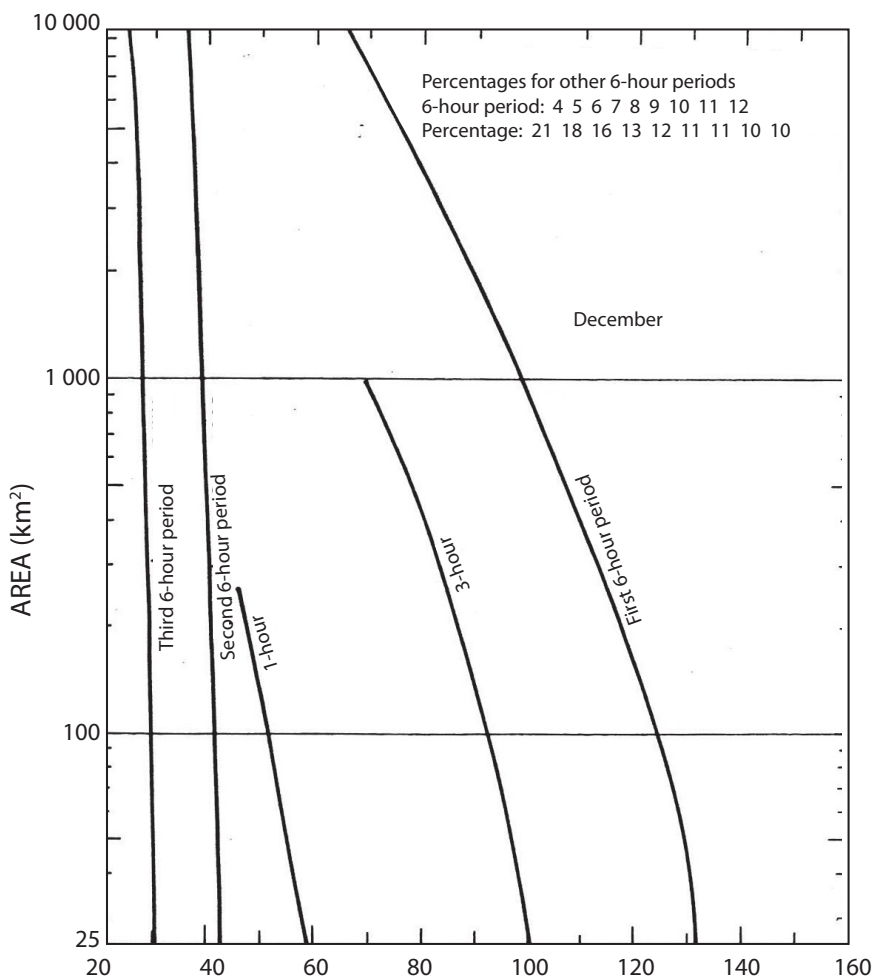


Figure 3.17. Variation of convergence PMP index with basin size and duration for December  
(United States Weather Bureau, 1961a)

While modification of non-orographic PMP is used more often than the orographic separation method, it is being described in less detail because descriptions have been published in reports on studies made for the Hawaiian Islands (Schwarz, 1963), the Tennessee River basin (Schwarz, 1965; Zurndorfer and others, 1986), the region between the Continental Divide and the 103rd meridian (Miller and others, 1984b) and the Mekong River basin (United States Weather Bureau, 1970). The orographic separation method could not be used in these study areas for the reasons cited below.

In the Hawaiian Islands, isolated peaks or short ridges are relatively ineffective in lifting moist air as required by the orographic model. Observations indicate that streamlines are diverted horizontally as well as being lifted vertically in such terrain.

The Tennessee River basin includes multiple ridges at various angles to moisture inflow directions. Critical inflow directions vary from south-west to south-east. Moisture inflow from any direction in this range can produce heavy rainfalls in some portion of the basin. Another obstacle to the use of the orographic model here is the relatively large variability of storm wind direction with height, so simple wind profiles, as used effectively for the Sierra Nevada slopes in California, are not appropriate.

The orographic model could not be used for the Mekong River basin for several reasons. In regions near the tropics, precipitation variation with topography is different from that in middle latitudes. Atmospheric moisture is near saturation levels, and slopes are important in setting the locations for heavy rains. Also, atmospheric instability is generally greater. Laminar wind flow across mountain barriers, which results in the heaviest rainfalls near the highest elevations, is not supported by observations. Another obstacle is that typhoons, which set the level of PMP for durations up to 3 days, show no simple relation between wind speed and rainfall, so that maximization for wind is difficult.

The orographic portion of the region between the Continental Divide and the 103rd meridian is composed of the eastward facing slopes of the Rocky Mountains. The laminar flow model could not be used in this region for two reasons. First, examination of the vertical wind profile in storms shows the wind veers from easterly in the lowest several hundred metres to south-west to west near the nodal surface. The laminar flow model assumes a nearly constant wind inflow direction. Second, storms in this region have a stronger convective

component than is compatible with the laminar flow concept.

Modification of non-orographic PMP for orography as used in a study for the Tennessee River basin above Chattanooga, Tennessee (Schwarz, 1965), is described below. The procedures as used in generalized estimates of PMP for the Tennessee River basin (Zurndorfer and others, 1986), the United States between the Continental Divide and the 103rd meridian (Miller and others, 1984b) and for thunderstorm rainfall in the Columbia River basin in north-western United States (United States Weather Bureau, 1966) are described in Chapter 5. The procedures used in the Hawaiian Islands (Schwarz, 1963) and the Mekong River basin (United States Weather Bureau, 1970), are described in Chapter 6, which discusses procedures appropriate for tropical regions.

### **3.4.2      Tennessee River basin above Chattanooga, Tennessee**

A study for the Tennessee River basin covered the 55 426 km<sup>2</sup> area above Chattanooga, Tennessee and a 20 668 km<sup>2</sup> sub-basin in the lower portion just above Chattanooga (Schwarz, 1965). Topography of the larger basin varies from the rugged mountains of the southeastern portion with peaks above 1 500 m to a relatively smooth central valley extending from south-west to north-east. Northwest of the valley lies a series of parallel ridges extending from south-west to north-east with peaks to about 1 000 m. Chief moisture sources are the Gulf of Mexico about 600 km to the south, and the Atlantic Ocean about 500 km to the south-east. A typical orographic rainfall pattern for southwesterly winds is shown in Figure 3.18. The values shown are ratios of orographic to non-orographic precipitation as estimated from a study of several major storms.

The approach described below is the one used for estimating PMP for these two basins. Other approaches could have been used with equally valid results.

#### **3.4.2.1    Topographic effects**

A major consideration in assessing topographic effects was whether they would produce a net increase or decrease of average basin PMP as compared with that to be expected if there were no mountains. Increases, of course, would be related to slopes exposed to moisture inflow, while decreases would be associated with sheltered or lee areas. The question is: what would be the net effect on the basin as a whole?

Mean annual precipitation was used as the first basis for comparison. Observed basin average precipitation indicated a net basin-wide increase of about 10 per cent above estimates for surrounding non-orographic areas.

February, March and August were selected for estimating topographic effects on monthly rainfall volume. The larger basin was divided into three zones (Figure 3.19):

- A: A zone of minimal topographic effects;
- B: An orographic depletion zone;
- C: An orographic intensification zone.

The average precipitation in zone A was used as a base. The mean precipitation for each of the three months indicated a net topographic depletion for the winter months based on the zone B decrease overcompensating for the orographic zone C increase.

A similar comparison based on the mean of seven unusually wet months selected from the January–April season in six different years showed no appreciable difference between precipitation in depletion zone B and that in intensification zone C.

Daily station rainfalls averaged over the Tennessee River basin above and below Chattanooga were used as an auxiliary indicator of net orographic effects. The area above Chattanooga can be likened topographically to zones B and C, and the area below to zone A (Figure 3.19). Comparison of the means of the series of monthly maximum daily averages showed a net deficit for the basin above Chattanooga.

Although mean annual precipitation indicated a modest orographic intensification, the more extreme precipitation data tended to negate such intensification. The net effects, if any, are apparently small and it was assumed that there was no net topographic effect on the volume of precipitation for the basin as a whole.

### 3.4.2.2 Derivation of PMP

About three dozen major storms scattered throughout the eastern half of the country were maximized, and generalized charts of PMP were prepared for south-eastern United States. It developed that March storms provided controlling PMP values for the basins, and a map of 24-hour 25 900 km<sup>2</sup> March PMP was drawn (Figure 3.20). The PMP value for the centre of the 20 668 km<sup>2</sup> sub-basin was then read from this map, and adjusted upward slightly, on the basis of depth-area relations of observed storms, for the difference in area size. The 24-hour March PMP for the sub-basin was thus determined to be 357 mm.

### 3.4.2.3 Seasonal variation

Study of outstanding storms of the region indicated that, for the basin sizes involved, a March storm would be more likely to produce PMP than would summer tropical storms. Thus, the seasonal variation curve was established with 100 per cent indicated for mid-March. Other precipitation data, such as wettest 7-day periods and months, rainfall-frequency data, and some unpublished generalized PMP estimates for 51 800 km<sup>2</sup> were used in setting the seasonal variation for the larger basin. Tropical storms, which

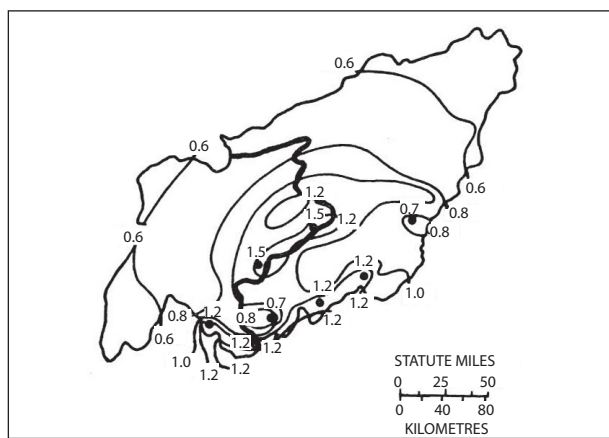


**Figure 3.18. Typical orographic rainfall pattern for southwesterly winds. Isolines indicate ratios of orographic to non-orographic rainfall (Schwarz, 1965)**

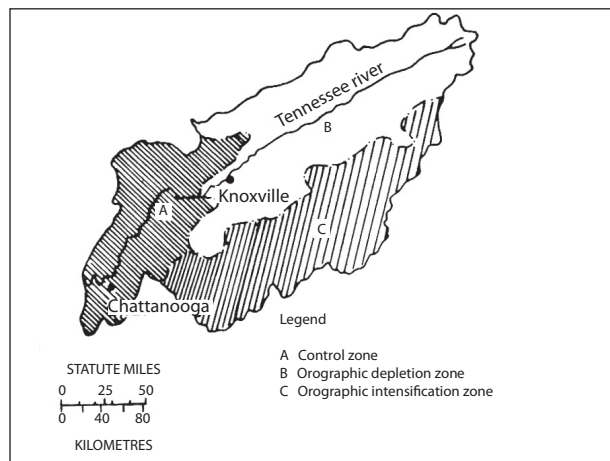


**Figure 3.19. Basin subdivisions for check of topographic effects on basin-wide precipitation volume (Schwarz, 1963)**

usually occur with near-maximum dewpoints, were adjusted to the basin location on the basis of decreased rainfall with distance inland of observed storms. This tropical storm data aided in establishing summer PMP magnitudes. The seasonal variation was first determined for the larger basin, because of previous studies for that size area, and then applied to the sub-basin as described below. Figure 3.21 shows the adopted seasonal variation of PMP for the 55 426 km<sup>2</sup> basin as a percentage of March PMP.

A seasonal variation curve of the ratio of 24-hour storm rainfall for 55 426 km<sup>2</sup> to that for 20 668 km<sup>2</sup>, the areas of the two project basins, was based on some two dozen major storms in the southeastern part of the country. This ratio curve (Figure 3.22) was used to estimate PMP for the larger basin from that for the smaller, with an additional reduction of about 2 per cent for the north-eastwardly displacement of the centre of the large basin. This small adjustment was based on PMP values indicated by Figure 3.20. Application of the basin centre adjustment and area ratio for March to the sub-basin PMP (357 mm) yielded a 24-hour March PMP of 284 mm for the larger basin.

The seasonal variation curve of Figure 3.21 was then applied to the 24-hour March PMP for the larger basin to obtain 24-hour PMP for April to September as shown on line 5 of Table 3.4. These PMP values were then adjusted for area by the reciprocal of the ratio curve of Figure 3.22 to yield April to September 24-hour PMP for the sub-basin (line 2, Table 3.4).

#### 3.4.2.4 Depth-duration relations

Depth-duration relations, particularly 6-hour/24-hour and 72-hour/24-hour rain ratios, of over 100 outstanding storms in the eastern part of the

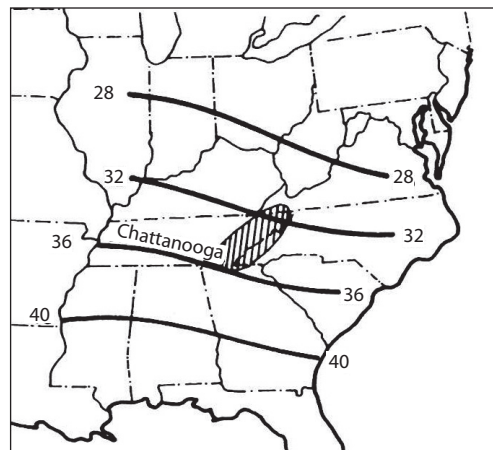


**Figure 3.20. March 24-hour 25 900 km<sup>2</sup> PMP (cm; after Schwarz, 1965)**

country were examined. Although the storms occurred in various months during the March–July period, no seasonal trend was indicated. The adopted depth–duration curves (Figure 3.23) show slight differences for basin size. These curves were used to adjust the 24-hour PMP values of Table 3.4 to 6-hour and 72-hour amounts.

#### 3.4.2.5 Geographic distribution of PMP

It was stated earlier that there was no net decrease or increase of basin rainfall as compared with surrounding areas. This does not mean that there are no topographic effects. Any examination of a number of storms shows that the distribution is definitely affected by the topography. In rugged terrain, topographic effects result in more or less distinct storm rainfall patterns, with appreciable differences between patterns attributable chiefly to wind direction and storm movement.

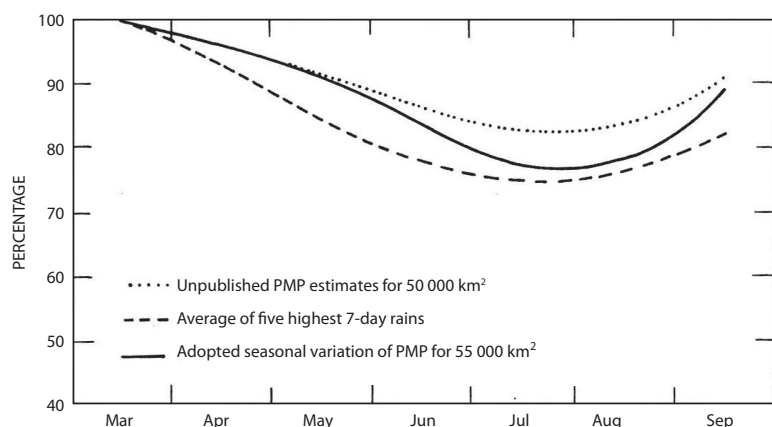


**Figure 3.21. Seasonal variation of PMP for 55 426 km<sup>2</sup> as percentage of March PMP (Schwarz, 1965)**

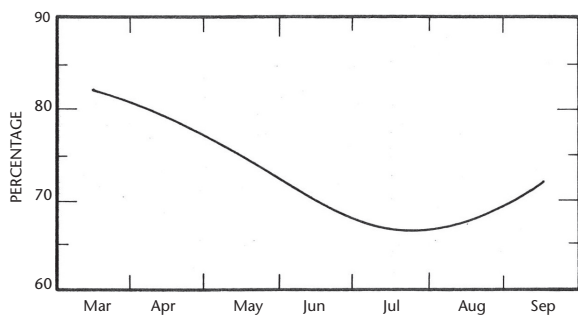


**Figure 3.22. Depth-area ratios (55 426 / 20 688 km<sup>2</sup>) for 24-hour rainfall (Schwarz, 1965)**

The PMP values of Table 3.4 merely represent average depths of basin PMP, and provide limiting rainfall volumes for various possible PMP storm patterns. Examination of isohyetal patterns for a number of outstanding storms over the project basins, together with streamflow data, indicated several critical rainfall patterns for the larger basin. Figure 3.24 presents one of these patterns for the 6-hour March PMP.

In order to minimize the work involved in determining pattern configurations and resulting runoff, any selected pattern is generally considered applicable to all durations, with only the isohyet values changing. Isohyet values for the pattern of Figure 3.24 were obtained by the relation of Figure 3.25, which applies to the maximum, or first, 6-hour PMP increment. Similar relations were developed for other 6-hour increments and for 72 hours. These relations were derived in a manner similar to that described in section 2.11.3, with the so-called within-basin, or typical, depth-area curves, like those of Figure 2.14, patterned after outstanding storms in or transposable to the project basins.

Isohyet values for the PMP storm pattern of Figure 3.24 are given in Table 3.5. The isohyet values for the maximum, or first, 6-hour PMP increment of the storm pattern of Figure 3.24 were obtained as follows. The total area enclosed by each isohyet was obtained by planimetry. The area was then used to enter the nomogram of Figure 3.25 on the ordinate scale. The corresponding ratio of isohyet value to basin PMP was then obtained by laying a straight edge across the nomogram at the proper ordinate value and reading the ratio below the intersection of the straight edge and the appropriate basin area curve. This ratio was then applied to the basin PMP to obtain the isohyet value.

Isohyet values for other 6-hour PMP increments were obtained in a similar fashion from similar ratio relations except that the ratios were applied to corresponding 6-hour PMP increments. Thus, for example, the isohyet values for the second 6-hour PMP increment were determined from a corresponding ratio relation, like that of Figure 3.25, and the second 6-hour PMP increment as indicated by the appropriate depth-duration curve from Figure 3.23.

The effect of geographic distribution of rainfall on runoff generally decreases as basin size decreases. The simple oval-shaped pattern of Figure 3.26 was considered appropriate for the sub-basin. Isohyet values were determined as described above.

### 3.4.2.6 Time distribution of PMP

The procedures just described yielded 6-hour rainfall incremental values or maps for the 12 periods in the 72-hour PMP storm for the Tennessee River basin above Chattanooga, Tennessee, in any given month in the March–September season. The ordering of 6-hour increments was based on descending order of magnitude and not on chronological

**Table 3.4. Probable maximum precipitation (mm) for Tennessee River basin above Chattanooga, Tennessee (Schwarz, 1965)**

Line no.	Duration (hours)	March	April	May	June	July	August	September
<i>Sub-basin (20,688 km<sup>2</sup>)</i>								
1	6	178	177	174	171	164	167	178
2	24	357	354	349	342	334	334	356
3	72	517	513	506	496	484	484	516
<i>Total basin (55,426 km<sup>2</sup>)</i>								
4	6	128	123	116	107	98	99	114
5	24	284	273	259	239	219	222	253
6	72	426	409	388	358	328	332	379

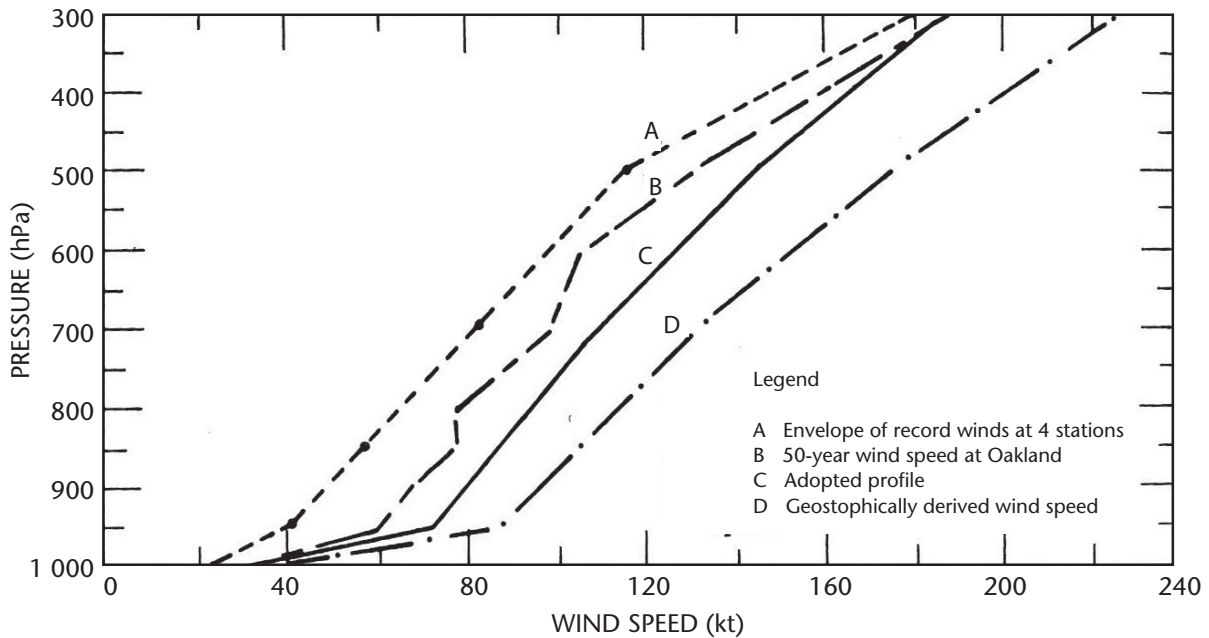


**Figure 3.23. Depth–duration relations in percentage of 24-hour rainfall (Schwarz, 1965)**

sequence. Storm experience in the Tennessee River basin, which provides guidelines for reasonable time sequences, generally indicates a strong tendency for several bursts of rainfall during a 72-hour storm. Within a typical burst, the largest two or three 6-hour increments usually occur in succession.

The following criteria were recommended for this basin (Schwarz, 1965) on the basis of the above

guidelines. It does not necessarily provide PMP for all durations but generally conforms to observed storm sequences.

The four largest 6-hour increments of the 72-hour PMP storm were grouped in one 24-hour sequence; the middle four, in a second 24-hour sequence; and the four smallest, in a third 24-hour sequence.

The four 6-hour increments within each of these three 24-hour sequences were arranged as follows: second largest next to largest, the third largest adjacent to these, and the fourth largest at either end.

The three 24-hour sequences were arranged with the second largest next to largest, with the third at either end. Any possible sequence of the three 24-hour periods was determined acceptable with the exception of that which would place the smallest 24-hour increment in the middle.

A sample arrangement that follows these criteria is shown in Table 2.4. This arrangement does not maintain PMP magnitude for the 30-, 36-, 42-, 54-, 60- and 66-hour durations. If it is desired to maintain PMP values for all durations, however, any sequence of  $n$  6-hour increments should consist of the  $n$  highest 6-hour values (see section 2.12 for general discussion on temporal distribution).

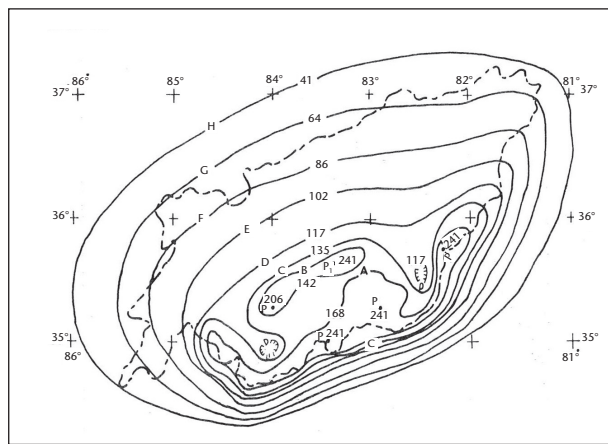


**Figure 3.24. Six-hour PMP storm pattern (mm) for maximum 6-hour increment for total basin (55 426 km<sup>2</sup>) (Schwarz, 1965); isohyet values are applicable to the March PMP**

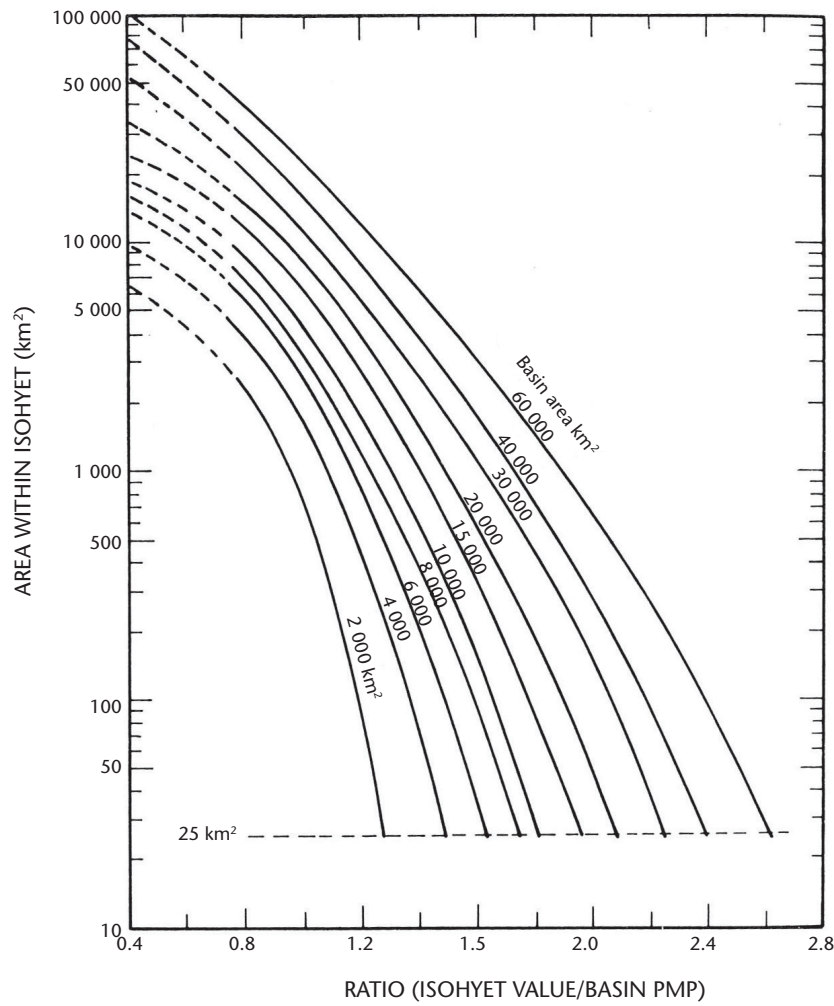


**Figure 3.25. Nomogram for obtaining isohyet values for maximum 6-hour rainfall increment in pattern storms**

**Table 3.5. Isohyet values (mm) for 6-hour March PMP storm pattern of Figure 3.24**

	<i>Isohyet</i>									
	A	B	C	D	E	F	G	H	P1	P2
72 hours	498	470	439	378	371	333	290	241	688	584
1st 6 hours	168	142	135	117	102	86	64	41	241	206
2nd 6 hours	79	76	71	69	64	58	53	41	107	89
3rd 6 hours	53	53	51	46	43	41	40	38	71	61
4th 6 hours	41	41	38	36	33	30	28	25	56	48
2nd day <sup>a</sup>	99	99	91	61	81	74	69	61	135	114
3rd day <sup>b</sup>	58	58	53	51	46	43	41	36	79	66
Total area enclosed by isohyet (km <sup>2</sup> )	7 120	1 640	18 370	27 530	39 320	55 880	78 000	107 950	2	2

<sup>a</sup> For successive 6-hour values use 32, 27, 22 and 19 per cent of 2nd day.

<sup>b</sup> For successive 6-hour values use 29, 26, 23 and 22 per cent of 3rd day.

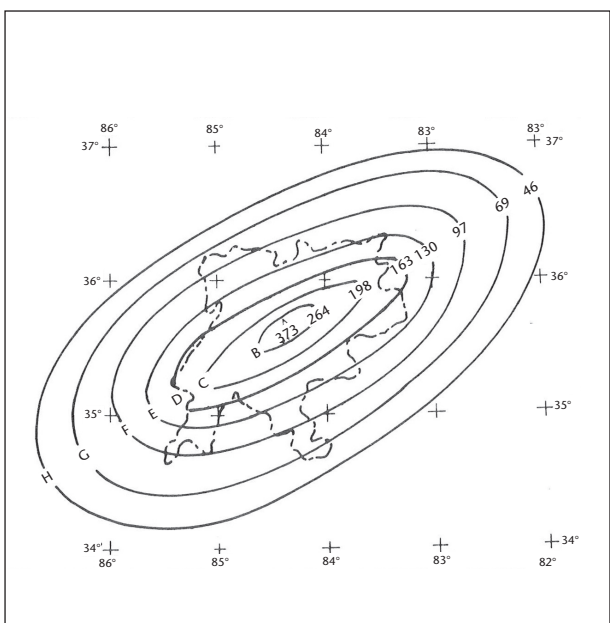


**Figure 3.26.** PMP storm pattern for maximum 6-hour increment for sub-basin ( $21\,000\text{ km}^2$ ; Schwarz, 1965); isohyet values are applicable to March

3.5

## **CAUTIONARY REMARKS ON ESTIMATING PMP IN OROGRAPHIC REGIONS**

The cautionary remarks of section 2.13 apply also to orographic regions concerning adequacy of storm sample, comparison with record rainfalls, consistency of estimates, regional, areal, and durational smoothing, seasonal variation, and areal distribution. As stated in section 1.3.3, the examples given are not intended for direct application. In addition, the following cautionary remarks must be considered.

### 3.5.1

## **Basic data deficiencies**

Precipitation networks in orographic regions are relatively sparse compared with those in non-orographic regions, which are generally more heavily populated. Furthermore, in mountainous areas, most gauges are located in settlements at relatively low elevations along rivers or in broad valleys. Very few are located on steep slopes or at high elevations. To these shortcomings may be added the usual deficiencies of gauge measurements, which are likely to be at

a maximum in mountainous terrain. Consequently, precipitation data are not only relatively sparse and sometimes inaccurate, but are generally biased and therefore do not represent adequately the effects of orographic influences on precipitation distribution. This shortcoming affects the reliability of various relationships required for estimating PMP, such as precipitation–elevation and depth–area relations. The situation may be alleviated by referring to orographically adjusted seasonal precipitation maps or precipitation-frequency maps prepared considering topographic effects in determining distribution of precipitation (sections 3.1.3 and 3.1.4). Also, it is sometimes possible to use rainfall–runoff relations to obtain areal estimates of storm rainfall that may be more accurate than indicated by observed precipitation data alone.

### **3.5.2 Orographic separation method**

The orographic separation method for estimating PMP (section 3.3) involves additional problems besides those just mentioned, since it requires enough upper-air data to obtain reliable extreme values. Model test requirements for upper-air soundings near the inflow side of the test area and for sufficient concurrent precipitation data for the test area further limit the applicability of the model.

Of the regions where the orographic model has been tested, best results were obtained for the continuous, high and favourably oriented (with respect to moisture inflow) Sierra Nevada in California. The model computes orographic precipitation under the assumption of laminar airflow. Orographic regions, where major storms occur in the cool seasons, are more likely to meet the required conditions.

This model is not well suited for regions or seasons with predominantly unstable atmospheric conditions. Studies for regions near the tropics indicate that the laminar flow model may be particularly unsuited for estimating PMP there as well. Indirect approaches, such as that used for the Tennessee River basin study (section 3.4.2), are more likely to yield reliable estimates of PMP for such regions.

Section 3.3.5 cautioned against over-maximizing and cited some precautions. To these may be added the use of conservative envelopment of the various factors involved in the procedure whenever this technique is required.



## CHAPTER 4

### STATISTICAL ESTIMATES

A statistical estimation method is used for deriving probable maximum precipitation (PMP) approximately for small areas. While the method is basically a frequency analysis method, it is different from traditional frequency analysis methods in two important respects. First, it focuses on a wide region, rather than a single station or single watershed, in order to seek a storm that approximates the physical upper limit of precipitation (the maximum observed rainfall). Second, frequency analysis methods are used to determine the statistics of extremes and this method involves the application of the process of enveloping. These two points are highlighted in Figure 4.1, which shows smooth enveloping of data from around 2 700 stations (90 per cent of which are located in the United States of America).

The essence of the method is storm transposition, but instead of transposing the specific rainfall amount of one storm, an abstracted statistic  $K_m$  is transposed. (The transposition is achieved by looking up the value of  $K_m$  in Figure 4.1 using a corrected average  $\bar{X}_n$  for the design station.) The transposition correction is estimated using the average  $\bar{X}_n$  and the coefficient of variability  $C_v$  (see Equation 4.3).

The method identifies the enveloping value of  $K_m$  from the observed data in a wide region (mainly in the United States) as the probable maximum value corresponding to PMP. It assumes that the PMP has been observed at the station that provided the  $K_m$  value.

#### 4.1 USE OF STATISTICAL PROCEDURE

Statistical procedures for estimating PMP may be used wherever sufficient precipitation data are available, and are particularly useful for making quick estimates, or where other meteorological data, such as dewpoint and wind records, are lacking. The procedure described below is not the only one, but it is the process that has received the widest acceptance. It is used mostly for making quick estimates for basins of no more than around 1 000 km<sup>2</sup>, but has been used for much larger areas. It is convenient because it requires considerably less time to apply than the meteorological, or traditional, approach, and one does not have to be a meteorologist to use it. A major shortcoming of the procedure is that it

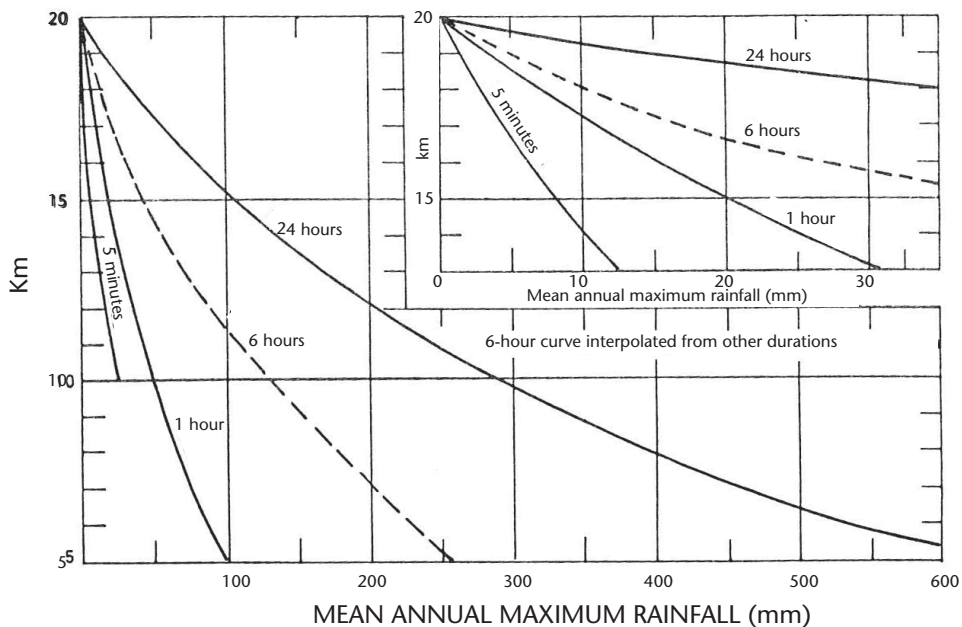


Figure 4.1.  $K_m$  as a function of rainfall duration and mean of annual series (Hershfield, 1965)

yields only point values of PMP and thus requires area-reduction curves for adjusting the point values to areas of various size. A second problem is determining the appropriate value to use for  $K$ , a statistical variable that depends on the frequency distribution of extreme-value hydrological data. Different  $K$  values have been used by various investigators (Dhar and Damte, 1969; McKay, 1965).

## 4.2 DEVELOPMENT OF PROCEDURE

### 4.2.1 Basis

The procedure as developed by Hershfield (1961a, 1961b) and later modified (1965) is based on the general frequency equation (Chow, 1961):

$$X_t = \bar{X}_n + K S_n \quad (4.1)$$

where  $X_t$  is the rainfall for return period  $t$ ,  $\bar{X}_n$  and  $S_n$ , are, respectively, the mean and standard deviation of a series of  $n$  annual maxima, and  $K$  is a common statistical variable, which varies with the different frequency distributions fitting extreme-value hydrological data.

If the maximum observed rainfall  $X_m$  is substituted for  $X_t$ , and  $K_m$  for  $K$ ,  $K_m$  is then the number of standard deviations to be added to to obtain  $X_m$ , or

$$X_t = \bar{X}_n + K_m S_n \quad (4.2)$$

The initial determination of an enveloping value of  $K_m$  was based on records of 24-hour rainfall for some 2 700 stations in the climatological observation programme. Values of  $\bar{X}_n$  and  $S_n$  were computed by conventional procedures, but the maximum recorded rainfall at each station was omitted from the computations. The greatest value of  $K_m$  computed from the data for all stations was 15. It was first thought that  $K_m$  was independent of rainfall magnitude, but it was later found to vary inversely with rainfall: the value of 15 may be too high for areas of generally heavy rainfall and too low for arid areas. Values of  $K_m$  for other rainfall durations were later determined (Hershfield, 1965), and its variation with  $\bar{X}_n$  for durations of 5 minutes, 1, 6 and 24 hours is shown in Figure 4.1, which indicates a maximum  $K_m$  of 20. Other investigators (Dhar and Damte, 1969; McKay 1965) have used other values for  $K$  to estimate PMP (see Section 4.5).

### 4.2.2 Adjustment of $\bar{X}_n$ and $S_n$ for maximum observed event

Extreme rainfall amounts of rare magnitude or occurrence – for example, with return periods of 500 years or more – are often found to have occurred at some time during a much shorter period of record, such as 30 years. Such a rare event, called an outlier, may have an appreciable effect on the mean  $\bar{X}_n$  and standard deviation  $S_n$  of the annual series. The magnitude of the effect is less for long records than for short, and it varies with the rarity of the event, or outlier. This has been studied by Hershfield (1961b) using hypothetical series of varying length, and Figures 4.2 and 4.3 show the adjustments to be made to  $\bar{X}_n$  and  $S_n$  to compensate for outliers.

In these figures  $\bar{X}_{n-m}$  and  $S_{n-m}$  refer to the mean and standard deviation of the annual series computed after excluding the maximum item in the series, respectively. It should be noted that these relationships consider only the effect of the maximum observed event. No consideration was given to other anomalous observations.

### 4.2.3 Adjustment of $\bar{X}_n$ and $S_n$ for sample size

The mean  $\bar{X}_n$  and standard deviation  $S_n$  of the annual series tend to increase with length of record, because the frequency distribution of rainfall extremes is skewed to the right so that there is a greater chance of getting a large than a small extreme as length of record increases. Figure 4.4 shows the adjustments to be made to  $\bar{X}_n$  and  $S_n$  for length of record. There were relatively few precipitation records longer than 50 years available for evaluating the effect of sample size, but the few longer records available indicated adjustment only slightly different from that for the 50-year records.

### 4.2.4 Adjustment for fixed observational time intervals

Precipitation data are usually given for fixed time intervals, for example 8 a.m. to 8 a.m. (daily), 6 a.m. to noon (6-hourly), 3 a.m. to 4 a.m. (hourly). Such data rarely yield the true maximum rainfall amounts for the indicated durations. For example, the annual maximum observational day amount is very likely to be appreciably less than the annual maximum 24-hour amount determined from intervals of 1 440 consecutive minutes unrestricted by any particular observation time. Similarly, maxima from fixed 6-hour and hourly intervals tend to be less than maxima obtained from 360 and 60 consecutive 1-minute intervals, respectively, unrestricted by fixed beginning or ending times.

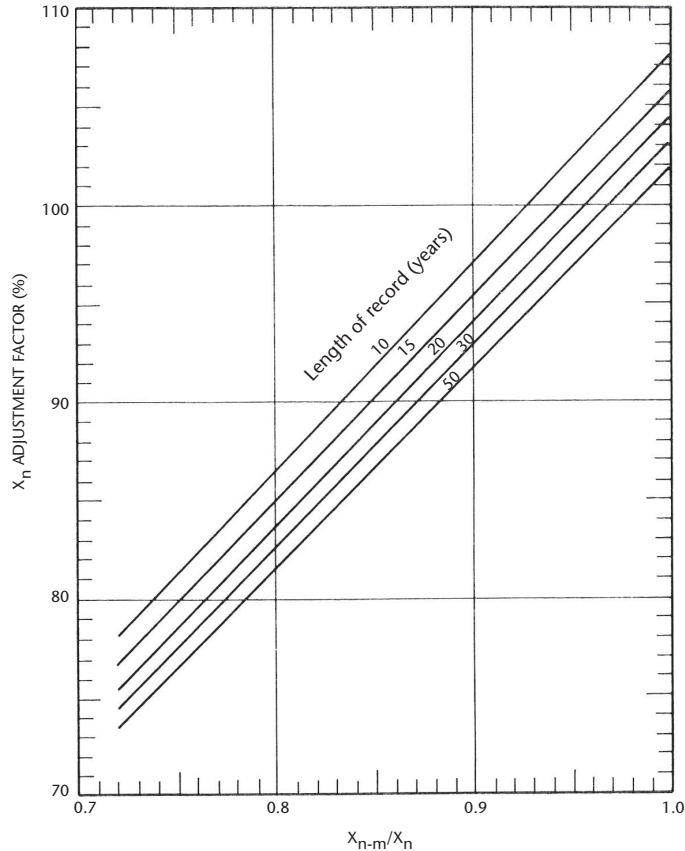


**Figure 4.2. Adjustment of mean of annual series for maximum observed rainfall (Hershfield, 1961b)**

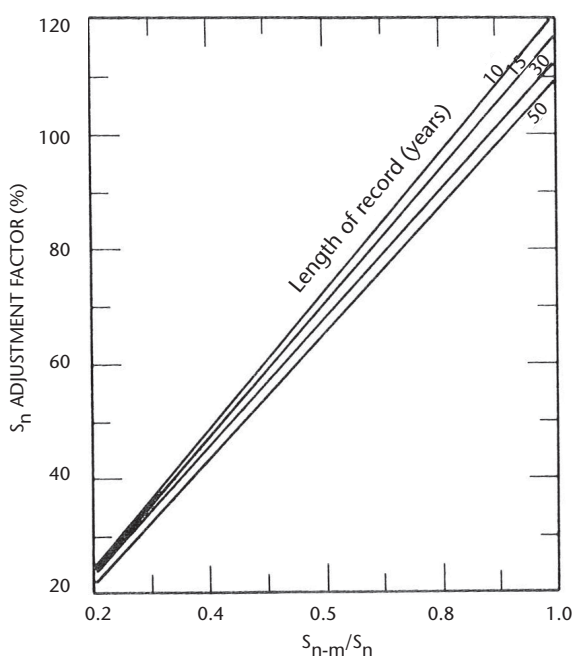


**Figure 4.3. Adjustment of standard deviation of annual series for maximum observed rainfall (Hershfield, 1961b)**

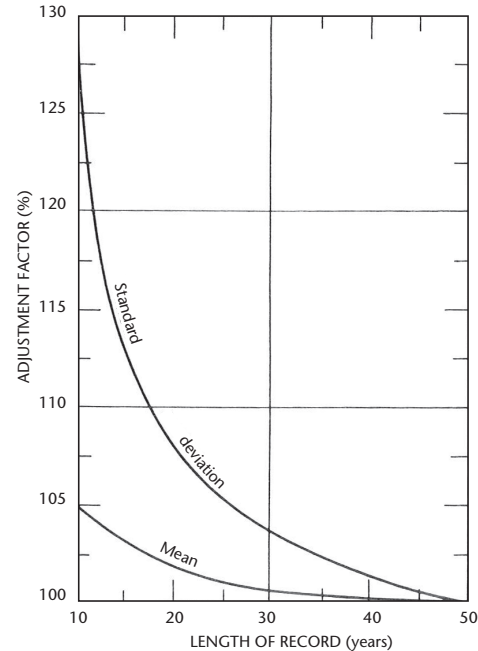


**Figure 4.4. Adjustment of mean and standard deviation of annual series for length of record (Hershfield, 1961b)**

Studies of thousands of station-years of rainfall data indicate that multiplying the results of a frequency analysis of annual maximum rainfall amounts for a single fixed time interval of any duration from 1 to 24 hours by 1.13 will yield values closely approximating those to be obtained from an analysis based on true maxima (Hershfield, 1961a). Hence, the PMP values yielded by the statistical procedure should be multiplied by 1.13 if data for single fixed time intervals are used in compiling the annual series. Lesser adjustments (Weiss, 1964; Miller, 1964) are required when maximum observed amounts for various durations are determined from two or more fixed time intervals (Figure 4.5). Thus, for example, maximum amounts for 6- and 24-hour periods determined from 6 and 24 consecutive 1-hour rainfall increments require adjustment by factors of only 1.02 and 1.01, respectively.

#### 4.2.5 Area-reduction curves

The procedure described here was developed for point rainfall data. Hence, its use requires some method for reducing the point values it yields to some required areal rainfall averages.

There are two types of depth-area relations (Miller and others, 1973). The first is the storm-centred relation, that is, the maximum precipitation occurring when the storm is centred on the area affected (Figure 4.6A). The second type is the

geographically fixed area relation where the area is fixed and the storm is either centred on it or displaced so only a portion of the storm affects the area (Figure 4.6B). Storm-centred depth-area curves represent profiles of discrete storms, whereas the fixed-area data are statistical averages in which the maximum point values frequently come from different storms. The storm-centred curves are appropriate for use with PMP studies.

There are many variations of the two basic depth-area relations (Court, 1961; United States Weather Bureau, 1960). Those for use with any PMP studies should be based on the depth-area-duration (DAD) characteristics of the storm types capable of producing the PMP in the region. The curves of Figure 4.7 are based on average values obtained from DAD analyses of important general storms over the western United States. The relation of Figure 4.7 is presented only as an idealized example and curves should be developed for the specific location of the project. For example, this relation does not show as much decrease with increasing area as would curves based on localized cloudbursts, and is therefore inappropriate for use where such storms would cause the PMP. They do not extend beyond 1 000 km<sup>2</sup> because extrapolation of point rainfall values becomes more unreliable as size of area increases. Necessity, however, has led to relations (McKay, 1965) relating point values to areas in excess of 100 000 km<sup>2</sup>. Point values are often assumed to be applicable to areas up to 25 km<sup>2</sup> without reduction.

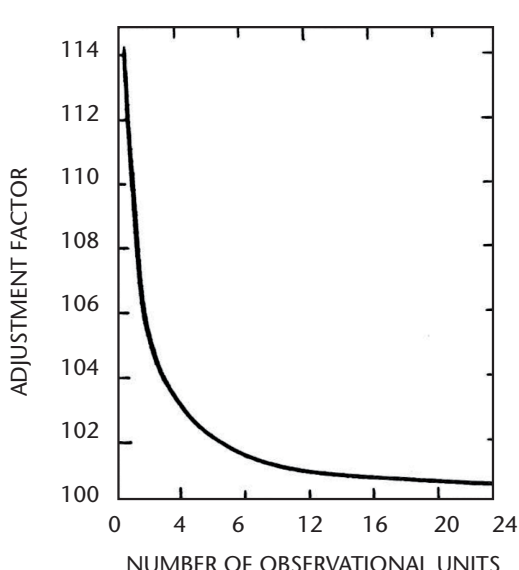
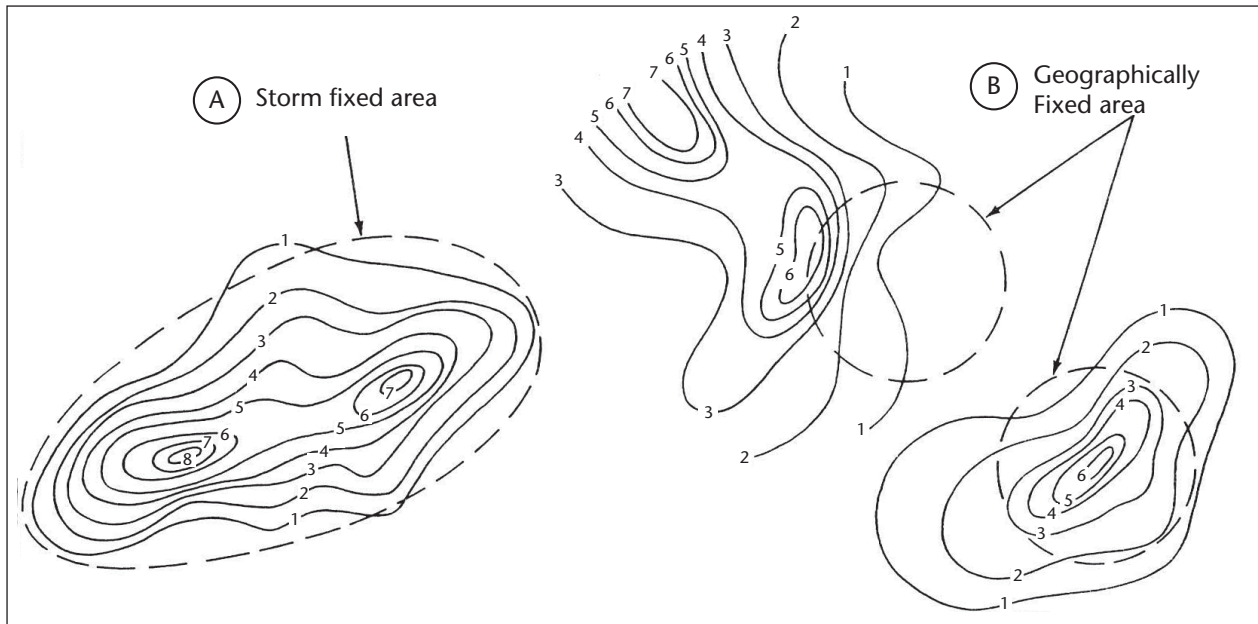


Figure 4.5. Adjustment of fixed-interval precipitation amounts for number of observational units within the interval (Weiss, 1964)

#### 4.2.6 Depth-duration relationships

Only daily measurements of precipitation are available for many regions. Various types of depth-duration relationships have been developed to show rainfall distribution within storms. Such relationships vary a great deal depending on storm type. For example, orographic rainfall will show a much more gradual accumulation of rainfall with time than will thunderstorm rainfall.

The maximum depth-duration relation of Figure 4.8 is based on rainfall amounts in heavy storms averaged over areas ranging up to 1 000 km<sup>2</sup> in Illinois, United States (Huff, 1967). This relation arranges the rainfall increments for various time intervals in decreasing order of magnitude and not in chronological order. In other words, the curve, a depth-duration curve, shows the greatest 3-hour amount in the first 3 hours, the second greatest 3-hour amount in the second 3-hour period, and so forth. This arrangement is not intended to represent the order in which the rainfall increments occurred, nor does it do so, except perhaps



**Figure 4.6.** Examples of (A) isohyetal pattern centred over basin as would be the case for storm-centred depth-area curves, and (B) two possible occurrences of isohyetal patterns over a geographically fixed area as would be the case in development of curves for a geographically fixed area (Miller and others, 1973)

accidentally, for an occasional storm. Studies of chronological distribution of rainfall within storms (the mass curve of rainfall) indicate no consistent pattern, with maximum intensities likely to occur during any period of the storm.

The depth-duration curve of Figure 4.8 is representative of convective storms in the central United States. Because of the variation of such relationships with storm type and geography, they should be developed from data for the same regions for

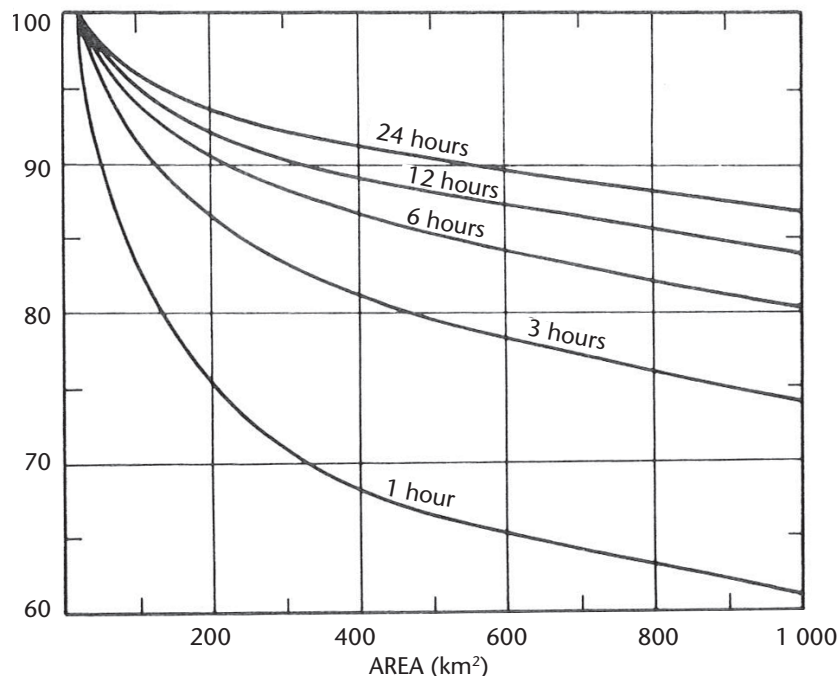


**Figure 4.7.** Depth-area, or area-reduction, curves for western United States (United States Weather Bureau, 1960)

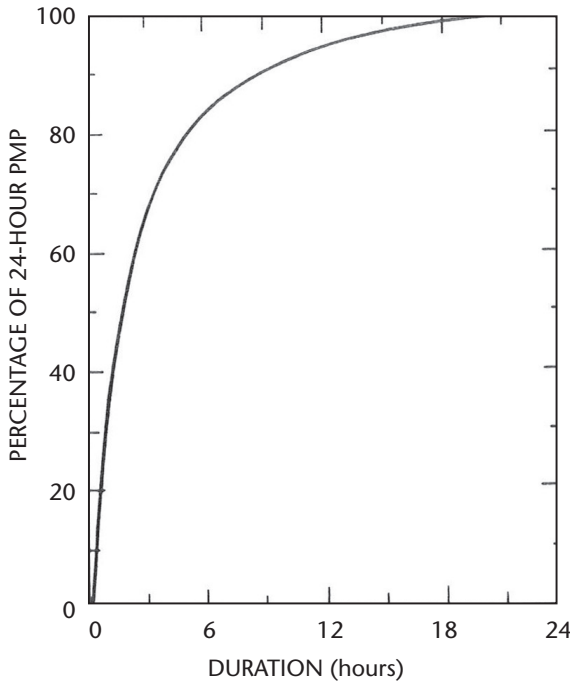


**Figure 4.8. Maximum depth-duration curve (Huff, 1967)**

which the PMP estimates are required. Figure 4.8 is presented here merely as an example and is not intended for general application. Figure 4.8, or similar relationships, should be used only when rainfall data for durations shorter than 24 hours are unavailable.

After the two means and standard deviations for each series and their respective ratios have been obtained as indicated in Table 4.1, estimation of PMP proceeds as follows:

- $\bar{X}_n$  and  $S_n$  are adjusted for maximum observed rainfall by means of Figures 4.2 and 4.3, respectively, and for record length by means of Figure 4.4.
- Values of  $K_m$  corresponding to adjusted values of  $\bar{X}_n$  for the various durations are obtained from Figure 4.1.
- Point values of PMP, or  $X_m$ , are computed as indicated by Equation 4.2.
- If basic rainfall data are for fixed time intervals, they are adjusted upward by applying the factor 1.13 for fixed observational periods or the factors 1.13, 1.02 and 1.01 to 1-, 6- and 24-hour amounts, respectively, compiled from hourly data (section 4.2.4).
- Point values of PMP are reduced to the proper areal value for the size of the basin using Figure 4.7, or a similar relation. (Note: if only 24-hour rainfall amounts are available, a maximum depth-duration curve, like that of Figure 4.8, can be used to estimate PMP for the shorter durations. The 34 and 84 per cent adjustments for the 1- and 6-hour amounts, respectively, would yield values of 155 and 382 mm, which are considerably higher than the 103 and 331 mm based on the actual data. Hence, Figure 4.8 does not very well represent the depth-duration characteristics of PMP indicated by the short-duration data for the problem basin.)

#### 4.3 APPLICATION OF PROCEDURE

It is assumed that a PMP estimate is required for a basin of 500 km<sup>2</sup>. Table 4.1 lists the annual maximum 1-, 6-, and 24-hour rainfall amounts (annual series) compiled from a hypothetical 25 year record of hourly precipitation data for a station in the problem watershed. The hourly values are thus for a clock hour – for example, 9 a.m. to 10 a.m. – and the 6-hour and 24-hour amounts consist of the greatest sums of 6 and 24 consecutive clock-hour rainfall increments, respectively.  $\bar{X}_{n-m}$  and  $S_{n-m}$  are the mean and standard deviation, respectively, of the annual series computed after excluding the maximum rainfall amount in each series.  $\bar{X}_n$  and  $S_n$  are for the series including all items. Means and standard deviations are computed by conventional methods and in actual practice should be compared with those of nearby stations for consistency. If inconsistent, another station should be used for estimating PMP.

#### 4.4 GENERALIZED ESTIMATES

Where precipitation networks are considered adequate, generalized PMP estimates may be made with relative ease by this procedure. The adjusted mean  $\bar{X}_n$  and standard deviation  $S_n$  are determined (Section 4.3) for each station, and the coefficient of variation ( $C_v$ , that is, the standard deviation divided by the mean), is then computed. Values of  $C_v$ , which is considered a more stable statistic than  $S_n$ , and are plotted on a map, and two sets of isolines are drawn. Values of PMP for any point on the map may then be obtained by estimating  $\bar{X}_n$  and  $C_v$  from their respective isolines and using the following relation:

$$X_m = \bar{X}(1 + K_m C_v) \quad (4.3)$$

By computing PMP for a fine grid of points, a map showing PMP values directly may then be constructed. Values of PMP, or  $X_m$ , obtained from

**Table 4.1. Computation of probable maximum precipitation (PMP)**

Year	Duration (hours)		
	1	6	24
1941	30	62	62
1942	19	38	60
1943	15	39	57
1944	33	108	112
1945	23	49	67
1946	19	39	72
1947	32	50	62
1948	24	30	61
1949	30	39	57
1950	24	38	69
1951	28	58	72
1952	15	41	61
1953	20	47	62
1954	26	68	82
1955	42	124	306
1956	18	43	47
1957	23	39	43
1958	25	48	78
1959	28	80	113
1960	25	89	134
1961	28	33	51
1962	46	72	72
1963	20	47	62
1964	14	34	53
1965	15	40	55
<i>n = 25</i>			
$\frac{\bar{X}_{n-m}}{\bar{X}_n}$	$\frac{24.0}{24.9} = 0.97$	$\frac{51.3}{54.2} = 0.95$	$\frac{69.3}{78.8} = 0.88$
$\frac{S_{n-m}}{S_n}$	$\frac{7.30}{8.00} = 0.91$	$\frac{19.5}{24.0} = 0.81$	$\frac{21.8}{51.9} = 0.42$
<i>Adjustment of means <math>\bar{X}_n</math> for maximum observed amount and record length:</i>			
	1 hour	6 hours	24 hours
From Figure 4.2	1.01	0.98	0.91
From Figure 4.4	1.01	1.01	1.01
Adjusted $\bar{X}_n$	25.4	53.6	72.4

**Table 4.1. (Continued)***Adjustment of standard deviations for maximum observed amount and record length*

	1 hour	6 hours	24 hours
From Figure 4.3	1.04	0.93	0.49
From Figure 4.4	1.05	1.05	1.05
Adjusted $S_n$	8.6	23.4	26.7
$K_m$ (Figure 4.1)	14	14	16

*Unadjusted point values of PMP from Equation 4.2*

1-hour PMP	= $25.4 + 14 \times 8.6 = 146$ mm
6-hour PMP	= $53.6 + 14 \times 23.4 = 381$ mm
24-hour PMP	= $72.4 + 16 \times 26.7 = 500$ mm

*Adjustment of PMP based on hourly data to true maximum values (see section 4.2.4)*

1-hour PMP	= $1.13 \times 146 = 165$ mm
6-hour PMP	= $1.02 \times 381 = 389$ mm
24-hour PMP	= $1.01 \times 500 = 505$ mm

(Note: if annual series data had been compiled from fixed observational time intervals instead of hourly data, the adjustment factor for all durations would have been 1.13.)

*Adjustment of point PMP to 500 km<sup>2</sup> (Figure 4.7)*

	1 hour	6 hours	24 hours
Adjustment factors	0.66	0.85	0.90
PMP for 500 km <sup>2</sup> (mm)	103	331	455

Equation 4.3 are subject to the same adjustments described in section 4.3.

#### 4.5 CAUTIONARY REMARKS

The curves of Figure 4.1 are based on observed data from approximately 2 700 stations. About 90 per cent of the stations were in the United States, where observations were taken at least daily for a period of at least 10 years. Consequently, they assume that PMP has already occurred at those stations, providing controlling values of  $K_m$ . As a matter of fact, there are several measurements of rainfall in the United States made at locations without official gauges that exceed the PMP values calculated from this statistical procedure (Riedel, 1977). One reason given for excluding these measurements in developing the procedure was that the accuracy of the measurements was somewhat questionable and that there were no precipitation records for the locations of occurrence from which to compute  $\bar{X}_n$  and  $S_n$ . Estimates of these

parameters for nearby stations indicated that use of a  $K_m$  value of 25 would have yielded PMP values enveloping any rainfall amounts ever observed in the United States. Computations of  $K_m$  for Canada (McKay, 1965) indicated a maximum value of 30 associated with a mean annual maximum 24-hour rainfall amount of 15 mm.

Further studies are needed to determine more reliable values of  $K_m$ . It appears likely, for example, that  $K_m$  may be related to other factors besides rainfall duration and mean of the annual series. In using the procedure, it should be kept in mind that the indicated  $K_m$  values based on limited data may be too high for some regions and too low for others, and care must be exercised in selecting a value of  $K_m$  for a particular study. In general, the procedure tends to yield values of PMP lower than those to be obtained from meteorological, or traditional, procedures.

In selecting a station for making a PMP estimate for a particular drainage basin, it is important that its precipitation record is reasonably representative.

Comparisons of  $\bar{X}_n$  and  $S_n$  or  $C_v$  with nearby stations are recommended. Odd values in the basic data should be examined and discarded if found spurious, or the record for another station should be used. However, care must be exercised not to remove an amount merely because it appears to be an outlier in the data series. Length of record should be considered also. A long record will yield generally more reliable PMP estimates than will a short record of comparable quality. Wherever possible, records of no less than 20 years should be used and records of less than 10 years should not be used at all.

Area-reduction and depth-duration curves, like those of Figures 4.7 and 4.8, respectively, should be developed directly from storm rainfall data in the region for which estimates are to be made. Use of generalized curves based on data from climatically similar regions, even if storm selection is limited to

storms of the type capable of producing PMP over the study region, introduces additional sources of error in the PMP estimates. The magnitude of this error, though undefined, can be appreciable.

Although the use of these procedures can provide results with minimum effort, they are generally not considered as reliable as those obtained by use of procedures based on a comprehensive meteorological analysis. Every effort should be made to complete additional studies to support the results obtained by statistical procedures. This is particularly true in regions with short records. Many national meteorological services utilize these results only for very preliminary estimates to be used in reconnaissance or feasibility studies.

Note: Professor Lin has some new points on statistical approach on PMP estimation, see reference (Lin and Vogel, 1993).

---



## CHAPTER 5

# GENERALIZED ESTIMATES

### 5.1

### INTRODUCTION

Methods for estimating PMP discussed in Chapters 2 and 3 can be used for individual watersheds and large regions that include numerous watersheds of various sizes. For the latter case, the estimation is called generalized or regional estimation. Some studies of regional generalization for PMP estimation for small watersheds are also performed using hydrometeorological methods (storm maximization and storm transposition), statistical estimation methods and frequency analysis methods. Generalized estimation is highlighted by the regional generalization (smoothing) of PMP estimates for watersheds of various sizes in a large region. It also includes the generalization of storm depth-area-duration (DAD) curves, the generalization (ellipses or circles) of the spatial distribution of PMP and the generalization (single-peak) of the temporal distribution of PMP.

Generalized estimates can be expressed with two similar modes. The first mode is the isoline map, which shows regional changes in PMP for a particular duration for watersheds with a particular size. Such an isoline map is the generalized or regional map of PMP. The second mode establishes a series of correlations that enable users to determine a PMP estimate for any ideal watershed. It may also draw one or more topographical change index maps of PMP for a particular duration for a particular part or regional area. Isoline maps are often used for non-orographic regions. The second mode is often used in watersheds where topography plays a critical role in the precipitation process.

In hydrometeorological practices today, people (Kennedy, 1982; Myers, 1967; Natural Environment Research Council (NERC), 1975; Rakhecha and Kennedy, 1985) tend to perform studies of regional generalization (Hansen and others, 1977; Miller, 1963; Miller and others, 1984b; Schreiner and Riedel, 1978; Schwarz, 1963; United States Weather Bureau, 1961a, 1961b and 1966; Zurndorfer and others, 1986; Ministry of Water Resources of the People's Republic of China, Ye and Hu, 1979; Minty and others., 1996), and then use the results or methods (United States National Weather Service, 1984; Hansen and others, 1982; Rakhecha and Kennedy, 1985; Zurndorfer and others, 1986) to estimate PMP for individual watersheds (Fenn, 1985;

Miller and others, 1984a; Rakhecha and Kennedy, 1985; Zurndorfer and others, 1986; Minty and others, 1996). Studies of regional generalization are time-consuming and costly, but have the following benefits:

- (a) Maximum use can be made of all data over a region;
- (b) Regional, durational and areal smoothing is done in a consistent fashion for the region;
- (c) Consistency between estimates for basins in the region is maintained;
- (d) Once completed, the best estimates for individual basins can be made accurately and easily.

The application of generalized estimation usually comes with a number of restrictions. Topographical changes tend to increase along with area sizes in watersheds, complicating the drawing of generalized PMP maps, especially in orographic regions. Owing to such difficulties, generalized estimation is usually confined to orographic regions smaller than 13 000 km<sup>2</sup> and non-orographic regions smaller than 52 000 km<sup>2</sup>. In addition, durations of PMP estimates are confined to less than 72 hours, because if precipitation durations are longer than 72 hours, it is hard to express the spatial distribution with a set of concentric ellipses and the temporal distribution with a single-peak process.

#### 5.1.1 Base maps

The choice of a suitable map base for developing and depicting the series of isohyetal maps for various area sizes and durations or the index charts for generalized estimates of PMP depends chiefly on the size of the region for which the estimates are to be made, the topography, and on the degree of detail to be shown on the final maps. Base maps with a scale of around 1 : 2 500 000 may be adequate for many non-orographic – that is, not extremely mountainous – regions, while a smaller scale, say 1 : 5 000 000, might be adequate for very flat terrain. Regions of rugged orography require a larger scale, usually no less than 1 : 1 000 000. Whatever the scale, the base maps should show the topography of the region. The final maps used for displaying the estimates may be reduced considerably, of course, but not so much as to make it difficult for the user to locate a basin for which an estimate is required. For this reason, the final maps should

show the scale, a scale in kilometres, a latitude-longitude grid, and boundaries of states, provinces/districts and countries.

## 5.2 ESTIMATES FOR NON-OROGRAPHIC REGIONS USING GENERALIZED MAPS

Estimates in non-orographic regions are prepared in the same manner as described in Chapter 2. The basic procedures are moisture maximization, transposition, and smoothing (envelopment) of observed storm rainfalls. Moisture maximization of observed storm precipitation adjusts individual storm amounts to their maximum potential. Transposition procedures are used to expand the storm data base and are either to a series of grid points or to the explicit storm transposition limits of the major storms in the region. In either case, depth-duration, depth-area, and regional smoothing of individual analyses are required to develop a consistent set of PMP maps.

### 5.2.1 Moisture maximization

The maximum atmospheric moisture available for storm maximization throughout a region is an important requirement for the development of generalized charts of PMP. For reasons given in section 2.2, maximum persisting 12-hour 1 000-hPa dewpoints are used as indices of the maximum amount of atmospheric water vapour available for maximizing storms. Generalized charts of these dewpoints (Figure 2.4) are therefore required for making the various adjustments involved in developing generalized PMP estimates. Details on the development of the charts and procedures used in moisture maximization calculations are given in sections 2.2 and 2.3, respectively.

### 5.2.2 Storm transposition

Storm transposition (section 2.5) plays an important role in the preparation of generalized PMP estimates. In any large region there are many areas that have not experienced or recorded outstanding storms of the magnitude observed in adjacent areas or elsewhere in the region, and transposable storms are adjusted to conditions in these deficient areas to supplement the inadequate record of major storms.

In estimating PMP for a specific basin, comprehensive meteorological analyses of major storms are made to determine whether the storms are transposable to the basin. The storms considered

transposable are then adjusted as required by the geographic features of that particular basin. In the preparation of generalized PMP charts, the boundaries, or limits, of the area of transposability (Figure 2.5) of each major storm are delineated. Each storm is then transposed within its area of transposability to locations indicated by grid points on a suitable base map (section 5.1.1) or to the boundaries of the area, or both. Transposition to grid points has the advantage of allowing ready comparisons between rainfall values from different storms. Transposition to storm limits has the advantage of determining transposed values at the limits of explicit transposition. If the grid point procedure is used, a particular grid point may be just beyond transposition limits. This may result in an underestimate at this point. If transposition to storm limits is used, the problems of discontinuities between adjacent locations are minimized.

Transposition of a storm from its place of occurrence to another location involves adjustments for differences in geographic features of the two locations (section 2.6). The need for elevation adjustment is minimized if the transposition limits are so delineated that differences in elevation greater than 300 m within the area of transposability are avoided. When this is done, the elevation adjustment discussed in section 2.6.2 is generally omitted.

#### 5.2.2.1 Storm transposition techniques

Once a suitable base map has been selected, it is necessary to select the system to use for portraying transposed storm values on the base map. Two systems have been used. The first uses a grid system over the region. The second uses the explicit storm transposition limits as a basis.

##### 5.2.2.1.1 Grid system

If transposition to grid points is preferred, the points are usually selected to conform with the latitude-longitude grid of the map. The points formed by the intersections of the grid lines (which actually do not have to be drawn) indicate the locations to which the maximized storms are transposed and the maximum values plotted. Enough maps are prepared so that there are maps for a representative number of area sizes and durations, the number depending on the range in area sizes and durations of PMP values to be displayed. For example, one map may be used for developing and displaying 6-hour PMP for 100 km<sup>2</sup> areas, another for the 24-hour PMP over 1 000 km<sup>2</sup> areas, and so forth. Regardless of the number of maps required, the use

of the same grid on all maps is advisable as it will minimize the work involved in storm transposition.

The fineness or coarseness of the grid depends on the topography. In very flat regions, a grid of 2 latitude degrees by 2 longitude degrees may be adequate. In mountainous regions, a 0.5 degree grid may be too coarse. It is not necessary to have a uniform grid over an entire region. If a region includes both flat and somewhat complex terrain, a coarse grid may be used over the flat area and a fine one over the less flat regions.

#### **5.2.2.1.2    *Storm transposition limits***

In this technique, the explicit transposition limits of all storms important for determining the PMP estimates for a region are outlined on a series of maps. As with the grid point system, several base maps are required in this technique to ensure that the range of area sizes and durations is adequately represented. The storm values are then transposed to a number of representative points along their explicit transposition limits. In some cases, supplementary values are determined within the region defined by the explicit transposition limits. The number of points selected depends upon the gradient of the transposed rainfall amounts.

#### **5.2.3        *Data smoothing (envelopment)***

In the preparation of a series of generalized PMP charts for a region, it is important that consistency of estimates be maintained within and between the various charts. It is unrealistic to expect variation in PMP between different durations and sizes of area to be irregular and erratic, and smoothing of computed PMP values is justified. Smoothing is in fact mandatory if consistency is to be achieved. The smoothing techniques used are similar to those described in section 2.8. This smoothing is termed implicit transposition.

##### **5.2.3.1      *Data smoothing (envelopment) for grid point technique***

In use of the grid point method, depth-duration and then depth-area smoothing are completed first. Then, the areally and durationally smoothed values are plotted on maps and regional smoothing done.

###### **5.2.3.1.1    *Depth-duration smoothing***

In depth-duration smoothing, maximum adjusted rainfall amounts for various durations and a specified size of area for each maximized and transposed

storm applicable to a particular grid point or location are plotted on a depth-duration diagram. Figure 2.10 is an example of such a diagram for 2 000-km<sup>2</sup> values at one grid point. The data plotted are the largest maximized rainfall values for each duration, and a smooth curve is drawn to envelop these values.

###### **5.2.3.1.2    *Depth-area smoothing***

Smoothing and envelopment across area sizes is similar to depth-duration smoothing. Here maximum adjusted rainfall values for various sizes of area and a specified duration for each maximized and transposed storm applicable to a particular grid point or location are usually plotted on a semi-logarithmic graph, with size of area being plotted on the log scale. Figure 2.11 shows such a plot for 24-hour PMP. The data plotted at 2 000 km<sup>2</sup> are the same data used in Figure 2.10 for the 24-hour duration.

###### **5.2.3.1.3    *Combined depth-area-duration smoothing***

Depth-area and depth-duration smoothing is sometimes performed in one operation. This is normally done by plotting the data for various durations and sizes of area on one chart like that of Figure 2.12, with each plotted point being labelled with the appropriate storm identification and duration. Smooth isopleths are then drawn.

The combined smoothing procedure is sometimes confusing because of the relatively large amount of data plotted for each duration and size of area. The procedure is simplified by first subjecting the data to separate depth-duration and depth-area smoothing as described in sections 5.2.3.1.1 and 5.2.3.1.2. The values plotted on the combination chart are then taken from the enveloping depth-duration and depth-area curves. There is then only one value for each duration and size of area, as shown in Figure 2.12.

###### **5.2.3.1.4    *Regional smoothing***

Isohyets of PMP are drawn to the smoothed storm rainfall values plotted at grid points on a map of the study region. Limits of transposition of storms will usually result in discontinuities between some adjacent grid points. Regional smoothing must, therefore, take into account the effect of an extreme storm beyond the limits of its area of transposability. This regional smoothing is termed implicit transposition. In drawing smooth isohyets, meteorological factors – such as moisture source, storm

tracks, moisture barriers, etc. – need to be considered. Some plotted values may be undercut while others may be over-enveloped. This is done when data appear inconsistent with nearby values, and to draw for them would result in unwarranted bulges or dips in otherwise smooth isohyets. If there are geographic factors, such as an extended range of rough hills in a plains region, to support suspected inconsistent data, isohyets should, of course, be drawn to the data. If data at individual grid points have been smoothed properly (sections 5.2.3.1.1 and 5.2.3.1.2), little over-envelopment or undercutting is required.

#### **5.2.3.2 Data smoothing (envelopment) for the storm limit transposition technique**

In using the procedure in which moisture maximized transposed values are computed for the explicit storm transposition limits, regional smoothing for a particular area size and duration is completed first. At selected locations, depth-area and depth-duration curves are prepared and durational smoothing is accomplished second, followed by areal smoothing.

##### **5.2.3.2.1 Regional smoothing**

Isohyets of PMP are drawn to the storm rainfall values plotted along the explicit storm transposition limits on the map for a particular area size and duration. In drawing smooth isohyets, meteorological factors – such as moisture source, storm tracks and moisture barriers – need to be considered. Some plotted values may be undercut, though these should be few. Some values may be enveloped. This is done when data appears inconsistent with nearby values, and to draw for them would result in unwarranted bulges or dips in otherwise smooth isohyets. If there are geographic factors, such as an extended range of rough hills in a plains region, to support apparently inconsistent values, isohyets should, of course, be drawn to the data. The isohyets should be drawn with a minimum of over-envelopment, and with smooth regular gradients. Sharp gradients should be supported by the meteorological factors or topographic gradients.

##### **5.2.3.2.2 Depth-duration smoothing**

At selected locations on the series of maps prepared, the precipitation values are read from the smooth isohyets drawn for durations for a specific area size. A representative number of locations should be selected. These need not be so plentiful as the number of points selected in the grid point method,

but should be representative geographically. These values are plotted on the graph with the duration on the horizontal axis and the rainfall amounts on the vertical axis. The values should be identified with a controlling storm wherever possible. A smooth curve is drawn to these data (Figure 2.10). If the data on the individual maps have been smoothed properly, little over-envelopment or undercutting of values from the maps is required.

##### **5.2.3.2.3 Depth-area smoothing**

Smoothing and envelopment across area sizes is similar to depth-duration smoothing. In this case, however, all precipitation depths for a particular duration from the series of maps for a particular area size are selected. The values should be from the same locations as used for the depth-duration smoothing. The values for the various area sizes are plotted on a semi-logarithmic graph, the size of area being plotted on the log scale. The plot is similar to that used for the grid point screening technique, except that enveloping values from the series of maps are plotted. If a particular storm provides a controlling value for a particular area size, this point is labelled on the graph. Again if the data on the individual maps have been smoothed properly, little over-envelopment or undercutting of the values is required.

##### **5.2.3.2.4 Combined depth-area-duration smoothing**

Depth-area and depth-duration smoothing are sometimes performed in one operation in this method as with the grid point procedure. This is normally done by plotting the data for the different area sizes and duration on one graph. Each point is labelled with the appropriate duration, and if a particular storm is controlling, that notation is made. A smooth set of curves is then drawn. Since the initial regional smoothing eliminates all but the most important storms, the depth-duration and depth-area smoothing are normally done simultaneously.

#### **5.2.3.3 Preparation of final map**

The depth-duration, depth-area and regional smoothing using transposition to grid points or explicit storm transposition limits can rarely be accomplished with a single step. Rather the process should be viewed as an iterative procedure where the steps are repeated until the best relation is developed for all relations. Generally, other physiographic factors are used in the regional smoothing to aid in establishing isohyetal gradients and patterns on the PMP charts (section 5.2.4).

### 5.2.3.3.1 *Cross-sectional profiles*

A useful step in preparation of the final charts is to plot cross-sections along latitude lines, longitude lines, or lines normal to steep gradients on the isohyetal maps. These are usually plotted as depth-area-duration diagrams. The precipitation depths are selected along the cross-section lines at reasonably short intervals. These values are then plotted on a semi-logarithmic graph. The points should form a set of smooth curves. When smooth curves do not result, adjustments are made to the original maps and the process of depth-area, depth-duration and regional smoothing repeated. This is also an iterative process with the procedures continuing until the best possible set of depth-area curves, depth-duration curves and regionally smoothed isohyetal maps are prepared.

### 5.2.3.3.2 *Maintenance of consistency between maps*

In order to maintain consistency between maps when several are to be drawn for various durations and sizes of area, it is recommended that successive maps in a series be superimposed on a light table, and isohyets adjusted as required to form consistent patterns for both maps. For example, the map of 6-hour PMP for 1 000 km<sup>2</sup> might be superimposed on that for 1-hour PMP for the same size area. The 6-hour PMP isohyets should, of course, indicate higher values at every point on the map. Also, there is usually no reason for an isohyet on one map to show a dip, or depression, while the isohyet at the corresponding location on another map of about the same duration and size of area in the series shows a bulge. Of course, as differences in duration and size of area increase, there may be gradual changes in patterns so that bulges eventually become dips or vice versa.

Maps for different sizes of area should be compared and fitted to each other in the same manner. For example, isohyets on a map of 24-hour PMP for 1 000 km<sup>2</sup> should everywhere indicate greater depths than those for 24-hour PMP for 10 000 km<sup>2</sup>.

If maps for various months are required, as well as the all-season envelope, seasonal smoothing is necessary. Seasonal variation was discussed in section 2.10.

### 5.2.4 *Supplementary aids*

Preparation of generalized PMP charts is often facilitated by supplementary considerations. These considerations apply only to isohyetal gradients

and patterns, and should have little or no effect on magnitude of PMP values throughout the region, though they may have an impact at some locations. In other words, they provide guidance on the gradient and shape of isohyets while moisture-maximized storm rainfall values provide information on the magnitude of PMP.

Guidance can be provided by various types of climatological data. For example, a chart of maximum observed 24-hour point rainfall values from long observational records should show some resemblance to a generalized chart of 24-hour PMP for any size of area up to about 1–1000 km<sup>2</sup>. Rainfall-frequency charts may also be used for guidance, although they are not as reliable an indicator of regional variation of PMP since frequency is involved rather than magnitude alone. Similar regional patterns may be found also between charts of maximum observed point rainfalls for relatively long durations, say three consecutive days, and generalized PMP charts for similar durations. For larger areas, say 10 000 km<sup>2</sup> to 50 000 km<sup>2</sup>, weekly or monthly averages over geographic regions such as climatic zones of similar area sizes, can provide guidance on gradients and orientation of PMP isolines.

Regional similarity of generalized PMP and precipitation-frequency patterns does not prevail in those regions where one type of storm produces a large number of moderate to heavy rainfalls, but a different type provides the truly outstanding amounts. An example of this lack of similarity is found on Hawaii Island. There, frequent heavy showers associated with north-east trade winds produce high rainfall-frequency values, while extreme rainfalls invariably occur with the breakdown of these trade winds, and generally with winds from a very different direction. This climatic feature is reflected in differences between generalized PMP and rainfall-frequency patterns (Figure 5.1).

### 5.2.5 *General remarks*

Much work is involved in the preparation of a series of generalized PMP charts for different durations, area sizes and months. Two different procedures are followed in presenting the results of regionalized or generalized estimates of PMP. One method is to prepare as few such charts as are absolutely required and to provide depth-duration, depth-area, and seasonal variation curves to adjust the chart PMP index values as required. Often, especially for small basin sizes, index charts of point values are prepared for 1-, 6- and 24-hour depth-duration diagrams (Figure 5.2) and area-reduction curves (Figure 4.7)

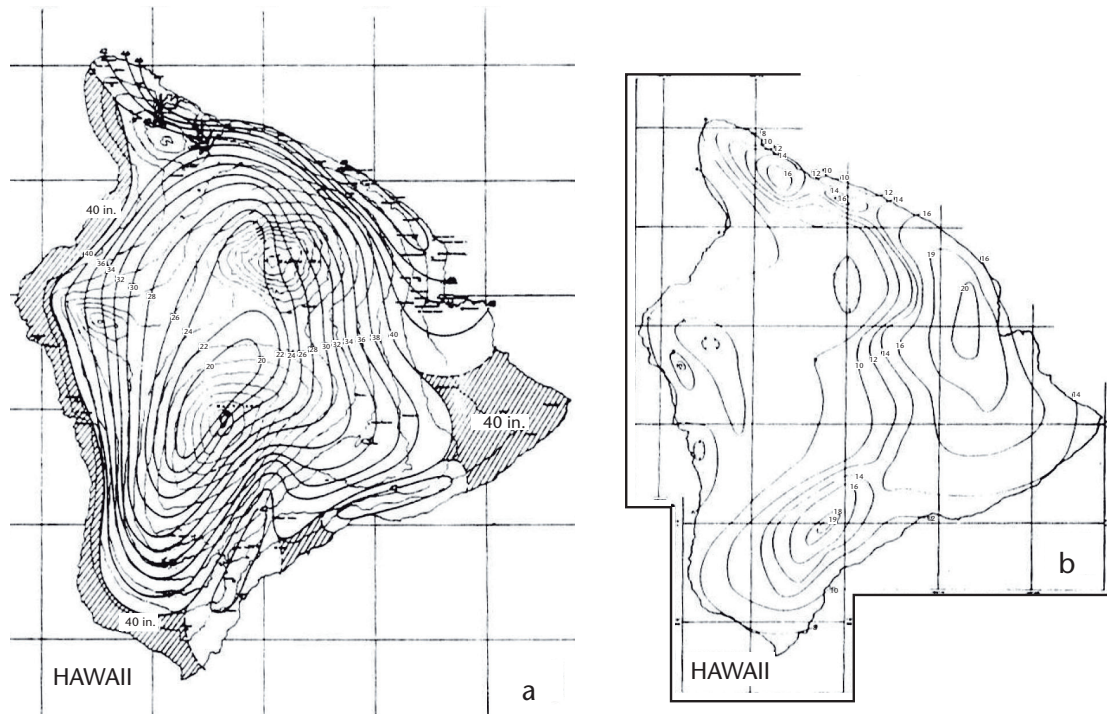


**Figure 5.1. Contrast in (a) PMP (Schwarz, 1963) and (b) 25-year rainfall patterns (United States Weather Bureau, 1962), both for 24-hour at a point, Island of Hawaii; particularly note differences on north-western coast**

were provided for making adjustments for other durations and basin sizes. The depth-duration diagrams (Figure 5.2) were based on maximized rainfall values from major storms over the western United States of America. A straight edge placed on either diagram so that it intersects the first and last verticals at the PMP values indicated on the maps for the corresponding durations will yield the PMP value for any intermediate duration by its intersection with the vertical for that duration. Thus, for example, if the 1- and 6-hour PMP values were 250 and 400 mm, respectively, a straight edge set at those values on the corresponding verticals of the diagram on the left side of Figure 5.2 would show a 2-hour PMP value of 300 mm. The depth-duration diagram of Figure 5.2 is based solely on storms from the western United States. In any other study, such diagrams should be based on the storms that have occurred over the study region. The area-reduction curves (such as Figure 4.7) could then be used to reduce the point values to average depths over the basin.

The second procedure is to develop charts for a range of area sizes and durations. Figure 5.3 shows the 25.9-km<sup>2</sup> 24-hour PMP map from a study for

the eastern United States (Schreiner and Riedel, 1978). In this procedure, the user may need to construct sets of depth-area-duration diagrams centred at the location of the basin. The PMP values plotted are selected from charts for various durations and representing standard storm area sizes both larger and smaller than the size of the basin. The storm-derived estimate of PMP is then adjusted to specific drainage characteristics. Isohyetal patterns and labels and appropriate temporal distributions are determined by use of an applications manual (Hansen and others, 1982; section 5.2.7).

### 5.2.6 Summary of procedural steps

The preparation of generalized or regionalized PMP estimates for non-orographic regions is summarized in the following steps:

- (a) Areas of transposability of major observed storms in the region of interest and surrounding areas are determined (section 5.2.2).
- (b) An adequate grid system is constructed transposition limits are outlined for all storms on a suitable base map or maps (section 5.2.2).

- (c) Depth-area-duration values of the selected major storms are maximized in place and transposed to grid points in their areas of transposability or to selected points along their explicit transposition limits. It is rarely necessary to transpose all storms to all grid points since adjustment of a few storms generally indicates which are likely to provide controlling (maximum) values at a particular grid point or set of grid points.
- (d) (i) If transposition to grid points is used, data at each point should be checked for durational and areal consistency, and smoothed (sections 5.2.3.1.1 and 5.2.3.1.2);  
(ii) If transposition to explicit storm transposition limits is used, draw isohyets to the values on several maps for the various area sizes and durations (Section 5.2.3.2.1).
- (e) (i) Draw preliminary isohyets to the values at each grid point. In drawing the isohyets, data at a few points may be undercut or over-enveloped if the data appear inconsistent with adjacent values and cause unwarranted bulges or dips in the otherwise smooth isohyets (section 5.2.3.1.4);  
(ii) The data of selected locations should be checked for duration and areal consistency (sections 5.2.3.2.2 and 5.2.3.2.3).
- (f) Whatever supplementary aids are available are used for spacing and shaping isohyets between grid points and maintain consistency between maps (section 5.2.4). Final isohyets should be smooth, with no unjustifiable dips, bulges, or gradients.
- (g) If maps are prepared for a range of area sizes and durations, the user will have the information necessary to develop smooth depth-area-duration relations so storm PMP values may be calculated for any desired basin. If a generalized chart of PMP for just one specific size of area and duration is prepared, index relations are provided so values for other area sizes and durations can be computed. PMP for other sizes of area and durations are then obtained from these relations, and any necessary depth-area-duration relations calculated for the location of the basin of interest.

### **5.2.7 Application of generalized or regionalized non-orographic PMP estimates to specific basins**

Regionalized, or generalized, estimates of PMP in non-orographic regions provide storm-centred values. It is necessary to develop specific procedures to apply to these storm-centred values to develop a

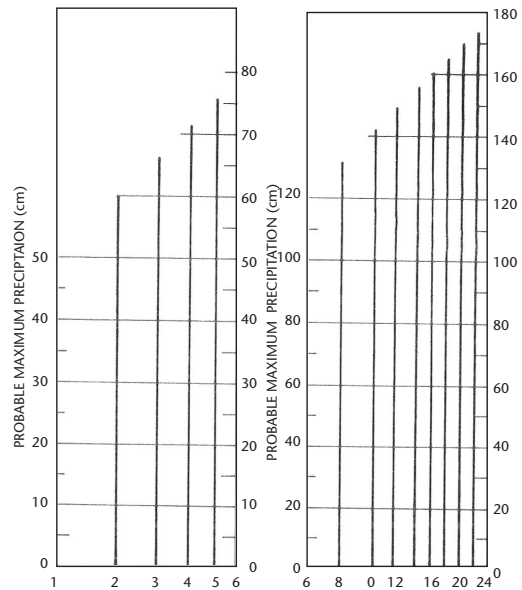


**Figure 5.2. Depth-duration interpolation diagrams from study for western United States (United States Weather Bureau, 1960)**

PMP estimate for a specific basin. These procedures are usually provided in an applications manual, which considers the shape and preferred orientations of the isohyetal pattern, the spatial distribution of the isohyetal pattern, and the preferred time distribution of the 6-hour increments of PMP. This is information is usually necessary for the determination of the peak discharge and total volume of the flood hydrograph to permit evaluations of the PMF for a particular location. Procedures described in this section are based on a study for the eastern United States (Hansen and others, 1982). They are based on information derived from major storms in the region and are applicable to non-orographic portions of the region. Variations in these procedures must be developed if they are to be used in orographic regions (section 5.3.6). It should be emphasized that the procedures described may be applicable in other regions, but specific results cannot be applied directly in other regions without detailed examination of data for that region and development of the necessary relations.

#### **5.2.7.1 Temporal distribution**

When applying PMP to determine the flood hydrograph, it is necessary to specify how the rain falls with time. Such rainfall sequences are termed the mass curve of rainfall of the storm. They are the accumulated rainfall plotted against the time since the beginning of the storm. Mass curves of rainfall observed in severe storms show a great variety of sequences of 6-hour rain increments. Certain

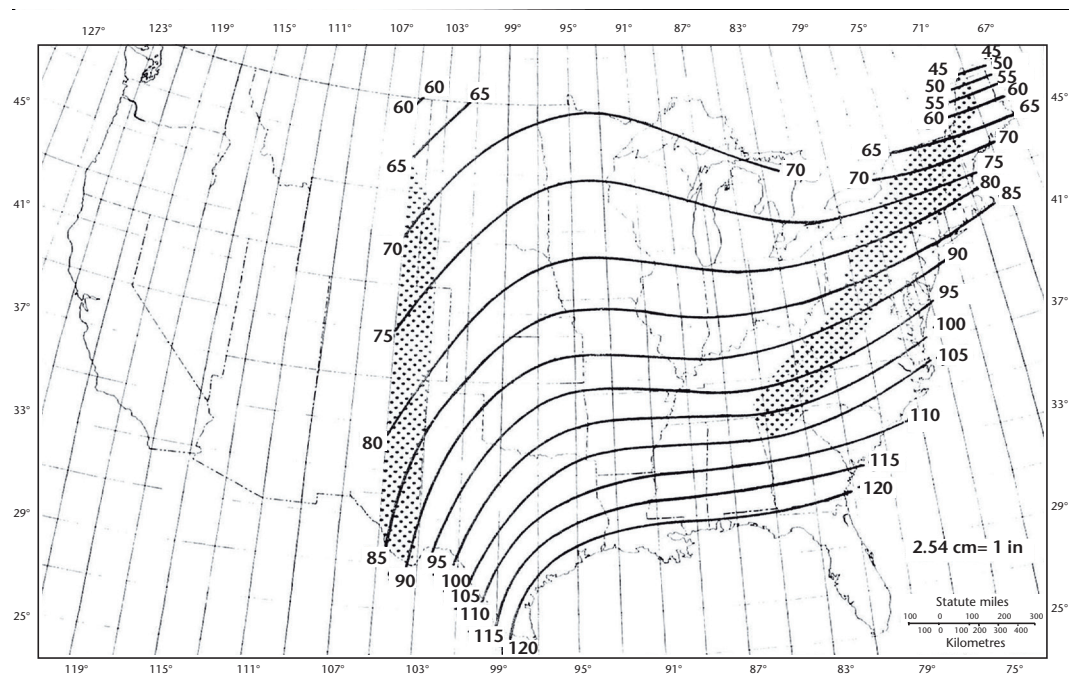


**Figure 5.3. All-season envelope of 24-hour 25.9 km<sup>2</sup> PMP (cm; Schreiner and Riedel, 1978); stippled areas are regions where orographic effects have not been considered**

sequences result in more critical flow (higher peak) than others. The normal practice is to consider the sequences of 6-hour rain increments in the most important storms in the region. For the eastern United States, guidance for recommending sequences for PMP was developed from 53 of the most important storms in the region. In this study, three criteria were used to select storms for consideration. First, the moisture-maximized storm rainfall had to be within 10 per cent of the PMP for the storm location. Second, the storm had to last for the entire 72-hour period of interest. Finally, the storm had to cover the full range of area sizes considered in the study (259 km<sup>2</sup> to 51 800 km<sup>2</sup>).

In these storms, the observed rainfall sequences were examined. A first step was to define the number of rain bursts within each storm. A rain burst was defined as one or more consecutive 6-hour rain increments for which each individual increment had 10 per cent or more of the 72-hour rainfall. Different results were obtained by redefining a rain burst as containing 20 per cent of the 72-hour rainfall. Still other results would be obtained if 5, 15, 25 per cent or some other value were used. Examination of the incremental rainfall sequences for each of the storms allowed compilation of some constructive information. There were three temporal characteristics of importance: (a) the number of bursts in each sequence; (b) the duration of each burst; and (c) the time interval

between bursts. Figure 5.4 shows examples of temporal sequences of 6-hour precipitation in five major storms. The first example of Figure 5.4, the storm of 6–8 June 1906, illustrates three temporal characteristics of interest in these storms using the definition of a burst as 10 per cent of the total storm rainfall. There are two bursts observed for the 259-km<sup>2</sup> area and three bursts for the 25–900-km<sup>2</sup> area. For the 259-km<sup>2</sup> area, the first rain burst is 12 hours long and the second is 6 hours long. These are separated by 6 hours. The first burst for the 25 900 km<sup>2</sup> area is 6 hours long, separated by 12 hours from the second burst of 12 hours, which in turn is separated by 6 hours from the last burst of 6 hours. The limited example of storms examined showed almost any arrangement could be found in the data. The storm centred at Council Grove, Kansas, showed daily bursts of 12 hours with lesser rains between. Another storm, not shown in Figure 5.4, at Warner, Oklahoma, showed the greatest 6-hour increments to be consecutive in the middle of the 72-hour rain sequence. To get PMP for all durations within a 72-hour storm requires that the 6-hour increments be arranged with a single peak. This seemed consistent with the observed rainfall sequences in the majority of these major storms. A 24-hour rain period was selected as being representative of the rain bursts in major storms. The rainfall was then divided into three 24-hour periods in the 72-hour storm. The following guidance was then given for

arranging the 6-hour increments of PMP within the 72-hour storm period for this particular region.

To obtain PMP for all durations:

- Individual 6-hour increments are arranged so that they decrease progressively to either side of the greatest 6-hour increment. This implies that the lowest 6-hour increment will be either at the beginning or the end of the sequence.
- The four greatest 6-hour increments are placed at any position in the sequence, except within the first 24-hour period of the storm sequence. The study of major storms shows maximum rainfall rarely occurs at the beginning of the sequence.

#### 5.2.7.2 Isohyetal patterns

The two most important considerations regarding an isohyetal pattern used to represent PMP rainfalls are:

- The pattern shape and how it is to be represented;
- The number and magnitude of the isohyets within the pattern.

In the study for the eastern United States (Hansen and others, 1982), 53 major storms were examined. It was apparent from this sample that the most representative shape for all such storms is that of an ellipse. The actual storm patterns in general are extended in one or more directions, primarily as a result of storm movement, and an ellipse having a particular ratio of major to minor axis is usually the best fit to the portion of the storm having the heaviest precipitation. The variation of shape ratios for the 53-storm sample is summarized in Table 5.1. Shape ratios of 2 are most common in this region, followed by those of 3 and 4. Of the storms summarized in Table 5.1, 62 per cent had shape ratios of 2 or 3. These ratios were also examined for regional bias, bias by magnitude of storm, or bias by total area size of the storm. In all cases, the preference was for a ratio of major to minor axis of 2 to 1 or 3 to 1. Since the majority of the storms considered had shape ratios of 2 or 3, an idealized elliptical isohyetal pattern with a ratio of major to minor axis of 2.5 to 1 was recommended for distribution of all 6-hour increments of precipitation over

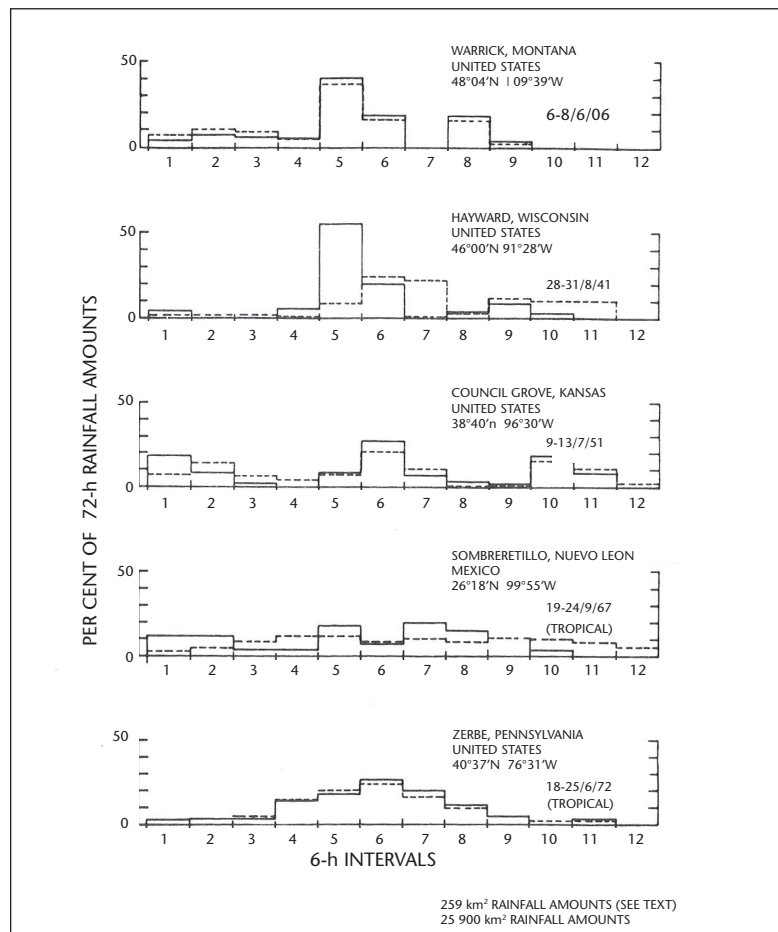


**Figure 5.4 Examples of temporal sequences of 6-hour precipitation in major storms in eastern and central United States (Hansen and others, 1982)**

non-orographic drainages of the eastern United States. This recommended pattern is shown in Figure 5.5. The pattern should be centred over a drainage to obtain the hydrologically most critical runoff volume. Since most drainages have irregular shapes, the pattern shape in Figure 5.5 will not fit exactly over any individual drainage, so there will generally be portions of the drainage that will not be covered by the pattern for a particular area size of PMP. The precipitation that lies outside the area of the PMP pattern is termed residual precipitation. It should be emphasized that residual precipitation is outside the area of the defined PMP storm pattern (section 5.2.7.5), but not necessarily outside the drainage. This residual precipitation is considered in developing the average depth over the basin and in the computations for any resulting flood hydrograph.

#### 5.2.7.3 Isohyetal orientation

It is possible to place the isohyetal pattern of the PMP storm over the drainage in any direction. However, this may not be meteorologically reasonable. In the eastern United States, the question was examined to determine if there were preferred orientations for major storms in the region. Figure 5.6 shows the resulting analysis of preferred orientations for major storms in the eastern United States, based on the orientation of several hundred large storms. In addition to the isolines of preferred orientations, the orientations of 31 selected major storms are shown. Because of the variability in the

**Table 5.1. Shape ratios of isohyetal patterns for 53 major rain events in the eastern United States\_ (Hansen and others, 1982)**

	Shape ratio								
	1	2	3	4	5	6	7	8	Total
Percentage of total	3.8	41.5	20.8	20.8	7.5	3.8	1.9	0	100
Accumulated percentage	4	45	66	87	94	98	100	100	

observed orientations of storms, any orientation within  $\pm 40^\circ$  of the isolines shown on the map was considered to be within the preferred orientation of major storms.

In the application of PMP to the specific drainage, therefore, full value of PMP was used for the range of orientations within  $\pm 40^\circ$  of the value read from the map (Figure 5.6). Beyond this range of orientation some reduction of the PMP would be expected. The percentage reduction was determined from the examination of major storms. Within various storm regions, the amount of precipitation in major storms was expressed as a percentage of the maximum value within that region (the value that was associated with the preferred orientation) and plotted on a series of graphs (not shown). These graphs were used to develop the relation for determining the adjustment factor to apply to isohyetal values (Figure 5.7). No reduction was applied to storms of less than  $777 \text{ km}^2$ , since this area was considered to

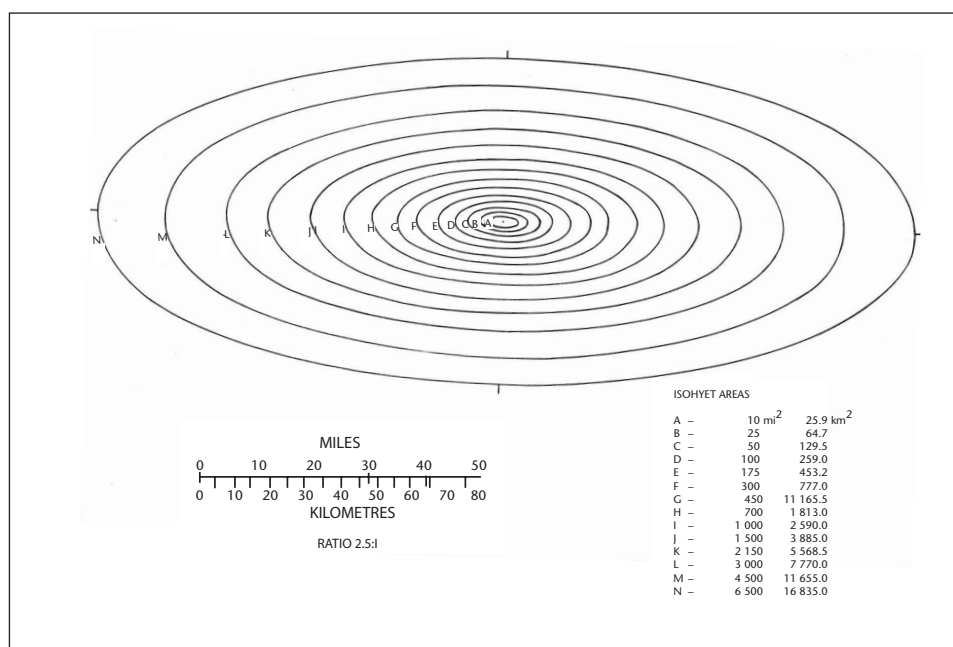


**Figure 5.5. Standard isohyetal pattern recommended for spatial distribution of PMP for the United States east of the 105th meridian (Hansen and others, 1982)**

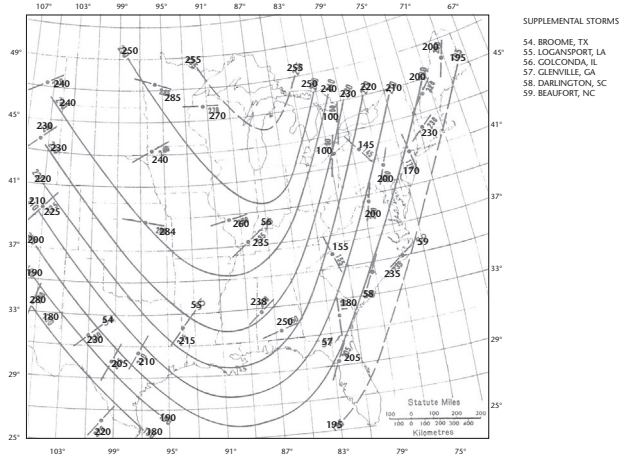


**Figure 5.6.** Analysis of isohyet orientations for selected major storms in United states east of the 105th meridian adopted as recommended orientation for PMP within  $\pm 40^\circ$  (Hansen and others, 1982)

be representative of a single thunderstorm or possibly a complex thunderstorm cell. These systems could be expected to occur with equal intensity at any orientation. It was determined that the maximum reduction would apply to an area of 7 770 km<sup>2</sup> or larger. Reductions between these two extremes were assumed to increase in a linear fashion.

#### 5.2.7.4 Isohyet values

Within observed storms in the eastern United States, rainfall for smaller areas within a storm providing controlling values for the large-area PMP storm will be less than the corresponding storm rainfall providing PMP values for small areas (Schreiner and Riedel, 1978). Therefore, the depth-area relation for PMP should not be used to determine the isohyet values for the PMP storm. The term adopted for the depth-area relations in the PMP storm is thus a within-storm relation, since it serves to represent a relation for which one storm determines the depth of precipitation over all area sizes less than the area of the PMP storm. It is also true for this region that for areas larger than the area of the PMP storm the precipitation is less than the PMP magnitude. The term adopted for this rainfall distribution is without-storm curves, or residual precipitation. Figure 5.8 shows a schematic of these relations. The within-storm/without-storm distribution of PMP for a drainage will fall somewhere between a flat average value (uniform distribution) and the depth-area relation of PMP. Record storm rainfalls show a wide variation in DAD relations between these extremes. They all indicate a sharp decrease with area size for the maximum 6-hour rainfall. The remaining 6-hour rainfall increments may vary from showing a decrease, an increase, or

no change with increasing area size. In most PMP studies, the 6-hour incremental values beyond the three greatest 6-hour increments are small enough that a uniform distribution is applied.

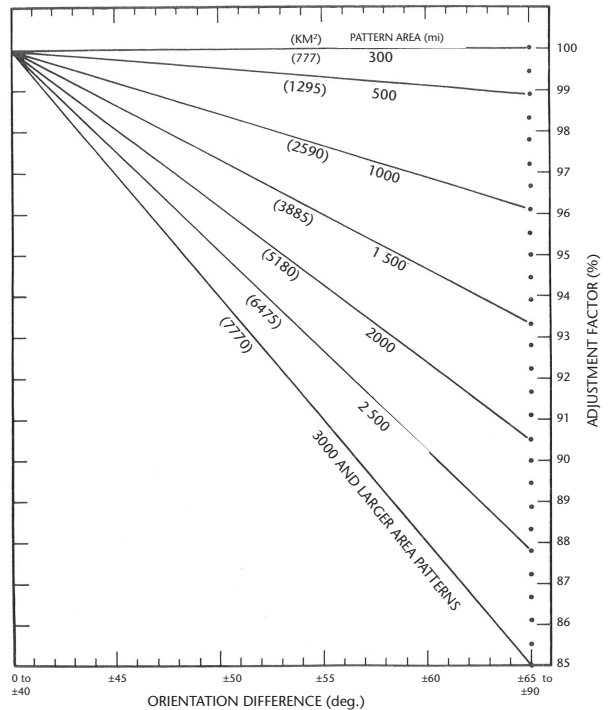


**Figure 5.7.** Model for determining the adjustment factor to apply to isohyet values as a result of placing the pattern in Figure 5.5 at an orientation differing from that given in Figure 5.6 by more than  $\pm 40^\circ$ , for a specific location (Hansen and others, 1982)

#### 5.2.7.4.1 Nomogram for isohyet labels for each of the largest three 6-hour increments

The procedure used to develop nomograms for providing isohyet labels is similar for each of the first three increments. In this section, the procedure used to develop the nomogram to provide isohyet labels for the maximum 6-hour period is discussed. The same procedure can be used for the next two largest increments. In some situations, the nomogram for the third increment is determined by interpolation between the second increment and a single average depth.

The first step is to select the largest storms in the region. Generally, all storms within some fixed percentage of the PMP depths are used, for example those storms with moisture-maximized depths within 10 per cent of the PMP values. Next, depth-area data for these storms are used to form all available ratios of depths. That is, the average precipitation depth for the 25.9-km<sup>2</sup> area is divided by the average precipitation depth for the 25.9-km<sup>2</sup>, 518-km<sup>2</sup>, 2 590-km<sup>2</sup>, 12 950-km<sup>2</sup>, 25 900-km<sup>2</sup> and 51 800-km<sup>2</sup> areas. The first of these ratios is, of course, unity. These within/without-storm average ratios, since they are done individually for each storm, are computed as a percentage of the respective storm area size precipitation amounts. The ratios obtained are then averaged and the average ratio plotted against area size. The relation

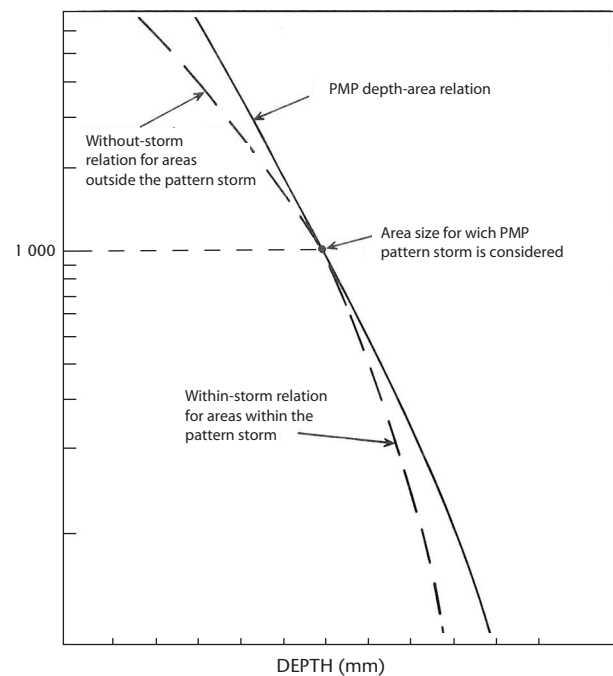


**Figure 5.8. Schematic diagram showing the relation between depth-area curve for PMP and the within/without-storm relations for PMP at 1 000 km<sup>2</sup> (Hansen and others, 1982)**

for the storms in the eastern United States (Hansen and others, 1982) is shown in Figure 5.9. The

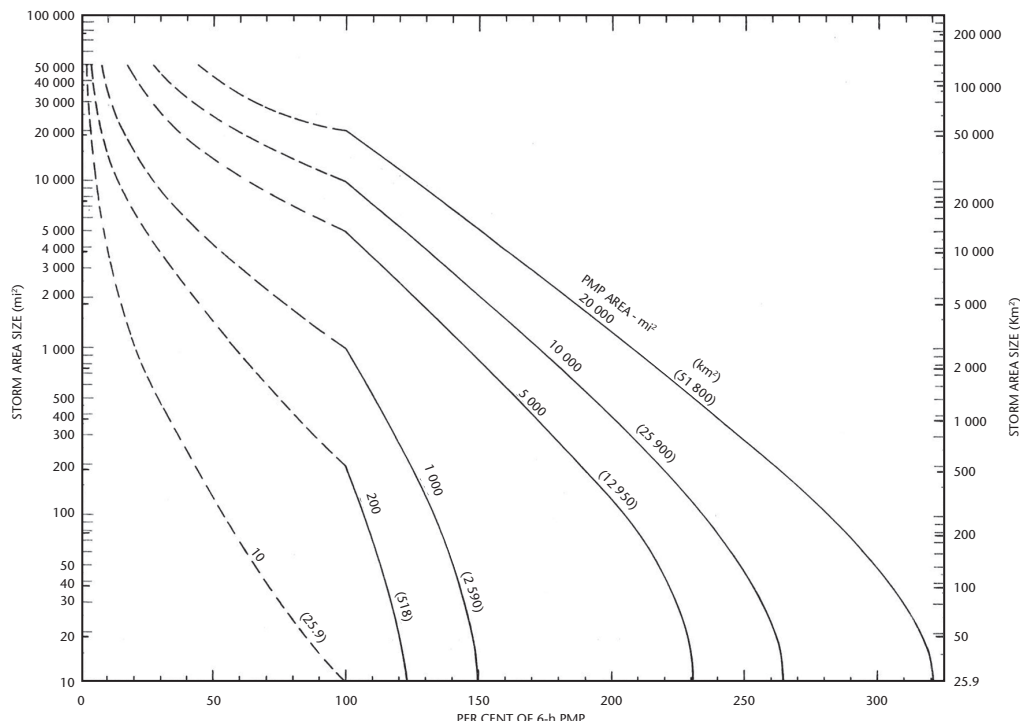


**Figure 5.9. Six-hour within/without-storm average curves for standard area sizes (Hansen and others, 1982)**

solid lines represent within-storm averages for areas less than that of the PMP storm, and the dashed lines represent without-storm averages for areas greater than the area of PMP storm, or the residual precipitation.

Now, by applying the curves in Figure 5.9 to the storm area average PMP from a generalized study at a specific location,  $37^{\circ}$  N  $89^{\circ}$  W, a set of curves of the form shown in Figure 5.10 can be obtained. The solid curves connect to 6-hour PMP for various area sizes. The short-dashed lines are the within-storm curves for areas less than the PMP area, and the long-dashed lines are the without-storm curves for areas larger than the PMP area. The curves of Figure 5.10 can then be used to develop isohyetal profiles as discussed in section 2.11.3. Isohyet profiles were developed for specific locations in the eastern United States. Those of Figure 5.11 are for  $37^{\circ}$  N  $89^{\circ}$  W. These profiles were then normalized

by converting them to a percentage of the greatest 6-hour increment of PMP for this location. The normalized isohyetal profiles were compared for several locations in the eastern United States and no consistent regional variation could be found. The various isohyetal profiles were combined, therefore, and a nomogram for determining the labels on the isohyet for the first 6-hour PMP increment and for the standard isohyet area sizes between 25.9 and 103 600  $\text{km}^2$  was developed (Figure 5.12).

#### 5.2.7.4.2 Isohyet labels for remaining 6-hour increments

For the fourth through to the twelfth increment in the 72-hour PMP storm, the average depth for the PMP increment is usually small and a use of that depth as an average value over the basin is sufficient. In regions where the increment is large, additional nomograms distributing the rainfall over

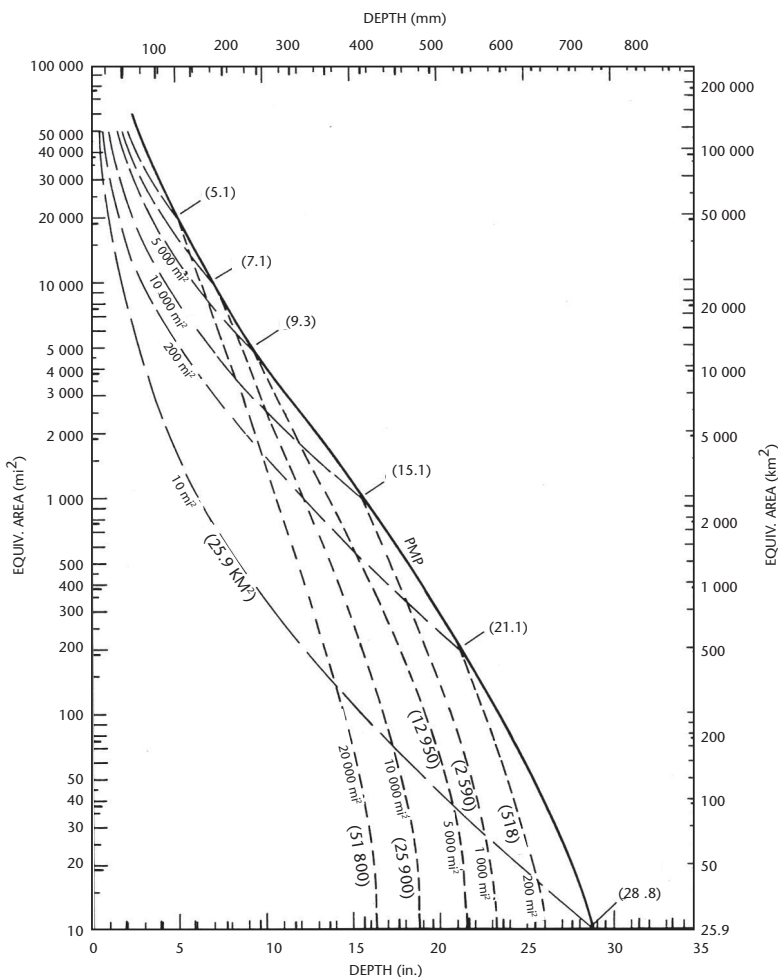


**Figure 5.10. Within/without storm curves for PMP at  $37^{\circ}$  N,  $89^{\circ}$  W Tennessee River basin over Chattanooga, Tennessee (Zurndorfer and others, 1986). W for standard area sizes (Hansen and others, 1982)**

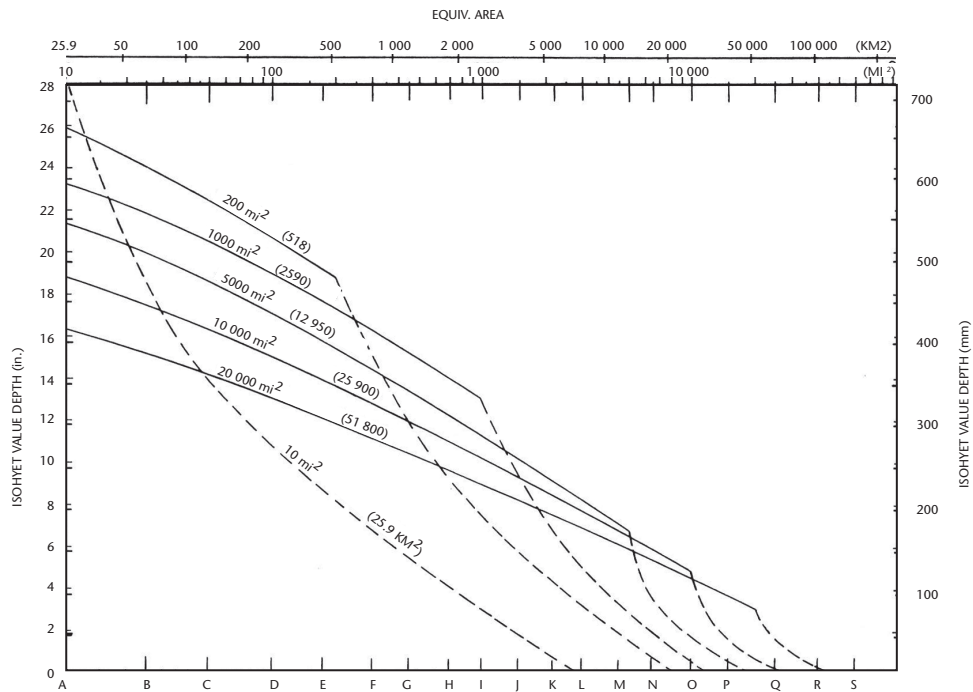


**Figure 5.11. Isohyetal profiles for standard area sizes at 37° N, 89° W (Hansen and others, 1982)**

the basin should be developed. Outside the PMP storm area the residual precipitation should continue to decrease. For the study in the eastern United States (Hansen and others, 1982), the tendencies from the nomograms for the first three increments were used to develop a nomogram (not shown) for computing isohyetal labels for residual precipitation for the remaining increments. A single nomogram was used for all nine increments.

#### 5.2.7.5 Selection of area of PMP storm for drainage

The selection of area of the PMP storm pattern is based on maximizing the volume of precipitation within the drainage. The maximum volume is a function of the PMP storm-pattern centring, of the irregularity of the basin's shape, and of the area size of PMP distributed over the drainage. The pattern centring is a decision of the meteorologist or others determining the individual drainage estimate. If there are no meteorological or topographical controls on the placement of the pattern, it is recommended that the pattern be centred so as to place as many complete isohyets within the drainage as possible. The irregularity of the drainage is fixed, and the area of the PMP storm pattern is the remaining variable. This optimum area is determined by a series of trials. A first step is to choose areas that are near those of a standard isohyet (section 5.2.7.2) in an idealized pattern (Figure 5.5)

and that are both larger and smaller than the area size of the drainage. Next, the volume of precipitation for each of the three greatest 6-hour increments of PMP for the area sizes chosen are computed and the total volume of rainfall over the drainage is determined. Then, additional areas on either side of the area size that gave the maximum volume are chosen and the volume corresponding to each of these is evaluated. By this trial process, and by plotting the results as area size (selected) versus volume (computed), the area size in which the volume reaches the maximum can be determined.

#### 5.2.7.6 Stepwise procedure

The procedures developed for determining maximum volume over the drainage utilizes the sum of the volumes for the largest three 6-hour increments of PMP. The example given below shows the procedure for the greatest increment. The procedure for the other two increments is the same.

- 6-hour incremental PMP:
  - Depth-area-duration data is obtained from generalized study (such as those represented in Figure 5.3) for the location of the drainage.
  - The data in (a)(i) is plotted on a semi-logarithmic graph (area on the log scale) and a smooth curve through points for common duration is drawn.

- (iii) Values for a set of standard area sizes both larger and smaller than the area sizes of the specific drainage are read off the curves from step (a)(ii).
  - (iv) For each of the standard pattern area sizes in step (a)(iii), the depth-duration data is plotted on a linear graph and a smooth curve is fitted to enable interpolation of values for intermediate durations.
  - (v) Incremental differences are obtained for each of the first three 6-hour periods through successive subtraction for each area size considered in (a)(iv).
- (b) Isohyetal pattern:
- (i) A tracing of the drainage should be placed over the isohyetal pattern developed. These should both be of the same map projection and scale. Placement should generally be done so as to put the maximum precipitation in the drainage. In most cases this condition is met by drainage-centring the isohyetal pattern.
  - (ii) The orientation of the pattern when placed on the drainage is determined.
  - (iii) The preferred orientation for PMP conditions is determined from Figure 5.6 at the location of the pattern centre. If the difference between the orientation from (b)(iii) and (b)(ii) is less than  $40^\circ$ , then no reduction factor needs to be considered for that placement of the isohyetal pattern over the drainage. If the orientation difference exceeds  $40^\circ$ , then it must

be decided whether the pattern is to be:

- a. placed at some angle to the drainage at which no reduction to isohyetal values used is required, or
  - b. aligned with the drainage and reduction made to the isohyetal values.
  - (iv) This step is carried out if no adjustment for orientation is needed. Having settled on the placement of the isohyetal pattern, the appropriate adjustment factor due to the orientation of the isohyets involved is determined from the model shown in Figure 5.7. Note that the amount of reduction is dependent upon the PMP storm area size (only areas larger than  $777 \text{ km}^2$  need to be reduced) and the difference in orientation. The adjustment factor is multiplied by the corresponding 6-hour incremental amounts from (a)(v) for each pattern area size to obtain incremental values reduced as a result of the pattern orientation.
- (c) Maximum precipitation volume:
- (i) The name of the drainage, drainage area, data of computation and increment (either first, second or third) is placed in the appropriate boxes at the top of the form shown in Figure 5.13.
  - (ii) The area size ( $\text{km}^2$ ) from (a)(iii) for which the first computation is made is placed under the heading at the upper left of the form.

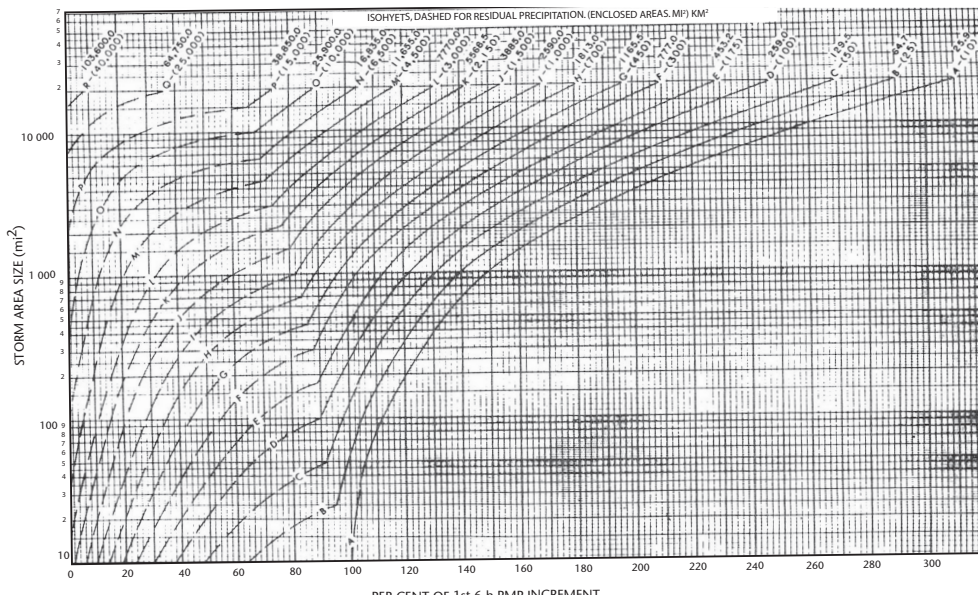


**Figure 5.12. Nomogram for the first 6-hour PMP increment and for standard isohyet area sizes between 25.9 and 103 600 km<sup>2</sup> (Hansen and others, 1982)**

- (iii) Column I contains a list of isohyet labels. Only as many as needed to cover the drainage are used.
- (iv) For the area size in (c)(ii), the corresponding percentages derived from the nomogram in Figure 5.12 for those isohyets needed to cover the drainage are listed in column II.
- (v) The value from (b)(iv) corresponding to the area size and increment of the computation is placed under the heading AMT (amount) in column III. Each of the percentages in column II is multiplied by the AMT at the head of column III to fill column II.
- (vi) Column IV represents the average depth between adjacent isohyets. The average depth of the A isohyet is taken to be the value from column III. The average depth between all other isohyets which

are totally included by the drainage is the arithmetic average of paired values in column III. For incomplete isohyets covering the drainage, the average depth between the isohyets should be estimated considering the percentage of the area between isohyets covered by drainage.

- (vii) Column V lists the incremental areas between adjacent isohyets. When the isohyets are completely enclosed by the drainage, the incremental area can be determined from the standard area sizes of the iso-hyetal pattern. For all other isohyets it is necessary to planimeter the area of the drainage enclosed by each isohyet and make the appropriate successive subtractions. The sum of all the incremental areas in column V should equal the area of the drainage.

Drainage:						Area:						Date:						
Area size	Iso.	Nomo.	Amt.	Avg. depth	$\Delta A$	$\Delta V$	Area size	Iso.	Nomo.	Amt.	Avg. depth	$\Delta A$	$\Delta V$					
A							A											
B							B											
C							C											
D							D											
E							E											
F							F											
G							G											
H							H											
I							I											
J							J											
K							K											
L							L											
M							M											
N							N											
O							O											
P							P											
Sum =						Sum =						Sum =						
Area size			Amt.				Area size			Amt.			Area size			Amt.		
A							A						A					
B							B						B					
C							C						C					
D							D						D					
E							E						E					
F							F						F					
G							G						G					
H							H						H					
I							I						I					
J							J						J					
K							K						K					
L							L						L					
M							M						M					
N							N						N					
O							O						O					
P							P						P					
Sum =						Sum =						Sum =						
Area size			Amt.				Area size			Amt.			Area size			Amt.		
A							A						A					
B							B						B					
C							C						C					
D							D						D					
E							E						E					
F							F						F					
G							G						G					
H							H						H					
I							I						I					
J							J						J					
K							K						K					
L							L						L					
M							M						M					
N							N						N					
O							O						O					
P							P						P					

Figure 5.13. Example of computation sheet showing typical format (Hansen and others, 1982)

- (viii) Column VI gives the incremental volume obtained by multiplying the values in column IV by those in column V. The incremental values are summed to obtain the total volume of precipitation in a drainage for the specified pattern area size in the first 6-hour period.
- (ix) Steps (c)(ii) to (c)(viii) are repeated for all the other pattern area sizes selected in (a)(iii).
- (x) The largest of the volumes obtained in (c)(viii) and (c)(ix) represent the preliminary maximum volume for the first 6-hour incremental period. The pattern area to which this volume relates can then be found. The area of the maximum volume can be used as guidance in choosing pattern areas to compute volumes for the second and third 6-hour incremental periods. Note: the second and third 6-hour incremental volumes can be computed by repeating steps (c)(i) to (c)(ix) using appropriate nomograms (not shown).
- (xi) The sum of values from the largest three 6-hour increments for corresponding area sizes are plotted in terms of volume versus area size (semi-logarithmic plot). The points are connected to determine the area size of the precipitation pattern that gives the maximum 18-hour volume for the drainage. This is the PMP storm area size.
- (d) Distribution of storm-area average PMP over the drainage:
  - (i) For the pattern area size for PMP determined in (c)(xi), the data from (a)(iii) is used to extend the appropriate depth-duration curve in (a)(iv) to 72 hours and values are read off the smooth curve for each 6-hour interval (6 hours to 72 hours).
  - (ii) Six-hour incremental amounts for data in (d)(i) are obtained for the fourth through to the twelfth 6-hour periods in accordance with (a)(v), and procedural steps (b)(i) to (b)(v) are followed to adjust these incremental values for isohyet orientation if needed.
  - (iii) Incremental average depths for each of the twelve 6-hour periods in the 72-hour storm are given by (d)(i) and (d)(ii). To obtain the values for the isohyets that cover the drainage, the first 6-hour incremental depth is multiplied by the first 6-hour percentages obtained from Figure 5.11 for the area sizes determined

in (c)(xi). Then the second 6-hour incremental depth is multiplied by the second 6-hour percentages from a nomogram similar to Figure 5.12, and so forth. As a result of this step, isohyet label values can be placed in a table similar to the template below (to the extent of which-ever isohyets cover the drainage):

	6-hour period											
	1	2	3	4	5	6	7	8	9	10	11	12
A	-	-	-	-	-	-	-	-	-	-	-	-
B	-	-	-	-	-	-	-	-	-	-	-	-
C	-	-	-	-	-	-	-	-	-	-	-	-

- (iv) To obtain incremental average depth over the drainage, the incremental volumes for the area size of the PMP pattern determined in (c)(xi) is computed. Divide each incremental volume by the drainage area (that portion covered by precipitation).

- (e) Temporal distribution:  
In the table in (d)(iv), (storm-area averaged) PMP has been spatially distributed according to increasing 6-hour periods. (Drainage-averaged PMP will be obtained by completing (d)(iv).) The increments in (d)(iii) are arranged according to a PMP depth-duration curve. The incremental values should be arranged according to the criteria of section 5.2.7.1.

## 5.3 ESTIMATES FOR OROGRAPHIC REGIONS

### 5.3.1 Introduction

In orographic regions the problems in deriving regionalized or generalized PMP charts are much more complex than for non-orographic areas. Differences in topography and its effects, storm types, amount of data available and so forth preclude the development of a standard basic procedure adaptable to the wide variety of situations encountered in making regionalized PMP estimates. One approach to such estimates is based on non-orographic PMP values modified for orography. The modification procedures differ for different situations. Since there is no standard procedure for modification, summarized examples from actual studies may provide some guidance on how this procedure is used to develop regionalized PMP

estimates. The examples presented in sections 5.3.2, 5.3.3, 5.3.4, 5.3.6 and 5.3.7 of this chapter were selected to represent a variety of conditions.

Another approach is the orographic separation method. In this approach, the convergence and orographic components of PMP are estimated separately and then combined. PMP estimates made by this method using a laminar flow model to estimate orographic PMP (United States Weather Bureau, 1961a, 1966), were discussed in detail in sections 3.2 and 3.3, and are not included here. The alternative procedure mentioned in section 3.1.6.1 for use of the orographic separation method (Hansen and others, 1977) is described in section 5.3.5.

### **5.3.2 PMP for drainages up to 259 km<sup>2</sup> in the Tennessee River basin**

A procedure for determining PMP for the entire eastern half of the Tennessee River basin above Chattanooga, Tennessee, was described in section 3.4.2. The western half is comprised of relatively low rolling hills. Generalized PMP estimates have been made for the entire basin for drainages up to about 7 800 km<sup>2</sup> (Zurndorfer and others, 1986). Because of a specific requirement for generalized PMP estimates for small basins up to about 259 km<sup>2</sup> and the fact that different types of storms are likely to produce PMP over small and large areas, separate investigations were conducted for small basins and for drainages between 259 and 7 800 km<sup>2</sup>. Only the estimates for the eastern half of the entire basin are described in this manual. The eastern half is referred to hereafter as the project basin. This section deals with estimates for the small basins. For the larger basins the estimates are discussed in section 5.3.3.

#### **5.3.2.1 Outstanding rainfalls over the eastern United States**

A record of 80 outstanding point rainfalls in the period 1924–1982 in or near the project basin, including a few estimates based on runoff computations, yielded a 1-hour amount and several 2- and 3-hour amounts of about 300 mm. Approximate elevations ranging from 200 to over 1 200 m were determined for most of these storms. No unique rainfall–elevation relation was evident. This suggested a procedure for estimating PMP that did not over-emphasize orographic influences on short-duration rainfalls. Neither was there any discernible geographic distribution of these outstanding values.

In order to supplement the basin data, a survey was made of intense small-area short-duration storms from several hundred storm studies for the eastern half of

the United States. Attention was given to all storms with 6-hour 25.9-km<sup>2</sup> rainfall exceeding 250 mm, particularly to those exceeding 350 mm. Some of these had durations of 24 hours. A study of 60 of the more severe storms indicated that most of them intensified during the night hours. This suggested that factors more important than daytime heating were generally responsible for these outstanding storms.

Information gained from the above investigations led to the following conclusions regarding small-area PMP storm types for the project basin:

- (a) The PMP storm type situation would involve a continuation of geographically fixed thunderstorms throughout a 24-hour period;
- (b) The PMP-type thunderstorm for durations of 1 hour or less shows only a small orographic effect, while that for the longer durations would be likely to produce more rainfall on slopes and adjacent valleys than over flat areas with no nearby slopes.

#### **5.3.2.2 Local topographic classification**

Examination of major storm sites on large-scale topographic maps (1 : 24,000) led to the following topographic classifications:

- (a) Smooth: Few elevation differences of 15 m in 0.5 km;
- (b) Intermediate: Elevation differences of 15 to 50 m in 0.5 km;
- (c) Rough: Elevation differences exceeding 50 m in 0.5 km.

Although the entire south-eastern portion of the project basin is classified as rough, there were variations in rainfall potential across the area. Some peaks reached almost 2 000 m and some ranges sheltered large valleys, which required consideration of other features besides roughness in order to assess the topographic effects on the intense summer rainfalls. The effect of local topography on rainfall is discussed in section 5.3.2.3.

#### **5.3.2.3 Broad-scale topographic effects**

Broad-scale topographic effects on rainfall were determined by analysis of maps of maximum observed and 100-year daily rainfalls. Mean annual and seasonal precipitation maps were also examined. After some experimentation, the following concepts evolved and were adopted:

- (a) First upslopes: A mountain slope facing the lowlands in a direction east to south-west

(moisture-inflow directions) with no intervening mountains between the slope and the moisture source (that is, the Gulf of Mexico and the Atlantic Ocean);

- (b) Secondary upslopes: A secondary upslope high and steep enough to increase precipitation, but partially shielded from moisture sources by a lower mountain range with an elevation between crests of at least 500 m;
- (c) Sheltered areas: These are defined as valleys having moisture-inflow barriers of 600 m or higher;
- (d) Depression: The elevation difference between the barrier crest and a point in the sheltered area is the depression of that point.

Terrain classifications in the project basin are delineated in Figure 5.14. Analysis of summer rainfall amounts for the various classifications led to the adoption of the following guides on topographic effects on PMP:

- (a) Precipitation increases of 10 per cent per 300 m from sea level to 800 m on first upslopes, with no further increases above 800 m;
- (b) Increases of 5 per cent per 300 m from sea level to all elevations on secondary upslopes;
- (c) Decreases of 5 per cent per 300 m of depression in sheltered areas.

#### 5.3.2.4 PMP depth-duration curves for 2.6 km<sup>2</sup>

Point rainfalls measured at regularly reporting precipitation gauges are likely to be less than the maximum point rainfalls experienced. It is for this reason supplementary precipitation surveys are conducted after most major storms. These surveys usually reveal

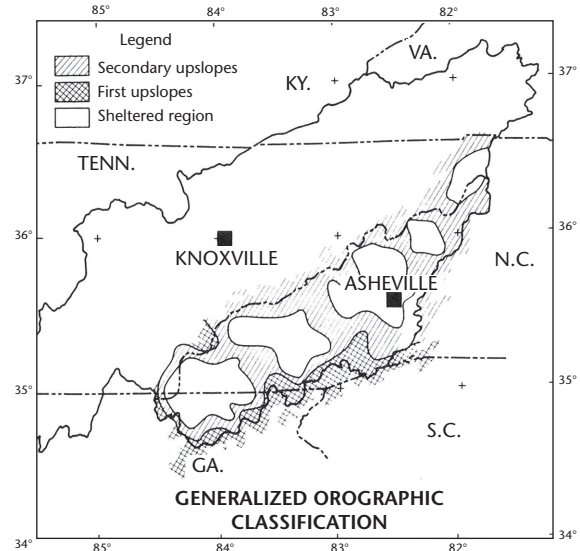


**Figure 5.14. Topography classified on basis effect on rainfall, Tennessee River basin above Chattanooga, Tennessee (Zurndorfer and others, 1986)**

significantly larger amounts. These maximum point values are considered to apply to average depths over 2.6 km<sup>2</sup>, the smallest basin size assigned for study. Maximum observed point, or 2.6-km<sup>2</sup>, rainfalls for durations up to 12 hours in the eastern half of the country were transposed and maximized as described in Chapter 2. Outstanding maximized and observed values were plotted against duration (Figure 5.15), and curves (solid lines) were drawn to 6 hours for smooth and rough terrain (section 5.3.2.2).

The following concepts and principles were observed in constructing the two depth-duration curves. Over

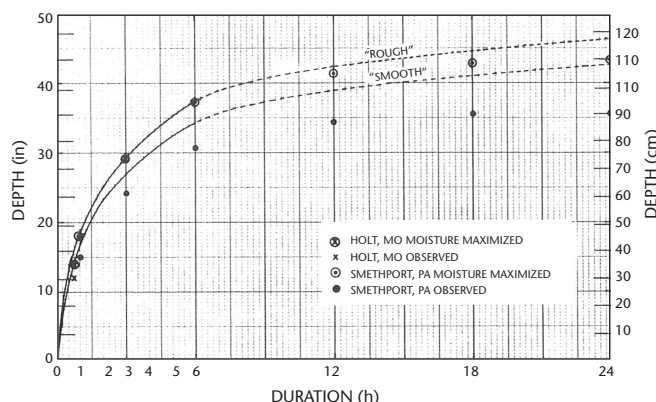


**Figure 5.15. Adopted 2.6-km<sup>2</sup> PMP with supporting data, Tennessee River basin; dashed lines are extrapolations based on relation of Figure 5.16, smooth curve applies uncorrected only to 100 per cent line of Figure 5.18 (Zurndorfer and others, 1986)**

areas of  $2.6 \text{ km}^2$  and for durations of a few tens of minutes, maximum rainfall rates depend on extreme upward velocities associated with vigorous thunderstorms. These high velocities are related to storm dynamics, and topographic effects are negligible. Hence, the same maximum intensities may be expected within the same air mass over various types of terrain. As duration increases, terrain roughness becomes increasingly important. First, upslopes and roughness accentuate upward velocities. Secondly, intense thunderstorms tend to remain in one place longer over a topographically favourable site than over smooth terrain, where they drift with the wind or propagate laterally by their own dynamics. Finally, the probability of continued rainfall after an intense thunderstorm is enhanced by terrain roughness.

The basic PMP values of Figure 5.15 are applicable to the southern edge of the project basin. Smooth PMP in rough terrain is hypothetical, but serves as an index for consistent application of adjustments for orographic effects (sections 5.3.2.2 and 5.3.2.3.).

Experience with severe storms throughout the country was useful in shaping the depth-duration curves beyond 6 hours. The adopted curve of Figure 5.16 was developed to extend the 6-hour curves from 6 to 24 hours (dashed lines in Figure 5.15).

### 5.3.2.5 Adjustment for moisture and latitudinal gradient

A moisture adjustment chart was developed for the relatively smooth north-western section of the project basin. This chart (Figure 5.17) was based on assessment of mean dew points and maximum persisting 12-hour dew points. Analysis indicated a gradient of about  $1^\circ\text{C}$  from the extreme south-western corner of the total basin (outside the area shown) to the north-eastern corner. This gradient corresponds to a difference in rainfall of about 10 per cent, according to the usual model for convective rain in extreme storms (United States Weather Bureau, 1960). Figure 5.17 shows the moisture index lines, in percentages, for adjusting PMP values.

A latitudinal gradient chart (Figure 5.18) was developed for the mountainous portion of the project basin. This chart was based on rainfall-frequency gradients resulting primarily from sheltering by mountains. Moisture effects were incorporated.

### 5.3.2.6 Six-hour $2.6 \text{ km}^2$ PMP index map

The concepts and charts discussed above were used to develop the 6-hour  $2.6 \text{ km}^2$  PMP index map

(Figure 5.19) for the project basin. Six-hour PMP values from Figure 5.15 of 874, 912 (interpolated), and 950 mm were assigned to smooth, intermediate and rough terrain categories, respectively, and

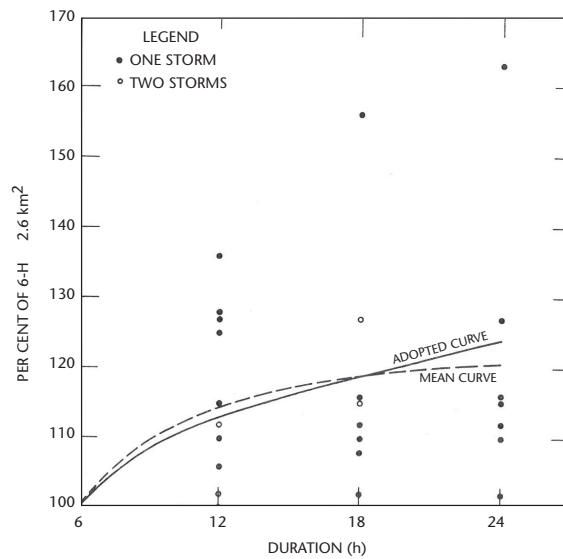


Figure 5.16. PMP depth-duration curves for basins up to  $259 \text{ km}^2$  in Tennessee River basin  
(Zurndorfer and others, 1986)

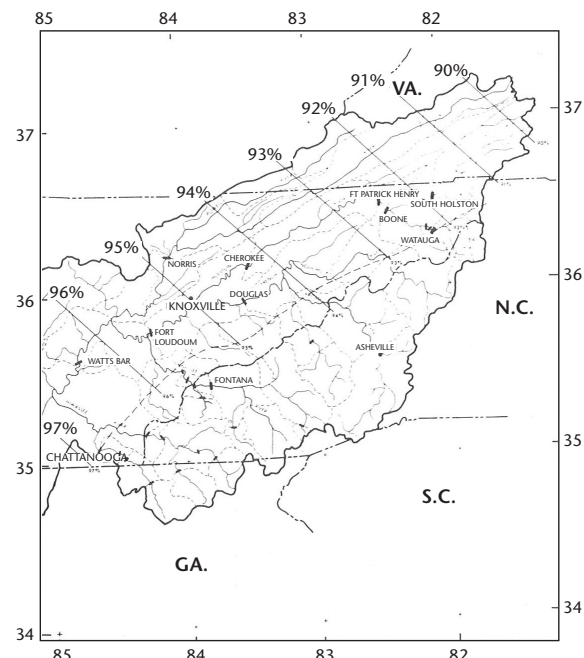
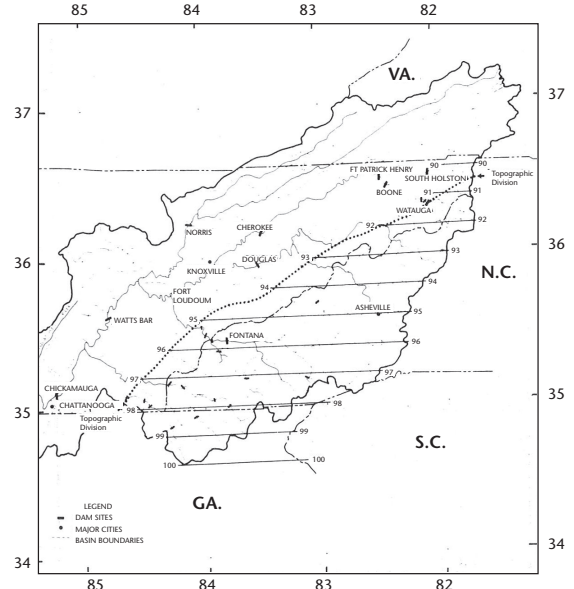


Figure 5.17. Moisture index chart for north-western portion of Tennessee River basin over Chattanooga, Tennessee (Zurndorfer and others, 1986)

multiplied by adjustment factors indicated in Figures 5.17 and 5.18. Isohyets were drawn with steepest gradients corresponding to the greatest changes in elevation. This placed steepest gradients where mountains rise from valley floors. Different adjustments for south-eastern and north-western portions of the basin (Figures 5.17 and 5.18) resulted in some discontinuity at their common boundary, which was smoothed out in drawing isohyets. A depth-duration relation (Figure 5.20) was developed from a number of PMP depth-duration curves, such as Figures 5.15 and 5.16, so that 6-hour PMP could be adjusted to other durations. A depth-area relation (Figure 5.21) was constructed from intense small-area storm data for adjusting the 2.6-km<sup>2</sup> PMP values to other sizes of area.

### 5.3.2.7 Time distribution of rainfall

Observed extreme small-area storms in the project basin have generally been one-burst events in which little rain followed the extreme 3-hour rainfall, that is storm experience pointed to the occurrence of a 24-hour rainfall in a single burst. The following guidelines were therefore suggested for critical sequences:



**Figure 5.18. Latitudinal rainfall gradient (in per cent) in south-eastern portion of Tennessee River basin above Chattanooga, Tennessee (Zurndorfer and others, 1986)**

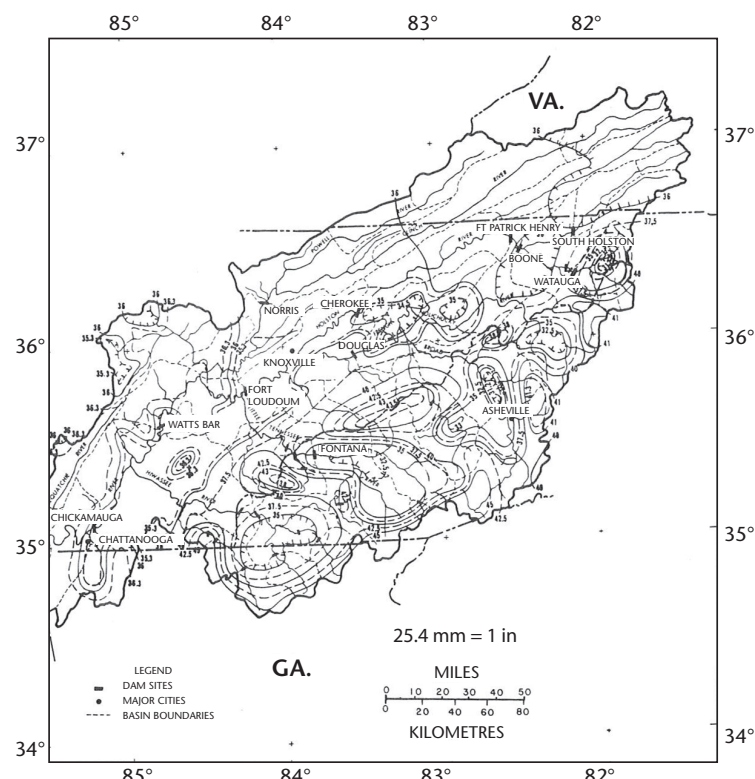


**Figure 5.19. Six-hour 2.6-km<sup>2</sup> PMP (inches) for Tennessee River basin above Tennessee River basin over Chattanooga, Tennessee (Zurndorfer and others, 1986)**

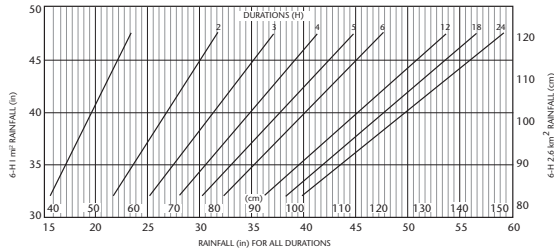


**Figure 5.20. Nomogram for depth–duration relations for 24-hour PMP storms, Tennessee River basin (Zurndorfer and others, 1986)**

- (a) For 6-hour rainfall increments in a 24-hour storm, the four increments should be arranged with the second-highest next to the highest, the third-highest adjacent to these two, and the fourth-highest at either end. This still allows various arrangements, and the most critical is that which would yield the most critical streamflow.
- (b) For 1-hour increments in the maximum 6-hour increment, any arrangement is acceptable, so long as it keeps the two highest 1-hour amounts adjoined, the three highest 1-hour amounts adjoined, and so forth.

### 5.3.2.8 PMP for specific basins

PMP for specific basins is estimated by the following steps:

- (a) The basin on Figure 5.19 is outlined, and the mean 6-hour 2.6-km<sup>2</sup> PMP for the basin is determined.
- (b) Figure 5.20 is used to obtain PMP for durations up to 24 hours.

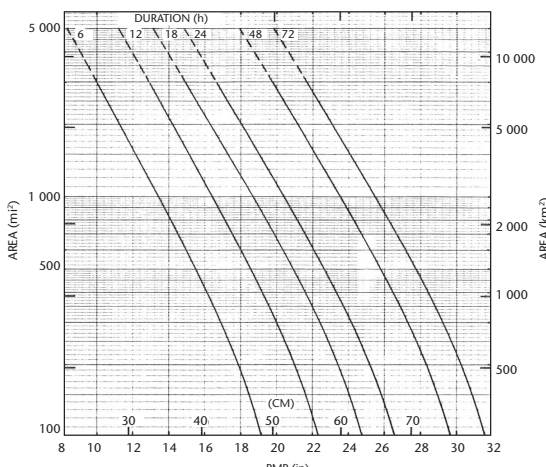


**Figure 5.22. Non-orographic PMP at Knoxville, Tennessee (Zurndorfer and others, 1986)**

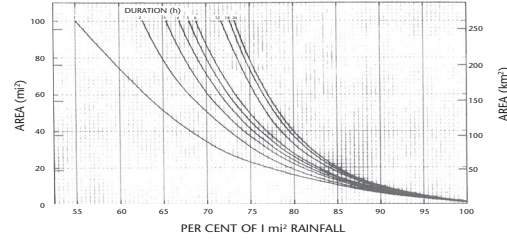


**Figure 5.21. Depth–area relations for small basin estimates, Tennessee River basin (Zurndorfer and others, 1986)**

- (c) Figure 5.21 is used to adjust 2.6-km<sup>2</sup> PMP for basin size.
- (d) A smooth enveloping depth–duration curve is constructed from data obtained in (c), and 1-hour increments are determined for the four 6-hourly increments of the 24-hour storm.
- (e) Suggested critical time sequences (section 5.3.2.7) include: (i) hourly increments in the maximum 6-hour period: 6, 5, 4, 3, 1, 2, where 1 refers to the maximum 1-hour increment; and (ii) 6-hourly increments in a 24-hour storm: 4, 2, 1, 3, where 1 now refers to maximum 6-hour increment. Spatial distribution of rainfall is usually not required for basins of less than 259 km<sup>2</sup>. If needed, the techniques discussed in section 5.3.3 can be used to distribute the rainfall.

### 5.3.3 PMP for drainages from 259 km<sup>2</sup> to 7 770 km<sup>2</sup> in the Tennessee River basin

The discussion which follows refers only to the Tennessee River basin above Chattanooga, Tennessee (Zurndorfer and others, 1986). The topography and moisture sources were discussed above, and topographic classifications are shown in Figure 5.14.

#### 5.3.3.1 Derivation of non-orographic PMP

PMP was derived in the manner described in section 3.4.2. Storms for the eastern part of the country were maximized in place and enveloping isohyets constructed, thus applying an implicit transposition. PMP maps like that of Figure 3.20 were constructed for a number of area sizes and durations, with isohyets not only enveloping the data on each chart, but also showing smooth progression with varying area size and duration. Values read from these charts for the location of Knoxville, Tennessee, were used to develop the basic PMP depth–area–duration relations of Figure 5.22. The 24-hour 2 590-km<sup>2</sup> chart (not shown) was converted

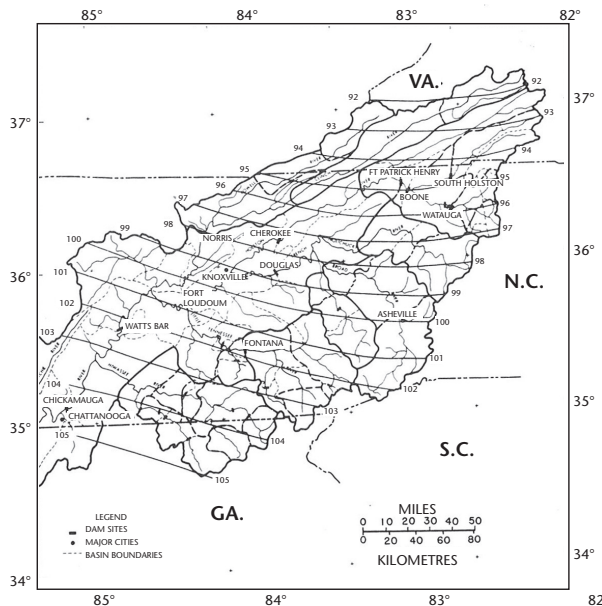


**Figure 5.23.** Twenty-four-hour 2 590-km<sup>2</sup> PMP percentiles of Knoxville Airport value (meteorological observations made at airport, about 16 km south of Knoxville; Zurndorfer and others, 1986)

to percentages of the value at Knoxville (Figure 5.23). Multiplication of the depth-area-duration values of Figure 5.22 by the percentages of Figure 5.23 yields non-orographic PMP at various locations in the basin.

### 5.3.3.2 Terrain and orographic influences on PMP

Five indicators of terrain and orographic influence on precipitation were considered in adjusting non-orographic PMP.

Mean annual precipitation was one indicator. A hypothetical mean annual non-orographic precipitation map (not shown) was constructed by eliminating the influence of the Appalachian mountain chain by smooth extrapolation of isolines of mean annual precipitation from surrounding non-orographic regions. This map supports the generalized PMP percentile lines of Figure 5.23.

A chart of 2-year 24-hour rainfalls (Figure 5.24) based on data from some 600 stations in and near the basin was developed. Although index relations based on physiographic factors were not developed to aid in interpolation between stations, topographic maps were used to aid in the analysis. Extreme monthly rains were also plotted and the resultant maps (not shown) analysed to assess terrain effects.

Another indicator of orographic influence was the comparison of the small-basin PMP chart of Figure 5.19 with the chart (not shown) reconstructed under the assumption that the smooth

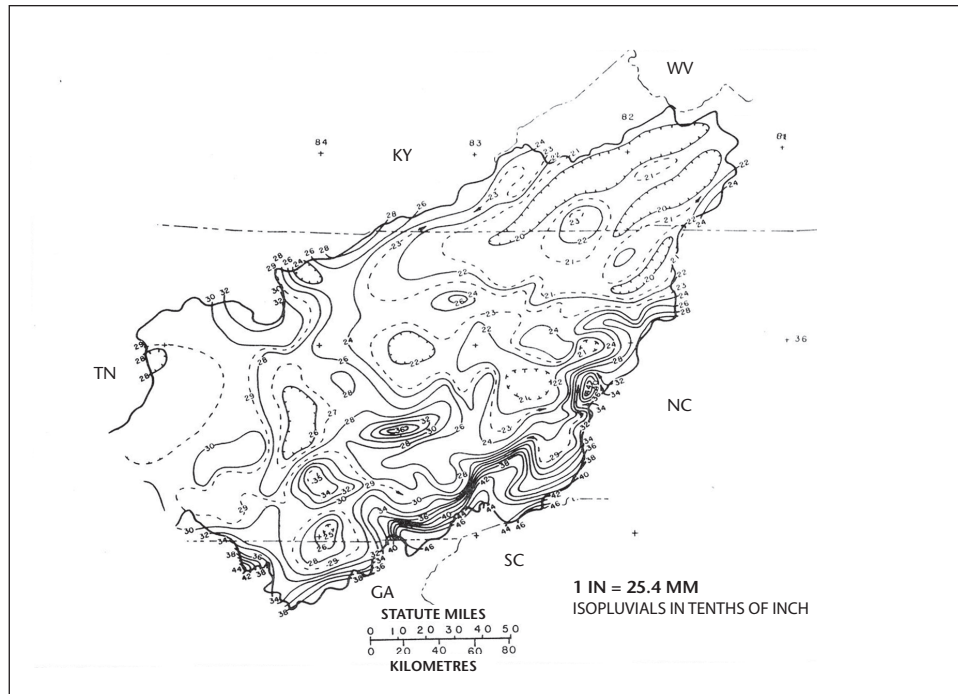


**Figure 5.24.** Two-year 24-hour precipitation-frequency map (tenths of inches) for eastern Tennessee River basin (Zurndorfer and others, 1986)

classification applied to the entire basin. Non-orographic PMP depth-area-duration values (Figure 5.22) were adjusted by the ratio of PMP index chart values (Figure 5.19) to 6-hour smooth PMP (Figure 5.15) adjusted for basin location (Figure 5.17 or 5.18).

The optimum inflow direction for heavy rains was another index. Over a basin of no more than approximately 259 km<sup>2</sup>, it is presumed that the optimum wind direction for unobstructed inflow of moist air and for enhancement by ground roughness prevails during the PMP storm. In larger basins, the optimum direction for precipitation may differ from one part of the basin to another because of varying terrain features. The wind direction most critical for the basin as a whole is defined as the direction that is most favourable over the largest portion of the basin. Figure 5.25 shows the optimum moisture-inflow directions for local areas in the mountainous eastern portion of the region. The largest percentage of a problem basin with the same optimum wind direction is determined from Figure 5.25. An adjustment factor for the optimum wind inflow is related to this percentage value by Figure 5.26, which was developed empirically after a number of PMP estimates for specific basins had been made.

### 5.3.3.3 Terrain stimulation adjustment

The procedures discussed in sections 5.3.2 and 5.3.3 interface at the 259 km<sup>2</sup> basin size. The estimates for the smaller area are based upon extreme thunderstorm events. Estimates for the larger area sizes are controlled by large-area general storms. If only large-area storms are considered in developing PMP estimates for area sizes just slightly larger than 259 km<sup>2</sup>, the PMP amounts will be somewhat underestimated. This results from the exclusion of small-area high-intensity storm events from consideration. Adjustments to the estimates that are derived from large area storms only reflect the terrain classification. Rough and intermediate terrain tends to fix convective cells in one place and cause rainfall amounts to increase. Figure 5.27 shows the terrain classifications for the eastern half of the Tennessee River basin. From this map, the percentage of each basin with the various terrain classifications of rough, intermediate or smooth can be determined. These percentages are used in the nomogram of Figure 5.28 to determine a percentage adjustment for terrain stimulation effects on large-storm rainfall. The adjustments for the rough and intermediate terrain classifications are added to obtain a total terrain adjustment in cases where the basin contains both types of terrain

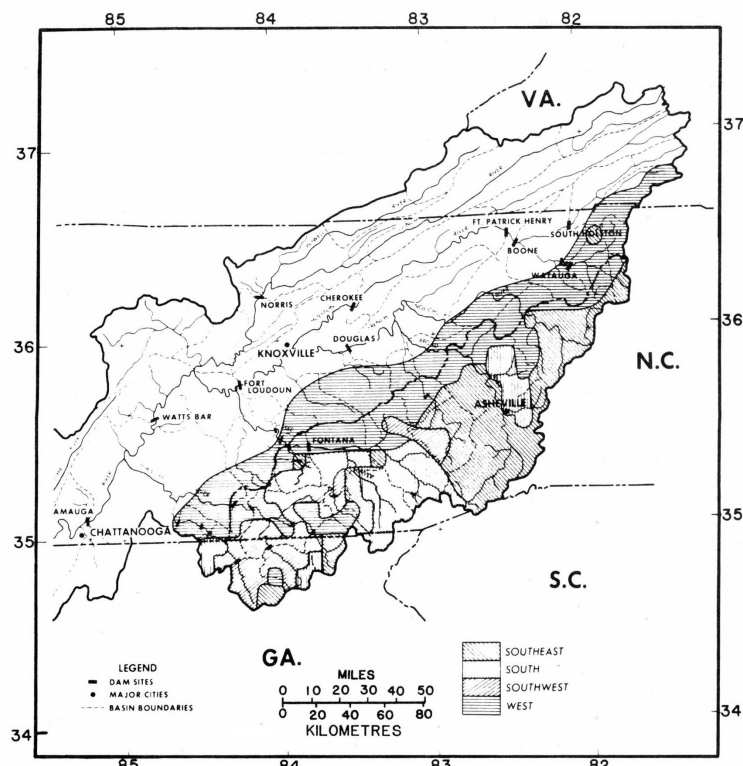
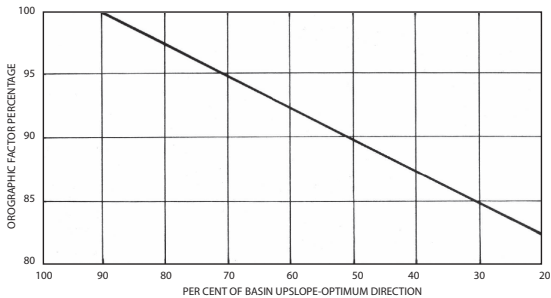


Figure 5.25. Optimum wind directions for heavy rains (Zurndorfer and others, 1986)



**Figure 5.26. Adjustment chart for optimum wind inflow direction for south-eastern mountainous portion of Tennessee River basin over Chattanooga, Tennessee (Zurndorfer and others, 1986)**

classification. Since the adjustment is related to the effects of terrain on convective cells within the larger-area storm, the adjustment decreases with increasing area size (Figure 5.29). This adjustment is termed the terrain stimulation factor (TSF).

A second adjustment factor is required in the mountainous eastern region in order to account for the effects of upslopes and sheltering. This second factor is referred to as the broad-scale orographic factor (BOF) and is the sum of weighted percentages of a

basin covered by first upslopes, secondary upslopes and sheltered regions as determined by using Figure 5.14. The respective weights for these three categories are 0.55, 0.10 and 0.05, obtained through regression analyses of orographic intensification factors determined for 18 basins. These factors were based on detailed evaluation of terrain effects for these basins and subjective comparisons of the mean annual precipitation to the mean annual non-orographic precipitation ratios.

For any basin in the mountainous east region, the total adjustment factor (TAF) is the sum of the TSF and the BOF. The non-orographic PMP determined from Figure 5.22, geographically adjusted to the site, is then multiplied by the TAF to obtain the total PMP.

#### 5.3.3.4 Adjustment for PMP at interface ( $259 \text{ km}^2$ )

When different generalized procedures are developed to estimate PMP for ranges of area sizes, estimates for basins near the interface in area sizes may differ. These inequalities result from the differing evaluation of topography. Sample computations of PMP in the vicinity of  $259 \text{ km}^2$ , the interface between the methods described in sections 5.3.2 and

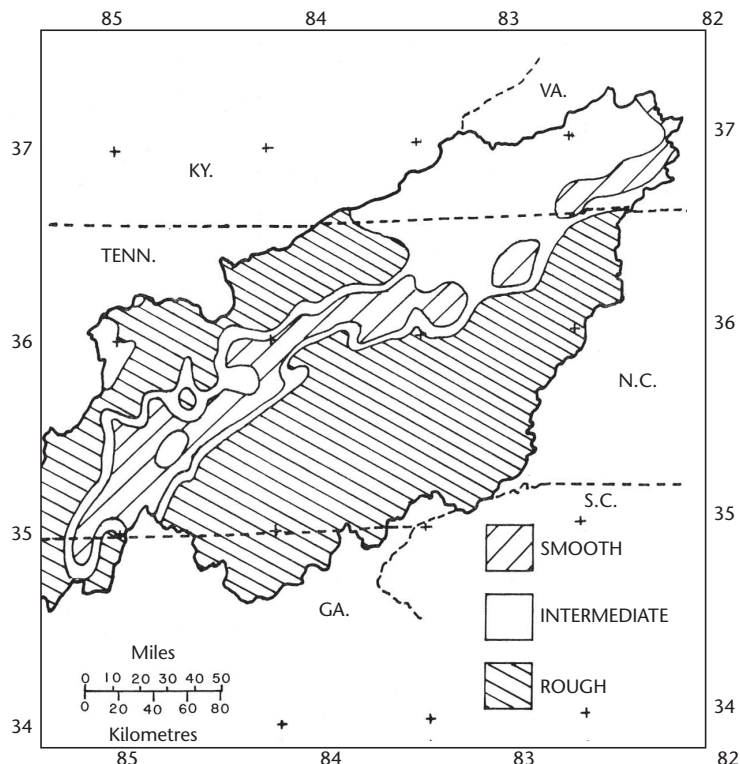


**Figure 5.27. Illustration of terrain classification for the eastern Tennessee River basin (Zurndorfer and others, 1986)**

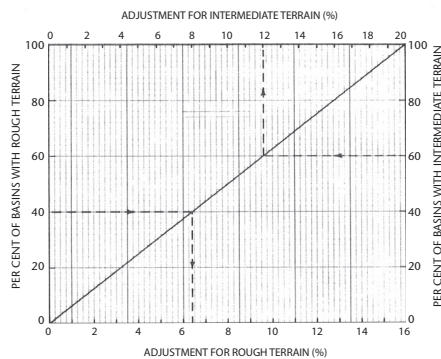


**Figure 5.28. Nomogram for determining terrain adjustments for basins larger than 259 km<sup>2</sup>**  
(Zurndorfer and others, 1986)

5.3.3, have shown that for basins in the mountainous east, differences between the two procedures may be 10 per cent to 20 per cent. In particular, for basins between 259 and 285 km<sup>2</sup> that are primarily upslopes, a reduction to BOF adjustment is necessary, as shown in Figure 5.30.

Reduction of discontinuities at the interface is necessary to enable smoothing of depth-area relations throughout the range of area sizes needed for proper application of the procedures outlined in section 5.2.7.

The entire procedure for estimating PMP for specific basins is outlined in section 5.3.3.6.

### 5.3.3.5 Areal and time distribution

The relationships described above yield the volume of PMP for specified area sizes and various durations. Geographic distribution of PMP within problem basins is determined by developing the isohyetal pattern of an idealized or typical representative storm and providing nomograms for obtaining isohyetal values, then adjusting for the effects of topography. The procedure is described in section 5.3.3.6. Critical sequences of 6-hour and 24-hour rainfall increments may be arranged as described in section 3.4.2.6.

### 5.3.3.6 PMP for specific basins

For the relatively smooth north-western portion of the total Tennessee River basin, referred to as the non-mountainous east (unhatched regions of Figure 5.25), PMP estimates are obtained from the basin PMP at Knoxville (Figure 5.22) and the regional adjustment (Figure 5.23). The stepwise procedure follows. Individual steps needed to compute basin average PMP – steps (a) to (g) – may be followed more easily by referring to

the example computation for the 7 542 km<sup>2</sup> Clinch River basin above South Holston Dam, Tennessee, in Table 5.2.

- (a) From Figure 5.22, 6-, 12-, 18-, 24-, 48- and 72-hour values of non-orographic PMP for the basin size are obtained.
- (b) The percentage adjustment indicated in Figure 5.23 is obtained for the centre of the problem basin, and used to multiply values obtained in (a).
- (c) A smooth enveloping depth-duration curve is constructed from the adjusted values of (b), and 6-hour increments for the 72-hour PMP are obtained.
- (d) From Figure 5.27, the percentage of intermediate and rough terrain within the basin for the respective portions of the basin is determined. Figure 5.28 for each of these percentages is entered to obtain the terrain adjustments for this basin. These adjustments are combined. Figure 5.29 for the area size of the basin (7 542 km<sup>2</sup>) is entered to get an areal adjustment. If the basin size were less than 285 km<sup>2</sup>, the areal adjustment would have to be multiplied by the combined adjustment from

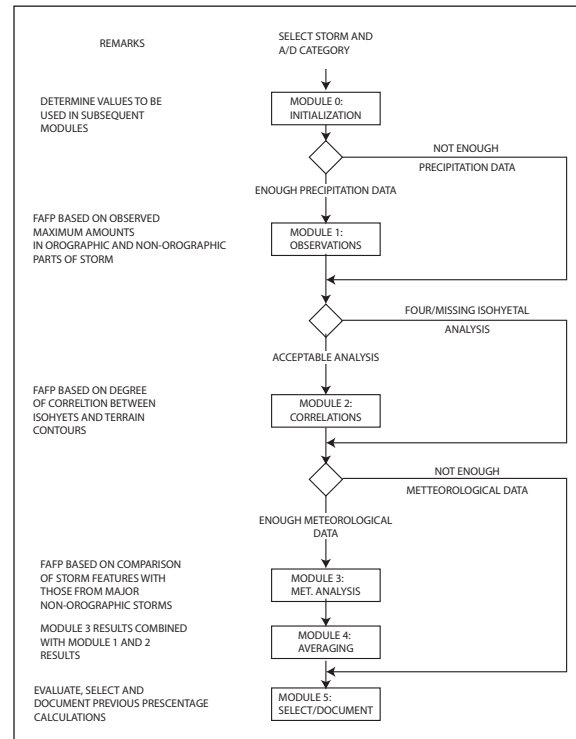


**Figure 5.29. Variation of terrain roughness adjustment (Figure 5.28) with basin size**  
(Zurndorfer and others, 1986)

**Table 5.2. Sample computation of PMP precipitation estimates for the 7 542 km<sup>2</sup> Clinch River basin above Norris Dam, Tennessee. Centre of basin is 36°42' N 82°54' W.**

Line	Item and source	Duration (hours)					
		6	12	18	24	48	72
1	Unadjusted PMP (Figure 5.22; mm)	259	333	386	432	508	561
2	Adjustment for location (Figure 5.23)	0.94	0.94	0.94	0.94	0.94	0.94
3	Basin PMP, unadjusted for terrain	243	313	363	406	478	527
4	Compute terrain stimulation factor (TSF)	Basin is 62% intermediate, 12% adjustment from Figure 5.28 Basin is 35% "rough". 5% adjustment from Figure 5.28 Total adjustment = 12% + 5% = 17% From Figure 5.29, adjustment for 7 542 km <sup>2</sup> basin = 0.25 TSF = 0.25 × 0.17 = 0.0425					
5	Compute broad-scale orographic factor (BOF) from Figure 5.14 (if required)	This step is not required in this example					
6	Total adjustment factor (TAF) = TSF + BOF + 1.00 (rounded to nearest 0.05)	1.05	1.05	1.05	1.05	1.05	1.04
7	PMP = TAF × basin PMP (smoothed)	255	328	381	426	502	553

Figure 5.30 to obtain the terrain stimulation factor (TSF). If this basin had been located in the mountainous east, the TSF would need to be further modified for sheltering and optimum wind direction effects.

- (e) For basins in the mountainous east (not applicable in the example in Table 5.2), Figure 5.14 is used to obtain the percentages of primary upslopes, secondary upslopes and sheltered areas within the basin. These percentages are multiplied by the respective factors 0.55, 0.10 and 0.05. The results are added and rounded to the nearest 0.05 to obtain the broad-scale orographic factor (BOF).
- (f) The numbers obtained in (d) and (e) are combined plus 1.00 to obtain the total adjustment factor (TAF). This factor is rounded to the nearest 0.05. The TAF equals the TSF in the non-mountainous east.

$$\text{TAF} = \text{TSF} + \text{BOF} + 1.00$$

- (g) The TAF from (f) is multiplied by the values from (c). A depth-duration diagram is plotted and a smooth curve is fitted for final results. The results are the basin-averaged PMP. This establishes the magnitude of PMP only, and in highly orographic regions – for example, the mountainous east – the pattern of areal distribution is also modified by topographic

effects. The resulting isohyetal pattern must be planimetered to obtain the volume of the PMP within the basin.

Note: The procedure of determining the areal distribution of the basin averaged PMP is based on the generalized procedures outlined in the applications manual (Hansen and others, 1982) discussed in section 5.2.7. Following the procedure discussed in that section one can determine the storm area size that produces the maximum precipitation volume within the drainage. This is the PMP storm area. Section 5.2.7.4 described how to obtain labels for the isohyets of the PMP storm. This gives the areal



**Figure 5.30. Adjustment applied to broad-scale orographic factor for areas near the interface between procedures for areas less than and greater than 259 km<sup>2</sup> (Zurndorfer and others, 1986)**

distribution for the non-orographic PMP over the drainage.

Since most orographic precipitation is likely to occur over ridges and slopes surrounding or within the drainage in orographic regions, the areal distribution procedure for total PMP in the Tennessee River drainage relocates the non-orographic pattern centre toward the maximum 2-year 24-hour amount within the basin. This is in agreement with storm experience in this region. When applying this warping method in other regions, one should carefully evaluate the criteria for storm relocation. The following steps describe the orographic warping of the non-orographic elliptical pattern.

- (h) The non-orographic PMP storm pattern is displaced to the location of the maximum 2-year 24-hour precipitation amount within the basin in such a manner as to have the greatest proportion of central isohyets contained within the basin. The relocated pattern centre is kept at least 16 km inside the basin border. The orientation may be the same as, or different from, the non-orographic pattern. No further reduction for orientation is made for orientations differing from preferred storm orientations.
- (i) The 6-hour incremental pattern in (h) is adjusted to maintain the same volume of PMP as obtained for the basin-centred pattern from the procedure for non-orographic precipitation discussed above (Hansen and others, 1982). The adjustment is done by multiplying the isohyet labels by the ratio of the displaced volume to the basin-centred volume.
- (j) The displaced adjusted pattern from (i) is overlaid onto the 2-year 24-hour precipitation analysis from Figure 5.24. The 2-year 24-hour isohyets covering the basin are converted into a percentage of the 2-year 24-hour isohyet that passes through the centre of the displaced elliptical pattern.
- (k) For a fine grid of points, or at intersections of the 2-year 24-hour isopercental analysis and the displaced elliptical isohyetal pattern, the product of the two analyses is computed.
- (l) The resulting values obtained from (k) are analysed, considering both the 2-year 24-hour analysis and a topographic map as guidance. The resulting analysis should provide a pattern that is warped considerably from the elliptical pattern (the degree of warping changes with each 6-hour increment).

(m) The warped pattern in (l) is replanimetered to obtain a new volume and compare this with the volume in (i). If differences of more than a few per cent occur, the isohyet values are adjusted to correct the volume to that of (i).

Steps (h) to (m) are repeated for each 6-hour incremental pattern.

When displacing and warping isohyetal patterns, two procedural cautionary steps should be taken. First, isohyetal patterns over sub-basins within the total basin should be planimetered to ensure the results for the total basin PMP do not provide a larger volume over the sub-basin than a PMP computed specifically for the sub-basin. Second, the central isohyets should be reviewed against the small-area PMP (section 5.3.2) for the location of the isohyetal pattern to ensure that these isohyet values do not exceed the PMP for those smaller areas.

#### **5.3.4 PMP estimates for the United States between the Continental Divide and the 103rd meridian**

This is a topographically complex region that extends from the western edge of the Great Plains of eastern Montana, Wyoming, Colorado, and New Mexico through the slopes of the eastward-facing Rocky Mountains, to the crest that separates the Pacific Ocean and Gulf of Mexico drainages, the Continental Divide. The mountainous portion of this region contains narrow and broad valleys, some exposed directly to moisture-bearing winds and others almost completely sheltered. It is also a complex region meteorologically. The extreme rainfall amounts in this region result from a wide range of storm types: for example, the southern portion of the region is primarily influenced by decadent tropical storms, while farther north the extreme rainfall events result from extratropical cyclones. In all portions of the region, extreme convective events are an important factor in extreme rainfall events for short durations over small areas. The terrain within the study region had a marked effect upon the procedures used to develop the PMP estimates (Miller and others, 1984b). A procedure was developed that enabled PMP for this diverse terrain to be analysed in a consistent fashion. The procedure has some similarities to those which have been used in other studies for the western United States. First, the convergence precipitation in all major storms in the region are estimated. The convergence precipitation amounts are then moisture-maximized and transposed to all regions where similar storms have occurred. The moisture-maximized transposed

values are then adjusted for the variation in terrain effects throughout the region.

#### 5.3.4.1 Storm separation method

In orographic regions, transposition of storms is generally limited to those places where the terrain and meteorological characteristics are the same as those at the place where the storm occurred. Concern for terrain homogeneity has restricted transpositions in most previous studies for orographic regions to very limited regions. In an effort to expand this region of transposability, it was desirable to identify the amount of precipitation from individual storms which resulted solely from atmospheric forces, termed free atmospheric forced precipitation (FAFP). The procedure assumes that in non-orographic regions the precipitation, or FAFP, would be solely the result of atmospheric forces. In orographic areas, the procedure assumes that the basic storm mechanism is unaffected when terrain feedback is removed. The method estimates the percentages of precipitations caused by topography and those caused by atmospheric dynamics based on analysis and assessment on observed precipitation data, isohyetal maps and the quantity and quality of all the existing meteorological data. Figure 5.31 is a flowchart of the method, details of which are outlined in Hydrometeorological Report (HMR) No. 55A (Hansen and others, 1988).

The first step is to select the area size and duration of interest (A/D category). The percentage of the storm precipitation resulting from topographic effects generally tends to increase with longer durations and larger area sizes. The first determination of the relation of the free atmospheric forced precipitation to orographic precipitation in a particular storm is based upon consideration of the observed precipitation amounts (Module 1). A comparison is made between the maximum observed precipitation in the non-orographic region to the maximum observed precipitation in the orographic region of the storm. Usually, as the difference between these two amounts decreases, the greater the convergence or FAFP in a particular storm.

A second evaluation is based on the storm convergence component of the isohyetal pattern (Module 2). The isohyetal pattern is compared with the terrain contours within the region. In this comparison, the higher the degree of correlation between topographic features and the isohyetal pattern in the region of the isohyet which encompasses the rainfall for the area of interest, the greater the amount of orographic precipitation within the storm.

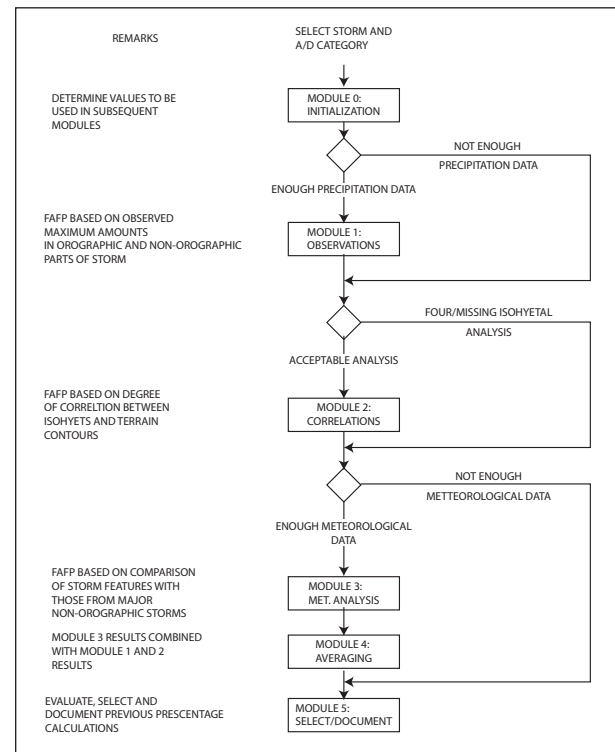


Figure 5.31. Schematic flow chart for storm separation method (Miller and others, 1984b)

A third method for evaluation of convergence involves a detailed consideration of the meteorological factors important in producing convergence precipitation (Module 3). Those factors present in the particular storm are compared with those present in major storms of record in non-orographic regions. Considerable effort should be expended in a detailed re-analysis of surface and upper-air charts where these may be crucial in estimating the percentage of convergence rainfall in a particular storm.

In the storm separation method, percentages are also determined by averaging the percentage obtained from use of the isohyetal analysis with that from the meteorological analysis and from the analysis of the precipitation observations with the meteorological analysis (Module 4). Five percentages are produced by this method if sufficient observational data, isohyetal and meteorological analyses are available. The selection of the final percentage is based on first quantifying the degree of confidence one has in how well the storm fits the assumptions underlying each step, and second on how well the data available for each step serve the purpose of that step. If percentages are considered equally reliable, the evaluation that results in the highest percentage of convergence or FAFP is chosen.

After the determination of the convergence precipitation (FAFP) for all of the major storms in the region, the 24-hour convergence precipitation values were moisture-maximized and transposed to all other locations where similar storms have occurred. Transposition limits were determined as discussed in section 2.5. The precipitation amounts were increased or decreased based upon the differences in available precipitable water. In this study, no adjustments for change in precipitable water or changes in elevation of 300 m or less were made, and an adjustment of only one half of the available precipitable water for differences in elevation beyond the first 300 m (section 2.6.4.2). Figure 5.32 shows the analysed moisture-maximized convergence precipitation map for central and eastern Colorado. This map shows, as expected, a general decrease towards the west, the region of increasing elevation. The lowest precipitation amounts are shown along the Continental Divide, where, in general, elevations are the highest.

#### 5.3.4.2 Orographic factor $T/C$

It was necessary to adjust the convergence precipitation for the variation in orographic effects that occurs over this region. The variation of the orographic factor was determined from the 100-year 24-hour precipitation frequency maps from National Oceanic and Atmospheric Administration (NOAA) Atlas 2 (Miller and

others, 1973). A first step of this procedure was to determine the non-orographic portion, or convergence component  $C$ , of the 100-year precipitation frequency amounts. The procedure used was to examine the map to find regions of minimal values in plains regions and broad valleys. These were considered to experience the least amount of influence of orographic effects. Smooth isolines of the convergence component were then drawn for the regions, assuming these minimum values reflected only the convergence precipitation. These isolines would reflect solely the decrease of convergence potential away from the moisture source, generally toward the west and north in this region. Figure 5.33 shows an example of this convergence portion of 100-year 24-hour precipitation for the state of New Mexico east of the Continental Divide.

The orographic factor was then determined by dividing the total 100-year 24-hour precipitation frequency amount  $T$  by that amount determined to be convergence precipitation  $C$ . This was done for a variable grid over the region with the closest spacing in regions of tight gradient on the precipitation-frequency maps. A portion of the resulting map, for Colorado east of the Continental Divide, is shown in Figure 5.34. There is generally some orographic effect on precipitation throughout this study region, but there is little or none on the western limits of the Great Plains or in some broad river valley bottoms.

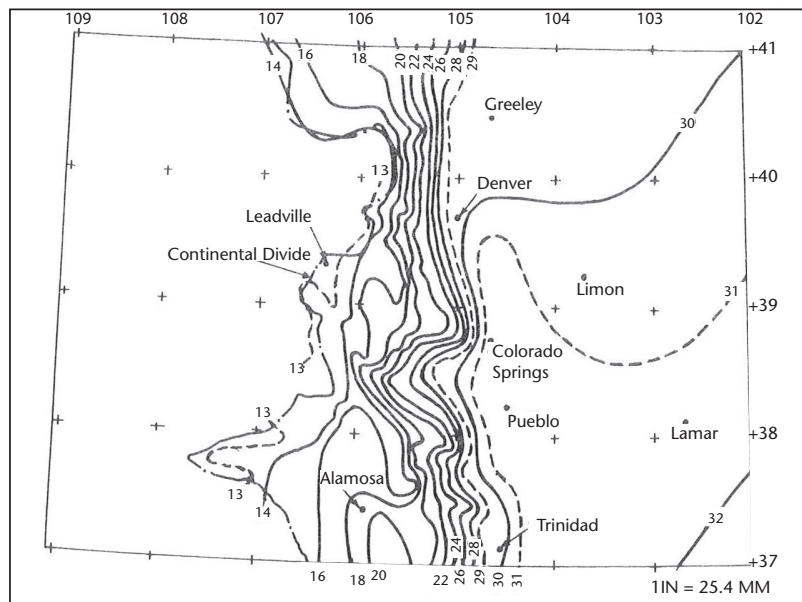


**Figure 5.32. Moisture-maximized convergence precipitation (inches) map for state of Colorado east of Continental Divide (Miller and others, 1984b)**

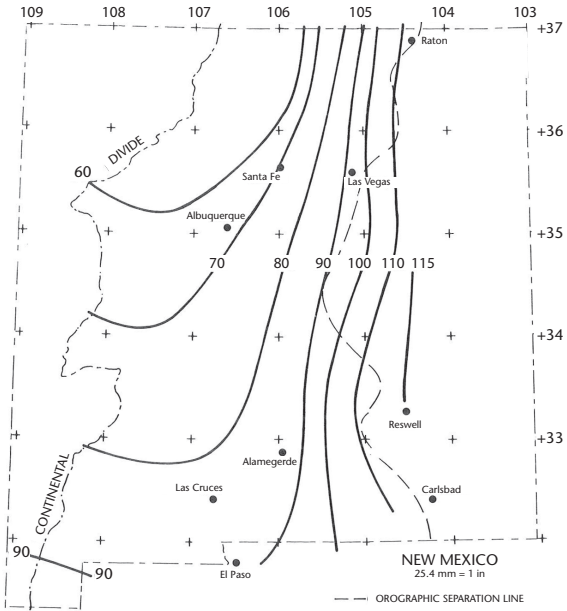


**Figure 5.33. Convergence component of the 100-year 24-hour precipitation-frequency values (tenths of inches) for the state of New Mexico east of the Continental Divide (Miller and others, 1984b)**

#### 5.3.4.3 Storm intensity factor $M$

Precipitation at any location in a mountainous region is the result of both the atmospheric forces associated with the storm and the vertical lift imparted by the air flow against the mountain slopes. This latter effect on storm precipitation can be considered relatively constant in any specific location. There is some variation related to the magnitude of the inflow wind normal to the orographic barrier, but this is relatively small in relation to the variation of the dynamic forces during the storm. To adjust the orographic factor for this varying effect, a storm intensity factor was needed. This factor  $M$  is defined as the amount of rainfall in the most intense portion, or core portion, of the storm divided by the amount of rainfall in the duration of the storm under consideration. Although durations from 1 to 72 hours were required for this study, the primary focus of the investigation was to determine the 24-hour 25.9 km<sup>2</sup> precipitation. For this region, the most intense portion of this 24-hour period was determined to be approximately 6 hours, based on an examination of data from major storms within the region. The storm intensity factor is therefore a 6-hour amount divided by the 24-hour amount for each of the major storms within the region. There is some geographic variation in this factor through

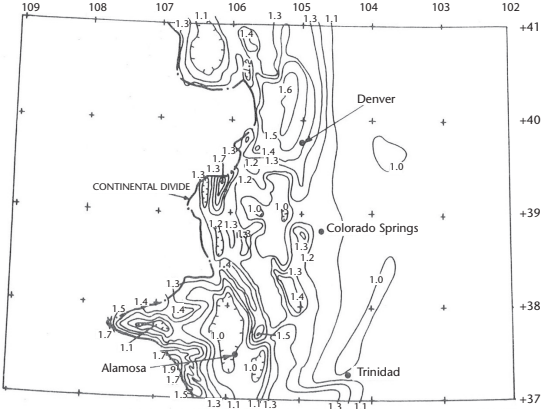


**Figure 5.34. Orographic factor ( $T/C$ ) map for the state of Colorado east of the Continental Divide (Miller and others, 1984b)**

the region based on the meteorological characteristics of storms. An example of geographic variation is shown for the state of Montana east of the Continental Divide in Figure 5.35.

#### 5.3.4.4 Computation of PMP

The three factors discussed in sections 5.3.4.1 to 5.3.4.3, were used to obtain a final estimate of PMP. The equation used is:

$$\text{PMP} = \text{FAFP} \# \left( M^2 \left( 1 - \frac{T}{C} \right) \right) + \frac{T}{C} \quad (5.1)$$

where FAFP is free atmospheric forced precipitation (section 5.3.4.1);  $M$  is the storm intensity factor (section 5.3.4.3);  $T/C$  is the orographic factor (section 5.3.4.2)

This formulation decreases the effect of the orographic intensification factor ( $T/C$ ) as the storm becomes more convective. That is, in regions where a storm is primarily of a convergence nature as reflected by highly convective activity within the major storms of record, the orographic intensification factor is reduced in effectiveness. In regions where more generally uniform rainfall prevails, such as is characteristic of the mountain slopes,  $T/C$  becomes increasingly important. It also minimizes the effect of the orographic intensification factor in the most intense or core period of the storm. Using this equation and a varying grid over the region, estimates of total PMP were computed. The resulting grid point values were analysed to provide a generalized chart of 24-hour 25.9-km<sup>2</sup> PMP for the region of the United States between the Continental Divide and the 103rd meridian. Figure 5.36 shows a portion of this map for northern New Mexico east of the Continental Divide. Values for

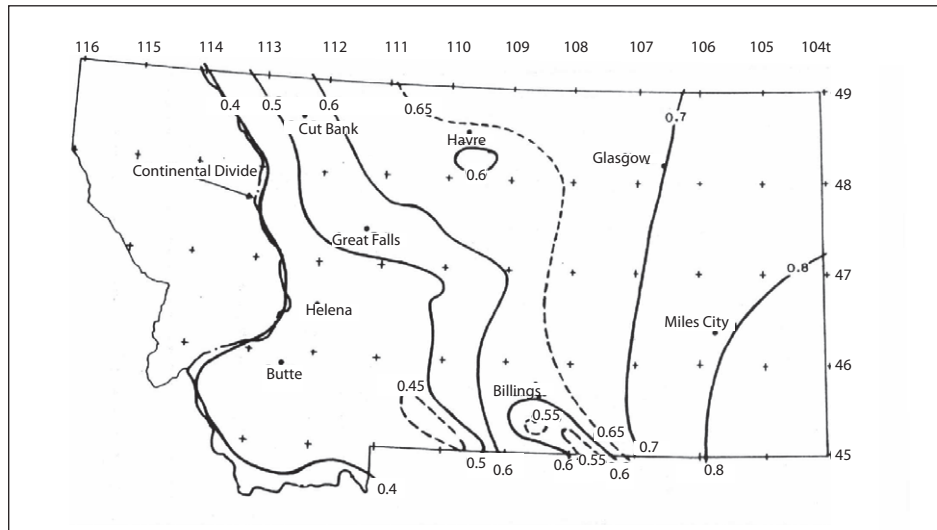


**Figure 5.35. Storm intensity factor ( $M$ ) for the state of Montana east of the Continental Divide (Miller and others, 1984b)**

other durations were obtained by use of ratios related to basic 24-hour 25.9-km<sup>2</sup> PMP estimates.

#### 5.3.4.5 Depth-area relations

The index maps prepared for this study were for 25.9 km<sup>2</sup> at 1-, 6-, 24-hour and 72-hour durations. It is generally necessary in developing PMP estimates for a region, to provide values for a range of area sizes. Depth-area relations were developed to enable estimates to be obtained for area sizes up to 51 800 km<sup>2</sup> in non-orographic regions and to 12 950 km<sup>2</sup> in orographic regions. The depth-area relations were based on depth-area characteristics

of major storms in the region between the Continental Divide and the 103rd meridian. The variety of storms than can produce the PMP within the region and the complexity of the topography required subdividing this region into several sub-regions. first division was the major river basins within this total study region. There were five major combinations of river basins that were used, extending from the Missouri and Yellowstone rivers in the north to the Pecos and Canadian rivers and middle Rio Grande in the south (see Table 5.3). A second separation was between orographic and non-orographic regions. Each of these was separated into primary and secondary, or sheltered, regions. A

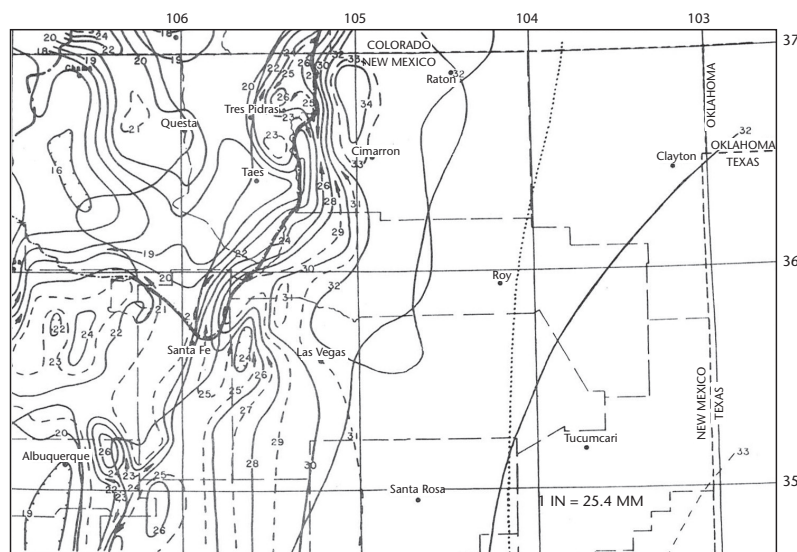


**Figure 5.36. Twenty-four-hour 25.9-km<sup>2</sup> PMP estimates (inches) for the northern portion of the state of New Mexico east of the Continental Divide**

schematic diagram of the final separation into sub-regions is shown in Figure 5.37. An example of the depth-area relation for the orographic portion of the Missouri and Yellowstone River basins is shown in Figure 5.38.

### 5.3.5 PMP estimates for the Colorado River and Great Basin drainages of the south-western United States

Estimation of PMP in this region of the south-western United States (Hansen and others, 1977) used the orographic separation method (section 3.1.6). First, essentially non-orographic or convergence PMP was estimated from major convergence storms in non-orographic portions of the region. Orographic PMP was then determined.

In this region, the laminar flow model discussed in section 3.2.2 is inappropriate. Along the west coast of the United States, where the laminar flow model has been applied (United States Weather Bureau, 1961a, 1966), the mountains form an almost unbroken barrier to windflow. One of the major causes of rainfall along the western coast of the United States is the lifting of moist stable air over this barrier. There are also a large number of representative rainfall measurements available for calibrating the model. In the Colorado River and Great Basin drainages moisture transport into the region involves air with greater instability than along the west coast, and the orographic model with its assumed laminar flow has only very limited applicability. Much of the rainfall in major storms in this region results in the initiation of convective activity, including thunderstorms, along the mountain slopes. The terrain also is much more complex, with short mountain ridges that present various aspects and thus angles to the inflow winds. Because of these factors, the orographic wind flow model has very limited use.

The orographic precipitation estimates were based on variations in observed precipitation and terrain effects. The development of the convergence precipitation estimates in this region was completed in a manner similar to that for California and discussed in section 3.3.4. It will not be repeated in this chapter. Since the development of the orographic component of the precipitation uses indirect procedures, a brief description will be given.

#### 5.3.5.1 Orographic precipitation index

The initial estimate of the orographic component of PMP over the Colorado River and Great Basin (Hansen and others, 1977) was based on the

**Table 5.3. Major river basins within the region of the central United States between the Continental Divide and the 103rd meridian used for depth-area relations**

Sub-region	River basins
A	Missouri and Yellowstone rivers
B	North Platte River
C	South Platte River
D	Arkansas River and Upper Rio Grande
E	Pecos and Canadian rivers and middle Rio Grande

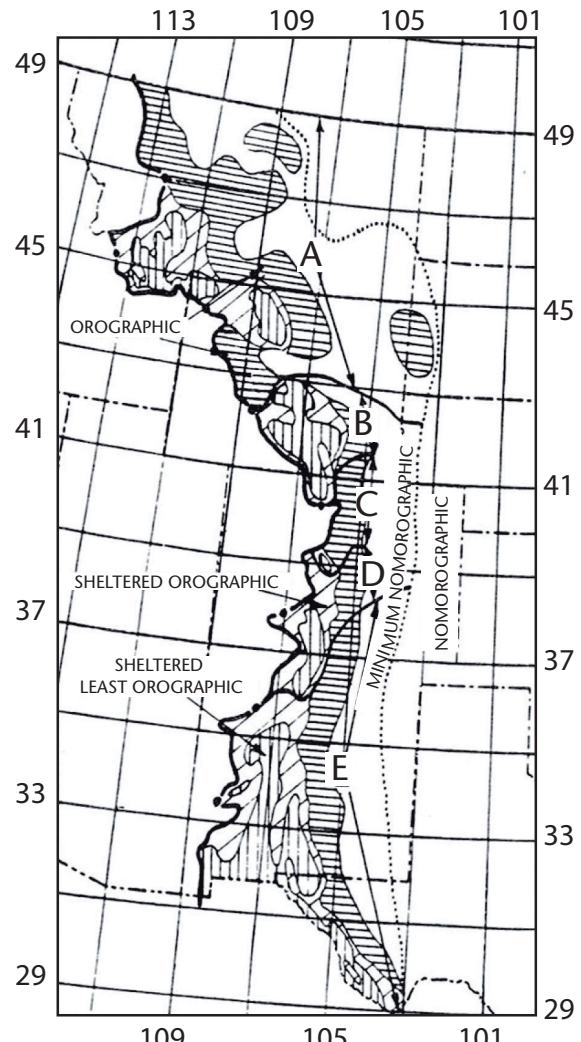


**Figure 5.37. Schematic diagram of the sub-regional system used in developing depth-area-duration relations (Miller and others, 1984b)**

100-year 24-hour  $25.9 \text{ km}^2$  precipitation frequency values from NOAA Atlas 2 (Miller and others, 1973). A 100-year 24-hour rainfall of 102 mm over the nearly flat area of south-western Arizona and south-eastern California was assumed to be entirely convergence rainfall. Comparable convergence values over minimally orographic portions of the study region were estimated by first applying reductions for effective barrier and elevation. The total 100-year 24-hour rainfall was then expressed as a percentage of this convergence component. This percentage was then applied to the convergence component of PMP to obtain a first approximation to the orographic effects. Implicit in this procedure is the assumption that the orographic and convergence components of PMP have the same relation to each other as the relation between the orographic and convergence components of the 100-year 24-hour rainfall, each appropriately adjusted for elevation and barrier.

#### 5.3.5.1.1 *Modifications of the first approximation to the orographic precipitation index*

Several factors were used to provide guidance in modifying the first approximation to the orographic PMP index. The first of these were rain ratios for line segments across ridges in the region. The rain ratio is the rate of change in rainfall per 305 m divided by the base elevation rainfall. This rain ratio is one index to the variation of rainfall with elevation and is related to the low-elevation amounts. Various rain ratios were computed based on the 100-year 24-hour rainfall, mean annual precipitation, mean seasonal precipitation, and maximum observed values. A modification of this rain ratio was based upon mean monthly rainfalls adjusted by a frequency of rain versus elevation relation. This ratio was not greatly different from, but generally slightly smaller than, rain ratios not adjusted by the frequency of rainfall relations. Rain ratio profiles were also computed for several major storms in the region. As a basis for a comparison, all ratios were plotted on graphs, using distance from the ridge for the  $x$ -coordinate. Also plotted on the graphs were the terrain profiles. Similar ratios were also computed for the region beyond the ridge to the valley on the lee side. Using this information, the region was divided into three separate terrain categories: (a) most orographic; (b) least orographic; and (c) intermediate orographic.

In the areas of most orographic effects, the gradient of PMP was maintained at about twice the gradient in the rain ratios of 100-year 24-hour rainfall and mean annual precipitation. In the least orographic

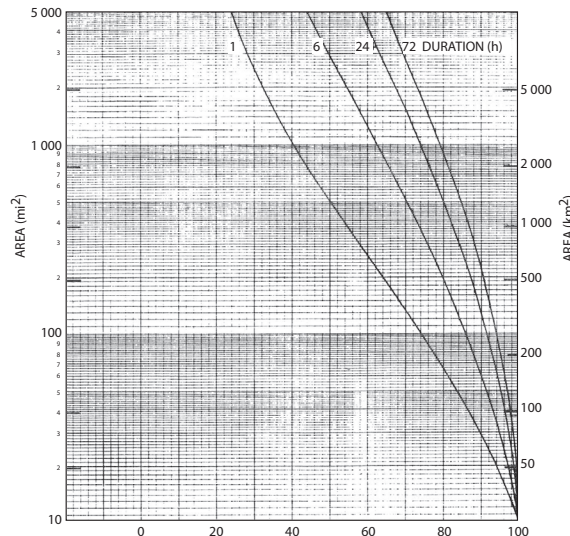


**Figure 5.38. Depth-area-duration relation for orographic region of Missouri and Yellowstone River basins (Miller and others, 1984b)**

regions, orographic PMP had a lower limit of 25.4 mm. Orographic rainfall in these regions is attributed to either spillover from upwind regions or the generalized influence of smaller hills that make up a part of most areas classified as least orographic. In intermediate orographic areas, isoline gradient was maintained at about the same as for the rainfall ratios. Figure 5.39 shows a portion of the orographic index PMP map for southern Arizona, south-western New Mexico and south-eastern California.

#### 5.3.5.2 Variation with basin size

In a previous study (United States Weather Bureau, 1961a) using the orographic separation method, variation with basin size was related to steepness, height, length, orientation and exposure of each slope to moisture bearing winds. The assumption is that there is a limit to the lateral extent over which moisture can be transported over mountain slopes without a decrease in intensity. This decrease was assessed by a study of the variation of pressure gradients with distance between stations that take pressure observations. In the inter-mountain portion of the western United States, inflow from several directions must be considered in determining the magnitude and gradient of orographic PMP for the entire storm period. For any particular 6-hour period of the PMP storm over a given drainage, however, the winds would generally be from one direction. Thus, they would have their maximum orographic influence on slopes normal to that direction only. An approximate method was determined to take into account both the reduction due to a lateral

extent for the basin, and the fact that at a given time slopes in only one direction can be maximally effective. This procedure was to analyse depth-area relations of most orographically influenced rainfalls from major storms of record in the region. Figure 5.40 shows the variation of orographic PMP with basin size developed from these storms.

### 5.3.5.3 Durational variation

Variation of orographic precipitation with duration depends on the durational variation of winds and moisture. The variation of maximum 6-hour incremental winds at the 500-hPa and 900-hPa pressure levels for Tucson, Arizona, were used as a guide for the durational decay of wind. The durational variation of maximum moisture was based on consideration of the highest persisting 12-hour 1,000-hPa dewpoints for seven stations throughout the Colorado River and Great Basin drainages. The maximum persisting 1,000-hPa dewpoints for 6, 12, 24, 36, 48, 60 and 72 hours for each of 12 months at each of seven stations were expressed in centimetres of precipitable water assuming a saturated atmosphere with a pseudo-adiabatic lapse rate. This dewpoint variation was combined with wind decay for the total durational variation for orographic PMP (Figure 5.41). For locations between the two latitudes shown, a linear interpolation was recommended. These durational decays were verified by comparison with variation in precipitation in major storms in the south-western part of the United States. Another comparison was to develop ratios of maximum observed 6- to 24-hour and

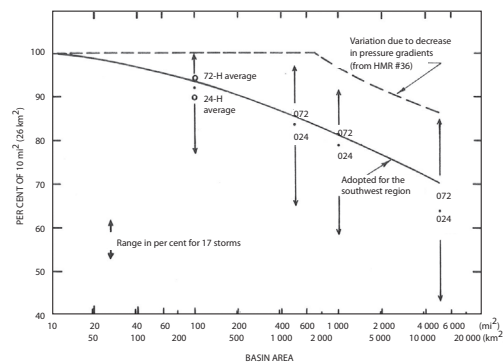


Figure 5.40. Variation of orographic PMP with basin size for Colorado River and Great Basin drainages (Hansen and others, 1977)

72- to 24-hour precipitation. These comparisons confirmed the adopted durational variation.

### 5.3.5.4 Combination of orographic and convergence PMP

The orographic PMP discussed in the preceding sections can be computed for any basin in the Colorado River and Great Basin drainages of south-western United States. This orographic component of PMP is combined with the convergence component of PMP for the basin to obtain an estimate of total PMP. The convergence PMP is developed as discussed in section 3.3.4. In the development of the convergence component of PMP only those storms that are consistent with general storms that produced large orographic precipitation amounts are considered.

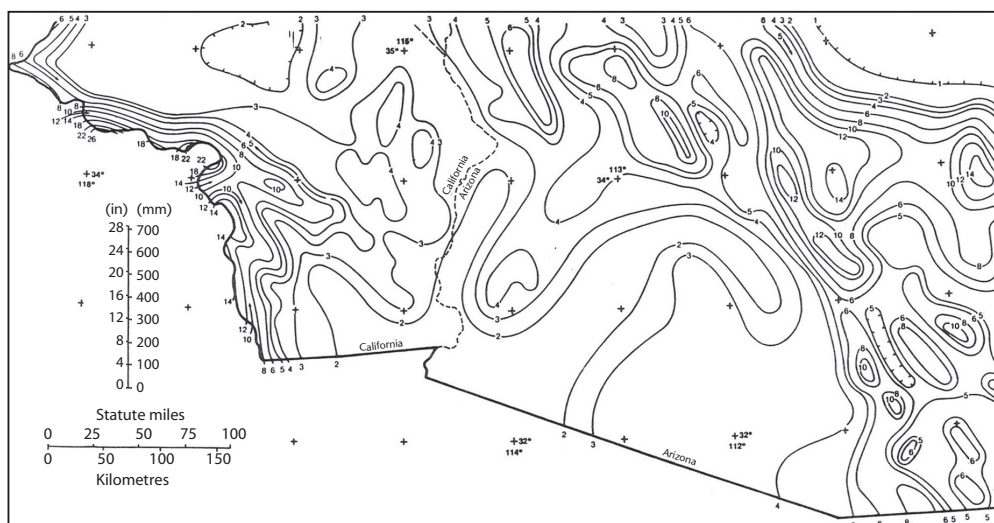
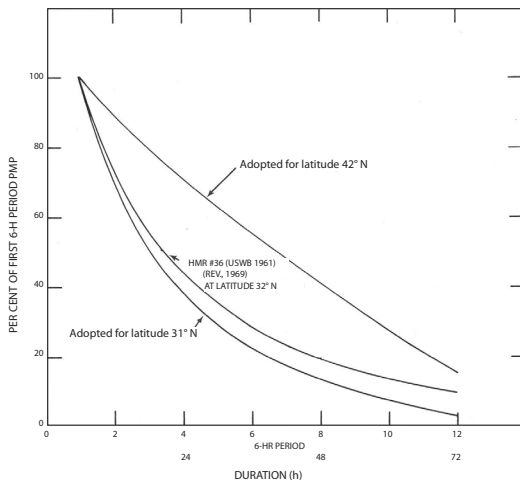


Figure 5.39. Twenty-four-hour 25.9 km<sup>2</sup> orographic PMP (inches) for southern Arizona, south-western New Mexico and south-eastern California (Hansen and others, 1977)



**Figure 5.41. Adopted durational variation in orographic PMP for Colorado River and Great Basin drainages (Hansen and others, 1977)**

### 5.3.6 PMP estimate for drainage above Dewey Dam, Johns Creek, Kentucky

In a generalized study for the eastern United States (Schreiner and Riedel, 1978), only convergence or non-orographic precipitation was determined. An orographic region, the Appalachian Mountains, was stippled on the maps presenting the results and the study recommended that individual estimates be prepared for individual basins in this region to consider orographic effects. Two such studies have been completed (Fenn 1985; Miller and others, 1984a). In each study, the procedures developed for the region between the Continental Divide and the 103rd meridian (Miller and others, 1984a) were adapted. In that study (section 5.3.4) convergence PMP was developed and then adjusted for orographic effects. In the eastern United States, convergence PMP is obtained by applying procedures of the *Applications Manual* (Hansen and others, 1982) discussed in section 5.2.7 to the generalized PMP estimates for the region (Schreiner and Riedel, 1978). The procedures used to develop the orographic intensification factors were similar in each instance. In the estimate for the Deerfield River basin (Miller and others, 1984a), precipitation stations were located in the basin and data from these stations were used to develop the required orographic factor. In the Johns Creek basin (Fenn, 1985), there were no precipitation stations in the basin and indirect procedures were required.

#### 5.3.6.1 Orographic factor T/C

Values of  $C$  (section 5.3.4.2) throughout the region were calculated first. Figure 5.42 shows the isolines

of convergence of 100-year 24-hour rainfall for a portion of the central United States. The region where elevations are greater than 1 000 ft (305 m) is hatched and the portion of this region where orographic effects are considered significant is indicated by the stippling. The project basin is on the western edge of the orographic region and is outlined in Figure 5.42. The 100-year 24-hour precipitation-frequency values were calculated for all regularly reporting stations within the region shown in Figure 5.42. The values outside the orographic region can be considered to be due entirely to convergence. The values within the orographic region result from a combination of convergence and orographic influence. Examination of all data indicated maxima of convergence 100-year 24-hour values at the western and eastern edges of the analysis region. Joining these eastern and western regions with smoothly varying isolines produced a trough of lower values in the centre of the region. Along 37° N, the value of  $C$  was approximately 10 per cent lower than at the western edge and approximately 20 per cent lower than at the eastern edge. A 1 000-hPa value of  $C$  of 160 mm for the centroid of the basin can be determined from the analysis.

Since there were no precipitation stations located in the basin, it was necessary to determine the total 100-year 24-hour precipitation-frequency value for the basin by use of proxy stations. The topography was examined and separated into three topographic classifications: lowlands, representing the valley floor below about 220 m; uplands, representing the more rugged terrain above about 300 m; and a transition area in between. The lowlands comprised 32 per cent of the basin and the upland area comprised 43 per cent of the basin. The remaining 25 per cent was a transition zone between the two. Next, the 100-year 24-hour precipitation-frequency values

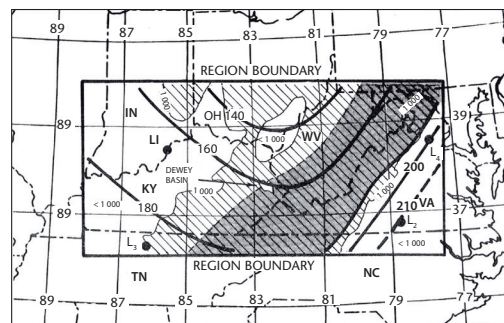


**Figure 5.42. Isolines on convergence 100-year 24-hours rainfall (cm) for central United States (Fenn, 1985)**

for all stations around the basin were plotted and the topography examined. There were ten “close-in stations” characterized by topographic settings similar to the three categories that were characteristic of the basin. The elevations used to separate these were the same as those used within the basin. Variations of both the convergence precipitation from the map of the Figure 5.42 and total precipitation values determined for the individual stations were adjusted to the elevation of the centroid of each of the topographic classifications. Using these values, a weighted value for  $T/C$  of 1.13 for the 24-hour duration is determined for the basin.

To obtain values of  $T/C$  for durations other than 24 hours, data from other regions were used. Regions were selected where the 100-year 24-hour and 6-hour precipitation-frequency values had been analysed, the value of  $T/C$  based on the 100-year 24-hour amounts was 1.13, and the region was at approximately the same latitude and distance from the moisture source as the Johns Creek basin. In addition, the topography was selected to be, as near as possible, comparable with that around Johns Creek and the three proxy regions. The locations selected were in the foothills of the front range of the Rocky Mountains in Colorado and northern New Mexico. There were some differences in the climatology of rainfall between Johns Creek and the three regions and also some difference in topographic settings. However, the storm types which produced the PMP for this area size are similar in these two regions. For these locations, a value of  $T/C$  for 6 hours of 1.11 was determined. As the duration decreases, the value for  $T/C$  should approach 1. Using this assumption and the values of  $T/C$  for 6- and 24-hour values of  $T/C$  for the durations between 1 and 72 hours were determined. These values are shown in Table 5.4.

### 5.3.6.2 Storm intensity factor $M$

The storm intensity factor is related to the length of the core event (the period of most intense precipitation) during the PMP storm (see section 5.3.4.3). Examination of the major storms in the regions surrounding the Johns Creek drainage (Fenn, 1985) suggests the length of the core event  $r$  for some durations is slightly different from those found in other regions for some durations (Miller and others, 1984a, 1984b). The duration of  $r$ , for selected total periods of precipitation  $h$  is shown in Table 5.5. The storm intensity factor  $M$  is the ratio of the precipitation during the period  $r$  to the precipitation during  $h$ . These precipitation amounts are the

non-orographic PMP values read from the maps of the generalized study for the region (Schreiner and Riedel, 1978) for an area size approximately that of the basin. The values of  $M$  computed from these values, and thus appropriate to the Johns Creek basin, are shown in Table 5.6.

### 5.3.6.3 Computation of PMP for Johns Creek basin

The procedure used to compute the total PMP for the Johns Creek basin is the same as that used for the orographic region between the Continental Divide and the 103rd meridian. The procedure uses Equation 5.1, shown in section 5.3.4.4. The equation was developed considering only the relationships between atmospheric forces and orographic effects. It should be generally applicable where the climatic regime, storm types, and topography are not completely dissimilar to the mid-latitude United States. The only requirement would be to develop the orographic factor  $T/C$  and the storm intensity factor  $M$  using the relations for major storms within the region. In this study (Fenn, 1985), the convergence precipitation adjusted for depletion in moisture availability and for the orientation and basin shape of the Johns Creek basin with the  $T/C$  and  $M$  factors discussed in the preceding two sections produces total PMP values shown in Table 5.7. These values are also shown in percentages of storm-centred PMP determined directly from the generalized or regional study (Schreiner and Riedel, 1978) for the area size of the basin. The combined effect of orographic intensification and reduction for the barrier to moist air inflow and non-concurrence of the elliptical isohyetal pattern with the basin shape results in a small decrease from the results taken directly from the generalized study. With other basins, the combined effect could be different and the net result could be an increase or an even larger reduction.

### 5.3.7 Generalized estimation of PMP for local storms in the Pacific Northwest region of the United States

#### 5.3.7.1 Brief introduction

A small-area, short-duration storm may be the centre of a large-area precipitation or an isolated event independent of a large-area precipitation. The former is called a non-local storm and the latter a local storm. The definition of local storm in this section is a storm with a duration less than 6 hours and an area less than 1 300 km<sup>2</sup> that has nothing to do with a large-area storm. Extreme local storms in the Pacific Northwest region of the United States are atmospheric convergence phenomena and are mostly

thunderstorm rains. Storm moistures mostly come from the west and the south-west. Regions featuring large-scale ascendant movements provide some conditions for thunderstorm rains, but strong ascendant movements also need support from convection activities. Convective storms, however, mainly depend on stable thermodynamic conditions, which play a critical role in the resulting convection intensity. Direct surface heating in the Pacific North-west region leads to strong convection instability, which causes local extraordinary thunderstorm rains. The main season (June–August) of thunderstorm rains in the region with a high frequency during the day (afternoon) support this view. Low-altitude convergence caused by storm gusts plays a critical role in the recurrence process of multi-grid storm bursts. The content of this section is taken from HMR No. 57 (Hansen and others, 1994). Steps applied in the Columbia River basin, the Snake River basin and the Pacific Coast watershed may be a guide for other regions.

### 5.3.7.2 Moisture maximization

After studies of each characteristic of local storms in the Pacific North-west region and meteorological conditions influencing it, it is believed that the humidity required by local storms is not as pervasive and long-lasting as that required by non-local storms. Continuous moisture supplement is scarce, so the duration of representative dewpoints of storms should be consistent with cases in which storm time intervals are short. For storm moisture maximization and adjustment, methods similar to those for non-local storms are used, that is, moisture maximization and adjustment are performed with maximum durative surface dewpoints during a time interval as a scale of the moisture content of local storms. Nonetheless, different practices exist. First, the main rainfall time interval of local storms is 3–4 hours, so the maximum durative 3-hour dewpoints during the storm period are regarded as indicators of moisture maximization and adjustment. Second, the direction of moisture inflows is not certain during the local storm period, so the selection of locations of representative dewpoints is

**Table 5.4. Values of  $T/C$  at the centroid of the drainage above Dewey Dam, Johns Creek, Kentucky**

$T/C$	Duration (hours)					
	1	6	12	24	48	72
	1.04	1.11	1.12	1.13	1.14	1.15

**Table 5.5. Estimated duration of intense precipitation  $t$  for selected total length of precipitation period (Fenn, 1985)**

$r$ (hours)	Duration (hours)					
	1	6	12	24	48	72
	0.75	3	4.5	6	8.5	10.5

**Table 5.6. Storm intensity factor  $M$  for selected durations (Fenn, 1985)**

$M$	Duration (hours)					
	1	6	12	24	48	72
	0.881	0.788	0.776	0.774	0.773	0.772

not restricted by inflow directions. Third, to better reflect characteristics of moistures of local storms, the selection of dewpoints should be at stations within 80 km of the storm site.

The largest local storms in the Pacific North-west region of the United States occur from April to October, especially June–August, during which time the amount of precipitation is also the greatest. Three-hour duration maximum dewpoints are highest in the south and the south-east in June–August, when they reach 24°C or 25°C. They are lowest in the north-west, but may still reach 16°C to 18°C.

### 5.3.7.3 Elevation adjustment and horizontal transposition adjustment

The methods used for local storm elevation adjustment and horizontal transposition adjustment are identical to those for non-local storm adjustment.

### 5.3.7.4 PMP precipitation depth-duration relation

During local extraordinary storms in the Pacific North-west region of the United States, continuous moisture supply is scarce due to regional geographical features. As a result, those local storms usually cause the largest storms in the first hour with their total precipitation durations seldom exceeding

**Table 5.7. PMP of the drainage above Dewey Dam, Johns Creek, Kentucky**

	Duration (hours)					
	1	6	12	24	48	72
PMP (mm)	190	492	591	607	760	779
Percentage of total estimation value	85	95	96	97	98	98

6 hours. According to studies of temporal variations in 99 local storms in the North-west region, the ratio between 6 hours and 1 hour is about 1.10 to 1.15.

### 5.3.7.5 PMP precipitation depth-area relation

Based on HMR No. 43 (United States Weather Bureau, 1966) and HMR No. 49 (Hansen and others, 1977) and studies of data on extreme local storms in the North-west region, the precipitation depth-area relation has been corrected. The current precipitation depth-area relation is shown in Figure 5.43. The adopted generalized local storm isohyet map is shown in Figure 5.44. Using both of these, the spatial distribution of PMP of local storms with particular durations and areas may be determined.

### 5.3.7.6 One-hour 2.6 km<sup>2</sup> PMP map of the North-west region

#### 5.3.7.6.1 Analysis of results

An index map of 1-hour 2.6-km<sup>2</sup> PMP for elevations up to and including 1 830 m is provided in HMR No. 57 (Hansen and others, 1994; Figure 5.45)

The highest values of local storm PMP are found over the extreme south-eastern portions of the region in the Snake River basin, where a maximum of almost 250 mm reaches nearly to the Idaho border. A broad maximum of 200 to 230 mm in local storm PMP is evident through the

Snake River basin along the Idaho border with a concomitant dip over the Rockies. Local storm PMP values decrease generally to the north and west across the region, falling to about 150 mm in the Cascades east of Seattle. This is in response to both decreased moisture and diminished intensity of solar radiation. The minimum local storm PMP, about 80 mm, occurs in the Olympic Peninsula in Washington. This value increases to a little over 130 mm southward along the coast, at the Oregon-California border. These lower values are due to the destabilizing effect of the cool, moist layer of surface air resulting from interaction with the cool Pacific Ocean waters along the coast.

#### 5.3.7.6.2 Comparison with other studies

HMR No. 43 (United States Weather Bureau, 1966) calculated summer thunderstorm PMP for areas of the Columbia River basin east of the Cascades. The procedures used in that study vary significantly from those utilized in the current study. A brief review of the salient differences in procedures and results will serve to emphasize the types of changes involved.

Compare the estimate results of HMR No. 57 (Hansen and others, 1994) and HMR No. 43 (United States Weather Bureau, 1966) for 1-hour 2.6-km<sup>2</sup> PMP in inches east of the Cascades. In the majority of the region the difference between the two estimates is less than 130 mm. Slightly larger differences, however, appear in the study area

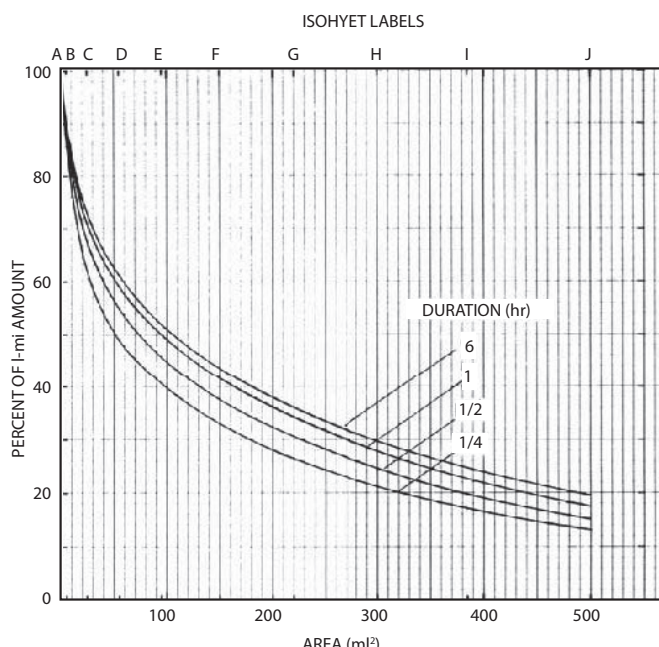
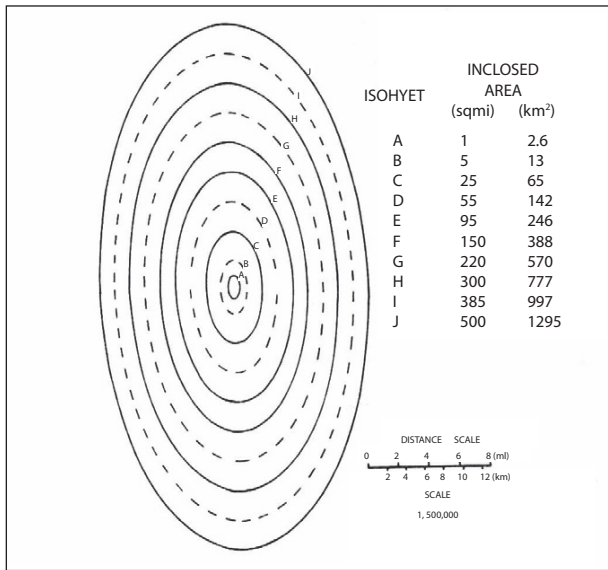


Figure 5.43. Depth-area relations for local storm PMP Pacific Northwest states



**Figure 5.44. Idealized isohyetal pattern for local storm PMP areas up to 1 300 km<sup>2</sup> (Hansen and others, 1977)**

from around central Washington to the Canadian border. The new study results in PMP from 25 to 40 mm lower.

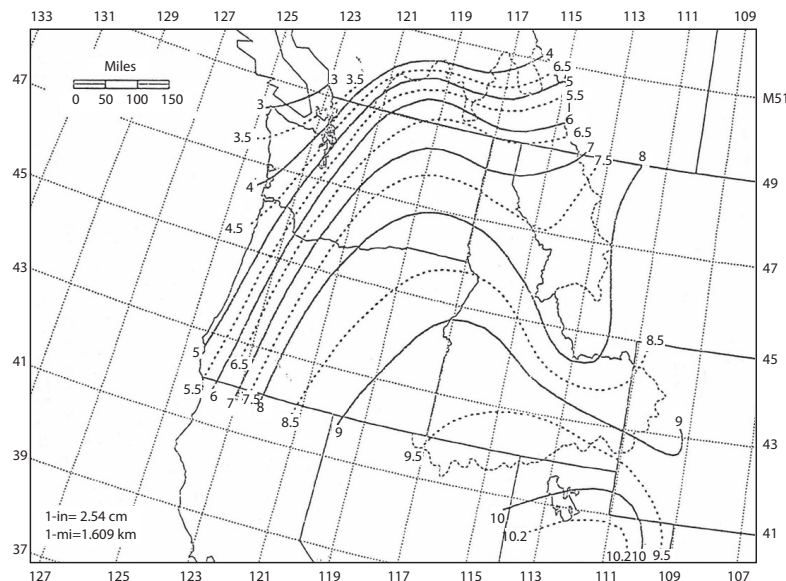
Comparisons were also made with adjoining studies, including HMR No. 49 (Hansen and others, 1977) and HMR No. 55A (Hansen and others, 1988). Some of the different assumptions regarding elevation and durational characteristics have already been discussed.

Relative to HMR No. 49 (Hansen and others, 1977), the differences in 1-hour 2.6-km<sup>2</sup> PMP are near zero in extreme northern Utah, becoming more positive moving westward to a maximum of around +40 mm along the California–Oregon border area. The primary reason for this discrepancy may come from transposing the Morgan, Utah, storm throughout the southern portions of the Northwest. HMR No. 49 (Hansen and others, 1977) and the present study support a preferred seasonality of storms and do not attempt to apply seasonal curves or nomograms.

No significant PMP differences exist in local storm PMP between the current study and HMR No. 55A (Hansen and others, 1988). No major new storms were found within this general area which would cause any increase in PMP to be made, and no evidence was revealed which might indicate a lowered estimate. Seasonality for HMR No. 55A (Hansen and others, 1988) showed a distinct summer maximum in extreme local storms, a finding in agreement with this.

#### 5.3.7.7 Estimating procedure of local storm PMP for specific basin

- The 1-hour 2.6-km<sup>2</sup> PMP for elevations at or below 1 830 m is determined by locating the basin on Figure 5.45 and determining the basin average 1-hour 2.6-km<sup>2</sup> PMP local storm index PMP. Linear interpolation is assumed to be applicable.



- (b) To adjust for mean drainage elevation, determine the mean elevation of the drainage in question. No adjustment is necessary for elevations of 1 830 feet or less. If the mean elevation is greater than 1 830 m, reduce the index PMP from (a) by 9 per cent for every 300 m above the 1 830-m level.
- An example of the elevation adjustment is as follows. Take a basin with a mean elevation of 2 650 m, (820 m above 1 830 m). The reduction factor would be 24.3 per cent ( $2.7 \times 9$ ) in this case.
- (c) To adjust for durations, the 2.6-km<sup>2</sup> local storm PMP estimates for durations less than 1 hour and up to 6 hours are obtained as a percentage of the 1-hour amount from (b). The PMP of all durations can be obtained by multiplying the results from (b) by the percentage of all durations.
- (d) Adjustment for basin area is determined using the percentage reductions at 0.25, 0.50, 0.75, 1, 3, and 6 hours for the area of the basin from Figure 5.43. These are multiplied by the respective results from (c), and a smooth curve drawn for the plotted values in order to obtain estimates for durations not specified.
- (e) Temporal distribution is ascertained using reviews of local storm temporal distributions for this region. These show that most storms have durations of less than 6 hours and that the greatest 1-hour amount occurs in the first hour. The recommended sequence of hourly increments is as follows: arrange the hourly increments from largest to smallest as directly obtained by successive subtraction of values and read from the smooth depth-duration curve.
- (f) Areal distribution of local storm PMP is derived using the percentages in Figure 5.44 and Table 5.8. In the event of choosing this option,

(c) and (d) can be ignored and the results from (b) (or (a), if no elevation adjustment is made) are multiplied by each of the percentage factors in Table 5.8. The results represent the labeled isohyets of the idealized pattern placed over the specific drainage.

Once the labels have been determined for each application, the pattern can be moved to different placements on the basin. In most instances, the greatest volume of PMP will be obtained when the pattern is centred in the drainage. However, peak flows may actually occur with placements closer to the drainage outlet.

### 5.3.7.8 Example of local-storm PMP estimation

This example shows the application of the above steps to determine the local storm PMP for the White River basin above Mud Mountain Dam (1 041 km<sup>2</sup>).

- (a) The basin outline is placed on Figure 5.45 and the basin average 2.6-km<sup>2</sup> 1-hour PMP is read as 161 mm.
- (b) The average drainage elevation is below 1 830 m although higher elevations occur near the border of the basin. No adjustment is needed for this basin.
- (c) Durational 2.6-km<sup>2</sup> values are obtained as shown in Table 5.9.
- (d) The areal reduction factors are obtained from Figure 5.43 for 1 041 km<sup>2</sup> to give basin average PMP at the durations indicated. Multiply the respective factor by the results of (c) as shown in Table 5.10.
- (e) The temporal distribution is given by plotting the results of (d) as shown in Figure 5.46 and reading off smoothed hourly values. Note that

**Table 5.8. PMP profile values (accumulative percentage of 1-hour 2.6-km<sup>2</sup> amount)**

Isohyet	Duration (hours)								
	0.25	0.50	0.75	1	2	3	4	5	6
A	50.0	74.0	90.0	100.0	110.0	112.0	114.0	114.5	115.0
B	32.0	53.0	67.0	74.8	83.5	85.5	87.5	88.0	88.5
C	22.0	37.5	48.0	56.0	63.0	65.0	66.0	66.5	67.0
D	17.0	28.5	38.0	43.0	48.0	49.5	50.5	51.0	51.5
E	12.0	21.0	28.0	32.2	37.0	38.0	38.0	39.0	39.5
F	7.5	14.0	19.0	22.4	25.0	25.7	25.7	26.7	27.2
G	5.0	8.5	12.0	14.0	16.2	16.7	16.7	17.7	18.2
H	2.0	3.5	5.0	6.5	8.3	8.8	8.8	9.8	10.3
I	0.4	0.7	1.0	1.2	2.2	2.7	2.7	3.7	4.2
J	0.2	0.3	0.4	0.5	1.0	1.5	1.5	2.5	3.0

the smoothed values may differ slightly from the calculated values as shown in Table 5.11. These increments are arranged in the recommended sequence for front-loaded local-storm PMP. See Figure 5.46 for the temporal distribution relation.

- (f) If the areal distribution provided by the idealized elliptical pattern in Figure 5.44 is needed, the isohyet labels are determined by reference to Table 5.8. In this example, the result from (a) of 161 mm is multiplied by each percentage in Table 5.8 to get the label values in Table 5.12.

The isohyet label values given in Table 5.12 are to be applied to the isohyetal pattern shown in Figure 5.44 for each duration. The pattern may be placed over the drainage in order to maximize the precipitation volume into the drainage, or it may be positioned so as to obtain a maximized peak runoff.

### 5.3.8 PMP estimation in California, United States

#### 5.3.8.1 Profile

HMR No. 58 (Corrigan and others, 1998) and HMR No. 59 (Corrigan and others, 1999) present procedures of estimating PMP for California. The reports introduce two methods of estimation: the general storm method and the local storm method. The general storm method is used to estimate PMP for durations from 1 hour through to 72 hours (1 hour, 6 hours, 12 hours, 24 hours, 48 hours and 72 hours) for watersheds with area sizes from 26 km<sup>2</sup> to 26 000 km<sup>2</sup>; the local storm method is used to estimate PMP for durations from 15 minutes to 6 hours for watersheds with area sizes under 1 300 km<sup>2</sup>. It is recommended that both methods be employed when estimating PMP for watersheds

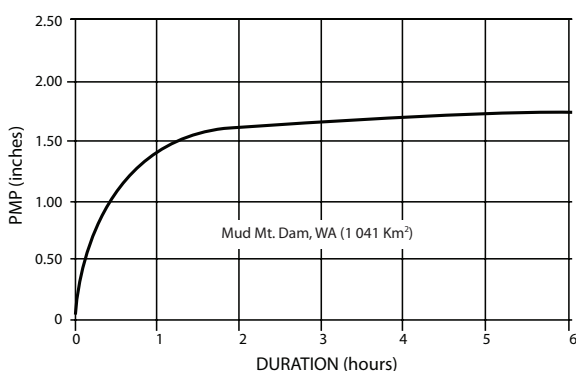


Figure 5.46. Temporal distribution relation for Mud Mountain Dam

Table 5.9. PMP values of each duration in drainage mean 2.6 km<sup>2</sup>

	Duration (hours)								
	0.25	0.50	0.75	1	2	3	4	5	6
Percentage	50	74	90	100	110	112	114	114.5	115
PMP (mm)	81	119	145	161	178	181	184	185	185

Table 5.10. Drainage average PMP value for each duration

	Duration (hours)					
	0.25	0.50	0.75	1	3	6
Percentage	16.0	19.0	21.0	22.0	23.0	24.0
PMP (mm)	13	23	30	36	42	44

Table 5.11. Increments of drainage average PMP value for each duration

	Hourly intervals					
	1	2	3	4	5	6
PMP (mm)	35.1	39.4	41.7	43.2	43.9	44.5
Increments (mm)	35.1	4.30	2.30	1.50	0.80	0.50

with area sizes under 1 300 km<sup>2</sup> and then the larger of the two be used as the design PMP for the watershed.

The generalized DAD method is still employed for estimating the PMP of general storms. For the separation of orographic rains, Equation 5.1 is rewritten as:

$$\text{PMP} = K \# \text{FAFP} \quad (5.2)$$

where

$$K = M^2 \left( 1 - \frac{T}{C} \right) + \frac{T}{C} \quad (5.3)$$

The reports give isoline maps for FAFP, T/C, M and K. A 26-km<sup>2</sup> 24-hour PMP isoline map was ultimately drawn on a 1 : 1 000 000 California map.

The PMP isoline map indicates longitudes, latitudes and some major places in addition to the boundaries of sub-regions. A generalized DAD curve is available in each of the sub-regions, so they are called DAD regions below.

If the studied watershed is located in more than one DAD region, then PMP for the sub-basin in each DAD region should be computed separately before determining PMP for the entire watershed using the area weighting method. For example, suppose a watershed whose area is 100 units includes three

**Table 5.12. Isohyetal label values (mm) for local-storm PMP, White River, Washington (1 041 km<sup>2</sup>)**

Isohyet (area in km <sup>2</sup> is shown in brackets)	Duration (hours)								
	0.25	0.50	0.75	1	2	3	4	5	6
A (2.6)	80.8	119.4	145.3	161.4	177.5	180.6	80.8	119.4	145.3
B (13)	51.6	85.6	108	120.7	134.6	137.9	51.6	85.6	108
C (65)	35.6	60.5	77.5	90.4	101.6	104.9	35.6	60.5	77.5
D (142)	27.4	46	61.2	69.3	77.5	79.8	27.4	46	61.2
E (246)	19.3	33.8	45.2	51.8	59.7	61.2	19.3	33.8	45.2
F (389)	12.2	22.6	30.7	36.1	40.4	41.4	12.2	22.6	30.7
G (570)	8.1	14.6	19.3	22.6	26.2	26.9	8.1	14.6	19.3
H (777)	3.3	5.6	8.1	10.4	13.5	14.2	3.3	5.6	8.1
I (997)	0.8	1	1.5	2	3.6	4.3	0.8	1	1.5
J (1 295)	0.3	0.5	0.8	0.8	1.5	2.5	0.3	0.5	0.8

sub-basins whose areas are 70, 20 and 10 units, respectively. The three sub-basins are located in different DAD regions. As a result, the PMP for the entire watershed,  $R$ , is:

$$R = \frac{70R_1 + 20R_2 + 10R_3}{100} \quad (5.4)$$

where  $R_1$ ,  $R_2$  and  $R_3$  are PMPs for the three sub-basins, respectively.

For moisture maximization under the local storm method, the representative dewpoint is set to be the 3-hour maximum persisting value. A 2.6-km<sup>2</sup> 1-hour PMP isoline map was ultimately drawn on the California map.

### 5.3.8.2 Procedure and example computation of estimating PMP with the general storm method

Estimating PMP with the general storm method includes six steps that will be introduced below one by one. Meanwhile, a full explanation of the process of computing PMP for a watershed is given, with the Auburn watershed in California as an example. The Auburn watershed is on Folsom Lake and located in the Sierra region (that is, the No. 5 DAD region), with an area of 2 520 km<sup>2</sup>.

#### 5.3.8.2.1 Drawing the boundary

The boundary of the watershed is drawn on the 1 : 1 000 000 California map, a step that can be done with GIS software. Since the studied object is the Auburn watershed, the boundary of that watershed is drawn on the 1:1 000 000 map and superposed with the generalized 24-hour PMP isoline map, as is shown in Figure 5.47.

#### 5.3.8.2.2 Estimating PMP

The networked watershed map is superimposed with the 24-hour PMP isoline map, PMP is calculated for each network in the watershed through the superimposed PMP isoline map for it, and then the area weighting method is employed to find the PMP for the entire watershed. Spatial changes to local estimates of PMP need to be considered in the size of the network on the determination of a reasonable PMP value for the basin. This step can also be performed through GIS software or other commercial software, which can make more accurate analyses on PMP changes with space and therefore obtain more accurate PMP values.

According to the corresponding precipitation depth on the PMP isoline in Figure 5.47, the 24-hour mean PMP for the Auburn watershed is 603 mm.

#### 5.3.8.2.3 Relationship between precipitation depth and duration

Figure 5.48 illustrates the boundary of each DAD region (seven sub-regions) of California. If the studied region is in a particular DAD region, the relationship between precipitation depth and duration for the corresponding region is read from Table 5.13. Note that the values in Table 5.13 refer to the ratios of PMP for that duration to PMP for 24-hour duration, that is, the coefficient of precipitation-depth conversion. Hence, the values in Table 5.13 should be multiplied by the 24-hour PMP obtained in section 5.3.8.2.2 above to obtain the PMP for each standard duration.

Except for a tiny part of its area, which is near the dam site, the Auburn watershed is basically in the

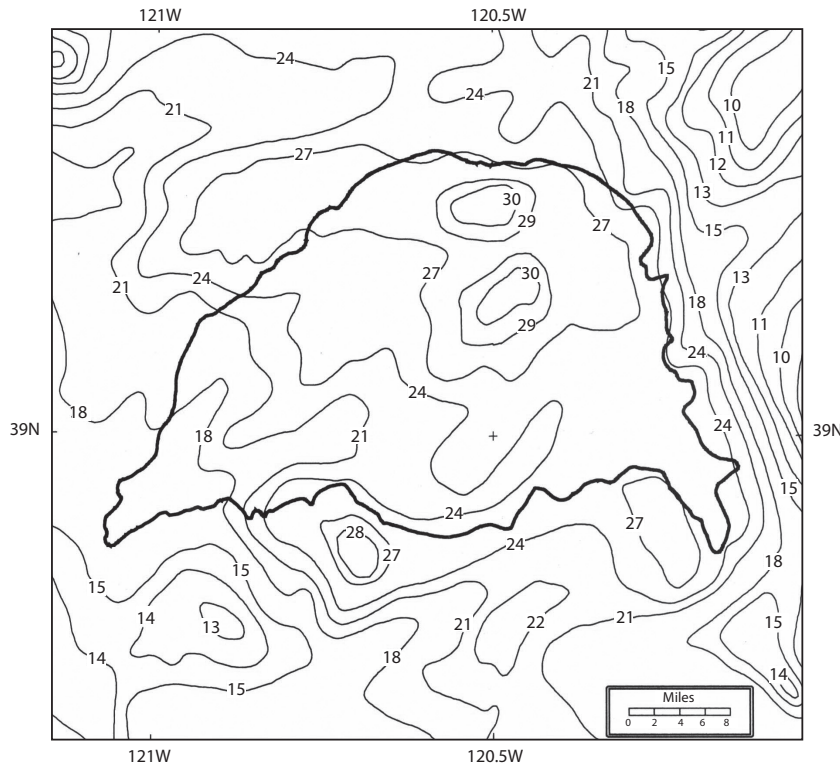


**Figure 5.47. Twenty-four-hour PMP isoline map for Auburn watershed (inches)**

Sierra region (region 5). The 24-hour PMP is multiplied by the coefficient of precipitation depth conversion for region 5 from Table 5.13 to obtain the PMP for each duration, as shown in Table 5.14.

#### 5.3.8.2.4 Coefficient of area reduction

A table is available for the coefficient of area reduction for each duration for each sub-region (the coefficient for any area size can be obtained by simple linear interpolation). Table 5.15 lists only the coefficients of area reduction for the Sierra Nevada region. The coefficient of area reduction for

each duration is multiplied by the PMP for the corresponding duration obtained in section 5.3.8.2.3 above. If the watershed is in more than one DAD region, then coefficient of area reduction for each DAD region is found the area weighting method is employed to obtain the coefficient of area reduction for the entire watershed.

Table 5.15 is interpolated to get the coefficient of area reduction for the 2 520 km<sup>2</sup> Auburn watershed, with the results listed in Table 5.16. Then PMP for each duration in section 5.3.8.2.3 is multiplied by its corresponding coefficient of area reduction to get the areal mean PMP for the watershed, again with the results listed in Table 5.16.

The duration is placed on the horizontal axis and the areal mean PMP on the vertical axis and the curve of the relationship between the areal mean PMP and the duration for the Auburn watershed is drawn (see Figure 5.49).

#### 5.3.8.2.5. PMP growth curve

The PMP growth curve is drawn for a particular duration using the following method: the duration is taken as the horizontal axis and the precipitation depth as the vertical axis and a smooth duration-precipitation depth curve is drawn with PMP for

**Table 5.13. Coefficients of duration – precipitation depth conversion for each DAD region in California**

	Duration (hours)					
	1	6	12	24	48	72
North-west (1)	0.10	0.40	0.73	1.0	1.49	1.77
North-east (2)	0.16	0.52	0.69	1.0	1.40	1.55
Central Coast (3)	0.13	0.45	0.74	1.0	1.45	1.70
Central Valley (4)	0.13	0.42	0.65	1.0	1.48	1.75
Sierra (5)	0.14	0.42	0.65	1.0	1.56	1.76
South-west (6)	0.14	0.48	0.76	1.0	1.41	1.59
South-east (7)	0.30	0.60	0.86	1.0	1.17	1.28

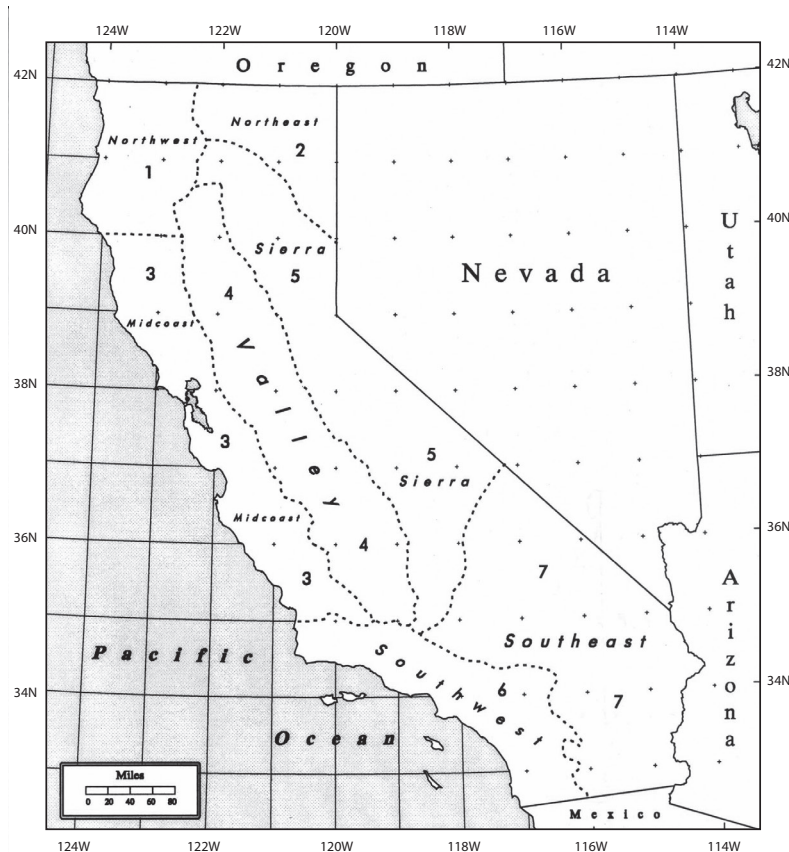


Figure 5.48. California DAD region map

each duration obtained in section 5.3.8.3.4. It is allowed to increase (or decrease) 12.25 mm when drawing the curve because of errors of rounding in the previous steps. When drawing the hydrograph of the 6-hour time interval PMP, 6-hour PMP is taken as PMP for the first time interval; 6-hour PMP is subtracted from 12-hour PMP to get PMP for the second time interval; and, by analogy, 66-hour PMP is subtracted from 72-hour PMP to get PMP for the twelfth time interval.

The accumulated PMP hydrograph for 6-hour duration is extracted from Figure 5.48 to obtain the PMP hydrograph by time interval (one time interval equals 6 hours), with the results listed in Table 5.17.

Table 5.14. Calculated result of PMP for each duration in Auburn

	Duration (hours)					
	1	6	12	24	48	72
Coefficient of precipitation depth conversion	0.14	0.42	0.65	1.00	1.56	1.76
PMP (mm)	86	262	406	625	975	1100

#### 5.3.8.2.6. Temporal and areal distribution of PMP

- (a) Temporal distribution of PMP is not discussed much in HMR No. 58 (Corrigan and others, 1998), and it is recommended that the generalized hyetograph based on historical extraordinary storms be employed for the distribution. Section 5.3.8.2.5 has already converted the 72-hour PMP into a hydrograph of 6-hour time-interval PMP. The guidelines for placing PMP for each time interval are as follows:
  - (i) the largest 24-hour rainfalls (consisting of the top four 6-hour rainfalls) are placed together;
  - (ii) the largest and the second-largest 6-hour rainfalls are centred among the largest 24-hour rainfalls, with the third-largest and the fourth-largest values beside them;
  - (iii) the largest 24-hour rainfalls may be in the front, centred or at the back, while the other eight 6-hour rainfalls may be placed beside them randomly.
- (b) Areal distribution of PMP is identified with the generalized method, that is, isohyetal maps are generalized from multi-year observed data on large storms. The isohyetal map for storms tends

to be elliptical. Two characteristic quantities – the form ratio and the orientation of the rain axis – are used to generalize the isohyetal map.

The temporal distribution of 72-hour PMP for the Auburn watershed is obtained from the above-mentioned guidelines for placing the PMP hydrograph and the time-interval rainfall hydrograph in section 5.3.8.2.5 (see Figure 5.50).

As for the areal distribution, the generalized areal distribution map for the region is employed. No detailed introduction is given herein.

### 5.3.8.3 Procedure and example computation of estimating PMP with the local storm method

There are two parts to the process of estimating PMP with the local storm method:

- (a) Calculate the mean PMP for the watershed, excluding its areal distribution;

**Table 5.15. Area-duration-reduction coefficients for Sierra Nevada region (percentage)**

Area (km <sup>2</sup> )	Duration (hours)					
	1	6	12	24	48	72
26	100.00	100.00	100.00	100.00	100.00	100.00
130	88.00	89.00	90.00	91.00	92.50	94.00
260	82.50	84.00	85.50	87.00	89.25	91.25
520	76.75	78.75	80.75	82.75	85.50	88.25
1 300	69.25	71.75	74.25	77.00	80.50	83.50
2 600	63.25	66.25	69.25	72.25	76.25	79.75
5 200	57.00	60.00	63.50	67.00	71.25	75.25
13 000	47.50	51.00	55.00	59.00	63.50	68.00
26 000	40.00	44.00	48.00	52.50	57.50	62.00

**Table 5.16. Coefficient of area reduction and areal mean PMP for Auburn watershed**

Coefficient of area reduction	Duration (hours)					
	1	6	12	24	48	72
PMP (mm)	56	175	284	450	752	879

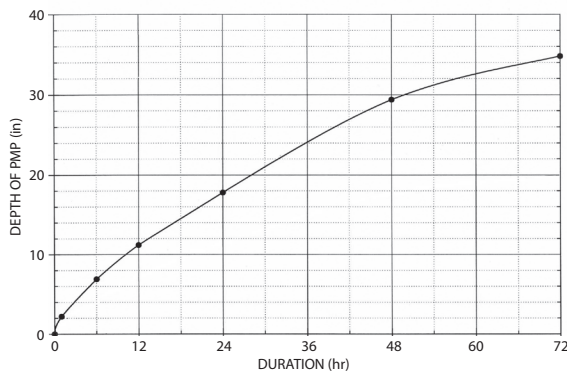


**Figure 5.49. Curve of relationship between areal mean PMP and duration for Auburn watershed**

- (b) Identify the areal distribution of PMP based on the hydrograph of a large storm in the watershed.

Below is an introduction to the procedure of estimating PMP with the local storm method, using the Wash watershed as an example which details the computation process. Located in south-eastern California, the Wash watershed has an area of 434 km<sup>2</sup>. In Figure 5.51, the area surrounded by the thick line is the Wash watershed.

- (a) The PMP value for the watershed for local storms with 1-hour duration and storm area of 2.6 km<sup>2</sup> is identified by the watershed being positioned on Figure 5.52 and then by means of linear interpolation.

The centre of gravity of the Wash watershed is at 33.75° N 114.75° W. By conducting interpolations in Figure 5.52, PMP for the point representing local storms with 1-hour duration and storm area of 2.6 km<sup>2</sup> is found to be 290 mm. Since PMP for the region does not change much with location, interpolation is feasible; if PMP changes much with location, then the mean PMP value must be obtained by conducting more detailed analyses on data from the NOAA.

- (b) The correction to mean watershed elevation is determined by first identifying the mean elevation of the watershed under study. If the mean elevation is equal to or less than 1 830 m, no correction is needed; if it is greater than 1 830 m, 9 per cent is subtracted from the PMP calculated in (a) for every 305 m of the part that is above the 1 830-m mark. Figure 5.53 also presents the corrected percentages of moisture content in air columns for different mean watershed elevations that are greater than 1 830 m, that is, the ratio of the moisture content at the elevation to the moisture content in air columns at the mean watershed elevation (1 830 m).

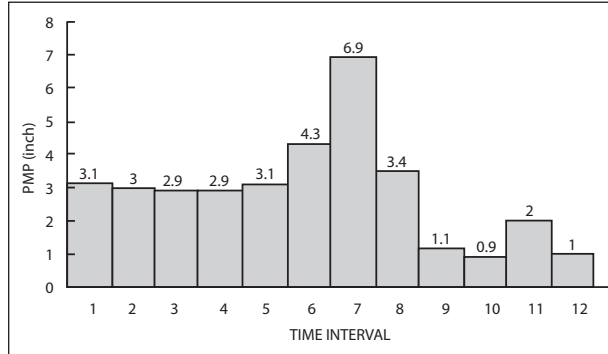
**Table 5.17. Accumulated PMP hydrograph and time-interval hydrograph for the Auburn watershed**

	Duration (hours)												
	6	12	18	24	30	36	42	48	54	60	66	72	
Accumulated PMP hydrograph (mm)	169	274	358	434	510	583	654	725	774	801	826	848	
PMP time-interval hydrograph (mm)	169	105	83	76	76	74	71	71	49	27	25	22	

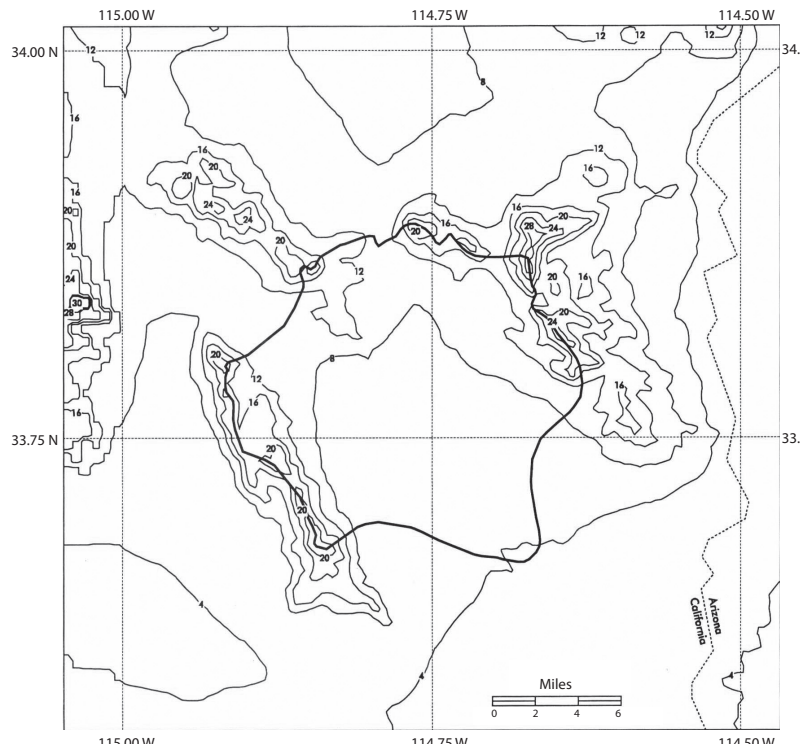
For example, if the mean elevation of a particular watershed is 2 650 m, 820 m higher than 1 830 m, then the reduction amount equals 24.3 per cent (2.7 times 9 per cent). In other words, PMP values obtained from (a) must be multiplied by 76 per cent, which can also be shown from Figure 5.53: the corresponding ratio of the pseudo-adiabat at an elevation of 2 652 m is about 76.4 per cent.

In this example computation, the mean elevation of Wash watershed is far below 1 830 m, so it is unnecessary to conduct any correction to mean watershed elevation.

- (c) The duration is corrected as follows. PMP for durations shorter than 1 hour can be found from Figure 5.54, which shows the PMP for various durations as a percentage of 1-hour PMP. For coefficients of correction to the 1-hour PMP for durations longer than one hour, the correction

**Figure 5.50. Temporal distribution of 72-hour PMP for Auburn watershed**

type for the watershed needs to be identified. The correction types include A (1.15), B (1.5), C (1.3) and D (1.4). Figure 5.55 is the isoline

**Figure 5.51. California Wash watershed**

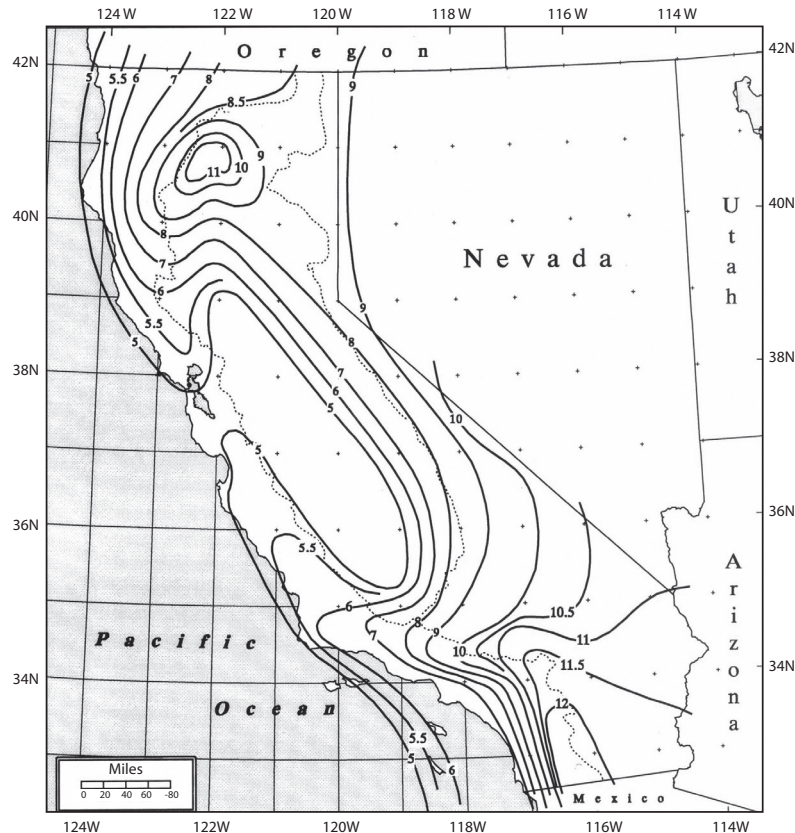


**Figure 5.52. Isoline map of PMP for California for local storms with 1-hour duration and storm area of  $2.6 \text{ km}^2$**

map of the watershed correction types for California. Values in the figure are the ratios of 6-hour PMP to 1-hour PMP. As for specific operations, the correction type of the watershed is first identified from Figure 5.55, and then the coefficients of correction for durations of 1 hour to 6 hours for corresponding types of watershed are obtained from Figure 5.54.

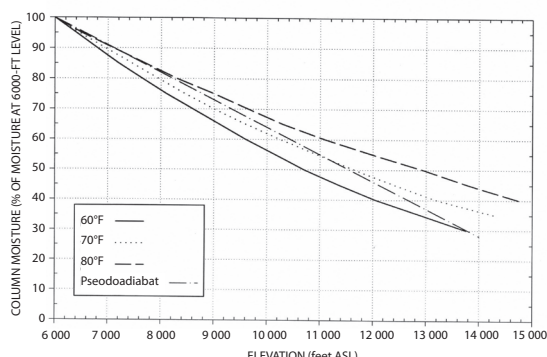


**Figure 5.53. Corrected percentage of moisture content in air columns for different watershed elevations**

It can be seen from Figure 5.54 that the Wash watershed requires C-type correction. The coefficients of correction for different durations for the C type are found in Figure 5.54. These are multiplied by PMP with correction to the mean watershed elevation in (b) (there is no correction as per (b) in this example, so the results in (a) are employed directly) to obtain PMP for each duration for a storm area of  $2.6 \text{ km}^2$  for the Wash watershed (see Table 5.18).

(d) Correction for watershed area size is performed using figures available for the coefficients of area reduction (area size  $< 1,295 \text{ km}^2$ ) for corrections of types A, B, C and D. Figure 5.56 presents the coefficients of area reduction corresponding to corrections of type C.

The coefficient of area reduction for a storm area of  $432 \text{ km}^2$  converted from  $2.6 \text{ km}^2$  is obtained from Figure 5.56 (in fact, the coefficient is unrelated to the watershed area size and is related only to the ratio of 6-hour PMP to 1-hour PMP). The PMP for the corresponding duration in (c) is multiplied by the coefficient to get the PMP with correction for watershed area size (see Table 5.19).

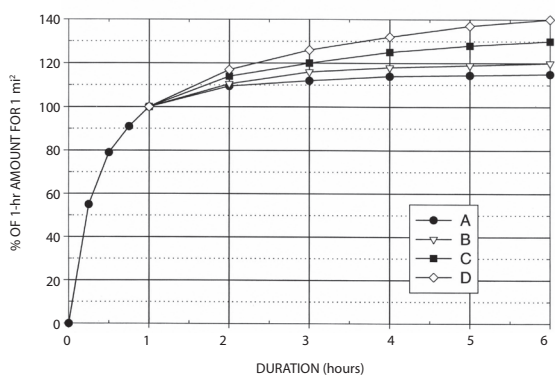


**Figure 5.54. Coefficients of correcting PMP for different durations**

A smooth curve of PMP is drawn for each duration in Table 5.19, as is shown in Figure 5.57.

- (e) Temporal distribution is determined as follows. Analyses of multiple storms in the region show that the duration of storms in the region tends to be less than 6 hours, and that the 1-hour maximum rainfall tends to occur in the first hour. As a result, the guidelines for the temporal distribution of PMP for the region are to put the 1-hour maximum rainfall in the first time interval, put the second-greatest 1-hour rainfall in the second time interval and so forth.

The accumulated PMP hydrograph is read from Figure 5.57 and results are shown in the first row of Table 5.20. Then the PMP for the previous time interval is subtracted from the PMP for the one after that to get the PMP hydrograph by time interval (with an interval length of 1 hour), and results are shown in the second row of Table 5.20.

The sequencing of PMP for each time interval in Table 5.20 is in line with the above-mentioned guideline for the temporal distribution, so it is unnecessary to make adjustments.

- (f) Areal distribution can be determined using tables available for the percentages of isohyets corresponding to corrections of types A, B, C and D of rainfall values on the elliptical isohyets (Table 5.21 is for a type-C correction). Their matching determinate isohyets in Figure 5.58 can be used to determine the areal distribution of PMP for the local storm. The ratios of the major axes to the minor axes of the elliptical isohyets in Figure 5.58 all equal 2 : 1, and the percentages in the four tables refer to the ratios of the precipitation depths of the isohyets to PMP for local storms with correction to mean watershed elevation (if no correction is needed, they are the ratios of precipitation depths to the PMP for local storms calculated in (a)). The isohyetal map must be superposed with the 1 : 500 000 watershed map before calculating the mean PMP for the watershed based on it. Once it is finalized, the isohyetal map can be transposed into the watershed. Different orientations will lead to different areal distributions of PMP, of course, thereby leading to different calculated results of areal PMP. The maximum PMP value will be obtained if the isohyetal map is placed at the centre of the watershed; a large peak flood will be obtained if the isohyetal map is placed near the exit section of the watershed.

In addition, it needs to be explained that each of the four tables (of which Table 2.21 (type-C correction) is an example) applies to one of types A, B, C or D. Meanwhile, the percentages shown in the tables apply only to PMP for local storms with 1-hour duration and storm

**Table 5.18. Results of corrected PMP for different durations for the Wash watershed**

	Duration (hours)								
	0.25	0.50	0.75	1	2	3	4	5	6
Coefficient of correction for each duration	0.55	0.79	0.91	1.00	1.14	1.20	1.25	1.28	1.30
PMP (mm)	160	229	264	290	330	348	363	371	376

**Table 5.19. Results of PMP for the Wash watershed with correction to area size**

	Duration (hours)				
	0.25	0.50	1	3	6
Coefficient of area reduction	0.31	0.37	0.43	0.50	0.54
PMP (mm)	51	84	124	175	203

**Table 5.20. Accumulated PMP hydrograph and time-interval hydrograph for the Wash watershed**

	Duration (hours)					
	1	2	3	4	5	6
Accumulated PMP hydrograph (mm)	124	155	175	188	196	203
PMP time-interval hydrograph (mm)	124	30	20	13	8	8

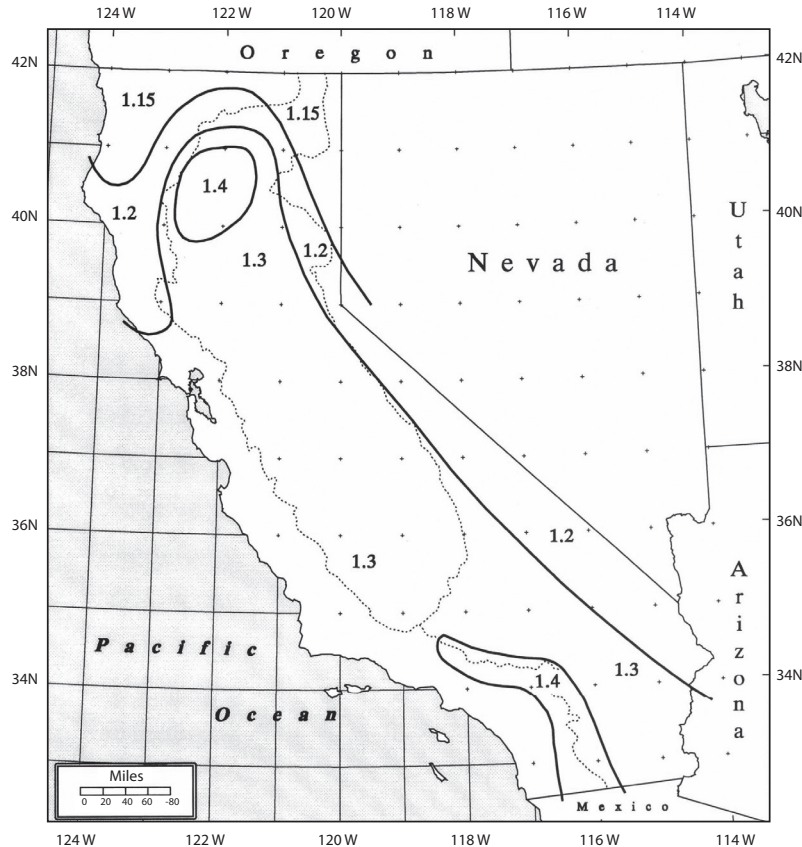


**Figure 5.55. Isoline map of watershed correction types**

area of  $2.6 \text{ km}^2$ , so they must be multiplied by the PMP obtained in (a) or (b). In this example computation, PMP for the local storm is 290 mm and requires type-C correction. To get the isohyetal map for 6-hour duration for the watershed similar to Figure 5.58, 290 mm is multiplied by the percentage corresponding to 6 hours in Table 5.21. Since the area of

the Wash watershed is  $434 \text{ km}^2$ , its isohyets are calculated from A (the surrounding area is  $2.6 \text{ km}^2$ ) to G (the surrounding area is  $570 \text{ km}^2$ ). See Table 5.22 for the precipitation-depth value corresponding to each isohyet.

The shape of the Wash watershed will not be perfectly superposed with the isohyetal map, that

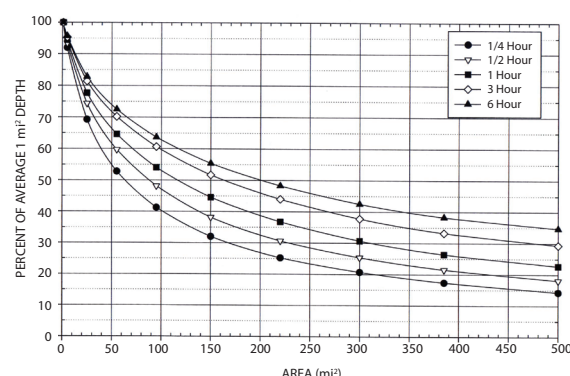


**Figure 5.56. Coefficients of area reduction corresponding to Type C**

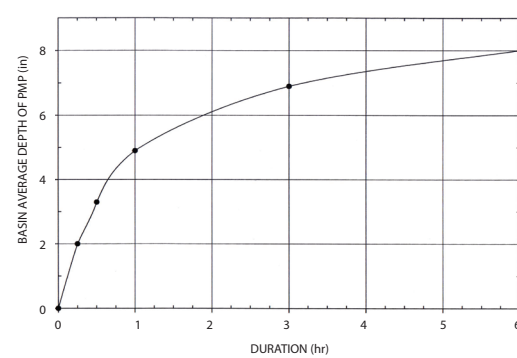


**Figure 5.57. Curve of duration-area PMP relationship for the watershed**

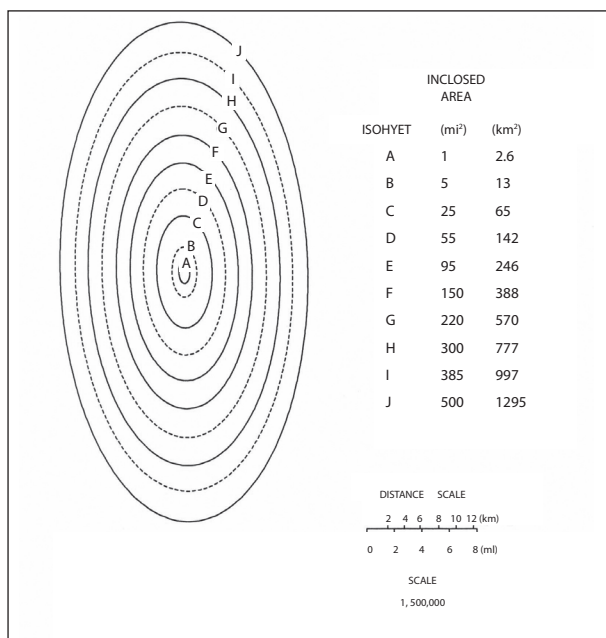


Figure 5.58. Generalized isohyetal map of PMP

is, it does not possess the 2 : 1 ratio of major axis to minor axis of the elliptical isohyet. Therefore, when the isohyet is placed onto the Wash watershed (which is irregularly shaped), the areal mean PMP calculated based on it is smaller than the areal PMP obtained in (d), however it is placed.

### 5.3.9 Topographic adjustment

For storms with durations of 24 hours and more, the effect of the different terrain between the storm and target locations will produce different effects on the rainfall at the two sites. A storm that occurred over a hilly area would produce more rainfall if it had occurred over a more elevated region. A topographic adjustment is factored in to take into account the different topographic influences on the rainfall. In regions where rainfall intensity-duration-frequency (IDF) data is available, the index rainfalls with average recurrence intervals and durations similar to the observed events can be used to objectively determine the effect of different terrain between the storm and target locations on the rainfall. This technique involves evaluating the ratio of the index rainfalls at the target and storm locations. The following example illustrating this technique is taken from Wang B.H. (1986), and describes how the rainfall IDF field can be used in transposing a storm from Montana to the Cheesman basin. Figure 5.59 shows isohyets of a storm over Montana transposed to the Cheesman basin. Figures 5.60 and 5.61 show the grids of 100-year 24-hour rainfall over the Montana and Cheesman catchments respectively.

In Figure 5.60, the Cheesman catchment outline has been shown to locate the grid points where computations are required.

The transposed storm rainfall at each grid point (as shown in Figure 5.62) is calculated by multiplying the grid point values from (a) by the ratio of the 100-year 24-hour rainfall grid over Cheesman to the 100-year 24-hour rainfall grid over Montana.

Therefore,

$$R_c = R_s \# \frac{\text{IDF}_c}{\text{IDF}_s}$$

where  $R_c$  denotes the rainfall grid over the target catchment;  $R_s$  denotes the rainfall grid over the storm location;  $\text{IDF}_c$  denotes the rainfall intensity-duration-frequency grid over the target catchment; and  $\text{IDF}_s$  is the rainfall intensity-duration-frequency grid over the storm location.

In this case the maximum storm rainfall isohyet of 406 mm near the north-eastern portion of the catchment has been reduced to 330 mm because

Table 5.21. Percentages of isohyets corresponding to type-C correction

Isohyet	Duration (hours)									
	0.25	0.50	0.75	1	2	3	4	5	6	
A	55	79	91	100	114	120	125	128	130	
B	44	66	77.6	86	100	106	111	114	116	
C	26	44	53.6	61	74	81	86	89	91	
D	17	31	40.2	46.5	58	65	70	73	75	
E	11	20	26.8	32.5	42	49	54	57	59	
F	6.6	13	19	24	32	38	43	46	48	
G	6.5	11	14	16	23	28	33	36	38	
H	5.0	8.0	10.5	12	17.5	21.5	25.5	29	31	
I	3.0	6.0	8.5	10.5	16	20	24	27.5	30	
J	2.5	5.5	8.0	10	15	19	23	26.5	29	

Table 5.22. Isohyet values for the Wash watershed

Precipitation depth (mm)	Isohyet						
	A	B	C	D	E	F	G
376	376	336	263	217	171	139	376

the 100-year 24-hour rainfall over Cheesman is less than the 100-year 24-hour rainfall over Montana.

## 5.4 ESTIMATION OF PMP FOR SHORT DURATIONS AND SMALL AREAS IN AUSTRALIA

### 5.4.1 Introduction

Only a small number of intense short-duration storms have been documented in Australia due to sparse rain gauge networks with few recording rain gauges. The few storms which have been documented indicate that rainfall potential in Australia is similar to that in the United States. This has led to the introduction of a procedure to estimate PMP in Australia using a method of adjusted United States data (Australian

Bureau of Meteorology, 1985), known as the generalized short-duration method (GSDM). Since 1985, this method has been refined and revised twice (Australian Bureau of Meteorology, 1994, 2003).

### 5.4.2 Comparison of record storms in Australia and the United States

Basic to any procedure for using data from another region of the world is a comparison of the meteorology of storms in the different regions and their depth-area-duration characteristics. In each region considered here, extreme rainfall amounts for short durations and small areas will be produced by large, efficient and virtually stationary thunderstorms, or by part of a meso-scale or synoptic-scale storm system with embedded cumulonimbus cells. The precipitation is considered to be a function of the available moisture and a convergence factor.

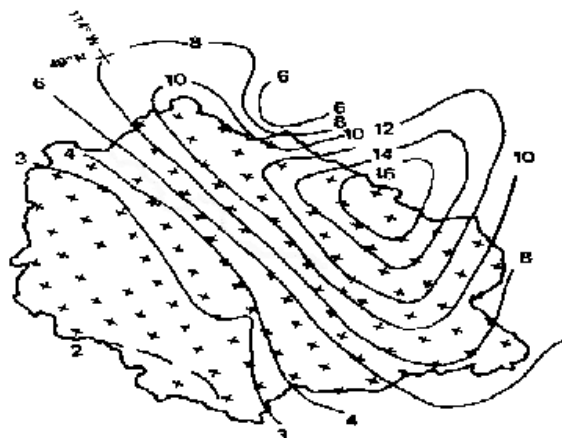


Figure 5.59. Montana storm isohyets (inches) transposed to Cheesman basin



Figure 5.61. Cheesman 100-year 24-hour rainfall (inches)



Figure 5.60. Montana 100-year 24-hour rainfall (inches)



**Figure 5.62. Grid of rainfall depth (inches) of Montana storm transposed over the Cheeseman basin multiplied by the ratio of the grids of Figures 5.61 to 5.60**

While severe local storms are reported frequently in Australia, adequate data from detailed rainfall analyses are possible for only a few. Maximum observed data from those for which a depth-area-duration analysis was possible are shown in Table 5.23. Excluded from consideration for this table are those storms that have occurred in the tropical and subtropical coastal strips. Table 5.24 provides data on notable point rainfall values for durations from a few minutes to several days. These data support the concept that rainfall potential for short durations and small areas is similar to the potential in the United States.

#### 5.4.3 Use of GSMD depth-area-duration data

Synoptic meteorological analyses, together with observations by radar and satellite of severe storms in Australia, have permitted determination of areas of Australia subject to the use of adjusted United States depth-area-duration data (Figure 5.63). Between the zones where storm duration is limited to either 3 hours or 6 hours is an intermediate zone. The storm duration in this zone is determined either by linear interpolation between the other zones or by use of other meteorological analysis. The enveloping depth-area-duration curves (Figure 5.64) were developed using the highest recorded rainfall depths in the United States plus those of a phenomenal storm near Dapto in New South Wales (Shepherd and Colquhoun, 1985),

adjusted to a common moisture charge, equivalent to a dewpoint of 28.0°C. Two sets of curves are provided: one is representative of smooth terrain and the other of rough terrain. Rough terrain is characterized as areas where elevation changes of 50 m or more within horizontal distances of 400 m are common. The rough category is intended for use mainly for basins on the windward slopes of steep hills facing the ocean.

The curves of Figure 5.64 are considered applicable to elevations below 1 500 m. Above this elevation, a reduction of 5 per cent per 300 m is applied.

##### 5.4.3.1 Geographic variation

The curves of Figure 5.64 have been adjusted to a common moisture base, equivalent to a dewpoint temperature of 28.0°C. The extreme annual 24-hour persisting dewpoint temperatures over Australia have been used to create a dewpoint chart, and these dewpoint values were revised in 2001. This chart was then used to develop an index to adjust the depth-area-duration data for available moisture. The index was obtained by calculating the ratio of the precipitable water associated with the extreme annual dewpoint to that of the base dewpoint temperature of 28.0°C. A chart showing the reduction index is shown in Figure 5.65.

##### 5.4.3.2 Distribution of PMP in time

The temporal distribution of the PMP should be based on extreme storms characteristic of the region (Figure 5.66). This distribution is patterned after the Woden Valley, Australian Capital Territory storm of 26 January 1971 and the Melbourne, Victoria storm of 17 February 1972. These two storms each resulted from severe thunderstorm cells.

**Table 5.23. Notable observed depth-area-duration data (mm) for Australia (derived from data in Australian Bureau of Meteorology, 1985)**

	0.5	1.5	3
1	114 <sup>c</sup>	300 <sup>c</sup>	
10	85 <sup>c</sup>	99 <sup>b</sup>	222 <sup>c</sup>
50	72 <sup>c</sup>	87 <sup>b</sup>	195 <sup>a</sup>
100	66 <sup>c</sup>	78 <sup>b</sup>	190 <sup>a</sup>
500	49 <sup>c</sup>	180 <sup>a</sup>	
1 000	42 <sup>c</sup>	170 <sup>a</sup>	

<sup>a</sup> Storm of 20 March 1900, Molong, New South Wales

<sup>b</sup> Storm of 26 January 1971, Woden Valley, Australian Capital Territory

<sup>c</sup> Storm of 2 March 1983, Dutton, South Australia

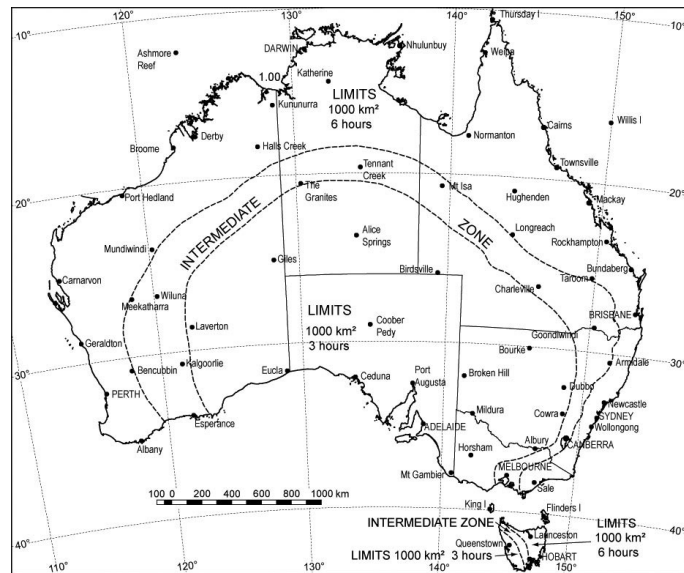


**Figure 5.63. Zones for use with the generalized short-duration method (Australian Bureau of Meteorology, 2003)**

#### 5.4.3.3 Distribution of PMP in space

The design spatial distribution for convective storm PMP is given in Figure 5.67. It is based on the distribution provided by the United States Weather Bureau (1966) and the second edition of the Manual on PMP (WMO-No. 332) but has been modified in light of Australian experience. It assumes a virtually stationary storm and can be oriented in any direction with respect to the catchment. Instructions for the application of the spatial distribution are as given in Australian Bureau of Meteorology (2003). The spatial distribution diagram has no projection.

For simplicity and consistency of application, it is recommended that PMP depth be distributed using a step-function approach. This means that the depth has a constant value at all points in the interval between consecutive ellipses (or within the central ellipse), and steps to a new constant value at each new ellipse. This constant value between ellipses is the mean rainfall depth for that interval and is derived by the procedure described below. Further information on the rationale behind this method may be found in Taylor and others (1998).

##### 5.4.3.3.1 *Instructions for the use of the spatial distribution diagram*

- To position the spatial distribution diagram (Figure 5.67), its size is enlarged or reduced to match the scale of the catchment outline

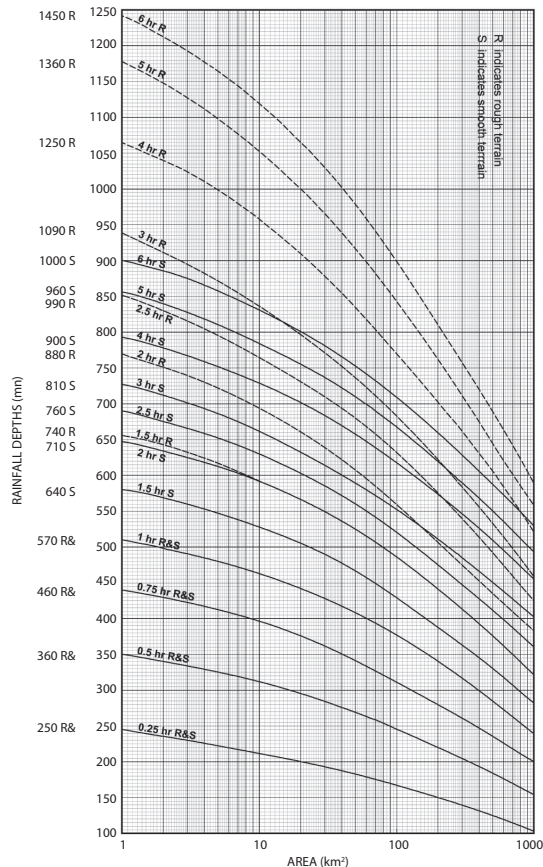


**Figure 5.64. Generalized short-duration method depth-duration-area curves (Australian Bureau of Meteorology, 2003)**

**Table 5.24. Some notable point rainfall totals recorded in Australia  
(Australian Bureau of Meteorology, 1994, as amended 1996)**

Date	Location	Duration	Rainfall (mm)
3 May 1942	Adelaide, South Australia	2 minutes	11
26 October 1960	Tamborine Village, Queensland	4 minutes	18
25 June 1901	Karridale, Western Australia	5 minutes	22
15 January 1977	Tewkesbury, Tasmania	12 minutes	32
22 December 1960	Fairbairn, Australian Capital Territory	15 minutes	20
3 March 1969	Croker Island, Northern Territory	15 minutes	42
24 December 1959	Sunbury, Victoria	18 minutes	40
25 March 1974	Cunliffe, South Australia	20 minutes	61
11 November 1969	Bonshaw, New South Wales	40 minutes	174
30 March 1961	Deer Park, Victoria	60 minutes	102
2 March 1983	Dutton, South Australia	2 hours 15 minutes	228
2 March 1983	North Dutton, South Australia	3 hours	330
6 January 1980	Binbee, Queensland	4 hours 30 minutes	607
18 February 1984	Wongawilli, New South Wales	6 hours	515
4 January 1979	Bellenden Ker Top, Queensland	24 hours	960
5 January 1979	Bellenden Ker Top, Queensland	2 days	1 947
8 January 1979	Bellenden Ker Top, Queensland	8 days	3 847

map. The spatial distribution diagram is overlaid on the catchment outline and move it to obtain the best fit by the smallest possible ellipse. This ellipse is now the outermost ellipse of the distribution.

- (b) The area of catchment lying between successive ellipses is determined ( $C_{i(\text{between})}$ ), where the  $i^{\text{th}}$  ellipse is one of the ellipses A to J. Where the catchment completely fills both ellipses, this area is the difference between the areas enclosed by each ellipse as given in Table 5.25:

$$C_{i(\text{between})} = \text{Area}_i - \text{Area}_{i-1}$$

Where the catchment only partially fills the interval between ellipses, a geographic information system (GIS), planimetry or a similar method is used to determine this area.

- (c) The area of catchment enclosed by each ellipse is determined ( $C_{i(\text{enclosed})}$ ) by:

$$C_{i(\text{enclosed})} = \sum_{k=A}^i C_{k(\text{between})}$$

The area of the catchment enclosed by the outermost ellipse will be equal to the total area of the catchment.

- (d) The initial mean rainfall depth enclosed by each ellipse is obtained using the  $x$ -hour initial mean rainfall depth (IMRD $_i$ ) for each area enclosed by successive ellipses ( $C_{i(\text{enclosed})}$ ) from (c).

Where the catchment completely fills an ellipse ( $C_{i(\text{enclosed})} = \text{Area}_i$ ), the  $x$ -hour initial mean rainfall depth for this area is determined from Table 2.3. Where the catchment only partially fills an ellipse ( $C_{i(\text{enclosed})} < \text{Area}_i$ ), the  $x$ -hour initial mean rainfall depth for that area is determined from the appropriate depth-area-duration (DAD) curves (Figure 5.64).

Note that no initial mean rainfall depths are required for ellipses I and J because the areas of these ellipses are greater than 1 000 km $^2$  which is the areal limit of the DAD curves.

- (e) The adjusted mean rainfall depth (AMRD $_i$ ) is obtained by multiplying the IMRD $_i$  by the moisture adjustment factor (MAF) and the elevation adjustment factor (EAF):

$$\text{AMRD}_i = \text{IMRD}_i \# \text{MAF} \# \text{EAF}$$

The adjusted mean rainfall depth for the area enclosed by the outermost ellipse will be equal to the (unrounded) PMP for the whole catchment.

- (f) The volume of rain enclosed by each oval is determined by multiplying the area of the catchment enclosed by each ellipse ( $C_{i(\text{enclosed})}$ ) from (c) by the AMRD $_i$  for that area from (e) to obtain the volume of rainfall over the catchment and within each ellipse ( $V_{i(\text{enclosed})}$ ):

$$V_{i(\text{enclosed})} = \text{AMRD}_i \# C_{i(\text{enclosed})}$$

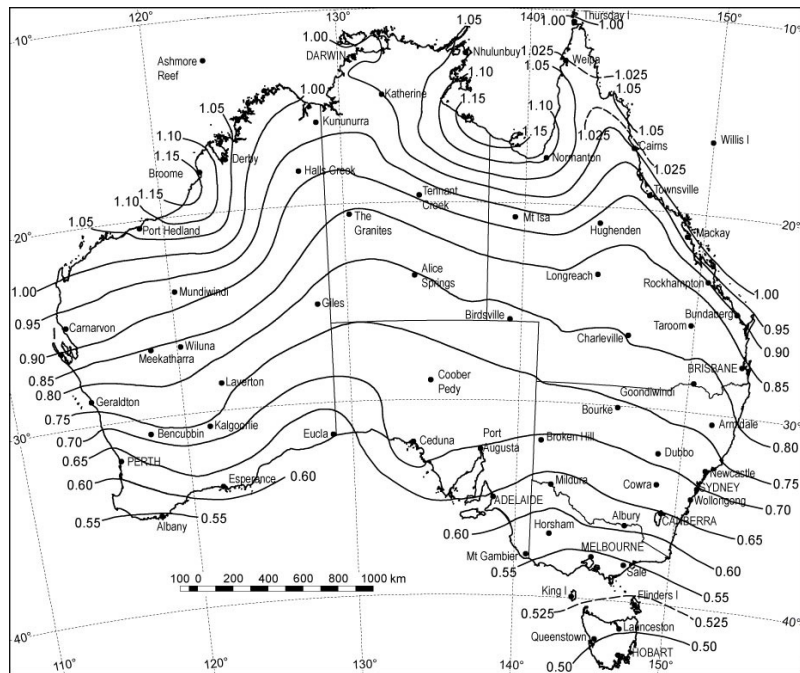


**Figure 5.65. Reduction factor for geographic variation from extreme moisture (Australian Bureau of Meteorology, 2003)**

- (g) The volume of rainfall between successive ellipses ( $V_{i(\text{between})}$ ) is obtained by subtracting the consecutive enclosed volumes ( $V_{i(\text{enclosed})}$ ):

$$V_{i(\text{between})} = V_{i(\text{enclosed})} - V_{i-1(\text{enclosed})}$$

The volume of rainfall within the central ellipse has already been obtained (f).

- (h) The mean rainfall depth between successive ellipses ( $\text{MRD}_{i(\text{between})}$ ) is obtained by dividing the volume of rainfall between the ellipses ( $V_{i(\text{between})}$ ) (g) by the catchment area between them ( $C_{i(\text{between})}$ ) (b):

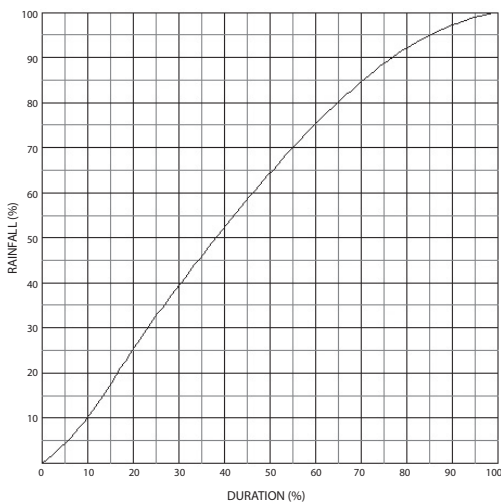


**Figure 5.66. Temporal distribution for use with PMP estimates derived using the generalized short-duration method (Australian Bureau of Meteorology, 2003)**

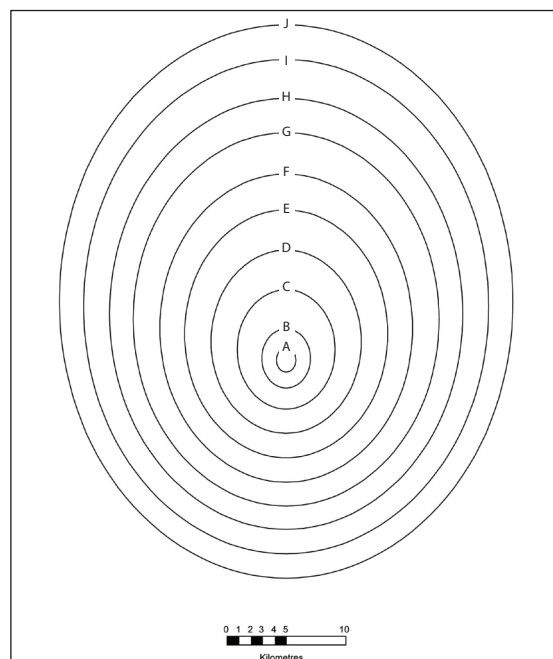


**Figure 5.67. Generalized short-duration method spatial distribution**

**Table 5.25. Initial mean rainfall depths enclosed by ellipses A–H in Figure 5.67**

Ellipse label	Area enclosed (km <sup>2</sup> )	Area between (km <sup>2</sup> )	Initial mean rainfall depth (mm)										
			Duration (hours)										
			0.25	0.5	0.75	1	1.5	2	2.5	3	4	5	6
<i>Smooth</i>													
A	2.6	2.6	232	336	425	493	563	628	669	705	771	832	879
B	16	13.4	204	301	383	449	513	575	612	642	711	765	811
C	65	49	177	260	330	397	453	511	546	576	643	695	737
D	153	88	157	230	292	355	404	459	493	527	591	639	679
E	280	127	141	207	264	321	367	418	452	490	551	594	634
F	433	153	129	190	243	294	340	387	422	460	520	562	599
G	635	202	118	174	223	269	314	357	394	434	491	531	568
H	847	212	108	161	208	250	293	335	373	414	468	506	544
<i>Rough</i>													
A	2.6	2.6	232	336	425	493	636	744	821	901	1 030	1 135	1 200
B	16	13.4	204	301	383	449	575	672	742	810	926	1 018	1 084
C	65	49	177	260	330	397	511	590	663	717	811	890	950
D	153	88	157	230	292	355	459	527	598	647	728	794	845
E	280	127	141	207	264	321	418	480	546	590	669	720	767
F	433	153	129	190	243	294	387	446	506	548	621	664	709
G	635	202	118	174	223	269	357	417	469	509	578	613	656
H	847	212	108	161	208	250	335	395	441	477	541	578	614

$$\text{MRD}_i = \frac{V_{i(\text{between})}(g)}{C_{i(\text{between})}(b)}$$

- (i) Other PMP durations are determined by repeating steps (a) to (h) for other durations.

#### 5.4.3.4 Seasonal variation

The storms associated with short-duration PMP estimates are assumed to be summer or early autumn thunderstorms. In some regions of Australia, summers are very dry and winter storms of lesser magnitude may be more critical for design purposes; this is true for south-western Australia. A seasonal variation curve for this region based on the variation of the moisture determined from the monthly extreme persisting 24-hour dewpoints expressed as a percentage of the annual extreme appears in Figure 5.68. These are based on the

maximum of the monthly values at 12 sample stations across southern Australia.

It is applicable to catchments south of 30° S and with an area less than 500 km<sup>2</sup>.

#### 5.4.4 Steps to calculate short-duration small-area PMP

The following steps can be followed to determine PMP for a basin.

- The terrain classification of the basin is determined.
- PMP duration permissible at the location of the basin is determined (Figure 5.63).
- PMP for the duration specified or permitted for the area of the basin is determined

- (Figure 5.64). If the required duration cannot be determined directly from Figure 5.64, values for durations from 0.5 hours to 6 hours are plotted on a semi-logarithmic graph and interpolated using the curve of best fit drawn to the data.
- (d) Reduction factor for the location of the basin is determined (Figure 5.65).
  - (e) A reduction factor of 5 per cent per 300 m for elevations above 1 500 m is applied.
  - (f) If seasonal values are needed for a catchment smaller than 500 km<sup>2</sup> and located south of 30° S, an adjustment factor from Figure 5.67 is applied.
  - (g) If an isohyetal pattern is needed, the procedures discussed in section 5.4.3.3 are applied.

## 5.5 ESTIMATION OF PMP FOR LONGER-DURATION STORMS IN AUSTRALIA

### 5.5.1 Introduction

There are two generalized methods of PMP estimation for use with longer-duration storms in Australia: the generalized south-east Australia method (GSAM; Minty and others, 1996) and the revised generalized tropical storm method (GTSMR; Walland and others, 2003). Figure 5.69 shows the boundaries between the application regions of the methods. A novel approach was applied in Australia that simplifies the generalization and implementation processes by taking advantage of an Australia-wide rainfall intensity–frequency–duration database (Institution of Engineers, Australia, 1987) as well as advances in computing technology. This approach vastly simplifies the parametrization of the effect of orography on rainfall and is easily applied if such intensity data is available in the region of interest.

The hydrometeorological section of the Australian Bureau of Meteorology first embarked on the development of the GSAM (Minty and others, 1996) for regions not influenced by tropical storms. The methods and procedures used in the development of the GSAM were then applied to storms of tropical origin, superseding the previous approach of Kennedy and Hart (1984). The revised method was completed in 2003 (Walland and others, 2003).

Both methods follow the same basic approach. As generalized methods, they are founded on a thorough historical search of storm data in the relevant parts of the continent over the available record. In Australia, some 100 years worth of data were searched and around 100 significant rainfall

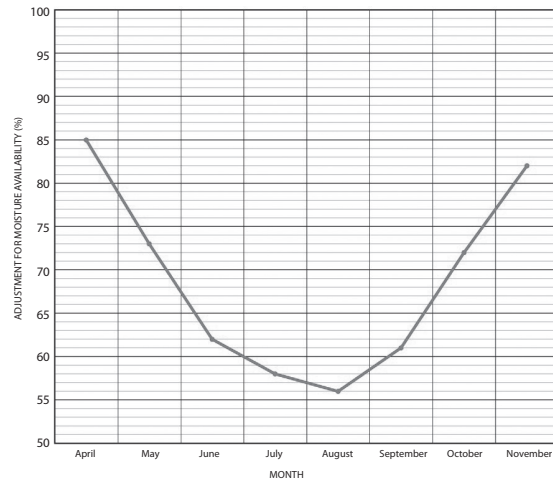


**Figure 5.68. Monthly percentage moisture adjustment for southern Australia (south of 30° S); areal limit is 500 km<sup>2</sup>.**

occurrences were selected for use with each of the generalized methods. A database of this size allows sampling storms of a large variety of durations and extents in a wide variety of locations. The location-specific components of each individual storm were then identified and removed, allowing the modified storm to be freely transposed across relevant regions and enabling the enveloping of the storm data.

As shown in Figure 5.69, generalized PMP methods are now available for all regions of Australia except the west coast of Tasmania.

### 5.5.2 Establishment of the storm database

#### 5.5.2.1 Storm selection

When searching for historical rainfall data, sources such as (a) published reports including: storm descriptions, tropical cyclone reports, lists compiled for other projects, and flood damage reports; (b) previous PMP studies; and (c) computerized searches of the rainfall archive, were utilized. Procedures were developed to interrogate the Australian Bureau of Meteorology rainfall archive and extract data for all the rainfall-recording stations within defined regions. The data were ranked according to the highest falls and examined to determine whether the high rainfall totals were widespread. In addition, rainfall totals were compared to the 72-hour 50-year rainfall intensity (Institution of Engineers, Australia, 1987) at the station location. This assisted the storm ranking, as it gave a measure of the rarity of an event at its location.

A final database for the GSAM contained 110 significant rainfall events, while that for GTSMR contained 122 events.

#### 5.5.2.2 Data quality control

The quality control of the storm data was a time-consuming, but essential, component of the construction of the database. It included temporal and spatial consistency checks of the rainfall data. Instances were found of faults such as rainfall totals being recorded on the wrong date, unmarked accumulated totals and the location of a station being changed over the period of the station's record. The original rainfall observation booklets were retrieved from the Commonwealth Archives for stations at the centre of the largest storms. Comments by observers concerning rain gauge overflow were noted particularly. All relevant data about the investigation of high rainfall occurrences, flood damage, dam break reports and so forth were collected and added to the database. The spatial consistency was checked by eye from geographically grouped lists for the GSAM and from geographic plots for the GTSMR.

#### 5.5.2.3 Storm analysis and gridding

The rainfall totals for the total storm duration were then plotted at a scale suitable for overlay on a topographic map and analysed. The isohyets of the analysed storm were then digitized. The strings of latitude and longitude values representing the isohyets were interpolated to a regular grid using a spline function, in the manner of Canterford and others (1985). The gridded data were contoured

and replotted at the scale of the original analysis and overlaid on top of it for direct comparison. The parameters of the spline function were adjusted and extra shaping isohyets were digitized, in a recursive procedure, until a satisfactory reproduction of the original analysis was achieved. For storms with isohyets extending across the coastline and over the sea, where no data existed, a land-sea mask was applied to the gridded data, which set the values over the sea equal to zero.

#### 5.5.2.4 Storm temporal distributions

In order to find the maximum percentages of the total storm rainfall that fell within the standard durations and standard areas, it was necessary to eliminate the restriction imposed by the 24-hour (9 a.m. to 9 a.m.) rainfall observing period of the vast majority of stations. Where possible, this was achieved by imposing a 3-hourly distribution on the 24-hour distribution for a storm and extracting the maximum percentages for a duration and area from this unrestricted pattern.

To construct the 3-hourly distributions, daily rainfall records, 3-hourly rainfall observations from the synoptic station network, individual storm studies and, principally, the pluviograph archive were used. As with the storm analyses, the data used to construct the temporal distributions were checked for temporal and spatial consistency. In this procedure, however, stations recording anomalous rainfall depths were deleted from the list.

Temporal distributions were determined for a set of polygons approximating the standard areas

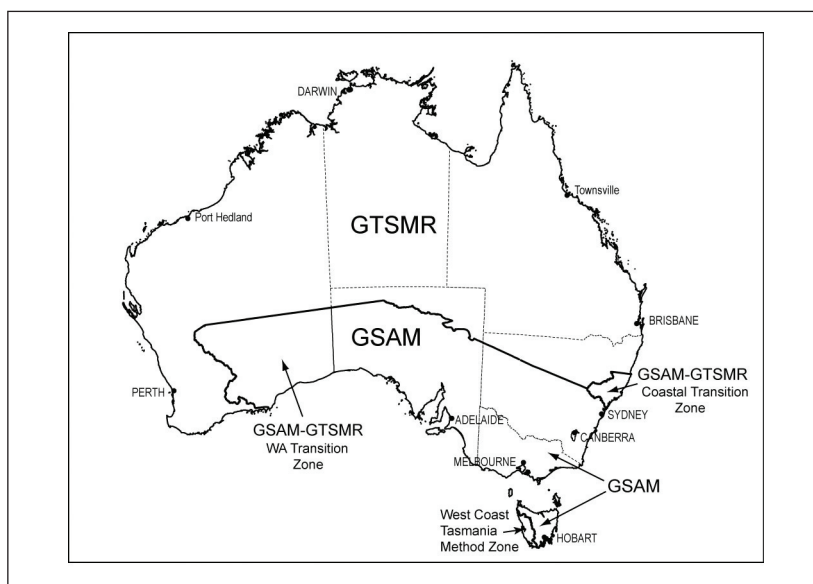


**Figure 5.69. Boundaries between PMP methods**

surrounding each storm centre, as shown in Figure 5.70. The standard areas chosen for the GSAM were 100, 500, 1 000, 2 500, 5 000, 10 000, 20 000, 40 000 and 60 000 km<sup>2</sup>; the GTSMR added 100 000 and 150 000 km<sup>2</sup>. The daily rainfall depths within each specified polygon were then averaged using an areal weighting technique. The result of this procedure was a series of daily (9 a.m. to 9 a.m.) percentages of the total storm depth, for each polygon area. The 3-hourly temporal distribution was then imposed on this daily distribution. This procedure thus provided a series of 3-hourly percentages of the total storm depth for each polygon area. Percentages at the exact standard areas were determined by interpolation between the polygon areas. The final step in the construction of the storm temporal distributions was to determine the maximum percentages of the total storm depth that fell within the standard durations of 6, 12, 24, 36, 48, 72, 96 and 120 hours, that is, the maximum 6-hour percentage, the maximum 12-hour percentage and so on. The GTSMR standard durations extend to 144 hours.

#### 5.5.2.5 Depth-area-duration analysis

The maximum depth-area curve of each gridded storm was constructed by counting the number of grid points between evenly incremented isohyets from the maximum to the minimum isohyet, calculating the arithmetic mean rainfall per interval and determining a running-average rainfall depth and cumulative area over all intervals. The area

calculations are based on the number of grid points counted and the known resolution of the grid. Once the depth-area curve for the total storm duration had been calculated, the depths at standard areas were determined by interpolation. These were then multiplied by the percentage depths in the storm temporal distributions as obtained in section 5.5.2.4 to produce a set of depth-area curves at standard durations and standard areas.

#### 5.5.2.6 Storm dewpoint temperatures

To ensure that a storm dewpoint temperature is representative of the rain-producing airmass of a storm, surface dewpoint temperatures from a number of stations were averaged where possible. Suitable stations were either on the trajectory of the moisture inflow to the storm or in the area of the storm peak itself, and had recorded high dewpoint temperatures persisting over a period of 6 to 24 hours. Care was taken to ensure that these surface dewpoint temperatures were not contaminated by rain. Where the station elevation was above 100 m, the surface dew points were reduced pseudo-adiabatically to 1 000-hPa values (United States Weather Bureau, 1951).

In the process of estimating a storm dewpoint temperature a considerable amount of judgement was required: in determining the moisture inflow direction, the influences of local topography, the timing of the precipitation process, the relevance of dewpoint temperature persistence, the

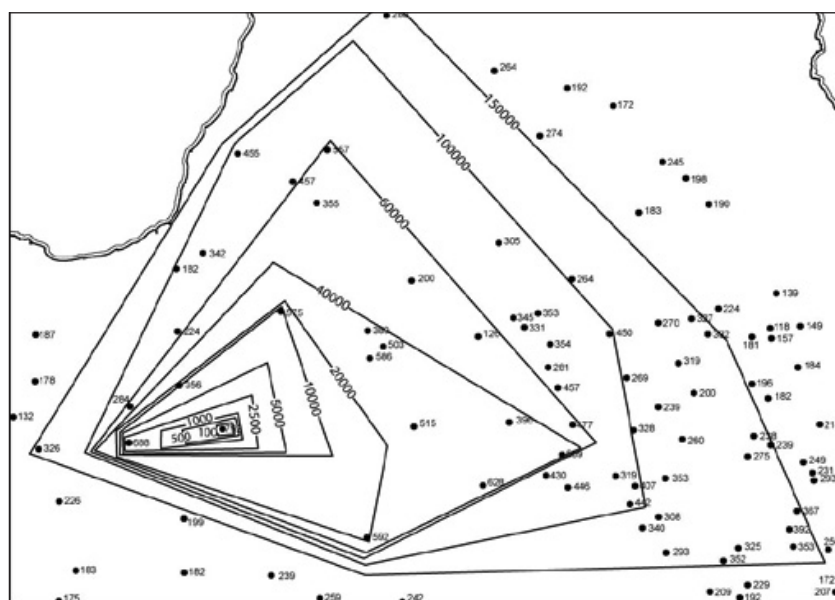


Figure 5.70. An example of a set of standard area polygons as applied to the 6-day storm, 18–23 January 1974

representativeness of surface measurements to the layer where precipitation was forming, and the quality of individual observations. Weighing these various factors and determining a single estimate of storm dewpoint temperature was very subjective. Given that all other sources of inaccuracy had been minimized, no more accuracy than around 2°C could be achieved.

### 5.5.3 Generalizing the storm database

The task of generalizing the storm database was primarily one of identifying and removing the site-specific components of each storm so that the storm could be transposed to other locations.

#### 5.5.3.1 Regions, zones and homogeneity

The region of GSAM applicability is south-eastern Australia and the boundary extended to cover that part of Australia outside the region of applicability of the method of Kennedy and Hart (1984). The geographical boundary between the two methods follows the boundaries of certain drainage basins.

The GSAM region was subsequently divided into two zones, coastal and inland. This division reflects a working hypothesis that within the two zones the mechanisms by which large rainfalls are produced are genuinely different. The corollary is that within each zone there is an assumed homogeneity: storms in the zonal database can occur anywhere within the zone.

With the introduction of the GTSMR (Walland and others, 2003) the geographical boundary between the two methods was maintained but the GTSMR region was divided into new zones: coastal, inland and a winter-only zone in the south-west corner of the continent. As for the GSAM, the GTSMR zones are based on an examination of the geographical extent of various storm-producing mechanisms. In practice, this meant a coastal zone where any mechanism operating in the tropics may be the principal influence and an inland zone where only monsoonal lows would be expected to produce extreme rainfall.

The boundaries between the methods and zones are shown in Figure 5.71.

#### 5.5.3.2 Depth-area-duration analysis

The size, shape and orientation of the analysed isohyets of a storm are influenced by a number of site-specific features: topographic influences, moisture inflow direction, and storm movement. Quantifying each storm in terms of a set of DAD curves, as outlined in section 5.5.2.5, effectively removes the specifics of the spatial distribution of each storm.

#### 5.5.3.3 Topographic enhancement of rainfall

The most original feature of the generalized methods is the application of a technique loosely based on concepts and practices expressed in various United States Hydrometeorological Reports (United

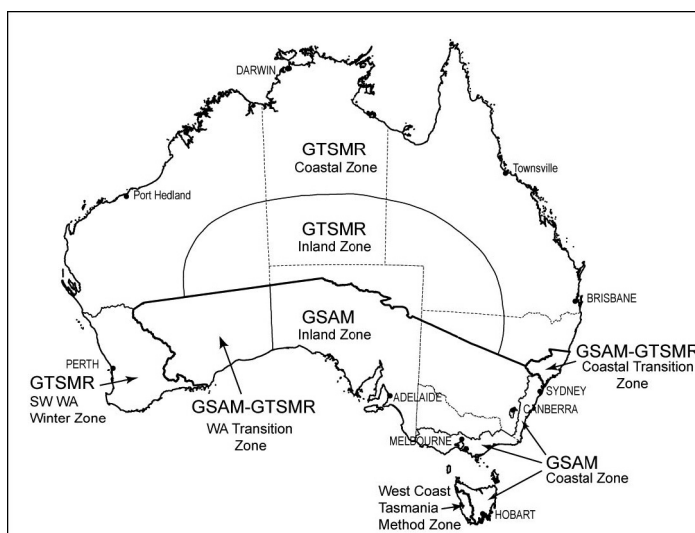


**Figure 5.71. Boundaries between PMP methods and zones – GTSMR**

States Weather Bureau, 1966; United States National Weather Service, 1977, 1984) and in Wang B.H. (1986).

Two basic concepts are introduced: the primary concept is that storm is divided into two parts, that is a part due to convergence and a part due to topographic influences, while the secondary concept is that rainfall frequency analyses can be used as a measure of the topographic influences operating in an area.

Rainfall intensity frequency analyses have been constructed for the Australian region as part of *Australian Rainfall and Runoff* (Institution of Engineers, 1987) and the Australian Bureau of Meteorology holds a gridded version of the maps in a package called computerized design IFD (intensity-frequency-duration) rainfall system (CDIRS). An example of these data is given in Figure 5.72.

Variation in rainfall intensity over the area of this figure is largely an indication of the average variation in the topographic influences on rainfall production, in relatively rare (the average recurrence interval (ARI) is 50-years), medium duration (72 hours) rainfall events. The rainfall intensities over areas that are not affected by topography can be considered as deriving from convergence precipitation alone. The values over areas that are affected by topography derive from both convergence and topographic precipitation. The ratio of values from topographic to non-topographic areas in the same general region is a measure of the average enhancement of rainfall due to topography.

To estimate the topographic enhancement factor of a storm the following approximate equality has been used:

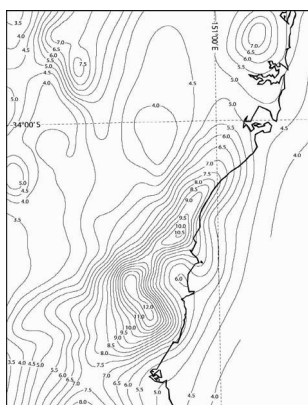


**Figure 5.72. Seventy-two-hour 50-year rainfall intensities over central NSW coast. Isopleths in mm/hour.**

$$\frac{\text{Total rainfall intensity}}{\text{Convergence rainfall intensity}} \approx \frac{\text{Total storm depth}}{\text{Convergence storm depth}}$$

In practice, the  $\approx$  was replaced by  $=$ , but the approximate nature of the relationship was kept in mind. Thus, the convergence and topographic components of a storm were defined as:

$$\begin{aligned} \text{Convergence storm depth} &= \\ \text{Total storm depth} &\# \frac{\text{Convergence rainfall intensity}}{\text{Total rainfall intensity}} \end{aligned}$$

$$\begin{aligned} \text{Topographic storm depth} &= \\ \text{Total storm depth} &- \text{Convergence storm depth} \end{aligned}$$

In the course of the development of the methods, a number of approaches to evaluating the convergence component were tried. Ultimately, it was decided to construct a map of the convergence component of the 72-hour 50-year rainfall intensities over the whole continent. This was done by pinpointing those locations where values were considered to be unaffected by topographic influences and manually interpolating between these points. For inland Australia this was a relatively simple task but over the mountainous areas far more judgement was required. A section of the resulting field is shown in Figure 5.73.

The isopleths of this field were then digitized and gridded using the technique established for the gridding of the storm isohyets. The ratio of the total rainfall intensity field to its convergence component could then be calculated on a grid point by grid point basis. Likewise, the convergence component of each storm could be calculated by dividing the total storm rainfall depth at each storm grid point by the coincident rainfall intensity ratio. Depth-area curves can now be drawn for both the total storm and convergence component of each storm.

The decision to use the 72-hour 50-year rainfall intensity field to estimate the topographic enhancement factor for all storms was based on the following considerations:

- The 72-hour 50-year field is the most accurate of the six basic rainfall frequency analyses developed for *Australian Rainfall and Runoff*;
- A duration of 72 hours is about the middle of the duration range required for the GSAM;
- An ARI of 50 years is about the mean of the range of ARIs for storms of the GSAM storm database.

#### 5.5.3.4 Moisture maximization and standardization

Moisture maximization is “the process of adjusting observed precipitation amounts upward based

upon the hypothesis of increased moisture inflow to the storm" (WMO-No. 332). The maximized storm rainfall is the rainfall that would have occurred if maximum moisture inflow for a particular location at a particular time of year had been available to the storm.

The technique of moisture maximization requires knowledge of two quantities:

- (a) The maximum or extreme moisture that could possibly occur at a particular location and time of year, indicated by the extreme 24-hour persisting dewpoint temperature;
- (b) The moisture available to the storm as indicated by the storm dewpoint temperature and derived in section 5.5.2.6.

The extreme 24-hour persisting dewpoint temperatures are obtained using long-term climatological data and an updated set of monthly values for Australia has been in use since 2001.

Storm and extreme persisting dewpoint temperatures can be related to precipitable water values with the use of look-up tables (for example, WMO-No. 332). The moisture maximization factor is defined as the ratio of the extreme precipitable water corresponding to the extreme dewpoint temperature to the storm precipitable water corresponding to the storm dewpoint temperature. Thus,

$$MF = \frac{EPW}{SPW}$$

where MF is the moisture maximization factor; EPW is the extreme precipitable water corresponding to the extreme dewpoint temperature; SPW is the storm precipitable water corresponding to the storm dewpoint temperature.

The highest extreme dewpoint temperature for the same location as the storm dewpoint temperature within  $\pm 28$  days of the date of the storm commencement was chosen. Storm convergence precipitation was maximized by multiplying by the maximization factors.

The concept of moisture maximization assumes that the relationship between increased moisture and increased precipitation is linear, at least with relatively small increases in moisture. The extent to which storm efficiency could be altered by changes in moisture is not known, however it is reasonable to assume that small changes in moisture inflow would have a minimal impact on storm efficiency while large changes in moisture inflow may well affect storm efficiency significantly. Excessively large moisture maximization factors are therefore to be avoided as they may alter the storm dynamics. It is common practice to set a limit on the maximization factor. In the past, this limit has ranged from 1.5 to 2.0. For the GSAM, the limit imposed was 1.8. For the GTSMR storms, five storms had ratios in excess of 1.8; one of which was 1.96, determined for a well-documented storm. Hence, the GTSMR maximization factor limit was set at 2.0.

To remove the site-specific feature of moisture content requires moisture standardization: storm

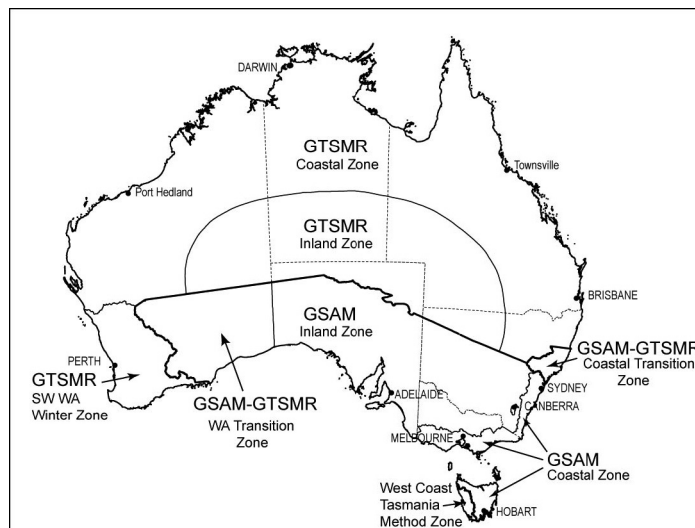


**Figure 5.73. Convergence component of 72-hour 50-year rainfall intensities over central NSW coast. Isopleths are in mm/hour.**

moisture content is increased to the level of a standard extreme dewpoint temperature for the zone rather than for the storm location. In essence standardization is equivalent to transposition of each storm from its original location to a common hypothetical location. Since this is purely a transposition in terms of moisture content, standardization is only valid for the convergence component of a storm. A standardization factor is calculated in an analogous fashion to the maximization factor: it is the ratio of the precipitable water value at the standard extreme dewpoint temperature to that of the storm extreme dewpoint temperature. It is worth noting that the only essential difference between moisture maximization and standardization is in the imposition of a limit on the maximization factor.

Dividing Australia into two method regions and dividing each region further into application zones effectively limited the transposability of the storms in space. A similar limitation on their transposability in time was also considered necessary, as storm type is correlated with season as much as with geographical zone. For this reason the GSAM storm database was divided into four seasonal groups with four different standard extreme dewpoint temperatures, and the GTSMR storm database was divided into two seasonal groups with two different standard extreme dewpoint temperatures. These standards were chosen on the basis of the annual variation of the extreme 24-hour persisting dewpoint temperature within the method regions.

For the GSAM, this annual oscillation was approximated by four irregular step functions. The timespan of each step was chosen on the basis of the gradient of the oscillation curve and the desire to minimize the range of associated dewpoint temperatures within each step. The groupings, therefore, are not truly seasonal. This precaution kept the effects of standardization of the database reasonably consistent from group to group. The values of these seasonal standard extreme dewpoint temperatures are typical of the northern extremities of the GSAM region, so that the standardization factors, in general, are greater than 1.0. The standard steps are shown in Figure 5.74, with the annual variation in extreme dewpoint temperature at Brisbane for comparison.

A similar process of standardization was applied to storms in the GTSMR database. The storms were standardized to a two-season function shown in Figure 5.75. It is based on the extreme 24-hour persisting dew-point values at Broome, a station with long records in a region of high monthly

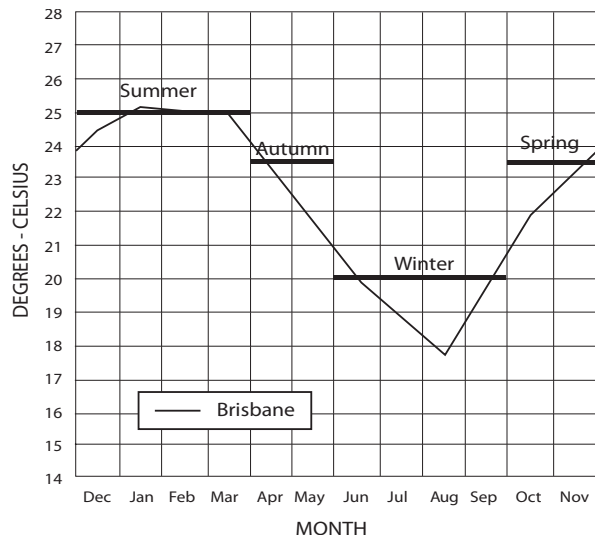


**Figure 5.74. Extreme monthly 24-hour persisting dew-point temperature for Brisbane and the standard extreme persisting dew-point temperatures for the GSAM seasons**

extreme persisting dewpoint values.

#### 5.5.3.5 Geographic variation in decay of storm mechanism

The GTSMR uses an additional adjustment factor. Removal of the effects of topography and moisture maximization and standardization was sufficient in the case of the GSAM to generalize the storms such that they could be transposed within the region. However, the GTSMR region is much bigger and the type of storm that generates extreme rainfall scenarios, particularly in the coastal zone, is a tropical cyclone. In general, the tropical storms have a greater energy source to draw on in the warm moist air over the ocean and so the further they are located from this source of energy, the more reduced in magnitude they will be. In order for the storm mechanisms to be able to be transposed within the zone, this additional geographic variation needs to be considered.

A useful way of quantifying this is to take the intensity-frequency-duration (IFD) information from the Institution of Engineers, Australia (1987) as the basis for the geographic variation of rainfall intensity over the country, it being the best information currently available for this purpose. The IFD data, however, represents rainfall variability due to topography and moisture as well as the residual geographic variability that needs to be captured. The component of the rainfall contributed by moisture and by topography must be removed from the IFD data so as not to

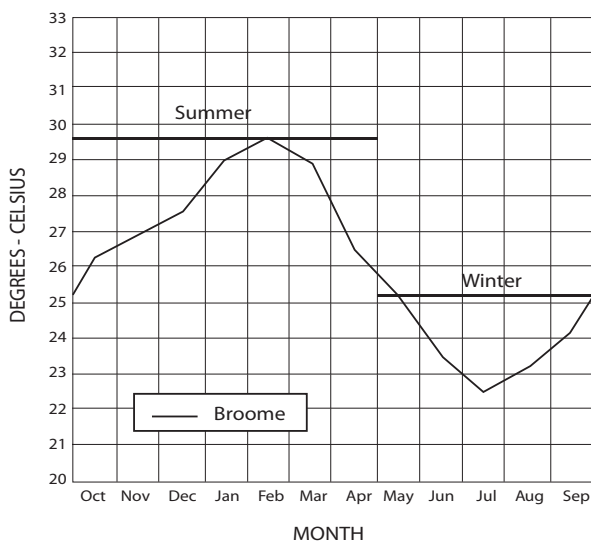


**Figure 5.75. Extreme monthly 24-hour persisting dew-point temperatures for Broome and the standard extreme persisting dew-point temperatures for the GTSMR seasons**

double-count it. The convergence intensity data (section 5.5.3.3), which present rainfall intensity assuming Australia is flat, serves to remove the effect of topography on rainfall. The existing information on maximum persisting dewpoints can be used to help remove the effect of moisture based on the following hypothesis:

$$R_c \approx \text{Smooth IFD}_a \# \left( \frac{\text{EPW}_{\text{Australia}}}{\text{EPW}_a} \right)$$

where  $R_a$  is the residual IFD value at point  $a$ ; Smooth IFD $_a$  is the flatland IFD value at point  $a$ ; EPW<sub>Australia</sub> is the depth of precipitable water equivalent to the extreme 24-hour persisting dewpoint for Australia (the extreme 24-hour persisting dewpoint at Broome being chosen as it has the highest dewpoints in Australia at a reliable station, 29.5°C  $\leftrightarrow$  118.9 mm); EPW $_a$  is the depth of precipitable water equivalent to the extreme 24-hour persisting dewpoint at point  $a$ .

Having standardized the IFD information for topography and moisture, what remains is any residual geographic variation due to other effects such as distance from the coast, distance from the equator, and the effect of barriers to preferential flow, along with any other more subtle variations.

To get the residual IFD data into a form that is usable, it is scaled into an amplitude factor based on supporting data (sea surface temperature (SST) and observed events). The distribution of amplitude is also smoothed to remove noise. The distribution

of the resulting factor, known as the decay amplitude, is shown in Figure 5.76.

An important element of scaling and smoothing the data was the choice of where to position the southernmost latitudes for unmodified storms (and their coastal intersections), that is, those with a decay factor of 1.0. This was made partly on the basis of SST information, making the conservative assumption that the 25°C–26°C isotherm in SST is approximately the ocean temperature at which a tropical cyclone above the ocean can maintain its full potential. The latitude of this isotherm is therefore used to indicate where the southern extent of unmodified storm strength should lie. The basic asymmetry between the east and west coast in terms of the amplitude is replicated in the SST data.

Also considered was the location of some of the larger tropical cyclones that have reached higher latitudes. As part of the smoothing process, an example on the east coast was used to confirm the southern extent of the 1.0 value of the decay amplitude whilst a west coast example confirmed that the 1.0 value boundary should extend slightly further south.

### 5.5.3.6 Enveloping the depth-area-duration curves

The final step in generalizing the GSAM and GTSMR storm databases was to draw an enveloping curve to each standard-duration set of maximized, standardized convergence component depth-area curves for storms within the same PMP method region and

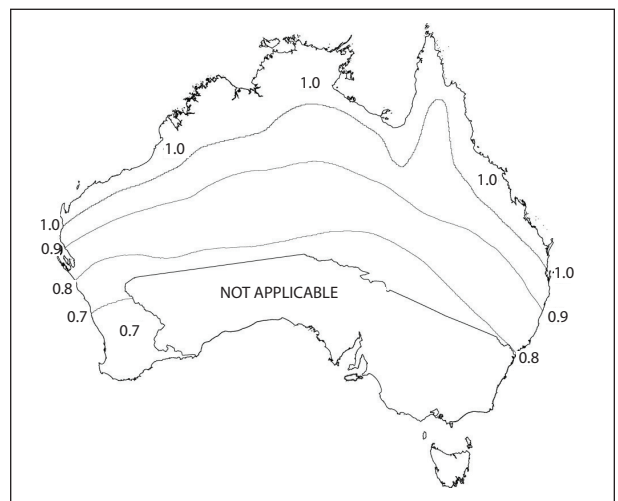


**Figure 5.76. The distribution of amplitude factors defining the degree of mechanism decay expected over the GTSMR zone**

zone. Enveloping effectively creates a single hypothetical storm of maximum moisture content and maximum efficiency from the database, that is, the standard convergence component of a PMP storm. The envelopment process can be best depicted visually (see Figure 5.77).

The drawing of the enveloping curves was carried out in a similar manner for the two generalized methods. Enveloping curves were drawn over the depth-area information to represent the theoretical maximum depth for each of the method zones and their relevant season across the range of standard durations. The next step was to combine all the depth-area curves for a particular zone onto a single plot. The curves were smoothed to remove inconsistencies or unlikely scenarios such as having a lower rainfall depth at a longer duration. Generally, the 24-hour, 48-hour and 72-hour curves were used to guide decisions on adjusting the shape of other curves as these are the most reliable, being based on the largest quantity of data. The enveloping process was designed to remove inconsistencies in depth and it was an iterative process.

As part of the GSAM development, the influence of the density of rain gauges on isohyets was tested. A data analysis of storms was used to establish the adjustment coefficient of small-area rainfall depth shown in Table 5.26. A similar test of storm analyses from the GTSMR database did not show any clear trends so no such adjustment was applied.

In total, 57 envelope curves were constructed for the GSAM: eight durations for each of the two zones and four seasons, except for inland spring for which

there was only one recorded storm and therefore one curve, at 24 hours. The GTSMR produced 25 envelope curves: six durations for each of the three zones, plus an additional duration for the coastal summer zone and the coastal zone having curves for two seasons.

#### 5.5.4 PMP estimation technique for a particular watershed

The final stage in the development of the two generalized methods was the establishment of a general technique for estimating PMP from the envelope curves of the generalized storm database. To estimate the PMP of a catchment, the catchment-specific features of the PMP storm must be derived and combined with the convergence component of the PMP storm as derived from the design DAD curves for the appropriate method, zone, season and duration. The catchment-specific features of the PMP storm were identified as:

- (a) storm type;
- (b) topographic influences;
- (c) local moisture availability;
- (d) mechanism decay (for the GTSMR only).

The features are interrelated, as are the techniques developed for reconstructing them.

##### 5.5.4.1 Catchment area and location

An accurate specification of the catchment location is required to determine which of the generalized methods to apply and into which geographic application zone it falls. The catchment boundary and

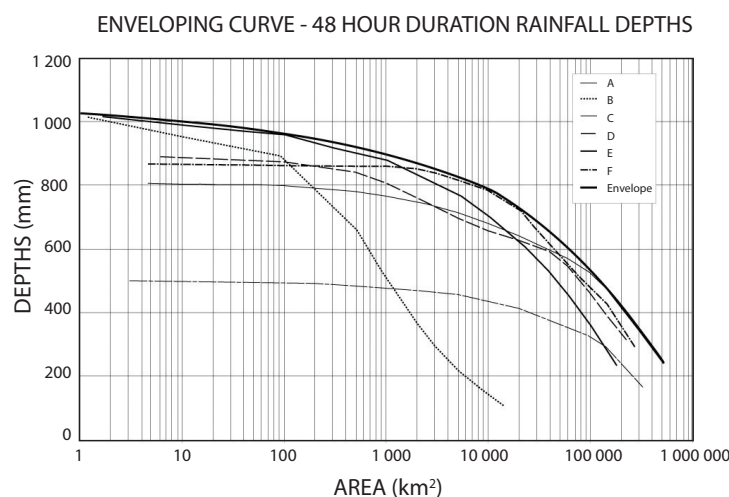


**Figure 5.77. An example of the enveloping process for a set of storms (A–F) defined by depth-area curves of their convergence component**

**Table 5.26. Small-area adjustments used in the GSAM (percentage)**

	Area (km <sup>2</sup> )				
	1	10	100	1 000	10 000
Inland (upper limit of values used)	50.0	37.5	25.0	12.5	0.0
Coastal (values used)	15.0	10.0	5.0	0.0	0.0

the area it encloses are required in order to obtain the convergence component from the appropriate DAD curves.

Catchment outlines can be hand-drawn on topographic maps, digitized and gridded. The area can then be calculated from the number of grid points within the catchment outline and the known resolution of the grid. More recently, catchment outlines are prepared and displayed via GIS and a script applied to calculate the area enclosed.

#### 5.5.4.2 Convergence component PMP estimates

Once the catchment area and location have been determined, the standard convergence component envelope depths from the appropriate zonal database can be interpolated between the standard areas to the area of the catchment.

Transposition of the standard PMP convergence rainfall from the standard hypothetical location to the location of the catchment requires adjustment of the depths for the different moisture potentials of the two locations. A moisture adjustment factor (MAF) is calculated in an analogous fashion to the standardization factor: it is the ratio of the precipitable water at the catchment extreme dewpoint temperature to that at the standard extreme dewpoint temperature.

$$\text{MAF} = \frac{\text{EPW}_{\text{catchment}}}{\text{EPW}_{\text{standard}}}$$

where EPW<sub>catchment</sub> is the extreme precipitable water associated with the catchment extreme dewpoint temperature; EPW<sub>standard</sub> is the extreme precipitable water associated with the standard extreme dewpoint temperature. Since there are seasonal standard extreme dewpoint temperatures, four for the GSAM and two for the GTSMR, corresponding seasonal catchment extreme dewpoint temperatures are required. One technique is to take the centroid of the catchment as the catchment

location and determine the seasonal extreme dewpoint temperatures for this latitude and longitude. A more recent practice is to derive catchment average values using GIS.

The envelope depths from each seasonal group were then multiplied by these catchment moisture adjustment factors. For each duration, a catchment PMP convergence depth was defined as the maximum of these depths across all seasons.

When applying the GTSMR to a catchment, the decay amplitude must be applied. Multiplying the convergence depth by this factor takes into account the geographic variation in the decay of the storm mechanism.

Thus the catchment PMP convergence component is obtained. The catchment-specific feature of the storm type is included by virtue of the zone in which the catchment is located and by virtue of the season which provides the greatest convergence depths at the area and location of the catchment for a given duration. Moisture content is included by virtue of the moisture adjustment factors for the catchment location. Finally, for catchments within the GTSMR region, the decay in the storm mechanism is included by virtue of the decay amplitude.

#### 5.5.4.3 Estimating the topographic component of the PMP storm

The remaining adjustment that needs to be made in order to progress from the catchment PMP convergence component to the catchment PMP depth is to reconstruct the topographic component of the PMP storm at the catchment. The method for doing this is analogous to that for removing the same component for the storms in the database (section 5.5.3.3) and involves modifying the catchment PMP convergence component by the topographic adjustment factor (TAF).

$$\text{Catchment PMP depth} =$$

$$\text{Catchment PMP convergence depth} \# \text{TAF}$$

$$\text{where: TAF} = \frac{\text{Total rainfall intensity}}{\text{Convergence rainfall insensity}}$$

However, because it was considered that the PMP event would have a greater convergence component than orographic component when compared with the storms in the database, which typically had an average recurrence interval of 50 to 100 years (see Klemes, 1993; Minty and others, 1996), some adjustment to the original TAF (section 5.5.3.3) was considered necessary. This was based

on evidence comparing extreme rainfall over high and low topography in the GSAM database as well as evidence of truly extreme rainfall over the globe. As a result, a formula to calculate a modified topographic enhancement factor for PMP storms was devised and this is used for both generalized methods. The details are presented in Table 5.27.

Modified topographic enhancement factors were then calculated at each of the grid points within the catchment. The catchment average of these provided the catchment PMP topographic enhancement factor.

#### 5.5.4.4 Catchment PMP estimates

Finally, total PMP depths were calculated by multiplication of the catchment PMP convergence components by the catchment PMP topographic enhancement factor. The total PMP depths were then plotted against duration and a final envelope drawn to these. Catchment PMP estimates are taken from this final envelope. An example is given in Figure 5.78.

The rationale for the final enveloping of the PMP estimates is that:

- (a) the storm databases are necessarily incomplete and cannot provide the form of the PMP design storm in total;
- (b) PMP estimates for different durations may derive from different seasons and there has been no attempt to envelope the database across seasons.

#### 5.5.4.5 Design spatial distribution of the PMP storm

The design spatial distribution for the PMP storm is simply given by the field of modified topographic enhancement factors over the catchment. An example is given in Figure 5.79.

#### 5.5.4.6 Design temporal distribution of the PMP storm

Design temporal distributions of the PMP storm were developed from the storm temporal distributions constructed by the method described in section 5.5.2.4.

For the GSAM, design temporal distributions were developed in a cooperative effort between the Australian Bureau of Meteorology and the Rural Water Commission of Victoria. The work is extensively documented in Nathan (1992). For each standard area and duration, and separately for

each zone, the average variability method of Pilgrim and others (1969) was applied to the storm temporal distributions to derive design temporal distributions for the PMP storm. It was considered that the temporal distribution of rainfall in a PMP storm would be smoother than that of an average storm in the GSAM database. Accordingly, the temporal distributions derived by the average variability method were smoothed using the method described by Nathan (1992).

The GTSMR provides for two sets of temporal distributions that can be applied to the catchment PMP depths. Firstly, a set derived by applying the average variability method to the 10 storms with depths approaching closest to the PMP depth at each standard area and standard duration; and secondly, the real storm patterns for these 10 storms from the appropriate zone, which can be used for additional analysis.

In assigning a design temporal distribution to a catchment PMP depth, the distribution for the standard area closest to the area of the catchment is used; there is no interpolation between areas.

### 5.6 GENERALIZED ESTIMATION OF 24-HOUR POINT PMP IN CHINA

#### 5.6.1 Brief introduction

A catastrophic cloudburst occurred in the west of Henan Province, China, from 5 to 7 August 1975. The maximum 24-hour rainfall amount reached 1 060 mm in Linzhuang, the storm centre. The maximum 3-day rainfall amount was as high as 1 605 mm and the 24-hour 10 000 km<sup>2</sup> areal rainfall was greater than 400 mm. The catastrophic cloudburst led to serious flooding. To ensure the safety of flood control at reservoirs, Chinese water and power departments and meteorological departments worked together in order to compile a 24-hour point PMP isoline map of China in 1976 and 1977 (Ye and Hu, 1979).

For PMP estimation, three types of methods were

**Table 5.27. Topographic enhancement factors**

Value of $x$	Value of $X$
$x \leq 1.0$	$X = 1.0$
$1.0 < x \leq 1.5$	$X = x$
$1.5 < x \leq 2.5$	$X = 0.5x + 0.75$
$x > 2.5$	$X = 2.0$

used: storm meteorological factor maximization, statistical estimation and storm frequency analysis. A rational value was selected as the result that was adopted.

### 5.6.2 24-hour extraordinary precipitations in China

120 000 station years of observed rainfall data from Chinese hydrological and meteorological departments were processed and studied. Extremes of maximum 24-hour point rainfalls exceeded 500 mm, which all occurred east of 103 °E. Among these, the largest is 1 748.5 mm, which occurred at Mount Ali, Taiwan, in 1996; records in Hainan Province and Guangdong Province also exceeded 900 mm. Records at multiple points in the west and north of the Sichuan Basin exceeded 400 mm, with a maximum of 578.5 mm. However, the difference between values in the south and north of China is not large. Maximum 24-hour storm rainfalls observed along the Haihe River, the Yellow River and the Huaihe River in the north of China exceeded 700 mm, while the record of maximum 24-hour rainfalls in north-east China (north of 40 °N) reached 657.9 mm. Orography has small effects on the average of short-duration storms, but it has strong effects on the average distribution of mid- to long-duration storms (Wang J., 2002). Studies of relations between extremes of short- and long-duration storms and orography in China had the same conclusions (Zhang, 1988).

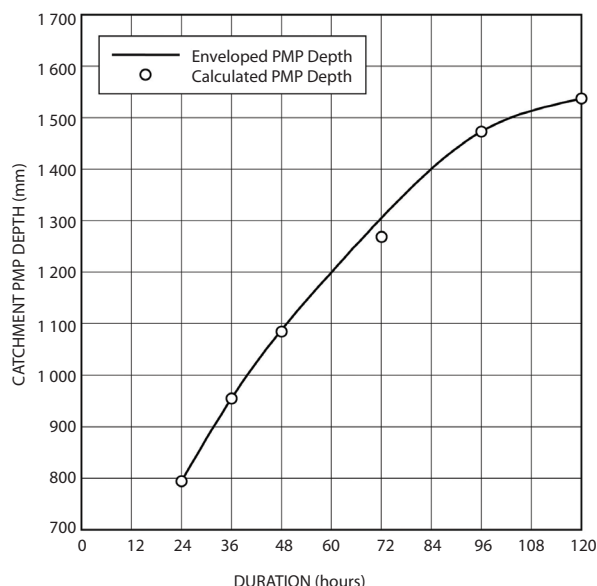


**Figure 5.78. Enveloping process to define PMP depth across a range of durations for a specific catchment area**

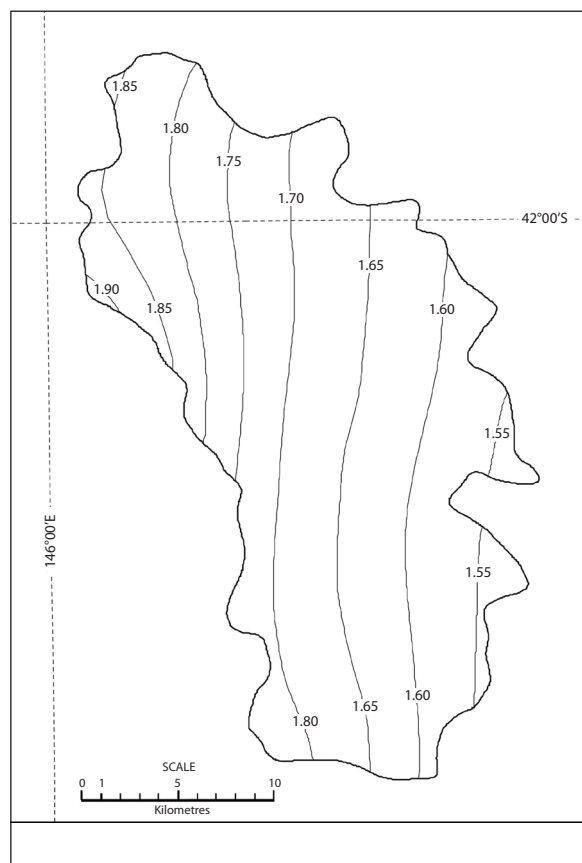


**Figure 5.79. Example of a GSAM design spatial distribution**

Data on more than 100 large storms were used in the study. Those data were all results of timely and careful surveys and therefore were reliable. For example, five surveys and re-surveys were performed (Zheng and others, 1979). It was validated that 8–12 hour rainfalls at five places in Wushenqi, which is on the border between Inner Mongolia and Shaanxi Province, exceeded 1 000 mm between 9 a.m. 1 August and 6 a.m. 2 August, 1977. Among these, the 8-hour rainfall reached 1 050 mm in the village of Shilanaohai. Some surveyed rainfalls were more than twice as high as the records of storms observed nearby, with some even exceeding worldwide records.

Provinces such as Henan, Shaanxi, Sichuan and Guizhou used results of historical flood surveys to trace values or magnitudes of historical storms. Those data are valuable references for regions that are short of data on large storms. Valuable storm information can be found from historical literature.

Based on processed data on storms and meteorological factors, as well as isoline maps that are drawn with the statistical parameters of storms, a

province is broken down into level 1 and level 2 storm areas based on geographical and topographical characteristics. Such a breakdown can be used as the basis for classifying storm transposition, storm statistical parameter synthesis and storm DAD relations.

### 5.6.3 Maximization method of meteorological factors of storms

Moisture maximization is performed for 24-hour large storms that are observed, surveyed or transposed. Methods discussed in section 2.3.4 are used for moisture maximization. When the historical maximum dewpoint is not large enough, 50-years-at-a-time dewpoint temperatures are also used as the maximum index. When storm transposition is performed, elevation and displacement adjustments need to be made. If it is believed that it is impossible to reach the probable maximum value using only moisture maximization, meteorological factors such as the moisture transportation rate may also be used for further maximization.

### 5.6.4 Statistical estimation method

Based on the idea of Hershfield's statistical estimation method (1961a, 1961b, 1965) the following formula is used to calculate PMP at each station:

$$\text{PMP} = \bar{X}_m (1 + \phi_{mm} C_{vn})$$

where  $\bar{X}_m$  and  $C_{vn}$  are the average and the coefficient of variation calculated from an  $n$ -year series including the maximum  $X_m$ ;  $\phi_{mm}$  is the enveloping value of  $\phi_m$ , the deviation coefficient calculated from an  $n$ -year series including the maximum  $X_m$ .

It is easy to see that in this method, the enveloping value  $\phi_{mm}$  is used to replace  $K_m$  in Hershfield's statistical method.

### 5.6.5 Storm frequency estimation method

#### 5.6.5.1 Storm data

More than 15 years of records from rainfall stations were applied. In regions where observation stations were scarce, more than 10 years of data from stations were also used for reference. For the years when large storms happened at adjacent stations, interpolation was done based on the same-time storm rainfall isoline map. As for data consisting of only daily rainfall records, the multi-year average was multiplied by 1.13 to convert into the multi-year average of maximum 24-hour rainfalls.

#### 5.6.5.2 Return period

Return periods of large storms observed or surveyed may be indirectly estimated based on recurrence periods of corresponding floods of small rivers near storm centres. Also, they may be ranked by size according to the total number of years of observation at each station in the storm homogeneous region. Sometimes, it may be estimated based on topographical and geomorphic changes caused by storms and comparison with storm records at home and abroad.

#### 5.6.5.3 Frequency curve and statistical parameters

A Pearson Type III curve was used as the frequency curve of storms. The average and the coefficient of variability  $C_v$  were determined according to the frequency curve on the probability grid paper under the principle of point group centres. It was specified that the deviation coefficient  $C_s = 3.5C_v$ .

To reduce the error of the result of frequency analysis on data from a single station, regional synthesis was applied. If storm observation series of each station in the storm homogeneous region could be believed to come from the same overall distribution independently and randomly, then the average line and corresponding statistical parameters of the storm frequency curve of each station could be regarded as the common statistical characteristics of each station. The method can be used directly in small ranges in plains. Nonetheless, in large ranges in orographic regions or plains, difference among stations should be considered properly based on the above-mentioned averaging and rules of the regional distribution of statistical parameters.

#### 5.6.5.4 Drawing the storm frequency isoline map

Draw the isoline maps of the average and  $C_v$  value of annual maximum 24-hour point rainfalls based on calculated averages and values for each station and considering geographical locations, ground elevations, topographical characteristics and characteristics of the distribution of meteorological factors such as moisture and thermodynamics. Superpose the two isoline maps and compare them to see if their high and low sections and trends are rational. After smoothing, read the average and the  $C_v$  value of each station, calculate their 10 000-year return period values and draw isoline maps of 10 000-year return period values of annual maximum 24-hour point rainfalls. If results are irrational, make corrections by modifying the average and the  $C_v$  value. Results of the calculation can be regarded

as class-two estimation results of PMP at the calculation point.

### 5.6.6 Drawing 24-hour point PMP isoline maps

#### 5.6.6.1 Analysis and determination of statistical results

The following analyses should be performed on the various PMP estimates at each station to select a consistent value.

- (a) The relative reliability of each result should be assessed from perspectives such as data availability and assumptions of method, and the results of estimation by various methods at the same place should be analysed.
- (b) The rationality of the regional distribution of PMP estimates in different places should be analysed by comparing the distribution map of records of the largest storms observed or surveyed, the distribution map of the isolines of storm statistical parameters or the precipitation with a particular frequency (100-year or 10 000-year return period) and the distribution maps of factors such as meteorology and orography that are related to the formation of storms.

#### 5.6.6.2 Steps in drawing isoline maps

The main steps in drawing isoline maps were as follows:

- (a) Most provinces selected the centres of large storms observed or surveyed. After calculations with multiple methods and then comprehensive analysis, 24-hour PMP values of these point rainfalls were determined and used as values of supporting points.
- (b) The values of the supporting points were used to determine corresponding values of locations of rainfall stations according to certain correlations. Then provincial isoline maps were drawn and used as the initial estimates.
- (c) The rationality of the initial estimates were analysed and isoline maps of various statistical parameters were compared to adjust them and draw correction maps.

Some provinces directly selected a large number of calculation points, performed estimations with multiple methods, and then adopted selected values as the points for drawing isoline maps. Then they performed a rationality check and correction and drew correction maps.

- (d) The country was broken down into nine sections, with each section containing three to

five provinces. The correction maps of all the provinces were pieced together; magnitudes of PMP of the provinces were harmonized along with isoline values and trends in border regions; isoline maps of all the provinces were modified; 24-hour PMP isoline maps of all the points in all the sections were drawn.

- (e) Finally, isoline maps of all the sections were adjusted and pieced together to create the national isoline map. Figure 5.80 shows the 24-hour point PMP isoline map of China.

### 5.6.7 Application of the 24-hour point PMP isoline map

The 24-hour point PMP isoline map of China is applicable to watersheds with areas less than 1 000 km<sup>2</sup>. Firstly, probable maximum point storm rainfalls of the design time intervals of the watershed where the study project is located are calculated based on the isoline map. Then, the corresponding areal mean rainfalls of the time intervals on the corresponding given watershed area are calculated based on the point-area relationship of the storm. Finally, the temporal distribution of PMP is determined based on a certain typical or generalized map.

The calculation of PMP of  $t$  points of design time intervals is conducted as follows:

$$\text{PMP}_t = \text{PMP}_{24} \# t^{1-n}$$

where  $n$  is the storm depression index, which is a term used in Chinese hydrological engineering and is the exponent  $n$  in the relation

$$a_{t,p} = \frac{s_p}{t^n}$$

where  $s_p$  is the average rainfall intensity in one hour with probability  $p$ ; and  $a_{t,p}$  is the average rainfall intensity in  $t$  hours with probability  $p$ .

While completing the 24-hour point PMP isoline maps in their own regions, all the provinces offered a set of auxiliary charts for the DAD relation and the temporal distribution of storms in their regions for use in project designs. Table 5.28 shows the point-area relation of storms in Henan Province, China.

### 5.7 NOTES

Generalized or regional estimates of PMP are representative for individual basins having topographic features similar to the generalized topography used

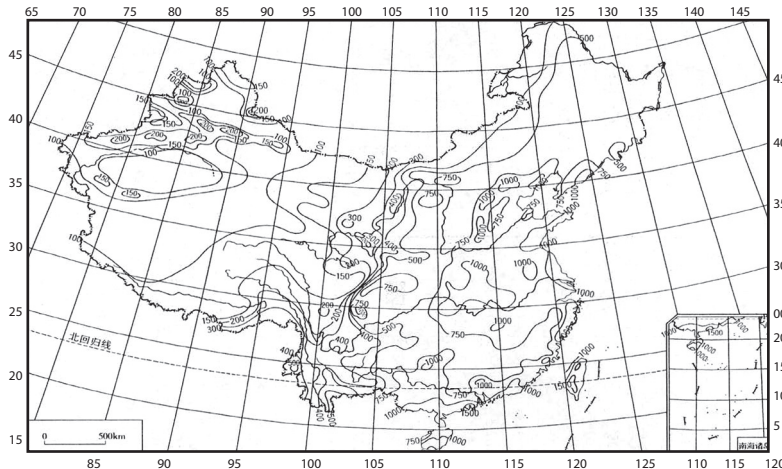


**Figure 5.80. Twenty-four-hour point PMP in China (mm; Wang J., 2002)**

in deriving the estimates. PMP for individual basins with different features may be considerably modified from the generalized values, especially in orographic regions. If there are differences, these should be evaluated and the value from the generalized or regional study modified. Generalized estimates for the larger basins of the size range considered in this chapter are less likely to require modifications of the results of regional studies. These larger basins usually have average topographic features similar to those on which the generalized estimates are based. Smaller basins, on the other hand, may have topographic features entirely unlike the general features of the area in which they are located, and generalized estimates therefore tend to more frequently require modifications.

The step-by-step procedures given in this manual for developing regional PMP values or estimates for specific basins serve merely to summarize some of the methods used in deriving PMP estimates and the techniques used for applying the results to specific basins. They are not intended to enable the reader to obtain PMP values for specific basins in the regions covered by the examples. For this reason, only those charts and tables required for illustrating the approaches used are included. Additional charts and tables would be required for making complete PMP estimates for specific basins.

Other equally valid approaches besides those represented by the examples shown have been used for developing generalized estimates. As mentioned earlier, the approach used depends on the geography of the project region and the amount and quality of required data. Basic data requirements for reliable estimates are adequate precipitation networks, dewpoint and wind data. A thorough knowledge of the meteorological characteristics of storms likely to govern PMP limits is an important requirement. This knowledge is most important where basic data are sparse.

The cautionary remarks of section 2.13 relative to adequacy of the storm sample, comparison with record rainfalls, consistency of estimates, seasonal variation and areal distribution apply to generalized estimates.

**Table 5.28. Point-area relation of PMP with different durations in orographic regions in Henan Province, China**

Duration (hours)	Point	Area ( $\text{km}^2$ )				
		100	200	300	500	1 000
1	1.00	0.89	0.82	0.75	0.65	0.52
6	1.00	0.91	0.85	0.80	0.73	0.62
24	1.00	0.92	0.87	0.84	0.78	0.70

# CHAPTER 6

## ESTIMATES FOR TROPICAL REGIONS

This chapter discusses probable maximum precipitation (PMP) procedures that are considered applicable within about  $30^{\circ}$  of the equator, the region commonly referred to as the humid tropics or the tropical rainy climates. Excluded from this chapter are high mountain areas where snowfall is an important factor and arid or semi-arid regions generally found in the interior of large landmasses.

### 6.1 MODIFICATION OF COMMON TEMPERATE-LATITUDE PROCEDURES

When estimating PMP for humid tropical regions or tropical rainy climates, the greatest difficulty is a shortage of rainfall stations. As a result, it is necessary to supplement rainfall data with indirect measurements from satellites, etc. In addition, the transposition range needs to be enlarged by transposing existing observed data on large storms in regions within  $30^{\circ}$  north and south of the equator. Moreover, meteorological conditions for storms in tropical regions are different from those in temperate latitudes because abnormal sea surface temperatures play a critical role in moisture changes and the generation of large storms.

Despite these difficulties, the basic steps used for PMP estimation in mid-latitude regions – such as moisture maximization, transposition, spatial and temporal maximization and methods for enveloping – can still be applied, with corrections for tropical regions. This chapter discusses which elements need to be corrected, based on a combination of PMP studies on Hawaiian Islands, the Lower Mekong basin in Viet Nam, India and the Chang-huajiang River basin on Hainan Island, China. Included are meteorological studies in the regions, analyses on depth-area-duration (DAD) relationships from regional storms as well as moisture extremes, wind structures, and other key factors for the process of precipitation generation.

#### 6.1.1 Meteorological storm analysis

The initial step in preparation of PMP estimates is a thorough understanding of the meteorology of major storms throughout the region. A starting point is a synoptic analysis of meteorological conditions associated with important rain events. All

surface and upper air charts should be used to make an analysis of the meteorological situation that is as comprehensive as possible. Using upper-level charts is particularly important in tropical regions. Data from all layers should be examined. In some instances, important information can be obtained from the 300- or 200-hPa charts. These charts can usually be obtained from the various national meteorological services. Particular attention should be given to the primary cause of the rain event – for example, thunderstorm, tropical cyclone, or monsoon. Tracks of tropical storms have been published for some regions of the world (Arakawa, 1963; Chin, 1958; Crutcher and Quayle, 1974; Koteswaram, 1963; Lourens, 1981; Neumann and others, 1981; United States Department of Defense, 1960). Date and location comparison of large rainfall amounts with tropical storm locations along appropriate tracks can aid in identifying rainfalls that may be caused by such storms.

Other factors that should be evaluated to the greatest possible extent are:

- (a) location of moisture sources;
- (b) amount and vertical distribution of the wind bringing moisture into the storm area;
- (c) the vertical distribution of temperature and information on cloud structure and cloud tops.

Data from various regions that are subject to the same type of storms – for example, tropical storms – should be utilized to develop the best analysis of storm structure (Schwarz, 1972; Schwerdt and others, 1979). To the extent that data are available, all dynamic features of the major storms should be analysed. In some instances, data from global weather experiments can be used to aid in the examination of storm structure. The advent of meteorological satellites has made a significant contribution to synoptic analysis in tropical regions. Over many parts of the tropics, satellite sensors provide the only comprehensive source of meteorological data.

It should be emphasized that knowledge of the meteorology of severe storms that have occurred over the region is a requirement for any of the PMP estimation approaches being considered. It is also during this preliminary phase of storm analysis that

appropriate storm transposition limits should be determined (sections 2.5 and 6.1.5).

### 6.1.2 DAD analysis

A DAD analysis of all the major storm rainfalls should be completed. The standard procedure for making these analyses is described in the *Manual for Depth-Area-Duration Analysis of Storm Precipitation* (WMO-No. 237). Since rain gauge networks may be sparse in tropical regions, maximum use must be made of indirect measurements to supplement observed rainfall amounts. Satellite measurements can provide valuable information on both areal extent of rain areas and the magnitude of the rainfall (Barrett and Martin, 1981; Falansbee, 1973; Negri and others, 1983; Scofield and Oliver, 1980).

Some completed studies provide basic information that can be utilized in other regions. Kaul (1976) has provided information on maximum point precipitation for Indonesia. Extreme point rainfalls in Jamaica have been listed by Vickers (1976). Heavy rainfalls from hurricanes that occurred in the United States have been summarized for the period 1900–1955 by Schoner and Molansky (1956). Schoner (1968) used this and other unpublished studies to examine the climatic regime of hurricanes in coastal regions of eastern United States. Several studies (Dhar and Bhattacharya, 1975; Dhar and Mandal, 1981; Dhar and others, 1980) provide information on extreme rain events in India.

### 6.1.3 Moisture maximization

Moisture maximization in temperate climates has relied on two assumptions: first, the atmosphere in major storms is saturated and can be represented by the pseudo-adiabatic lapse rate that is determined by the surface dewpoint; second, the maximum moisture available over a region can be determined from the surface dewpoint assuming a saturated atmosphere with a pseudo-adiabatic lapse rate (Riedel and others, 1956, United States Weather Bureau, 1960). These assumptions may not be valid in all tropical regions.

For rain situations, several investigations have found differences between precipitable water estimated from surface dewpoints and that computed from radiosonde observations. Clark and Schloellar (1970) found observed precipitable water to be approximately 1.5 cm less than indicated by dewpoint data for rain days. In the Hawaiian Islands, Schwarz (1963) found the difference to be approximately 2.0 cm for rain days. In Malaysia, Mansell-Moullin (1967) also found that the surface

dewpoint overestimated the precipitable water measured by a radiosonde.

Miller (1981) examined the assumption of a saturated atmosphere with a pseudo-adiabatic lapse rate during maximum moisture conditions using the precipitable water records at Merida, Mexico, for the periods January 1946 to December 1947 and October 1956 to December 1972, inclusive. For these periods, the maximum observed precipitable water for each half-month (Ho and Riedel, 1979) was compared with the precipitable water computed from the surface dewpoint at the time of the radiosonde ascent, assuming a saturated atmosphere with a pseudo-adiabatic lapse rate. Figure 6.1 shows this comparison for the layer from the surface to 500 hPa. A correlation coefficient for the relation shown is significant at the 5 per cent level. A similar relation (Figure 6.2) shows a comparison for the layer between the surface and 850 hPa.

Two comparisons are shown in Figure 6.2:

- (a) when the maximum precipitable water was observed in the layer from the surface to 850 hPa;
- (b) when the maximum precipitable water was observed in the layer from the surface to 500 hPa.

For most observed values in Figure 6.2, the precipitable water based upon the surface dewpoint slightly underestimates that computed from radiosonde observations. Only at the extreme upper end of the relation does the surface dewpoint tend to overestimate observed values.

The comparisons discussed in the preceding two paragraphs are not conclusive, but this limited evidence suggests that the assumption of a saturated atmosphere with a pseudo-adiabatic lapse rate based upon a surface dewpoint may not always be valid in the tropical climates for either storm or maximum moisture situations. In the region where PMP is to be estimated, similar comparisons between surface moisture measurements and precipitable water computed from rawinsonde observations should be made for both storm and maximum moisture conditions before storms are moisture maximized. As part of these investigations, studies should be made to determine the layer of the moist air inflow most critical for the precipitation process in major storms. It may be more realistic to base the moisture adjustment on variations in a particular layer of the atmosphere, rather than the total column.

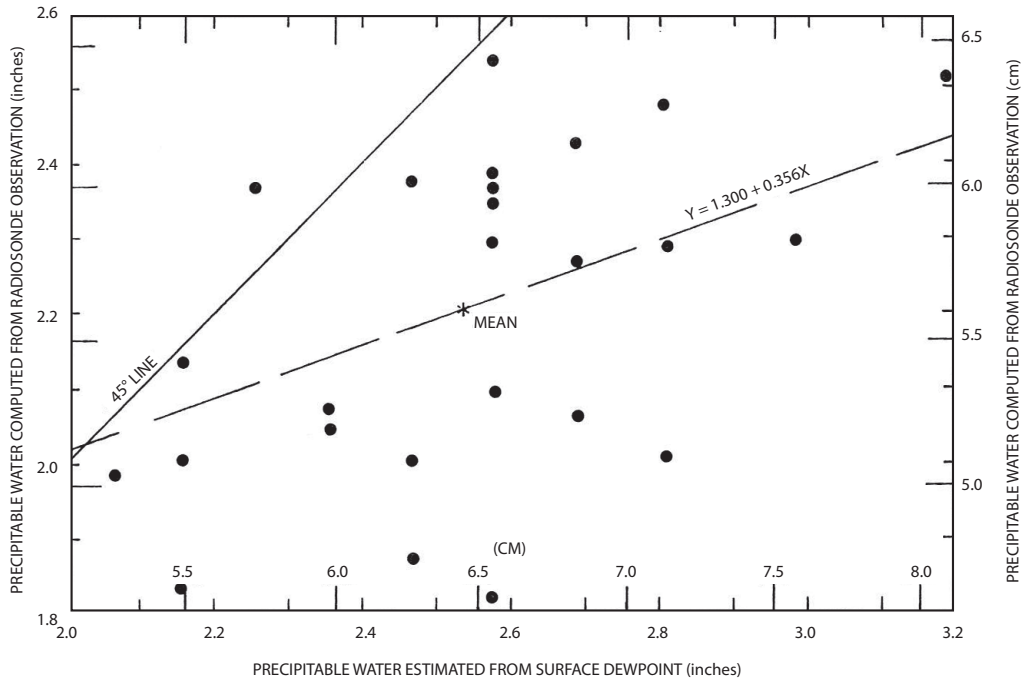


**Figure 6.1.** Comparison (Miller, 1981) of observed and estimated precipitable water for Merida, Mexico for layer from surface to 500 hPa; observed values computer from radiosonde observations using data by 500-hPa layers; estimated values determined using surface dewpoint at time of radiosonde observations and assuming a saturated pseudo-adiabatic lapse rate

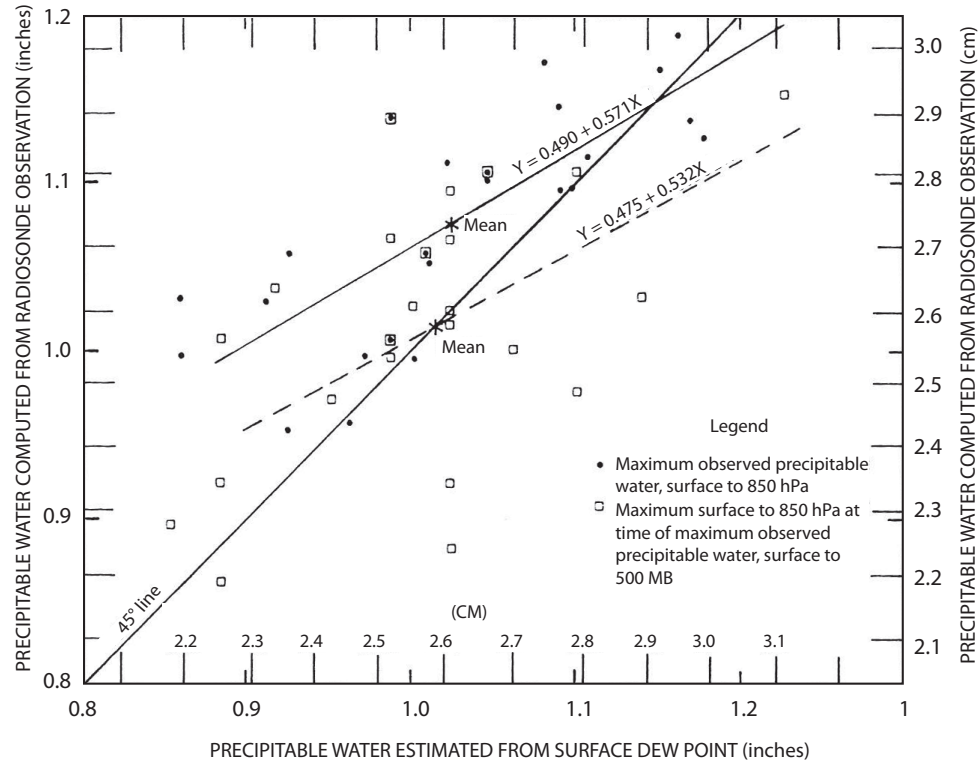


**Figure 6.2.** Comparison (Miller, 1981) of maximum semi-monthly precipitable water computer from radiosonde observations and that estimates from the surface dewpoint at the time of observation for Merida, Mexico; the period of record is January 1946 to December 1947 and October 1957 and December 1972

The adjustment of storm rainfall by the ratio between the moisture observed in the storm and the maximum that has been observed in the region assumes that storms do occur with varying moisture conditions. In some tropical regions, there may be little variation in the available moisture supply when this is evaluated using surface dewpoints. However, Brunt (1967) has found that cyclone rainfall is significantly correlated with dewpoint.

#### 6.1.3.1 Sea-surface temperatures

Some studies have suggested that anomalous sea-surface temperatures play an important role in moisture variations and subsequent heavy rainfall events (Namias, 1969). Schwarz (1972) suggests the variation in sea-surface temperature needs to be considered when estimating PMP over broad regions where tropical storms are important. Pyke (1975) concluded in a study of heavy rainfall amounts over the south-western United States that sea-surface temperature anomalies were important in determining the magnitude of the rain event. Sea-surface temperature condition may be a more appropriate measure for moisture maximization of storms in tropical regions than observed surface dewpoints.

Statistical analysis of precipitable water amounts and dewpoint observations in temperate climates have shown the maximum observed values used for moisture maximization approximate the 1 per cent chance event (United States Weather Bureau, 1961a). For sea-surface temperatures, an anomalous value or some statistical measure might be more appropriate than mean values. One possibility would be the use of the standard deviation of the series of sea-surface temperatures – for example, one or two standard deviations above the mean. One study (Rakhecha and Kennedy, 1985) used a value of 3°C above the long-term mean sea-surface temperatures.

Whatever technique is used for moisture adjustment, extreme adjustments should be avoided. In most studies in the United States, adjustments in excess of 170 per cent have not been used. The average moisture adjustment for the major storms in the non-orographic eastern two-thirds of the United States is approximately 134 per cent with a range from 105 to slightly greater than 150 per cent. Significantly lower ratios might suggest either that there is little variability in storm potential or that simple moisture adjustment is inadequate and other maximizations steps might be required.

#### 6.1.4 Wind maximization

The wind maximization technique is the same as that used in temperate regions. It was discussed in detail in section 2.4 and is not repeated here. Modification of the procedure would be required only if studies done to determine maximum inflow layers indicate a particular layer is most important for moisture inflow to the storm. If this were ascertained, then the wind maximization procedure should be restricted to that layer. Before a wind maximization process is applied to rainfall amounts, studies should be undertaken to validate the relation between increased wind speed and increased rain.

#### 6.1.5 Storm transposition

The storm transposition procedures used in temperate latitudes are applicable to tropical regions. In temperate latitudes, where many storms occur over a region, it is usually possible to consider a meteorologically homogeneous region that is contiguous to the problem basin. In general, an adequate storm sample is available if the region encompasses several hundred thousand square kilometres and the period of record is at least 40 years. In most instances, contiguous homogeneous regions of this size do not occur in tropical climates. While storms from a nearby geographic region are preferable, knowledge of storm dynamics is becoming sufficiently advanced to permit a broadening of transposition limits to contain non-contiguous units large enough to contain an adequate storm sample. Schwarz (1972) suggested that data from many continents could be combined to develop reliable estimates of PMP. Figure 6.3 shows the extensive nature of the region Schwarz proposed based upon the occurrence of tropical cyclones.

The thunderstorm-infested fixed convergence area (TIFCA) is another storm type that has been found to occur over a large section of the tropics. It has been used in the development of PMP estimates in the Hawaiian Islands (Schwarz, 1963) and in South-East Asia (Kennedy, 1976). The assessment that these or other storm types would be important in a particular region would be determined in the comprehensive meteorological analysis of the major storms (section 6.1.1).

Transposition adjustments in temperate climates are based only on moisture variation between the storm location and the basin or region to which the storm is being transposed. This is appropriate in contiguous regions in temperate climates where there are significant moisture gradients. The

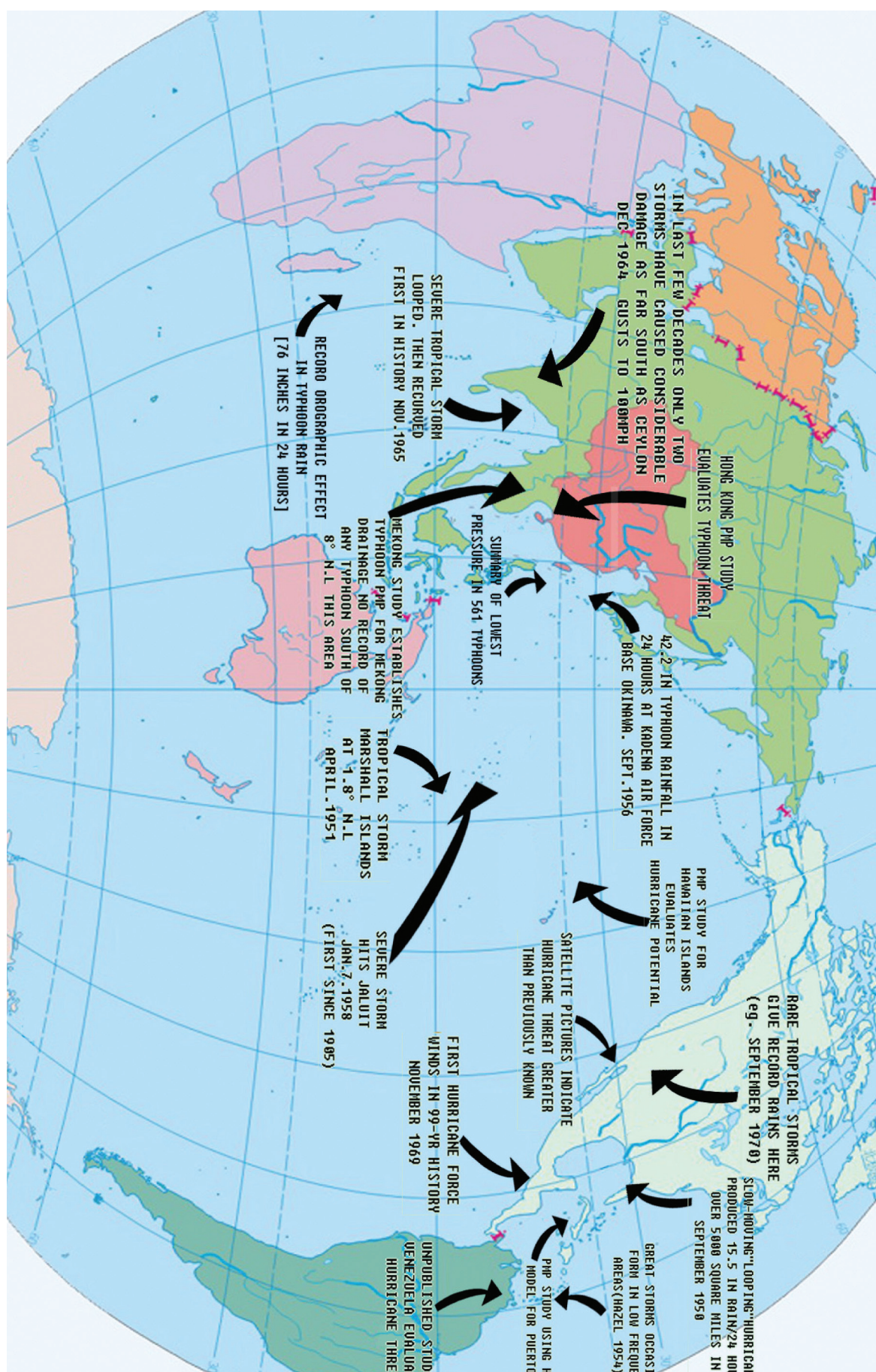


Figure 6.3. Extreme events related to tropical storms (Schwarz, 1972)

procedures are discussed in sections 2.5 and 2.6. When considering non-contiguous regions, particularly those that are spread over widely separated regions, other adjustments may be used. The differences in tropical storm PMP values between various regions will be related to variations in sea-surface temperature, tropical storm intensity, and orographic effects (Schwarz, 1972). For variations in other storm types – for example, TIFCA – other factors related to the dynamics of the storm processed should be considered. Factors that can be utilized are:

- (a) strength of inflow winds into the storm;
- (b) cloud height or cloud top temperatures that can be derived from satellite, radar or aircraft data;
- (c) instability measures or horizontal temperature gradients.

If direct measures of the geographic variations in storm dynamics are not available, indirect measures are frequently used. A commonly used factor is the transposition of the moisture maximized precipitation amount expressed as the per cent of the normal annual or seasonal precipitation. If annual or seasonal precipitation is used, adjustment of this factor by the number of rainy days above some threshold value – for example, 6 mm – would tend to minimize the influence of the frequency of small storms. Another rainfall factor that can be used as a transposition index is the rainfall frequency value for some duration, for example the 50-year, 24-hour value. A rainfall-frequency event for a single recurrence interval and duration selected for an appropriate duration minimizes the problem associated with normal or annual seasonal precipitation. It does not yield, however, complete information about the difference in storm potential between regions. A more complete approach based on rainfall-frequency information would use a combination of the central tendency – this is, the mean of the annual series – and some measure of the dispersion – that is, the standard deviation.

#### **6.1.6 Sequential and spatial maximization**

In temperate climates, many storms have occurred as a result of different storm mechanisms within a region and the variability of moisture between storms is relatively large. In these regions, the increase of total storm experience to the storm that would have occurred with maximum available moisture produces an estimate of the upper limit of rainfall that has been accepted as realistic. With a large storm sample, it can be reasonably assumed

that some storms have occurred with a near-optimum combination of all rain-producing factors other than moisture. In tropical regions, where the variation of storm types and moisture availability is generally less, simple maximization for moisture may not produce realistic estimates even when combined with liberal transposition procedures. Sequential and spatial maximization can be an important tool. Although the techniques do not differ from temperate climates, considerable judgement must be exercised in developing appropriate meteorological sequences of storms. The particular storms considered need not have occurred over the same basin to be considered in a sequential or spatial maximization procedure. It is sufficient to find sequences of similar storms that have occurred within the basin and then to develop meteorologically reasonable minimum time sequences to make the transition from one selected large storm event to the second.

## **6.2 PMP ESTIMATES FOR INDIVIDUAL REGIONS**

Fewer PMP studies have been completed for tropical regions than for temperate climates. Consequently, the procedures have not been as fully developed. The following sections discuss some completed studies (Rakhecha and Kennedy, 1985; Schwarz, 1963; United States Weather Bureau, 1970) that outline possible approaches.

### **6.2.1 Hawaiian Islands PMP**

Drainage areas in the Hawaiian Islands are generally less than 120 km<sup>2</sup>. Isolated peaks extend above 3 000 m for two of the islands, and to about 1 200 m for the three other islands. Numerous investigations have indicated that winds tend to flow around rather than over the higher mountain peaks. Record-breaking rainfall situations feature complex thunderstorms and disturbances of the normally prevailing easterly trade winds. The optimum situation was, therefore, determined to be (Schwarz, 1963) a relatively fixed zone of convergence with imbedded regenerative smaller areas of intense vertical motion of the size and intensity associated with thunderstorms (TIFCA). Examination of 156 cases of daily Hawaiian rainfalls exceeding 300 mm disclosed that about 60 per cent were associated with thunderstorms. Thunderstorms were thus revealed as important products of extreme rainfalls, although, as a general weather feature, severe thunderstorms are relatively uncommon in the Hawaiian Islands.

### 6.2.1.1 Non-orographic PMP

A basic non-orographic station, or point, 24-hour PMP of 1 000 mm shown in Figure 5.1, was based on the following considerations:

- The value agreed with worldwide extreme observed non-orographic rainfalls in tropical and subtropical regions influenced by tropical cyclones, with due consideration for Hawaii's location and limitation on moisture availability;
- It enveloped maximum observed rainfall amounts in Hawaii by a reasonable margin;
- It approximated the value obtained from multiplying the enveloping  $P/M$  ratio (ratio of storm precipitation to maximum moisture) and appropriate cool-season moisture.

Additional support was provided by an earlier estimate of PMP for Puerto Rico (United States Weather Bureau, 1961b), which is located at about the same latitude as Hawaii.

### 6.2.1.2 Slope intensification of rainfall

An empirical relation showing rainfall intensification with slope was developed from observed rainfall data in somewhat comparable terrain. These data indicated a decrease in the elevation of maximum rainfall amounts as rainfall intensity increased and an increase of rainfall with ground slope. Precipitation data from various parts of the world were used to determine the general variation in rainfall intensification with ground slope shown in Figure 6.4.

Greatest intensification is shown for intermediate values of slope (about 0.10–0.20). There is almost no intensification for slopes greater than about 0.25. Such steep slopes in this region are generally found at the higher elevations, where winds tend to circumvent the peaks so that there is little large-scale lifting of air over the peaks.

The dashed lines in Figure 6.4 apply to a column of saturated air with a 1 000-hPa temperature of 23°C, and show the depletion of moisture with increasing ground elevation. Thus, for any point on the intensification curve, or any given slope, the elevation at which moisture depletion negates rainfall intensification can be determined readily. For example, the critical elevation for a slope of 0.17 is about 1 000 m. Above 1 500 m, moisture depletion outweighs slope intensification for all slopes. This is shown in Figure 6.5, which combines the effects of slope intensification and moisture depletion to provide a slope and elevation adjustment to the basic 24-hour point PMP of 1 000 mm.

### 6.2.1.3 Generalized PMP estimates

Generalized estimates of 24-hour point ( $2.6 \text{ km}^2$ ) PMP are presented in Figure 5.1. Climatological data showing spillover and other orographic effects were used to modify the results indicated by the relation in Figure 6.5. Ratios of PMP to 100-year rainfall were examined and adjustments made to avoid unrealistically high or low ratios.

DAD relations (Figure 6.6) for extending the basic PMP values to durations of 30 minutes–24 hours

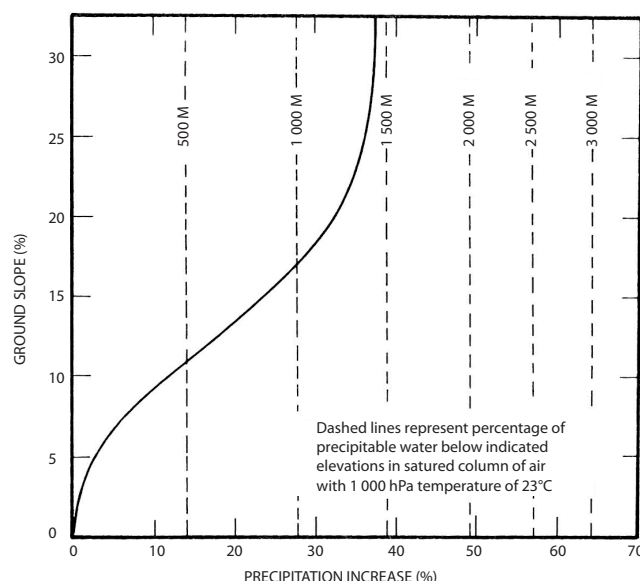
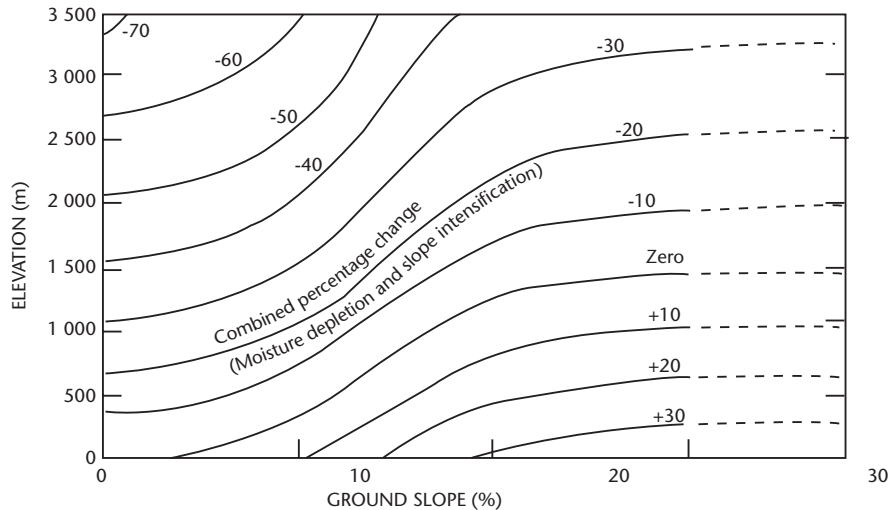


Figure 6.4. Rain intensification for ground slopes (Schwarz, 1963)



**Figure 6.5. Adjustment of non-orographic PMP for elevation and slope, Hawaiian Islands (Schwarz, 1963)**

and to areas up to 500 km<sup>2</sup> were derived mainly from Hawaiian storms. No seasonal variation curve was required since the greater efficiency and lower moisture of cool season storms balanced the lower efficiency and greater moisture of summer season storms.

PMP for a specific basin is obtained by planimetering the area within the basin on the 24-hour point PMP chart (Figure 5.1) to obtain the 24-hour basin-average PMP. The DAD relation from Figure 6.6 is then used to obtain PMP values for other durations.

## 6.2.2

### PMP for the lower Mekong River basin in South-East Asia

Generalized estimates of PMP were made for drainages from 5 000 to 25 000 km<sup>2</sup> in the Mekong River basin south of the Chinese border at about 22° N latitude (Figure 6.7; United States Weather Bureau, 1970). This part of the basin is referred to generally as the Lower Mekong. The procedure used in making these estimates provides an example of how data from one part of the world may be used to estimate PMP for a region with inadequate data.

#### 6.2.2.1 Mean seasonal precipitation map

A rough approximation of regional variation of rainfall potential may be gained from mean seasonal or annual precipitation maps. A map of mean rainfall was developed for the May–September season, that is, the south-west monsoon period, which produces most of the annual rainfall for much of the Lower Mekong. Rainfall observations provided the primary basis for the seasonal map. As usual, few observations were available for mountainous areas.

Where data are severely limited in mountainous regions, as was the case in the Mekong basin, determination of the detailed effects of topography on precipitation is a practically impossible task. In such situations, the best relations that can be developed are based on extensive smoothing of topography. Figure 6.8 shows the generalized topography of the Mekong drainage area and the locations of precipitation stations.

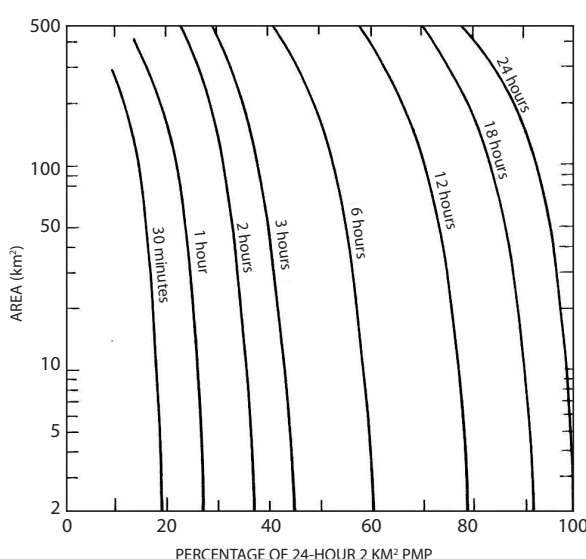


**Figure 6.6. Variation of index PMP with basin size and duration, Hawaiian Islands (Schwarz, 1963)**

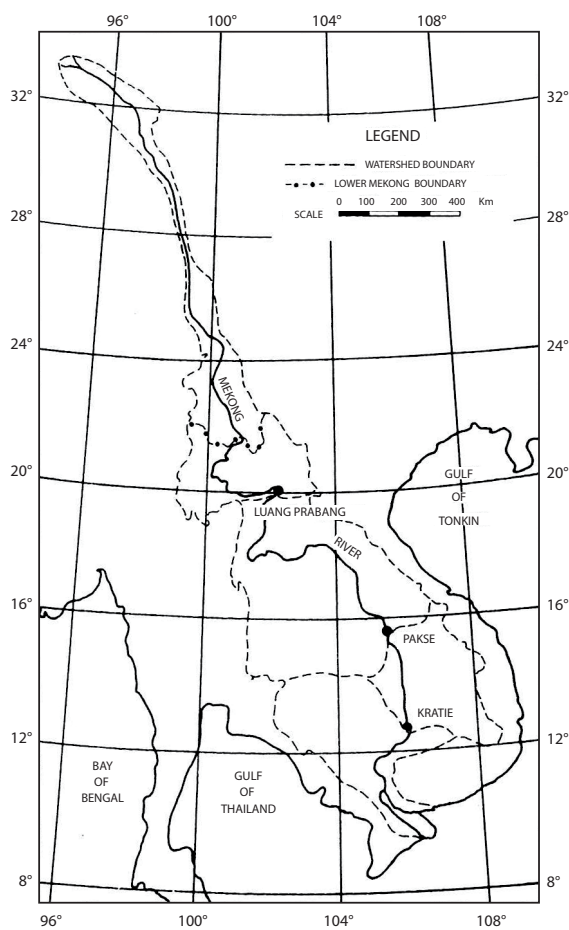


**Figure 6.7. Mekong River basin and sub-basins**  
(United States Weather Bureau, 1970)

Topographic effects on seasonal rainfall distribution were assessed on the basis of the limited data and on past experience gained from study of these effects in regions with adequate data. Comparisons of mean rainfalls at a few pairs of stations in the Mekong River basin, critically selected to reflect different topographic effects within each pair, provided guidance. These comparisons, plus experience, led to the following guidelines:

- For mountain slopes facing south to west, with no nearby mountain barriers to moisture inflow, mean seasonal rainfall approximately doubles in the first 1 000 m rise in elevation. Except for extremely steep slopes extending to high elevations, no further increase was indicated;
- Upslopes near the coast, outside the basin but bounding it, produce spillover rainfall over limited areas in the basin;
- Sheltered areas immediately to the lee of mountain barriers receive about half the rainfall observed upwind of the barriers.

The above guidelines, plus general guidance from some streamflow data, supplemented observed rainfall data in the construction of the mean May–September rainfall map (Figure 6.9). Mean rainfall maps for August and September, the wettest months, were constructed in a similar fashion.

#### 6.2.2.2 The typhoon as a PMP prototype

Typhoons are the most important producers of rains with several days duration in the Lower Mekong for the range of basin sizes considered in this example. Such storms, approaching the Mekong basin from the east, produce the heaviest general rainfalls in the basin in spite of mountain barriers between the coast and the eastern border of the basin. Rainfalls from typhoon Vae (21–22 October 1952), in the southern portion of the Lower Mekong basin, and Tilda (21–25 September 1964), near the middle, are foremost examples. Large-area rainfalls from these storms, after adjustment as described below, approximate the greatest values from tropical storms throughout the world.

With the idea of adapting the more abundant DAD rainfall data from tropical storms along the United States coast to the Mekong drainage, the massiveness (size and intensity), speed of movement and other features of tropical storms affecting the two regions were compared. Also compared were average maximum 1-day point rainfalls from tropical storms in the United States and in the Pacific Ocean, including the Viet Nam coast. Values along the Viet Nam coast were about 20 per cent greater, but the excess was attributed to topographic influences absent in the coastal regions of south-eastern United States. The comparisons suggested that non-orographic tropical storm rainfall potential was about the same for the two regions.

#### 6.2.2.3 Adjustment of United States tropical storm rainfalls

Two adjustments were made to the United States tropical storm DAD data to make them applicable to the Viet Nam coast. First, the storm data were moisture maximized for a persisting 12-hour dew point of 26°C, the highest value for United States coastal regions affected by tropical storms. Second, an adjustment was made for the decrease of tropical storm rainfall with distance inland. This adjustment is discussed in the following section. The adjusted data and enveloping DAD curves are shown in Figure 6.10. The DAD curves were considered to represent non-orographic PMP just off the Viet Nam coast.

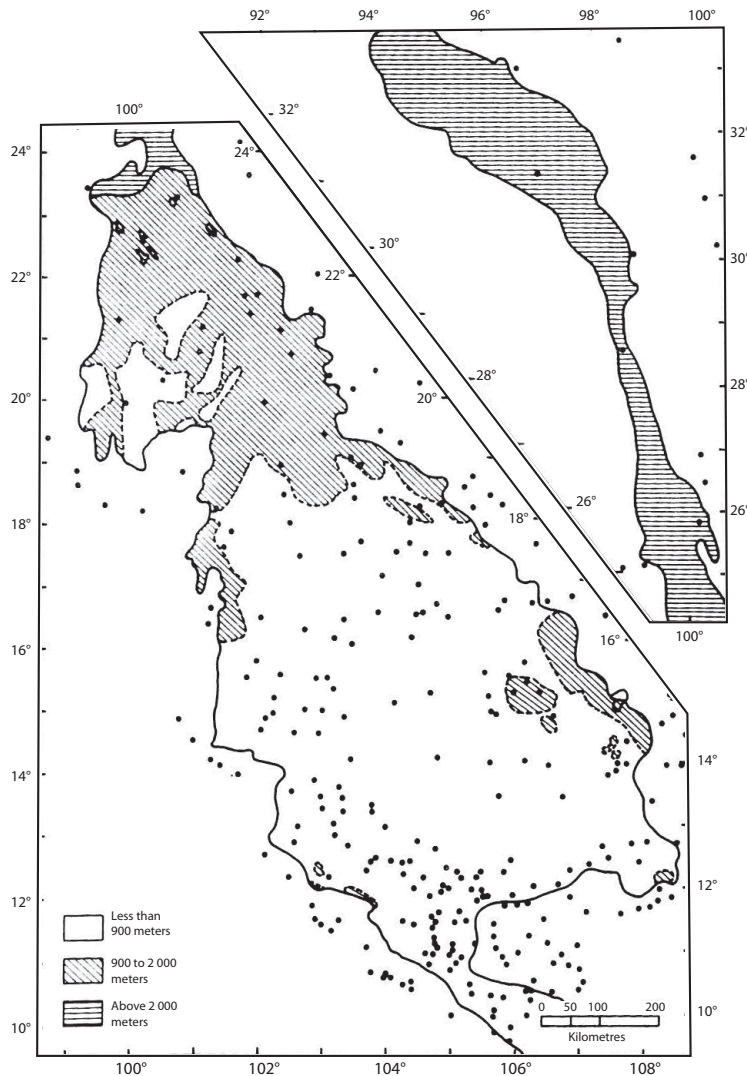


**Figure 6.8. Generalized topography of Mekong River basin; dots show location of precipitation stations (United States Weather Bureau, 1970)**

#### 6.2.2.4 Adjustment of Viet Nam tropical storm rainfalls

Since the non-orographic PMP DAD curves of Figure 6.10 applied only to the Viet Nam coast, the indicated values had to be modified for occurrence in the Mekong basin. The following adjustments were thus required:

- (a) distance inland;
- (b) moisture source;
- (c) latitude;
- (d) moisture-inflow barriers;
- (e) basin topography.

#### 6.2.2.4.1 Adjustments for distance inland and moisture source

The general decrease in tropical storm rainfall with distance inland previously developed in another study (Schwarz, 1965) was considered applicable to South-East Asia. Approximately 60 United States storms in mostly non-orographic regions were used. Figure 6.11 shows the adjustment for the Lower Mekong in percentages of the PMP values off the coast.

While typhoons approach the Mekong basin from an easterly direction, the wind circulation brings in moisture from the southerly and easterly directions. The few analysed storms in the basin clearly

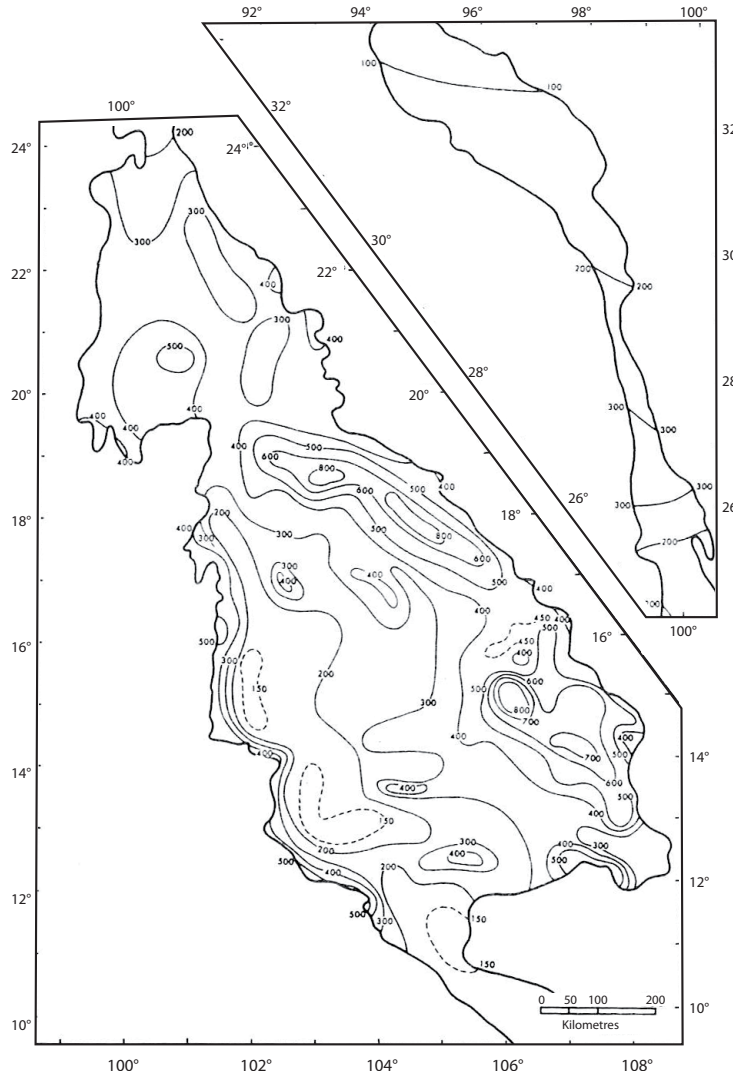


**Figure 6.9. Mean May–September (south-west monsoon season) precipitation (mm; United States Weather Bureau, 1970)**

demonstrate multiple sources of moisture. Thus, the distance inland adjustment (Figure 6.11) incorporates a weighting of the generalized decrease for moisture-inflow direction for the region south of 17° N. A weight of one-third was given to distance inland from the south coast and two-thirds to distance from the south-east to east coasts.

#### 6.2.2.4.2 *Adjustment for latitude*

Typhoon rainfall potential must decrease to about zero near the equator. The literature reports few cases south of 10° N. It was assumed typhoons could maintain full intensity as far south as 15° N. The need for maintaining a high typhoon rainfall potential in southerly reaches of the basin is

supported by the October 1952 storm that occurred in the basin near 12° N. The adopted adjustment is shown in Figure 6.12.

##### 6.2.2.4.3 *Adjustment for barrier*

In addition to generalized decrease in rainfall with distance in non-orographic regions, it was necessary to consider decrease within the basin due to moisture-inflow barriers. The decrease varies with height of barriers and their uniformity, that is whether they are continuous or have breaks, or passes. Moisture inflow from a southerly direction reduces the depleting effect of the eastern coastal mountains. The eastern barrier was therefore considered to reduce rainfall to the west by half

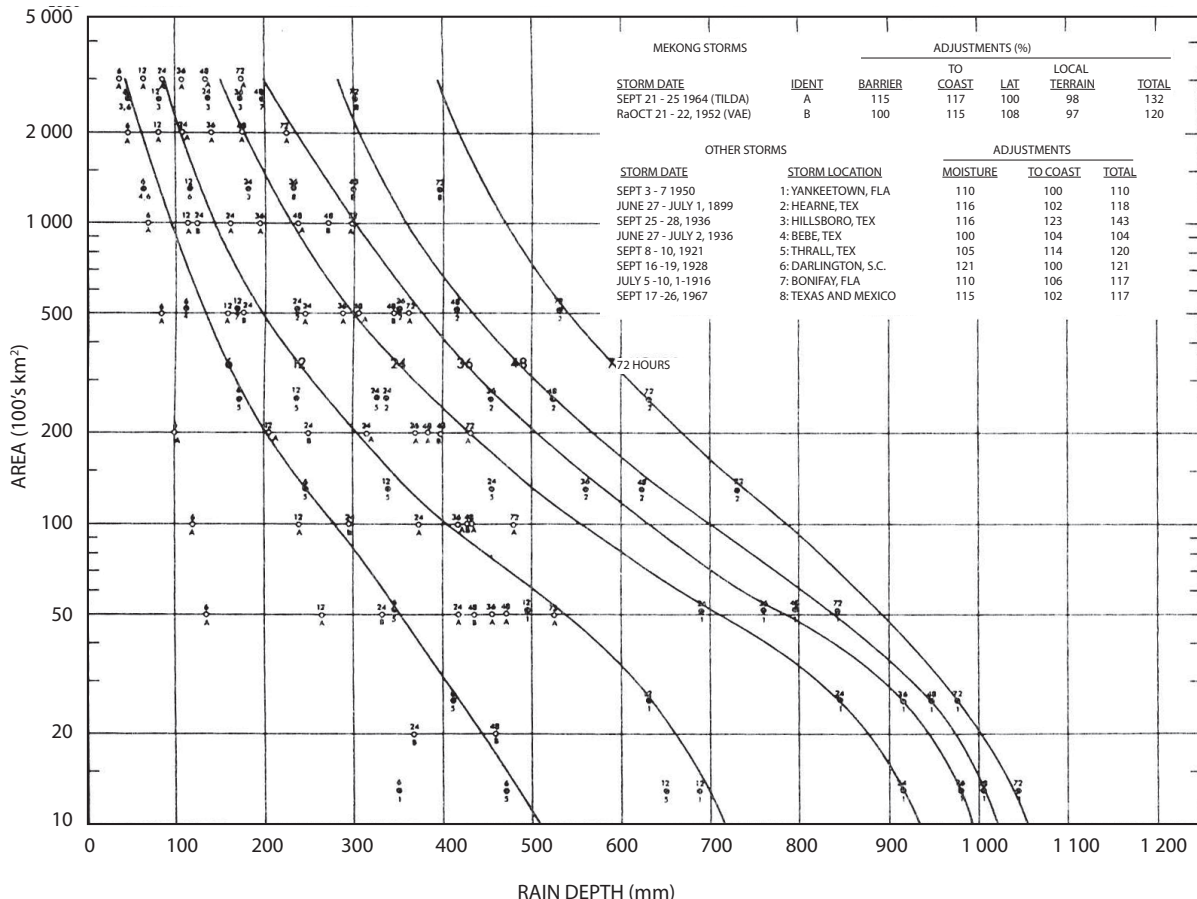


**Figure 6.10. Depth-area-duration curves of PMP on Viet Nam coast (United States Weather Bureau, 1970)**

the usual barrier reduction. Figure 6.13 shows the adopted adjustment applicable to coastal rainfall values.

#### 6.2.2.4.4 Adjustment for basin topography

Typhoon Tilda (section 6.2.2.2) produced increased rainfall along south-west facing slopes in the basin. This is consistent with the assumption that moisture from southerly or south-westerly directions, with relatively low intervening inflow barriers, must be considered in assessing regional variations in PMP. As an aid for evaluating topographic effects for these inflow directions, ratios of high- to low-elevation mean May–September precipitation were used as primary indices. A bias in the mean seasonal precipitation map (Figure 6.9), resulting from more frequent precipitation at high elevations, precluded direct use of variations in seasonal precipitation as an indication of variations in a 3-day storm. Comparison of rainy day station amounts suggested an increase with elevation of about 60 per cent of that

indicated by mean seasonal values for application to typhoon PMP.

Another adjustment of monsoon season rainfall ratios involved consistency with the one-half effectiveness adopted for the eastern barrier adjustment. This implied that south-west slopes were effective for only one-half of the storm duration. The rainfall elevation relation thus becomes 30 per cent of that indicated on the map. A mean seasonal low-elevation rainfall value of 1 200 mm was used as a basic non-orographic value. Percentage increases for typhoon rainfall on windward slopes and decreases on lee regions as indicated by south-west monsoon season rainfall (Figure 6.9) are shown in Figure 6.14.

#### 6.2.2.4.5 Combined adjustment

Combination of the above adjustments (Figures 6.11–6.14) produced the combined adjustment chart of Figure 6.15, which relates to coastal Viet Nam typhoon rainfall values equated to 100 per cent.

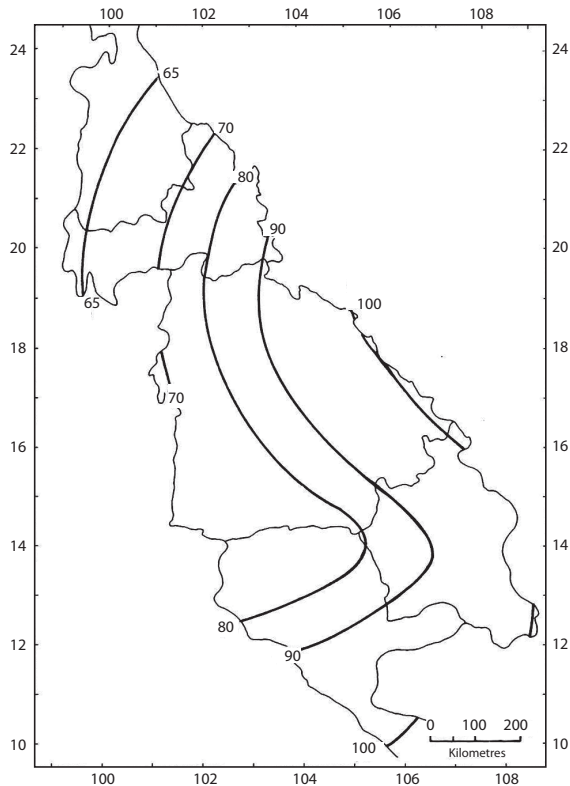


**Figure 6.11. Adjustment (percentage) of coastal typhoon rainfall for distance inland (United States Weather Bureau, 1970)**

#### 6.2.2.5 Generalized estimates of PMP

The 24-hour 5 000-km<sup>2</sup> coastal PMP values of Figure 6.10 were multiplied by the combined adjustment percentages of Figure 6.15 to obtain the generalized PMP map of Figure 6.16. PMP values for basin sizes between 5 000 and 25 000 km<sup>2</sup> from Figure 6.10 were expressed as percentages of the 24-hour 5 000-km<sup>2</sup> PMP. These percentages were then used to construct the curves of Figure 6.17.

#### 6.2.2.6 Time distribution

Examination of hourly records of intense rainfalls in the Mekong basin showed various sequences of 6-hour increments during a storm period. Those associated with tropical storms, for example, Tilda (September 1964), had rain bursts lasting up to 30 hours with greatest intensities near the centre of the burst. Some stations reported double bursts with an intervening lull of 6 to 18 hours.

Strictly speaking, in order to maintain PMP magnitude no lulls can be allowed in a sequence of 6-hour

rainfall increments during the PMP storm. In other words, the greatest, second greatest, etc., down to the twelfth greatest must be arranged in an ascending or descending order such that the highest increments always adjoin. Such a sequence is unrealistic in this region, however, and that described in section 3.4.2.6 was recommended as essentially conforming to requirements for the 72-hour PMP storm.

#### 6.2.2.7 Areal distribution

Isohyetal patterns for 6-hour rainfall increments in observed storms have various configurations. Some approach simple concentric circles or ellipses, while others are complicated, often with centres of high and low rainfall in close proximity to each other. An elliptical pattern, similar to that of Figure 3.26, was recommended for the four greatest 6-hour rainfall increments. Uniform areal distribution was recommended for the remaining 48 hour of the storm.

Within a 3-day period, the isohyetal centre of a major storm usually moves along the storm path. In the most extreme rainfalls, however, the storm may become almost stationary. It is therefore

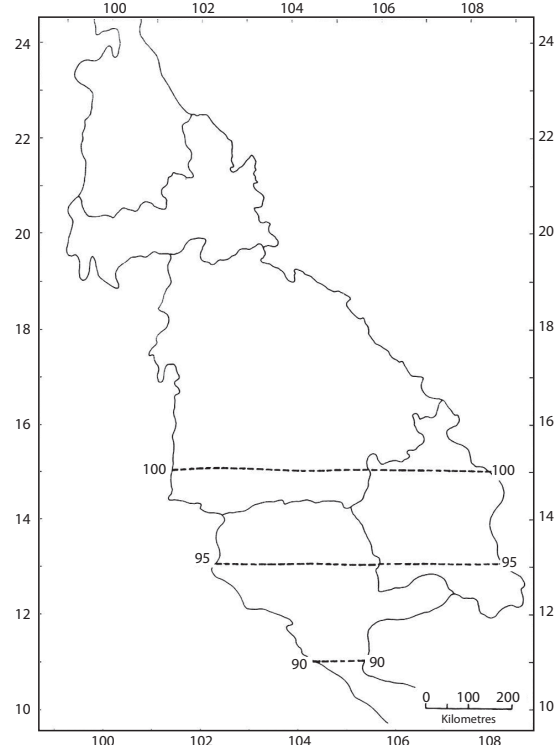


**Figure 6.12. Latitude adjustment of typhoon rainfall as percentage of values at 15° N (United States Weather Bureau, 1970)**

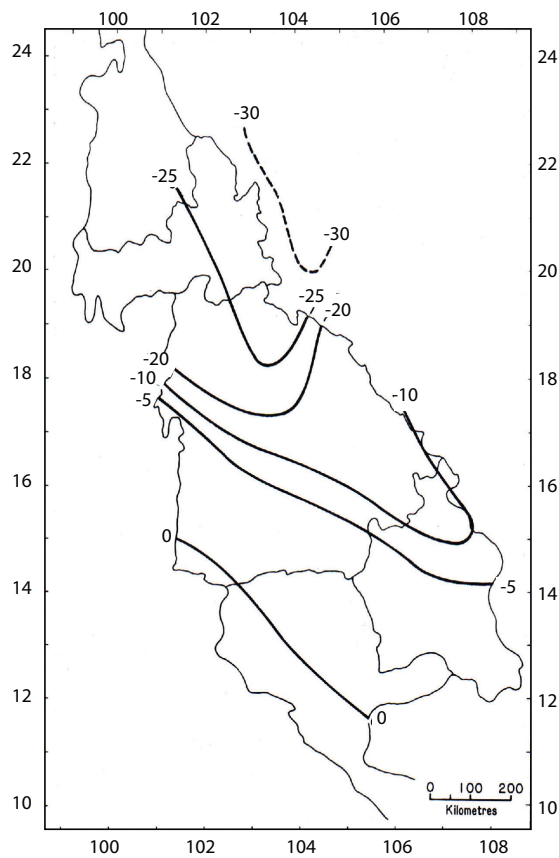


**Figure 6.13. Barrier adjustment of typhoon rainfall (percentage decrease; United States Weather Bureau, 1970)**

considered reasonable to have the isohyetal centre over the same location for a 24-hour period in the PMP storm.

DAD relationships in the heaviest tropical storm rainfalls of the Mekong basin and the United States were used to establish isohyetal values for the selected pattern. Particular attention was given to maximum 6- and 24-hour rainfalls. For these durations, consistent depth-area curves were constructed for standard area sizes of 5 000, 10 000, 15 000 and 25 000 km<sup>2</sup>.

With the 6- and 24-hour relations established, the second and third heaviest rainfall increments were computed proportional to PMP increments at standard size areas. The dashed curves of Figure 6.18 represent adopted depth-area relations for key basin sizes and durations. The solid curves are based on Figure 6.10. The storm depth-area curves and PMP DAD data were used to develop nomograms like that of Figure 6.19 for

evaluating isohyetal values. Such nomograms are derived by the procedure described in section 2.11.3, the only difference being that isohyetal values were converted into percentages of average rainfall enclosed by the respective isohyets and presented as a nomogram instead of in a table.

#### 6.2.2.8 PMP for specific basins

PMP for specific basins (see cautionary remarks, section 6.3) is estimated using the following steps:

- Lay out basin outline of Figure 6.16 and determine average 24-hour, 5 000-km<sup>2</sup> PMP for the basin.
- From Figure 6.17, read percentages of 24-hour, 5 000 km<sup>2</sup> for 6, 12, 18, 24, 48 and 72 hours for the basin area.
- Multiply basin average 24-hour, 5 000-km<sup>2</sup> PMP from (a) by the percentages of (b) to obtain basin PMP.
- Use data from (c) to construct a smooth depth-duration curve, and read off 6-hour PMP increments for the entire 72-hour storm.
- Arrange 6- and 24-hour increments as described in section 6.2.2.6.
- Use selected elliptical isohyetal pattern (not shown) to distribute the four greatest 6-hour rainfall increments. Centre and orient pattern over the problem basin so as to obtain most critical runoff, which usually results with greatest rainfall volume within the basin. Enter Figure 6.19 with basin area, and read percentage values for each isohyet, P to E, for the maximum 6-hour increment. Multiply the maximum 6-hour PMP increment of (e) by these percentages to obtain isohyetal values in millimetres. Values for second, third, and fourth PMP increments are obtained in a similar manner from similar nomograms (not shown).

### 6.2.3 Estimation of PMP for India

#### 6.2.3.1 Introduction

The PMP over most of India will be the result of either tropical cyclones or monsoonal depressions. These storms have occurred over almost all of India except the far southern extremity and northern areas bordered by the Himalayas. Thus, virtually the entire sub-continent can be treated as meteorologically homogeneous for the transposition of storm rainfall (Rakhecha and Kennedy, 1985). The limits to the transposition area are

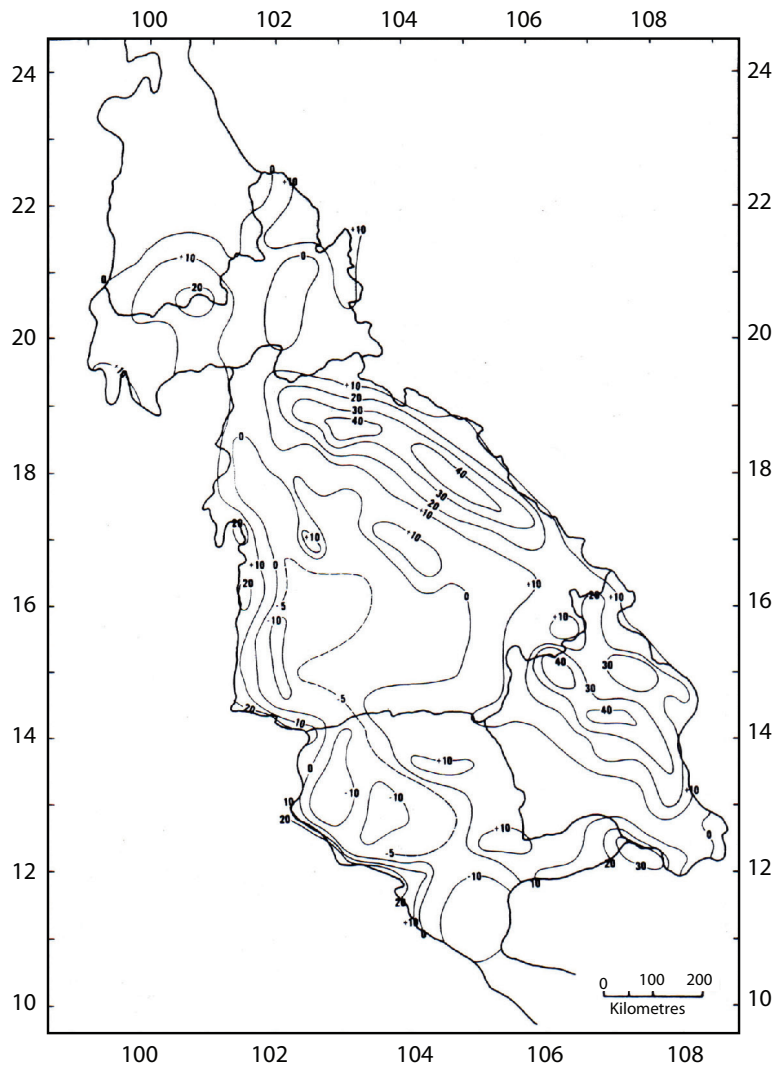


**Figure 6.14.** Adjustment of typhoon rainfall (United States Weather Bureau, 1970) for basin topography (percentage increase or decrease relative to low-elevation south-west monsoon rainfall over flat terrain)

shown in Figure 6.20. Three such storms are most important in developing the PMP estimates: 17–18 September 1880 over north-west Uttar Pradesh; 26–28 July 1927 over Gujarat; and 2–4 July 1941 over Dharampur, Gujarat. The locations of these storms are shown in Figure 6.20. The observed DAD values for these storms are shown in Figure 6.21.

#### 6.2.3.2 Initial non-orographic PMP values

The rainfall during most significant storms occurred during a period of very little or no movement of the storm system. These storms occurred over a region of little topography. In fact, the storms of 1927 and 1941 were primarily over areas

that were almost flat. This led to the development of non-orographic PMP values applicable to the flat coastal areas.

Moisture maximization of observed rainfall depths was used in the development of PMP for India. Dewpoint temperatures are less variable in India than in temperate climates, but there is some variation in available moisture from year to year due to changes in sea-surface temperature. The highest persisting 24-hour dew-point temperatures were obtained from approximately 25 representative stations and an interim map constructed using these values. Australian data showed extreme dewpoint temperatures are about 4°C lower than extreme sea-surface temperatures. This result was

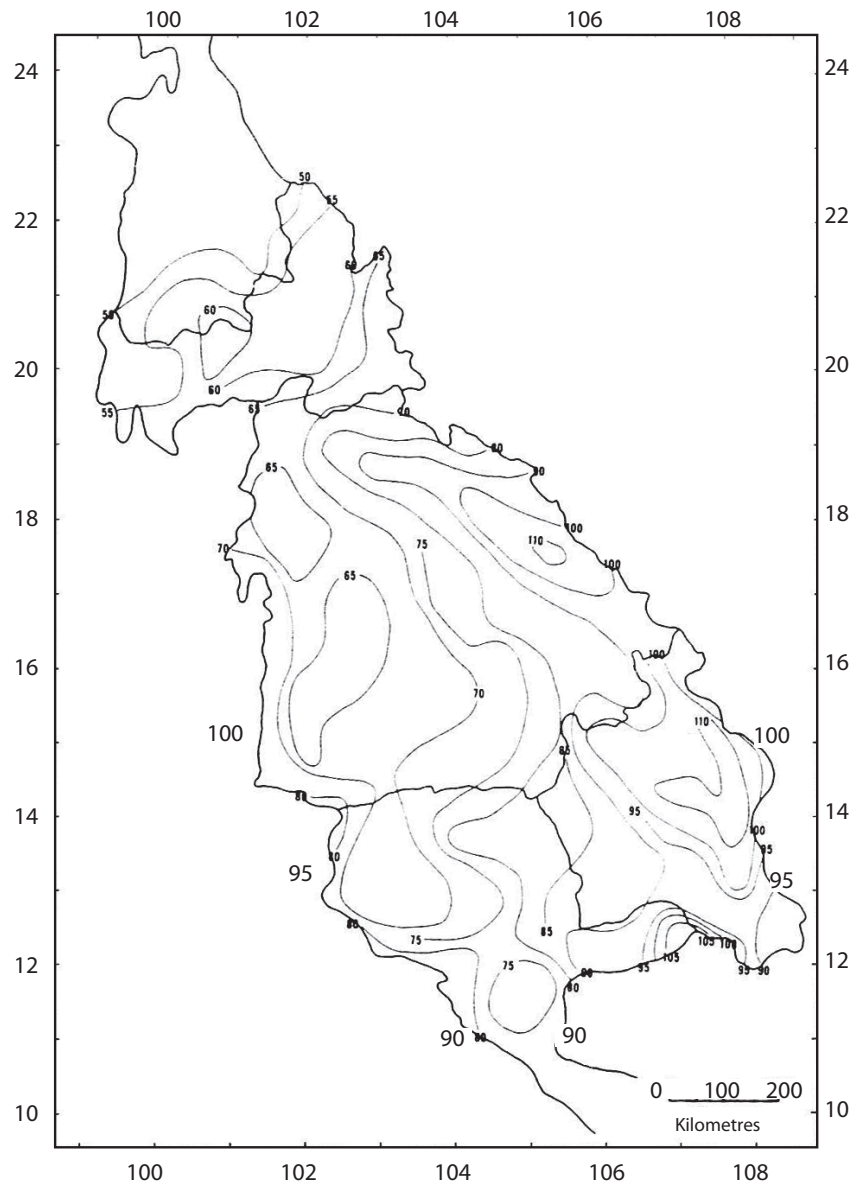


**Figure 6.15. Total adjustment (percentage) of coastal typhoon rainfall (combined adjustments of Figure 6.11 to 6.14; United States Weather Bureau, 1970)**

used to adjust coastal values assumed to be low due to limited record lengths. This concept also influenced alignments of isopleths along the coast. The resulting extreme dewpoint isopleths are shown in Figure 6.22. These extreme dewpoint values were used for moisture adjustment of storms.

#### 6.2.3.3 Adjustments to initial non-orographic PMP values

The alternative procedure discussed in section 2.3.4.2 was used for moisture adjustment over barriers. Since tropical storms are dependent on the continued supply of moisture, an adjustment for

distance that air travels over land is also required. This adjustment, based on one developed by Schwarz (1965) was modified by rainfall data recorded in major Indian storms (Figure 6.23). Any terrain effects on the rainfall amounts were removed by use of the adjustments discussed in section 5.3.2.3.

#### 6.2.3.4 Final non-orographic PMP values

Non-orographic PMP values for a maximum persisting 24-hour dew point of 30°C were obtained by applying the factors discussed above to observed rainfall amounts. These values are shown in

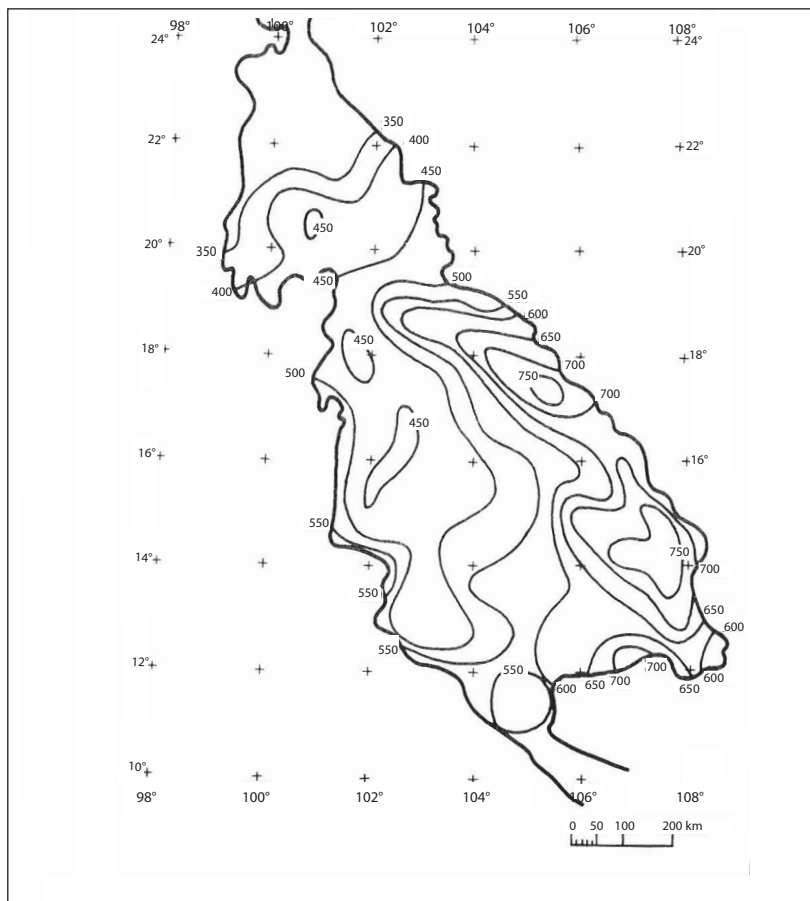


**Figure 6.16. PMP (mm) for 24 hours over 5 000 km<sup>2</sup>**  
**(United States Weather Bureau, 1970)**

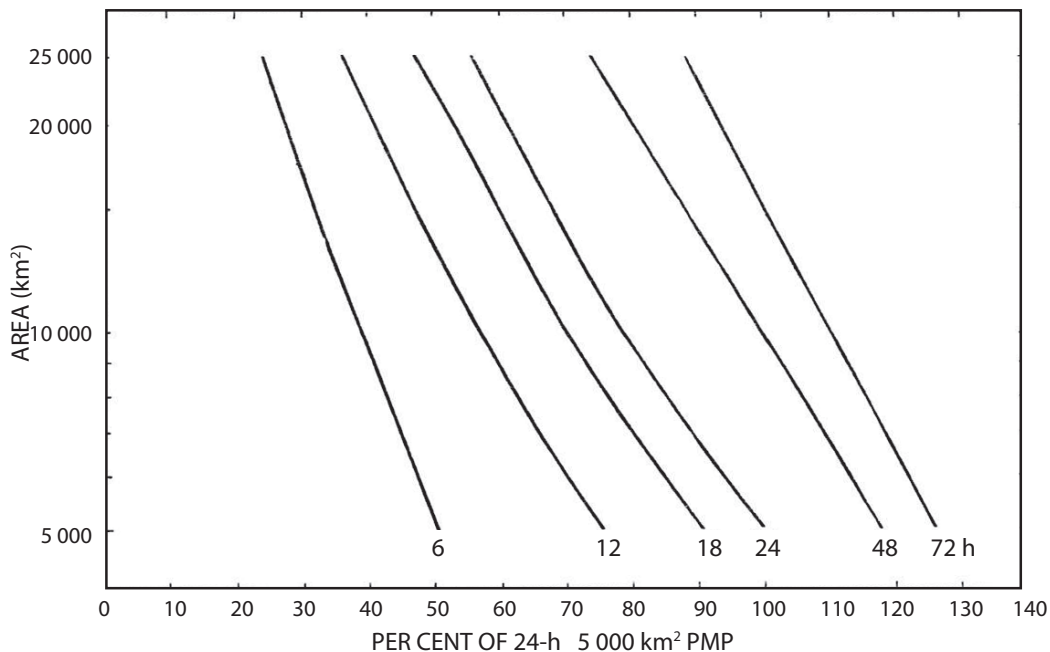


**Figure 6.17. Depth-area-duration values of PMP in per cent of 24-hour 5 000 km<sup>2</sup> PMP** (United States Weather Bureau, 1970)

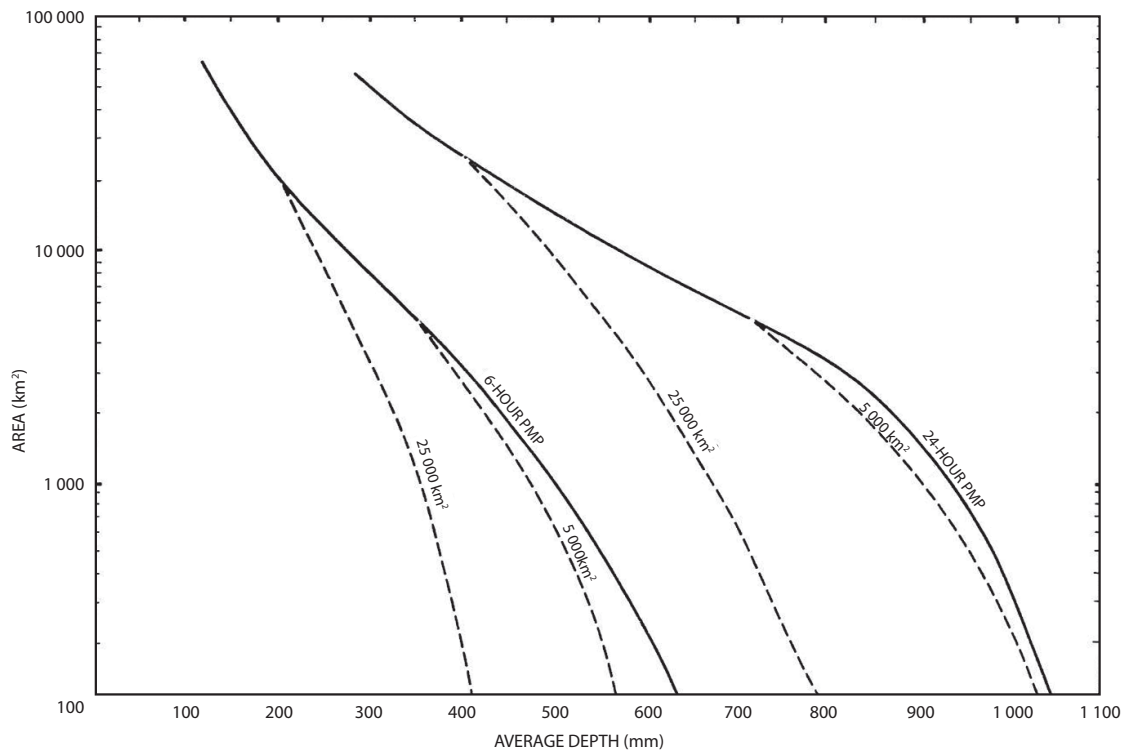


**Figure 6.18.** PMP (solid lines) and key depth-area curves typical of major tropical storms  
(United States Weather Bureau, 1970)

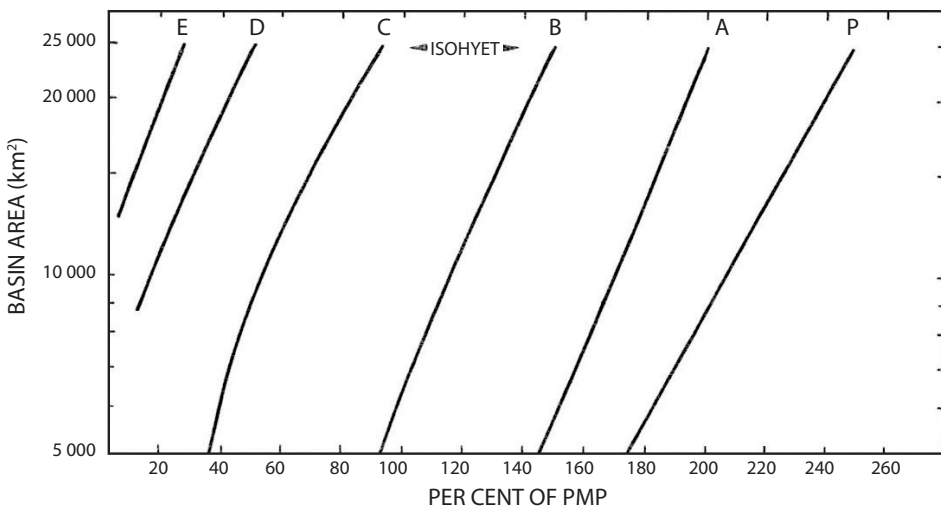


**Figure 6.19.** Isohyetal values for maximum 6-hour increment of PMP storm as percentage of average rainfall for area enclosed (United States Weather Bureau, 1970)

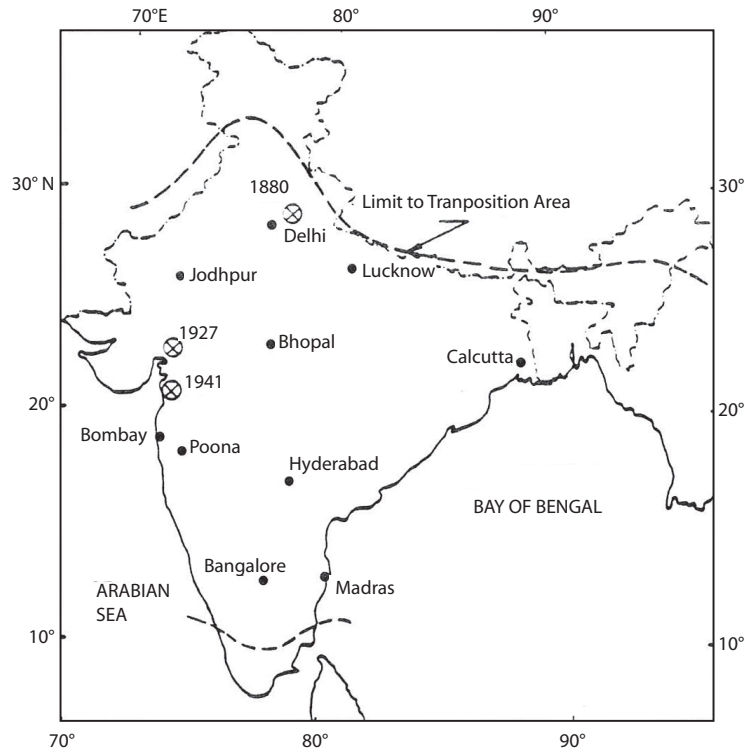


**Figure 6.20. Location of three major storm centres over India and their transposition limits (Rakhecha and Kennedy, 1985)**

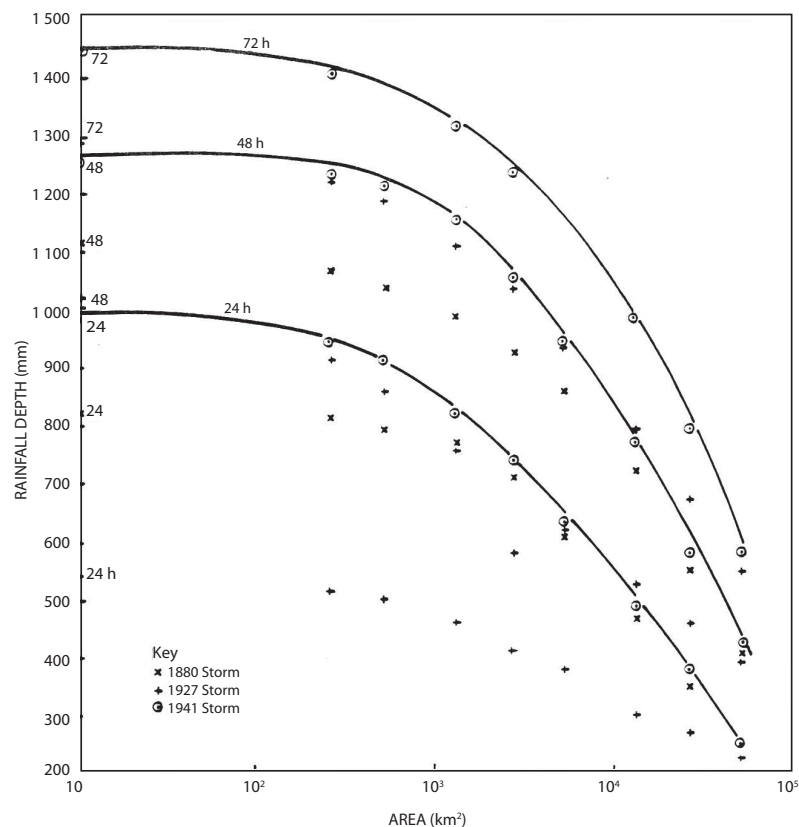


**Figure 6.21. Maximum observed DAD rainfall values for three major storms in India (Rakhecha and Kennedy, 1985)**

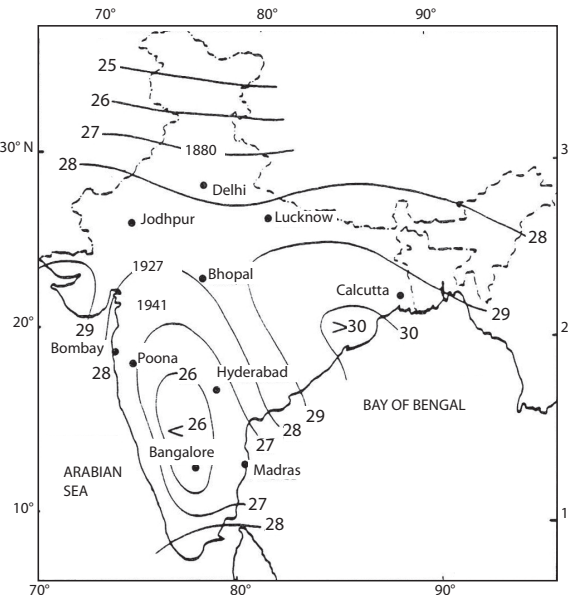


**Figure 6.22. Extreme persisting 24-hour point dewpoint temperatures over India (Rakhecha and Kennedy, 1985)**

Figure 6.24 and are applicable to flat land at sea level next to the coast. The final values shown include regional durational and areal smoothing. Values for individual basins can be obtained by use of these curves and the adjustments discussed in the preceding paragraph.

#### 6.2.4 Estimating PMP for Chambal, Betwa, Sone and Mahi watersheds in India

##### 6.2.4.1 Introduction

Chambal, Betwa, Sone and Mahi watersheds are all located in the central west of India. There are no mountain chains in any of the watersheds. PMP estimation for the four watersheds is presented in *Dam Safety Assurance and Rehabilitation Project Generalized PMP Atlas, Phase 1* (Water and Power Consultancy Services (India) Limited, 2001). The statistical estimation method was used for small watersheds, the generalized DAD method for medium to large watersheds, and the method of precipitation depth-duration analysis for large watersheds.

##### 6.2.4.2 Estimating PMP for small watersheds

Hershfield's (1961a, 1961b, 1965) statistical estimation method was used to estimate PMP for small watersheds. This method is also commonly used to check results of PMP for small to intermediate watersheds determined rough hydrometeorological methods. It was used to estimate the annual 1- and

2-day maximum PMP for Chambal, Betwa, Sone and Mahi watersheds.

To estimate PMP for 1-day duration, the frequency factors for rainfalls with 1-day duration at all the rainfall stations were calculated and drawn on the watershed map. Table 6.1 lists the frequency factors  $K_m$  for rainfalls with 1-day duration in the four watersheds. The enveloping values of  $K_m$  were determined from the mean annual maximum rainfall series. The frequency factor did not show a regional distribution, but decreased as rainfall increased, hence the enveloping curves of increasing  $K_m$  for decreasing were drawn for the four watersheds. PMP was determined from the  $K_m$  for each rainfall stations. The daily rainfalls used to determine PMP were observation-day (8.30 a.m. to 8.30 a.m.) rainfalls, so it was recommended that the correction coefficient 1.13 provided by WMO should be used for determining PMP. Table 6.2 lists PMP for 1-day duration for two of the watersheds.

The method of estimating PMP for 2-day duration was identical to that used for PMP for 1-day duration, but it was the annual 2-day maximum rainfall series that was selected, for which the 2 days must be 48 continuous hours. Table 6.1 lists the frequency factors for rainfalls with 2-day durations in Chambal, Betwa, Sone and Mahi watersheds, and Table 6.2 lists PMP for 2-day duration for Chambal and Betwa watersheds calculated through the statistical method.

##### 6.2.4.3 Estimating PMP for medium to large watersheds

The generalized DAD method was used to estimate PMP for medium to large watersheds, with specific

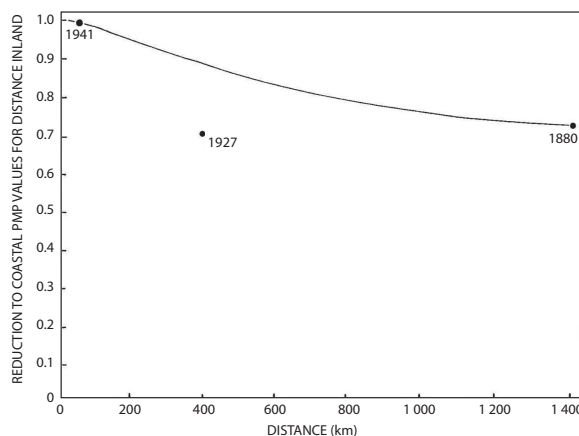


**Figure 6.23. Adjustment factor for distance from coast for non-orographic PMP values in India (Rakhecha and Kennedy, 1985)**

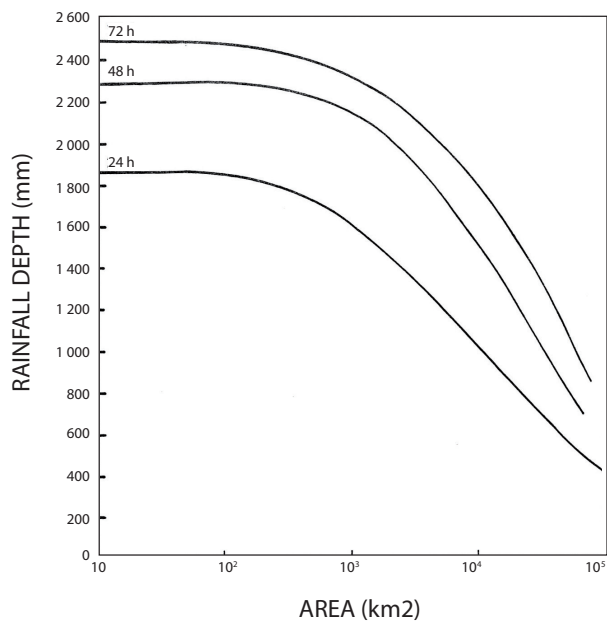


**Figure 6.24. Normalized PMP DAD curves for India  
(Rakhecha and Kennedy, 1985)**

practices differing from the traditional United States practices. Below is a brief introduction to the practices used focusing on the Chambal watershed.

#### 6.2.4.3.1 Description of the Chambal watershed

The Chambal River is one of the Yamuna's major tributaries, which also include the Kali Sindh, Parvati, Kunar and Kunwari rivers. The Chambal River originates from Mhow (located in the Indore region of Madhya Pradesh with a mean watershed elevation of 854 m) in the Vindhya Mountains. From its headstream, the Chambal River flows northward and is 320 km long in Madhya Pradesh, 226 km long in Rajasthan, 251 km along the border between Madhya Pradesh and Rajasthan, and 117 km along the border between Madhya Pradesh and Uttar Pradesh, with a total length of 960 km.

Table 6.3 shows the control watershed area of each tributary in the Chambal watershed.

**Table 6.1. Frequency factors  $K_m$  for Chambal, Betwa, Sone and Mahi watersheds**

No.	Series mean (mm)	Frequency factor $K_m$	
		1-day duration	2-day duration
1	50	12.80	11.70
2	60	12.24	11.26
3	70	11.74	10.82
4	80	11.3	10.44
5	90	10.88	10.12
6	100	10.40	9.80
7	110	10.08	9.48
8	120	9.70	9.16
9	130	9.34	8.94
10	140	9.06	8.82
11	150	8.90	8.70
12	160	8.62	8.54
13	170	8.49	8.38
14	180	8.37	8.28
15	190	8.20	8.24
16	200		8.20
17	210		8.16
18	220		8.12
19	230		8.10

**Table 6.2. PMP for 1- and 2-day durations for Chambal and Betwa watersheds**

Chambal watershed			Betwa watershed		
Station	1 day (mm)	2 days (mm)	Station	1 day (mm)	2 days (mm)
Bidhuna	491	591	Kanpur	527	759
Bhind	558	625	Chandianallah	620	672
Ambah	483	570	Banda	555	725
Dholpur	459	590	Damoh	530	636
Morena	493	583	Borina	594	631
Jaura	599	623	Jabalpur	663	865
Bijaypur	809	1 063	Sager	913	967
Shahabad	646	881	Bhilsa	567	717
Shivpuri	639	833	Bhopal	730	913
Guna	978	1 064	Sehore	669	965
Lalitpur	752	886	Narsingarh	630	768
Tikamgarh	616	851	Lalsot	444	516
Gwalior	553	647	Sapotra	527	679
Pichhore	519	651	Tonk	571	629
Nowgans	643	751	Sawai	753	910
Chhatarpur	603	782	Sheopur	587	736
Panna	760	1 083	Jahazpur	533	710
Satna	590	907	Kotaah	566	619
Jhansi	643	738	Mangrol	662	816
Rai	864	995	Bhilwara	559	637
Alaunj	530	603	Nimbahera	592	850
Derapur	655	807	Chechat	564	603
Hamirpur	648	774			

#### 6.2.4.3.2 *Weather systems affecting the Chambal watershed*

The annual rainfall is greatly varied within the Chambal watershed, increasing from 700 mm in the north-west to 1400 mm in the south. The rainfall during the south-western monsoon accounts for 85 per cent of the annual rainfall, with July and August having the largest rainfalls. Monsoon depressions from the Bay of Bengal bring large-area, long-duration rainfalls in the watershed. Slowly moving troughs, which commonly turn in the Chambal watershed, bring abundant rainfalls. The India Meteorological Department (IMD) divides the Chambal watershed into a number of sub-basins as listed in Table 6.4.

The isohyetal map for the Chambal watershed was based on a 1 : 1 000 000 watershed map. There were about 95 rainfall stations outside and 177 inside the watershed.

#### 6.2.4.3.3 *Storm analysis*

Several storms with large effects on the Chambal watershed and its sub-basins were selected from storms recorded in the India Daily Weather Report. Relevant rainfall data were collected from rainfall stations inside and outside the watershed.

The daily mean rainfall and the 1-, 2- and 3-day maximum rainfalls for the rainy period at each

**Table 6.3. Catchment areas in the Chambal watershed**

No.	River (or tributary)	Catchment area (km <sup>2</sup> )
1	Main Chambal	46 073
2	Banas	48 577
3	Kali Sindh	25 741
4	Parvati	14 122
5	Kunar	4 507
6	Kunwari	7 610

sub-basin were calculated. The rules of classification defined by IMD were followed to designate the rainfall threshold for each duration. Storms whose rainfall exceeded the threshold were extracted for isohyetal analyses. Ultimately, 24 storms (with a daily rainfall at the storm centre of between 225 mm and 396 mm) were selected for analysis from among the 95 in the Chambal watershed. These 24 storms were used to conduct 1-day isohyetal analyses. Similarly, 2- and 3-day isohyetal analyses were conducted using 17 and 10 storms, respectively.

The three storms for which the DAD enveloping curves were drawn occurred on 27–29 June 1945, 22–23 July 1971 and 22–24 July 1986. They were all caused by the trough movement from the Bay of Bengal.

#### 6.2.4.3.4 Estimating PMP

The following steps are applied in estimating PMP:

- (a) Drawing the DAD curve:
  - (i) a. The DAD curve is drawn for each typical storm;
  - b. The DAD curves for the three extraordinary storms in 1945, 1971 and 1986 are drawn.
- (ii) As a result, the typical storms that controlled the DAD enveloping curves were:

**Table 6.4. Sub-basin location in the Chambal watershed**

Sub-basin no.	Location
404	Up Chambal River to Kotah dam site
405	From Kotah Dam to the intersection of the Chambal and Banas rivers
406	Banas River
407	From the intersection of the Chambal and Banas rivers to the Yamuna River

- a. 1-day duration: DAD enveloping curve was 29 June 1945;
- b. 2-day duration: DAD enveloping curves were 28–29 June 1945 and 22–23 July 1971;
- c. 3-day duration: DAD enveloping curves were 27–29 June 1945 and 22–24 July 1986.

(iii) Rainfall on the DAD enveloping curve is called the standard project storm (SPS). Table 6.5 lists the SPS by standard area size for the Chambal watershed.

- (b) Calculating the storm maximization factor and adjustment factor by region:

- (i) The moisture maximization factor (MMF) is calculated by

$$\text{MMF} = (W_2)_{h1}/(W_1)_{h1}$$

where  $h_1$  is the mean watershed elevation of the region where the typical storm occurs;  $(W_1)_{h1}$  is the precipitable water for the part of the catchment beyond the elevation  $h_1$  to which the representative dew point for the typical storm (or the storm region)  $d_1$  corresponds;  $d_2$  occurs at the same location and month as  $d_1$ .

Table 6.6 shows the MMF of the three typical storms for drawing the DAD enveloping curves.

- (ii) The location adjustment factor (LAF) is calculated by

$$\text{LAF} = (W_3)_{h1}/(W_2)_{h1}$$

where  $(W_3)_{h1}$  is the precipitable water for the part of the catchment beyond the elevation  $h_1$  to which the maximum dew point for the storm transposed region  $d_3$  corresponds. When  $d_3 > d_1$  then  $\text{LAF} \neq 1$ .

- (iii) The barrier adjustment factor (BAF) is calculated using

$$\text{BAF} = (W_3)_{h2}/(W_3)_{h1},$$

where  $h_2$  is the mean elevation of the transposed region;  $(W_3)_{h2}$  and  $(W_3)_{h1}$  are the precipitable water for the parts of the catchment beyond the elevations  $h_2$  and  $h_1$ , respectively, to which the maximum dew point for the transposed region  $d_3$  corresponds. When  $h_2 > h_1$  then  $\text{BAF} < 1$ ; when  $h_2 = h_1$  then  $\text{BAF} = 1$ . Storm transposition is not recommended if the elevation difference between the transposed region and the storm occurrence region  $\Delta h$  is greater than 1 000 m.

**Table 6.5. SPS for the Chambal watershed in India**

Watershed	Area size (km <sup>2</sup> )	SPS (mm)		
		1 day	2 days	3 days
	5 000	320	424	472
	10 000	294	380	424
	20 000	258	338	380
	30 000	238	320	350
	40 000	220	300	324
	50 000	203	280	310
Chambal	46 073	208	285	314
Banas	48 577	206	282	312
Kali Sindh	25 741	244	330	362
Parvati	14 122	278	360	403
Kunar	4 507	324	438	480
Kunwari	7 610	307	404	443

- (iv) The moisture adjustment factor (MAF) is calculated using

$$\text{MAF} = \text{MMF} \times \text{LAF} \times \text{BAF}$$

If it is unnecessary to calculate MMF, LAF and BAF separately, MAF can be calculated with the following simplified relation

$$\text{MAF} = (W_3)_{h2}/(W_1)_{h1}$$

- (v) The area reduction factor (ARF) is obtained from area and precipitation depth analyses for a number of large storms. ARF for watershed areas between 0 and 10 000 km<sup>2</sup> are listed in Table 6.7. The ARF value is the ratio between the areal rainfall and the rainfall at the storm centre, for the given area. ARF for any

area can be obtained through interpolating the ARF/area relationship curve drawn for the particular area and its ARF in the table.

- (c) Estimating PMP for design watershed:

- (i) If the DAD curve for the typical storm is available for the design watershed or its surrounding regions, PMP is determined by the precipitation depth  $R$  (found using the area of the design watershed) multiplied by MMF, that is,

$$\text{PMP} = \text{MMF} \times R$$

Table 6.8 lists PMP from the standard areas of the Chambal watershed determined through moisture maximization.

- (ii) If there is no DAD curve available for the design watershed or its surrounding regions, the rainfall  $R$  is determined by looking up the DAD enveloping curve. Since the project has involved storm transportation, both displacement adjustment and barrier adjustment should be applied. Therefore, PMP is calculated using the equation

$$\text{PMP} = \text{MMF} \times \text{MAF} \times \text{BAF} \times R$$

- (d) Estimating PMP for each grid point:

To facilitate networking, the Chambal, Betwa, Sone and Mahi watersheds were divided into a

**Table 6.6. Moisture maximization factors for three typical storms**

Storm occurrence date	MMF	Storm area
27–29 June 1945	1.29	404, 405, 406, 407 and 408
21–23 July 1971	1.31	404, 405, 406 and 407
22–24 July 1986	1.29	404, 405, 406, 407 and 408

Note: The storm area numbers in the table are the watershed numbers.

**Table 6.7. Area reduction factor for storms in the Chambal watershed**

<i>Area (km<sup>2</sup>)</i>	<i>ARF</i>	<i>Area (km<sup>2</sup>)</i>	<i>ARF</i>	<i>Area (km<sup>2</sup>)</i>	<i>ARF</i>
0.0	1.000	700.0	0.966	5 000.0	0.833
100.0	0.994	800.0	0.961	6 000.0	0.811
200.0	0.989	900.0	0.956	7 000.0	0.790
300.0	0.983	1 000.0	0.951	8 000.0	0.773
400.0	0.978	2 000.0	0.906	9 000.0	0.760
500.0	0.974	3 000.0	0.878	10 000.0	0.748
600.0	0.970	4 000.0	0.854		

1° longitude and latitude grid, and the above-mentioned method was then used to calculate PMP for the standard area of each grid. The Chambal and Betwa watersheds are presented below as an example.

(i) MAF was calculated for the storm that occurred on 27–29 June 1945 and transposed into each grid of the Chambal and Betwa watersheds. This storm covered the whole Chambal and Betwa watersheds, so it could be transposed into any grid of either watershed.

The relevant values were determined to be:  $d_1 = 25.7^\circ\text{C}$ ;  $d_2 = 28.5^\circ\text{C}$ ;  $h_1 = 400 \text{ m}$ ;  $(W_1)_{h1} = 84.0 - 8.0 = 76.0$ ;  $(W_2)_{h1} = 108 - 10.0 = 98.0$ ; MMF =  $(W_2)_{h1}/(W_1)_{h1} = 1.29$ . Table 6.9 lists the MAF for each grid.

(ii) PMP was determined for the standard area of either Chambal or Betwa watershed (2 500 km<sup>2</sup>, 5 000 km<sup>2</sup>, 7 500 km<sup>2</sup> and 10 000 km<sup>2</sup>) using the above-mentioned method (see Table 6.10).

**Table 6.8. Calculated results of PMP for the Chambal watershed**

<i>Watershed</i>	<i>Area (km<sup>2</sup>)</i>	<i>PMP (mm)</i>		
		<i>1 day</i>	<i>2 days</i>	<i>3 days</i>
	5 000	413	555	609
	10 000	379	498	547
	20 000	333	436	490
	30 000	307	413	452
	40 000	284	387	418
	50 000	362	361	400
Chambal	46 073	268	368	405
Banas	48 577	266	364	402
Kali Sindh	25 741	315	426	467
Parvati	14 122	359	472	520
Kunar	4 507	418	574	619
Kunwari	7 610	396	529	571

#### 6.2.4.4 Estimating PMP for super large watersheds

PMP for super large watersheds are usually estimated with the method of precipitation depth-duration analyses. Since actual conditions for all super large watersheds are different, there is no unified method of estimation.

#### 6.2.4.5 Temporal distribution of storms

The temporal distribution of PMP is determined through generalizing, evening and smoothing of multiple typical storms.

#### 6.2.4.6 Example application

A water resources project was planned for the Kanhar River in Sone watershed. Its control watershed area was to be 6 020 km<sup>2</sup>. One of the largest storms to happen in the watershed occurred on 29 August 1940. The enveloping curve for Sone watershed was used to find the enveloping value of the precipitation depth for 1-day duration for 6 020 km<sup>2</sup>, which was 360 mm. The watershed grids were 23° 84°, 24° 83° and 24° 84° and the MAF for these three grids were 1.04, 1.28 and 1.33, respectively, with a mean of 1.217. Hence, PMP for the watershed was 438 mm.

**Table 6.9. MAF for each grid of either Chambal or Betwa watershed**

<i>Geographic coordinate of grid</i>		<i>d<sub>3</sub></i> (°C)	<i>(W<sub>3</sub>)<sub>h1</sub></i> (mm)	<i>h<sub>2</sub></i> (m)	<i>(W<sub>3</sub>)<sub>h2</sub></i> (mm)	LAF	BAF	MAF
<i>Latitude</i> (°)	<i>Longitude</i> (°)							
23	76	29.0	102.0	400	102.0	1.04	1	1.34
23	77	29.0	102.0	400	102.0	1.04	1	1.34
23	78	30.0	109.0	400	109.0	1.11	1	1.43
23	79	30.5	113.0	400	113.0	1.15	1	1.48
24	75	29.5	104.0	400	104.0	1.06	1	1.37
24	76	30.0	109.0	400	109.0	1.11	1	1.43
24	77	30.0	109.0	400	109.0	1.11	1	1.43
24	78	30.5	113.0	400	113.0	1.15	1	1.48
24	79	30.0	109.0	400	109.0	1.11	1	1.43
24	80	29.5	104.0	400	104.0	1.06	1	1.37
25	74	29.0	102.0	400	102.0	1.04	1	1.34
25	75	29.0	102.0	400	102.0	1.04	1	1.34
25	76	29.0	102.0	400	102.0	1.04	1	1.34
25	77	29.0	102.0	400	102.0	1.04	1	1.34
25	78	30.0	109.0	400	109.0	1.11	1	1.43
25	79	30.0	109.0	400	109.0	1.11	1	1.43
25	80	29.5	104.0	400	104.0	1.06	1	1.37
26	75	26.5	81.0	400	81.0	0.83	1	1.07
26	76	28.0	93.0	400	93.0	0.95	1	1.22
26	77	27.0	86.0	400	86.0	0.88	1	1.14
26	78	29.0	102.0	400	102.0	1.04	1	1.34
26	79	29.0	102.0	400	102.0	1.04	1	1.34
27	76	27.0	86.0	400	86.0	0.88	1	1.13

Note: The mean elevation of each grid is equal to or less than 400 m, and there is no barrier elevation between the transposed region and the storm occurrence region, so  $h_2 = h_1$  for all grids.

**Table 6.10. PMP for each grid of either Chambal or Betwa watershed**

Geographic coordinate of grid		MAF	PMP for 1-day duration for each area (km <sup>2</sup> )			
Latitude (°)	Longitude (°)		2 500	5 000	7 500	10 000
23	76	1.34	458	429	411	394
23	77	1.34	458	429	411	394
23	78	1.43	489	458	439	420
23	79	1.48	506	474	454	435
24	75	1.37	469	438	421	403
24	76	1.43	489	458	439	420
24	77	1.43	489	458	439	420
24	78	1.48	506	474	454	435
24	79	1.43	489	458	439	420
24	80	1.37	469	438	421	403
25	74	1.34	458	429	411	394
25	75	1.34	458	429	411	394
25	76	1.34	458	429	411	394
25	77	1.34	458	429	411	394
25	78	1.43	489	458	439	420
25	79	1.43	489	458	439	420
25	80	1.37	469	438	421	403
26	75	1.07	366	342	328	315
26	76	1.22	417	390	375	359
26	77	1.14	390	365	350	335
26	78	1.34	458	429	411	394
26	79	1.34	458	429	411	394
27	76	1.13	386	362	347	332

## 6.2.5 PMP estimation for the Daguangba Project in Hainan Island, China

### 6.2.5.1 Introduction

Located between longitude 108°–110° E and latitude 18°–20° N, Hainan Island has a tropical island climate that is slightly continental. The Daguangba Project is located in the south-west of Hainan Island in the Changhuajiang River basin. It has an above-dam-site watershed area of 3 498 km<sup>2</sup>. Analysis of records of storms in the Daguangba watershed between 1951 and 1983 with 24-hour rainfall amounts larger than 200 mm showed that they were all caused by typhoons. As a result, PMP estimation for the Daguangba Project study focused on the impact of typhoon storms.

### 6.2.5.2 Estimation of orographic components of storms in the Changhuajiang River basin

The generalized estimation method was used for PMP estimation for the Daguangba Project. Since the watershed was in an orographic region, the orographic component was separated from observed storms in order to facilitate generalizing the convergence component of the storms.

Analysis of the geographical distribution of extremes of storm rainfalls with various durations in China showed variations in the orographic effects. Differences between regions in rainfalls less than 1 hour are small and orography has no marked effect on these storms. For time intervals from 1–24 hours or longer, orography has an increasing effect on the enhancement of storms.

Due to different moisture inflows, the rainfall differences between windward slopes and leeward slopes are larger. Based on this understanding, the time-interval orographic enhancement factor method was used (Lin, 1988). The method estimates orographic rains at different time intervals using statistics of observed storms at different time intervals.

In the actual estimation, the average orographic enhancement factor  $\bar{f}_{\Delta t}(x, y)$  was calculated using the following equation:

$$\bar{f}_{\Delta t}(x, y) \approx \frac{\bar{R}_{\Delta t}(x, y)}{\bar{R}_{0\Delta t}} \quad (6.1)$$

where  $\bar{R}_{\Delta t}(x, y)$  is the multi-year average of observed rainfalls at the point  $(x, y)$  in the time interval  $\Delta t$ ;  $\bar{R}_{0\Delta t}$  is the average convergence component of storms in the time interval  $\Delta t$ .

The convergence component of storms at the point  $(x, y)$  in the time interval  $\Delta t$  can be expressed as:

$$R_{0\Delta t}(x, y) \approx \frac{R_{\Delta t}(x, y)}{\bar{f}_{\Delta t}(x, y)} \quad (6.2)$$

where  $R_{0\Delta t}(x, y)$  is the convergence component of storms at the point  $(x, y)$  in the  $\Delta t$  time interval;  $R_{\Delta t}(x, y)$  is the actual storm rainfall at the point  $(x, y)$  in the time interval  $\Delta t$ ;  $\bar{f}_{\Delta t}(x, y)$  is the average orographic enhancement factor at the point  $(x, y)$  for the  $\Delta t$  time interval.

Thus, according to the size and the shape of the drainage in question and the number of the rain gauge stations available in the drainage a denser grid of calculation was formed in such a way to cover the drainage completely. Now, the area-averaged PMP for a drainage and for a period of  $\Delta t$  can be written as:

$$PMP_{\Delta t, A} = \frac{1}{m \times n - k} \sum_1^m \sum_j^n PMP_{0\Delta t}(x_i, y_i) \cdot \bar{f}_{\Delta t}(x_i, y_i)$$

where the  $PMP_{0\Delta t}(x_i, y_i)$  represents the contribution of a node in the drainage in  $\Delta t$  time to the area-averaged convergence PMP when the PMP occurs (note, here the  $PMP_{0\Delta t}(x_i, y_i)$  is not equal to the point-PMP( $x_i, y_i$ ) of the node), while  $m$  and  $n$  are the numbers of  $\Delta x_i$  and  $\Delta x_t$  respectively, and the  $k$  value is the number of nodes which are located outside the drainage.

When estimating PMP for the Daguangba watershed of the Changhuajiang River, isoline maps (Ye and Hu, 1979) of averages of the annual maximum 6-h, 21-, 24-hour and 3-day point storms in China were used to compute the average orographic enhancement factor  $\bar{f}_{\Delta t}(x, y)$ . A number of rainfall

stations without apparent orographic disturbances were identified in the storm moisture inflow direction where the storm occurred. The annual maximum rainfall averages in the time interval  $\Delta t$  for these stations were used to calculate the average for the group of stations.

In this instance,  $11 \times 7 = 77$  nodes (see Figure 6.25) were set up surrounding the centre of the Changhuajiang River basin. Five rainfall stations in flat coastal regions west and south of the basin were selected to be comparison stations for studying the enhancement effects of orography. Averages of the annual maximum 6-, 12- and 24-hour rainfall extremes of 72 nodes were calculated. The calculated values of the nodes were compared with the group-station averages of the selected five stations, and time-interval orographic enhancement factors of all the time intervals and nodes were obtained. Results of the calculation showed that average enhancement extents of the orography of the Daguangba watershed for 6-, 12- and 24-hour storms were 8.7, 14.6 and 22.1 per cent, respectively. Within 24 hours, the orographic enhancement effect on storms increased with storm duration.

#### 6.2.5.3 DAD relations of PMP for non-orographic regions on Hainan Island

Data from the following three areas were considered:

- (a) Data on the watershed: analysis of 15 typhoon storms affecting the Changhuajiang River basin, and meteorological data, showed three storm centres in the Daguangba watershed. They were in Sanpai in the lower reaches, Qilinchang in the middle reaches and Baoguo in the upper reaches. Moisture inflows were

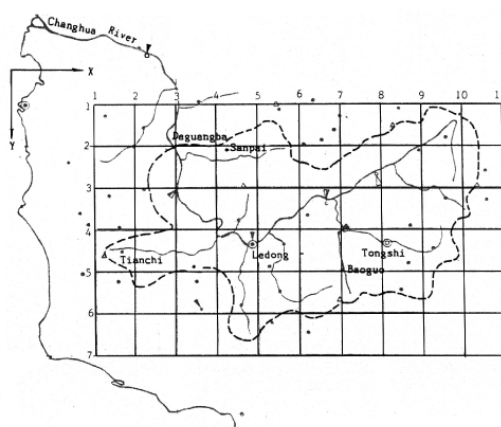


Figure 6.25. Calculation grids of Changhuajiang River Basin (Lin, 1988)

from the south-west throughout storm periods. DAD relations for the largest typhoon storms observed in non-orographic regions on Hainan Island were established using data from the five largest typhoon storms and deducting orographic effects.

- (b) Data from south-eastern coastal regions in China were transposed: a storm that occurred in Chaoqiao, a coastal region in Jiangsu Province, on 4–5 August 1960 had a maximum 24-hour and 3-day rainfall of 822 mm and 934 m, respectively; a second storm occurred in Wuyang, Guangdong Province, on 21–22 September 1976 with maximum 24-hour and 3-day rainfall of 794 mm and 1 092 mm, respectively. The two typhoon storms were transposed to Hainan Island after their DAD relations were moisture adjusted.
- (c) Data from the United States were transposed: DAD relations of extreme typhoon storms in the south-eastern coastal plain of the United States were also transposed to Hainan Island after moisture maximization and adjustment, for the following reasons. The latent energy of extreme typhoon storms in the South China Sea is approximate to that of extreme typhoon storms in the Atlantic Ocean (Hydrometeorological Report No. 46, United States Weather Bureau, 1970) and thermal and dynamic force

conditions affecting the South China Sea and the Gulf of Mexico as well as typhoon speeds and frequencies in the two regions were similar. The average of maximum 24-hour typhoon storm series on Hainan Island was 27 per cent larger than that of the south-eastern and southern plains of the United States, largely due to topographic effects and the difference in moisture content.

After moisture adjustment and enveloping, data on DAD relations of typhoon storms in the plain regions were converted into enveloping curves of DAD relations of maximized typhoon storms applicable to non-orographic regions on Hainan Island. The set of enveloping curves could be regarded as DAD relations of PMP for non-orographic regions in the Changhuajiang River basin, as is shown in Table 6.11.

#### 6.2.5.4 Estimation of 24-hour PMP for Daguangba watershed

##### 6.2.5.4.1 DAD curve of 24-hour PMP for designs for non-orographic regions in the Changhuajiang River basin

The storm DAD curve of 24-hour PMP for non-orographic regions in the Changhuajiang River

**Table 6.11 DAD enveloping relations of typhoon storm extremes in non-orographic regions on Hainan Island (Lin, 1988)**

Area (km <sup>2</sup> )	Precipitation depth of each duration (mm)			
	6 hour	12 hour	24 hour	72 hour
Point	751	879	1 197	1 389
100	697	836	1 129	1 304
300	646	807	1 081	1 236
700	580	789	1 042	1 188
1 000	548	779	1 023	1 165
2 000	478	728	966	1 107
3 000	434	672	903	1 051
4 000	399	619	837	1 003
5 000	376	565	776	944
7 000	335	493	662	886
10 000	303	430	549	850

basin was established using data from 24-hour typhoon storms in non-orographic regions in the Hainan Island region and those that were transposed, as well as DAD relations of PMP for non-orographic regions on Hainan Island. The precipitation depth of the DAD curve for an area equal to the watershed area was the same as the PMP for non-orographic regions on Hainan Island. The average precipitation depth for areas larger or smaller than the watershed area was smaller than PMP for the same areas in non-orographic regions on Hainan Island. The DAD curve was called the DAD curve of 24-hour PMP for designs for non-orographic regions in the Changhuajiang River basin.

#### 6.2.5.4.2 *Spatial distribution of 24-hour PMP for non-orographic regions in the Changhuajiang River basin*

According to an analysis of observed typhoon storms in the Changhuajiang River basin, the isohyetal map was nearly elliptical. Calculations of ratios between major and minor axes showed that the storm isohyetals tended to change from ellipses to circles with increasing area size. After establishing the average isohyetal distribution of the typhoon storms, the PMP isohyetal model for the typhoon storms was designed using the DAD curve of 24-hour PMP for designs for non-orographic regions in the Changhuajiang River basin, as is shown in Figure 6.26. When estimating

PMP for the watershed, the direction of the major axis was  $225^\circ$  and the centre was the watershed centre according to the direction of moisture inflow.

#### 6.2.5.4.3 *Adjustment of typhoon intensity*

After landing, typhoons get weaker as they move inland. The 50-year persisting maximum 12-hour dewpoint temperature was selected as an index for the adjustment. The dewpoint isoline maps formed closed rings along the coastline of Hainan Island, descending from the coastline to the centre of the island. The largest decrease was 9 per cent.

#### 6.2.5.4.4 *Comprehensive adjustment coefficient*

The adjustment coefficient for the distance to the coast and the time-interval orographic enhancement factor were merged into the comprehensive adjustment coefficient. Table 6.12 lists comprehensive adjustment coefficients for 24-hour storms in the Changhuajiang River basin.

#### 6.2.5.4.5 *PMP estimation*

Figure 6.25 was placed at the watershed centre of Daguangba, and the 24-hour  $PMP_{0\Delta t}(x, y)$  for non-orographic regions on the grid points were calculated using linear interpolation.  $PMP_{\Delta t}(x, y)$  on the grid points could be determined using Table 6.12 and Equation (6.2). The isoline map of 24-hour

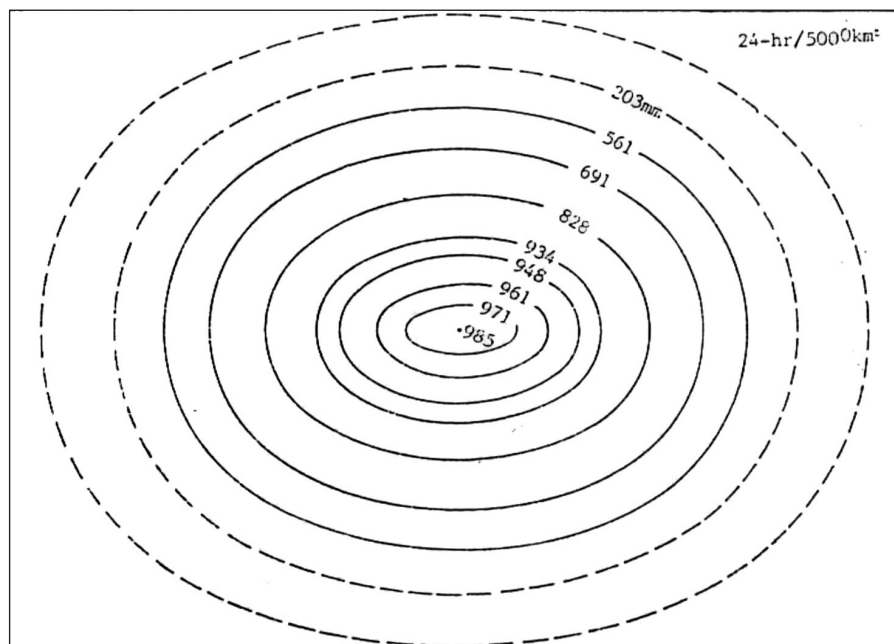


**Figure 6.26. Isohyetal map of 24-hour 5 000 km<sup>2</sup> PMP for non-orographic regions on the Changhuajiang River Basin (Lin, 1988)**

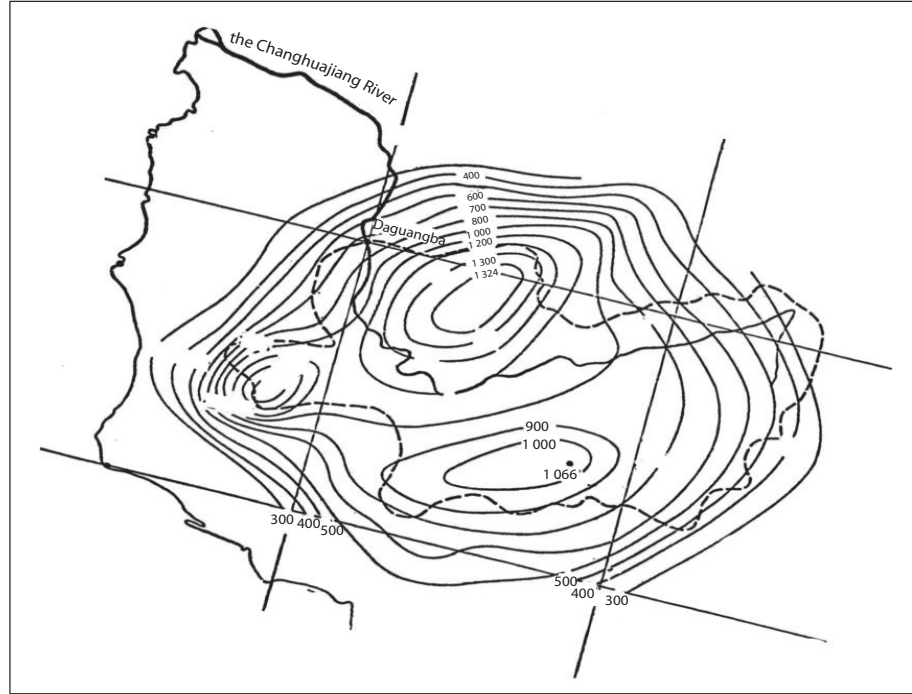


**Figure 6.27. Storm isoline map of 24 hour PMP for the Changhuajiang River basin on Hainan Island (Lin, 1988)**

PMP for the above-mentioned watershed of Daguangba could be drawn. According to Figure 6.27, there were three storm centres, which were completely consistent with the three storm-rich regions in the watershed. The shape of the storm isohyets was an irregular ellipse, whose major axis was in the north-east-south-west direction and was consistent with the trend of the Wuzhi Mountains on the north-west side.

#### 6.2.5.4.6 Temporal distribution of 24-hour PMP

According to the observed data, the smallest time interval was 6 hours. The largest 6-hour and 12-hour precipitations were equal to the PMP. Among the largest 24-hour precipitations, the largest and the second largest 6-hour precipitations were adjacent and in the middle of the event.

**Table 6.12. Comprehensive adjustment coefficient for 24-hour storms in the Changhuajiang River basin of Hainan Island (Lin, 1988)**

y-axis point data no.	x-axis point data no.										
	1	2	3	4	5	6	7	8	9	10	11
1	1.04	1.09	1.15	1.27	1.38	1.55	1.08	1.10	1.27	1.42	1.08
2	1.00	1.05	1.21	1.48	1.65	1.22	1.08	1.13	1.02	1.06	1.10
3	1.03	0.96	1.00	1.39	1.38	1.03	0.98	1.00	1.07	1.28	1.15
4	1.28	1.27	1.12	1.11	1.10	0.96	0.99	1.00	1.09	1.06	1.31
5	1.72	1.84	1.10	0.98	0.91	1.10	1.16	1.09	1.07	0.97	1.18
6	1.44	1.13	1.02	1.12	1.12	1.11	1.13	1.16	0.90	0.84	0.84
7	1.02	0.81	0.78	1.20	1.22	1.12	1.13	1.15	1.11	0.84	0.85

### 6.2.5.5 Analysis of the rationality of PMP estimates

#### 6.2.5.5.1 Comparison with observed storm records in the watershed

The storm that occurred on 7–9 September 1963 was the largest actual storm in the watershed with the maximum 24-hour watershed areal mean precipitation depth up to 308 mm. The ratio between it and the 24-hour PMP areal mean precipitation depth, 880 mm, was 0.35. The maximum 24-hour precipitation depth in Qilinchang, one of the storm centres in the watershed, occurred on 13 June 1974 with a value of 783 mm. The maximum 24-hour precipitation depth in Baoguo occurred on 8 September 1963 with a value of 688 mm. The maximum 24-hour precipitation depth in Sanpai occurred on 2 July 1964 with a value of 593 mm. The 24-hour PMP values of the three centres were 1 100, 1 066 and 1 150 mm, respectively. Their ratios were 0.712, 0.645 and 0.516, respectively. It can be seen that the ratios of the two areal mean precipitation depths and the storm centres were acceptable.

#### 6.2.5.5.2 Comparison with 24-hour PMP for mid-to large-scale water projects in China

According to the enveloping curve of the relationship between 24-hour PMP and area sizes for 44 mid- to large-scale water projects in China, the PMP value for area sizes equal to that of the Daguangba watershed is 720 mm. The ratio between the 24-hour PMP value for Daguangba and the corresponding enveloping value is 1.22. Given 24-hour storm records in the Changhuajiang River basin, such a case is likely to occur.

#### 6.2.5.5.3 Comparison with generalized PMP for the Gulf of Mexico coast in the south-eastern United States

The depth-area relationship of generalized PMP for the Gulf of Mexico coast in the south-eastern United States (Schreiner and Riedel, 1978) reflects PMP for non-orographic regions in the area. This relationship and the 24-hour PMP for the same area in the Daguangba watershed are slightly larger than the 24-hour convergence-component PMP in the Daguangba watershed, with a ratio of about 1.09 between the two. The former is a value on storm areas, while the latter is a value on watershed areas, which gets smaller due to the effects of residual rains. Therefore, it may be believed that 24-hour PMPs for the two regions are equivalent.

### 6.3 CAUTIONARY REMARKS

The procedures for estimating PMP were developed originally for temperate latitudes. Most studies have been completed for basins in these latitudes. The procedures have recently been applied to tropical regions. The procedures have not been as thoroughly tested for these regions. The user, therefore, should exercise care in applying these procedures directly. Much is still to be learned about developing PMP estimates in tropical regions. The user should also review the cautionary remarks and notes in Chapters 2 to 5. The comments on adequacy of storm sample, length of record, comparison with record rainfalls, consistency of estimates and other factors apply equally in tropical regions.

## CHAPTER 7

# ESTIMATION OF PMP USING THE WATERSHED-BASED APPROACH AND ITS APPLICATION IN CHINA

### 7.1

#### INTRODUCTION

As mentioned in section 1.4.2, there are two approaches and several methods that can be used for probable maximum precipitation (PMP) estimation. Examples presented in this chapter use the watershed-area based approach developed in China (Wang G., 1999). As discussed in section 1.1, the objective of estimating PMP is to determine the probable maximum flood (PMF), which is critical for engineering design purposes of a specific project. For example, in the case of a reservoir with a large storage capacity and a small flood discharge capability, the flood volume is critical to the design of the project. In this case, the critical PMF is usually of long duration, and the associated weather system supplying the corresponding PMP might typically be a cluster of frontal cyclones over a long duration. If a reservoir has a small storage capacity and a large flood discharge capability, the critical factor is that the peak flow has a shorter duration and the associated meteorology generating the PMP may be a single weather system, such as a tropical cyclone and thunderstorm, of short duration and high intensity. It is thus important to be aware of the critical events for the specific watershed.

The Ministry of Water Resources (MWR; 1980) and the Changjiang Water Resources Commission (CJWRC; 1995) present watershed-area based methods of estimating PMP for PMF requirements associated with a particular project in the design watershed. Detailed discussions of these methods are also available in other literature (for example, Zhan and Zhou, 1983; Wang G., 1999). The WMO report *Estimation of Maximum Floods* (1969a) establishes the basis for many of the ideas presented here in sections 7.5, 7.6, and 7.7.

### 7.2

#### OVERVIEW OF THE APPROACH

##### 7.2.1

##### Main characteristics

There are five main characteristics of this approach:

- (a) All calculations, including the areal mean precipitation depth and its spatial and temporal distributions, are derived specifically for the design watershed.

- (b) All significant historical storm and flood data over the available period are obtained through field surveys and from the literature.
- (c) The most appropriate method and storm (for example critical duration, type) for estimating the storm rainfall is determined.
- (d) More than one method is applied to determine a range of reasonable results (advisable).
- (e) Finally, the reasonableness of results are assessed to ensure the resulting estimates are realistic.

##### 7.2.2 Process

The sequential process for determining PMP/PMF is shown in Figure 7.1. This chapter focuses on presenting the local model method (local storm maximization), the transposition model method (storm transposition) and the combination model method (spatial and temporal storm maximization). These methods are applicable to PMP estimation under different orographic conditions and with different precipitation durations in medium and large watersheds. The rational method (the theoretical model) is applicable only to small and medium areas and is not discussed here.

##### 7.2.3

##### Project characteristics and design requirements

The PMF information required for typical project designs include three key factors: the flood peak, flood volume and flood hydrograph. Different projects, however, focus on different aspects: for reservoirs with small storage capacities and large discharges the flood peak is critical; for reservoirs with large storage capacities and small discharges, the flood volume is critical; and for reservoirs with small storage capacities and small discharges, all three factors are important. Consequently, the relevant information on the planned project should first be assessed in order to select the right method for estimating PMP as well as the critical extraordinary storms/floods.

##### 7.2.4

##### Analysis of watersheds, characteristics of storms and floods, and meteorological causes

The objective of this analysis is to determine the types and behaviour of systems that generate storms and floods in the design watershed to assist with

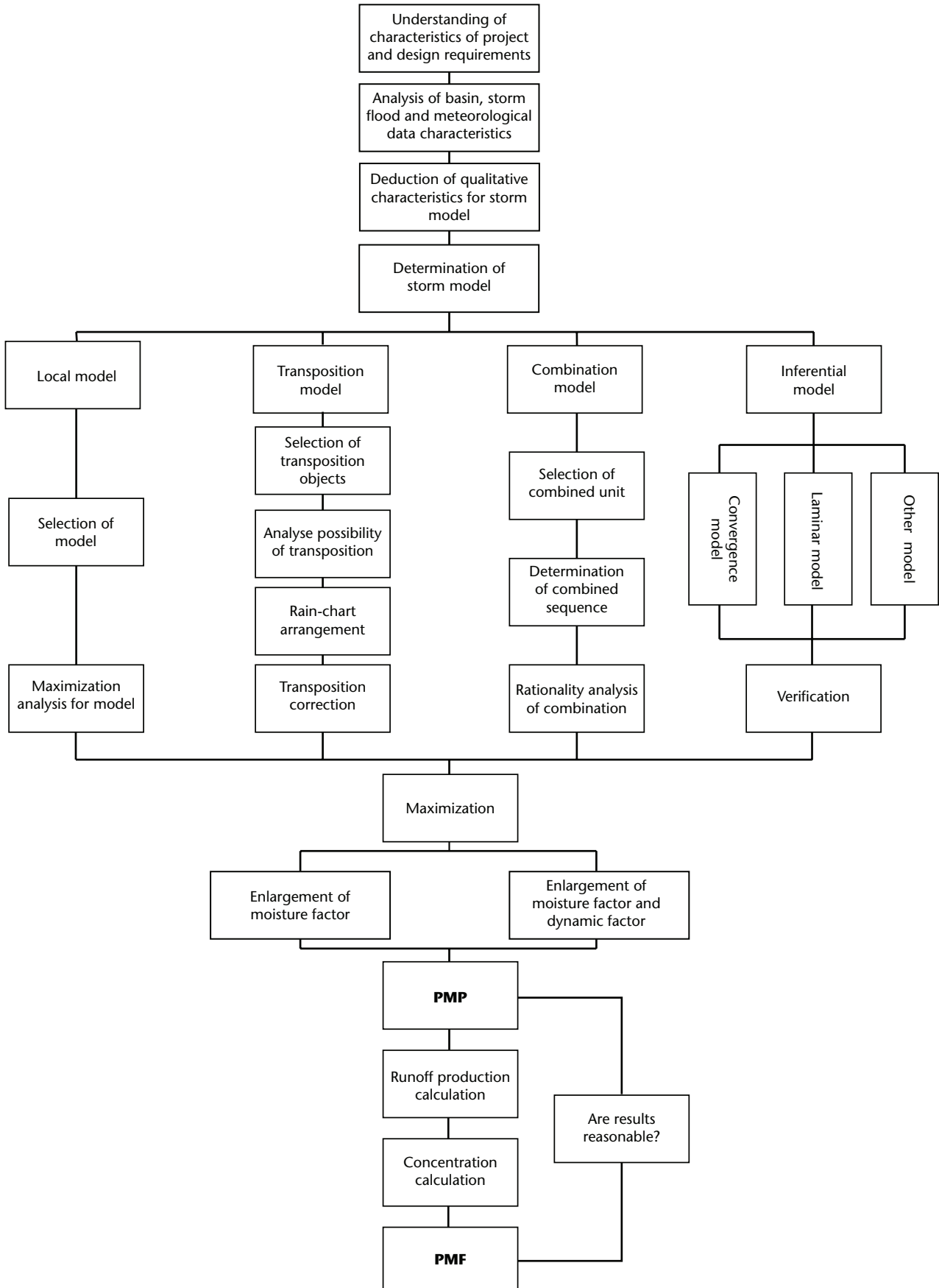


Figure 7.1. The process for PMP and PMF estimation (Wang G., 1999)

determining the right PMP estimation method, and to check the accuracy of the resulting estimates. The analysis covers: geographic, orographic and climatic conditions; basic types of storms and floods; the synoptic causes of storms/floods; and the characteristics of their spatial and temporal distribution in the watershed.

Geographic, orographic and climatic conditions combine to provide the macroscopic background for the formation of storm and floods.

It is important to know what types of storms and floods occur in the design watershed so that the qualitative characteristics of storm models can be deduced through a comprehensive analysis based on the design requirements of a particular project.

## **7.2.5 Deducing qualitative characteristics of storm models**

### **7.2.5.1 Importance of correct storm model**

The method used to determine PMP introduced in this chapter is maximization. There are two key issues here: the first is determining the storm models and the second is selecting parameters of maximization. The first part is critical since it forms the basis of the study. Choosing the storm model correctly means that the physical basis for the PMP/PMF required in a particular project is sound, thereby increasing the reliability of the PMP/PMF results.

### **7.2.5.2 Qualitative characteristics**

Qualitative characteristic assessments of PMP storm models should include three points: the occurrence season of the storm; the type of significant weather generating the storm, including the circulation type and the storm weather system; and details for the storm, including the duration, temporal distribution, isohyetal distribution, storm area and location of the storm centre.

### **7.2.5.3 Methods for determining characteristics**

An understanding of the required characteristics of the PMP storm models can be obtained by considering the design requirements of the project, data about the relevant significant weather systems, observed storms and floods in and around the design watershed – both surveyed and recorded in literature, as well as the characteristics of the watershed. Specific details are presented in the following example.

## **7.2.5.4 Example of qualitative characteristic analysis – San-Hua region, China**

Methods of deducing qualitative characteristics of storm models are explained for the San-Hua region – a watershed area of 41 615 km<sup>2</sup> between Sanmenxia and Huayuankou on the Yellow River (Wang G., 1999) are outlined in this section.

### **7.2.5.4.1 Analysis based on project requirements**

Analysis of PMF in the San-Hua region aims to provide a hydrological basis for the arrangement of a flood-control system in the lower reaches of the Yellow River. In this region, floods with high peaks and large volumes are critical to flood control. According to historical analyses, it is the flood peak and the flood volume over a duration of 5 days that is critical for this project.

### **7.2.5.4.2 Analysis based on flood data observed in the watershed**

Collection of flood data in the San-Hua region started in 1919. According to statistical data, large floods occurred in 1937, 1954, 1957, 1958 and 1982. These can be categorized as midsummer longitudinal type floods (1937, 1954, 1958 and 1982) and a midsummer latitudinal type flood (1957) according to the circulation type, the weather system responsible for the storm and the storm area distribution.

The midsummer longitudinal type floods are formed by storms that are caused by north-south shear lines, sometimes interacting with a typhoon to produce high peaks and large volumes. When such storms happen, the maximum 1-hour rainfall often exceeds 100 mm, and the 24-hour rainfall exceeds 700 mm, with the storm area in a longitudinal, elongated, narrow distribution. The storm area typically extends to the middle and upper reaches of the Huaihe River in the south and to the lower and middle reaches of the Fenhe River in the north, spanning the entire watershed of the San-Hua region longitudinally. In the San-Hua region, the storm centre is often over the middle and upper reaches of the Yihe River and Luohé River, the lower and middle reaches of the Qinhe River, or in the region between Sanmenxia and Xiaolangdi along the main branch of the Yellow River. The duration of precipitation for such a storm might be around 7 days, while the main burst duration associated with the storm (the areal mean rainfall is 50 mm or greater in the San-Hua region) is approximately 3 days. Such storms often occur in July and August when the watershed is already wet from previous rains.

#### 7.2.5.4.3 *Analysis based on flood data in the watershed, both surveyed and recorded in literature*

There is a great deal of literature on rainfall and floods in the San-Hua region over the past 2,600 years. The region is in the heartland of China, and since 770 B.C., nine dynasties have had their capitals located in Luoyang, an ancient city in the region. Since 1953, many flood surveys for the main rivers and tributaries in the region have been carried out, yielding a great deal of valuable data. Based on this record, extraordinary floods occurred in the San-Hua region in 184 B.C., and 223, 271, 722, 1482, 1553 and 1761 A.D.

According to the available literature, these historical floods can be categorized into two types, similar to those from recent years. The longitudinal type storms feature longer durations, higher intensities and wider storm areas. For example, the flood of 1761 was similar to 1958 and 1982. Its characteristics were as follows (for details see Wang G., 1999, pp. 112–113):

- (a) Precipitation duration was approximately 10 days.
- (b) The within-storm burst associated with the storm was approximately 5 days.
- (c) The 5-day storm had two peaks, with the smaller one preceding the larger one. The information was obtained from an extensive historical study.
- (d) The storm area was spatially distributed along a meridional, elongated, narrow region. From an extensive literature review, the synoptic situation was categorized as a longitudinal midsummer type in terms of the circulation type, and north-south shear lines in terms of the storm weather system.

Analysis based on available literature shows that the peak flood for the 1761 Yellow River event was about 30 000 m<sup>3</sup>/s in Heigangkou and rose to 32 000 m<sup>3</sup>/s in Huayuankou, of which 26 000 m<sup>3</sup>/s was from the San-Hua region. The recurrence period for an event of this magnitude was estimated to be in excess of 400 years.

#### 7.2.5.4.4 *Analysis based on data on extraordinary floods in similar neighbouring watersheds*

According to flood data observed along the Haihe River, a neighbouring watershed, extraordinary floods in the Haihe River watershed have characteristics similar to those in the San-Hua region. An

example is the catastrophic cloudburst on the Haihe River on 1–10 August 1975. Its circulation type was the longitudinal midsummer type; the storm weather system was a northerly trough and a southerly vortex followed by north-south shear lines; the storm area was distributed like a longitudinal belt. The precipitation duration was 10 days, with most of the rainfall falling in 7 days (3–9 August).

#### 7.2.5.4.5 *Analysis based on watershed characteristics*

With a watershed area of 41 615 km<sup>2</sup>, the San-Hua region is located at 110–114° E and 34–37° N, and is between the two main plateaus of China. The terrain varies greatly in the watershed: there are mountains in the north, west and south and an opening in the east that acts like a funnel. The Yellow River runs through from west to east. The main river branches in the region include the Yihe River and the Luohe River in the south and the Qinhe River in the north.

The terrain in the San-Hua region favours moisture inflow from the south-east. The funnel-like ascending terrain in the region assists with the formation of intense, large storms. The shape of the watershed in the San-Hua region looks like a butterfly flying eastward (Figure 7.2). Storms formed by north-south shear lines can cover the entire watershed, thus facilitating the formation of large floods.

Meanwhile, the observed data show that centres of storms formed by north-south shear lines occur mostly in mountainous areas, where conditions for runoff yield and concentration further facilitates the formation of large floods.

#### 7.2.5.4.6 *Analysis based on the synoptic situation*

Generally speaking, the basic characteristic of the longitudinal midsummer type system is that meridional circulations dominate in mid-and high-latitude regions in Asia, such that southerly flow (warm and wet) and northerly flow (cold and dry) interchange, leading to storms with large areas, high intensities and long durations.

Specifically in this situation, the east of northern China and the Sea of Japan are both under the influence of stable subtropical anticyclones and the eastward movement of westerly troughs is hampered (between 850 hPa and 700 hPa). There is strong southerly flow bringing warm, moist air on the west side of subtropical anticyclones. Influenced by such circulation, north-south shear lines appear frequently in the San-Hua region. To the east of the

San-Hua region (see Figure 7.3: the San-Hua region is located in the middle of the shaded area), the south-eastern wind prevails, and the topography of the San-Hua region is such that the elevation increases gradually from east to west, and thus enables the lifting of the warm and wet air mass, and also the formation of heavy rainstorms.

The above six key points are summarized in Table 7.1, which shows the required characteristics for storm models of PMP/PMF in the San-Hua region. Only a flood derived from the PMP that is determined using storm models with these characteristics is the high-peak and large-volume PMF that meets design requirements of the project.

#### 7.2.5.5 Similar work in other countries

Most practices in other countries for estimating PMP require the qualitative assessment of characteristics of storm models. For example, in Hydrometeorological Report (HMR) No. 46, the United States transposed typhoon rainstorms in the south-eastern coastal region of the country to the Mekong River basin for PMP estimation (United States Weather Bureau, 1970, 6.2.2). In HMR Nos 55A, 57 and 59, storms are categorized into local and general storms and PMP estimation is performed using generalized estimation (Hansen and others, 1988, 1994; Corrigan and others, 1998).

The Australian Bureau of Meteorology also categorizes storms according to duration and location, and uses different models for each in PMP studies. It formulated the Generalized Short Duration Method (GSDM; Australian Bureau of Meteorology, 1994) for short duration storms (less than 6 hours). Furthermore, it separates longer duration storms into tropical weather systems and subtropical weather systems and applies different generalized approaches to each. For storms occurring in the region of Australia where tropical storms are the most significant, the Generalized Tropical Storm Method (GTSM), revised in 2003, is applied (Walland and others, 2003). In regions where a subtropical weather system is the most significant rain-producing system, the Generalized Southeast Australia Method (GSAM) is applied (Minty and others, 1996).

In studies of PMP for the Indus River basin, Pakistan, the PMF for the basin can be deduced from observed data. Essentially, it has been determined that PMF results from tropical depressions in the Bay of Bengal, and the time the PMF is most likely to occur is between mid-August and late September.

In one case of PMP estimation in Korea, four typhoon rainstorms are selected for generalized studies, since extraordinary storms and floods in the country are caused by typhoons (Kim and others, 1989).

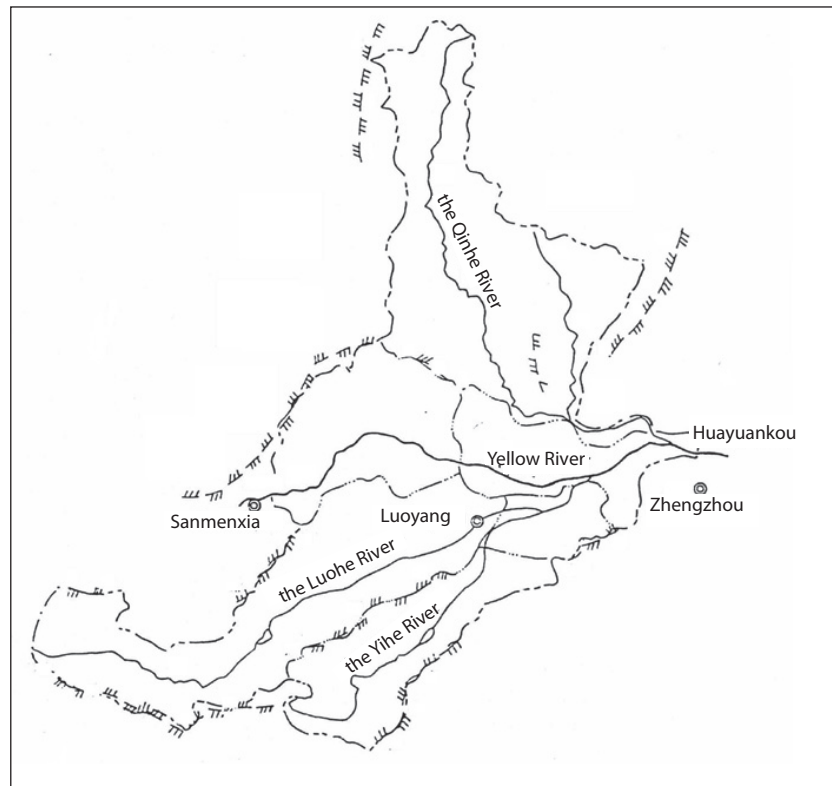


Figure 7.2. Diagram of the shape of the San-Hua region watershed on the Yellow River (Wang G., 1999)

**Table 7.1. Qualitative characteristics of PMP storm model in the San-Hua region of the Yellow River**

No.	Description	Characteristics	
1	Season the storm occurred	July–August	
2	Weather cause	Atmospheric circulation type	Meridional midsummer
3		Storm weather system	Taking north–south shear lines as the dominant factor
4		Rain field distribution type	North–south strip distribution
5		Scope of rain field within the basin	Widespread precipitation within the San-Hua region basin
6	Rain type	Location of centre of storm	<p>Yiluhe River Middle reaches</p> <p>Qinhe River Middle reaches</p> <p>Mainstream reach Sanmenxia-Xiaolangdi region</p>
7	Precipitation duration	Continuous precipitation	Approximately 10 days
		Storm duration	5 days
8	Storm temporal distribution type	Double and main peaks appear later	

### 7.2.6 Comprehensive analysis using multiple methods

There are many methods available for determining PMP for the design watershed. The most common include the local model, the transposition model and combination model methods. For large watersheds, the major temporal and spatial combination method and storm simulation method based on historical flood are used for determining PMP.

Each method has its own theoretical basis as well as advantages, disadvantages and applicable conditions. Moreover, each method provides further options (for example: several typical storms or maximization methods are available for the local model method; the transposition model method can use several storms for transposition; the combination model method can use several combination methods). As a result, multiple methods or schemes, selected on data availability, should be used for comparative purposes. This will illuminate inconsistencies or contradictions. Then, a comprehensive analysis should be performed on results obtained from each method or scheme, enabling rational selection of PMP/PMF results to be used in the project design. Such a practice can also avoid the bias of results obtained with a single method or scheme, hence avoiding the situation in which the PMP/PMF result is underestimated.

The principle of “multiple methods, comprehensive analysis and rational selection” should be encouraged for hydrological engineering calculations.

### 7.2.7 Realistic results check

Methods for checking whether PMP/PMF results are realistic include the following six steps. The first two steps must be followed, but the remaining four steps are optional depending on data availability.

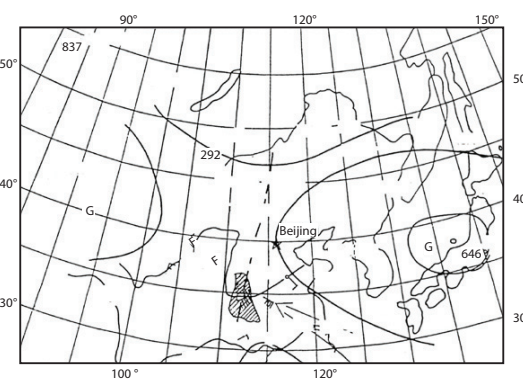


**Figure 7.3. Generalized 700-hPa storm effect system map for 8 p.m. (Beijing time) 16 July 1958 in the catastrophic cloudburst period in the San-Hua region on the Yellow River (Wang G., 1999)**

### 7.2.7.1 Checking each step

Basic data and the processing and applicability of methods used should be checked thoroughly during each step of the calculation process.

The representation and reliability of the basic data should be checked, including the uncertainty/error introduced through any analysis techniques. It is important to ascertain whether data on extraordinary storms/floods in and around the design watershed were available and taken into account.

It is also important to check that an appropriate model storm is used for the region and project in question. For local models, the check should ensure that the model storm represents the largest possible storm of this type for this region. For transposition models, the check should focus on the limits of where a storm could realistically be transposed and, in particular, the orographic correction applied. For combination models, the check should focus on the appropriateness of the combination schemes.

For the maximization process, the check should focus on the applicability of the methods for maximization and whether the selection of maximization parameters is reasonable.

For PMF, the check should focus on whether the selection of methods and parameters for the calculation of runoff yield and concentration is reasonable. In addition, attention should be paid to whether there are risks of dam breaks as well as overflows and bursts at dykes along the river when the water level is high.

### 7.2.7.2 Comparison with historical extraordinary storms/floods in the watershed

For a particular watershed, the probability of extraordinary storms/floods occurring is small in any short period of time. However, the probability becomes much larger over a long period of time. It is thus reasonable to assume that for any particular watershed or station, the longer the historical record and assessment of storms and floods, the closer the estimated maximum design value will be to reality. PMP/PMF estimates can be compared with data on historical extraordinary storms and floods (inclusive of those observed, surveyed or recorded in literature) for the watershed. Clearly, the total rainfall for the PMP estimate and the flood peak and flood volume of PMF should not be less than those of extraordinary storms and floods that have happened in the history of the watershed.

Nonetheless, in areas with a long historical record, PMP/PMF should also not be excessively large when compared with historical extraordinary storms/floods. Whilst it is most unlikely that a PMP will have occurred in the watershed, extraordinary storms and floods should provide some guidance of what is possible. This statement will clearly become more appropriate the larger the area of transposition or the longer the historical record of data. In China, where records are commonly available for a period of approximately 600 years, observed estimates generally begin to converge towards the PMP (Wang G., 1999).

### 7.2.7.3 Comparison with adjacent watersheds

For a particular period of record, the probability of the occurrence of large storms/floods for a given watershed is small, but the probability increases if a wider area is considered, for example, a region having similar characteristics to the design watershed. In regions with similar geographical characteristics, the larger the region of reasonable transposition of storms and floods, the closer the results will be to the actual PMP. Therefore, PMP/PMF results should be compared with those derived in adjacent watersheds.

If PMP/PMF estimates are available for adjacent watersheds, these results can be compared with the design watershed to see whether there is general agreement.

### 7.2.7.4 Comparison with historical estimation results

If PMP/PMF estimates are available from previous studies in the watershed or region, current estimates can be compared with those. The comparison should highlight the differences in terms of data and methods of estimation. It should then be possible to rationalize the new PMP/PMF estimates with the changes in current procedure, for instance PMP estimates may have increased due to the application of a generalized method as opposed to a local storm approach, which may have incorporated new data on significant storms not within the immediate region. In such a case, it is anticipated and quite acceptable that the estimates would increase.

### 7.2.7.5 Comparison with worldwide storm and flood records

Worldwide storm and flood records may be used to approximate PMP/PMF. It would be surprising, therefore, if PMP/PMF estimates, assuming a

comparable watershed, were significantly beyond the enveloped curve.

According to PMF analysis on more than 600 projects in the United States, attached to the 1977 edition of the *Guide to Regulations* issued by the Nuclear Regulation Commission (NRC), the enveloping curve of peak floods in the country has not exceeded the worldwide flood record (Wang G., 1999).

#### 7.2.7.6 Comparison with results of frequency analysis

Storm and flood frequency analysis is an important approach for determining a design flood; the extreme values may be compared with PMP/PMF results.

The precondition for such a comparison is that the data series for the frequency analysis is long (typically more than 50 years). Furthermore, it should be representative of long-term streamflow characteristics.

Meanwhile, care should be taken when selecting the frequency model and method for parameter estimation.

Strictly speaking, the estimated storm/flood with a low frequency of occurrence and PMP/PMF are obtained by two different approaches and both have errors, so no fixed relationship between the two is likely to exist. As a result, it should not be a requirement that PMP/PMF should be larger than or smaller than a storm/flood with a defined frequency. As long as data and processes in each key step are reasonable throughout the analysis and calculation of PMP/PMF, the value should be regarded as being reasonable even if it is less than a 1 000-year storm/flood (Wang G., 1999).

#### 7.2.7.7 Similar work in other countries

In HMR Nos 55A, 57 and 59 (Hansen and others, 1988; Hansen and others, 1994; Corrigan and others, 1998), PMP estimates were compared with large storms observed in the region, PMP in adjacent regions, historical PMP estimates and the 100-year rainfall in the region, in the United States. In HMR No. 55A (Hansen and others, 1988) and HMR No. 59 (Corrigan and others, 1998), PMP results were compared with the PMP of local storms and general storms.

In estimating the PMP/PMF of the Indus River basin, Pakistan, statistical checks were used to assess the relative magnitude of the PMF estimates. The

frequency analysis indicated that the PMF of the basin was not far from a 200-year flood, raising concerns that the PMF was underestimated.

### 7.3 LOCAL MODEL METHOD

#### 7.3.1 Applicable conditions

If there is a long record of rainfall data available for the design watershed, an individual significant storm could be selected to represent an efficient dynamic mechanism that could then be maximized to estimate PMP. This method is not appropriate when there is limited data, as the probability of identifying a storm representing the greatest possible rainfall is remote.

#### 7.3.2 Model selection

This process generally reduces to a search through observed storm data to identify the largest rainfall event with characteristics matching those required for a particular project (see Table 7.1 for an example).

#### 7.3.3 Model suitability analysis

An assessment of the selected storm is made to see how serious the resultant flood was compared with other floods in the watershed, particularly in terms of the flood control project (for example, the flood storage capacity needs to be large or the flood discharge capacity of the reservoir needs to be large).

#### 7.3.4 Model maximization

##### 7.3.4.1 Summary

If the selected storm is a high-efficiency storm, only moisture maximization is required. However, with limited data from which to select storms, local models do not always provide for high-efficiency storms and both the moisture factor and the dynamic factor need to be maximized.

To minimize subjectivity in maximizing the moisture and the dynamic factors, the 100-year value from a frequency analysis can be used. The selection of the frequency model in deriving the moisture and dynamic maximization factors does not tend to impact on the estimate of the PMP.

Observed data show that the relationship between the moisture factor and the dynamic factor for a storm is complex, and that they can almost be

regarded as independent. The probability of two independent events (each with a probability of 0.01) occurring simultaneously is 0.0001. Hence, the two factors are used to ensure the PMP represents very rare conditions.

#### 7.3.4.2 Selection of maximum moisture adjustment factor

An annual series of dewpoints corresponding to the largest storm in the watershed for each year in the record can be identified. The 100-year value of the dew point is used in the estimation of the PMP.

#### 7.3.4.3 Selection of maximum dynamic adjustment factor

##### 7.3.4.3.1 Methods for denoting the dynamic factor

There are many methods for denoting the dynamic factor. For example, the precipitation efficiency  $\eta$  (hereinafter called the efficiency), is a useful representation. It can be defined as follows (Wang G., 1999):

$$\eta = \frac{K_F(V_{12}W_{12} - V_{34}W_{34})}{W_{12}} \quad (7.1)$$

where  $K_F$  is the watershed constant;  $V_{12}$ ,  $V_{34}$ ,  $W_{12}$  and  $W_{34}$  are the wind speed and the precipitable water of the inflow and the outflow respectively (as shown in Figure 7.4).

This can be approximated by:

$$\eta = \frac{P}{W_{12}t} = \frac{I}{W_{12}} \quad (7.2)$$

where  $P$  is the watershed's average precipitation depth with duration of  $t$ ;  $I$  is the rainfall intensity.

Based on Equation 7.2, the efficiency is the precipitation-moisture ratio ( $P/W_{12}$ ) with duration of  $t$ .

##### 7.3.4.3.2 Advantages of the efficiency factor

(a) This representation of the dynamic factor is physically conceptualized clearly.

Equation 7.1 shows that the efficiency  $\eta$  is the ratio of the net moisture input to the design watershed per unit time ( $V_{12}W_{12} - V_{34}W_{34}$ ) and the precipitable water for the inflow,  $W_{12}$ . In other words, the efficiency is the ability of the storm weather system to convert the precipitable water of the inflow  $W_{12}$  into rainfall.

Equation 7.2 shows that the efficiency  $\eta$  is the ratio of the rainfall  $I$  amount in the design watershed per unit time and the precipitable

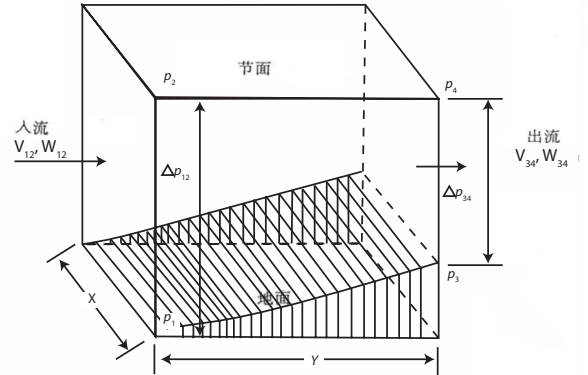


Figure 7.4. Watershed sketch

water for the inflow  $W_{12}$ . Essentially, it is also the ability of the storm weather system to convert the precipitable water of the inflow  $W_{12}$  into the rainfall  $I$ .

- (b) The efficiency calculation is based on the average rainfall amount in the watershed, as it is the only indicator that is able to indirectly reflect air convergence and vertical motion in the entire design watershed. Such an indicator is necessary as there are currently no methods of directly determining optimal air convergence or vertical motion.
- (c) Since the efficiency calculation is based on rainfall data and dewpoints observed at the surface, it is relatively easy to calculate to a high degree of precision. There are a large number of ground observation stations, where measurements are easily taken and there are long series of relatively high-precision data. Upper air data are measured with much greater difficulty and expense at a small number of stations and thus exhibit generally shorter series and lower precision.

##### 7.3.4.3.3 Selection of probable maximum efficiency

Based on storm and flood data observed in the design watershed, the efficiency of the storm resulting in the largest flood each year is determined. Then a frequency analysis is performed and the 100-year value is regarded as the probable maximum efficiency.

#### 7.3.4.4 Model maximization

The moisture maximization  $P_m$  follows the formula:

$$P_m = \frac{\eta_m}{\eta} \frac{W_{12m}}{W_{12}} \frac{S}{S'} \quad (7.3)$$

There are two methods of maximization, as follows:

- (a) The first method is the same-multiple maximization, that is, the entire storm process is maximized using the product of the efficiency ratio and the moisture maximization ratio in a particular time interval. The method is applicable to determining PMP for up to 12 hours.
- (b) The second method is the per-time-interval control and maximization, that is, the maximum efficiency in each time interval is found on the efficiency-time relation graph and then the control and maximization is performed for each time interval. The method is applicable to determining PMP for durations longer than 12 hours (Table 7.4 and 7.5).

### 7.3.5 Example calculations

An analysis using the same-multiple maximization method over the San-Hua region on the Yellow River is presented as an example.

#### 7.3.5.1 Deducing qualitative characteristics of PMP storm models

This step directly makes use of the results from 7.2.5.4, which are summarized in Table 7.1.

The storm duration is set to be 5 days.

#### 7.3.5.2 Model selection

The top three observed floods in the San-Hua region – occurring in August 1954, July 1958 and August 1982 – show similar characteristics as Table 7.1, so they can all be selected as representatives for the local model. The July 1958 storm, which formed the largest peak flood, is regarded as the main storm for the local model. The areal mean rainfall amount of the 5 days is shown in Table 7.2.

The storm has a recurrence period of about 50 years, so it is not a high-efficiency storm. As a result, the moisture factor and the dynamic factor both need to be enlarged.

#### 7.3.5.3 Selection of dewpoints

Dewpoints representative of the storms are selected and traditional methods are used to calculate the average moisture from the stations on the inflow side of the storm, just at its edge.

The representative dew point (1 000 hPa) of the July 1958 storm is 24.4°C.

#### 7.3.5.4 Calculating the efficiency of the typical storms

The daily maximum precipitation efficiency in the San-Hua region is calculated using Equation 7.2. The average elevation of the San-Hua region watershed is 655 m (194 grid points are calculated). The calculated efficiency is 3.35 %/h (Table 7.3).

#### 7.3.5.5 Determining maximization parameters

Since data on storms observed in the San-Hua region are not adequate, frequency analysis methods are used to determine the probable maximum moisture and dynamic factors.

After calculation, the average of representative dewpoints of the storms is 24.1°C, the coefficient of variability  $C_v$  is 0.04, the deviation coefficient  $C_s$  is  $2C_v$  and the 100-year value is 26.5°C. The average daily maximum efficiency is 2.46 %/h,  $C_v = 0.50$ ,  $C_s = 3C_v$  and the 100-year value is 6.60 %/h.

#### 7.3.5.6 Calculating maximization amplification

The calculation of moisture amplification  $K_W$ , efficiency amplification  $K_\eta$ , and a combined amplification  $K_{W\eta}$  is shown in Table 7.4.

#### 7.3.5.7 Maximizing typical storm

To get the 5-day PMP for the San-Hua region watershed use the joint maximization amplification of moisture and efficiency  $K_{W\eta} = 2.37$  (Table 7.4) to maximize daily rainfalls (Table 7.2) of the selected typical storm (Table 7.5).

Note that the same calculations were done on the 1954 and 1982 typical storms but these are omitted here.

**Table 7.2. The areal mean rainfall amount of the July 1958 storm in the San-Hua region on the Yellow River**

	Date (in July 1958)					Total
	14	15	16	17	18	
Rainfall amount (mm)	7.2	34.1	61.7	13.1	30.0	146.1

**Table 7.3. Table of calculation of efficiencies of the July 1958 typical storm in the San-Hua region on the Yellow River**

Daily maximum rainfall		1 000-hPa dewpoint $T_d$ ( $^{\circ}$ C)	Precipitable water $W$ (mm)			Efficiency $\eta$ (%/h)	
$P$ (mm)	$I$ (mm/h)		1 000 hPa – 200 hPa	1 000 hPa – 655 m	655 m – 200 hPa	1 000 hPa – 200 hPa	655 m – 200 hPa
(1)	(2)	(3)	(4)	(5)	(6) = (4) – (5)	(7) = (2)/(4)	(8) = (2)/(6)
61.7	2.57	24.4	76.8	13.5	63.3	3.35	4.06

**Table 7.4. Calculation of moisture and efficiency amplifications of the July 1958 typical storm in the San-hua Region on the Yellow River**

Case	1 000 hPa dewpoint $T_d$ ( $^{\circ}$ C)	Precipitable water $W$ (mm)		Efficiency $\eta$ (%/h)		Amplification		
		1 000 hPa – 200 hPa	655 m – 200 hPa	1 000 hPa – 200 hPa	655 m – 200 hPa	$K_w$	$K_\eta$	$K_{w\eta}$
(1)	(2)	(3)	(4)	(5)	(6)	(7) = 76.5/63.3	(8) = 7.94/4.06	(9) = (7) × (8)
Design	26.5	92.0	76.5	6.60	7.94	1.21	1.96	2.37
Typical	24.4	76.8	63.3	3.35	4.06			

## 7.4 TRANSPOSITION MODEL METHODS

### 7.4.1 Applicable conditions

This method is applicable to cases in which data on an extraordinary storm observed are available for regions around the design watershed. The rainfall and the spatio-temporal distribution of the storm are moved to the design watershed with necessary corrections (adjustments). It is then used as a typical storm, which is maximized properly to determine PMP.

### 7.4.2 Selection of transposed storms

The selection of transposed storms should follow the conclusions (Table 7.1) of the analysis on qualitative characteristics of PMP storm models in the design watershed as outlined in section 7.2.5. Here, the focus should be on weather causes.

In deducing qualitative characteristics, if the conclusion is, for example, that the weather system of PMP is typhoons, the transposed storms should be selected from typhoon rainstorms. Likewise, if the deduced weather system of PMP is the frontal surface or the shearing vorticity, then the transposed objects should be selected from frontal storms or shearing vorticity storms.

### 7.4.3 Transposition possibility analysis

Transposition possibility analysis forms the basis of storm transposition. In generalized estimation, there are two methods for solving transposition possibility issues: the first is compartmentalizing meteorological homogeneous zones; the second is performing studies for specific extraordinary storms and determining their transposable ranges, that is, drawing transposition borderlines (Hansen and others, 1988). When performing PMP estimation for a particular design watershed, any research results associated with the above two methods should be utilized; if there are no such results, specific analysis on the design watershed needs to be done. The transposition possibility problem is solved by analysing and comparing similarities – in terms of climate, weather, geography and topography – between the design watershed and the

**Table 7.5. Five-day PMP in the San-Hua region on the Yellow River**

	Duration (days)					Total
	1	2	3	4	5	
Areal mean rainfall (mm)	17.1	80.8	146.2	31.0	71.1	346.2

transposed object region; the greater the similarity, the higher the transposition possibility, and vice versa (Wang G., 1999).

#### 7.4.3.1 Comparison of geographical and climatic conditions

This comparison focuses is on differences between the two regions in terms of geographical location (latitude) and distance to the sea. If the two regions are close to each other geographically, they will have similar climatic and moisture conditions. Separate analysis can be performed to confirm whether climatic and moisture conditions are similar. If geographical conditions (the same latitude belt) and climatic conditions (the same climatic characteristics, especially the annual precipitation and the annual distribution) are similar, the distance of transposition can be widened.

#### 7.4.3.2 Comparison of orographic conditions

The orographic characteristics of the regions should be assessed, followed by a comparison of the two regions' orographic characteristics to establish if they have similar orographic conditions.

When storm weather systems cross high mountains the moisture and dynamic conditions change. Therefore, storm transposition should avoid going across high mountains. Transpositions with an elevation difference greater than 800 m should be avoided in most cases (see section 2.6.3). The elevation difference of the transposition of strong local thunderstorm rains or typhoon storms can be determined through analysis of the storm path. Where there are high mountains, transpositions can be performed along mountain ridges.

Terrain in orographic regions is usually complex and has a variety of impacts on the weather systems. In addition, the impact of terrain on precipitation works best under favourable weather system configurations. Therefore, specific analysis should be performed on specific conditions when determining the transposable elevation difference.

To study if the terrains in two regions are different enough to cause great changes in weather systems and storm structures, comparison of 3-D spatial structures of similar weather systems in the two regions can be analysed, or the actual rainfalls of similar weather systems in the two regions can be assessed. Orographic corrective calculations are performed to account for the degree of the orographic effects.

#### 7.4.3.3 Comparison of spatio-temporal distribution characteristics of storms (floods)

The characteristics of transposed storms – such as storm season, duration, temporal distribution as well as the range and distribution of the storm area – should be compared with the same characteristics of large storms that have occurred in the design watershed.

Such analysis should be based on historical records from the design watershed and data from historical extraordinary storm floods surveyed in the field. Historical extraordinary storms with characteristics very similar to those of the transposed storms can usually be found in the watershed.

In addition, in cases where the design watershed and the transposed storm are adjacent, analysis on the contemporaneity of storms and floods can be performed. In other words, observed data and literature can be checked to see if large storms and floods occurred simultaneously (or almost simultaneously) in the two regions. If this is the case, it suggests that storms caused by weather systems of the same type are likely to occur simultaneously in the two regions.

#### 7.4.3.4 Comparison of weather causes

Storms should be analysed to verify that weather conditions similar to those of the transposed storms have occurred or can occur in the design watershed. If similar storms have occurred, then the transposed storms can occur in the design watershed, and can be transposed. Analysis of the weather related similarity of the transposed storms and design watershed storms focuses mainly on examining historical weather maps to see if the two storm sets are similar in terms of circulation types and weather systems.

Similarities between weather causes of historical floods and storms in the transposition source region and the transposition destination region can be indirectly determined through storms and floods recorded in literature. This includes records about storms, floods and weather conditions such as high temperatures, droughts and winds in related regions.

#### 7.4.3.5 Comprehensive judgement

The above-mentioned four comparisons should not be treated separately. They should be extensively considered together, based on principles of synoptic meteorology and analysis of weather maps.

#### 7.4.4 Spatial distribution of rainfall map

Spatial distribution of rainfall is the process of moving the isohyetal map of the transposed storm to the design watershed.

Specific operations begin by analysis of the spatial distribution of actual storms. Existing data on storms in the design watershed (observed, surveyed or recorded in literature) are used to find general rules regarding the locations of centres and axials of storms that are similar, in terms of weather causes, to the transposed storm. These are then adjusted to fit the project.

Transposition of isohyetals should fit into the large-scale terrain of the design watershed. The storm centre should fit into small-scale terrains (such as river mouths).

#### 7.4.5 Transposition adjustment

Transposition adjustment is the quantitative estimation of rainfall changes caused by differences between the design watershed and the transposed storm region, in terms of conditions such as regional shapes, geographical locations and terrains. Methods of orographic adjustment vary with orographic conditions.

##### 7.4.5.1 Common methods

Transposition adjustments can be performed with methods introduced earlier in the manual. In this section, the comprehensive orographic correction method applicable to storm transpositions in orographic regions (Wang G., 1999) is the focus.

##### 7.4.5.2 Comprehensive orographic correction method

In this method, storms in orographic regions are represented in two parts – weather system rains (weather system convergence components) and orographic rains (orographic convergence components).

Given that the weather system rain remains the same before and after the transposition, and the post-transposition efficiency increment is the difference between the orographic rains in the two regions, then the post-transposition rainfall equals the original storm weather system rain with moisture correction plus the orographic rain in the design region, that is:

$$R_B = \frac{W_B}{W_A} (R_A - R_{Ad}) + R_{Bd} \quad (7.4)$$

where  $R_A$  and  $R_B$  are the total rainfall of the transposition source region and the design region, respectively;  $W_A$  and  $W_B$  are the precipitable water of the transposition source region and the design region, respectively;  $R_{Ad}$  and  $R_{Bd}$  are the orographic rains of the transposition source region and the design region, respectively.

$R_{Ad}$  and  $R_{Bd}$  are based on a full analysis of the regions' topographic effects on precipitations. They should be estimated using proper methods selected according to meteorological, topographic and rainfall data conditions. Existing methods for determining orographic rains may be conducted through either of two approaches – empirical comparison and theoretical computation – in order to make mutual comparisons and reasonable selections.

The empirical comparison approach involves comparing the rainfalls in the plains and the mountainous regions, respectively, and comparing the topographic profile and the rainfall profile.

##### 7.4.5.2.1 Comparing the rainfalls in the plains and the mountainous regions

Rainfalls are different in plains and mountainous regions covered by the same weather system. The difference in the mean rainfalls between the regions can be viewed as caused by topography.

Let the mean rainfall of the stations in the plain be  $\bar{R}_p$  and the mean rainfall of the stations in the mountainous region be  $\bar{R}_s$ , then the orographic rain  $\bar{R}_d = \bar{R}_s - \bar{R}_p$ . Note that the selected groups of stations must be representative of the regions.

This method typically applies to the separation of orographic rains for windward slopes.

##### 7.4.5.2.2 Comparing the topographic profile and the rainfall profile

As is shown in Figure 7.5, the rainfall profile curve rises along the real line to point *a* past the sharp growth point *c*, which is not far from the turning point of the topographic profile. The imagined plain rainfall profile is extended along the broken line according to the trend (gentle slope) of the plain rainfall distribution. It is assumed that the separated plain rainfall centre can be superposed with the observed rainfall centre. Hence, section *ab* in Figure 7.5 can be viewed as the value of the separated orographic rain. In this method, the assumption that the two centres can be superposed often brings errors.

In addition, different inflow directions will lead to different orographic rain values, so inflow winds must be analysed to find a reasonable major inflow wind direction. The method requires that rainfall data distributed along the elevation be available in the inflow direction.

Both  $R_{Ad}$  and  $R_{Bd}$  can be determined through the difference between average rainfalls of plains and orographic regions covered by the same weather system, or comparison between orographic profiles and rainfall profiles, or theoretical calculation approaches (Gao and Xiong, 1983).

For a comprehensive orographic correction method, calculations can also be based on grid points.

#### 7.4.6 Example calculations

The Yahekou Reservoir is located on the south-eastern slope of Funiu Mountains in the upper reaches of the Baihe River, Henan Province, China. It features a control area of 3 035 km<sup>2</sup>. To ensure the safety of the dam, PMP/PMF needs to be estimated. According to the analysis of data observed, surveyed and recorded in the literature, the PMP/PMF in the watershed should be caused by the penetration of typhoons from the West Pacific Ocean into the watershed under stable longitudinal circulation types. The critical precipitation duration is 3 days. For this example, the transposition model method needs to be used to determine PMP. Steps of analysis and calculation are as follows (CJWRC, 1995).

(a) Selecting the transposed storm:

A study of rainfall data observed over the past decades shows that in the upper reaches of the Huaihe River, more than 100 km east of the design watershed, a historically rare extraordinary storm occurred on 5–7 August 1975. The maximum 3-day rainfall reached 1 605 mm in Linzhuang, the storm centre, where the maximum 24-hour, 12-hour, 6-hour and 1-hour rainfalls were 1 060 mm, 954 mm, 830 mm and 173 mm, respectively. The storm was caused by a typhoon, which turned into a depression after landing. That storm was selected as the transposed storm.

(b) Transposition possibility analysis:

(i) Comparison of geographical and climatic conditions:

The Baihe River basin is near the region where the August 1975 storm occurred. At the same latitude, both regions fall into the northern subtropical monsoon climate zone. They are similar to each

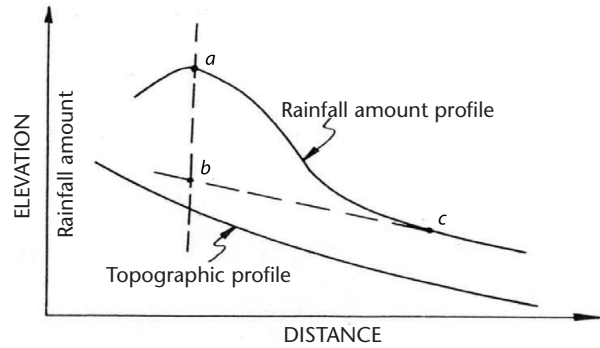


**Figure 7.5. Diagram of topographic and rainfall profiles**

other in terms of the annual rainfall, the annual number of days of precipitation and the annual number of days of storms. The main storm season is July and August. Both have a maximum absolute humidity of above 40 hPa, which means that they are both high-humidity regions. Therefore, the two regions are similar in terms of geographical location and share the same climatic background.

(ii) Comparison of weather systems:  
The August 1975 storm was primarily caused by typhoon no. 7503 turning into a stable thermal low. A study of typhoon path maps since 1884 showed that two typhoon paths passed Henan Province, in 1943 and 1944, both of which were more westerly than the path of the August 1975 typhoon, suggesting that typhoons are likely to reach the Baihe River basin. The basin and the August 1975 storm area are at the same latitude, where circulations are stable. Possible transposition relies on whether the storm can be successfully transposed 100 km west. According to experience in weather analysis, it is probable that the circulation of the August 1975 storm could have moved 100 km westward. In other words, if extraordinary storms occur in the Baihe River basin, their circulations can remain stable.

(iii) Comparison of orographic conditions:  
The August 1975 storm area was between plains and orographic regions. Linzhuang, the storm centre, is in an orographic belt that is surrounded by shallow mountains on three sides with an opening east to north-east. Such an orographic belt helps to draw in east to north-east air currents.

The orography in the upper reaches of the Baihe River was less favourable for the August 1975 typhoon system than it was for the August 1975 storm area. Nonetheless, there is no large orographic barrier higher than 1 000 m between the two regions, so transposition is possible. Orographic correction may be performed for the difference in orographic conditions.

(c) Spatial distribution of rainfall map:

The distribution is determined by placing the Linzhuang storm centre in a belt in the watershed where storms occur frequently and optimizing the amount of precipitation that would occur over the basin. This is achieved by turning the storm axis 20° clockwise. The measured 24-hour areal mean precipitation depth of the design watershed is 560 mm.

(d) Transposition correction:

Since the two regions are at the same geographical location and share the same moisture conditions, no location correction is needed. Barrier elevation correction is needed, since there are barriers with an average elevation of 800 m between the storm area and the design watershed, and the average elevation of the storm area is 200 m. A tracing of air particles tracks over the storm location shows that most of the moisture comes from the south-east. The average sea level 12-hour dew point of multiple stations on the south-eastern edge of the storm area (25.8°C) is selected as the representative dew point. The two regions share the same historical maximum dew point (28°C). The correction coefficient of barrier elevations is calculated as follows:

$$K_2 = \frac{(W_{Bm})_{ZB}}{(W_{Bm})_{ZA}} = \frac{(W_{28})_{800}}{(W_{28})_{200}} = \frac{105 - 20.0}{105 - 5.00} = 0.85 \quad (7.5)$$

where  $K_2$  is the water vapour corrected coefficient of elevation or inflow barrier elevation,  $W_{Bm}$  is the maximum precipitable water of the design watershed,  $( )_{ZB}$  is the surface elevation or barrier elevation of the design region, and  $( )_{ZA}$  is the transposed region surface elevation.

(e) Maximization calculation:

Since the August 1975 storm is a rare extraordinary storm, it may be regarded as a high-efficiency storm. Therefore, only moisture maximization is needed. Its maximum coefficient is given by:

$$K_3 = \left( \frac{W_{Bm}}{W_B} \right)_{200} = \left( \frac{W_{28}}{W_{25.8}} \right)_{200} = \frac{105 - 5.00}{86.6 - 4.80} = 0.85 \quad (7.6)$$

where  $K_3$  is the maximum coefficient, and  $W_B$  is the precipitable water of the design watershed.

After barrier correction and maximization, the comprehensive correction coefficient of the design watershed is:

$$K = K_2 \times K_3 = 0.85 \times 1.22 = 1.04 \quad (7.7)$$

The areal rainfall measured after the August 1975 storm multiplied by the above coefficient and transposed to the design watershed with its axis turned gives the required PMS.

#### 7.4.7 **Storm transportation for arid and semi-arid regions**

##### 7.4.7.1 **Storm characteristics**

The moisture content of sand is low and precipitation is scarce in arid and semi-arid regions, where storms show the following characteristics:

- (a) Storms of long durations and large areas have low frequencies. Meanwhile, storms of short durations and small areas have high frequencies and much sharper rainfall intensities, some of which even exceed those in humid regions.
- (b) Storms change greatly from year to year. Extraordinary storms seldom occur in long-term observations at stations. These storms are only occasionally observed at a minority of the stations and come with rare frequencies – the return periods can be from several hundred to ten thousand years.
- (c) Either the spatial or the temporal distribution of a storm is somewhat uneven. In addition, the station density is far smaller than in humid regions. As a result, it is hard to observe violent local storms of short durations, especially the storm centre.

Due to these characteristics, estimation of PMP for arid and semi-arid regions primarily depends on storm transposition (Wang Y. and Wang W., 2000).

##### 7.4.7.2 **Characteristics of PMP estimation**

- (a) Surveyed data on extraordinary storms should be used as control point data for extension and amplification.
- (b) There are large differences in terms of causes and characteristics between storms with long dura-

tions and large areas and those of short durations and small areas. They should be differentiated and analysed by area size of the design watershed. For example, if the area size of the design watershed is large, storms with long durations and large areas are selected. Differences between these two storm types are also large in terms of design duration and storm point area relationship. These characteristics should be taken into account when deducing the storm model and qualitative characteristics.

- (c) Local thunderstorms receive small effects from the topography and elevation and therefore have large transposable areas. According to some studies, they are usually transposable within an elevation difference of 1 500 m.
- (d) Both moisture and efficiency maximization should be carefully considered. Some extraordinary storms may be believed to have approached their highest efficiencies and only moisture maximization be needed. Individual storms on the enveloping curve of worldwide storms with the same duration need to be studied carefully to see if maximization is needed. In addition, the actual storm duration should be adopted instead of the standard duration when calculating the efficiency (Wang Y. and Wang W., 2000).

## 7.5 COMBINATION MODEL STORM METHOD

### 7.5.1 Applicable conditions

This method is applicable to cases where data on a number of observed large storms are available for the design watershed.

In this method, two or more storms are reasonably combined under principles of synoptic climatology and weather forecast experience to form a new sequence of ideal extraordinary storms, which are then used as typical storms to determine PMP.

The mode of combination is typically temporal, but may also be spatial when necessary, or both temporal and spatial. By temporal combination, rainfall processes of two or more storms are realistically linked together. While combining, a reasonable interval should be kept to enable the previous weather process to evolve into the next one. By spatial combination, isohyetal maps of two or more storms are reasonably pieced together. During the sequencing, a reasonable amount of time should be kept between storm events. The combined events should appear possible.

The key to the combination model method is that the combination sequence definition and its rationale should be plausible.. To do this correctly, it is necessary to be familiar with general climatic characteristics and abnormal climatic conditions in the studied watershed, as well as theories and experience in mid- to long-term evolvement of weather processes. Therefore, it is important to get recommendations from local meteorological organizations (Ministry of Water Resources, 1980; Zhan and Zhou, 1983; Wang G., 1999).

### 7.5.2 Combination methods

The storm time (temporal) combination method is introduced here. This method includes the similar process substitution method and the evolvement trend analysis method.

#### 7.5.2.1 Similar process substitution method

##### 7.5.2.1.1 Basic concept

The similar process substitution method uses an extraordinary (or large) storm that features persistent extremely (or relatively) abnormal precipitation as a typical process. One or more precipitations in the typical process with small rainfalls are substituted with one or more storm processes with very similar circulation types – almost the same weather systems – and large rainfalls, thereby forming a new storm sequence.

For example, the original typical storm process is  $A \rightarrow B \rightarrow C$ . A serious storm process  $M$ , which has a circulation type and a storm weather system similar to those of  $B$ , may be used to substitute  $B$ , forming a storm process  $A \rightarrow M \rightarrow C$ .

The key factors in this method are the selection of the typical process and the determination of the principles of similar process substitution.

##### 7.5.2.1.2 Selection of the typical process

The selection of the typical process is performed based on observed flood processes. Generally, the storms selected as typical processes feature:

- (a) flood durations that correspond to the storm design time interval;
- (b) high peaks;
- (c) large volumes;
- (d) serious floods in the lower to upper reaches;
- (e) similar circulations and storm weather systems;
- (f) good hydrometeorological data. Those typical storm processes are formulated into a process sequence with units of 24 hours (or 12 hours).

Note that the storm characteristics of the selected typical year should be in accordance with analysis of the qualitative characteristics of PMP in the design watershed described in section 7.2.5.

#### **7.5.2.1.3 Principles of similar process substitution**

To minimize randomness, similar process substitution should adopt the following four principles:

- (a) Large circulation types should be similar. Large circulation types are those that have direct effects on the storm weather system in the region, such as location of long wave troughs and ridges and subtropical highs, as well as their intensities.
- (b) Weather systems that cause storms should be identical – processes included in the substitution must fall into the same type of weather systems.
- (c) Rain types and their evolvement should be similar. During the substitution, special attention must be paid to rain types, their evolvement and the rain axes direction, especially the locations of storm centres and their movement paths.
- (d) Storm seasons should be identical – storms included in the substitution should have the exact same seasons.

Principles of combination may also be determined through comprehensive analysis and induction of storm causes, large circulation types and weather systems in the design watershed, and the application of elements of synoptic meteorology and experience in forecasting.

#### **7.5.2.1.4 Procedure**

The step-by-step procedure of the similar process substitution method is as follows:

- (a) Select the typical year – methods for the selection have been discussed in 7.5.2.1.2.
- (b) Categorize weather processes of the typical year – determine the weather processes (such as the low vortex shear line type, the westerly trough type, the typhoon type and more) that occur in the typical year.
- (c) Substitute with similar processes – based on storm weather processes of the typical year, substitute processes that have small rainfalls in the design time interval with similar processes selected from historical storms that have large rainfalls, thereby forming a sequence of severe storm processes, which acts as the basis of PMP.

### **7.5.2.2 Evolvement trend analysis method**

#### **7.5.2.2.1 Basic concept**

In this method, combinations are made from the development trends of synoptic situations. One or several consecutive weather processes in observed data with the largest rainfall is used, and smaller events are built around the largest to form the combination or sequence. Synoptic weather and analytical techniques are used to form the combination.

For example, the original sequence of storm weather processes is  $D \rightarrow E \rightarrow F$ , and there is now a more severe storm weather process  $G$ . In terms of circulation types and weather systems,  $F$  and  $G$  are different, but it is possible for  $F$  to evolve into  $E$  – according to deduction based on elements and experience in synoptic meteorology – so  $D \rightarrow E \rightarrow G$  is possible.

Keys factors to successful application of this method are the selection of the largest rainfall event in the combination method and suitable analysis of weather systems evolution. This method is used to combine two or three storms only as the randomness increases when the combination time is too long.

#### **7.5.2.2.2 Selection of the base point of the combination**

Methods for the selection of the base point of the combination are identical to those used in the selection of the typical process in the similar process substitution method (section 7.5.2.1.2).

#### **7.5.2.2.3 Principles of weather systems evolution analysis**

With the evolution method, the storm combination is performed based on circulation evolution characteristics. To perform a suitable analysis the following two principles should be considered:

- (a) In-depth analyses on the main types of extraordinary, consecutive storm weather processes that have occurred in the design watershed should be performed as the starting point of the combination. For example, the maximum 10-day precipitations in the Lancang River basin are primarily caused by the continuous occurrence of shearing vorticity, while the maximum 30-day precipitations in the Huaihe River basin are primarily caused by continuous shearing vorticity processes, but may also be affected by typhoons.

(b) Characteristics of the conversion of circulation types and storm weather systems should be fully understood. This should include experience in weather analyses, and characteristics of storm weather systems. Special attention needs to be given to ensuring the time lag between events is meteorologically plausible.

#### 7.5.2.2.4 Procedure

- (a) Weather types (storm weather systems) affecting precipitations in the design watershed based on weather maps are classified. They are named based on key characteristics, such as shearing vorticity, westerly trough and typhoon. All weather processes during a selected period are ranked and possible storm sequences are created in a reasonable manner.
- (b) Flow fields and humidity fields of typical storm processes are analysed to learn their circulation characteristics and moisture transportation.
- (c) Comprehensive dynamic maps are drawn (of, for example, the location and the intensity of the blocking system, paths of vortexes and cyclones, frontal system evolvement, and cold and warm air movements), and the cause of the storm process is thereby determined.
- (d) Rainfall distribution maps and discharge hydrographs corresponding to severe weather processes are drawn.
- (e) Several storm processes are selected through analysis and comparison, that have large precipitations and are favourable for generating severe floods. These are combined into a new storm sequence using meteorological judgement for floods.

#### 7.5.3 Analysis of combination scheme rationality

For both methods – the similar process substitution method and the evolvement trend analysis method – the rationality of the combination scheme needs to be analysed after it is determined. This can be done via synoptic meteorology, climatology and study of historical extraordinary storm floods.

##### 7.5.3.1 Analysis based on synoptic meteorology

For combinations with many elements, the overall rationality of the combined sequence needs to be checked based on the evolvement of historical weather type sequences in the flood period. For combinations with few elements (two or three elements), the check should focus on the rationality of the interval between two elements and the

possibility of the conversion of the first element into the second one in terms of the combination of synoptic situations. For combinations with long durations (one to two months), the check can also be done in terms of characteristics of seasonal changes in atmospheric circulations.

In regions affected by westerly belts, for example, the westerly circulation index of the combined sequence can be calculated and compared with typical years for large floods. At low latitudes, locations and intensities of subtropical anticyclones as well as changes to the configurations and intensities of major system members of high-altitude deformation fields, with special attention to the preservation and development of blocking systems, can be assessed.

##### 7.5.3.2 Analysis based on climatology

The combined sequence can be compared with days of storms, locations of storm centres, storm extremes, characteristics of spatio-temporal distributions and so on in the design watershed. There should be no large contradictions between the two. Meanwhile, the combined sequence can also be compared with the distribution of storm extremes as well as corresponding synoptic situations, moisture conditions, etc., in adjacent watersheds in the same climate zone.

##### 7.5.3.3 Comparison with historical extraordinary storm floods in the watershed

The storm duration, temporal distribution, storm area distribution, locations of major storm areas, etc. of the combined storm sequence is compared to historical extraordinary storms in the watershed to confirm that key characteristics are reflected.

#### 7.5.4 Combination model maximization

A combination model itself not only extends durations of actual typical storms, but also increases the typical precipitation total. This can be considered maximization of some sort, so it can usually be regarded as a high-efficiency storm, for which only moisture maximization is needed to determine PMP. In most cases, only major elements are maximized.

#### 7.5.5 Example calculations

##### 7.5.5.1 Similar process substitution method

The Manwan project on the Lacang River, Yunnan Province, China is a dam with a height of 132 m, a

total reservoir capacity of 1.05 billion m<sup>3</sup> and an installed capacity of 1.5 million kW. A great deal of observed data on large storms are available for this watershed. Kunming Survey and the Design Institute derived PMP for the project using the combination model method in the 1980s (Wang G., 1999).

#### 7.5.5.1.1 *Basin profile*

The above-dam-site watershed area is 114 500 km<sup>2</sup> in Manwan and the river is 1 575 km long. In the north-south direction, the basin is long and narrow and tapers in from the north to the south. The latitude difference is about 9.5°. It spans two climate zones.

The part of the basin north of the Liutongjiang River (with a watershed area of 83 000 km<sup>2</sup>) is high (with an average elevation of 4 510 m) and the climate belongs to the Qinghai-Tibet Plateau. This part is affected mainly by the westerly-belt weather system, and the weather systems that cause precipitations are mainly westerly troughs and shearing vorticities. Precipitation magnitudes are usually small with low intensities. The spatio-temporal distribution does not change much.

The reach between the Liutongjiang River and the dam site in Manwan (with a watershed area of 31 500 km<sup>2</sup>) is characterized by a *puna* (high, dry, cold plateau) and a subtropical transitional climate. With a wide range of altitudes, the reach is in the famous Hengduan Mountain region (with an average watershed elevation of 2 520 m), which features multi-layer climates and an observed maximum 1-day precipitation of 163.7 mm. As a result, weather systems of storms in the region mainly include shearing, low troughs, cold fronts, low vortexes, Bay of Bengal monsoon depressions, Bay of Bengal storms and equatorial convergence zones. Moistures come from the Bay of Bengal in the Indian Ocean. In rainy seasons, southwest monsoon circulations are the main moisture transportation currents.

#### 7.5.5.1.2 *Determination of PMP key characteristics*

According to an analysis of observed and surveyed data on storm floods in the watershed, in combination with project requirements, PMP for the Manwan project should have key characteristics as listed in Table 7.6.

#### 7.5.5.1.3 *Storm combination*

Using the similar process substitution method of combination, a storm that occurred in late August

1966 was selected as the typical year. Its storm process and the corresponding synoptic situation are shown in Table 7.7. Under the principle of similar process substitution, the storm process on 22–24 July 1955 was used to substitute the one on 25–27 August 1966; the storm process on 24–26 July 1972 was used to substitute the one on 28–30 August 1966. Information on each year's storms is shown in Table 7.8. The combined 10-day areal mean rainfall was 177.1 m.

#### 7.5.5.1.4 *Analysis on rationality of the combination model*

According to the information in Tables 7.7 and 7.8, the combined and substituted storms complied with the principles of similar process substitution and key characteristics of PMP listed in Table 7.6.

In addition, according to a typical-year 10-day 500 hPa average circulation map and a combined storm 10-day 500 hPa average circulation map (not

**Table 7.6. Key characteristics of PMP for the Manwan project**

Item	Characteristics	
Atmospheric circulation type	Asian-Europe two-ridge and one-trough type (the west of Baikal Lake is a wide trough area)	
The storm weather system	Shearing vorticity and monsoon depression	
Scope of rain field within the basin	Widespread precipitation within the basin	
Location of main rain field	The middle reach between the Liutongjiang River and the Jiajiuhe River	
Precipitation duration	Continuous precipitation Areal rainfall ≥ 20 mm	10 days Over 5 days
Storm temporal distribution type	Triple peaks in a saddle-like shape with the main peak ahead	
Storm occurrence period	July–August	

included in this manual), average trough-ridges and locations of subtropical anticyclones in the East Asia region were very similar. After the combination, mid-latitude areas maintained the dual-ridge and single-trough circulation type. This indicates that after the similar process substitution, the circulation type did not vary greatly, indicating that such a combination was possible and rational. Meridional circulations of the combined average circulation field were enhanced, which was favourable for the north-south exchange of cold and warm air and the enhancement of storm intensity.

#### 7.5.5.1.5 Maximization of combination model

The 10-day rainfall of the combined storm was 177.1 mm, which was 34.1 per cent larger than the

typical-year 10-day rainfall (132.1 mm). Nonetheless, it was smaller than the 10-day storm rainfall (215 mm) of the historically largest flood, which occurred in 1750. The combined storm also didn't reach the PMP magnitude of the 1750 flood peak (16 000 m<sup>3</sup>/s at the Jiajiu station), so it was necessary to maximize physical factors.

Based on watershed characteristics and meteorological data, the moisture inflow index method (introduced in section 2.4.3) was used to maximize both the August 1966 storm and the July 1972 storm by 3 days. The ultimate 3-day PMP of the combined storm was 127.4 mm, while the 10-day PMP was 280 mm (Table 7.8). The latter was inconsistent with the post-moisture-maximization result of the back-induced 10-day storm rainfall of the 1750 flood,

**Table 7.7. Table of typical storm process sequence in Manwan in 1966**

Date	August 1966										Total
Item	21	22	23	24	25	26	27	28	29	30	
Areal rainfall (mm)	14.1	23.1	18.2	21.6	9.6	5.4	10.6	7.8	7.1	13.2	132.1
Circulation type	Dual-ridge and single-trough										
500 hPa	Shearing				Southern sub-trough shearing vorticity			Shearing trough (vorticity)			
Weather system	700 hPa	Shearing vorticity				Shearing vorticity			Shearing		
Ground	Tibet monsoon depression				Plateau cold front and Burma monsoon depression			Burma monsoon depression and plateau cold front			

**Table 7.8. Table of combined storm process sequence using similar process substitution method for the 1966 typical storm in Manwan**

Date	August 1966				July 1955			July 1972			Total
	21	22	23	24	22	23	24	24	25	36	
Areal rainfall (mm)	14.1	23.1	18.2	21.6	10.1	28.6	15.6	12.5	18.5	14.8	177.1
Circulation type	Dual-ridge and single-trough				Dual-ridge and single-trough			Dual-ridge and single-trough			
500 hPa	Shearing				Low trough (vortex)			Shearing trough			
Weather system	700 hPa	Shearing vorticity				Shearing vorticity			Shearing		
Ground	Tibet monsoon depression				Burma monsoon depression			Ground plateau cold front and Tibet monsoon depression			
PMP (mm)	14.1	46.8	36.8	43.8	10.1	28.6	15.6	23.1	34.1	27.6	280.0

258–279.5 mm, suggesting that the PMP estimate is suspect as it may be underestimated.

#### 7.5.5.2 Weather system evolution method

For a large watershed along the upper reaches of the Changjiang River in China, a storm that occurred on 1–13 July 1981 was combined with one that occurred on 15–29 July 1982 using the evolvement trend analysis method to derive PMP (CJWRC, 1995).

The continuity of weather processes was analysed to determine whether synoptic situations of the two processes could be linked together and whether the former process could evolve into the latter.

##### 7.5.5.2.1 *Analysis of the possibility of synoptic situations evolvement between the two processes*

The two processes selected to be linked together occurred on 13 July 1981 and 15 July 1982. The large circulation types of these two processes were similar. Locations of troughs and ridges at mid- to high-latitudes were nearby, as shown in Figures 7.6 and 7.7. Both the New Siberia region and Okhotsk featured ridges of high pressure, and between them were troughs. Subtropical anticyclones were latitudinally distributed. Ridge lines were between 25–26° N.

The differences between the 13 July 1981 and 15 July 1982 processes were: the troughs in 1981 were slightly more westward and northward than those in 1982; ridges of high pressure in the New Siberia region were slightly more westward; ridges were

north-south in 1981 and north-east–south-west in 1982; and subtropical anticyclones were more westward in 1982 than in 1981. According to synoptic meteorology experience and the rule that troughs and ridges at high latitudes move from the west to the east, northern ridge lines of high pressure will change from north-south to north-east–south-west during the eastward movement of ridges of high pressure, forcing troughs on the Baikal Lake to move south-eastward along the ridges. As a result, circulation types begin to change.

The weather system on 5–7 June 1956 was also very similar (see Figures 7.8 and 7.9).

##### 7.5.5.2.2 *Analysis of the possibility of circulation type evolvement*

The circulation type on 9–13 July 1981 was the Baikal large trough type, but it changed into the dual-trough and single-ridge type from 14 July onwards. The circulation type on 15–20 July 1982 was also the dual-trough and single-ridge type. The two storms were identical not only in circumfluence type but also in rain types, which were both East Sichuan movement type. Therefore, linking 13 July 1981 with 15 July 1982 complied with observed atmospheric circulations.

##### 7.5.5.2.3 *Analysis of the possibility of storm weather systems evolvement*

Weather systems of the storms on 13 July 1981 and 15 July 1982 were both shearing vorticity, and system locations were also similar. Low vortexes in 1982 were slightly weaker and more eastward than in 1981. As weather systems evolve from the west

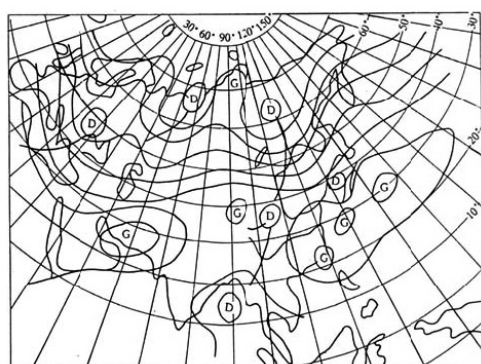


**Figure 7.6. 500-hPa situation map for 13 July 1981 (MWR and others, 1995)**

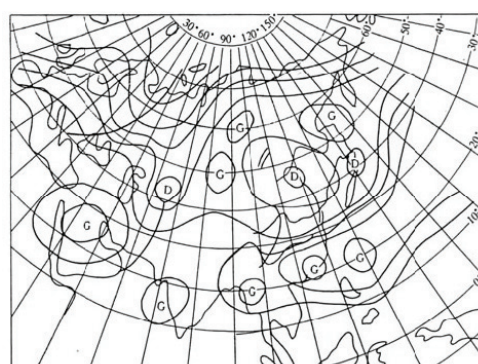


**Figure 7.7. 500-hPa situation map for 15 July 1982 (MWR and others, 1995)**

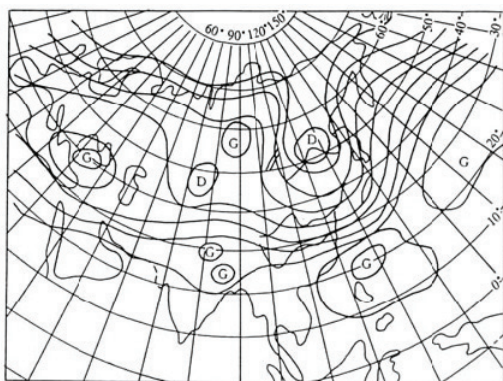


**Figure 7.8. 500-hPa situation map for 5 June 1956  
(MWR and others, 1995)**

to the east, it would have been possible that the weather system on 13 July 1981 could have moved eastward and got weaker and evolved into the location of the weather system on 15 July 1982.

#### 7.5.5.2.4 *Post-combination analysis of storm spatio-temporal distribution*

After the combination, the storm was first in the north-east-south-west rain belt on the Tuojiang River and the Jialingjiang River, then moved eastward to the Three Gorges region. It moved out 2 days later, causing the Tuojiang River and the Jialingjiang River floods to meet, generating large peaks. To study the spatio-temporal distribution of such storms, statistics were gathered about 27 large floods with precipitations in the Three Gorges reach. Among them, 12 precipitations had moved in from the Jialingjiang River. There were eight large storms on the Jialingjiang River that brought large storms in the Three Gorges reach. Descriptions of the rains for the 1870 historical flood indicate that it was also of this type. The storm distribution and trend on 5–7 June 1956 were very similar to those of the combined storm (Figures 7.10 to 7.13). This all suggested that linking the 13 July 1981 process with the 15 July 1982 process was reasonable.

## 7.6 PMF ESTIMATION

### 7.6.1 Introduction

The essential issue of deriving PMF from PMP is how to convert the design rainfall for a particular watershed into the design flood for the outlet section (or the dam site of the reservoir). This issue

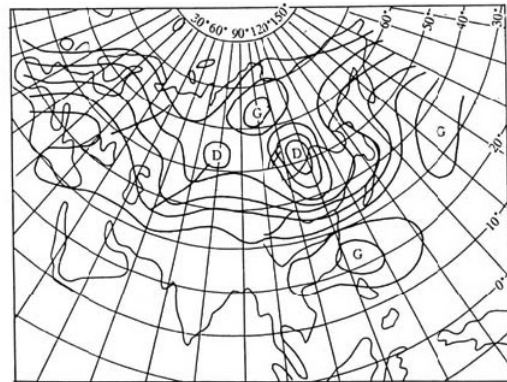


**Figure 7.9. 500-hPa situation map for 6 June 1956  
(MWR and others, 1995)**

can be solved using rainfall-runoff modelling methods. These methods estimate flood characteristics based on rainfall data. There are numerous methods available to convert rainfall to runoff, from a simple empirical correlation to the complex watershed models. Users can select the model they need based on: specific conditions (mainly data conditions) of the design watershed; suitability of the approach; and methods with which they are familiar (Wang G., 1999; CJWRC, 1993; CJWRC, 1995).

A brief overview of deriving PMF from PMP is given herein. Specific methods for estimation are only briefly described and references exist that provide much more detail (United States Department of the Interior, 1992; United States Army Corps of Engineers, 1996).

### 7.6.2 Basic assumption for deriving PMF from PMP

The basic assumption is that the flood discharge resulting from the PMP is the PMF. When deriving PMF from PMP, special attention should be given to establishing what type of storm mechanism results in the PMP (including the storm volume and its spatio-temporal distribution) that produces the overall PMF required by a design project. One of the most important steps is to establish the qualitative characteristics of the ideal or model storm, which has been described in section 7.2.5.

### 7.6.3 Characteristics of runoff yield and flow concentration with PMP

Some studies indicate that runoff yield and flow concentration of discharge have distinct characteristics associated with the PMP design storm (Hua, 1984). These characteristics are noteworthy.

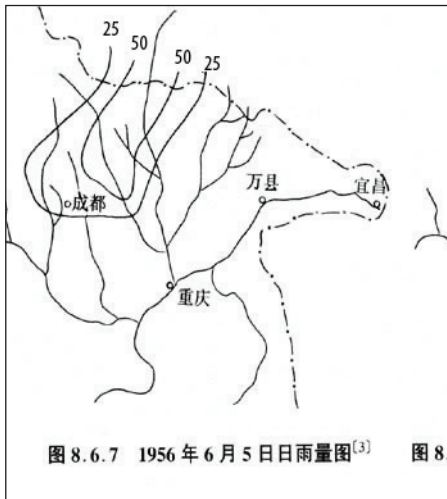


Figure 7.10. Daily rainfall map on 13 July 1981

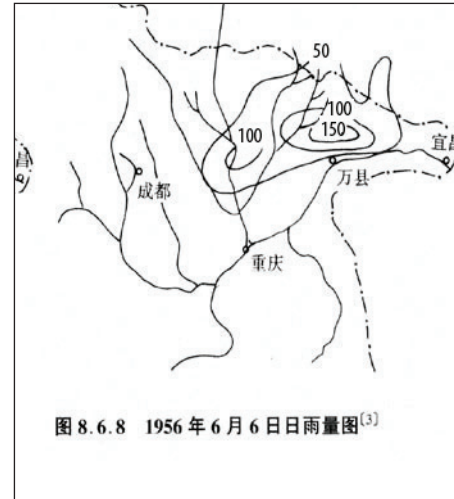


Figure 7.11. Daily rainfall map on 15 July 1982

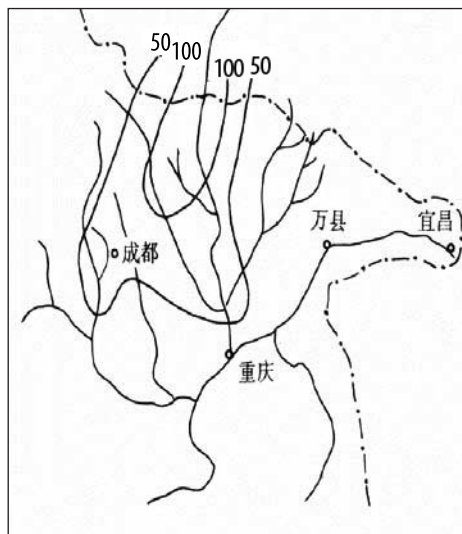


Figure 7.12. Daily rainfall map on 5 June 1956

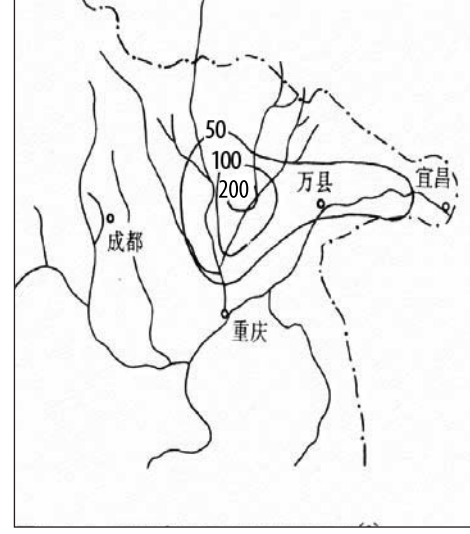


Figure 7.13. Daily rainfall map on 6 June 1956

### 7.6.3.1 Characteristics of runoff yield

The rainfall intensity and volume of a PMP storm are large and concentrated compared with average storms. In terms of runoff yield, the runoff coefficient is extraordinarily large and tends to exceed the observed maximum, especially in drought regions. Therefore, the importance of the runoff yield calculation in PMF estimation is much smaller than in hydrological forecasting. Since the PMP rainfall is far beyond the basin's maximum initial loss, the error caused by the loss-deduction calculation is a tiny percentage of the value of PMP. As a result, the calculation error has relatively minor effect on the estimation of the PMF, even if simple methods are used to estimate the loss.

### 7.6.3.2 Characteristics of flow concentration

Observed data indicate that, in cases of large floods, the discharge velocity tends to be constant, or close to constant, in the high-water-level part of the stage-discharge curve of the outlet section in the watershed. It can be shown theoretically that when the discharge velocity ( $V$ ) for high stage is constant,  $dV/dA = 0$ , where  $A$  is the area of the section. This infers that the discharge velocity is equal to the wave velocity and the time of concentration is a constant. As a result, under PMF conditions, simple addition of confluences can be used to calculate the discharge of PMF. The simplest method is through the use of Sherman's unit hydrograph to derive the flow concentration in the watershed and the Muskingum method for channels.

Since the flood is very large under PMF conditions, special attention must be paid to the impact of dam-break and overtopping and rupturing of dykes along channels in the upper reaches during PMF conditions.

#### 7.6.4 Methods for converting PMP into PMF

There are two types of methods for converting PMP into PMF.

The first type is the traditional unit hydrograph method. Sherman's unit hydrograph is used in most cases. Large watersheds are typically broken into a number of sub-watersheds, for which unit hydrographs are used to ascertain the outflow hydrographs. Then the Muskingum method is used to route the sub-watershed hydrographs to the outlet section. The base flow is also added to obtain the flood hydrograph or PMF.

The second type is the river-basin or hydrological process models. Such models are numerous, with the key differences relating to the number of factors considered for the runoff-production part. Minor differences also exist in the estimation of the flow concentration. Sherman's or Nash's unit hydrographs are commonly used to estimate discharge from the watershed, or sub-watershed, with the Muskingum method, or similar approaches, being used to route flows downstream. Given the extreme magnitude associated with PMP, it is often considered unnecessary to adopt complex models to describe the process for the estimation of the PMF.

#### 7.6.5 Influence of antecedent conditions

Both Linsley and others (1975) and Zhan and Zhou (1983) assert that PMP is an unusually large event, and it is unnecessary that the most extreme initial conditions be adopted for the estimation of the PMF. Given the storms/floods that result in the PMP/PMF are very large, the influence of estimating antecedent rainfalls, base flow and moisture conditions will usually have little effect on PMF values.

Generally, the antecedent rainfall ( $P_a$ ) for humid regions is set equal to the maximum watershed loss ( $I_m$ ), or  $P_a = I_m$ . In other words, the initial losses are set as zero (Wang B.H., 1984, 1988). For arid and semi-arid regions,  $P_a = \frac{2}{3}I_m$  as a safety measure (Wang G., 1999).

Base flow resulting from underground water reserves usually has a minor effect on PMF. Various approaches exist to estimate base flow contributions. For example, the base flow can be estimated as the minimum

daily average discharge among the maximum monthly runoffs for the particular month of the year associated with the time of occurrence of the PMF (Wang B.H., 1988). It can also be determined using on the base flow for the observed typical flood hydrograph for that period of the year.

### 7.7 ESTIMATION OF PMP/PMF FOR LARGE WATERSHEDS

#### 7.7.1 Introduction

Deriving PMP/PMF for large watersheds (above 50 000 km<sup>2</sup>) poses specific difficulties. For large watersheds, especially those larger than 100 000 km<sup>2</sup>, flood durations are typically as long as 5 to 10 days. Since existing storm data are not sufficient for such watersheds, neither the local model method nor the transposition model method works in most cases. As a result, the combination model method is usually used.

Major disadvantages of the combination model method are: when combined elements are excessive and combination durations are too long, it is not easy to demonstrate the rationality of the combined sequence; and when it comes to maximization, it is hard to determine which combined elements should be maximized.

Also, channels tend to be thousands of kilometres long, while the average watershed width is usually hundreds of kilometres. As a result – due to the large difference in geographical locations, plus the effects of mountains and other orographic features – climatic characteristics and causes of storm weather are different across the lower, middle and upper reaches, or between one part and another part of the watershed. It is difficult to reflect such differences when determining model storms and establishing appropriate model maximization.

In the 1970s and 1980s, some organizations in China provided two methods applicable to the above-mentioned situations. They are the major temporal and spatial combination method (MTSCM) and the storm simulation method based on an historical flood (SSMF; Wang G., 1999).

#### 7.7.2 Major temporal and spatial combination method

##### 7.7.2.1 Introduction

The main idea of this method is to solve the part that has a great impact on PMF for the design region

with hydrometeorological methods and solve the part that has a small impact with hydrological methods.

The hydrometeorological methods are the same as those used for estimation of PMP introduced in Chapters 2, 3 and 5 and sections 7.3–7.5 in Chapter 7.

The hydrological methods include calculations based on the space inflow proportion or the temporal distribution proportion in typical floods, the correlation method (regional flood volume correlation or short- and long-term-interval flood volume correlation), the method of transport capacity control of the upper reach, and so on.

The parts having a great or small impact are:

- (a) In terms of flood sources (or space), the section having a great impact is the main source region where PMF is formed, and the other regions have little impact;
- (b) In terms of flood hydrographs (or time), the part having a great impact is the discharge hydrograph for the largest flood volume that has a great impact on the flood control of the project in a short time interval (for example, 5 days) within the duration of the design flood (for example, 12 days), and the discharge hydrographs for the other time interval (for example,  $12 - 5 = 7$  days) have little impact.

## 7.7.2.2 Procedure

### 7.7.2.2.1 PMP/PMF for major reaches

General steps for estimating PMP/PMF for major reaches are:

- (a) According to the type of storm, the watershed above the design section A (Figure 7.14) is divided into two parts, that is, the reach above section B and below section B, referred to as the BA reach.
- (b) PMP is derived for the BA reach with direct methods.
- (c) Runoff yield and concentration calculations on PMP is performed for the BA reach and the base flow is added to acquire an estimate of the PMF for the BA reach.
- (d) The corresponding flood above section B under the condition of the occurrence of PMF in the BA reach is obtained using hydrological methods. Flows are routed to the design section A, and added to the PMF hydrograph for the BA reach, and the result is the PMF hydrograph for the design section A.

### 7.7.2.2.2 Estimating PMF for long time intervals

General steps are as follows:

- (a) PMF is determined for the major time interval  $t_1$  of the time interval  $T$  of the design flood using direct methods.
- (b) Methods for the calculation of the flood for the remaining time interval  $t_2 = T - t_1$  depend on the size of the basin. Hydrological methods are used when the size of the basin is small.
- (c) Flood hydrographs obtained from the above two steps are pieced together to obtain PMF for the time interval of the design flood.

### 7.7.2.3 Example calculations

Tables 7.9 and 7.10 show the watershed conditions for four key projects in China and methods for deriving PMP/PMF.

Estimations for the Qikou and Sanmenxia projects were determined by the Survey and Design Institute, the Yellow River Conservancy Commission. Estimates for the Ertan and Manwan projects were made by the Chengdu Survey and Design Institute and the Kunming Survey and Design Institute of the Ministry of Water Resources (Wang G., 1999).

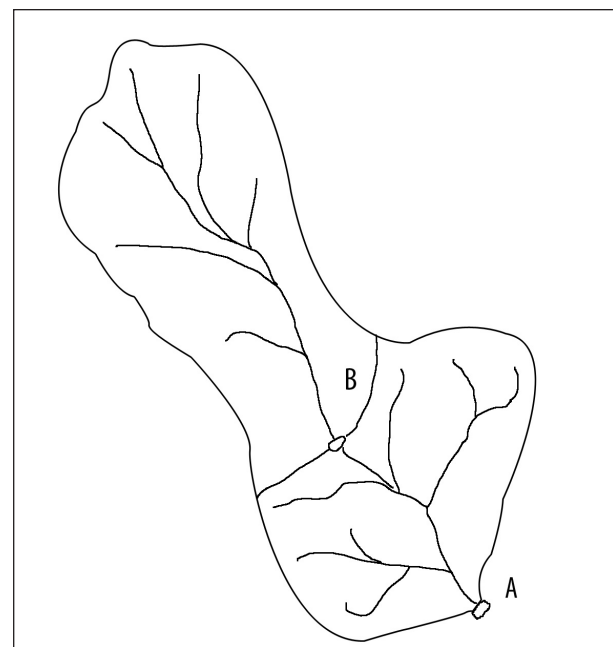


Figure 7.14. Watershed diagram of design project A

### 7.7.3 Storm simulation method based on an historical flood

#### 7.7.3.1 Introduction

Historical floods are extraordinary floods that are typically greater than observed records, found through field surveys, literature and archival research. Their return periods are typically more than 100 years with a minority of them more than 1 000 years.

For historical floods in some countries, the flood hydrograph and major characteristics of corresponding storms can be determined for the peak flood and also the flood volume. Such historical floods can be used to derive PMP/PMF through the storm simulation method for historically extraordinary floods (Zhao and others, 1983; Jin and Li, 1989).

This method can also be used to derive PMP/PMF for some large watersheds where hydrological stations were set up early. This is only the case if the largest flood in the observed data occurred in the early period of the hydrological station and there were scarce rainfall stations at that time, making it hard to use it to derive PMP/PMF.

#### 7.7.3.2 Principles

Storms corresponding to rare historical extraordinary floods can be regarded as high-efficiency storms. If those high-efficiency storms can be reconstituted through trial calculations with the watershed rainfall runoff model, followed by moisture maximization, then PMP is determined (Wang, 1999, 2005a). Conversion of the PMP into a flood yields PMF.

#### 7.7.3.3 Procedure

The peak flood, the flood hydrograph and the major source region of the historical extraordinary flood are known conditions. The spatio-temporal distribution and the representative dewpoint of its corresponding storm need to be determined.

##### 7.7.3.3.1 *Estimation of the spatio-temporal distribution of the storm corresponding to the historical flood*

Key points on methods for estimating the spatio-temporal distribution are as follows:

- The weather cause (including the circulation type and the storm weather system), the storm

**Table 7.9. Watershed profiles for four key projects in China**

River		Yellow River	Yellow River	Yalongjiang River	Lancang River
Project		Qikou	Sanmenxia	Ertan	Manwan
Watershed area (km <sup>2</sup> )		430 900	688 421	116 360	114 500
River length (km)		3 893	4 439	1 467	1 579
Maximum straight line length of the watershed (km)	West–east	1 470	1 480	137*	104*
	North–south	480	870	950*	1 100
Major reach	Name	Hekou Town, Qikou	Hekou Town, Sanmenxia	Ya'an, Xiaodeshi	Liutongjiang River, Jiajiu
	Area (km <sup>2</sup> )	44 934	320 513	50 633	31 600
Climatic features	Major reach	Subtropical monsoon climate	Subtropical monsoon climate	Transitional frigid zone to subtropical zone climate	Transitional frigid zone to subtropical zone climate
	Upstream section within the reach	Qinghai-Tibet Plateau climate	Qinghai-Tibet Plateau climate	Qinghai-Tibet Plateau climate	Qinghai-Tibet Plateau climate
Major weather systems for extraordinary storms	Major reach	South-east shear line	South-west–north-east shear line	Shearing vorticity	Monsoon depression typhoon and subtropical anticyclone edge
	Upstream section within the reach	South-west–north-east shear line	Same as above, but different occurrence time	Westerly trough shearing vorticity	Low vortex and shearing

\* Average watershed width and length

**Table 7.10. Methods for deriving PMP/PMF for four key projects in China**

	Project	Name			
		Qikou	Sanmenxia	Ertan	Manwan
Method for deriving PMP for major region	Design duration (d)	12	12	3	10
	Major time interval	Days	5	5	5
	Method for deriving PMP	Hydro-meteorological methods	Hydro-meteorological methods	Hydro-meteorological methods	Hydro-meteorological methods
Method for deriving PMF for entire watershed	Remaining time interval			Hydrological methods	Hydrological methods
	Major reach	Major time interval	Hydro-meteorological methods	Hydro-meteorological methods	Hydro-meteorological methods
	Remaining time interval		Hydrological methods $W_5 - W_{12}$	Hydrological methods $W_5 - W_{12}$	Hydrological methods
Upstream section within the reach		Hydrological methods (the discharge is based on the discharge capacity of dykes along the Inner Mongolia reach)	Hydrological methods (the discharge is based on the discharge capacity of dykes along the Inner Mongolia reach)	Hydrological methods (the average of the observed maximum and the surveyed maximum)	Hydrological methods (the discharge is based on the typical inflow proportion in 1966)

area distribution, the location of the major storm area, the storm trend and the rough storm temporal distribution are estimated based on data on storm floods recorded in literature and survey field notes.

- (b) Several large storms that are of the same type and in the same season as the historical extraordinary flood are selected from the observed data under a principle that states if weather causes of storms are similar in a particular region in a particular season, then basic characteristics of those storms are similar.
- (c) Selected storms are ranked into a combined storm sequence according to the rough storm temporal distribution of the historical extraordinary flood estimated above.
- (d) Runoff yield and concentration for the combined storm sequence is calculated through the rainfall runoff model in order to determine the flood hydrograph. This should approximate the hydrograph of the historical flood (it should approximate the historical flood in terms of the flood peak and the flood volume of the major time interval). Its source region should also approximate that of the historical flood. If the approximations are inaccurate, the storm sequence should be adjusted properly (temporally and spatially) till the derived flood hydrograph approximates the hydrograph of

the historical flood. The duration-area distribution of the storm is that of the storm corresponding to the historical flood.

At this step, the rainfall runoff model needs to be verified by observed data on large floods.

#### 7.7.3.3.2 *Estimation of the representative dewpoint of the storm corresponding to the historical flood*

The representative dewpoint of the storm corresponding to the historical flood can be approximated by an extraordinary storm selected from among observed data on large storms in the region, which has the same weather cause as the one that caused the historical flood. It may also be determined through the correlation between representative dewpoints of storms of the same type and the maximum 1-day areal mean precipitation depth plotted in the design watershed.

#### 7.7.3.4 *Example calculations*

Multiple methods were used to estimate PMF for the Three Gorges Project (the controlled watershed area is one million square kilometres), including the storm simulation method for historically extraordinary floods. An extraordinary flood in July 1870 was simulated to generate a storm, which was then maximized.

#### 7.7.3.4.1 Flood specifications

The flood that occurred in the upper reaches of the Changjiang River in July 1870 was a rare extraordinary flood. There was a large amount of data available for the flood. A large-scale field survey found more than 500 flood mark points along the Changjiang River and its branches. 91 inscriptions were found along the 754-km reach, from Hechuan to Yichang. In addition, there were reports to the Imperial Palace, history books about water conservancy and literature published by nearly 800 counties and prefectures. According to an analysis of these data, the flood was primarily from the Jialingjiang River and the reach from Chongqing to Yichang. Its storm characteristics included: long duration, high intensity and wide coverage; the storm location was steady and slowly moved eastward. The storm was a result of several consecutive strong south-west low vortexes moving along south-west–north-east shear lines under a steady meridional environment background and favourable topographic conditions. It was representative of an extreme flood-generating storm on the Changjiang River.

According to surveys and analysis of data from the literature, the flood process was of the double-peak type, with the major peak ahead and the minor peak behind. The flood peak and the flood volume at the Yichang station (near the dam site of the Three Gorges Project) are shown in Table 7.11.

According to the literature and archival research, the flood was the largest observed since 1153, more than an 840-year period, along the Three Gorges reach. According to research on ancient floods, this event was the worst for 2 500 years.

#### 7.7.3.4.2 Storm simulation

According to the literature, the extraordinary flood on the Changjiang River in July 1870 was a result of rainfall along the lower portion of the Jinshajiang River plus a seven-consecutive-day storm over a large area of Sichuan Province. In terms of temporal and regional distribution, the storm could be broken down into two processes: one from 13–17 July and the other from 18–19 July. The first process focused on the Jialingjiang River region, and the other focused on south-east Sichuan and the Chongqing–Yichang section in the upper reaches of the Changjiang River. The storm was in a south-west–north-east belt distribution, covering a wide range from the lower portion of the Jinshajiang River to the middle reaches of the Hanjiang River. The storm centre was somewhere in the middle reaches of the Jialingjiang River and the Qujiang River.

**Table 7.11. Peak and volume of the flood at Yichang station in 1870 (CJWRC, 1997)**

Flood peak ( $m^3/s$ )	Flood volume ( $10^9 m^3$ )			
	3-day	7-day	15-day	30-day
105 000	26.5	53.7	97.5	165.0

According to dates in rainfall records of county annals, the storm moved slowly from west to east: it was on the Fujiang River on 13 July; moved to Hechuan County on the Jialingjiang River on 14 July, lasting 3 days there; then moved to the east of Sichuan after 15 July; finally focusing on the east of Sichuan and Wan County from 17–20 July. The overall storm duration was about 7 days.

The spatio-temporal distribution of the storm corresponding to the flood can be quantitatively simulated based on the qualitative descriptions about the duration-area distribution of the storm in July 1870 and the flood hydrograph of the Yichang station. The procedure used is described below.

Records made in 1870 were compared with twentieth-century records about storm processes to find a number of large storms of the low shearing

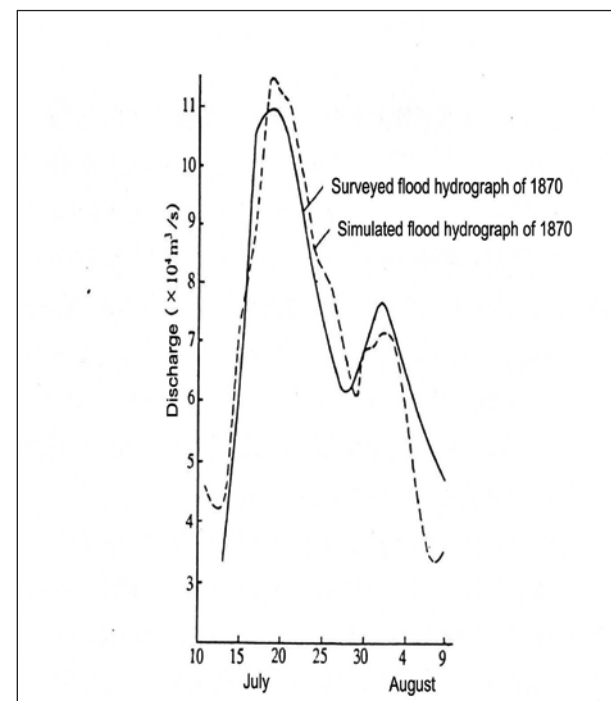


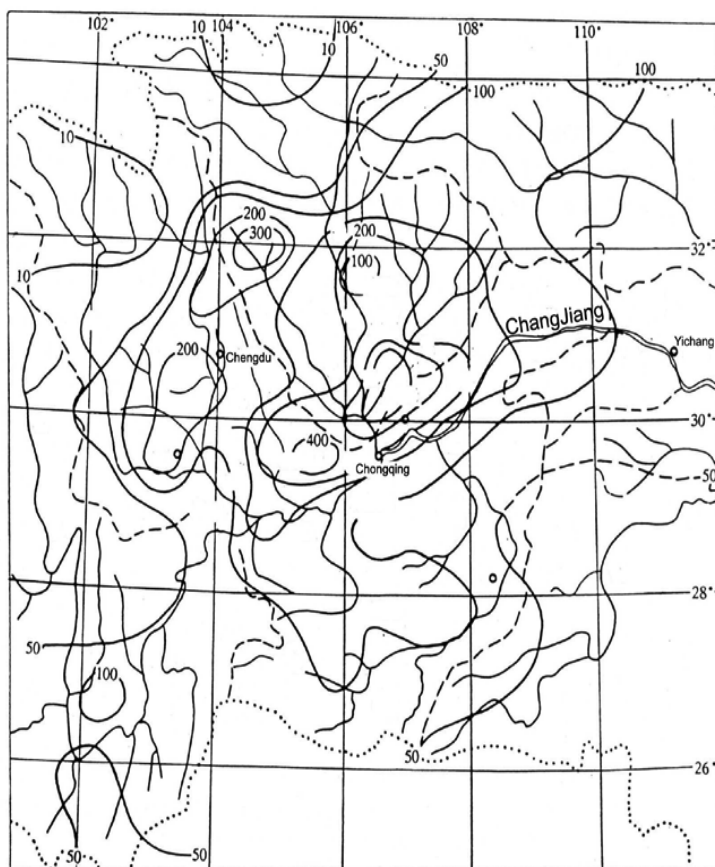
**Figure 7.15. Flood hydrograph of Yichang station in 1870 (Zhao and others, 1983)**

**Table 7.12. Simulated 1870 storm sequence**

Day order	1	2	3	4	5	6	7	8	9	10	11	12	13	14	15	16	17	18	19	20
Simulated storm	1957																	1956		
Sequence date	6.21	22	23	24	25	26	27	28	29	30	7.1	2	3	4	5	6	7	6.16	6.26	27
Day order	21	22	23	24	25	26	27	28	29	30	31	32	33	34	35	36	37	38	39	40
Simulated storm	1956	1973	1957	1937		1957	1937	1965		1957		1974								
Sequence date	6.28	6.30	7.3	7.14	15	7.2	7.16	7.7	8	7.18	19	7.31	8.1	2	3	4	8.8	9	8.16	17
Day order	41	42	43	44	45	46	47	48	49	50	51	52	53	54	55	56	57	58	59	60
Simulated storm	1974																			
Sequence date	18	8.10	11	12	13	14	15	16	17	18	19	20	21	22	23	24	25	26	27	28

vorticity type with their centres along the lower and middle reaches of the Jialingjiang River. The daily rainfall maps of those observed large storms were pieced together according to the trend of the storm in July 1870. Rainfalls before and after the

extraordinary storm process were arranged according to the rise-and-fall trend in the flood hydrograph of the Yichang station in July 1870, thereby forming a combined storm sequence. The flood hydrograph of the Yichang section was established

**Figure 7.16. Simulated rainfall isoline for 13–19 July 1870 (Zhao and others, 1983)**

through the calculation of runoff yield and time of concentration. If the calculated process is similar to the surveyed flood process, then the combined storm sequence can represent the actual storm sequence that led to the large flood on the Changjiang River in 1870, thereby quantitatively determining the extraordinary storm process that led to the extraordinary flood.

Before the simulation and trial calculation of runoff yield and concentration, the scheme for these calculations was verified with observed data from 25 July to 2 September 1974. It turned out that all calculation errors were less than 9 per cent. After 60 trial calculations, the simulated flood process approximated the surveyed flood process (Figure 7.15). The simulated storm sequence that was ultimately selected is shown in Table 7.12. Days 21 to 27 are the extraordinary storm that led to the extraordinary flood peak in Yichang in 1870. The duration is 7 days, and the total rainfall distribution of the simulated process is shown in Figure 7.16.

#### 7.7.3.4.3 Maximization

According to descriptions in the literature about the extraordinary storm that led to the flood peak in 1870, it was reasonably assumed to be a high-efficiency storm, so only moisture maximization was needed.

Moisture for the storm was from the Indian Ocean and the South China Sea. Owing to data conditions, the moisture inflow direction could only be from the Guiyang station. Its representative dewpoint was 20°C. After being corrected to a 1 000 hPa dewpoint, it was 24.5°C. The historical maximum

**Table 7.13. PMF estimate for Three Gorges (Yichang) – scheme of simulating 1870 historical flood (Jin and Li, 1989)**

Daily average discharge ( $m^3/s$ )	7-day flood volume ( $10^9 m^3$ )	15-day flood volume ( $10^9 m^3$ )
120 000	63.00	110.9

dewpoint at the 1 000 hPa elevation at the Guiyang station was 26.2°C, so the coefficient of moisture maximization  $K$  was given by:

$$K = \frac{(W_{Td})_m}{W_{Td}} = 1.17 \quad (7.8)$$

Using that coefficient, the 5-day rainfalls that led to the flood peak were maximized.

Considering the fact that the annual maximum flood volume of long durations includes those of short duration on the Changjiang River, a precipitation process for the minor peak was replaced for the major peak, in addition to moisture maximization, thereby forming the PMP series.

#### 7.7.3.4.4 Probable maximum flood

The reach above Yichang was divided into 18 areas, and the calculation of runoff yield and flow concentration was done for each of them. The flood process for each area was calculated by typical year or unit hydrograph. The travel time of the channel was calculated using the Changjiang Basin Planning Office flow concentration curve (linear flow concentration curve) formula. The PMF estimate was ultimately obtained as shown in Table 7.13.

## ACKNOWLEDGEMENTS

As chief author of the manual, I would like to express my appreciation to the many people who contributed to the revision of this manual.

First, my sincere admiration goes to the authors of the first and second versions of the manual. The content of these versions set an important benchmark in probable maximum precipitation (PMP) estimation and provided the primary basis for this revision. The authors of the first version are J.L.H Paulhus, J.F. Miller, J.T. Riedel, F.K. Schwarz and C.W. Cochrane. J.F Miller is the author of the second version.

Second, there were many experts who provided valuable suggestions and opinions during the revision. The following people contributed to the preparation of the draft of the Chinese edition of this manual: Wang Juemou, Wang Jiaqi, Sun Shuangyuan, Yang Yuandong, Liu Heng, Zhang Youzhi, Dong Zengchuan, Wu Zhiyao, Xu Qianqing, Chen Jiaqi, Wen Kang, Chen Qinglian, Ma Xiufeng and Wang Zhengxiang. The following people made significant contributions to the modification and editing of the English edition of this manual: Paul Pilon (Canada), Louis C. Schreiner (USA), David Walland (Australia), Cristina Moyano (Argentina), Van-Than-Va Nguyen (Canada), Shaukat Ali Awan (Pakistan), Aaron F. Thompson (Canada), Alistair McKerchar (New Zealand) and Bruce Stewart (Australia).

Third, I was the beneficiary of tremendous support from the Chinese hydrometeorological staff who provided their skills and expertise for the

compilation of this manual. This support included Gao Zhiding, Wang Yu, the experts on PMP and floods appointed by WMO, Wang Chunqing (the translator for report revisions and the interpreter of international conferences), Wang Yufeng, Liu Zhansong, Wang Junliang, Zhang Zhihong, Li Baoguo, Li Rong ronj, Lei Ming, He Shunde, Wang Nei, Liu Hongzhen, Song Weihua and Ma Yingping. These people assisted with: the collection, reorganization and translation of literature, material and information from the Internet; receiving and dispatching and translation of e-mails; and copying, typing, drawing and checking the various versions of the manual.

Finally, I would also like to acknowledge the strong support of the WMO Secretariat in organizing meetings, undertaking the organization of the review and final editing of the manual.

Wang Guoan

CHy-XI Expert for WMO on PMP/PMF  
Professor Senior Engineer  
Yellow River Engineering Consulting Co. Ltd.

109 Jinshui Road  
Zhengzhou  
China 450003

Fax: 86 371 65959236  
E-mail: wangga@yrec.cn, g\_a\_wang@163.com

---



## ANNEXES

### ANNEX I. TABLES OF PRECIPITABLE WATER IN A SATURATED PSEUDO-ADIABATIC ATMOSPHERE

As stated in Chapter 2, precipitable water is a term used mostly by hydrometeorologists for expressing the total mass of water vapour in a vertical column of the atmosphere. It represents the depth of liquid water that would accumulate at the base of the column if all its water vapour were condensed. The term is a misnomer since no natural process can condense or precipitate all the water vapour in the atmosphere, and substitute terms such as liquid equivalent of water vapour or liquid water equivalent are sometimes used.

The general formula for computing precipitable water,  $W$ , in cm, is:

$$W = \frac{\bar{q}\Delta p}{g\ell} \quad (\text{A.1.1})$$

where  $\bar{q}$  is the mean specific humidity in g/kg of a layer of moist air;  $\Delta p$  is the depth of the layer in hPa;  $g$  is the acceleration of gravity in cm/s<sup>2</sup>; and  $\ell$  is the density of water, which is equal to 1 g/cm<sup>3</sup>.

In most hydrometeorological work the atmosphere is assumed to contain the same amount of water vapour as saturated air with saturation pseudo-adiabatic temperature lapse rate. The precipitable water in various layers of the saturated atmosphere can be determined and listed in tables or in nomogram form. Table A.1.1 presents values of precipitable water (mm) between the 1 000-hPa surface and various pressure levels up to 200 hPa in a saturated pseudo-adiabatic atmosphere as a function of the 1 000-hPa dewpoint. Table A.1.2 lists similar values for layers between the 1 000-hPa surface, assumed to be at zero elevation, and various heights up to 17 km. Table A.1.3 gives values of precipitable water (mm) in the atmosphere between the indicated pressure and 300 hPa. Table A.1.4 provides mixing ratios along specified pseudo-adiabats for specified 1 000-hPa dewpoints at given elevations in metres above 1 000 hPa. These are used in the moisture adjustment for barrier discussed in section 2.3.4.2.

**Table A.1.1. Precipitable water (mm) between 1 000-hPa surface and indicated pressure (hPa) in a saturated pseudo-adiabatic atmosphere as a function of the 1 000-hPa dew point (°C)**

Pressure (hPa)	Temperature (°C)																															
	0	1	2	3	4	5	6	7	8	9	10	11	12	13	14	15	16	17	18	19	20	21	22	23	24	25	26	27	28	29	30	
990	0	0	0	0	0	0	1	1	1	1	1	1	1	1	1	1	1	1	1	1	1	1	1	2	2	2	2	2	2	2	2	3
980	1	1	1	1	1	1	1	1	1	1	1	1	2	2	2	2	2	2	2	3	3	3	3	3	4	4	4	4	5	5	5	
970	1	1	1	1	1	2	2	2	2	2	2	2	3	3	3	3	3	4	4	4	4	5	5	5	5	6	6	7	7	7	8	
960	1	2	2	2	2	2	2	2	3	3	3	3	3	4	4	4	4	5	5	5	6	6	6	7	7	8	8	9	9	10	11	
950	2	2	2	2	2	3	3	3	3	3	3	4	4	4	4	4	5	5	6	6	6	7	7	8	8	9	9	10	10	11	12	13
940	2	2	2	3	3	3	3	3	3	4	4	4	4	5	5	5	6	6	7	7	8	9	9	10	10	11	12	12	13	14	15	16
930	2	3	3	3	3	3	4	4	4	5	5	5	5	6	6	7	7	8	8	9	9	10	11	11	12	13	14	14	15	16	17	18
920	3	3	3	3	4	4	4	5	5	5	6	6	7	7	8	8	9	9	10	10	11	12	13	14	14	15	16	17	17	19	20	21
910	3	3	3	4	4	4	5	5	5	6	6	7	7	8	8	9	10	10	11	12	13	13	14	15	16	17	18	20	21	22	23	
900	3	4	4	4	5	5	6	6	6	7	7	8	9	9	10	11	11	12	13	14	15	16	17	18	19	20	22	23	24	24	24	
890	4	4	4	5	5	5	6	6	7	7	8	8	9	9	10	11	12	13	14	15	16	17	18	20	21	22	24	25	27	28		
880	4	4	4	5	5	6	6	7	7	8	8	9	9	10	11	12	12	13	14	15	16	17	19	20	21	23	24	26	27	29	31	
870	4	4	5	5	6	6	6	7	7	8	8	9	9	10	11	12	13	13	14	15	16	18	19	20	21	23	24	26	27	29	33	
860	4	5	5	6	6	6	7	7	8	9	9	10	11	12	12	13	14	15	16	18	19	20	21	23	24	26	28	29	31	33	36	
850	5	5	5	6	6	7	7	8	9	9	10	11	11	12	13	14	15	16	18	19	20	21	23	24	26	28	30	32	34	36	38	
840	5	5	6	6	7	7	8	8	9	10	10	11	12	13	14	15	16	17	19	20	21	23	24	26	28	30	32	34	36	38	40	
830	5	5	6	6	7	7	8	9	9	10	11	12	13	14	15	16	17	18	19	21	22	24	26	27	29	31	33	35	38	40	43	
820	5	6	6	7	7	8	8	9	10	11	11	12	13	14	15	17	18	19	20	22	24	25	27	29	31	33	35	37	40	42	45	
810	5	6	6	7	8	8	9	10	10	11	12	13	14	15	16	17	19	20	21	23	25	26	28	30	32	34	37	39	42	44	47	
800	6	6	7	7	8	8	9	10	11	12	12	13	15	16	17	18	19	21	22	24	26	28	29	32	34	36	38	41	44	46	49	
790	6	6	7	7	8	9	9	10	11	12	13	14	15	16	17	19	20	22	23	25	27	29	31	33	35	38	40	43	46	49	52	
780	6	7	7	8	8	9	10	11	11	12	13	14	16	17	18	19	21	23	24	26	28	30	32	34	37	39	42	45	48	51	54	
770	6	7	7	8	9	9	10	11	12	13	14	15	16	17	19	20	22	23	25	27	29	31	33	35	38	41	43	46	49	53	56	
760	6	7	7	8	9	10	10	11	12	13	14	15	17	18	19	21	22	24	26	28	30	32	34	37	39	42	45	48	51	55	58	
750	6	7	8	8	9	10	11	12	13	14	15	16	17	18	20	21	23	25	27	29	31	33	35	38	41	44	47	50	53	57	60	
740	7	7	8	9	9	10	11	12	13	14	15	16	18	19	20	22	24	26	28	30	32	34	37	39	42	45	48	51	55	59	62	
730	7	7	8	9	9	10	11	12	13	14	15	17	18	20	21	23	24	26	28	30	33	35	38	40	43	46	50	53	57	60	64	
720	7	7	8	9	10	11	11	12	13	15	16	17	18	20	22	23	25	27	29	31	34	36	39	42	45	48	51	55	58	62	66	
710	7	8	8	9	10	11	12	13	14	15	16	17	19	20	22	24	26	28	30	32	35	37	40	43	46	49	53	56	60	64	68	
700	7	8	8	9	10	11	12	13	14	15	16	18	19	21	23	24	26	28	31	33	35	38	41	44	47	50	54	58	62	66	70	

**Table A.1.1. (Continued)**

Pressure (hPa)	Temperature (°C)																														
	0	1	2	3	4	5	6	7	8	9	10	11	12	13	14	15	16	17	18	19	20	21	22	23	24	25	26	27	28	29	30
690	7	8	9	9	10	11	12	13	14	15	17	18	20	21	23	25	27	29	31	34	36	39	42	45	48	52	55	59	63	68	72
680	7	8	9	10	10	11	12	13	15	16	17	19	20	22	24	25	27	30	32	34	37	40	43	46	49	53	57	61	65	69	74
670	7	8	9	10	11	11	12	14	15	16	17	19	20	22	24	26	28	30	33	35	38	41	44	47	51	54	58	62	67	71	76
660	8	8	9	10	11	12	13	14	15	16	18	19	21	23	24	26	29	31	33	36	39	42	45	48	52	55	60	64	68	73	78
650	8	8	9	10	11	12	13	14	15	16	18	19	21	23	25	27	29	31	34	37	39	42	46	49	53	57	61	65	70	75	80
640	8	8	9	10	11	12	13	14	15	17	18	20	21	23	25	27	29	32	35	37	40	43	46	50	54	58	62	67	71	76	81
630	8	8	9	10	11	12	13	14	16	17	18	20	22	24	26	28	30	32	35	38	41	44	47	51	55	59	63	68	73	78	83
620	8	9	9	10	11	12	13	14	16	17	19	20	22	24	26	28	30	33	36	38	42	45	48	52	56	60	65	69	74	79	85
610	8	9	9	10	11	12	13	15	16	17	19	20	22	24	26	28	31	33	36	39	42	45	49	53	57	61	66	71	76	81	87
600	8	9	9	10	11	12	13	15	16	17	19	21	23	25	27	29	31	34	37	40	43	46	50	54	58	62	67	72	77	82	89
590	8	9	10	10	11	12	14	15	16	18	19	21	23	25	27	29	32	34	37	40	43	47	51	55	59	63	68	73	78	84	90
580	8	9	10	11	11	13	14	15	16	18	19	21	23	25	27	30	32	35	38	41	44	48	51	55	60	64	69	74	80	85	91
570	8	9	10	11	12	13	14	15	16	18	20	21	23	25	27	30	32	35	38	41	45	48	52	56	61	65	70	75	81	87	93
560	8	9	10	11	12	13	14	15	17	18	20	21	23	26	28	30	33	36	39	42	45	49	53	57	61	66	71	77	82	88	94
550	8	9	10	11	12	13	14	15	17	18	20	22	24	26	28	30	33	36	39	42	46	49	53	58	62	67	72	78	83	90	96
540	8	9	10	11	12	13	14	15	17	18	20	22	24	26	28	31	33	36	39	43	46	50	54	58	63	68	73	79	85	91	97
530	8	9	10	11	12	13	14	15	17	18	20	22	24	26	28	31	34	37	40	43	47	50	55	59	64	69	74	80	86	92	99
520	8	9	10	11	12	13	14	16	17	19	20	22	24	26	29	31	34	37	40	43	47	51	55	60	64	70	75	81	87	93	100
510	8	9	10	11	12	13	14	16	17	19	20	22	24	26	29	31	34	37	40	44	48	51	56	60	65	70	76	82	88	95	102
500	8	9	10	11	12	13	14	16	17	19	20	22	24	27	29	32	34	37	41	44	48	52	56	61	66	71	77	83	89	96	103
490	8	9	10	11	12	13	14	16	17	19	21	22	25	27	29	32	35	38	41	45	48	52	57	61	66	72	78	84	90	97	104
480	8	9	10	11	12	13	14	16	17	19	21	23	25	27	29	32	35	38	41	45	49	53	57	62	67	73	78	85	91	98	105
470	8	9	10	11	12	13	14	16	17	19	21	23	25	27	29	32	35	38	42	45	49	53	58	62	68	73	79	85	92	99	106
460	8	9	10	11	12	13	14	16	17	19	21	23	25	27	30	32	35	38	42	45	49	54	58	63	68	74	80	86	93	100	108
450	8	9	10	11	12	13	14	16	17	19	21	23	25	27	30	32	35	39	42	46	50	54	58	63	69	74	81	87	94	101	109
440	8	9	10	11	12	13	15	16	17	19	21	23	25	27	30	33	35	39	42	46	50	54	59	64	69	75	81	88	95	102	110
430	8	9	10	11	12	13	15	16	17	19	21	23	25	27	30	33	36	39	42	46	50	55	59	64	70	76	82	88	96	103	111
420	8	9	10	11	12	13	15	16	18	19	21	23	25	27	30	33	36	39	43	46	50	55	60	65	70	76	82	88	96	104	112
410	8	9	10	11	12	13	15	16	18	19	21	23	25	27	30	33	36	39	43	47	51	55	60	65	71	77	83	90	97	105	113
400	8	9	10	11	12	13	15	16	18	19	21	23	25	28	30	33	36	39	43	47	51	55	60	65	71	77	84	90	98	105	114
390	8	9	10	11	12	13	15	16	18	19	21	23	25	28	30	33	36	39	43	47	51	56	60	66	71	77	84	91	98	106	115
380	8	9	10	11	12	13	15	16	18	19	21	23	25	28	30	33	36	39	43	47	51	56	61	66	72	78	85	92	99	107	115
370	8	9	10	11	12	13	15	16	18	19	21	23	25	28	30	33	36	40	43	47	51	56	61	66	72	78	85	92	100	108	116
360	8	9	10	11	12	13	15	16	18	19	21	23	25	28	30	33	36	40	43	47	51	56	61	66	72	79	85	93	100	108	117
350	8	9	10	11	12	13	15	16	18	19	21	23	25	28	30	33	36	40	43	47	52	56	61	67	73	79	86	93	101	109	118
340	8	9	10	11	12	13	15	16	18	19	21	23	25	28	30	33	36	40	43	47	52	56	61	67	73	79	86	93	101	109	119
330	8	9	10	11	12	13	15	16	18	19	21	23	25	28	30	33	36	40	43	47	52	56	61	67	73	79	86	94	102	110	119
320	8	9	10	11	12	13	15	16	18	19	21	23	25	28	30	33	36	40	44	48	52	57	62	67	73	80	87	94	102	111	120
310	8	9	10	11	12	13	15	16	18	19	21	23	25	28	30	33	36	40	44	48	52	57	62	67	73	80	87	94	102	111	120
300	8	9	10	11	12	13	15	16	18	19	21	23	25	28	30	33	36	40	44	48	52	57	62	67	74	80	87	95	103	111	121
290	8	9	10	11	12	13	15	16	18	19	21	23	25	28	30	33	36	40	44	48	52	57	62	68	74	80	87	95	103	112	121
280	8	9	10	11	12	13	15	16	18	19	21	23	25	28	30	33	36	40	44	48	52	57	62	68	74	80	88	95	103	112	121
270	8	9	10	11	12	13	15	16	18	19	21	23	25	28	30	33	36	40	44	48	52	57	62	68	74	81	88	95	104	112	122
260	8	9	10	11	12	13	15	16	18	19	21	23	25	28	30	33	36	40	44	48	52	57	62	68	74	81	88	96	104	113	122
250	8	9	10	11	12	13	15	16</td																							

**Table A.12. Precipitable water (mm) between 1 000-hPa surface and indicated height (m) above that surface in a saturated pseudo-adiabatic atmosphere as a function of the 1 000-hPa dew point (°C)**

Height (m)	1 000 hPa Temperature (°C)																															
	0	1	2	3	4	5	6	7	8	9	10	11	12	13	14	15	16	17	18	19	20	21	22	23	24	25	26	27	28	29	30	
200	1	1	1	1	1	1	1	1	1	1	1	1	1	1	1	1	1	1	1	1	1	1	1	1	1	1	1	1	1	1	1	1
400	2	2	2	2	2	2	3	3	3	3	3	3	3	3	3	3	3	3	3	3	3	3	3	3	3	3	3	3	3	3	3	3
600	3	3	3	3	4	4	4	4	4	4	4	4	4	4	4	4	4	4	4	4	4	4	4	4	4	4	4	4	4	4	4	4
800	3	3	4	4	4	5	5	5	5	5	5	5	5	5	5	5	5	5	5	5	5	5	5	5	5	5	5	5	5	5	5	5
1 000	4	4	4	5	5	5	6	6	6	6	6	6	6	6	6	6	6	6	6	6	6	6	6	6	6	6	6	6	6	6	6	6
1 200	4	5	5	6	6	6	7	7	7	7	7	7	7	7	7	7	7	7	7	7	7	7	7	7	7	7	7	7	7	7	7	7
1 400	5	5	6	6	6	7	7	7	7	7	7	7	7	7	7	7	7	7	7	7	7	7	7	7	7	7	7	7	7	7	7	7
1 600	5	6	6	7	7	7	8	8	8	8	8	8	8	8	8	8	8	8	8	8	8	8	8	8	8	8	8	8	8	8	8	8
1 800	6	6	7	7	7	8	8	9	9	9	10	11	12	13	14	15	16	17	18	19	20	21	22	23	24	25	26	27	28	29	30	
2 000	6	7	7	8	8	9	9	10	11	11	12	13	14	15	16	17	18	19	20	21	22	23	24	25	26	27	28	29	30	31		
2 200	7	7	8	8	9	9	10	10	11	12	13	14	15	16	17	18	19	20	21	22	23	24	25	26	27	28	29	30	31	32		
2 400	7	8	8	8	9	9	10	10	11	12	13	14	15	16	17	18	19	20	21	22	23	24	25	26	27	28	29	30	31	32		
2 600	7	8	8	8	9	9	10	10	11	12	13	14	15	16	17	18	19	20	21	22	23	24	25	26	27	28	29	30	31	32		
2 800	7	8	8	8	9	9	10	11	11	12	13	14	15	16	17	18	19	20	21	22	23	24	25	26	27	28	29	30	31	32		
3 000	8	8	8	8	9	9	10	10	11	12	13	14	15	16	17	18	19	20	21	22	23	24	25	26	27	28	29	30	31	32		
3 200	8	8	8	8	9	9	10	10	11	12	13	14	15	16	17	18	19	20	21	22	23	24	25	26	27	28	29	30	31	32		
3 400	8	8	8	8	9	9	10	10	11	12	13	14	15	16	17	18	19	20	21	22	23	24	25	26	27	28	29	30	31	32		
3 600	8	8	8	8	9	9	10	10	11	12	13	14	15	16	17	18	19	20	21	22	23	24	25	26	27	28	29	30	31	32		
3 800	8	8	8	8	9	9	10	10	11	12	13	14	15	16	17	18	19	20	21	22	23	24	25	26	27	28	29	30	31	32		
4 000	8	9	10	10	11	11	12	12	13	14	15	16	17	18	19	20	21	22	23	24	25	26	27	28	29	30	31	32	33			
4 200	9	9	10	10	11	12	12	13	14	15	16	17	18	19	20	21	22	23	24	25	26	27	28	29	30	31	32	33	34			
4 400	9	9	10	10	11	12	12	13	14	15	16	17	18	19	20	21	22	23	24	25	26	27	28	29	30	31	32	33	34			
4 600	9	9	10	10	11	12	12	13	14	15	16	17	18	19	20	21	22	23	24	25	26	27	28	29	30	31	32	33	34			
4 800	9	9	10	10	11	12	12	13	14	15	16	17	18	19	20	21	22	23	24	25	26	27	28	29	30	31	32	33	34			
5 000	8	9	10	10	11	12	12	13	14	15	16	17	18	19	20	21	22	23	24	25	26	27	28	29	30	31	32	33	34			
5 200	8	9	10	10	11	12	12	13	14	15	16	17	18	19	20	21	22	23	24	25	26	27	28	29	30	31	32	33	34			
5 400	8	9	10	10	11	12	12	13	14	15	16	17	18	19	20	21	22	23	24	25	26	27	28	29	30	31	32	33	34			
5 600	8	9	10	10	11	12	12	13	14	15	16	17	18	19	20	21	22	23	24	25	26	27	28	29	30	31	32	33	34			
5 800	8	9	10	10	11	12	12	13	14	15	16	17	18	19	20	21	22	23	24	25	26	27	28	29	30	31	32	33	34			
6 000	8	9	10	10	11	12	12	13	14	15	16	17	18	19	20	21	22	23	24	25	26	27	28	29	30	31	32	33	34			
6 200	8	9	10	10	11	12	12	13	14	15	16	17	18	19	20	21	22	23	24	25	26	27	28	29	30	31	32	33	34			
6 400	8	9	10	10	11	12	12	13	14	15	16	17	18	19	20	21	22	23	24	25	26	27	28	29	30	31	32	33	34			
6 600	8	9	10	10	11	12	12	13	14	15	16	17	18	19	20	21	22	23	24	25	26	27	28	29	30	31	32	33	34			
6 800	8	9	10	10	11	12	12	13	14	15	16	17	18	19	20	21	22	23	24	25	26	27	28	29	30	31	32	33	34			
7 000	8	9	10	10	11	12	12	13	14	15	16	17	18	19	20	21	22	23	24	25	26	27	28	29	30	31	32	33	34			
7 200	8	9	10	10	11	12	12	13	14	15	16	17	18	19	20	21	22	23	24	25	26	27	28	29	30	31	32	33	34			
7 400	9	10	10	11	12	12	13	14	15	16	17	18	19	20	21	22	23	24	25	26	27	28	29	30	31	32	33	34	35			
7 600	9	10	10	11	12	12	13	14	15	16	17	18	19	20	21	22	23	24	25	26	27	28	29	30	31	32	33	34	35			
7 800	9	10	10	11	12	12	13	14	15	16	17	18	19	20	21	22	23	24	25	26	27	28	29	30	31	32	33	34	35			
8 000	9	10	10	11	12	12	13	14	15	16	17	18	19	20	21	22	23	24	25	26	27	28	29	30	31	32	33	34	35			
8 200	9	10	10	11	12	12	13	14	15	16	17	18	19	20	21	22	23	24	25	26	27	28	29	30	31	32	33	34	35			
8 400	9	10	10	11	12	12	13	14	15	16	17	18	19	20	21	22	23	24	25	26	27	28	29	30	31	32	33	34	35			
8 600	9	10	10	11	12	12	13	14	15	16	17	18	19	20	21	22	23	24	25	26	27	28	29	30	31	32	33	34	35			
8 800	9	10	10	11	12	12	13	14	15	16	17	18	19	20	21	22	23	24	25	26	27	28	29	30	31	32	33	34	35			
9 000	9	10	10	11	12	12	13	14	15	16	17	18	19	20	21	22	23	24	25	26	27	28	29	30	31	32	33	34	35			
9 200	9	10	10	11	12	12	13	14	15	16	17	18	19	20	21	22	23	24	25	26	27	28	29	30	31	32	33	34	35			
9 400	9	10	10	11	12	12	13	14	15	16	17	18	19	20	21	22	23	24	25	26	27	28	29	30	31	32						

TABLE A.1.3. Precipitable water (mm) in column of air above specified heights (m) as a function of the 1 000 hPa temperature (°C) (revised May 1981)

Height above MSL (m)	Temperature (°C)										
	0.0	0.5	1.0	1.5	2.0	2.5	3.0	3.5	4.0	4.5	5.0
0 (1000 hPa)	8.1	8.7	9.2	9.7	10.3	10.8	11.4	11.9	12.5	13.1	13.7
100	7.5	8.1	8.6	9.2	9.8	10.3	10.8	11.4	11.9	12.5	13.1
200	7.0	7.5	8.1	8.6	9.2	9.8	10.3	10.8	11.3	11.9	12.4
300	6.5	7.0	7.5	8.0	8.6	9.2	9.7	10.2	10.7	11.3	11.8
400	6.1	6.5	7.0	7.5	8.1	8.6	9.1	9.6	10.1	10.7	11.2
500	5.7	6.1	6.5	7.0	7.6	8.1	8.6	9.1	9.6	10.1	10.6
600	5.3	5.7	6.1	6.6	7.1	7.6	8.1	8.6	9.1	9.6	10.0
700	4.9	5.3	5.7	6.2	6.7	7.2	7.7	8.2	8.6	9.1	9.5
800	4.5	4.9	5.3	5.8	6.3	6.8	7.2	7.7	8.1	8.6	9.0
900	4.2	4.6	4.9	5.4	5.9	6.4	6.8	7.2	7.6	8.1	8.5
1 000	3.9	4.3	4.6	5.0	5.5	5.9	6.3	6.8	7.2	7.6	8.0
1 100	3.6	4.0	4.3	4.7	5.1	5.5	5.9	6.4	6.8	7.2	7.6
1 200	3.4	3.7	4.0	4.4	4.8	5.2	5.6	6.0	6.4	6.7	7.1
1 300	3.1	3.4	3.7	4.2	4.5	4.9	5.2	5.6	6.0	6.3	6.7
1 400	2.9	3.2	3.5	3.9	4.3	4.6	4.9	5.3	5.7	6.0	6.3
1 500	2.7	3.0	3.3	3.7	4.0	4.3	4.6	4.9	5.3	5.7	6.0
1 600	2.5	2.8	3.1	3.4	3.7	4.0	4.3	4.6	5.0	5.4	5.7
1 700	2.3	2.6	2.9	3.2	3.4	3.7	4.0	4.3	4.7	5.0	5.3
1 800	2.1	2.4	2.7	3.0	3.2	3.5	3.8	4.1	4.4	4.7	5.0
1 900	1.9	2.2	2.4	2.7	2.9	3.2	3.5	3.8	4.1	4.4	4.7
2 000	1.7	1.9	2.2	2.4	2.7	2.9	3.2	3.5	3.8	4.1	4.4
2 100	1.5	1.7	1.9	2.2	2.4	2.7	3.0	3.3	3.5	3.8	4.1
2 200	1.4	1.6	1.7	2.0	2.2	2.4	2.7	3.0	3.3	3.5	3.8
2 300	1.3	1.4	1.6	1.8	2.0	2.2	2.5	2.8	3.0	3.2	3.5
2 400	1.2	1.3	1.5	1.6	1.8	2.0	2.3	2.5	2.8	3.0	3.3

TABLE A.1.3. (Continued)

Height above MSL (m)	Temperature (°C)										
	10.5	11.0	11.5	12.0	12.5	13.0	13.5	14.0	14.5	15.0	15.5
0 (1000 hPa)	22.1	23.3	24.6	25.9	27.2	28.5	29.8	31.2	32.6	34.1	35.6
100	21.1	22.3	23.5	24.8	26.0	27.2	28.5	29.8	31.2	32.7	34.1
200	20.1	21.2	22.4	23.6	24.8	26.0	27.3	28.5	29.8	31.3	32.7
300	19.1	20.2	21.4	22.5	23.7	24.9	26.2	27.4	28.6	29.9	31.3
400	18.2	19.3	20.4	21.5	22.7	23.9	25.1	26.2	27.4	28.7	30.0
500	17.4	18.5	19.5	20.6	21.8	23.0	24.1	25.2	26.3	27.5	28.9
600	16.7	17.7	18.7	19.7	20.9	22.0	23.1	24.2	25.3	26.4	27.7
700	15.9	16.8	17.8	18.8	19.9	21.1	22.2	23.3	24.4	25.4	26.6
800	15.2	16.0	16.9	17.9	19.0	20.1	21.2	22.3	23.4	24.5	25.6
900	14.5	15.3	16.1	17.1	18.1	19.2	20.3	21.4	22.5	23.6	24.7
1 000	13.8	14.5	15.3	16.3	17.3	18.3	19.4	20.4	21.5	22.5	23.6
1 100	13.1	13.8	14.6	15.5	16.5	17.5	18.5	19.5	20.5	21.5	22.6
1 200	12.5	13.2	13.9	14.8	15.7	16.7	17.6	18.6	19.6	20.6	21.7
1 300	11.9	12.6	13.3	14.1	14.9	15.8	16.8	17.7	18.7	19.7	20.8
1 400	11.3	12.0	12.7	13.4	14.2	15.1	16.0	16.9	17.8	18.8	19.8
1 500	10.8	11.4	12.0	12.7	13.5	14.3	15.2	16.1	17.0	17.9	18.9
1 600	10.2	10.8	11.4	12.0	12.8	13.6	14.5	15.4	16.3	17.1	18.0
1 700	9.7	10.2	10.8	11.4	12.2	13.0	13.8	14.7	15.6	16.4	17.3
1 800	9.2	9.7	10.3	10.9	11.6	12.4	13.2	14.0	14.9	15.7	16.5
1 900	8.7	9.2	9.8	10.4	11.1	12.9	12.6	13.4	14.2	15.0	15.8
2 000	8.2	8.7	9.3	9.9	10.6	11.4	12.1	12.8	13.5	14.3	15.1
2 100	7.8	8.3	8.8	9.4	10.1	10.8	11.5	12.2	12.9	13.7	14.5
2 200	7.4	7.9	8.4	9.0	9.6	10.3	11.0	11.7	12.4	13.1	13.8
2 300	7.0	7.5	8.0	8.6	9.2	9.9	10.5	11.2	11.9	12.5	13.2
2 400	6.6	7.1	7.6	8.2	8.8	9.5	10.1	10.7	11.4	12.0	12.7

TABLE A.1.3. (Continued)

Height above MSL (m) (1000 hPa)	Temperature (°C)										
	20.5	21.0	21.5	22.0	22.5	23.0	23.5	24.0	24.5	25.0	25.5
0 (1000 hPa)	54.8	57.1	59.5	62.1	64.9	67.9	71.0	74.3	77.5	80.8	84.3
100	52.9	55.3	57.6	60.2	62.9	65.9	68.8	72.0	75.2	78.6	82.0
200	51.2	53.5	55.8	58.3	61.0	63.8	66.7	69.8	72.9	76.3	79.7
300	49.5	51.7	54.1	56.5	59.1	61.9	64.7	67.7	70.7	74.4	77.5
400	47.8	50.0	52.4	54.8	57.3	60.0	62.7	65.7	68.7	72.0	75.3
500	46.2	48.4	50.8	53.1	55.5	58.1	60.8	63.7	66.6	69.9	73.2
600	44.7	46.8	49.1	51.4	53.8	56.3	58.9	61.8	64.7	68.0	71.3
700	43.1	45.2	47.6	49.8	52.1	54.6	57.1	60.0	62.9	66.1	69.3
800	41.6	43.7	46.0	48.2	50.5	52.9	55.3	58.1	61.0	64.2	67.4
900	40.2	42.3	44.5	46.6	48.8	51.2	53.6	56.3	59.1	62.3	65.5
1 000	38.8	40.8	43.0	45.1	47.3	49.5	51.8	54.5	57.3	60.4	63.6
1 100	37.4	39.3	41.4	43.6	45.7	47.9	50.1	52.7	55.4	58.5	61.8
1 200	36.0	37.9	39.9	42.2	44.3	46.4	48.4	51.0	53.7	56.7	60.0
1 300	34.8	36.6	38.6	40.8	42.8	44.9	46.9	49.4	52.0	55.0	58.1
1 400	33.6	35.3	37.3	39.5	41.5	43.4	45.3	47.8	50.4	53.4	56.4
1 500	32.2	34.0	36.0	38.1	40.0	41.9	43.8	46.2	48.7	51.8	54.8
1 600	31.1	32.8	34.6	36.7	38.6	40.4	42.3	44.7	47.2	50.3	53.2
1 700	30.0	31.6	33.4	35.4	37.3	39.1	41.0	43.3	45.7	48.7	51.6
1 800	28.9	30.5	32.2	34.2	36.1	37.9	39.7	42.0	44.4	47.2	50.0
1 900	27.9	29.5	31.2	33.1	34.9	36.7	38.5	40.7	43.0	45.8	48.5
2 000	26.8	28.4	30.1	32.0	33.8	35.5	37.3	39.5	41.8	44.4	47.0
2 100	25.9	27.5	29.0	30.8	32.5	34.4	36.2	38.3	40.5	43.0	45.5
2 200	25.0	26.5	27.9	29.6	31.3	33.2	35.0	37.1	39.3	41.8	44.2
2 300	24.0	25.5	26.9	28.6	30.2	32.1	34.0	36.0	37.2	40.0	42.6
2 400	23.1	24.5	26.0	27.6	29.3	31.1	33.0	35.0	37.1	39.3	41.6

21.5    22.0    22.5    23.0    23.5    24.0    24.5    25.0    25.5    26.0    26.5    27.0    27.5    28.0    28.5    29.0    29.5    30.0

Temperature (°C)

**TABLE A.1.4. Mixing ratios along pseudo-adiabats for specified 1 000-hPa dew points and elevations in meters above the 1 000-hPa level**

<i>Height above 1000 hPa level (m)</i>	<i>Dewpoint (°C)</i>																				
	10	11	12	13	14	15	16	17	18	19	20	21	22	23	24	25	26	27	28	29	30
0	7.7	8.2	8.8	9.4	10.1	10.8	11.5	12.3	13.1	14.0	14.9	15.9	16.9	18.0	19.1	20.3	21.6	23.0	24.4	25.9	27.6
100	7.5	8.0	8.6	9.2	9.9	10.6	11.3	12.1	12.9	13.8	14.7	15.7	16.7	17.8	18.9	20.1	21.4	22.7	24.1	25.8	27.3
200	7.4	7.9	8.5	9.1	9.7	10.4	11.1	11.8	12.8	13.5	14.4	15.4	16.4	17.5	18.6	19.8	21.1	22.5	23.9	25.4	27.1
300	7.2	7.7	8.3	8.9	9.5	10.2	10.9	11.6	12.4	13.3	14.2	15.2	16.2	17.3	18.4	19.6	20.9	22.2	23.6	25.1	26.8
400	7.0	7.5	8.1	8.7	9.3	10.0	10.7	11.4	12.2	13.1	14.0	15.0	16.0	17.0	18.1	19.3	20.6	22.0	23.4	24.9	26.5
500	6.8	7.3	7.8	8.5	9.1	9.8	10.5	11.2	12.0	12.8	13.7	14.7	15.7	16.8	17.9	19.1	20.4	21.7	23.1	24.6	26.2
600	6.7	7.2	7.7	8.3	8.9	9.6	10.3	11.0	11.8	12.6	13.5	14.5	15.5	16.6	17.7	18.9	20.1	21.5	22.9	24.4	26.0
700	6.5	7.0	7.5	8.1	8.7	9.4	10.1	10.8	11.6	12.4	13.3	14.3	15.3	16.3	17.4	18.6	19.9	21.2	22.6	24.1	25.7
800	6.3	6.8	7.3	7.9	8.5	9.1	9.8	10.5	11.3	12.2	13.1	14.0	15.0	16.1	17.2	18.4	19.6	21.0	22.4	23.9	25.4
900	6.1	6.6	7.2	7.7	8.3	8.9	9.6	10.3	11.1	11.9	12.8	13.8	14.8	15.8	16.9	18.1	19.4	20.7	22.1	23.6	25.2
1 000	6.0	6.5	7.0	7.5	8.1	8.8	9.5	10.2	10.9	11.7	12.6	13.6	14.6	15.6	16.7	17.9	19.1	20.5	21.9	23.4	24.9
1 100	5.8	6.3	6.8	7.4	8.0	8.6	9.3	10.0	10.7	11.5	12.4	13.3	14.3	15.4	16.5	17.7	18.9	20.2	21.6	23.1	24.6
1 200	5.7	6.1	6.6	7.2	7.8	8.4	9.1	9.8	10.5	11.3	12.2	13.1	14.1	15.1	16.2	17.4	18.6	20.0	21.4	22.9	24.4
1 300	5.5	6.0	6.5	7.0	7.8	8.2	8.9	9.6	10.3	11.1	12.0	12.9	13.9	14.9	16.0	17.2	18.4	19.7	21.1	22.6	24.1
1 400	5.3	5.8	6.3	6.8	7.4	8.0	8.7	9.4	10.1	10.9	11.8	12.7	13.8	14.6	15.7	16.9	18.1	19.5	20.9	22.3	23.8
1 500	5.2	5.8	6.1	6.8	7.2	7.8	8.5	9.2	9.9	10.7	11.6	12.5	13.4	14.4	15.5	16.7	17.9	19.2	20.6	22.1	23.6
1 600	5.0	5.5	6.0	6.5	7.0	7.6	8.3	9.0	9.7	10.5	11.4	12.3	13.2	14.2	15.3	16.5	17.7	19.0	20.3	21.7	23.3
1 700	4.9	5.3	5.8	6.3	6.9	7.5	8.1	8.8	9.5	10.3	11.2	12.1	13.0	14.0	15.0	16.2	17.4	18.7	20.1	21.6	23.1
1 800	4.7	5.1	5.6	6.1	6.7	7.3	7.9	8.6	9.3	10.1	10.9	11.8	12.7	13.7	14.8	16.0	17.2	18.5	19.8	21.2	22.8
1 900	4.8	5.0	5.5	6.0	6.5	7.1	7.7	8.4	9.1	9.9	10.7	11.6	12.5	13.5	14.6	15.7	16.9	18.2	19.6	21.0	22.5
2 000	4.4	4.8	5.3	5.8	6.3	6.9	7.5	8.2	8.9	9.7	10.5	11.4	12.3	13.3	14.3	15.5	16.7	18.0	19.3	20.7	22.3

## ANNEX II. THE WORLD'S GREATEST KNOWN RAINFALLS

World-record and near-record rainfalls are listed in Table A.2.1 and Table A.2.2, respectively. The relation between values and durations in Table A.2.1 is illustrated in Figure A.2.1, and an enveloping curve equation is given as follows (Wang G. and others, 2006):

$$R = 491 D^{0.452}$$

where the rainfall,  $R$ , is measured in mm and the duration,  $D$ , is measured in hours.

Extreme rainfalls in Tables A.2.1 and Table A.2.2 may be used to decide the general level of PMP in certain places. Nonetheless, these values contain only a few storm types and special geographic and topographic conditions, so their applicability is limited. Values with durations ranging from 12 hours to 2 years in Table A.2.1 come from tropical storms in La Réunion in the Indian Ocean and Cherrapunji in India. Typhoons, or what are called cyclones in La Réunion, run across steep mountains more than 3 000 m high and lead to favourable precipitation conditions. Cherrapunji is located on the southern side of Qinghai-Tibet Plateau and on the northern side of the Brahmaputra alluvial plain. Abundant moisture from the Bay of Bengal results in the formation of extraordinary storms with long durations. Table A.2.1 and Table A.2.2 list

near-record rainfalls in Taiwan Province of China, Jamaica and the Philippines, all of which are islands.

Most rainfalls with durations shorter than 12 hours in Table A.2.1 and Table A.2.2 are caused by typhoons (hurricanes) or strong local convection (thunderstorms).

Since the values listed are mostly from tropical storms, they should not be used as indicators of PMP magnitude in regions not prone to such storms. Obviously, small-area PMP in cold climates or over basins well protected by orographic barriers and located far enough from their coasts so as not to be affected by spillover will fall considerably below the values listed in these two tables.

Table A.2.3 shows the maximum observed depth-area-duration data for China, the United States of America and India. Table A.2.4.1 shows the maximum and near-record known depth-area-duration data for southern and northern China. Table A.2.4.2 shows depth-area-duration data of long-duration and large-area extraordinary storms in China. Table A.2.5 shows the maximum observed depth-area-duration data for the United States. Table A.2.6 shows the maximum observed depth-area-duration data for India.

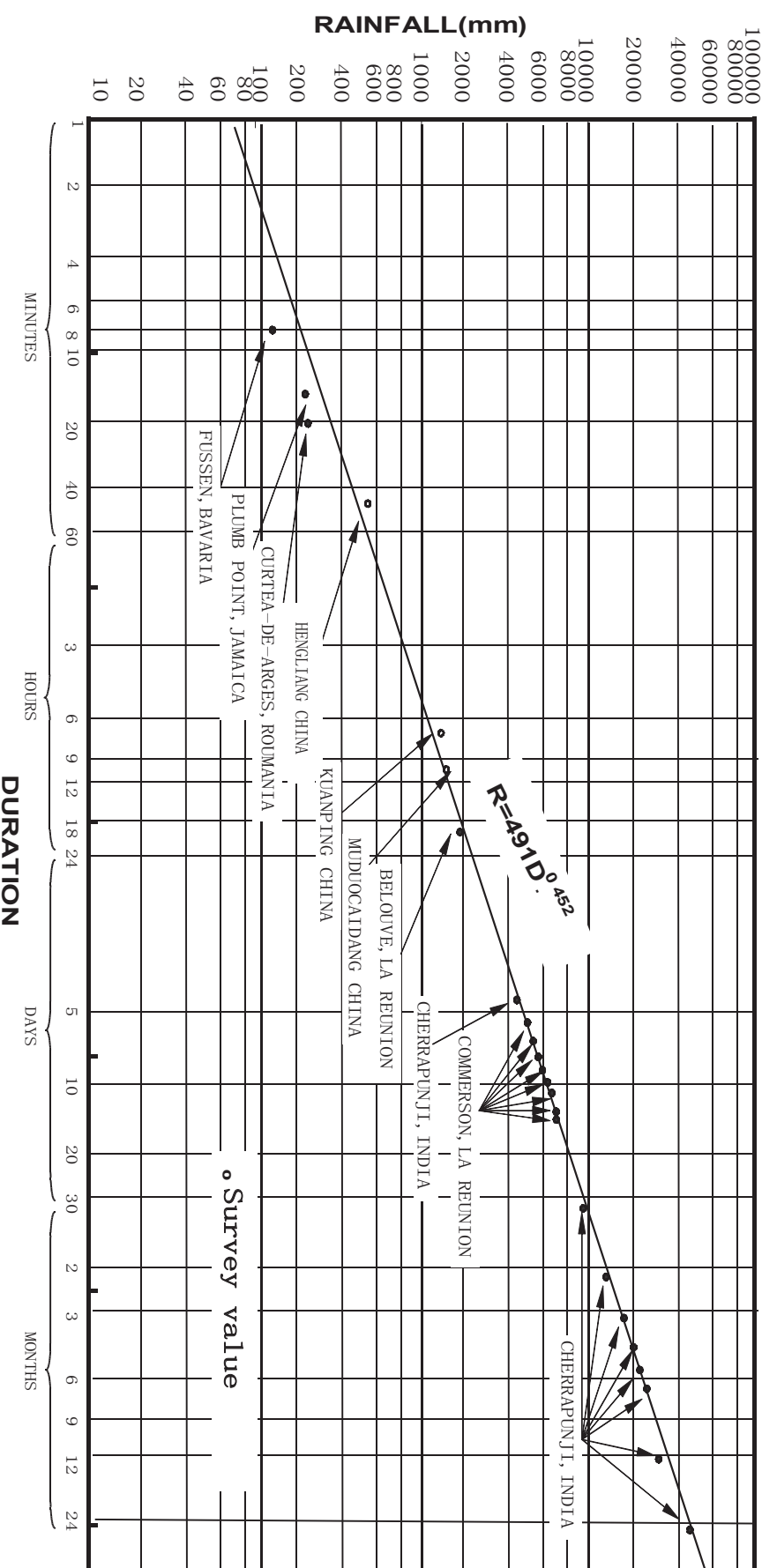


Figure A.2.1. World's greatest known point rainfalls (Wang G. and others, 2006)

**Table A.2.1. World's greatest known point rainfalls**

No.	Duration	Depth (mm)	Location	Date	Reference
1	1 minute	38	Barot, Guadeloupe	26 November 1970	WMO-No. 332
2	5 minutes	64	Haynes Canyon, California, United States	2 February 1976	Wang J., 2002
3	8 minutes	126	Fussen, Bavaria	24 May 1920	WMO-No. 332
4	15 minutes	198	Plumb Point, Jamaica	11 May 1916	WMO-No. 332
5	20 minutes	206	Curtea-de-Arges, Romania	7 July 1889	WMO-No. 332
6	30 minutes	280 <sup>a</sup>	Sikeshu, Hehei, China	3 July 1974	Wang J., 2002
7	42 minutes	305	Holt, Missouri, United States	22 June 1947	WMO-No. 332
8	44 minutes	472 <sup>a</sup>	Hengliang, Gansu, China	18 July 1991	Wang J., 2002
9	2 hours	489 <sup>a</sup>	Yujiawanzi, Nei Monggol, China	19 July 1975	Wang J., 2002
10	2 hours 10 minutes	483	Rockport, West Virginia, United States	18 July 1889	WMO-No. 332
11	2.5 hours	550 <sup>a</sup>	Bainaoabao, Hebei, China	25 June 1972	Wang J., 2002
12	2 hours 45 minutes	559	D'Hanis, Texas ,United States	31 May 1935	WMO-No. 332
13	3 hours	600 <sup>a</sup>	Duanjiazhan, Hebei, China	28 June 1973	Wang J., 2002
14	4 hours 30 minutes	782	Smethport, Pennsylvania, United States	18 July 1889	WMO-No. 332
15	6 hours	830	Linzhuang, Henan, China	7 August 1975	Wang J., 2002
16	6 hours	840 <sup>a</sup>	Muduocaidaing, Nei Monggol, China	1 August 1977	ABOM, 1994
17	7 hours	1 300 <sup>a</sup>	Kuanping, Shanxi, China	9 July 1998	Wang J., 2002
18	9 hours	1 087	Belouve, La Réunion	28 February 1964	WMO-No. 332
19	10 hours	1 400 <sup>a</sup>	Muduocaidang, Nei Monggol, China	1 August 1977	Wang J., 2002
20	12 hours	1 340	Belouve, La Réunion	28–29 February 1964	WMO-No. 332
21	18 hours 30 minutes	1 689	Belouve, La Réunion	28–29 February 1964	WMO-No. 332
22	24 hours	1 825	Foc Foc, La Réunion	15–16 March 1952	WMO-No. 332
23	2 days	2 467	Aurere, La Réunion	7–9 April 1958	WMO-No. 168

**Table A.2.1 (Continued)**

No.	Duration	Depth (mm)	Location	Date	Reference
24	3 days	3 130	Aurere, La Réunion	6–9 April 1958	WMO-No. 168
25	4 days	3 721	Cherrapunji, India	12–15 September 1974	WMO-No. 168
26	5 days	4 301	Commerson, La Réunion	23–27 January 1980	WMO-No. 168
27	6 days	4 653	Commerson, La Réunion	22–27 January 1980	WMO-No. 168
28	7 days	5 003	Commerson, La Réunion	21–27 January 1980	WMO-No. 168
29	8 days	5 286	Commerson, La Réunion	20–27 January 1980	WMO-No. 168
30	9 days	5 692	Commerson, La Réunion	19–27 January 1980	WMO-No. 168
31	10 days	6 028	Commerson, La Réunion	18–27 January 1980	WMO-No. 168
32	11 days	6 299	Commerson, La Réunion	17–27 January 1980	WMO-No. 168
33	12 days	6 401	Commerson, La Réunion	16–27 January 1980	WMO-No. 168
34	13 days	6 422	Commerson, La Réunion	15–27 January 1980	WMO-No. 168
35	14 days	6 432	Commerson, La Réunion	15–28 January 1980	WMO-No. 168
36	15 days	6 433	Commerson, La Réunion	14–28 January 1980	WMO-No. 168
37	31 days	9 300	Cherrapunji, India	1–31 July 1861	WMO-No. 332
38	2 months	12 767	Cherrapunji, India	June–July 1861	WMO-No. 332
39	3 months	16 369	Cherrapunji, India	May–July 1861	WMO-No. 332
40	4 months	18 738	Cherrapunji, India	April–July 1861	WMO-No. 332
41	5 months	20 412	Cherrapunji, India	April–Aug 1861	WMO-No. 332
42	6 months	22 454	Cherrapunji, India	April–Sept 1861	WMO-No. 332
43	11 months	22 990	Cherrapunji, India	January–November 1861	WMO-No. 332
44	1 years	26 461	Cherrapunji, India	August 1860–July 1861	WMO-No. 332
45	2 years	40 768	Cherrapunji, India	1860–1861	WMO-No. 332

<sup>a</sup> Survey value

**Table A.2.2. World's near-record rainfalls**

No	Duration	Depth (mm)	Location	Date	Reference
1	1 minute	31	Unionville, Maryland, United States	4 July 1956	WMO-No. 332
2	5 minutes	63	Porta Bello, Panama	28 November 1911	WMO-No. 332
3	10 minutes	87	Xiao Guanshan, Taiwan Province of China	2 February 1976	Wang J., 2002
4	14 minutes	100	Galveston, Texas, United States	4 June 1871	WMO-No. 332
5	15 minutes	117	Bengshan, Fujian, China,	4 July 1992	Wang J., 2002
6	20 minutes	120 <sup>a</sup>	Danianzi, Nei Monggol, China	6 May 1982	Wang J., 2002
7	40 minutes	235	Guinea, Virginia, United States	23 August 1906	WMO-No. 332
8	60 minutes	401 <sup>a</sup>	Shangdi, Nei Monggol, China	3 July 1975	Wang J., 2002
9	70 minutes	440 <sup>a</sup>	Gaojiahe, Gansu, China	12 August 1985	Wang J., 2002
10	90 minutes	430 <sup>a</sup>	Boligou, Hebei, China	25 June 1973	Wang J., 2002
11	3 hours	381	Port Elizabeth, South Africa	1 September 1965	WMO-No. 332
12	3 hours	406	Concord, Pennsylvania, United States	5 August 1843	WMO-No. 332
13	3 hours	495	Linzhuang, Henan, China	7 August 1975	Wang J., 2002
14	4 hours	584	Basseterre, St. Kitts, West Indies	12 January 1880	WMO-No. 332
15	4 hours	642	Linzhuang, Henan, China	7 August 1975	Wang J., 2002
16	4 hours	740	Shihetou, Shandong, China	4 August 1958	Wang J., 2002
17	6 hours	689	Dongxikou, Guangdong, China	10 June 1979	Wang J., 2002
18	7 hours	686	Shinlian, Taiwan, China	17 October 1967	WMO-No. 332
19	8 hours	796	Alishan, Taiwan, China	31 July 1996	Wang G., 1999
20	9 hours	890	Alishan, Taiwan, China	31 July 1996	Wang G., 1999
21	10 hours	983	Alishan, Taiwan, China	31 July 1996	Wang G., 1999
22	11 hours	1 076	Alishan, Taiwan, China	31 July 1996	Wang G., 1999
23	12 hours	1 158	Alishan, Taiwan, China	31 July 1996	Wang G., 1999
24	13 hours	1 246	Alishan, Taiwan, China	31 July 1996	Wang G., 1999
25	14 hours	1 322	Alishan, Taiwan, China	31 July 1996	Wang G., 1999
26	15 hours	1 370	Alishan, Taiwan, China	31 July 1996	Wang G., 1999
27	16 hours	1 405	Alishan, Taiwan, China	31 July 1996	Wang G., 1999
28	17 hours	1 474	Alishan, Taiwan, China	31 July 1996	Wang G., 1999
29	18 hours	1 538	Alishan, Taiwan, China	31 July 1996	Wang G., 1999
30	18 hours	1 589	Foc Foc, La Réunion	30 December 1899	ABOM, 1994

Table A.2.2. (Continued)

No.	Duration	Depth (mm)	Location	Date	Reference
31	20 hours	1 697	Foc Foc, La Réunion	7–8 January 1966	ABOM, 1994
32	21 hours	1 635	Alishan, Taiwan Province of China	31 July 1996	Wang G., 1999
33	22 hours	1 780	Foc Foc, La Réunion	7–8 January 1966	ABOM, 1994
34	23 hours	1 694	Alishan, Taiwan Province of China	31 July 1996	Wang G., 1999
35	24 hours	1 749	Alishan, Taiwan Province of China	31 July–1 August 1996	Wang G., 1999
36	24 hours	1 672	Xinliao, Taiwan Province of China	17 October 1967	WMO-No. 332
37	39 hours	1 585	Baguio, Philippines	14–16 July 1911	WMO-No. 332
38	2 days	1 987	Alishan, Taiwan Province of China	31 July–1 August 1996	Wang G., 1999
39	2 days	2 259	XinLiao, Taiwan Province of China	17–18 October 1967	WMO-No. 332
40	2 days	2 086	Bowden Pen, Jamaica	22–23 January 1960	WMO-No. 332
41	2 days	1 616	Cherrapunji, India	14–15 June 1876	WMO-No. 332
42	2 days 15 hours	2 010	Baguio, Philippines	14–17 July 1911	WMO-No. 332
43	3 days	2 749	Xinliaojiao, Taiwan Province of China	17–19 October 1967	WMO-No. 332
44	3 days	2 528	Bowden Pen, Jamaica	22–24 January 1960	WMO-No. 332
45	3 days	2 759	Cherrapunji, India	12–14 September 1974	WMO-No. 332
46	3 days 15 hours	2 210	Baguio, Philippines	14–18 July 1911	WMO-No. 332
47	4 days	2 789	Bowden Pen, Jamaica	22–25 January 1960	WMO-No. 332
48	4 days	2 587	Cherrapunji, India	12–15 June 1876	WMO-No. 332
49	5 days	2 908	Silver Hill Plantation, Jamaica	5–9 November 1909	WMO-No. 332
50	5 days	2 899	Cherrapunji, India	12–16 June 1876	WMO-No. 332
51	6 days	3 112	Silver Hill Plantation, Jamaica	5–10 November 1909	WMO-No. 332
52	6 days	3 032	Cherrapunji, India	11–16 June 1876	WMO-No. 332
53	7 days	3 331	Cherrapunji, India	24–30 June 1931	WMO-No. 332
54	7 days	3 277	Silver Hill Plantation, Jamaica	4–10 November 1909	WMO-No. 332
55	8 days	3 430	Cherrapunji, India	24 June–1 July 1931	WMO-No. 332
56	8 days	3 429	Silver Hill Plantation, Jamaica	4–11 November 1909	WMO-No. 332
57	8 days	3 847	Bellenden Ker, Queensland, Australia	1–8 January 1979	ABOM, 1994
58	15 days	4 798	Cherrapunji, India	24 June–8 July 1931	WMO-No. 332

<sup>a</sup> Survey value

**Table A.2.3. Maximum observed depth-area-duration data for China, the United States and India  
(average rainfall in mm) (Wang J., 2002)**

Duration	Country	Area ( $\text{km}^2$ )							
		Point	100	300	1 000	3 000	10 000	30 000	100 000
1 hour	China	401	267	167	107	72			
	United States	224	178	150	125	96			
3 hours	China	600	447	399	297	196			
	United States	478	410	370	315	245			
6 hours	China	840	723	643	503	350	127		
	United States	627	550	490	410	325	228	135	73
12 hours	China	1 400	1 050	854	675	512	212	115	47
	United States	757	700	660	630	540	325	190	118
24 hours	China	1 748	1 192	1 142	1 045	850	435	306	155
	United States	983	930	880	850	740	460	290	180
	India	987		940	850	720	540	365	
3 days	China	2 749	1 775	1 600	1 410	1 150	940	715	420
	United States	1 148	1 080	1 020	970	860	660	520	365
	India	1 448		1 400	1 340	1 240	1 040	750	
5 days	India	1 615		1 510	1 420	1 330	1 180	900	
7 days	China	2 749	1 805	1 720	1 573	1 350	1 200	960	570

**Table A.2.4.1. Maximum and near-record known depth-area-duration data for northern and southern China (Wang J., 2002)**  
**(a) Areal mean rainfall (mm)**

Duration	Region	Area ( $\text{km}^2$ )							
		0	100	300	1 000	3 000	10 000	30 000	100 000
1 hour	North	*401 <sup>SD</sup>	*267 <sup>GJ</sup>	*167 <sup>GJ</sup>	*107 <sup>LZ</sup>				
		253 <sup>DS</sup>	162 <sup>LZ</sup>	145 <sup>LZ</sup>	95 <sup>TJ</sup>				
	South	245 <sup>dsk</sup>	185 <sup>md</sup>	136 <sup>dh</sup>	105 <sup>dh</sup>	*72 <sup>dh</sup>			
		176 <sup>dh</sup>	155 <sup>dh</sup>	111 <sup>zd</sup>	85 <sup>zd</sup>	41 <sup>tt</sup>			
3 hours	North	*600 <sup>Dj</sup>	*447 <sup>Lz</sup>	*399 <sup>LZ</sup>	*297 <sup>LZ</sup>	120 <sup>MD</sup>			
		495 <sup>LZ</sup>	446 <sup>ZJ</sup>	343 <sup>ZJ</sup>	204 <sup>DZ</sup>	98 <sup>YW</sup>			
	South	435 <sup>dsk</sup>	328 <sup>md</sup>	305 <sup>dh</sup>	260 <sup>dh</sup>	*196 <sup>dh</sup>			
		346 <sup>dh</sup>	325 <sup>dh</sup>	264 <sup>lh</sup>	203 <sup>lb</sup>	105 <sup>tt</sup>			
6 hours	North	*840 <sup>MD</sup>	*723 <sup>LZ</sup>	*643 <sup>LZ</sup>	*503 <sup>LZ</sup>	240 <sup>MD</sup>	*127 <sup>MD</sup>		
		830 <sup>LZ</sup>	630 <sup>MD</sup>	512 <sup>MD</sup>	405 <sup>MD</sup>	239 <sup>IS</sup>			
	South	689 <sup>dsk</sup>	560 <sup>dh</sup>	524 <sup>dh</sup>	456 <sup>dh</sup>	*350 <sup>dh</sup>			
		588 <sup>dh</sup>	512 <sup>dsk</sup>	390 <sup>tc</sup>	292 <sup>wy</sup>	218 <sup>cq</sup>			
12 hours	North	*1 400 <sup>MD</sup>	*1 050 <sup>MD</sup>	*854 <sup>MD</sup>	*675 <sup>MD</sup>	400 <sup>MD</sup>	*212 <sup>MD</sup>	*115 <sup>MD</sup>	*47 <sup>MD</sup>
		954 <sup>LZ</sup>	833 <sup>LZ</sup>	763 <sup>LZ</sup>	658 <sup>LZ</sup>	310 <sup>IS</sup>			
	South	779 <sup>wy</sup>	735 <sup>bs</sup>	705 <sup>bs</sup>	630 <sup>bs</sup>	*512 <sup>bs</sup>			
		771 <sup>bs</sup>	715 <sup>dh</sup>	696 <sup>dh</sup>	612 <sup>dh</sup>	500 <sup>dh</sup>			
24 hours	North	1 400 <sup>MD</sup>	1 050 <sup>MD</sup>	854 <sup>MD</sup>	738 <sup>LZ</sup>	629 <sup>LZ</sup>	*435 <sup>LZ</sup>	214 <sup>ZM</sup>	122 <sup>EH</sup>
		1 060 <sup>LZ</sup>	929 <sup>LZ</sup>	850 <sup>LZ</sup>	675 <sup>MD</sup>	496 <sup>ZM</sup>	345 <sup>HG</sup>	200 <sup>LW</sup>	120 <sup>LW</sup>
	South	*1 748 <sup>al</sup>	*1 192 <sup>bs</sup>	*1 142 <sup>bs</sup>	*1 045 <sup>bs</sup>	*850 <sup>bs</sup>	430 <sup>ns</sup>	*306 <sup>ns</sup>	*155 <sup>ns</sup>
		1 673 <sup>xl</sup>	958 <sup>al</sup>	810 <sup>al</sup>	752 <sup>als</sup>	660 <sup>als</sup>	344 <sup>zd</sup>	206 <sup>dx</sup>	145 <sup>bs</sup>
3 days	North	1 605 <sup>LZ</sup>	1 554 <sup>LZ</sup>	1 442 <sup>LZ</sup>	1 280 <sup>LZ</sup>	1 080 <sup>LZ</sup>	805 <sup>LZ</sup>	535 <sup>LZ</sup>	245 <sup>ZM</sup>
		1 457 <sup>ZM</sup>	1 340 <sup>ZM</sup>	1 272 <sup>ZM</sup>	1 139 <sup>ZM</sup>	947 <sup>ZM</sup>	692 <sup>ZM</sup>	450 <sup>ZM</sup>	135 <sup>QI</sup>
	South	*2 749 <sup>xl</sup>	*1 775 <sup>al</sup>	*1 600 <sup>al</sup>	*1 410 <sup>bs</sup>	*1 150 <sup>bs</sup>	*940 <sup>ns</sup>	*715 <sup>ns</sup>	*420 <sup>ns</sup>
		1 987 <sup>al</sup>	1 610 <sup>bs</sup>	1 535 <sup>bs</sup>	1 220 <sup>al</sup>	1 060 <sup>ns</sup>	880 <sup>bs</sup>	515 <sup>bs</sup>	272 <sup>kt</sup>
7 days	North	2 050 <sup>ZM</sup>	*1 805 <sup>ZM</sup>	*1 720 <sup>ZM</sup>	*1 573 <sup>ZM</sup>	*1 345 <sup>ZM</sup>	1 020 <sup>ZM</sup>	780 <sup>ZM</sup>	524 <sup>ZM</sup>
		1 631 <sup>LZ</sup>	1 554 <sup>LZ</sup>	1 445 <sup>LZ</sup>	1 300 <sup>LZ</sup>	1 095 <sup>LZ</sup>	830 <sup>LZ</sup>	545 <sup>LZ</sup>	275 <sup>SZ</sup>
	South	*2 749 <sup>xl</sup>	1 775 <sup>al</sup>	1 600 <sup>al</sup>	1 410 <sup>bs</sup>	*1 350 <sup>ns</sup>	*1 200 <sup>ns</sup>	*960 <sup>ns</sup>	*570 <sup>ns</sup>
		1 987 <sup>al</sup>	1 610 <sup>bs</sup>	1 535 <sup>bs</sup>	1 400 <sup>ns</sup>	1 150 <sup>bs</sup>	880 <sup>bs</sup>	589 <sup>ds</sup>	440 <sup>ds</sup>

Notes: (1) Southern China and northern China are bounded by Qin Lin and Huaihe.  
(2) Survey storms which occurred at Heng Liang Gansu in 1991 (44 minutes, 472 mm) and at Kuanping, Shan Xi in 1998 (6–7 hours, 1 300 mm) are not listed.  
(3) The meaning of superscripts of rainfall values are listed in Table A.2.4.1(b).  
(4) \* Maximum value of each duration for China.

**Table A.2.4.1 (b) Location of storm centre**

<i>Region</i>	<i>Mark</i>	<i>Location</i>	<i>Latitude (N)</i>	<i>Longitude (E)</i>	<i>Catchment</i>	<i>Date</i>
South	al	Alishan	23° 31	120° 44	Taiwan Province of China	31 July 1996
	als	Alishan	23° 31	120° 44	Taiwan Province of China	7 August 1959
	bs	Baishi	24° 33	121° 13	Taiwan Province of China	10 September 1963
	cq	Chaoqiao	32° 18	121° 09	Changjiangkou	4 August 1960
	dh	Dahushan	23° 29	120° 38	Taiwan Province of China	7 August 1959
	ds	Dashuihe	30° 57	116° 38	Changjiang	13 July 1969
	dx	Dongxiang	28° 14	116° 36	Boyanghu	17 August 1953
	dsk	Dongxikou	23° 27	116° 51	Guangdong	10 June 1979
	kt	Ketan	31° 14	117° 08	Changjiang	14 July 1969
	lb	Liban	19° 08	109° 36	Hainan	20 July 1977
	lh	Laohutan	21° 35	107° 54	Beibuwan	11 July 1960
	ls	Luoshan	29° 40	113° 22	Changjiang	25 June 1954
	md	Maodong	21° 48	111° 32	Guangdong	12 May 1979
	ns	Nihi*	29° 56	110° 46	Linshui	4 July 1935
North	tc	Tianchi	18° 45	108° 52	Hainan	17 July 1983
	tt	Tantou	28° 15	120° 54	Zhejiang	27 August 1973
	wy	Wuyang*	21° 22	110° 41	Guangdong	21 September 1976
	xl	Xinliao	24° 35	121° 45	Taiwan Province of China	17 October 1967
	zd	Zhidao	19° 11	109° 23	Hainan	20 July 1977
	DJ	Duanjiazhuang*	40° 20	114° 35	Hebei	28 June 1973
	DS	Dashicao	34° 17	109° 37	Weihe	20 June 1981
	DZ	Dazhangzhuang	39° 17	117° 14	Haihe	25 July 1978
	EH	Erhe*	45° 06	127° 19	Songhuajiang	29 July 1966
	GJ	Gaojiahe	34° 51	104° 40	Weihe	12 August 1985
	HG	Huanggou	40° 17	124° 37	Yalujiang	4 August 1958
	JS	Jieshou	33° 16	115° 21	Yinghe	1 July 1972
	LW	Liuyu	33° 39	118° 05	Huaihe	12 August 1974
	LZ	Linzhuang	33° 03	113° 39	Huaihe	7 August 1975
	MD	Mudoucaidang*	38° 55	109° 24	Huanghe	1 August 1977
	QL	Qilier	44° 31	127° 12	Songhuajiang	6 August 1956
	SD	Shangdi*	42° 16	119° 08	Xiliaohe	3 July 1975
	SZ	Shiziping	38° 12	113° 46	Ziyahe	3 August 1956
	TJ	Tangjiatun*	39° 57	122° 18	Liaodong Island	27 July 1981
	YW	Yaowangmiao	40° 47	120° 09	Liaodongwan	19 July 1963
	ZJ	Zhangjiafangzi*	41° 52	113° 13	Neimenggu	19 July 1959
	ZM	Zhanghong	37° 22	114° 13	Ziyahe	4 August 1963

Notes: (1) Date is the occurrence time of the maximum 24-hour rainfall.

(2) \* Centre site of survey storm.

**Table A.2.4.2. Depth-area-duration data of long-duration and large-area extraordinary storms in China (average rainfall in mm) (Wang J., 2002)**

Main region	Date	Duration (days)	Storm centre Point	Area (km <sup>2</sup> )						
				1 000	3 000	10 000	30 000	100 000	300 000	1 000 000
Songhuajiang	1 July–31 August 1957	62	Lishugou	598.1	540	505	480	420		
Haihe	July–August 1939	62	Changping	1 137.2	1 100	965	850	735	630	
Haihe	2–8 August 1963	7	Zhanghong	2 050	1 573	1 345	1 020	780	524	
Huanghe	13 August – 13 September 1981	32	Sandagu	394.9	330	310	265	200		
Huaihe	6–20 July 1957	15	Fucheng	817.4	747	710	667	611		
Huaihe	4–8 August 1975	5	Linzhuang	1 631.1	1 300	1 095	830	545		
Changjiang	14–23 August 1981	10	Huaishu	806.0	725	665	595	500	355	210
Changjiang	1–10 July 1935	10	Nishi	1 650*	1 430	1 370	1 240	970	590	
Jianghuai	28 June – 27 July 1931	30	Taixian	987.7	830	740	700	580	430	
Jianghuai	May 1954	31	Huangshan	1 037	850	750	660	610	545	478
Jianghuai	June 1954	30	Luoshan	1 047	1 000	955	860	735	650	560
Jianghuai	July 1954	31	Wudian	1 265	1 180	1 080	940	850	740	610
Jianghuai	May–July 1954	92	Huangshan	2 824.2	2 480	2 270	1 960	1 760	1 620	1 460
Jianghuai	15 May – 13 July 1991	60	Huangshan	1 644			1 250	1 100	1 000	890
M.Z.G.	12–24 June 1998	13	Aotou	1 636.1	1 198	1 088	1 012	911	662	620
Zhuijiang	14–26 June 1998	13	Huajiang	986	900	765	670	535		
Xinjiang	13–28 July 1996	16	Tianshan	231	200	190	180	160	115	82
										54

Notes: (1) Sandagu is located at Changjiang watershed.

(2) Rainfalls of storm centre are survey value.

(3) Jiang Huai includes Changjiang and Huaihe.

(4) M.Z.G relates to Fu Jian, Zhe Jiang and Jiang Xi.

**Table A.2.5. Maximum observed depth-area-duration data for the United States (WMO-No. 332)**  
**(a) Average rainfall in mm**

Area	Duration (hours)						
	6	12	18	24	36	48	72
26 km <sup>2</sup>	627 <sup>a</sup>	757 <sup>b</sup>	922 <sup>e</sup>	983 <sup>e</sup>	1 062 <sup>e</sup>	1 095 <sup>e</sup>	1 148 <sup>e</sup>
295 km <sup>2</sup>	498 <sup>b</sup>	668 <sup>e</sup>	826 <sup>e</sup>	894 <sup>e</sup>	963 <sup>e</sup>	988 <sup>e</sup>	1 031 <sup>e</sup>
518 km <sup>2</sup>	455 <sup>b</sup>	650 <sup>e</sup>	798 <sup>e</sup>	869 <sup>e</sup>	932 <sup>e</sup>	958 <sup>e</sup>	996 <sup>e</sup>
1 295 km <sup>2</sup>	391 <sup>b</sup>	625 <sup>e</sup>	754 <sup>e</sup>	831 <sup>e</sup>	889 <sup>e</sup>	914 <sup>e</sup>	947 <sup>e</sup>
2 590 km <sup>2</sup>	340 <sup>b</sup>	574 <sup>e</sup>	696 <sup>e</sup>	767 <sup>e</sup>	836 <sup>e</sup>	856 <sup>e</sup>	886 <sup>e</sup>
5 180 km <sup>2</sup>	284 <sup>b</sup>	450 <sup>e</sup>	572 <sup>e</sup>	630 <sup>e</sup>	693 <sup>e</sup>	721 <sup>e</sup>	754 <sup>e</sup>
12 950 km <sup>2</sup>	206 <sup>h</sup>	282 <sup>b</sup>	358 <sup>b</sup>	394 <sup>e</sup>	475 <sup>i</sup>	526 <sup>i</sup>	620 <sup>i</sup>
25 900 km <sup>2</sup>	145 <sup>h</sup>	201 <sup>j</sup>	257 <sup>k</sup>	307 <sup>k</sup>	384 <sup>i</sup>	442 <sup>i</sup>	541 <sup>i</sup>
51 800 km <sup>2</sup>	102 <sup>h</sup>	152 <sup>j</sup>	201 <sup>k</sup>	244 <sup>k</sup>	295 <sup>i</sup>	351 <sup>i</sup>	447 <sup>i</sup>
129 000 km <sup>2</sup>	64 <sup>e,m</sup>	107 <sup>n</sup>	135 <sup>k</sup>	160 <sup>k</sup>	201 <sup>k</sup>	251 <sup>r</sup>	335 <sup>r</sup>
259 000 km <sup>2</sup>	43 <sup>m</sup>	64 <sup>o,m</sup>	89 <sup>k</sup>	109 <sup>k</sup>	152 <sup>p</sup>	170 <sup>p</sup>	226 <sup>q</sup>

**(b) Meaning of storm codes**

Storm	Date	Location of centre	Genesis
a	17–18 July 1942	Smethport, Pennsylvania	
b	8–10 September 1921	Thrall, Texas	
e	3–7 September 1950	Yankeetown, Florida	Hurricane
h	27 June – 4 July 1936	Bebe, Texas	
i	27 June – 1 July 1899	Hearne, Texas	
j	12–16 April 1927	Jefferson Parish, Iowa	
k	13–15 March 1929	Elba, Alabama	
m	22–26 May 1908	Chattanooga, Oklahoma	
n	15–18 April 1900	Eutaw, Alabama	
o	19–22 November 1934	Millry, Alabama	
p	29 September – 3 October 1929	Verson, Florida	Hurricane
q	5–10 July 1916	Bonifay, Florida	Hurricane
r	19–24 September 1967	Cibolo Creek, Texas	Hurricane

**Table A.2.6. Maximum observed depth-area-duration data for India (average rainfall in mm)  
(Wang G. and others, 2005)**

Area (km <sup>2</sup> )	Duration (days)						
	1	2	3	4	5		
(1)	(2) <sup>b</sup>	(3) <sup>b</sup>	(4) <sup>b</sup>	(5) <sup>b</sup>	(6) <sup>a</sup>	(7) <sup>b</sup>	(8) <sup>a</sup>
point	987	1 270	1 448	1 499	1 554	1 524	1 615
259	945	1 248	1 410	1 435	1 450	1 485	1 525
518	904	1 225	1 380	1 405	1 375	1 460	1 480
777	870	1 200	1 335	1 375	1 333	1 430	1 440
1 295	825	1 158	1 315	1 335	1 263	1 400	1 370
2 590	737	1 070	1 245	1 275	1 159	1 340	1 270
3 885	678	1 008	1 203	1 235	1 103	1 300	1 206
5 180	640	965	1 170	1 205	1 065	1 270	1 165
7 770	577	890	1 095	1 145	1 018	1 215	1 120
12 950	498	775	985	1 045	960	1 117	1 053
25 900	386	595	787	875	838	935	941
38 850	320	492	668	745	752	825	840
51 800	272	425	580	660	685	730	771
64 750	240	375	525	605	635	670	713

Notes: <sup>a</sup> Data in columns (6) and (8) are from the storm rainfall of 24–29 July 1927;

<sup>b</sup> The storm centre was at Dakor. Data in columns (2) to (5) and (7) are from the storm rainfall of 1–5 July 1941, with the storm centre at Dharampur.

### ANNEX III. THE WORLD'S GREATEST KNOWN FLOODS

World-record and near-record floods are listed in Table A.3.1 and Table A.3.2, respectively. The relation between peak floods and size of watersheds in Table A.3.1 is illustrated in Figure A.3.1. An enveloping curve equation is also given as follows (Wang G. and others, 2006):

$$\text{For } A < 300 \text{ km}^2 \quad Q_m = 154 A^{0.738}$$

$$\text{For } 300 \leq A \leq 3\,000\,000 \text{ km}^2 \quad Q_m = 1830 A^{0.316}$$

Where  $Q_m$  is the peak flood ( $\text{m}^3/\text{s}$ );  $A$  is the area size of the watershed ( $\text{km}^2$ ).

Maximum peak flow in Table A.3.1 and Table A.3.2 can be used to decide the general level of PMF for certain places. Like the world's greatest known rainfall, however, those flood values are mostly from areas whose geographic locations and topographic conditions are favourable to the formation of extraordinary floods, so they should only be used with caution.

The sources of flood values in Table A.3.1 and Table A.3.2 fall into five categories:

- (a) The World's Roof, Asia, the Eastern Hemisphere: the southern side (India, Bengal, Myanmar, Cambodia and Pakistan) and the south-eastern side (the Yangtze River, China) of the Tibetan Plateau. Extreme storms with long durations and large area sizes occur frequently here. The world's

flood extremes with collecting areas between 60 000 and 1 700 000  $\text{km}^2$  all occur in this area.

- (b) The east of Cordillera – a high mountain range along the Americas and on the east coast of the Pacific Ocean – and Brazil, the United States of America and Mexico on the west coast of the Atlantic Ocean in the Western Hemisphere. Floods in the Amazon River Basin, Brazil, are prominent, which might be related to its sector-like watershed area shape.
- (c) The Lena and Yenisei rivers, two large rivers in Russia. Extraordinary floods there are mostly caused by melted ice and snow (Duochino, 1991).
- (d) Island countries and coastal ones that are in the tropical zone or the subtropical zone and that are affected by typhoons (hurricanes), such as Australia, Madagascar, the Philippines, the Democratic People's Republic of Korea and the Republic of Korea, Japan, as well as Taiwan Province of China and Hainan Island, China.
- (e) Most flood extremes with small area sizes in the subtropical zone are caused by strong thermal convections (thunderstorms). Examples include the United States and China.

As a result, in PMF estimation, specific analyses must be made in combination with the specific conditions of the design watershed if flood values in Table A.3.1 and Table A.3.2 are to be compared with or used as indicators for PMF.

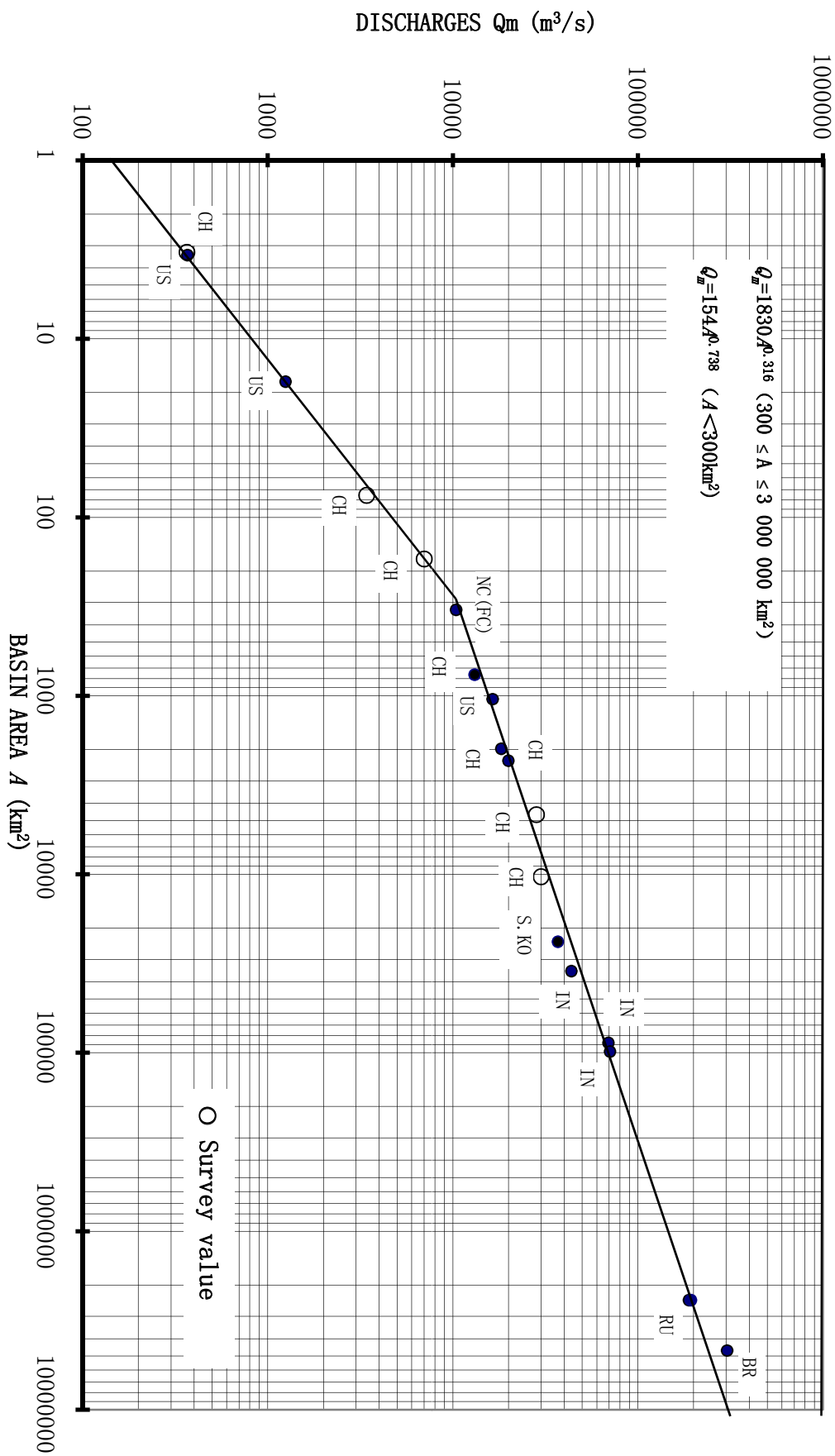


Figure A.3.1. World's greatest known floods (Wang G. and others, 2006)

**Table A.3.1. World's greatest known floods**

No.	Country	Station	Catchment area (km <sup>2</sup> )	Maximum discharge (m <sup>3</sup> /s)	Date	Reference
1	China	Taohe, Tamigou, Sunjiazhai	0.9	159 <sup>a</sup>	10/08/79	Hu and Luo, 1988
2	Puerto Rico (United States)	Q. de Los Cedros, Isabela	1.79	212	07/05/70	Wang G., 1999
3	United States	Humboldt River tributary, Nevada	2.2	251	31/05/73	Costa, 1987
4	China	Nangou, Shanxi	3.27	366 <sup>a</sup>	22/07/89	CCFDYRVNC, 1996
5	United States	Big Creek, near Waynesville, North Carolina	3.4	368	30/08/40	Crippen and Bue, 1977
6	China	Fenhe, Chengjiaqu	5.6	457 <sup>a</sup>	31/07/71	Luo and Shen, 1987
7	United States	Halawa, Hawaii	12	762	04/02/65	Rodier and Roche, 1984
8	United States	Lane Canyon, Oregon	13.1	807	26/07/65	Costa, 1987
9	United States	El Rancho Arroyo, near Pojoazue, New Mexico	17.4	1 250	22/08/52	Crippen and Bue, 1977
10	United States	Meyers Canyon, Oregon	32.9	1 540	13/07/56	Costa, 1987
11	United States	Bronco Creek, near Wikieup, Arizona	49.2	2 080	18/08/71	Costa, 1987
12	United States	Nelson Landing, El Dorado, Nevada	56.5	2 150	14/09/74	IAHS, 2003
13	United States	S.F. Waliua, Lihue Hawaii	58	2 470	15/04/63	Rodier and Roche, 1984
14	China	Nandujiang Baisha, Hainan	75.3	3 420 <sup>a</sup>	1894	Luo and Shen, 1987
15	Mexico	San Bartolo	81	3 000	30/09/76	Rodier and Roche, 1984
16	China	Dalinghe Tangtouhe, Shaohuyingzi	97.2	4 000	01/08/30	Luo and Shen, 1987
17	China	Minjiang, Xiyuanxi, Xiyuangong	142	4 600 <sup>a</sup>	17/09/09	Luo and Shen, 1987
18	China	Dalinghe Waziyuhe, Waziyu	154	5 320	01/08/30	Luo and Shen, 1987
19	China	Bohaian, Shihe, Xiaoshankou	171	7 000 <sup>a</sup>	01/07/94	Luo and Shen, 1987
20	Taiwan, China	Cho Shui, Taiwan	259	7 780	24/08/79	Rodier and Roche, 1984

**Table A.3.1 (Continued)**

No.	Country	Station	Catchment area (km <sup>2</sup> )	Maximum discharge (m <sup>3</sup> /s)	Date	Reference
21	France	Ouaieme, New Caledonia	330	10 400	24/12/81	Rodier and Roche, 1984
22	China	Huaihe Ruhe, Banqiao	762	13 100	07/08/75	Luo and Shen, 1987
23	United States	West Nueces River, Texas	1 041	16 400	14/06/35	Costa, 1987
24	China	Huaihe Pihe, Foziling	1 840	17 600	14/07/69	Feng, 1983
25	Taiwan, China	Wuxi Dadu, Taiwan	1 980	18 300	08/08/59	Feng, 1983
26	Taiwan, China	Zhuoshuixi, Jiji, Taiwan	2 310	20 000	01/08/96	Wang G., 1999
27	Japan	Shingu Oga	2 350	19 025	26/09/59	Rodier and Roche, 1984
28	Philippines	Cagayan Echague Isabella	4 244	17 550	1959	Rodier and Roche, 1984
29	China	Changhuajiang, Baoqiao, Hainan	4 634	28 300 <sup>a</sup>	1887	Luo and Shen, 1987
30	India	Madhopur, Ravi, Indus	6 087	26 050	01/09/88	IAHS, 2000
31	United States	Pecos Comstock, Texas	9 100	26 800	28/06/54	Rodier and Roche, 1984
32	China	Yihe Linyi	10 315	30 000 <sup>a</sup>	09/08/1730	Luo and Shen, 1987
33	People's Democratic Republic of Korea	Toedonggang Mirim	12 175	29 000	29/08/67	Rodier and Roche, 1984
34	China	Chang Jiang Lishui, Sanjiangkou	15 242	31 100	05/07/35	Luo and Shen, 1987
35	China	Qujiang, Fengtan	16 595	32 300 <sup>a</sup>	22/09/1847	Luo and Shen, 1987
36	India	Jhalawaw, Chambal, Ganga	22 584	37 000	08/69	IAHS, 2000
37	Republic of Korea	Han Koan	23 880	37 000	18/07/25	Rodier and Roche, 1984
38	India	Betwa Sahijna	44 870	43 800	26/07/71	Rodier and Roche, 1984
39	Madagascar	Mangoky Banyan	50 000	38 000	05/02/33	Rodier and Roche, 1984
40	China	Yalujiang Huanggou	55 420	44 800	11/08/1888	Hu and Luo, 1988

**Table A.3.1 (Continued)**

No.	Country	Station	Catchment area (km <sup>2</sup> )	Maximum discharge (m <sup>3</sup> /s)	Date	Reference
41	India	Gujarat, Wuyika	62 225	42 475	08/68	IAHS, 2000
42	India	Namada Garudeshwar	88 000	69 400	06/09/70	Rodier and Roche, 1984
43	India	Namada	98 420	70 790	1954	ICID, 1992
44	India	Godavari	299 320	78 690	17/09/59	ICID, 1992
45	India	Godavari at Polaeshwaram	307 800	87 250	08/07	IAHS, 2003
46	India	Godavari Dowlaishwaram	315 000	88 400	1959	Feng, 1983
47	Bengal	Brahmaputra Jiamuna	530 000	93 500	01/08/55	ICID, 1992
48	Bengal	Brahmaputra Bahadurabad	580 000	98 500	30/08/88	Feng, 1983
49	China	Changjiang Wanxian	974 900	108 000 <sup>a</sup>	18/07/1870	CJWRC, 1997
50	China	Changjiang Yitchang	1 005 500	105 000 <sup>a</sup>	20/07/1870	CJWRC, 1997
51	Bengal	Changes Baluliya	1 650 000	132 000	09/88	Feng, 1983
52	Russia	Lena Kusur	2 430 000	189 000	08/06/67	UNESCO, 1976
53	Russia	Lena Kusur	2 430 000	194 000	11/06/44	ICID, 1992
54	Brazil	Amazon Obidos	4 640 300	303 000 <sup>b</sup>	06/53	Wang G., 1999

<sup>a</sup> Survey values<sup>b</sup> This is a corrected value (original value is 370 000). Information was provided by Brazilian hydrologist Newton de Oliveira Carvalho in June 1991. Further details can be found in pages 432–433 of Wang G. (1999).

**Table A.3.2. World's near-record floods**

No.	Country	Station	Catchment area (km <sup>2</sup> )	Maximum discharge (m <sup>3</sup> /s)	Date	Reference
1	United States	San Rafae, San Rafae	3.2	250	16 January 1973	Rodier and Roche, 1984
2	China	Jinghe Lujigou, Lupo	4	304 <sup>a</sup>	1911	Luo and Shen, 1987
3	United States	Lake San Gorgonio, Beaumont	4.5	311	25 February 1969	Costa, 1987
4	China	Shuhe Guanfanghe, Guanfangjie	10.8	630 <sup>a</sup>	31 August 1907	Luo and Shen, 1987
5	China	Jialingjiang Xiaohebagou, Jieshang	14.2	867	July 1976	Luo and Shen, 1987
6	China	Fenhe Fupingshi, Kouzishang	15.0	893	31 July 1919	Luo and Shen, 1987
7	China	Yihe Junhe, Wujiazhuang	21.0	913 <sup>a</sup>	1 August 1926	Luo and Shen, 1987
8	China	Yellow River, Zhangjiagou, Zhangjiaping	24.8	996 <sup>a</sup>	1 August 1933	Luo and Shen, 1987
9	China	Hanjiang Tangbaihe, Dagongfen	36.6	1 070 <sup>a</sup>	June 1896	Luo and Shen, 1987
10	China	Yellow River, Meiligenggou, Meiligengzhao	39.4	1 640 <sup>a</sup>	1900	Luo and Shen, 1987
11	China	Hongruhe Shihe, Zushimiao	71.2	2 470	8 August 1975	Hu and Luo, 1992
12	France	Quateme Embouchure, New Caledonia	143	4 000	8 March 1975	Rodier and Roche, 1984
13	United States	Mail Trail Creek, Loma Alta, Texas	195	4 810	24 June 1948	Costa, 1987
14	China	Huaihe Shimantan	230	6 280	7 August 1975	Hu and Luo, 1992
15	United States	Seco Creek d' Hanis, Texas	368	6 500	31 May 1935	Costa, 1987
16	China	Shayinghe Shahe Zhongtang	485	8 550	10 August 1943	Luo and Shen, 1987
17	China	Hongruhe Zhentouhe Boshan	578	9 550	7 August 1975	Hu and Luo, 1992
18	China	Ningyuanhe Yaliang, Hainan	644	10 700	1946	Luo and Shen, 1987
19	China	Shayinghe Ganjianghe Feihe	746	11 300 <sup>a</sup>	June 1896	Luo and Shen, 1987
20	China	Shayinghe Guanzhai	1 124	14 700	8 August 1975	Hu and Luo, 1992

**Table A.3.2. (Continued)**

No.	Country	Station	Catchment area (km <sup>2</sup> )	Maximum discharge (m <sup>3</sup> /s)	Date	Reference
21	Mexico	Cithuatlan	1 370	13 500	27 October 1959	Rodier and Roche, 1984
22	Japan	Nyodo Lno	1 463	13 510	9 August 1963	IAHS, 2003
23	China	Nanduhe, Songtao, Hainan	1 480	15 700	21 July 1977	Feng, 1993
24	United States	West Nueces, Texas	1 800	15 600	14 June 1935	Rodier and Roche, 1984
25	India	Gujarat, Machu	1 930	16 310	11 August 1979	Wang G., 1999
26	Taiwan Province of China	Tam Shui, Taipei Bridge, Taiwan	2 110	16 700	11 September 1963	Hu and Luo, 1992
27	Japan	Shinguoga	2 251	19 030	26 September 1959	IAHS, 2003
28	Taiwan Province of China	Gaopingxi Jiugutang, Taiwan	3 075	18 000	8 August 1959	Hu and Luo, 1992
29	China	Zhemin Xiaoxi, Baiyan	3 255	19 200	31 July 1912	Luo and Shen, 1987
30	Philippines	Cagayan Echague Isabella	4 244	17 550	1959	IAHS, 2003
31	United States	Nueces Uvalde, Texas	5 043	17 440	June 1935	Linsley and others, 1975
32	Japan	Tone Yattajima	5 110	16 900	15 September 1947	Rodier and Roche, 1984
33	United States	Eel Scotia, California	8 060	21 300	23 December 1964	Rodier and Roche, 1984
34	Pakistan	Ravi, Jassar	10 000	19 240	5 October 1955	IAHS, 2003
35	China	Yalujiang Yunfeng	11 300	23 900	4 August 1960	Feng, 1993
36	Madagascar	Betsiboka Ambodiroka	11 800	22 000	4 March 1927	Rodier and Roche, 1984
37	Pakistan	Chenab, Marala	28 000	31 130	26 August 1957	IAHS, 2003
38	Pakistan	Jhelum, Mangla	29 000	31 100	1929	Costa, 1987
39	Pakistan	Jhelum, Mangla	31 000	30 850	10 September 1992	IAHS, 2003
40	India	Tapi, Kathur	64 000	36 500	6 September 1970	Rodier and Roche, 1984

**Table A.3.2. (Continued)**

No.	Country	Station	Catchment area (km <sup>2</sup> )	Maximum discharge (m <sup>3</sup> /s)	Date	Reference
41	China	Jialingjiang Beibei	156 142	57 300 <sup>a</sup>	16 July 1870	Hu and Luo, 1992
42	India	Godavari Dolaishwaram	309 000	78 800	17 September 1959	IAHS, 2000
43	Myanmar	Irrawaddy River	360 000	63 700	1877	ICID, 1992
44	Cambodia	Mekong River, Kratia	646 000	75 700	3 September 1939	ICID, 1992
45	Bengal	Brahmaputra Bahadurabad	800 000	81 000	6 August 1974	Wang G., 1999
46	Venezuela	Orinco, Puente Angostura	836 000	98 120	1892	Wang G., 1999
47	China	Changjiang Cuntan	866 559	100 000 <sup>a</sup>	15 July 1870	Hu and Luo, 1992
48	China	Changjiang Yitchang	1 005 500	96 300 <sup>a</sup>	1 August 1227	CJWRC, 1997
49	Russia	Yenisei Yijiaerka	2 440 000	154 000	June 1959	CSHE, 1984
50	Brazil	Amazon Obidos	4 640 300	250 000	June 1963	Rodier and Roche, 1984

<sup>a</sup> Survey values

## ANNEX IV. GLOSSARY

Many terms used in this report may be unfamiliar to users of this manual. It seems appropriate to provide a summary, listing for easy reference the more important terms used in the report and also some that may be helpful to the user in developing PMP studies.

**Adiabat** Curve of thermodynamic change taking place without addition or subtraction of heat. On an adiabatic chart or pseudo-adiabatic diagram, it is a line showing pressure and temperature changes undergone by air rising or sinking in the atmosphere without exchange of heat with its environment or condensation of its water vapour; a line, thus, of constant potential temperature. Also called a dry adiabat.

**Adiabatic** Referring to the process described by "adiabat".

**Adiabatic chart** Diagram in which temperature is plotted against pressure and on which adiabats are constructed.

**Adiabatic lapse rate** A lapse rate equal to the rate of change of temperature with height of unsaturated air adiabatically raised or lowered in the atmosphere; indicated by the adiabat, and equal to 1°C per 100 m, approximately. Also called the dry-adiabatic lapse rate.

**Advection** The process of transfer (of an air mass property) by virtue of motion. In particular cases, attention may be confined to either the horizontal or vertical components of the motion. The term is, however, often used to signify horizontal transfer only.

**Air mass** Extensive body of air approximating horizontal homogeneity, identified as to source region and subsequent modifications.

**Air-mass thunderstorm** A thunderstorm which is formed by convection within an air mass, usually by heating of the lower layers. By implication, it is one in the formation of which neither a front nor large-scale dynamical lifting of the air mass plays an important part.

**All-season** The largest or smallest value of a meteorological variable without regard to the time of the

year it occurred. In this report, all-season refers to the largest PMP estimate determined without regard to the time of year at which it may occur.

**Among-storm** A storm characteristic determined when values of various parameters are determined from different storms. An example is the ratio of 6-hour precipitation to 24-hour precipitation (a 6-hour to 24-hour ratio), where the 6-hour value is taken from a different storm than the 24-hour value.

**Atmospheric forces** The forces that result only from the pressure, temperature, and moisture gradients and their relative changes with time over a particular location.

**Barrier** A mountain range which partially blocks the flow of warm humid air from its oceanic region to a basin under study.

**Basin shape** The physical outline of the basin as determined from topographic charts or field survey.

**Cloudburst** A popular term for a very sudden and extremely heavy shower, often accompanied by thunder and hail. It is associated with strong upward and downward currents.

**Cold front** Front at which relatively colder air displaces warmer air.

**Combination model method** Reasonable combination of two or more transposable storms in the design watershed or surrounding regions based on principles and experience of synoptic meteorology in order to form a new ideal sequence of extraordinary storms, which then undergoes necessary transposition correction and maximization to estimate probable maximum precipitation for the design watershed.

**Composite maximization** Developing hypothetical severe precipitation events by joining together storms or storm bursts. Comprised of sequential maximization and spatial maximization.

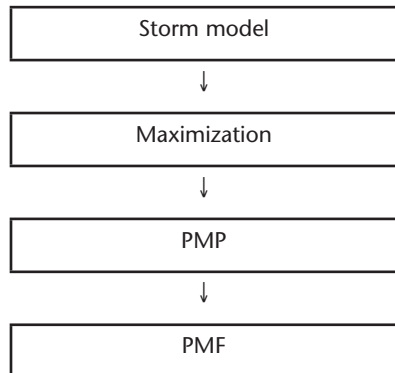
**Convective rain** Rainfall which is caused by the vertical motion of an ascending mass of air which is warmer than the environment. The horizontal

dimension of such a mass of air is generally of the order of 20 km or less and forms a cumulonimbus cloud. Convective rain is typically of greater intensity than either of the other two main classes of rainfall (cyclonic and orographic) and is often accompanied by thunder. The term is more particularly used in those cases in which the precipitation covers a large area as a result of the agglomeration of cumulonimbus masses.

**Convergence** Horizontal shrinking and vertical stretching of a volume of air, accompanied by net inflow horizontally and internal upward motion.

**Cyclone** That atmospheric pressure distribution in which there is a low central pressure relative to the surroundings. It is characterized on a synoptic chart by a system of closed isobars, generally approximately circular or oval in form, enclosing a central low pressure area. "Cyclonic circulation" is anti-clockwise in the northern hemisphere and clockwise in the southern hemisphere (the sense of rotation about the local vertical is the same as that of the earth's rotation).

**Deduction of qualitative characteristics of storm model** The PMP/PMF estimation method based on watershed area includes the main steps:



Obviously, identification of storm models is an important step in PMP estimation, in which qualitative characteristics (including storm type, synoptic meteorological cause, occurrence period, rain belt pattern, location of storm centre, storm duration, storm process pattern, and so forth) of storm models are first deduced. The deduction aims to ensure PMP/PMF derived by the storm model meets the requirements of a given project design for PMF while the overall analysis of PMP/PMF is based on reliable physical data, and overall, reliability of estimation results are therefore under control.

Deduction of qualitative characteristics of a storm model is based on the theory that PMP/PMF for a

given project in a watershed has only a single type of synoptic meteorological cause, and a great number of facts have proved the conclusion.

**Depth-area curve** Curve showing, for a given duration, the relation of maximum average depth to size of area within a storm or storms.

**Depth-area-duration values** Combination of depth-area and duration-depth relations.

**Dewpoint** The temperature to which a given parcel of air must be cooled at constant pressure and constant water-vapour content in order for saturation to occur.

**Drainage-averaged PMP** After the PMP storm pattern has been distributed across a specific drainage and a computational procedure applied, drainage-averaged PMP estimates are obtained. These average depths of precipitation include that portion of the PMP storm pattern that occurs over the drainage, both PMP and residual (see definition for residual precipitation).

**Effective elevation** The elevation at a point determined from a chart where topographic contours have been smoothed to reflect the effect of terrain of the precipitation process for a particular magnitude of storm. The actual elevation at the point may be either higher or lower than the effective elevation.

**General storm** A storm event which produces precipitation over areas in excess of around 1 300 km<sup>2</sup> and durations longer than 6 hours and is associated with a major synoptic weather feature.

**Hectopascal (hPa)** Unit of atmospheric pressure equal to 1,000 dynes/cm<sup>2</sup>, standard atmospheric pressure being 1013.2 hPa.

**Historical flood** Large floods that occurred before modern hydrological observation stations were set up. Moreover, some characteristics (dates of occurrence, flood levels and peak floods) can be determined through historical flood surveys.

**Historical flood survey** The water level and the discharge of a flood peak, and sometimes the volume, the process and the recurrence period of a flood, in a particular year decades ago, hundreds of years ago or even earlier are derived through analyses and calculations based on field surveys in a particular place or a particular reach, and if possible, surveys and researches in combination with relics (water marks on ancient buildings and steles) and records in literature.

**Historical storm** The precipitation process of a large flood that occurred before modern rainfall observation stations were set up. A storm process whose certain characteristics (occurrence date, storm magnitude, days of heavy raining and duration) can be determined through researches and analyses on rains and floods recorded in literature as well as records on droughts, floods, high temperatures and gales in surrounding regions.

**Hyetograph** A map or chart displaying temporal or areal distribution of precipitation, or a graph displaying the intensity of precipitation versus time.

**Inferential model method** A method of generalizing the 3-D structure of a storm weather system based on principles of synoptic meteorology in order to create a simplified physical equation that generates storms, and performing proper maximization to estimate probable maximum precipitation for the design watershed.

**Isohyet** Lines of equal value of precipitation during a given time interval.

**Isohyetal pattern** The pattern formed by the isohyets of an individual storm.

**Isohyetal orientation** The term used to define the orientation of precipitation patterns of major storms when approximated by elliptical patterns of best fit. It is also the orientation (direction from north) of the major axis through the elliptical PMP storm pattern.

**Lapse rate** Rate of change of temperature with height, either  $dT/dh$  or  $dT/dP$  where  $T$  is the temperature,  $h$  is the height and  $P$  is the pressure.

**Lift** Upward vertical motion. Also the upward vertical displacement required to saturate air by dry-adiabatic lift.

**Local model method** A method of selecting the process of an actual large storm with severe spatio-temporal distribution in the design watershed and then maximizing it properly to derive probable maximum precipitation for a particular season and a particular duration for the design watershed.

**Local storm** A storm event that occurs over a small area in a short time period. Precipitation rarely exceeds 6 hours in duration and the area covered by precipitation is less than around 1 300 km<sup>2</sup>. Frequently, local storms will last only 1 or 2 hours

and precipitation will occur over area sizes up to 500 km<sup>2</sup>. Precipitation in local storms will be isolated from general-storm rainfall.

**Major temporal and spatial combination method** The basic concept of this method is to treat the part of PMP which has the larger influence on PMF temporally (flood hydrograph) and spatially (flood source area) at the design section with hydrometeorological methods (maximization of local storms, storm transposition, storm combination, generalized estimation), and to treat the part of PMP which has the smaller influence with the common correlation method and the typical flood inflow proportional distribution method, in hydrological analysis. Obviously, this method, which can be regarded as a storm combination method, is an application of combination both in time and space. It only makes a detailed computation for the main part while making a rough computation for the secondary part.

**Mass curve** Curve of cumulative values of precipitation through time.

**Mixing ratio ( $w$ )** Ratio of the mass of water vapour to the mass of dry air in a given sample. The dimensionless ratio of mass of water vapour to the mass of dry air with which it is mixed.

$$w = 0.622 \frac{e}{p - e}$$

where  $w$  is the mixing ratio,  $p$  the atmospheric pressure,  $e$  the vapour pressure and 0.622 is the ratio of the molecular weight of water to the average molecular weight of dry air.

**Module** A self-contained unit of a complex procedure.

**Moisture maximization** The process of adjusting observed precipitation amounts upward based on the hypothesis of increased moisture inflow to the storm.

**Occluded front** Portion of the frontal surface (warm or cold) remaining in contact with the ground after the cold front has overtaken the warm front.

**Occlusion** Formation of an occluded front; a cyclonic system which has undergone the process of occlusion.

**Orographic rain** Rain which is caused entirely, or mostly, by the forced lift of moist air over high ground. Sometimes referred to as topographically induced rain.

**Precipitable water** The total atmospheric water vapour contained in a vertical column of unit cross-sectional area extending between any two specified levels, commonly expressed in terms of the height to which the liquid water would stand if the vapour were completely condensed and collected in a vessel of the same unit cross-section. The total precipitable water in the atmosphere of a location is that contained in a column or unit cross-section extending from the earth's surface all the way to the "top" of the atmosphere.

**Persisting  $n$ -hour dewpoint** The dewpoint value at a station that has been equalled or exceeded throughout a period of  $n$  consecutive hours. Durations of 12 or 24 hours are commonly used, though other durations may be used at times.

**Probable maximum precipitation (PMP)** Theoretically, the greatest precipitation for a given duration that is physically possible over a given watershed area or size of storm area at a particular geographic location at a certain time of the year, under modern meteorological conditions.

**Probable maximum flood (PMF)** The theoretical maximum flood that poses extremely serious threats to the flood control of a given project in a design watershed. Such a flood could plausibly occur in a locality at a particular time of year under modern meteorological conditions.

**Pseudo-adiabat** Line on thermodynamic diagram showing the pressure and temperature changes undergone by saturated air rising in the atmosphere, without ice-crystal formation and without exchange of heat with its environment other than that involved in assuming that the liquid water, formed by condensation, drops out.

**Pseudo-adiabatic** Referring to the process described by the pseudo-adiabat.

**PMP storm pattern** The isohyetal pattern that encloses the PMP area, plus the isohyets of residual precipitation outside the PMP portion of the pattern.

**Rawinsonde** A radiosonde which is tracked by radar or radio-theodolite to measure the wind aloft.

**Relative humidity** Ratio of actual water vapour content to saturation content, or total water vapour capacity, expressed as a percentage.

**Research on literature** Some characteristics (for example, storm occurrence dates, types and spatio-temporal distribution), sometimes even including

peaks, volumes and processes, of past floods can be deduced by applying the principles and experiences of modern hydrometeorology to literature and historic records (for example chorographies, ancient books, reports to emperors or empresses, epigraphs and newspapers). Such research can provide information on extraordinary floods that occurred before modern hydrological and meteorological observation stations were set up.

**Residual precipitation** The precipitation that occurs outside the area of the PMP portion of the PMP storm pattern placed on a drainage. Because of the irregular shape of a drainage, or because of the choice of a PMP pattern smaller in area than the area of the drainage, some of the residual precipitation can fall within a drainage. A particular advantage in the consideration of residual precipitation is that of allowing for the determination of concurrent precipitation, that is, the precipitation falling on a nearby drainage as compared with that to which the PMP pattern has been applied.

**Saturation** Upper limit of water vapour content in a given space; solely a function of temperature.

**Sequential maximization** The rearrangement of observed storms or portions thereof into a hypothetical sequence such that the time interval between storms is at a minimum in order to maximize values for given durations.

**Shear line** A narrow zone between two air masses where wind direction changes significantly over a relatively short distance.

**Sounding measurement** (by pibal, radiosonde, aircraft, or other means) of the vertical structure of the atmosphere above a station. Also the graph of the distribution of the elements with height or pressure.

**Spatial distribution** The geographic distribution of precipitation over a drainage according to an idealized pattern storm of the PMP for the storm area.

**Spatial maximization** The transposition of two separate storms or portions of them that occurred in or near a particular basin to one or more critical locations in the basin so as to obtain maximum runoff. In this procedure two separate storms or portions of storms are combined into a composite isohyetal pattern.

**Spillover** That part of orographically induced precipitation which is transported by the wind in a direction which has a horizontal component so

that it reaches the ground in the nominal rain shadow on the lee side of a ridge.

**Storm-centred** Describes a characteristic of a storm that is always determined in relation to the maximum value in the storm (storm centre) as compared with the same factor for some other duration and/or area of the storm. For example, a storm-centred depth-area ratio relates the average depth over some specific isohyetal area of the storm that encloses the centre of the storm to the amount at the storm centre.

**Storm depression index** A term used in Chinese hydrological engineering. It is the exponent  $n$  in the relation:

$$a_{t,p} = \frac{s_p}{t^n}$$

where:  $s_p$  is the average rainfall intensity in one hour with probability  $p$ ; and  $a_{t,p}$  is the average rainfall intensity in  $t$  hours with probability  $p$ .

**Storm profile** Vertical section through an isohyetal pattern, with distance from centre as abscissa and corresponding depth of precipitation as ordinate.

**Storm survey** Data on the volume, the precipitation process and the temporal distribution of one storm in a region or place are determined through visits, surveys and estimations when there is no rainfall observable in the region, or large storms occurred before stations were set up, or the rainfall at the storm centre was not observed due to a small density of stations and other reasons, or rainfall observation stations failed to observe large storms for certain reasons.

**Storm simulation method based on historical flood** The basic concept of this method is to simulate the storm, which is regarded as a high efficiency storm relevant to a historical extraordinary flood, then to derive PMP after maximizing moisture. Simulation is to derive the extraordinary storm relevant to a historical flood based on the incomplete temporal and spatial distribution information of the known extraordinary historical flood, using the synoptic theory and weather forecast experience, with the assistance of the watershed hydrological model and computer and through trial computation.

**Storm transposition** The hypothetical transfer or relocation of storms from the location where they occurred to other areas where they could occur. The transfer and mathematical adjustment of storm rainfall amounts from the storm site to another location is termed "explicit transposition". The

areal, durational and regional smoothing done to obtain comprehensive individual drainage estimates and generalized PMP studies is termed "implicit transposition".

**Synoptic** Showing the distribution of meteorological elements over an area at a given moment; for example, a synoptic chart.

**Temporal distribution** The time order in which incremental PMP amounts are arranged within the PMP storm.

**Transposition model method** This method involves the transposition of the rainfall and the spatio-temporal distribution of an actual large storm in surrounding regions (or the meteorological homogeneous zone) to the design watershed and its treatment as PMP for a particular season and a particular duration for the design watershed after transposition correction and proper maximization.

**Tropical cyclone** Specifically, a storm producing wind speeds in excess of 60 m/s (120 km/h); generally, a cyclone of tropical origin.

**Total storm area and Total storm duration** The largest area size and longest duration for which depth-area-duration data are available in the records of major storm rainfall.

**Vapour pressure** Pressure of the water vapour in a sample of air.

**Warm front** Front at which relatively warmer air replaces colder air.

**Warm sector** Sector of warm air bounded on two sides by the cold and warm fronts extending from a centre of low pressure.

**Wave** Localized deformation of a front, resembling a warm-sector formation, usually travelling along the front and sometimes developing into a mature cyclone.

**Within/without-storm depth-area relations** Relations that evolve from the concept that the depth-area relation for area-averaged PMP represents an envelopment of maximized rainfall from various storms, each effective for a different area size(s). The within-storm depth-area relation represents the areal variation of precipitation within a storm that gives PMP for a particular area size. Another way of putting this is to say that the storm that results in PMP for one area size may not give PMP for any other area size. Except for the area size that gives

PMP, the within-storm depth-area relation will give depths less than PMP for smaller area sizes.

Analogously, the without-storm depth-area relation represents the areal variation of precipitation for areas greater than the PMP storm and will give depths less than PMP for larger area sizes. This

concept is illustrated in the schematic diagram shown in Figure 5.8. In this figure, the curve of precipitation for areas in the PMP storm outside the area size of the PMP pattern describes a without-storm depth-area relation. The precipitation described by the without-storm relation is the residual precipitation.

---



## REFERENCES AND FURTHER READING

### REFERENCES

- Arakawa, H., 1963: *Typhoon Climatology as Revealed by Data of the Japanese Weather Service*. Technical Report No. 21, Japanese Meteorological Agency, Tokyo.
- Australian Bureau of Meteorology, 1985: *The Estimation of Probable Maximum Precipitation in Australia for Short Durations and Small Areas* (Bulletin No. 51). Canberra, Department of Science and Technology, Australian Government Printing Office.
- \_\_\_\_\_, 1991: *Temporal Distributions of Rainfall Bursts* (HRS Report No. 1). Hydrology Report Series, Melbourne.
- \_\_\_\_\_, 1992: *Analysis of Australian Rainfall and Rainday Data with Respect to Climate Variability and Change* (HRS Report No. 2), Hydrology Report Series, Melbourne.
- \_\_\_\_\_, 1994: *The Estimation of Probable Maximum Precipitation in Australia: Generalised Short-Duration Method* (Bulletin 53). Amended 1996, amended and revised 2003, Melbourne, [http://www.bom.gov.au/hydro/has/gsdm\\_document.shtml](http://www.bom.gov.au/hydro/has/gsdm_document.shtml)
- \_\_\_\_\_, 1995: *Catalogue of Significant Rainfall Occurrences Over Southeast Australia* (HRS Report No. 3). Hydrology Report Series, Melbourne.
- \_\_\_\_\_, 1998: *Temporal Distributions of Large and Extreme Design Rainfall Bursts Over Southeast Australia* (HRS Report No. 5). Hydrology Report Series, Melbourne.
- \_\_\_\_\_, 1999: *Rainfall Antecedent to Large and Extreme Rainfall Bursts Over Southeast Australia* (HRS Report No. 6). Hydrology Report Series, Melbourne, Australia.
- \_\_\_\_\_, 2001: *Development of the Method of Storm Transposition and Maximization for the West Coast of Tasmania* (HRS Report No. 7). Hydrology Report Series, Melbourne.
- \_\_\_\_\_, 2003: *Revision of the Generalised Tropical Storm Method for Estimating Maximum Precipitation* (HRS Report No. 8). Hydrology Report Series, Melbourne.
- \_\_\_\_\_, 2004: *Catalogue of Significant Rainfall Occurrences of Tropical Origin Over Australia* (HRS Report No. 9). Hydrology Report Series, Melbourne.
- Barrett, E.C. and D. W. Martin, 1981: *The Use of Satellite Data in Rainfall Monitoring*. London, Academic Press.
- Brunt, A.T., 1967: Space-time relations of cyclone rainfall in the north-east Australian region. *Civil Engineering Transactions, Institution of Engineers, Australia*, CE 10(1).
- Canterford, R.P., M.F. Hutchinson and L.H. Turner, 1985: *The Use of Laplacian Smoothing Spline Surfaces for the Analysis of Design Rainfalls*. Hydrology and Water Resources Symposium, 14–16 May, Sydney, Institution of Engineers.
- CCFDYRVNC (The Committee for Compiling Floods and Droughts in the Yellow River Valley and Northwest China), 1996: *Floods and Droughts in the Yellow River Valley*. Zhengzhou, Yellow River Conservancy Press.
- Changjiang Water Resources Commission (CJWRC), 1993: *Hydrologic Forecast Methods*. Second edition, Beijing, China Water Power Press.
- \_\_\_\_\_, 1997: *Hydrologic Research on the Three Gorges Project*. Wuhan, Hubei Science and Technology Publishing House.
- Changjiang Water Resources Commission (CJWRC), Hydrologic Office, the Ministry of Water Resources and Nanjing Hydrologic/Water Resources Research Institute, the Ministry of Water Resources, 1995: *Manual for Calculating Design Flood for Water Resources and Hydropower Projects*. Beijing, China Water Power Press.
- Chen, J., 2003: *Several Ideas on PMP*. Reports on Hydrology and Water Resources of Chen Jiaqi. Beijing, China Water Power Press.
- Chin, P., 1958: *Tropical Cyclones in the Western Pacific and China Sea Area from 1884 to 1953*. Technical Memoirs, Hong Kong, Royal Observatory.

- Chow, V.T., 1951: A general formula for hydrologic frequency analysis. *Transactions American Geophysical Union*, 32(2): 231–237.
- Clark, R.A. and H.E. Schloellar, 1970: *Problems of Inflow Design Flood Determination in the Tropics*. American Society of Civil Engineers, National Water Resources Engineering Meeting, 26–30 January 1970, Meeting Preprint 1117.
- Corrigan, P., D.D. Fenn, D.R. Kluck and J.L. Vogel, 1998: *Probable Maximum Precipitation for California – Calculation Procedures* (HMR No. 58). United States Department of Commerce, National Oceanic and Atmospheric Administration, Silver Spring, MD.
- , 1999: *Probable Maximum Precipitation for California* (HMR No. 59). United States Department of Commerce, National Oceanic and Atmospheric Administration, Silver Spring, MD.
- Costa, J.E., 1987: A comparison of the largest rainfall-runoff floods in the United States with those of the People's Republic of China and the World. *Journal of Hydrology*, 96: 101–115.
- Cotton, W.R., R.A. McAnelly and T. Ashby, 2003: *Development of New Methodologies for Determining Extreme Rainfall*. Fort Collins, CO, Colorado State University.
- Court, A., 1961: Area-depth rainfall formulas. *Journal Geophysical Research American Geophysical Union*, 66: 1823–1832.
- Crippen, J.R. and C.D Bue. 1977: *Maximum Floodflows in the Conterminous United States*. United States Government Printing Office, Washington.
- Crutcher, H.L. and R.G. Quayle, 1974: *Mariners Worldwide Guide to Tropical Storms at Sea*. Naval Weather Service NAVAIR 50-10-61, Asheville, NC.
- Cudworth, A.G., 1989: *Flood Hydrology Manual*. Water Resources Technical Publication, United States Department of the Interior, Bureau of Reclamation, Denver, CO.
- Dhar, O.N. and B.K. Bhattacharya, 1975: *A Study of Depth-Area-Duration Statistics of Severest Rainstorms over Different Meteorological Divisions of North Indian Plains*. Proceedings of the National Symposium on Hydrology, Roorkee.
- Dhar, O.N. and P.P. Damte, 1969: A pilot study for estimation of probable maximum precipitation using Hershfield technique. *Indian Journal of Meteorology and Geophysics*, 20(1): 31–34.
- Dhar, O.N. and B.N. Mandal, 1981: Greatest observed one-day point and areal rainfall of India. *Journal of Pure and Applied Geophysics*, 119(5): 922–933.
- Dhar, O.N., P.R. Rakhecha and B.N. Mandal, 1980: Rainstorms which contributed the greatest areal rain depths in India. *Archives for Meteorology, Geophysics, and Bioclimatology, Series A*, 29: 119–130.
- Dhar, O.N., and others, 1984: Most severe rainstorm of India – a brief appraisal. *Hydrological Science Journal*, 19(2): 119–229.
- Environmental Data Service, 1968: *Climatic Atlas of the United States*. Environmental Science Services Administration, United States Department of Commerce, Washington, DC.
- Falansbee, W.A., 1973: *Estimation of Average Daily Rainfall From Satellite Cloud Photographs*. NOAA Technical Memorandum NESS 49, National Environmental Satellite Service, National Oceanic and Atmospheric Administration, United States Department of Commerce, Washington, DC.
- Fenn, D.D., 1985: *Probable maximum precipitation estimates for the drainage above Dewey Dam, Johns Creek, Kentucky*. NOAA Technical Memorandum NWS Hydro 41, National Weather Service, National Oceanic and Atmospheric Administration, United States Department of Commerce, Silver Spring, MD.
- Gao Z. and X. Xiong, 1983: A method of calculating orographic rain correction in storm transposition, *Yellow River*, 5(5): 40–43.
- German Water Resources Association, 1983: *Contributions to the Choice of the Design Flood and to Probable Maximum Precipitation* (Publication No. 62), Hamburg (in German).
- Hansen, E.M., D.D. Fenn, P. Corrigan and J.L. Vogel, 1994: *Probable Maximum Precipitation – Pacific Northwest States Columbia River (including portions of Canada), Snake River and Pacific Coastal Drainages* (HMR No. 57). United States Department of Commerce, National Oceanic and Atmospheric Administration, United States Department of Army Corps of Engineers, United States Department of Interior Bureau of Reclamation, Silver Spring, MD.

- Hansen, E.M., D.D. Fenn, L.C. Schreiner, R.W. Stott and J.F. Miller, 1988: *Probable Maximum Precipitation Estimations – United States Between the Continental Divide and the 103rd Meridian* (HMR No. 55A). United States Department of Commerce, National Oceanic and Atmospheric Administration, United States Department of Army Corps of Engineers, United States Department of Interior Bureau of Reclamation, Silver Spring, MD.
- Hansen, E.M., L.C. Schreiner and J.F. Miller, 1982: *Application of Probable Maximum Precipitation Estimates – United States East of the 105th Meridian* (HMR No. 52). National Weather Service, National Oceanic and Atmospheric Administration, United States Department of Commerce, Washington, DC.
- Hansen, E.M., F.K. Schwarz and J.T. Riedel, 1977: *Probable Maximum Precipitation Estimates, Colorado River and Great Basin Drainages* (HMR No. 49). National Weather Service, National Oceanic and Atmospheric Administration, United States Department of Commerce, Silver Spring, MD.
- Hart, T.L., 1982: *Survey of Probable Maximum Precipitation Studies Using the Synoptic Method of Storm Transposition and Maximization*. Proceedings of the Workshop on Spillway Design, 7–9 October 1981, Conference Series No. 6, Australian Water Resources Council, Australian Department of National Development and Energy, Canberra, Australian Government Publishing Service.
- Hershfield, D.M., 1961a: *Rainfall Frequency Atlas of the United States*. Technical Paper No. 40, Weather Bureau, United States Department of Commerce, Washington, DC.
- \_\_\_\_\_, 1961b: Estimating the probable maximum precipitation. *Journal of Hydraulics Division: Proceedings of the American Society of Civil Engineers*, 87: 99–106.
- \_\_\_\_\_, 1965: Method for Estimating Probable Maximum Precipitation, *Journal of the American Waterworks Association*, 57: 965–972.
- Ho, F.P. and J.T. Riedel, 1979: *Precipitable Water Over the United States, Volume II Semimonthly Maxima*. NOAA Technical Report NWS 20, National Weather Service, National Oceanic and Atmospheric Administration, United States Department of Commerce, Silver Spring, MD.
- Hua S., 1984: Issues of Calculating Runoff Production and Confluence in Watersheds under PMP Conditions, *Journal of China Hydrology*, 1: 8–10.
- Huff, F.A., 1967: Time distribution of rainfall in heavy storms. *Water Resources Research*, 3: 1007–1019.
- Institution of Engineers, Australia, 1987: *Australian Rainfall and Runoff: A Guide to Flood Estimation* (D.H. Pilgrim, ed.), Barton, ACT.
- Jakob, D., R. Smalley, J. Meighen, K. Xuereb, and B. Taylor, 2008: *Climate Change and Probable Maximum Precipitation* (HRS Report No. 12). Hydrology Report Series, Australian Bureau of Meteorology, Melbourne.
- Jin R. and X. Li, 1989: Estimation of PMF in the reach between the Three Gorges Project and upstream reservoirs. *Journal of China Hydrology*, 6: 14–23.
- Luo C. and G. Shen, 1987: Records of largest floods and their geographic distribution in China, *Journal of Hydrology*, (5).
- Kaul, F.J., 1976: *Maximum Recorded Floods and Storms in Indonesia*. Water Resources Planning Guideline No. 7, Indonesia, Directorate of Planning and Programming Ministry of Public Works and Electric Power.
- Kennedy, M.R., 1976: *The Probable Maximum Precipitation from the Northeast Monsoon in Southeast Asia*. Symposium on Tropical Monsoons, 8–10 September 1976, Pune, India, Indian Institute of Tropical Meteorology, pp. 294–303.
- \_\_\_\_\_, 1982: *The Estimation of Probable Maximum Precipitation in Australia – Past and Current Practice*. Proceedings of the Workshop on Spillway Design, 7–9 October 1981, Conference Series No. 6, Australian Water Resources Council, Australian Department of National Development and Energy, Canberra, Australian Government Printing Office.
- Kennedy, M.R. and T.L. Hart, 1984: The estimation of probable maximum precipitation in Australia. *Civil Engineering Transactions, Institution of Engineers, Australia*, CE 26(1): 29–36.
- Kim, N.-W., S. Kim, and B.-H. Seoh, 1989. *Probable Maximum Precipitation Estimates of Korea*. Annual Report Vol. 1, Seoul, Korea Institute of Construction Technology, pp. 53–62.

- Klemes, V., 1993: *Probability of Extreme Hydrometeorological Events – a Different Approach, Extreme Hydrological Events: Precipitation Floods and Droughts*. Proceedings of the Yokohama Symposium, July 1993, International Association of Hydrological Sciences Publication No. 213.
- Koteswaram, P., 1963: *Movement of Tropical Storms over the Indian Ocean*. New Delhi, Indian Meteorological Department.
- Lin, B.Z., 1988: Application of the Step-Duration Orographic Intensification Factors Method to estimation of PMP for mountainous regions. *Journal of Hohai University*, (3): 40-51.
- Lin, B.Z., Vogel, J., 1993. A new look at the statistical estimation of PMP. *Engineering Hydrology, Proceedings of the ASCE Symposium*, San Francisco, USA, July 25-30, 1993.
- Linsley, R.K., M.A. Kohler and J.L.H. Paulhus, 1975: *Hydrology for Engineers*. New York, McGraw-Hill.
- Lott, G.A. and V.A. Myers, 1956: *Meteorology of Flood-producing Storms in the Mississippi River Valley* (HMR No. 34). Hydrometeorological Report, Weather Bureau, United States Department of Commerce, Washington, DC.
- Lourens, R.S., 1981: *Tropical Cyclones in the Australian Region, July 1909 to June 1980*. Meteorological Summary, Australian Bureau of Meteorology, Melbourne.
- Mansell-Moullin, M., 1967: The probable maximum storm and flood in a Malayan hill-catchment. *Assessment of the Magnitude and Frequency of Flood Flows*. Water Resources Series No. 30, New York, NY, United Nations, pp. 165–177.
- McKay, G.A., 1965: *Statistical Estimates of Precipitation Extremes for the Prairie Provinces*. Canada Department of Agriculture, Prairie Farm Rehabilitation Administration (PFRA) Engineering Branch, Canada.
- Miller, J.F., 1963: *Probable Maximum Precipitation and Rainfall-Frequency Data for Alaska*. Technical Paper No. 47, Weather Bureau, United States Department of Commerce Washington, DC.
- , 1964: *Two- to Ten-Day Precipitation for Return Periods of 2 to 100 Years in the Contiguous United States*. Technical Paper No. 49, Weather Bureau, United States Department of Commerce, Washington, DC.
- , 1981: *Probable Maximum Precipitation for Tropical Regions*. World Meteorological Organization Seminar on Hydrology of Tropical Regions, 11–15 May 1981, Miami, FL.
- Miller, J.F., R.H. Frederick and R.J. Tracey, 1973: *Precipitation Frequency Atlas of the Western United States*. NOAA Atlas 2 Vols I, II, III and IV, National Weather Service, National Oceanic and Atmospheric Administration, United States Department of Commerce, Silver Spring, MD.
- Miller, J.F., E.M. Hansen and D.D. Fenn, 1984a: *Probable Maximum Precipitation for the Upper Deerfield River Drainage Massachusetts/Vermont*. NOAA Technical Memorandum NWS Hydro 39, National Weather Service, National Oceanic and Atmospheric Administration, United States Department of Commerce, Silver Spring, MD.
- Miller, J.F., E.M. Hansen, D.D. Fenn, L.C. Schreiner and D.T. Jensen, 1984b: *Probable Maximum Precipitation Estimates – United States Between the Continental Divide and the 103rd Meridian* (HMR No. 55). National Weather Service, National Oceanic and Atmospheric Administration, United States Department of Commerce, Washington, DC.
- Ministry of Water Resources (MWR), 1980: *Regulation for Calculating Design Flood of Water Resources and Hydropower Projects SDJ22-79 (Trial)*. Beijing, China Water Power Press.
- Minty, L.J., J. Meighen and M.R. Kennedy, 1996: *Development of the Generalised Southeast Australia Method for Estimating Probable Maximum Precipitation* (HRS Report No. 4). Hydrology Report Series, Hydrometeorological Advisory Services, Australian Bureau of Meteorology, Melbourne.
- Morrison-Knudson Engineers Inc., 1990: *Determination of an Upper Limit design Rainstorm for the Colorado River Basin above Hoover Dam*. United States Department of the Interior, Bureau of Reclamation, Denver, CO.
- Myers, V.A., 1959: *Meteorology of Hypothetical Flood Sequences in the Mississippi River Basin* (HMR No. 35). Weather Bureau, United States Department of Commerce, Washington, DC.
- , 1962: Airflow on the Windward side of a Large Ridge. *Journal of Geophysical Research*, 67(11): 4267–4291.

- , 1967: *Meteorological Estimation of Extreme Precipitation for Spillway Design Floods*. Technical Memorandum WBTM HYDRO-5, Weather Bureau, Environmental Science Services Administration, United States Department of Commerce, Washington, DC.
- Namias, J., 1969: *Use of Sea-Surface Temperature in Long Range Prediction*. WMO Technical Note No. 103, World Meteorological Organization, Geneva.
- Nathan, R.J., 1992: The derivation of design temporal patterns for use with the generalized estimates of probable maximum precipitation. *Civil Engineering Transactions, Institution of Engineers, Australia*, CE 34(2): 139–150.
- National Environment Research Council (NERC), 1975: *Flood Studies Report*. Volumes I to V, London.
- Negri, A.J., R.F. Adler and P.J. Wetzel, 1983: *A Simple Method for Estimating Daily Rainfall From Satellite Imagery*. Preprint Volume Fifth Conference on Hydrometeorology, 17–19 October 1983, Tulsa, OK, American Meteorological Society, Boston, MA, pp. 156–163.
- Neumann, C.J., G.W. Cry, E.L. Caso and B.R. Jarvinen, 1981: *Tropical Cyclones of the North Atlantic Ocean, 1871–1980*. National Climatic Center, National Oceanic and Atmospheric Administration, United States Department of Commerce, Asheville, NC.
- Nordenson, T. J., 1968: *Preparation of Coordinated Precipitation, Runoff and Evaporation Maps*. Reports on WMO/IHD Projects, Report No. 6, World Meteorological Organization, Geneva.
- Pilgrim, D.H., I. Cordery and R. French, 1969: Temporal patterns of design rainfall for Sydney. *Civil Engineering Transactions, Institution of Engineers, Australia*, CE 11(1): 9–14.
- Pyke, C.B., 1975: *Some Aspects of the Influence of Abnormal Eastern Equatorial Ocean Surface Temperature Upon Weather Patterns in the Southwestern United States*. Final Report, United States Navy Contract N-0014-75-C-0126, Los Angeles, CA, University of California.
- Rakhecha, P.R. and M.R. Kennedy, 1985: A generalized technique for the estimation of probable maximum precipitation in India. *Journal of Hydrology*, 78: 345–359.
- Riedel, J.T., 1977: Assessing the probable maximum flood. 29(12): 29–34.
- Riedel, J.T., J.F. Appleby and R.W. Schloemer, 1956: *Seasonal Variation of the Probable Maximum Precipitation East of the 105th Meridian for Areas From 10 to 1000 Square Miles and Durations of 6, 12, 24, and 48 Hours* (HMR No. 33). Weather Bureau, United States Department of Commerce, Washington, DC.
- Riedel, J.T. and L.C. Schreiner, 1980: *Comparison of Generalized Estimates of Probable Maximum Precipitation with Greatest Observed Rainfalls*. NOAA Technical Memorandum No. NWS 25, National Weather Service, National Oceanic and Atmospheric Administration, United States Department of Commerce, Washington, DC.
- Riedel, J.T., F.K. Schwarz and R.L. Weaver, 1969: *Probable Maximum Precipitation Over the South Platte River, Colorado, and Minnesota River, Minnesota* (HMR No. 44). Weather Bureau, Environmental Science Services Administration, United States Department of Commerce, Washington, DC.
- Rodier, J.A. and M. Roche, 1984: World Catalogue of Maximum Observed Floods, IHP-II Project, A.2.7.2 IAHS-AISH Publication No. 143.
- Schoner, R.W., 1968: *Climatological Regime of Rainfall Associated with Hurricanes after Landfall*. ESSA Technical Memorandum WBTM ER-29, Weather Bureau, Environmental Science Services Administration, United States Department of Commerce, Garden City, NY.
- Schoner, R.W. and S. Molansky, 1956: *Rainfall Associated with Hurricanes*. National Hurricane Research Project Report No. 3, Weather Bureau, United States Department of Commerce, Washington, DC.
- Schreiner, L.C. and J.T. Riedel, 1978: *Probable Maximum Precipitation Estimates, United States East of the 105th Meridian* (HMR No. 51). National Weather Service, National Oceanic and Atmospheric Administration, United States Department of Commerce, Washington, DC.
- Schwarz, F.K., 1961: *Meteorology of Flood-Producing Storms in the Ohio River Basin* (HMR No. 38). Weather Bureau, United States Department of Commerce, Washington, DC.
- , 1963: *Probable Maximum Precipitation in the Hawaiian Islands* (HMR No. 39). Weather Bureau,

- United States Department of Commerce, Washington, DC.
- , 1965: *Probable Maximum and TVA Precipitation Over the Tennessee River Basin Above Chattanooga* (HMR No. 41). Weather Bureau, United States Department of Commerce, Washington, DC.
- , 1967: *The Role of Persistence, Instability and Moisture in the Intense Rainstorm in Eastern Colorado, June 14–17, 1965*. Technical Memorandum WBTM HYDRO-3, Weather Bureau, Environmental Science Services Administration, United States Department of Commerce, Washington, DC.
- , 1972: *A Proposal for Estimating Tropical Storm Probable Maximum Precipitation (PMP) for Sparse Data Regions*. Floods and Droughts Proceedings Second International Symposium in Hydrology, 11–13 September 1972, Fort Collins, CO.
- Schwerdt, R.W., F.P. Ho and R.W. Watkins, 1979: *Meteorological Criteria for Standard Project Hurricane and Probable Maximum Hurricane Windfields, Gulf and East Coasts of the United States*. NOAA Technical Report NWS 23, National Weather Service, National Oceanic and Atmospheric Administration, United States Department of Commerce, Washington, DC.
- Scofield, R.A. and V.J. Oliver, 1980: *Some Improvements to the Scofield/Oliver Technique*. Preprint Volume 2nd Conference on Flash Floods, 18–20 March 1980, Atlanta, GA, American Meteorological Society, Boston, MA, pp. 115–182.
- Shepherd, D.J. and J.R. Colquhoun, 1985: Meteorological aspects of an extraordinary flash flood event near Dapto, NSW. *Australian Meteorological Magazine*, 33(2): 87–102.
- Solomon, S.I., J.P. Denouville, E.J. Chart, J.A. Woolley and C. Cadou, 1968: The use of a square grid system for computer estimation of precipitation, temperature, and runoff. *Water Resources Research*, 4(5): 919–925.
- Taylor, B.F., L.J. Minty and J. Meighen, 1998: Modifications to the distribution of probable maximum precipitation in Bulletin 53, *Australian Journal of Water Resources*, 2(2).
- United Nations/World Meteorological Organization, 1967: *Assessment of the Magnitude and Frequency of Flood Flows*. Water Resources Series No. 30, New York, NY.
- United States Army Corps of Engineers, 1996: *Flood-Runoff Analysis*. New York, NY, American Society of Civil Engineers Press.
- United States Department of Defense, 1960: *Annual Typhoon Reports*. Fleet Weather Central-Joint Typhoon Warning Center, Guam, Mariana Islands.
- United States Department of the Interior, 1992: *Flood Hydrology Manual, A Water Resources Technical Publication*. Denver, CO, United States Government Printing Office.
- United States National Weather Service, 1977: *Probable Maximum Precipitation Estimates, Colorado River and Great Basin drainage* (HMR No. 49), Silver Spring, MD.
- , 1984: *Probable Maximum Precipitation for the Upper Deerfield Drainage Massachusetts/Vermont*. NOAA Technical Memorandum, NWS Hydro 39, Silver Spring, MD.
- United States Weather Bureau, 1947: *Generalized Estimates of Maximum Possible Precipitation Over the United States East of the 105th Meridian* (HMR No. 23) United States Department of Commerce, Washington, DC.
- , 1951: *Tables of Precipitable Water and Other Factors for a Saturated Pseudo-adiabatic Atmosphere*. Technical Paper No. 14, Asheville, NC.
- , 1952: *Kansas-Missouri Floods of June–July 1951*. Technical Paper No. 17, United States Department of Commerce, Washington, DC.
- , 1958: *Highest Persisting Dew Points in Western United States*. Technical Paper No. 5, United States Department of Commerce, Washington, DC.
- , 1960: *Generalized Estimates of Probable Maximum Precipitation West of the 105th Meridian*. Technical Paper No. 38, United States Department of Commerce, Washington, DC.
- , 1961a: *Interim Report-Probable Maximum Precipitation in California* (HMR No. 36). United States Department of Commerce, Washington, DC.
- , 1961b: *Generalized Estimates of Probable Maximum Precipitation and Rainfall-Frequency Data for Puerto Rico and Virgin Islands*. Technical Paper No. 42, United States Department of Commerce, Washington, DC.

- , 1962: *Rainfall Frequency Atlas of the Hawaiian Islands*. Technical Paper No. 43, United States Department of Commerce, Washington, DC.
- , 1966: *Probable Maximum Precipitation, Northwest States* (HMR No. 43). Environmental Science Services Administration, United States Department of Commerce, Washington, DC.
- , 1970: *Probable Maximum Precipitation, Mekong River Basin*, HMR No. 46, Environmental Science Services Administration, United States Department of Commerce, Washington, DC.
- Vickers, D.O., 1976: Very Heavy and Intense Rainfalls in Jamaica. *Proceedings of the Conference on Climatology and Related Fields, September 1966*, Mono, West Indies, University of West Indies.
- Walland, D.J., J. Meighen, K.C. Xuereb, C.A. Beesley and T.M.T. Hoang, 2003: *Revision of the Generalised Tropical Storm Method for Estimating Probable Maximum Precipitation* (HRS Report No. 8). Hydrology Report Series, Bureau of Meteorology, Melbourne.
- Wang, B.H., 1984: Estimation of probable maximum precipitation: case studies. *Journal of Hydraulics Division*, 110(10): 1457–1472.
- , 1986: *Probable Maximum Flood and its Application*. Chicago, IL, Harza Engineering Company.
- Wang, B.H., 1988: *Determination of Design Flood for Spillways*. Commission Internationale des Grands Barrages, Q.63–R.39.
- Wang, G., 1999: *Principles and Methods of PMP/PMF Calculations*. Beijing, China Water Power Press and Yellow River Water Resources Publishing House.
- , 2004: *Probable Maximum Precipitation: Approaches and Methodology*. Twelfth session of the Commission for Hydrology of the World Meteorological Organization, 20–29 October 2004, <http://www.yrce.cn/yrexport/whole.asp?id=wgan>. Published also 2006, *Yellow River*, 28(11): 18–20.
- , 2005a: Synopsis of advantages of PMP/PMF Study in China. *Yellow River*, 27(2): 1–5.
- Wang G, B. Li and J. Wang J, 2005: World's Greatest Known Point Rainfalls and Their Enveloping Curve Formula, <http://www.yrce.cn/yrexport/whole.asp?id=wgan>. Also published 2006: *Advances in Water Science*, 17(6):831–836.
- Wang, G., Wang, J., Li, B., 2006. Known maximum flood in the world and its envelope curve formula. *Yellow River*, 2006, 28(2): 1–5.
- Wang, J., 2002: *Rainstorms in China*. Beijing, China Water Power Press.
- Wang, Y. and W. Wang, 2000: *Hydropower Projects in China – Engineering Hydrology Volume*. Beijing, China Electric Publishing House.
- Water and Power Consultancy Services (India) Limited, 2001: *Dam Safety Assurance and Rehabilitation Project Generalized PMP Atlas, Phase I*.
- Weaver, R.L., 1962: *Meteorology of Hydrologically Critical Storms in California* (HMR No. 37). Weather Bureau, United States Department of Commerce, Washington, DC.
- , 1966: California storms as viewed by Sacramento radar, *Monthly Weather Review*, 94(1): 416–473.
- , 1968: *Meteorology of Major Storms in Western Colorado and Eastern Utah*. Technical Memorandum WBTM HYDRO-7, Weather Bureau, Environmental Science Services Administration, United States Department of Commerce, Washington, DC.
- Weiss, L.L., 1968: Ratio of true to fixed-interval maximum rainfall. *Journal of Hydraulics Division*, 90: 77–82.
- Wiesner, C.J., 1970: *Hydrometeorology*. London, Chapman and Hall Ltd.
- World Meteorological Organization, 1969a: *Estimation of Maximum Floods* (WMO-No. 233).TP 126, Technical Note No. 98, Geneva, pp. 9–17.
- , 1969b: *Manual for Depth-Area-Duration Analysis of Storm Precipitation* (WMO-No. 237). TP 129, Geneva.
- , 1973: *Manual for Estimation of Probable Maximum Precipitation* (WMO-No. 332). Operational Hydrology Report No. 1, (First edition) Geneva.
- , 1994: *Guide to Hydrological Practices (fifth edition)* (WMO-No. 168), Geneva.

- , 1975: *Hydrological Forecasting Practices* (WMO-No. 425). Operational Hydrology Report No. 6, Geneva.
- , 1986: *Manual for Estimation of Probable Maximum Precipitation* (WMONo.332). Operational Hydrology Report No. 1, Second Edition, Geneva.
- Xiong X. and Z. Gao, 1993: Estimation of probable maximum storm for Sanmenxia-Huayuankou Reach of the Yellow River. *Hohai University Transactions*, 21(3): 38–45.
- Xuereb, K.C., G.J. Moore and B.F. Taylor, 2001: *Development of the Method of Storm Transposition and Maximization for the West Coast of Tasmania* (HRS Report No. 7). Hydrology Report Series, Hydrometeorological Advisory Services, Australian Bureau of Meteorology.
- Ye Y. and M. Hu, 1979: *Issues in the Compilation of Isoline Maps of Probable Maximum Storms and Others in China*. Beijing, China Water Power Technology, No. 7, pp. 11–19.
- Yu J., 2001: Research on the application of generalized storm depth-area-duration method used in the United States to determine probable maximum precipitation in southwest China. *Design of Hydroelectric Power Station*, 17(1): 48–51.
- Zhan D. and J. Zhou, 1983: *Probable Maximum Precipitation and Flood*. Beijing, China Water Power Press.
- , 1984: Recent developments on the probable maximum precipitation estimation in China, in global water: science and engineering. The Ven Te Chow Memorial Volume, *Journal of Hydrology*, 68: 285–293.
- Zhao Y., Y. Zhang and L. Zhou, 1983: Analysis on extraordinary storms in the upper reach of the Changjiang River in 1870. *Journal of China Hydrology*, 3(1): 51–56.
- Zhang Y., 1982: Calculating probable maximum precipitation using net moisture transportation method. *Journal of China Hydrology*, 2(3): 38–40.
- Zhang Y. and Z. Wang, 1998: Estimating probable maximum storms in the middle and upper reaches of the Changjiang River using generalized depth-area-duration method. *Journal of China Hydrology*, 18(4): 13–18.
- Zheng W.S., W. Yi and Z. Yan, 1979: Survey and preliminary analysis on an extraordinary storm in Wushen County, Inner Mongolia, in August 1977. *Journal of China Hydrology*, 2: 45–49.
- Zurndorfer, E.A., E.M. Hansen, F.K. Schwarz, D.D. Fenn and J.F. Miller, 1986: *Probable Maximum and TVA Precipitation Estimates With Areal Distribution for the Tennessee River Drainages Less Than 3,000 Square Miles in Area* (HMR No. 56). National Weather Service, National Oceanic and Atmospheric Administration, United States Department of Commerce, Washington, DC.

## FURTHER READING

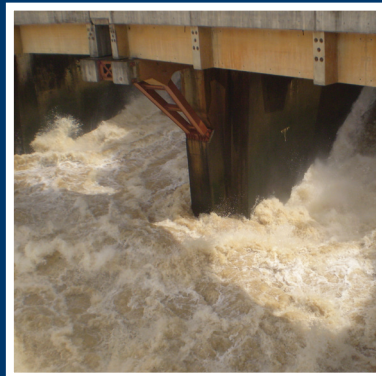
- Adil, M.A. and M.M. Suffi, 1964: *Probable Maximum Precipitation Over the Tarbela Dam Basin*. Scientific Note, 16, No. 3, Pakistan Department of Meteorology and Geophysics.
- Alexander, G.N., 1963: Using the probability of storm transposition for estimating the frequency of rare floods, *Journal of Hydrology*, 1(1): 46–57.
- ANCOLD, 1972: *Report on Safety and Surveillance of Dams*, Australian National Committee on Large Dams.
- Anon, 1977: Brazilian dam failures: a preliminary report. *Water, Power and Dam Construction*.
- , 1979: India's worst dam disaster. *Water, Power and Dam Construction*.
- Bell, G.J. and P.C. Chin, 1968: *The Probable Maximum Rainfall in Hong Kong*. Royal Observatory Technical Memoir No. 10, Royal Observatory, Hong Kong.
- Bell, G.J. and K.G. Tsui, 1973: Some typhoon soundings and their comparison with soundings in hurricanes, *Journal Applied Meteorology*, 12(1): 74–93.
- Benoit, R., P. Pellerin and Y. Larocque, 1997: *High-Resolution Modelling of Theoretical Meteorological Storm (PMS) Model*. Report prepared for B.C. Hydro, Maintenance, Engineering and Projects, British-Columbia Hydro Company, Vancouver, Canada.
- Bingeman, A.K., 2002: *Improving Safety Analysis for Hydrologic Structures by Using Physically-Based Techniques to Derive Estimates of Atmospherically Maximum Precipitation and Estimates of Frequency Curves*. Thesis available from the University of Waterloo, Waterloo, Ontario, Canada (civil engineering).
- Bond, H.G. and C.J. Wiesner, 1955: The floods of February 1955 in New South Wales, *Australian Meteorological Magazine*, No. 10: 1–33.
- Browning, K. A., 1968: The organization of severe local storms. *Weather*, Vol. 10: 439–434.
- Bruce, J.P., 1959: *Storm Rainfall Transposition and Maximization*, Proceedings of Symposium No. 1, Spillway Design Floods, Ottawa, Canada, National Research Council of Canada.
- , 1977: *New Directions in Hydrometeorology*. Robert E. Horton Memorial Lecture, Proceedings Second Conference on Hydrometeorology, 18–20 March 1980, Atlanta, Georgia. American Meteorological Society, Boston, MA.
- Bruce, J.P. and R.H. Clark, 1966: *Introduction to Hydrometeorology*. New York, Pergamon Press.
- Brunt, A.T., 1958: *Analysis of Two Queensland Storms*. Proceedings Conference on Extreme Precipitation, Melbourne, Australian Bureau of Meteorology.
- , 1963: *The Estimation of Extreme Precipitation – Current Problems and Aspects for Future Investigation*. Proceedings Hydrometeorological Discussion Group, September 1963, Melbourne, Australian Bureau of Meteorology.
- , 1964: *The Estimation of Areal Rainfall*. Australian Bureau of Meteorology Working Paper, Melbourne.
- , 1966: Rainfall associated with tropical cyclones in the northwest Australian region. *Australian Meteorological Magazine*, 14: 94–109.
- Canterford, R.P. and C.L. Pierrehumbert, 1977: *Frequency Distribution for Heavy Rainfalls in Tropical Hydrology Symposium*, Brisbane, Australia, Institution of Engineers.
- Charney, J.G. and A. Eliassen, 1964: On the growth of the hurricane depression. *Journal Atmospheric Science*, 21: 68–75.
- Commonwealth of Australia, Bureau of Meteorology, 1960: *A Long Lived Tropical Cyclone With an Unusual Track in Western Australia, Case 6 – Storm of March 1956*. Seminar on Rain, Vol. 1.
- , 1979: *Cyclone Joan – December 1975*.

- , 1982: *Estimation of Probable Maximum Precipitation, Morwell River Catchment Diversion Channel Project, Victoria.*
- Davis, D.R. and W.C. Bridges, 1972: Minimal tropical depression produces record rains and unprecedented floods. *Monthly Weather Review*, 100(4): 294–297.
- Dhar, O.N., P.R. Rakhecha and B.N. Mandal, 1960: Rainstorms which contributed greatest rain depths in India. *Archives for Meteorology, Geophysics, and Bioclimatology*, Series A.
- , 1976: *A Study of Maximum Probable Point Precipitation over Karnataka Region.* Proceedings of the Symposium on Tropical Monsoons, 8–10 September 1976, Pune, India, Indian Institute of Tropical Meteorology.
- , 1977: Estimation of design storm for the Subarnarekha Basin up to Chandil and Ghatsila dam sites. *Indian Journal of Power and River Valley Development*, XXVII (9): 338–343.
- , 1978: *A Study of Spillway Design Storm in Different Rainfall Regions of North Indian Plains.* Proceedings of the Symposium on Hydrology of River with Small and Medium Catchments, Vol. II.
- Dhar, O.N., P.R. Rakhecha, A.K. Kulkarni and G.C. Ghose, 1982: *Estimation of Probable Maximum Precipitation for Stations in the Western Ghats.* Proceedings of the International Symposium on Hydrological Aspects of Mountainous Watersheds, Roorkee, India.
- Dhar, O.N., A.K. Kulkarni and R.R. Mali, 1982: Estimation of maximum and probable maximum one-day point rainfall for Tamil Nadu. *Indian Journal of Power and River Valley Development*, 32(7): 117–124.
- Engman, E.T., L.H. Parmele and W.J. Gburek, 1974: Hydrologic impact of tropical storm Agnes. *Journal of Hydrology*, 22: 179–193.
- Fawkes, P.E., 1979: *Probable Maximum Flood for the Peace River at Site C.* Proceedings Canadian Hydrology Symposium-79, National Research Council, Ottawa, Canada.
- Flavell, D.R. and R.O. Lyons, 1973: *Probable Maximum Floods for the Fraser River at Hope and Mission,* Inland Waters Directorate, Environment Canada, Vancouver, Canada.
- Fletcher, R.D., 1951: Hydrometeorology in the United States. In: *Compendium of Meteorology*, American Meteorological Society, pp. 1033–1047.
- Ge, S., 1999: *Modern Flood Forecast Technologies.* Beijing, China Water Power Press.
- Gilman, C.S., 1964: Rainfall, Section 9. In: *Handbook of Applied Hydrology* (edited by V.T. Chow), New York, McGraw-Hill.
- Guo S., Zhou F. and Wang S., 2004: *Worldwide Research Progress and Assessment of PMP/PMF.* Water Resources and Hydropower Engineer Scientific National Key Experiment Office of Wuhan University.
- Hagen, V.K., 1982: *Re-evaluation of Design Floods and Dam Safety.* Fourteenth Congress on Large Dams, Rio de Janeiro, INCOLD.
- Hansen, E.M., 1987: Probable Maximum Precipitation for Design Floods in the United States, *Journal of Hydrology*, 96, pp. 267–278.
- , 1990: *Fifty Years of PMP/PMF.* Office of Hydrology National Weather Service, Silver Spring, MA.
- Harris, D.R., 1969: Cause and effect of the Tunisian floods. *Geographical Magazine*, 42(3): 229–230.
- Hawkins, H.F. and D.T. Rubsam, 1968: Hurricane Hilda 1964: II Structure and budgets of the hurricane on 1 October 1964. *Monthly Weather Review*, 96: 701–707.
- Henry, W.K., 1966: An excessive rainfall in Panama, October 1954. *Water Resources Research*, 2(4): 849–853.
- Hershfield, D.M. and W.T. Wilson, 1960: A comparison of extreme rainfall depths from tropical and non-tropical storms. *Journal of Geophysical Research*, 65(3): 959–982.
- Hounam, C.E., 1957: *Maximum Possible Rainfall Over the Cotter River Catchment.* Meteorological Study No. 10, Commonwealth of Australia, Department of Meteorology.
- , 1960: Estimation of Extreme Precipitation, *Journal of the Institution of Engineers, Australia*, 32(6).
- Hu, M. and C. Luo, 1988: *Historical Large Floods in China* (Vol. 1). Beijing, Cathay Bookshop.

- , 1992: *Historical Large Floods in China* (Vol. 2). Beijing, Cathay Bookshop.
- Institution of Engineers, Australia and ANCOLD, 1981: *A Catalogue of Design Flood Data for Australian Dams*. Institution of Engineers, Australia and Australian National Committee on Large Dams (ANCOLD).
- Knox, J.B., 1960: *Proceedings for Estimation Maximum Possible Precipitation*. Bulletin No. 88, State Department of Water Resources, CA.
- Koelzer, V.A. and M. Bitoun, 1964: Hydrology of spillway design floods: large structures-limited data, *Journal of Hydraulics Division, Proceedings of American Society of Civil Engineers*, Paper No. 3913, pp. 261–293.
- Lockwood, J.G., 1967: Probable maximum 24-h precipitation over Malaya by statistical methods. *Meteorological Magazine*, 96(1134): 11–19.
- McBride, J.L. and T.D. Keenan, 1980: *Climatology of Tropical Cyclone Genesis in the Australian Region*. WMO/ESCAP Symposium on Typhoons, Shanghai.
- Maksoud, H., P.E. Cabral and A. Garcia Occhipinti, 1967: *Hydrology of Spillway Design Floods for Brazilian River Basins with Limited Data*. International Committee on Large Dams, Ninth Congress, Istanbul.
- Mason, B., 1958: *The Theory of the Thunderstorm Model*. Proceedings Conference on Extreme Precipitation, Melbourne, Australian Bureau of Meteorology.
- , 1978: *The Physics of Clouds*. Clarendon Press, Oxford.
- Meaden, G.T., 1979: Point deluge and tornado at Oxford. *Weather*, 34(9): 358–361.
- Miller, J.F., 1973: *Probable Maximum Precipitation – The Concept, Current Procedures and Outlook, Floods and Droughts*. Proceedings of the Second International Symposium in Hydrology, 11–13 September 1972, Fort Collins, CO, Water Resources Publications.
- Miller, J.F., 1982: Precipitation evaluation in hydrology, Chapter 9. In: *Engineering, Meteorology, Fundamentals of Meteorology and Their Application to Problems in Environmental and Civil Engineering* (edited by E.J. Plate), Amsterdam, Elsevier Scientific Publishing Company.
- Mustapha, A.M. and P.M. Ojamaa, 1975: *Probable Maximum Flood – Red Deer River Flow Regulation Proposal*. Technical Services Division, Alberta Environment, Edmonton, Canada.
- Myers, V.A., 1967: *The Estimation of Extreme Precipitation as the Basis for Design Floods, Resume of Practice in the United States*, Extract of Publication No. 84, Symposium of Leningrad, International Association of Scientific Hydrology.
- Nicolini, M., Y. García Skabar, A.G. Ulke and A.C. Saulo, 2002: RAMS model performance in simulating precipitation during strong low-level jet events over South America. *Meteorologica, Special Issue for the South American Monsoon System*, 27: 89–98.
- Nicolini, M., P. Salio, J. Katzfey, J.L. McGregor and A.C. Saulo, 2002: January and July regional climate simulation over South America, *Journal of Geophysical Research-Atmospheres*, 107 (D22): 4637, doi:10.1029/2001JD000736
- Nicolini, M. and A.C. Saulo, 1995: *Experiments Using the LAHM/CIMA Model Over Argentina in Convective Situations: Preliminary Results of Precipitation Fields*. Programme Weather Prediction Research, PWPR No. 7 (WMO/TD No. 699), World Meteorological Organization, Geneva.
- Nicolini, M., A.C. Saulo, M. Torres Brizuela and J.C. Torres, 1997: *Simulation and Prediction of Mesoscale Precipitating Systems at CIMA*. CAS/JSC Working Group on Numerical Experimentation, Research Activities in Atmospheric and Oceanic Modelling, Report No. 25 (WMO/TD-No. 792), World Meteorological Organization, Geneva.
- Orgrosky, H.O., 1964: Hydrology of spillway design floods: small structures-limited data. *Journal of Hydraulics Division, American Society of Civil Engineers*, Paper No. 3914, pp. 295–310.
- Paegle, J., E.H. Berbery, R. Garreaud, T. Ammbrizzi, R. Porfirio da Rocha, P.L. Silva Dias, D. Herdies, J. Marengo, M. Seluchi, C. Campetella, C. Menendez, M. Nicolini, J. Ruiz and C. Saulo, 2004: Modelling studies related to SALLJEX. *CLIVAR Exchanges, Special Issue Featuring SALLJEX*, 9(1): 20–22.
- Panatoni, L. and J.R. Wallis, 1979: The Arno River flood study (1971–1976). *Transactions of the American Geophysical Union*, 60: 1–15.

- Paulhus, J.L.H. and C.S. Gilman, 1953: Evaluation of probable maximum precipitation. *Transactions of the American Geophysical Union*, 34: 701–708.
- Pierrehumbert, C.L. and M.R. Kennedy, 1982: *The Use of Adjusted United States Data to Estimate Probable Maximum Precipitation*. Proceedings of the Workshop on Spillway Design, 7–9 October 1981, Conference Series No. 6, Australian Water Resources Council, Australian Government Publishing Service, Canberra.
- Riehl, H. and H.R. Byers, 1958: *Flood Rains in the Bocono Basin, Venezuela*. Department of Meteorology, University of Chicago.
- Rui X., 2004: *Principles of Hydrology*. Beijing, China Water Power Press.
- Sarker, R.P., 1966: A dynamic model of orographic rainfall, *Monthly Weather Review*, 94(9): 555–572.
- Saulo, A.C. and M. Nicolini, 1995: Inclusión de la difusión vertical en un modelo regional de pronóstico: efecto sobre la precipitación, *Meteorología*, 20: 25–36.
- , 1998: The sensitivity of a LAM Model to an inclusion of a cloud fraction in an explicit representation of convection. *Atmospheric Research*, 47: 389–403.
- Scott, A.N., 1981: *PMP Estimation in Western Australia*. Proceedings Conference of Special Services Meteorologists, Melbourne, Internal Australian Bureau of Meteorology Report.
- Sherman, L.K., 1944: Primary role of meteorology in flood-flow estimating, discussion of paper. *Transactions American Society Civil Engineers*, 109: 331–382.
- Showalter, A.K., 1945: Quantitative determination of maximum rainfall. In: *Handbook of Meteorology* (F.A. Berry, E. Bollay and N.R. Beers, eds.). New York, McGraw-Hill, pp. 1015–1027.
- Singleton, F. and N.C. Helliwell, 1969: The calculation of rainfall from a hurricane. In: *Floods and Their Computation*, Vol. 1. International Association of Scientific Hydrology, Publication No. 84, pp. 450–461.
- Tripoli, G.J. and W.R. Cotton, 1980: A numerical investigation of several factors contributing to the observed variable intensity of deep convection over South Florida. *Journal of Applied Meteorology*, 19(9): 1037–1063.
- Tucker, G.B., 1960: Some meteorological factors affecting dam designs and construction. *Weather*, 15(1)..
- United Nations/World Meteorological Organization, 1967: *Assessment of the Magnitude and Frequency of Flood Flows*. Water Resources Series No. 30.
- Verschuren, J.P. and L. Wajtiw, 1980: *Estimate of the Maximum Probable Precipitation for Alberta River Basins*. Environment, Alberta, Hydrology Branch, RMD-8011.
- Wahler, W.A., 1979: *Judgment in Dam Design*. Proceedings, Engineering Foundation Conference: Responsibility and Liability of Public and Private Interests on Dams, American Society of Civil Engineers.
- Wang B., Z. Liu and Z. Gao, 2002: Probable maximum storms and floods in the reach of Yellow River between Xiaolangdi and Huayuankou. *Yellow River*, 10: 12–13
- Wang B., Y. Wang and H. Li, 2002: Study of precipitations for the extraordinary flood in the reach of Yellow River between Sanmenxia and Huayuankou in 1761. *Yellow River*, 10: 14–15
- Wang, B.H. and K. Jawed, 1985: Transformation of probable maximum precipitation to probable maximum flood. *Journal of Hydraulics Division*, 112(7): 547–567.
- Wang G., 1979: Approaches and knowledge of probable maximum flood analysis for sanmenxia-huayuankou reach of yellow river. *Yellow River*, 3: 14–19
- , 1991: Problems on design flood and flood criteria in China. *Journal of Hydraulic Engineering*, 171(4): 68–76.
- , 2002a: On flood prevention standard of reservoirs in China. *Journal of Hydraulic Engineering*, 12: 22–25.
- , 2002b: *Preliminary Study on Hydrologic Theorems, Laws and Hypotheses*. Zhengzhou, Yellow River Water Resources Publishing House.
- , 2004: Worldwide development and practice of PMP/PMF. *Journal of China Hydrology*, 24(5): 5–9.

- \_\_\_\_\_, 2005b: On rationality of basic frame of PMP/PMF calculation methods of the United States. *Yellow River*, 27(3): 20–22.
- \_\_\_\_\_, 2005c: Comparison of the PMP/PMF estimating methods between USA and PRC. *Journal of China Hydrology*, 25(5): 32–34.
- Wang G., X. Chen, Z. Gao and W. Yi, 1996: *Analysis and Calculation of Probable Maximum Flood for the Yellow River*. Water Science and Technology Series for the Yellow River (Hydrology for the Yellow River), Yellow River Water Resources Publishing House, Zhengzhou.
- Wang, G. and W. Li, 2002: *Rational Evaluation on the Results of Hydrological Design*. Zhengzhou, Yellow River Water Resources Publishing House.
- Wang, J., 1987a: Analysis on Statistics and Duration-Depth Relationship of Point Rainfalls of Short-Duration Storms in China. In: *Research on Hydrologic/Water Resources in Nanjing*, Ministry of Water Resources and Hydropower, Selected Papers on Hydrologic/Water Resources (1978–1985), China Water Power Press, Beijing, pp. 65–78.
- \_\_\_\_\_, 1987b: Study of design storms in China. *Journal of Hydrology*, 96: 279–291.
- \_\_\_\_\_, 2000a: *Proceeding of Hydrological Regime Prediction*. Zhengzhou, Yellow River Water Resources Publishing House.
- \_\_\_\_\_, 2000b: *Integrated Constrained Linear Prediction Model*. Zhengzhou, Yellow River Water Resources Publishing House.
- Wang, J. and M. Hu, 1984: Compilation of isoline maps for statistical parameters of short-duration storms in China. *Journal of China Hydrology*, 5: 1–7.
- \_\_\_\_\_, 1990: Distribution of point storm extremes in China. *Advances in Water Science*, 1(1): 2–12.
- \_\_\_\_\_, 1993: Distribution of areal rainfall extremes in China. *Advances in Water Science*, 4(1): 1–9.
- Wang, W., Y. Zhu and R. Wang, 1995: *Hydrology for Hydropower Station Projects*. Nanjing, Hohai University Press.
- Ward, J.K.G. and B. Harman, 1972: The Clermont storm of December 1916. *Civil Engineering Transaction, Institution of Engineers, Australia*, CE14: 153–7.
- Watanabe, K., 1963: *The Radar Spiral Bands and Typhoon Structure*. Proceedings of the Symposium on Tropical Meteorology, Rotorua, New Zealand.
- Wiesner, C.J., 1964: Hydrometeorology and river flood estimation. *Proceedings Institute of Civil Engineers*, 27: 153–67.
- \_\_\_\_\_, 1968: *Estimating the Probable Maximum Precipitation in Remote Areas*. Proceedings ANZAAS Congress, Christchurch, New Zealand.
- World Meteorological Organization, 1969: *Estimation of Maximum Floods* (WMO-No. 233). TP 126, Technical Note No. 98, Geneva.
- Yi, H.D., H.Z. Li and S.S. Li, 1980: On the physical conditions of occurrence of heavy rainfall and severe convective weather. *Bulletin American Meteorological Society*, 61(1).
- Yuan Z., 1990: *Watershed Hydrologic Models*. Beijing, China Water Power Press.
- Zhao R., 1984: *Watershed Hydrologic Simulation – Xinanjiang Model and North Shaanxi Model*, Beijing, China Water Power Press.
- Zhou, X., 1980: Severe storms research in China, *Bulletin American Meteorological Society*, 61(1).
- Zhuang Y.-L. and S. Lin, 1986: *Hydrologic Forecasts*. Beijing, China Water Power Press.



For more information, please contact:  
**World Meteorological Organization**

**Communications and Public Affairs Office**  
Tel.: +41 (0) 22 730 83 14/15 – Fax: +41 (0) 22 730 80 27  
E-mail: [cpa@wmo.int](mailto:cpa@wmo.int)

**Hydrology and Water Resources Branch**  
**Climate and Water Department**  
Tel.: +41 (0) 22 730 84 79 – Fax: +41 (0) 22 730 80 43  
E-mail: [chy@wmo.int](mailto:chy@wmo.int)

7 bis, avenue de la Paix – P.O. Box 2300 – CH-1211 Geneva 2 – Switzerland  
**[www.wmo.int](http://www.wmo.int)**